A new paradigm for Cerapodan Phylogeny : disentangling the origins of Marginocephalia and rediscussing Basal Iguanodontian relationships

Journal:	*Historical Biology*
Manuscript ID	GHBI-2020-0038
Manuscript Type:	Original Article
Date Submitted by the Author:	08-Mar-2020
Complete List of Authors:	Dieudonné, Paul-Emile; Universidad Nacional de Rio Negro, Instituto de Investigación en Paleobiología y Geología Cruzado Caballero, Penélope; Universidad Nacional de Río Negro, Instituto de Investigación en Paleobiología y Geología Godefroit, P; Royal Belgian Institute of Natural Sciences Tortosa, Thierry; Réserve Naturelle Nationale Sainte-Victoire, Conseil Départemental des Bouches-du-Rhône
Keywords:	Phylogeny, Cerapoda, Marginocephalia, Pachycephalosauria, Ornithopoda, Basal iguanodonts
Note: The following files were submitted by the author for peer review, but cannot be converted to PDF. You must view these files (e.g. movies) online.	
Supplemental material 4 - Complete datamatrix.nex Supplemental material 5 - Complete datamatrix without Yandusaurus.nex	

A new paradigm for Cerapodan Phylogeny : disentangling the origins of Marginocephalia and rediscussing Basal Iguanodontian relationships

Dieudonné, P.-E.[1*]; Cruzado-Caballero, P.[1, 2]; Godefroit, P.[3]; Tortosa, T.[4];

[1] *CONICET, Universidad Nacional de Río Negro. Instituto de Investigación en Paleobiología y Geología, General Roca, 8332, Rio Negro, Argentina;*

[2] *Grupo Aragosaurus-IUCA, Departamento de Ciencias de la Tierra, Área de Paleontología, Universidad de Zaragoza, Zaragoza, Spain;*

[3] *Directorate 'Earth and History of Life', Royal Belgian Institute of Natural Sciences, 1000, Brussels, Belgium.*

[4] *Réserve Naturelle Nationale Sainte-Victoire, Conseil Départemental des Bouches-du-Rhône, 52 avenue de Saint-Just, 13256 Marseille Cedex 20, France*

*Corresponding author : dpolmil@gmail.com

A new paradigm for Cerapodan Phylogeny : disentangling the origins of Marginocephalia and rediscussing Basal Iguanodontian relationships

Unaccurate taxon-grouping is augmented in numerical phylogenetic analyses by the missingness of the fossil record, uneveness of taxon-sampling, lack of data-compilation and insufficient revision of character scoring. Many authors disagree on the main ornithischian relationships at the family or even suborder level. This work attempts at providing a revised framework of the ornithischian phylogeny based on a strict bibliographic revision of one of the most recent iterations of the Butler et al. (2008 et seq) datamatrices. We improved the resolution of basal cerapods through the implementation of the Xu et al. datamatrix (2006). Heterodontosauridae is recovered as an unnatural paraphyletic family within Marginocephalia SERENO, 1986 progressively leading to the dome-headed 'true' pachycephalosaurs. 'Heterodontosauridae' falls within Pachycephalosauria in the sense of MARYANSKA and OSMOSLKA, 1974. Ornithopods origins remain unresolved and are pulled back to the early Jurassic. We provide an in-depth rediscussion of the phylogenetic relationships within Basal Iguanodontia based on our revised and augmented dataset. The validity of Rhabdodontomorpha is reassessed, and the origins of this clade and that of dryomorphs and elasmarians are rediscussed in the context of Basal Iguanodontian evolution.

Key-words: Phylogeny, Cerapoda, Marginocephalia, Pachycephalosauria, Ornithopoda, Basal iguanodonts.

Introduction

Ornithopoda and Marginocephalia are the two sister-Suborders of Cerapoda (Sereno 1986). Although widely accepted, Marginocephalia is one of the most weakly supported ornithischian group and there has been many hypotheses as to what regards their origins (Sereno 2000 ; Xu et al 2006 ; Butler et al. 2008). Similarly and despite of their huge evolutionnary success, the early phylogenetic relationships of Ornithopoda are an ever-lasting problem to dinosaur paleontologists (Sereno 1986 ; Sues and Norman 1990 ; Weishampel and Heinrich 1992 ; Butler et al. 2008 ; Boyd 2015 ; Bell et al. 2019). Researches dating back from about four decades have found that cursorial and sabre-toothed ornithischians – namely the Heterodontosauridae – shared similarities with ornithopods, pachycephalosaurs and ceratopsians (Santa Luca 1980 ; Cooper 1985 ; Sereno 1986 ; Sues and Norman 1990). However, results stemming from the first numerical phylogenetic analyses profoundly changed our conception on their phylogenetic affinities. After Sereno (1986) had erected the suborder Marginocephalia to group both Ceratopsia and Pachycephalosauria, the very first numerical phylogenetic analyses successively placed heterodontosaurids as basal ornithopods (Cooper 1985 ; Salgado et al. 1997), and unresolved at the base of Cerapoda with two MPTs placing them as either either basal ornithopods or the sister taxon of Marginocephalia (Norman et al. 2004). The large and comprehensive dataset of Butler et al. (2008) found heterodontosaurids as basal ornithischians, and their results largely influenced most subsequent authors. Yet, Butler et al. (2008, p. 23) recognized that their dataset was incomplete and claimed the need to implement other phylogenetic datasets to theirs, such as that of Xu et al. (2006) who had found heterodontosaurids as a basal sister taxon to Marginocephalia. However, such merging with the dataset of Xu et al. (2006) was never achieved. Throughout the past decade, the demultiplication of new ornithopod discoveries led to an increase of new ornithopods groups and families, with marked tendency to group

stratigraphically and geographically close taxa (Brown et al. 2013 ; Boyd 2015 ; Rozadilla et al. 2016). However, consensual results are rarely reached and phylogenies mostly fail to resolve ornithopod phylogenetic relationships when using an exhaustive taxonomic sampling (Boyd 2015 ; Herne et al. 2019 ; Cruzado-Caballero et al. 2019).

This arises questions as to wether this could be due to the actual fossil record lacunae, or to a lack of character scoring revision and data-compilation. At whichever cases, any of these possibilities might bring to an important, widely recongnized issue which is the long-branch attraction phenomenon. It occurs when longer branches – corresponding to better scored taxa – are erroneously clustered together because they share more characters in common than with other taxa for which those characters are partly or wholy missing (Felsenstein 1978, 2004). Inaccurate taxon-grouping especially occurs whenever missing characters or missing taxa within the tree are non-randomly distributed (Wiens 2005 ; Weishampel and Heinrich 1992). The largest weight-bearing ornithopods were for a long time the most complete and best described ones. They were also intuitively regarded as the 'most derived' ornithopods and grouped within Iguanodontia because of their quadrupedal stance and common loss of premaxillary teeth (e.g. Calvo et al. 2007 ; Butler et al. 2008). By contrast, the smaller ones were more scarcely recovered, less well preserved and known from more incomplete remains. They were thus scored for a smaller amount of characters within data-matrices (Weishampel and Heinrich 1992). The increased amount of new taxonomic descriptions and detailed osteological revisions allowed us to deal with this problem to some degree. We are now aware of many homoplasies that did actually occur throughout ornithopod evolution, especially to what regards graviportality, quadrupedy and premaxillary teeth loss (e.g. Winkler et al. 1997 ; Dieudonné et al. 2016). Yet, ornithopod relationships are still mostly unresolved (Bell et al. 2019 ; Rozadilla et al. 2019 ; Cruzado-Caballero et al. 2019).

This paper tries to adress the issues of incomplete data-compilation and erroneous character scoring that have been accumulated throughout past years. We merged a recent and exhaustively revised iteration of Butler et al. (2008) dataset with that of Xu et al. (2006), a set out n new theories on early cerapodan and basal iguanodontian origins.

Material and methods

This work is built on the line of phylogenetic datamatrices stemming from Butler et al. (2008), and more specifically uses a revised version of the Dieudonné et al. (2016) dataset (see character list and excel datamatrix in Supplemental material 1 and 2 respectively). Close attention was attached to the improvements, criticisms and modifications brought by Bell et al. (2019) on this datamatrix (see Supplemental material 3). Changes brought by Pol et al. (2011), Rozadilla et al. (2016); Andrzejewski et al. (2019); Rozadilla et al. (2019) on their respective dataset were also thoroughly considered. We merged this dataset with that of Xu et al. (2006) and revised each and every character scoring. Numerous corrections were brought on the character scoring based on a strict bibliographic revision; new characters were added, and some characters were also redefined (see Supplemental material 2, 3). Four out of the five ischial characters created by Gasca et al. (2014) - the first, third, fourth and fifth ones - were implemented to the present datamatrix. Characters #235 (also used by Cambiaso 2007 #59) and #236 from Han et al. (2018) were also implemented and completely recoded using a slightly modified definition. 35 new characters were created. We reintegrate 12 taxa which were previously coded in the series of Butler et al. (2008 *et seq.*) data-matrices. These are: *Laquintasaura venezuelae*, Ankylosauria, Stegosauria, *Isaberrysaura mollensis*, *Kulindadromeus zabaikalicus, Stenopelix valdensis, Chaoyangsaurus youngi*, *Liaoceratops yanzigouensis*, *Archaeoceratops oshimai*, *Wannanosaurus yansiensis*, *Goyocephale lattimorei*, *Homalocephale calathocercos*. We also add eleven taxa for the first time to this data-set: *Camptosaurus aphanoecetes*, *Convolosaurus marri*, *Eousdryosaurus nanohallucis*, *Kangnasaurus coetzeei*, *Mahuidacursor lipanglef*, *Morrosaurus antarcticus*, *Pachycephalosaurus wyomingensis*, *Prenocephale prenes*, *Stegoceras validum*, *Thescelosaurus assiniboiensis*, *Valdosaurus canaliculatus*. Psittacosauridae was also recoded and splitted as *Psittacosaurus major* and *Psittacosaurus mongoliensis*. *Dryosaurus altus* was

renamed "*Dryosaurus*" because it was actually based on specimens that are now attributed to *D. altus*, *Dryosaurus* cf. *altus* and *D. elderae* (Carpenter and Lamanna 2015; Carpenter and Galton 2018).

Character #110 (Ösi et al. 2012 #78) was newly treated as ordered, in addition to the already ordered characters #150 and #202 (from Ösi et al. 2012 #228 and #137 respectively). Characters #189, #201, #269, #272 (from McDonald et al. 2010 #87 and #113, Ösi et al. 2012 #135 and #174) were turned to unordered. The phylogenetic analysis was run under equally-weighted maximum parsimony using TNT (Tree Analysis using New Technology, Goloboff et al. 2008). A heuristic search of 1000 replications of Wagner trees (with random addition sequence) was performed, followed by a Tree Bisection Reconnection branch-swapping algorithm (holding 10 trees per replicate). Zero-length branches among any of the recovered most parsimonious trees (MPTs) were collapsed. *Herrerasaurus ischigualastensis* was used as the outgroup taxon. Bootstrap indices were obtained using TNT. After one run using an exhaustive set of taxa (nexus dataset in Supplemental material 4), we removed the wildcard taxon *Yandusaurus hongheensis* (nexus dataset in Supplemental material 5) to improve the overall resolution of the tree topology. We kept the 50% Majority Rule Consensus Tree (or 50% MRC) as our reference tree for subsequent analyses and discussion (see Fig. 1, 2). A table was built to show the phylogenetic definitions of each clade recovered in our analysis, and the characters that supported them (Supplemental material 6).

We performed three templeton tests in TNT (Templeton, 1983) with the TNT script developed by Alexander N. Schmidt-Lebuhn (2016) and tested for three alternative phylogenetic hypotheses with respect to our reference tree (Supplemental Material 7, see below). The first phylogenetic hypothesis tested for an arbitrary positioning of Heterodontosauridae as the closest monophyletic sister group of Genasauria as was the case prior to our study (Butler et al. 2008). The second hypothesis tested for the positioning of

Rhabdodontormopha at the base of Ankylopollexia, a hypothesis which we discuss further in this paper. The third alternative hypothesis tested for a breakage of Rhabdodontormopha consistent with the hypotheses of Bell et al. (2019) and Madzia et al. (2020), with *M. langdoni* and *F. dhimbangunmal* set within a monophyletic sister group of Ankylopollexia, and Rhabdodontidae left in the same positionning as in the 50% MRC (see Supplemental Material 7 for details on the results).

Results

Running the analysis with an exhaustive set of taxa results in the obtention of 20 MPTs. The basal ornithopods *Nanosaurus agilis*, *Jeholosaurus shangyuanensis*, *Haya griva*, *Changchunsaurus parvus* but also most non-iguanodontian ornithopods are found in politomy at the base of Cerapoda when viewing the strict consensus (results not shown). We remarked that *Yandusaurus hongheensis* is unstable and falls out of Ornithopoda 9 times out of 20 when viewing each MPT separately. The removal of *Y. hongheensis* greatly improves the overall resolution of the analysis. It allows to recover a monophyletic Ornithopoda, resolves the mutual relationships within the dome-headed pachycephalosaurs and reduces the number of MPTs to 10. The 50% Majority Rule Consensus (50% MRC) yields better resolved relationships within Elasmaria. It further recovers a monophyletic Rhabdodontidae with the Vegagete ornithopod as its basalmost member. Our reference tree was chosen as the 50% Majority-Rule Consensus tree (or "50% MRC" tree) with the prunning of *Yandusaurus hongheensis* (Fig. 1-2). This consensus has a tree length of 1389 steps (CI = 0.302, RI = 0.615).

Heterodontosaurids are - in any of our analyses and for the first time since fifteen years - resurected as basal members of Cerapoda (e.g. Cooper 1985 ; Weishampel and Heinrich 1992 ; Salgado et al. 1997 ; Norman et al. 2004). They are recognized as an unnatural paraphyletic grade of taxa stemming the dome-headed, 'true' pachycephalosaurs and should therefore be regarded as the basalmost members of Pachycephalosauria in the sense of MARYANSKA and OSMOLSKA, 1974. As in Sereno (2012), we recover the monophyletic subfamily Heterodontosaurinae that groups *Abrictosaurus consors*, *Heterodontosaurus tucki* and *Lycorhinus angustidens*. *Fruitadens haagarorum* is recovered as rooting Heterodontosaurinae but is excluded from Heterodontosaurinae because of specific characters that are discussed further below. The arbitrary positionning of a monophyletic

Heterodontosauridae at the base of Genasauria was found as significantly different from the reference tree in the Templeton Test (cf. Supplemental Material 7). The 'heterodontosaurids' *Tianyulong confuciusi* and *Echinodon becklesii* are recovered outside of Heterodontosaurinae as successive outgroups taxa to dome-headed pachycephalosaurs [Figure 1 near here].

Concerning iguanodontian ornithopods, our phylogenetic results show an overall similar topology to that found earlier by Calvo et al. (2007) and Barrett et al. (2011). Ornithopods giving rise to the clade Elasmaria are recovered as an intrinsically unresolved but separate lineage of gondwanan iguanodontians stemming from an early shoot of Late Jurassic dryosaurid-like ornithopods, amongst which is *Eousdryosaurus nanohallucis* (Escaso et al. 2014). For ease of the discussion we will refer to all of the taxa more derived than *Eousdryosaurus* as members of Elasmaria, although the original definition states that they should solely correspond to *Talenkauen*, *Macrogryphosaurus*, their common ancestor and all of their descendants (Calvo et al. 2007). The clade Rhabdodontomorpha DIEUDONNE et al. 2016 is again recovered as a separate monophyletic group despite of earlier criticisms (see Bell et al. 2019 and Supplemental Material 3). We discuss on the validity of the clade and re-establish its diagnosis below. The positionning of Rhabdodontomorpha at the base of Elasmaria and Dryomorpha can be subject of discussion. We propose a more derived position for this group and suggest it could have been derived from a close ankylopollexian ancestor based on character ressemblances with some Late Jurassic dryomorphs. The arbitrary positionning of Rhabdodontomorpha as the closest sister-taxon of Ankylopollexia is not significantly different from the topology of the reference tree (cf. templeton test, Supplemental Material 7). By contrast, the breakage of Rhabdodontomorpha with *Muttaburrasaurus langdoni* and *Fostoria dhimbangunmal* set as a monophyletic sister group of Ankylopollexia and rhabdodontids left as the basalmost iguanodontians is not sustained by

the templeton test and yields a significantly different results from the reference tree (cf. Supplemental Material 7). [Figure 2 near here].

Discussion

Heterodontosauridae : a controversial origin as basal ornithischians.

The dataset of Butler et al. (2008) invoked a number of shared traits between heterodontosaurids and *Herrerasaurus ischigualastensis*: v-shaped dentary symphysis (1), elongated penultimate manual phalanges (2) with pointed and claw-like ungueals (3), extensor pits on the anterodistal surface of manual phalanges (4), a medial tuberosity on the proximal articular end of the humerus (5), and a lack of mediolateral expansion of the distal extremity of tibia (6). Although the presence of distal extensor pits on manual phalanges, claw like manual ungueals, and mediolaterally unexpanded distal maleolli of tibiae are actually shared between *Herrerasaurus* and heterodontosaurids (Galton 2014, fig. 14C, O), the other three characters aren't. The dentary symphysis of *Herrerasaurus ischigualastensis* is straight, unexpanded and restricted to its very distal end (Sereno and Novas 1993, fig. 1F), which does not match with the massively butressed and v-shaped symphysis of *Heterodontosaurus tucki* (Norman et al. 2011, appendix 6.D). Contrary to heterodontosaurids, the penultimate phalanges of fingers II and III aren't longer than those from the first phalangeal row in *H. ischigualastensis* (Sereno 1993, fig. 13 and 15). The proximal tuberosity of humerus is deep, cleft-like and medially situated in *H. ischigualastensis* (Sereno 1993, fig. 4A-C), but it is shallow and centrally located in heterodontoaurids (Galton 2014, fig. 9L, M, O). Additionnally, there are many obvious differences between heterodontosaurids and basal ornithischians which argues in favor of placing heterodontosaurids within a much more derived position. The snout appearance of basal ornithischians such as *Lesothosaurus diagnosticus* (Sereno 1991) or *Isaberrysaura mollensis* (Salgado et al. 2017) is markedly elongated and bear many more teeth than that of heterodontosaurids and more derived neornithischians – to the sole exception maybe of derived ankylopollexians. A prominent and laterally projecting supra-acetabular crest encloses the femoral head into a cup-shaped

structure in all advanced archosaurs having achieved an upright limb-posture (Charig 1972). This supra-acetabular crest was later lost in neornithischian more derived than *Agilisaurus louderbacki* (e.g. Peng 1992, fig. 5). The lack of supra-acetabular flange in heterodontosaurids appears to be a weighty argument from a phylogenetic point of view, and regarding this feature as homoplastically acquired within basal Ornithischia is problematic (Barrett and Maidment 2011). Subsequently to the work of Butler et al. (2008) a number of characters shared by heterodontosaurids and marginocephalians continued to be alluded to in length, although these were listed as convergently acquired. Among them are the presence of three premaxillary teeth (Norman et al. 2011 ; Han et al. 2015), or the loss of the ischial obturator process (Galton et al. 2014).

A review of Marginocephalia

Marginocephalia : an historically weakly supported clade.

The first definitions of Marignocephalia were provided by Sereno (1984, 1986, 2000) and Maryanska and Osmolska (1985). The number of apomorphic characters originally listed went progressively reduced throughout the years, and passed from nine (Sereno 1984) to three in their latest definition (Sereno 2000). These three characters are as follow : the posterior extension of a parietosquamosal shelf obscures the occiput from a dorsal view (1), a median contact between the maxillae excludes the premaxillae from participation to the anterior margin of internal nares (2), the postpubic process is short and lacks the distal pubic symphysis (3). As we will see now, we consider that none of these characters are valid. We agree with Sues and Galton (1987) in that the parietosquamosal shelf of ceratopsians shows no close ressemblance with that of pachycephalosaurs. As Sereno (2000) noticed, the relative contribution of the parietal and squamosal to the parietosquamosal shelf is different wether we consider pachycephalosaurs or ceratopsians. In pachycephalosaurs, the parietal shelf is anteroposteriorly thick, and the parietal contribution to the parietosquamosal shelf is narrow

(e.g. *Stegoceras validum*, Gilmore 1924, pl. 4). In ceratopsians, the parietal shelf consists in a dorsoventrally wide and anteroposteriorly thin strap of bone (e.g. *Archaeoceratops oshimai* and *Yinlong downsi*, You and Dodson, 2003 ; Han et al. 2015). Moreover, the occiput is still visible from a dorsal view in primitive ceratopsians forms (e.g. *Yinlong downsi*, Han et al. 2015, fig. 4B). We are unaware of the plesiomorphic condition for a typical marginocephalian 'parietosquamosal shelf'. In regard of the above-mentionned differences we are forced to reject this character as a formal synapomorphic character of Marginocephalia. The second character looks confusing as actually, the premaxillae form contact with the internal nares in all marginocephalians and ornithischians so we disregarded this character pending further explanations. We concur with Sereno (2000) in that a postpubic reduction is shared between both ceratopsians (You and Dodson 2004) and *Homalocephale calathocercos*, the only 'true' pachycephalosaur for which a broken but likely very short postpubis is known (Maryanska and Osmolska 1974, fig. 5B). However, the finding of Heterodontosauridae within Pachycephalosauria in this analysis (see next chapter) drives us to reconsider the postpubic reduction as independently aquired in both pachycephalosaurians and ceratopsians lineages. Within pachycephalosaurian 'heterodontosaurids', *Tianyulong confuciusi* (Zheng et al. 2009) is the only one that features a similar post-pubic reduction. The postpubic process is as long as the ischium in *Heterodontosaurus tucki* (Galton 2014) and *Manidens condorensis* (Pol et al. 2011). We remark that post-pubic reduction occurred several times independently within Ornithischia. In addition to pachycephalosaurs and ceratopsians, it also occured in ankylosaurs (Vickarious et al. 2004), iguanodontoids (Norman 2004) and hadrosaurids (Horner et al. 2004). Marginocephalia has always suffered from weak character support (Sereno 1986, 2000). We here show that although all of the previously believed marginocephalian synapomorphies are no longer supported, many other apomorphic traits provide undisputable evidence for its existence.

Synapomorphic traits of Marginocephalia.

We confirm the validity of Marginocephalia and drastically increase its overall character support by notably finding Heterodontosauridae as a paraphyletic group of basal marginocephalians closer to the dome-headed, 'true' pachycephalosaurs than to Ceratopsia. Maryanska and Osmolska (1974) define pachycephalosaurs as all marginocephalians closer to *Pachycephaosaurus* than *Triceratops* (Sereno 1998). Following Maryanska and Osmolska (1974), heterodontosaurids should therefore be regarded as basal memebrs of Pachycephalosauria. 'Heterodontosaurids' lack the typically thickenned squamosals of formerly referred 'true' pachycephalosaurs (e.g. Sereno 2000). We will therefore informally refer to those marginocephalians fitted with a thickenned dorsal skull roof as 'eupachycephalosaurs'. The paraphyletic 'sabre-toothed' pachycephalosaurs devoid of thickenned dorsal skull roof will be referred here as 'heterodontosaurids' between quote marks, because this group isn't monophyletic anymore and therefore deemed invalid. We list as follow the newly recovered apomorphic characters that unite Marginocephalia.

The presence of three premaxillary teeth (#159) is shared by *Heterodontosaurus tucki* (Norman et al. 2011), *Abrictosaurus consors* (Sereno 2012, fig. 31), *Echinodon becklesii* (Sereno 2012, fig. 13C-D, 19), *Fruitadens haagarorum* (Butler et al. 2012, fig. 1), *Archaeoceratops oshimai* (You and Dodson 2003, p. 264), *Liaoceratops yanzigouensis* (Xu et al. 2002), *Yinlong downsi* (Han et al. 2015) and eupachycephalosaurs (Maryanska and Osmolska 1974, fig. 1A1, C1 ; Perle et al. 1982, p. 118). Those three premaxillary teeth were later lost progressively and possibly also several times within Marginocephalia : *Chaoyangsaurus youngi* has two premaxillary teeth (Zhao et al. 1999), psittacosaurids (e.g. Sereno 2010) and *Protoceratops andrewsi* (Brown and Schlaijker 1940) have none, *Tianyulong confuciusi* has two premaxillary teeth (Sereno 2012). The presence of a premaxilla-lacrimal contact (#17) is shared by *Heterodontosaurus tucki* (Norman et al. 2011,

fig. 8), *Tianyulong confuciusi* (Sereno 2012, p. 55), psittacosaurids (Sereno 2010, fig. 2.3, 2.7) and *Yinlong downsi* (Xu et al. 2006 #34; Han et al. 2015, fig. 8B). A potential apomorphic trait of Marginocephalia is an anterior midline contact between both maxillae that prevents the vomer from contacting the premaxillae (#29). It is actually observed in nearly all marginocephalians – to the exception of the basal ceratopsian *Yinlong downsi* for which such midline contact is dubious and possibly absent. A midline exclusion of the anterior vomeral head from the paired premaxillae is clearly observable in the pachycephalosaurs *Goyocephale lattimorei* (Perle et al. 1982, pl. 41.3B), *Prenocephale prenes* and *Stegoceras validum* (Maryanska and Osmolska 1974, fig. 1A3, C3), but also in the ceratopsians *Liaoceratops yanzigouensis* (Xu et al. 2002, fig. 1D). In *Heterodontosaurus tucki* the vomer would intercede in complex interlocking joint at the level of the premaxillae but prior to an intermaxillary contact, so a premaxillary-vomeral contact would be absent (Norman et al. 2011, p. 204, cf. sagittal reconstruction in fig. 10). In *Psittacosaurus major*, 'the vomer attaches to the dorsal surface of the maxillary symphysis' so we infer that there is a maxillary symphysis which prevents the vomer from contacting the premaxillae (You et al. 2008, p. 190). In *Yinlong downsi*, Han et al. (2015, p. 11) declares that 'the diamond-shaped rostral part of the vomers underlies and intercedes a short distance between the premaxillae at the rear of the premaxillary palate'. They further mention that 'the medial aspect of the articular peg [of maxilla] extends medial to the body of the maxilla; its surface is striated for articulation with either the vomer or contralateral maxilla' (Han et al. 2015, p. 12). They add that intermaxillary contact is not visible from a ventral view but could have occurred 'deep to the vomer' (Han et al. 2015, p. 12). This description recalls the complex interlocking contact of the vomer posteriorly to the short intermaxillary suture in *Heterodontosaurus tucki*, which is only visible from a sagittal section but not from a mere ventral view (Norman et al. 2011, fig. 9, 10). There remains a possibility that vomeral contact of *Y. downsi* resembles that of *H.*

tucki, although this cannot be ruled out from the available descriptions. *H. tucki* (Norman et al. 2011, appendix 3A, 4A-B), *M. condorensis* (Pol et al. 2011, fig. 2A-B), *Y. downsi* (Han et al. 2015, fig. 3A, 5A, 8A), *P. major* (You et al. 2008, fig. 1B), *W. yansiensis*, *P. prenes*, *S. validum*, *H. calathocercos* (Maryanska and Osmolska 1974, fig. 1A4, C4, D4), *G. lattimorei* (Perle et al. 1982, pl. 42.1), *P. wyomingensis* (Brown and Schlaikjer 1943, pl. 39), all have squamosals with a varyingly developped dorsolateral overhang (#69). Such lateral overhang seems absent or at most totally reduced to the posterior squamosal margin in the neoceratopsians such as *A. oshimai* (You and Dodson 2003, fig. 1E) and *L. yanzigouensis* (Xu et al. 2002, fig. 1A, C). The squamosal-quadrate articulation is set away from the posterodorsal squamosal border (#70) in *H. tucki* (Norman et al. 2011, appendix 3A, 4A-B), *M. condorensis* (Pol et al. 2011, fig. 2A-B), *Y. downsi* (Han et al. 2015, fig. 3A, 8A), *A. oshimai* (You and Dodson 2003, fig. 1A, C), *L. yanzigouensis* (Xu et al. 2002, fig. 1A, B), *W. yansiensis* (Butler and Zhao 2009, fig. 5C), *P. prenes*, *H. calathocercos*, *S. validum* (Maryanska and Osmolska 1974, fig. 1A4, C4, D4), *P. wyomigensis* (Brown and Schlaikjer 1943, pl. 39). The squamosal-quadrate articulation is set close to the posterodorsal border of the squamosal in psittacosaurids (You et al. 2008, Sereno, 2010, fig. 2.7), so we suggest that this trait was secondarily acquired in those latter taxa. The angular reaches the upper level of the mandibular ramus (#157) in the ceratopsians *A. oshimai* (You and Dodson 2003, fig. 1A-C), *L. yanzigouensis* (Xu et al. 2002, fig. 1A-B), *C. youngi* (Zhao et al. 2009, fig. 2A), and the pachycephalosaurs *H. tucki* (Norman et al. 2011, fig. 19A), *M. condorensis* (Pol et al. 2011, fig. 2C), *T. confuciusi* (Zheng et al. 2009, fig. 1D), *S. validum* (Gilmore 1924, pl. 1). In *Yinlong downsi*, the angular reaches the upper mandibular margin in the left side of IVPP V14530 and both sides of IVPP V18636 and IVPP V18686, (Han et al. 2015, fig. 3, 8A, 11A respectively), but not on the right side of IVPP V14530 (Han et al. 2015, fig. 2). We regard the latter variation as of little phylogenetic value, possibly related to either intrinsic

variability. As a whole, *Y. downsi* would bear a dorsoventrally tall angular as the aforementionned taxa. The angular is more than half the height of the mandibular ramus but does not reach its upper level in psittacosaurids (You et al. 2008, fig. 4 ; Sereno, 2010, fig. 2.7). Marginocephalians uniquely share the presence of 12 to 13 dorsal vertebrae (#202). This condition was actually reported for the ceratopsians *A. oshimai* (Dong and Azuma 1997, p. 78), *Y. downsi* (Han et al. 2018, fig. 2A), *Psittacosaurus mongoliensis* (Hailu and Dodson 2004, p. 487), but also for the basal pachycephalosaur *H. tucki* (Galton 2014, fig. 6B). *Y. downsi* (Han et al. 2018, fig. 5), *H. tucki* (Galton 2014, fig. 3A), *S. validum* (Gilmore 1924, pl. 9.1) all have an elongate and strap-like scapula, i.e. that is more than nine times as long as its minimum width at the level of the scapular neck (#223). The scapula is not strap-like in *P. mongoliensis* (Senter 2007). The total absence of ischial obturator process is an apomorphy of Marginocephalia (#291), as previously suggested by Gilmore (1924). The ischium of *Yinlong downsi* features a 'plate-like' distal expansion (Han et al. 2018, fig. 11E, G), but no real obturator process. *A. oshimai* (Dong and Azuma 1997, fig. 7), *S. valdensis* (Butler and Sullivan, 2009, fig. 3), *P. mongoliensis* (Osborn 1924, fig. 8), *S. valdensis* (Butler and Sullivan 2009, fig. 3), *P. prenes* (Maryanska and Osmolska 1974, pl. 25.3B), *S. validum* (Gilmore 1924, p. 35, fig. 3A), but also the heterodontosaurids *H. tucki* (Galton 2014, fig. 8J) and *T. confuciusi* (Zheng et al. 2009, supp. info. p. 5) all lack a tab-shaped obturator process. The postpubic shaft and prepubic process are widely open and almost on the same alignement in all marginocephalians for which such feature could be registered (#282). This is notably the case for the ceratopsians *Psittacosaurus mongoliensis* (Osborn 1924, fig. 8) and *Yinlong downsi* (Han et al. 2015, fig. 11E), and for the basal pachycephalosaur *H. tucki* (Galton et al. 2014, fig. 12F-G). Such feature could not be described in any other more derived pachycephalosaur. In *H. calathocercos*, the postpubic shaft is much probably extremely short, but is lacking (Maryanska and Osmolska 1974, fig. 5A5-8). Similarly to the alignement of the

prepubis and postpubic shaft, the proximal main axis of the ischial shaft falls right in the same axis as that of the ischial pubic peduncle in marginocephalians (#288). This character is formally reported in *H. tucki* (Galton 2014, fig. 12F, G), *M. condorensis* (Pol et al. 2011, fig. 1A-B), *S. validum* (Gilmore 1924, fig. 3A), *P. prenes* and *H. calathocercos* (Maryanska and Osmolska 1974, pl. 25.3B and pl. 29 respectively), *Y. downsi* (Han et al. 2018, fig. 11E, G), *Psittacosaurus mongoliensis* (Osborn 1924, fig. 8), *S. valdensis* (Butler and Sullivan 2009, fig. 3).

Heterodontosauridae and the origins of Pachycephalosauria.

Braincases are rarely observable, unless a sagittal section or Ct-Scan digital reconstruction is made. We remark that *Heterodontosaurus tucki* (Norman et al. 2011, fig. 2B) and *Stegoceras validum* (Snively and Theodor 2011, fig. 5B) share the relatively uncommon character of a braincase which basal axis angles to less than 35° with respect to the basioccipital and basisphenoid (#122). In *Psittacosaurus major* (You et al. 2008, fig. 2) and most other non-marginocephalian taxa, this angles is much steeper. The presence of a posterior caniniform premaxillary tooth (#163) and an anterior caniniform dentary tooth (#183) are outstanding features commonly found in nearly all "heterodontosaurids", except in *Abrictosaurus consors* (Sereno 2012, fig. 34, 35). Such trait is also found in the primitive eupachycephalosaur *Goyocephale lattimorei* (Perle et al. 1982, pl. 42.6, 42.9). Hou (1977, p. 3) cited an anterior caniniform dentary tooth in *Wannanosaurus yansiensis* which is now unfortunately lost (Butler and Zhao 2009). Its apex was not completely freed from matrix at the time of its description, and the whole tooth did not appear significatively enlarged apicobasally (Hou 1977, fig. 1). It seems that cervical centra of "heterodontosaurids" such as *Fruitadens haagarorum* (Carpenter and Galton 2018, fig. 5J, L) and *Heterodontosaurus tucki* (Galton 2014, fig. 4A) decrease in length posteriorly. A marked decrease is also observed between individually preserved cervical centra four and nine of *Pachycephalosaurus wyomingensis*

(Bakker et al. 2006, fig. 10B, 11B). Note that this character wasn't given a specific character state. It was coded the same as taxa for which there was neither posterior increase nor decrease in central length throught the neck (#200). The olecranon fossa of humerus is shallow to totally absent (#241) in the basal pachycephalosaurs *Fruitadens haagarorum* and *Heterodontosaurus tucki* (Santa Luca 1980; Galton 2014, fig. 9S, J respectively), as well as in the eupachycephalosaurs *Stegoceras validum* (Gilmore 1924, pl. 9.2, p. 34) and *Goyocephale lattimorei* (Perle et al. 1982, pl. 43.4A). In *Wannanosaurus yansiensis*, both the olecranon and coronoid fossae are told to be shallow, although as figured from a posterior view the olecranon fossa looks only very weakly depressed (Butler and Zhao 2009, fig. 8D). The subfamily "heterodontosaurinae" that was recovered by Sereno (2012) is also recovered in this analysis and is a valid monophyletic grouping.

Of note is that non-heterodontosaurine "heterodontosaurids" such as *Fruitadens haagarorum* (Butler et al. 2012), *Tianyulong confuciusi* (Zheng et al. 2009) and *Echinodon becklesii* (Owen 1858) present cranial and postcranial characters which make them more akin to dome-headed pachycephalosaurs than to heterodontosaurines, and heterodontosaurines are more akin to ceratopsians on those same respects. Most cerapods share the plesiomorphic condition of premaxillary teeth that are laterally offset with respect to an anteromedially deflected maxillary tooth row (#164). This is notably the case for the ceratopsians *Yinlong downsi* (Han et al. 2015, fig. 7A, B), the neoceratopsians *Archaeoceratops oshimai* and *Liaoceratops yanzigouensis* (Han et al. 2018, illustrations of characters #30(1) and #142), but also for the heterodontosaurine *Heterodontosaurus tucki* (Norman et al. 2011, fig. S5A). Although psittacosaurs lack premaxillary teeth, the anterior maxillary tooth row of *Psittacosaurus major* and *Psittacosaurus mongoliensis* is clearly inset medially with respect to their edentulous premaxillary wall (You et al. 2008, fig. 1C1; Sereno 2010, fig. 2.19F). However, the anterior maxillary tooth rows of non-heterodontosaurine heterodontosaurids

Fruitadens haagarorum (Butler et al. 2012, fig. 7C, D) and *Echinodon beclklesii* (Sereno 2012, fig. 12, 13) is not anteromedially deflected, so their maxillary row would have been aligned with the posterior premaxillary teeth. An alignment between premaxillary teeth and anterior maxillary teeth is clearly observed in the eupachycephalosaurs *Stegoceras validum*, *Prenocephale prenes* (Maryanska and Osmolska 1974, fig. 1A3, C3) and *Goyocephale lattimorei* (Perle et al. 1982, pl. 41.3). The teeth of non-heterodontosaurine heterodontosaurids are more triangular, "palmate", uniformly enamelled on both sides (Galton 1978, p. 143; Sereno, 2012; Butler et al. 2012) as also occur for eupachycephalosaurs (e.g. Butler and Zhao 2009, fig. 1B, E, 7C). By contrast, the crowns of the heterodontosaurines *Heterodontosaurus tucki* (Sereno 2012, fig. 55) and *Abrictosaurus consors* (Sereno 2012, fig. 32, 33) are higher, parallel-sided and much asymmetrically enameled. They are more reminiscent of the ceratopsians tooth crowns in those respects (e.g. *Yinlong downsi*, Han et al. 2015, fig. 21E; *Chaoyangsaurus youngi*, Zhao et al. 1999, fig. 3A). The non-heterodontosaurine "heterodontosaurids" *Echinodon becklesii* (Galton 1978, fig. 1D) and *Tianyulong confuciusi* (Zheng et al. 2009) share with the eupachycephalosaurs *Wannanosaurus yansiensis* (Butler and Zhao 2009, fig. 7A) and *Stegoceras validum* (Gilmore 1924, pl. 1; Sues and Glaton 1987, fig. 1A) the presence of a ventrolaterally extending coronoid that reaches a level ventral to the last dentary teeth. This outstanding feature is absent in *Heterodontosaurus tucki* (Norman et al. 2011, fig. 16). Concerning the postcranial skeleton, Sereno (2000, p. 482) had already listed the extremely short forearm – i.e. with an humerus forming less than half the length of the femur – as a pachycephalosaurian characteristic (#232). However, extreme shortening of the forelimb was also recovered in the non-heterodontosaurine "heterodontosaurid" *Tianyulong confuciusi* (Zheng et al. 2009), so this character might in fact characterize non-heterodontosaurine pachycephalosaurs. As for eupachycephalosaurs (cf. the broken although strongly reduced and splint-like post-pubis of

Homalocephale calathocercos, Maryanska and Osmolska, 1974, fig. 5A, pl. 29.2), the postpubis of *Tianyulong confuciusi* is extremely reduced (#285, Zheng et al. 2009, supp. info. p. 5). Finally, the distal fibular extremity of *Tianyulong confuciusi* (Zheng et al. 2009, p. 6) and *Stegoceras validum* (the only pachycephalosaur preserving a fibula, cf. Gilmore 1924, pl. 11.2) is splint-like (#316). Extreme forearm shortening, postpubis reduction and the presence of splint-like distal fibula are shared between *Tianyulong confuciusi* and eupachycephalosaurs and should therefore be regarded as plesiomorphic features of eupachycephalosaurs.

Marginocephalian plesiomorphies

Although Marginocephalia now appears better supported, there remains a high degree of uncertainties on what regards the origins and rooting of this suborder. *Changchunsaurus parvus*, *Haya griva*, *Jeholosaurus shangyuanensis* and *Nanosaurus agilis* were recovered as basal ornithopods in every MPTs but keeps being poorly supported. Their phylogenetic position might be subject to rapid changes with the addition and/or corrections of a few more characters. We hereafter discuss on a few characters plesiomorphic to Marginocephalia that were found as shared with both non-cerapodan-neornithischians and basal ornithopods.

The presence of an external mandibular fenestra (#154) is likely plesiomorphic to Marginocephalia, as a large external mandibular fenestra is present in *Agilisaurus louderbacki* at the boundary between the angular and surangular (Barrett et al. 2005, fig. 5). An external mandibular fenestra at the boundary between the surangular, angular and dentary is present in *Y. downsi* (Han et al. 2015, fig. 2), *L. yanzigouensis* (Xu et al. 2002, fig. 1A, B), *C. youngi* (Zhao et al. 1999, fig. 2A), psittacosaurids (Sereno 2010, fig. 2.7 ; You et al. 2008, fig. 4A-B), *L. angustidens* (Sereno 2012, fig. 79) and *A. consors* (Sereno 2012, p. 73, *contra* Thulborn 1974), *H. tucki* (Norman et al. 2011, appendix 6A), *T. confuciusi* (Zheng et al. 2009, fig. 1C-D). An external mandibular fenestra wasn't described for *A. oshimai*, although we suggest its possible presence in front of the angular (You and Dodson 2003, fig. 1A). The external

mandibular fenestra might have been secondarily lost in some pachycephalosaurs (Butler and Zhao 2009, p. 72 ; *S. validum*, Gilmore, 1924, pl.1), but not in *G. Lattimorei* in which it is still present (Perle et al. 1982, pl. 43C). 'Heterodontosaurids' (*H. tucki*, Galton 2014, fig. 3A), basal ceratopsians (*Yinlong downsi*, Han et al. 2018, fig. 1E), psittacosaurids (Osborn 1924, fig. 5) and other non-marginocephalians neornithischians such as *Jeholosaurus shangyuanensis* (Han et al. 2012, fig. 1A, C) share the presence of an extensive axis neural spine that covers up to the posterior margin of the third cervical centrum (#195). Note that although the axis neural spine of *Manidens condorensis* is elongated, it is also dorsoventrally oriented so that it would not have covered the third cervical centrum (Pol et al. 2011, fig. 1E). The axis neural spine of *C. youngi* is dorsoventrally tall but posteriorly unexpanded (Zhao et al. 1999, fig. 5B). In basal ceratopsians (e.g. Han et al. 2015, fig. 18B; Xu et al. 2002, fig. 1D), the pachycephalosaur *Homalocephale calathocercos* (Maryanska and Osmolska 1974, fig. 1D3), and cerapods such as *Haya griva* (Makovicky et al. 2011) but also *Thescelosaurus neglectus* (Boyd 2014), the ectopterygoid extensively contributes to the pterygo-palatine fenestra so the pterygoid is excluded from its margin (#129). In *Changchunsaurus parvus*, a small "postpalatine foramen" lies in contact with the ectopterygoid, pterygoid and palatine (Liyong et al. 2010, p. 208). However, and as deduced from the photograph (Liyong et al. 2010, fig. 6B), the ectopterygoid appears much expanded anteriorly so that the pterygoid doesn't make contact with the postpalatine foramen. Some pachycephalosaurs such as *Stegoceras validum* and *Prenocephale prenes* feature a reversed condition with respect to their marginocephalian ancestor in having a pterygoid that contributes to the pterygo-palatine fenestra (Gilmore 1924, pl. 5; Maryanska and Osmolska 1974, fig. 1A3, 1C3). In *Heterodontosaurus tucki*, the palatine branch of the pterygoid is poorly preserved and no specific mention of the pterygo-palatine fenestra is made except that the palatine branch of the pterygoid would be laterally sutured to the ectopterygoid (Norman et al. 2011, p. 208).

Norman et al. (2011, fig. 13) provide a conjectural ventral reconstruction of the skull, where the pterygoid participates to the pterygo-palatine fenestra. However, the right side of SAM-PK-K1332 (Norman et al. 2011, appendix 5.A) seems to feature a pterygo-palatine fenestra enclosed by the ectopterygoid and palatine. This nevertheless remains to be confirmed. The scapular blades of *Heterodontosaurus tucki* (Galton 2014, fig. 2A-B), *Tianyulong confuciusi* (Zheng et al. 2009, supp. info. p. 5, Sereno, 2012, p. 65), *Abrictosaurus consors* (Sereno 2012, p. 78), *Psittacosaurus mongoliensis* (Senter 2007, fig. 3J), *Stenopelix valdensis* (Butler and Sullivan 2009, fig. 5, see also discussion p. 30), *Stegoceras validum* (Gilmore 1924, pl. 9.1) are very weakly expanded distally (#222). *Yinlong downsi* appears polymorphic on what regards the expansion of its distal scapular blade, as two similarly-sized scapulae feature both the expanded and unexpanded conditions (IVPP V18678 and IVPP V18684, Han et al. 2018, fig. 5B-C). *Kulindadromeus zabaikalicus* (Godefroit et al. 2014, fig. S6A) and *Jeholosaurus shangyuanensis* (Han et al. 2012, fig. 2A) are the only early non-marginocephalian neornithischians featuring poorly expanded distal scapular blades.

Ornithopod relationships

A problematic origin.

The early temporal origin of Dryomorpha – exemplified by *Callovosaurus leedsi* from the Callovian of England (Ruiz-Omeñaca et al. 2007) and the Late Jurassic dryomorphs from the Morrison Formation of United States (e.g. Carpenter and Galton 2018) – have long set the whole ornithopod origin back to the mid-Jurassic. However, and paradoxically to their early radiation, dryomorphs are systematically placed in a derived position within the ornithopod tree. Other more primitive forms are mostly recovered from Mid to the Late Cretaceous stratas, thus creating huge ghost lineages at their bases. Our finding of 'heterodontosaurids' as basal members of Marginocephalia throws the ornithopod origins back to the early Jurassic. Although increasing the ghost lineage of every non-iguanodontian ornithopods, this result is coherent with the previous contention that the ornithopod radiation was more ancient than that of the Late Jurassic 'burst' of dryomorph forms (e.g. Weishampel and Heinrich 1992 ; McDonald et al. 2010 ; Boyd 2015). We newly coded *Kulindadromeus zabaikalicus* (Godefroit et al. 2014) - a neornithischian from the Bathonian of Siberia (Cincotta et al. 2019) - in our dataset, and noticeably found it as a basal ornithopod. The early age of this ornithopod is therefore coherent with our new tree topology. However, the early ornithopod record remains scarce, incomplete and represented by phylogenetically unstable taxa. *Yandusaurus hongheensis* ilustrates well this instability as it was successively recovered inside or outside of Cerapoda in the different MPTs (Supplemental Material 4). As a whole the phylogenetic relationships among basal ornithopods are still shrouded in mystery. We discuss as follow on the evolution of derived and better-represented groups of ornithopods. Our taxonomic sampling of Late-Jurassic basal iguanodontians was implemented through the addition of *Camptosaurus aphanoecetes* from the Morrison Formation of United States (Carpenter and Wilson 2008), and *Eousdryosaurus nanohallucis* from the Alcobaça Formation of Portugal

(Escaso et al. 2014). We significantly reduce the ghost-lineage at the base of Elasmaria, and regard these gondwanan ornithopods as derived from a Late-Jurassic dryosauroid-like offshoot akin to *Eousdryosaurus nanohallucis*. We discuss on the anatomical traits which justify the gondwanan ornithopod lineage leading to Elasmaria and the clade Dryomorpha. We finally rehabilitate the much debated and criticised clade Rhabdodontomorpha (Dieudonné et al. 2016 ; Bell et al. 2019). We will finally discuss on the phylogenetic rooting of Rhabdodontomorpha and its potential affinities with a camptosaurid-like ornithopod ancestor that wasn't recovered by our phylogenetic analysis.

Basal iguanodontian affinities of Eousdryosaurus nanohallucis

Eousdryosaurus nanohallucis is a relatively incomplete, although it is also a key taxon for untangling the phylogeny of Iguanodontia. *E. nanohallucis* bears marked affinities with elasmarians and dryosaurids. Our phylogenetic analysis resolves this taxon as rooting the elasmarian lineage. As previously argued by Escaso et al. (2014), *Eousdryosaurus* shares with *Elrhazosaurus nigeriensis* (Galton and Taquet 1982), *Dryosaurus altus* and *Dysalotosaurus lettowvorbecki* (Galton 1981), but also *Kangnasaurus coetzeei* (Cooper 1985) the presence of an anteriorly displaced *caudifemoralis longus* muscle scar on the medial side of its femur with respect to their fourth trochanter (#304). *Anabisetia saldiviai* was also described as bearing a *caudifemoralis longus* muscle scar anterodorsally displaced with respect to its pendant fourth trochanter (Coria and Calvo 2002, p. 506, fig. 7C). Let's remark that this feature is also shared with the more massively built basal camptosaurid *Draconyx loureoroi* (Mateus and Antunes 2001). The lesser trochanter of *Eousdryosaurus nanohallucis* is also high and reaches the upper level of the fourth trochanter (#298, Escaso et al. 2014, fig. 4), as also occurs in dryosaurids (Galton 1981, fig. 13C, 14C, I), *Anabisetia saldiviai* (Coria and Calvo 2002, fig. 7), and *Valdosaurus canaliculatus* (Barrett et al. 2011, pl. 1.4), but not in *Kangnasaurus coetzeei* (Cooper 1985, fig. 12A), *Morrosaurus antarcticus* (Rozadilla et al. 2016, fig. 2A)

and *Elrhazosaurus nigeriensis* (Galton and Taquet 1982). Let's remark that *Camptosaurus aphanoecetes* is polymorphic for this character (Carpenter and Wilson 2008, fig. 30). The cnemial crest of tibia of *Eousdryosaurus nanohallucis* projects anteriorly in a straight manner (Escaso et al. 2014, fig. 4M), in a similar way to the cnemial crest of *Anabisetia saldiviai*, *Morrosaurus antarcticus* (Cambiaso 2007, fig. 49D, 117E), *Talenkauen santacrucensis* (Rozadilla et al. 2019, fig. 24E), *Valdosaurus canaliculatus* (Barrett et al. 2011, fig. 7B, H), rhabdodontids (Dieudonné et al. 2016, fig. 9A2, C2) but also many other, more basal ornithopods (e.g. *Convolosaurus marri*, Andrzejewski et al. 2019, fig. 24I). As for some elasmarians (e.g. *Kangnasaurus coetzeei*, Cooper 1985, fig. 19 ; *Morrosaurus antarcticus*, Cambiaso 2007, fig. 52A), *E. nanohallucis* retains the primitive condition of a flat to broadly concave lateral surface of second metatarsal for resting against the third metatarsal. However, *E. nanohallucis* appears unspecialized in a number of features with respect to dryosaurids and elasmarian-like gondwanan ornithopods. For example, its caudal neural spines project posteriorly at an 'obtuse' angle superior to 50° (#208). A weak posterior bend of the proximal caudal neural spines is found in most ornithopods but also in camptosaurids (Carpenter and Wilson 2008, fig. 14), *Iguanodon bernissartensis* (Norman 1980, fig. 46), *Tenontosaurus tilletti* (Forster 1990, fig. 5A) and rhabdodontids (Weishampel et al. 2003, fig. 18D). This character is unknown for both *Morrosaurus antarcticus* and *Kangnasaurus coetzeei*. *Eousdryosaurus nanohallucis* retains the primitive trait of a proximally more developped articular surface on its first metatarsal (#334, Escaso pers. comm.), a feature that is shared with *Talenkauen santacrucensis* (Rozadilla et al. 2019, fig. S7E), *Anabisetia saldiviai* (Cambiaso 2007, fig. 120B) but also *Gasparinisaura cincosaltensis* (Cambiaso 2007, fig. 76C).

Similarities between basal dryomorphs, rhabdodontids and elasmarians.

Tenontosaurus and dryomorphans share some kinship with the gondwnanan ornithopod lineage leading to Elasmarians. *Talenkauen santacrucensis*, *Tenontosaurus* and dryomorphans share the exclusive presence of a relatively higher dentary tooth eruption rate, so there is no space left between adjacent functional teeth and their alveolar border (#174, Rozadilla et al. 2019, fig. 9 ; Thomas 2015, fig. 51, 52; Carpenter and Wilson 2008, fig. 5A, B; Norman 1980, fig. 9). As in *Tenontosaurus tilletti* (Thomas, 2015, fig. 2), *Camptosaurus dispar* (Gilmore 1909, fig. 2), *Dryosaurus* (Galton 1981, pl. 1) and *Iguanodon bernissartensis* (Norman 1980), the external nares of *Talenkauen santacrucensis* are enlarged posteriorly so they would have overlapped the maxilla posteriorly (#22, Rozadilla et al. 2019, fig. 2C, D). A gradual poterior lengthenning of cervical vertebrae (#200) is found in *Dryosaurus altus* (Carpenter and Galton 2018), *Camptosaurus dispar* (Carpenter and Galton 2018), elasmarians (Cruzado-Caballero et al. 2019), but also in the rhabdodontid *Zalmoxes robustus* (R.3841 in Nocpsa 1925: pl. 4.1A, 1C). Posterior cervical centra are not specially lengthenned in *Dysalotosaurus lettowvorbecki* (Janensch 1955, pl. 12.10), *Iguanodon bernissartensis* (Norman 1980, fig. 22) and *Tenontosaurus tilletti* (Forster 1990, fig. 1) although the latter is characterized by having increased its number of cervicals from nine to twelve. There is no posterior lengthenning of cervical centra either in more basal ornithopods (e.g. *Hypsilophodon foxii*, Galton 1974*a*, fig. 19 ; *Thescelosaurus neglectus*, Galton 1974*b*, pl. 3.3 ; *Convolosaurus marri* Andrzejewski et al. 2019, fig. 13B). As seen above, elasmarian ornithopods are similar to dryosaurids and *Draconyx loureoroi* in that they bear an anteriorly offset *caudifemoralis longus* muscle scar on the medial surface of their femur (#304). As formerly outlined by Rozadilla et al. (2016) the presence of a dominant proximal articular head of the third metatarsal (#328) is shared by the gondwanan elasmarian *Morrosaurus antarcticus*, *Kangnasaurus coetzeei*, *Anabisetia saldiviai*, but this is also the case in dryosaurids (Herne et al. 2018, fig. 32). This does not occur in the elasmarian *Talenkauen santacrucensis* (Rozadilla

et al. 2019) which has a third metatarsal of moderate size. Early dryomorphans such as *Dryosaurus altus* (Carpenter and Galton 2018, fig. 29B), *Camptosaurus dispar* (Carpenter and Galton 2018, fig. 14), but also ornithopods such as *Orodromeus makelai* (Scheetz 1999, fig. 12A) or the problematic taxon *Gasparinisaura cincosaltensis* (Coria and Salgado 1996; Cambiaso 2007, fig. 56A) all share with elasmarian ornithopods such as *Mahuidacursor lipanglef* (Cruzado-Caballero et al. 2019), *Talenkauen santacrucensis* (Rozadilla et al. 2019, fig. 13C, D), *Macrogryphosaurus gondwanicus* (Calvo et al. 2007, fig. 3) and *Anabisetia saldiviai* (Cambiaso 2007, p. 215, fig. 99) the presence of low and undevelopped cervical neural spines until their posteriormost cervical vertebrae (#194). Cervical neural spines are more prominent posteriorly in other ornithopods such as *Tenontosaurus tilletti* (Forster 1990, fig. 1), *Hypsilophodon foxii* (Galton 1974*a*, fig. 19), *Thescelosaurus neglectus* (Galton 1974*b*, pl. 3.3), *Convolosaurus marri* (Andrzejewski et al. 2019, fig. 13B). Of note is that the posteriormost cervical neural spine of *Dysalotosaurus lettowvorbecki* is higher than that of *Dryosaurus altus* (Janensch 1955, pl. 12.10). In *Muttaburrasaurus langdoni*, posterior cervicals weren't figured although they were described as getting slightly "stronger" from cervical five posteriorly (Bartholomai and Molnar 1981, p. 327). Weishampel et al. (2003, p. 83) suggest that the posterior cervical neural spines of *Zalmoxes robustus* were as tall as those of the anterior dorsal vertebrae, although they are preserved solely at their base.

Differences justifying an early divergence between elasmarian and dryomorphs

Rozadilla et al. (2016) already listed a number of traits that characterize derived elasmarians, such as for example a globular lateral surface of the greater trochanter (#300). However, there are a few oustanding difference which justify the early divergence between the lineage of gondwanan ornithopods leading to Elasmaria and basal dryomorphans. We remark that the sternal bones of *Mahuidacursor lipanglef* (Cruzado-Caballero et al. 2019) and *Macrogryphosaurus gondwanicus* (Calvo et al. 2007, fig. 6) markedly differ from those of all

other ornithopods. They are right-angled triangles closely apressed to each other along their medial edge, their paired anterior branch thin in close apression anteriorly and their posterolateral process is short and does not expand in a separate rod as in *Iguanodon bernissartensis* (#231). In *Iguanodon bernissartensis* the sternals are hatched-shaped with a posterolaterally extending process but with a wider semilunar anteromedial margin (Norman 1980, fig. 56). The sternals of *Dryosaurus altus*, *Camptosaurus dispar*, *Camptosaurus aphanoecetes, Tenontosaurus tilletti* and *T. dossi* are semi-lunar (Galton 1981, fig. 6M ; Winkler et al. 1997 ; Dodson and Madsen, 1981 ; Carpenter and Wilson 2008, fig. 18 ; Carpenter and Galton 2018, fig. 23N). Sternals are for now unknown in other iguanodontians, including rhabdodontids. The tibial cnemial crest of *Dryosaurus altus* (Galton 1981, fig. 16E), *Iguanodon bernissartensis* (Norman 1980, fig. 69A), and *Camptosaurus aphanoecetes* (Carpenter and Wilson 2008, fig. 31E) is curved outward to face laterally (#311), but that of *Tenontosaurus tilletti* (Forster 1990, fig. 20B), *Eousdryosaurus nanohallucis* (Escaso et al. 2014, fig. 4M), *Talenkauen santacrucensis* (Rozadilla et al. 2019, fig. 24E) and most other, more basal ornithopods is straight and faces anteriorly. *Tenontosaurus tilletti*, camptosaurids (Carpenter and Galton 2018, fig. 26Y, BB) and *Iguanodon bernissartensis* (Norman 1980, fig. 69D) share the possession of a sharply anteriorly projecting anteroproximal fibular process (#314). Dryosaurids (e.g. Galton 1981, fig. 17), *Eousdryosaurus nanohallucis* (Escaso et al. 2014, fig. 5A, B), elasmarians (Rozadilla et al. 2019, fig. 25B, E), *Muttaburrasaurus langdoni* (Bartholomai and Molnar 1981, fig. 10C), rhabdodontids (Weishampel et al. 2003, fig. 24E-F ; Godefroit et al. 2009, fig. 20E-F) and more primitive ornithopods all lack such anteroproximal process on their fibular head. The hands of *Tenontosaurus tilletti* (Forster 1990, fig. 14B), *Camptosaurus dispar* (Carpenter and Galton 2018, fig. 23B) and *Iguanodon bernissartensis* (Norman 1980, fig. 60) are outstanding in that their third digit is fitted with only three manual phalanges (#255), as opposed to four in other, more basal ornithopods (e.g.

Convolosaurus marri, Andrzejewski et al. 2019, fig. 20). Note that no manus comprising a complete third digit was described for now in dryosaurids, elasmarians or rhabdodontids. *Gasparinisaura cincosaltensis* is a problematic taxon and could be regarded as a close sister taxon to iguanodonts because it bears three phalanges on its third finger (Cambiaso 2007, fig. 65). However, it wasn't recovered as from the gondwanan ornithopod lineage leading to Elasmaria, probably because of its incompleteness and because it also possesses an array of basal, probably homoplastic features such as the lack of extensor groove on its distal femur. The proximalmost extremity of MT-II in iguanodonts such as dryosaurids (Herne et al. 2018, fig. 32H, I), *Tenontosaurus tilletti* (Forster 1990, fig. 22A), *Camptosaurus dispar* (Carpenter and Galton 2018, fig. 28JJ), *Iguanodon bernissartensis* (Norman 1980, fig. 70C) and rhabdodontids (Dieudonné et al. 2016, fig. 15C) feature a lateral step for resting upon a posteromedial protrusion of MT-III (#326). In *Anabisetia saldiviai*, the medial surface of the proximal MT-III is excavated to receive a lateral protrusion of MT-II, but the lateral surface of MT-II is smoothly concave dorsoventrally (Cambiaso 2007, fig. 120B). Such imbrication pattern is completely absent in *Morrosaurus antarcticus* (Cambiaso 2007, fig. 52A), *Eousdryosaurus nanohallucis* (Escaso et al. 2014, fig. 6), *Kangnasaurus coetzeei* (Cooper, 1985, fig. 19C), *Gasparinisaura cincosaltensis* (Salgado et al. 1997, fig. 5.6) and more basal ornithopods (e.g. *Hypsilophodon foxii*, Galton 1974*a*, fig. 57H).

A contentious but still valid Rhabdodontomorpha.

Rhabdodontormopha is a node-based clade of basal iguanodonts that was erected to group rhabdodontids – with *Rhabdodon priscus* chosen as their representative taxon – with the Australian *Muttaburrasaurus langdoni*, their most recent common ancestor and all of their descendents (Dieudonné et al. 2016). Madzia et al. (2018, supp. mat.) modified the definition of Rhabdodontomorpha authoritatively and without justification to a branch-based definition as the 'least inclusive group' comprising *Muttaburrasaurus langdoni*, *Rhabdodon priscus* and

all of their descendants. We insist on that we didn't aim at making a large-enough and inclusive group without any understanding of the characters implicitly upholding that group, just in order to avoid the possibility of being wrong. Should the apomorphic characters given to our node-based definition become invalid, plesiomorphic or homoplastic, then the name 'Rhabdodontomorpha' should definitively be abandonned and the group deemed polyphyletic. Yet, it is an euphemism to say that Rhabdodontomorpha was weakly supported, and perfectly understandable that Herne et al. (2019) and Bell et al. (2019) doubted on its validity. We call the lectors to reach supplemental materials 3 for a detailed discussion about the modifications brought by Bell et al. (2019) on our earlier datamatrix (Dieudonné et al. 2016), which directly regard the scoring of rhabdodontomorphs and *Muttaburrasaurus langdoni* more particularly. Five out of six apomorphic features originally cited for the clade are now regarded as invalid or uncertain. The group holds solely on behalf of the following unambiguous apomorphy: a mediolaterally thickenned dorsal margin of ilium at the level above the ischiac peduncle (Fig. 3). We here discuss on the additional apomorphic features which reaffirm the validity of Rhabdodontomorpha (see amended systematic definition). The ilia of *Muttaburrasaurus langdoni* and rhabdodontids are particularly similar and concentrate a number of apomorphic characters. In all of them, the outline of the dorsal iliac margin from a dorsal view is sigmoidal, with the postacetabular process deflected medialward and the preacetabular process deflected laterally (Weishampel et al. 2003, fig. 22C; Godefroit et al. 2009, fig. 13A-B, 18C; cf. also Fig. 3C for *M. langdoni*). As previously outlined (Dieudonné et al. 2016), the dorsal iliac margin of *M. langdoni* is mediolaterally broader and swollen from above the ischiac peduncle anteriorly (#267, Fig. 3C), and that of *Z. robustus* and *Z. shqiperorum* is mediolaterally swollen from above the postacetabular process all along (Weishampel et al. 2003, fig. 22C; Godefroit et al. 2009, fig. 13A, B; cf. also Fig. 3E). Such a broadenning over the dorsal iliac margin is quite unique in ornithopods. No rhabdodontomorph was ever

described or reported to bear a brevis shelf. Yet, *Z. shqiperorum* (Godefroit et al. 2009, fig. 18B, Fig. 3D) and *M. langdoni* (Fig. 3B) feature a similar, weak ridge on the ventromedial aspect of their postacetabular process. We refer such ridge as a remainder of reliquial brevis shelf that should characterize all rhabdodontomorphs (#270). Finally, the ischiac peduncle of ilium is uniquely anteroposteriorly long (#275) in *Muttaburrasaurus langdoni* (Fig. 3B) and rhabdodontids (Fig. 3D ; Weishampel et al. 2003, fig. 22A; Godefroit et al. 2009, fig. 18A-D). The finding of the Vegagete rhabdodontid in sister-relationship with *F. dhimbangunmal* in the semi-strict consensus (Fig. 2) is regarded as artefactual and probably related to the skeletal incompleteness of both specimens. *Fostoria* is unknown for the apomorphies that were listed for the Rhabdodontidae in the sense of our latest definition (Dieudonné et al. 2016). It is notably unknown for the presence or absence of bicipital sulcus as solely the mid-shaft region of its humerus is preserved, and not its proximal extremity (#233, supplemental material 3). The Vegagete ornithopod still holds as the earliest known rhabdodontid because of these characters and also because of its typically european geographic origin. We also note that the Vegagete ornithopod is recovered in monophyly with Rhabdodontidae to the exclusion of *F. dhimbangunmal* in the analysis resulting from implied character weighting (Fig. S4.4-5). *Fostoria dhimbangunmal* preserves little amount of overlapping characters with Rhabdodontomorpha and is positionned as a closer sister taxon to rhabdodontids on account of only a few characters. It shares with rhabdodontids a nearly vertical suture between its supraoccipital and opisthotics (#112, Bell et al. 2019, p. 6; Weishampel et al. 2003, fig. 10B ; Godefroit et al. 2009, fig. 4C, D), a character that is likely although not clearly referred in *Muttaburrasaurus langdoni*. *F. dhimbangunmal* is set slightly closer to rhabdodontids than *M. langdoni* on account of a single character which deals with the medioalterally broad and anteroposteriorly very short distal extremity of femur (#309, Fig. 3). The distolateral condyle length (not accounting for its posterolateral condylid) actually makes less than 40% of the

total distal width of the femur in *F. dhimbangunmal* (Bell et al. 2019, fig. 8E) and all rhabdodontids (Dieudonné et al. 2016, fig. 16). MDS-VG, 135 is a badly damaged distal extremity of femur and belongs to the largest individual of the Vegagete rhabdodontid (Fig. 3). It here as it closely matches the distal proportions found in other, smaller individuals from the same Vegagete locality, but also the distal femoral proportions of all other rhabdodontids (Dieudonné et al. 2016, fig. 15). In *M. langdoni* (Bartholomai and Molnar 1981, fig. 9G), *T. tilletti* (Forster 1990, fig. 19) and *C. aphanoecetes* (Carpenter and Wilson 2008, fig. 30E) the distal femora are still mediolaterally broad although their length-to-breadth proportions slightly exceeds 40%. [Figure 3 near here].

Questionnable rhabdodontomorphan ancestors

The above-mentionned traits characterizing Dryomorpha are rarely found in rhabdodontids or *Muttaburrasaurus langdoni*. We here point out features that are exclusively shared by *M. langdoni*, rhabdodontids and some basal dryomorphans. *M. langdoni* (Barthlomai and Molnar 1981, fig. 1C, contra Bell et al. 2019, cf. Supplemental materials 3) and rhabdodontids (Weishampel et al. 2003 ; Pincemaille-Quilleveré et al. 2006 ; Godefroit et al. 2009) share a reduced although still significant contribution of their suppraoccipital to the upper margin of the foramen magnum (#110). *Camptosaurus dispar* and *Dysalotosaurus lettowvorbecki* also retain the primitive condition of a reduced supraoccipital contribution to the upper margin of the foramen magnum (Gilmore 1909, fig. 4 ; Carenter and Lamanna, 2015, fig. 7E, 8E). This characters makes them more primitive than other laurasian dryomorphs such as *Dryosaurus* (Carenter and Lamanna 2015, fig. 4E) and *Iguanodon bernissartensis* (Norman 1980) in which the supraoccipital is excluded from the upper margin of the foramen magnum. This further make them differ from the Late Cretaceous north-american ornithopods *Tenontosaurus tilletti* (Thomas 2015, fig. 1), *Thescelosaurus neglectus* (Boyd 2014, fig. 4), and *Convolosaurus marri* (Andrzejewski et al. 2019, fig. 10) in which bar-like medial

processes are sent below their reverted 'T-shaped' supraoccipital. These processes completely exclude the supraoccipital from dorsal contribution to the upper margin of foramen magnum in *T. tilletti* and *T. neglectus*, but a complete exclusion of the supraoccipital is uncertain for *C. marri*. To the difference of *Tenontosaurus tilletti* (Thomas 2015, fig. 2), the quadratojugal of *Dryosaurus* (Galton 1983, pl.1), *Camptosaurus dispar* (Gilmore 1909, pl. 8), *Iguanodon bernissartensis* (Norman 1980, fig. 12A), *Muttaburrasaurus langdoni* (Bartholomai and Molnar 1981, p. 324) and *Zalmoxes robustus* (Weishampel et al. 2003) is devoid of quadratojugal foramen (#98). The exact location of that foramen is not known in the disarticulated skull of *Z. robustus*, but it was located at the boundary between the quadrate and quadratojugal in dryomorphs and *Muttaburrasaurus*. A paraquadratic/quadratojugal foramen is unknown in *Z. robustus* (Weishampel et al. 2003), although as in the aforementionned dryomorphs it could also have openned at the boundary between the quadratojugal and quadrate. Unlike dryomorphans, the anterolateral quadrate margin is not pierced for the passage of the quadratojugal foramen in rhabdodontids (Weishampel et al. 2003, fig. 7A ; Ösi et al. 2012, fig. 2C ; Carpenter and Lamanna 2015, fig. 13). The ilia of *Camptosaurus medius* (Carpenter and Galton 2018, fig. 24E, G), *Tenontosaurus tilletti* (Tennant 2013, fig. 25A, B), *Iguanodon bernissartensis* (Norman 1980, fig. 63), *Planicoxa venenica* (Carpenter and Galton 2008, fig. 49H), *Muttaburrasaurus langdoni* (Fig. 3A-B, Bartholomai and Molnar 1981, fig. 8A) and *Zalmoxes shqiperorum* (Fig. 3D, Godefroit et al. 2009, fig. 13C) are dorsally bulged and distinctly kinked above their pubic peduncle rather than more anteriorly, which induces a proximal downward deflection of the preacetabular process (#261). In *Camptosaurus aphanoecetes* (Carpenter and Lamanna 2015, fig. 10D, E) the downward curve of the dorsal margin of ilium occurs just anterior to the pubic peduncle. In *Zalmoxes robustus*, the dorsal bulge prior to the downward deflection of the preacetabular process is difficult to discern as the dorsal iliac margin is smoothly convex from above the

pubic peduncle anteriorly all along (Weishampel et al. 2003, fig. 23A, B). By contrast, the downward deflection of the preacetabular process occurs well anterior with respect to the pubic peduncle in the preacetabular process in dryosaurids and in the gondwanan elasmarians (Galton 1981, fig. 10A, L, 11A, C, J; Calvo et al. 2007, fig. 9B; Barrett, 2016, fig. 8; Rozadilla et al. 2019, fig. 22A). We note that in *Camptosaurus aphanoecetes* (CM 11337, Carpenter and Wilson 2008, fig. 30E) the distomedial condyle of femur protrudes more cranially than the distolateral condyle (#308). This feature is unknown in *E. nanohallucis* (Escaso et al. 2014) but is a common trait shared with many gondwanan iguanodontians such as *Anabisetia saldiviai* (Cambiaso 2007, fig. 116F, F'), *Kangnasaurus coetzeei* (Cooper 1985, fig. 16), *Muttaburrasaurus langdoni* (Bartholomai and Molnar 1981, fig. 9G), and rhabdodontids (Dieudonné et al. 2016). *Muttaburrasaurus langdoni* (Bartholomai and Molnar 1981, p. 332) was further reported to bear a cushion-shaped ulnare (#246), a trait exclusively shared with ankylopollexians (e.g. *Camptosaurus dispar*, *Camptosaurus aphanoecetes*, Carpenter and Wilson, 2008 fig. 23A, B ; *Iguanodon bernissartensis*, Norman 1980, p. 49). This contrasts with *Tenontosaurus tilletti* (Forster 1990, fig. 13B), the elasmarian *Mahuidacursor lipanglef* (Cruzado-Caballero et al. 2019, fig. 9) as well as all other more basal ornithopods. Unfortunately, no ulnare was ever described in any rhabdodontids up to now. Within Rhabdodontidae, the first metatarsal is currently known solely from the Vegagete rhabdodontid (Dieudonné et al. 2016, fig. 10). It is particularly noteworthy because of its distal head oriented medially and not anteriorly. Its extensor and flexor ligamentary fossae are directed mediodorsally and medioplantarly respectively. The first metatarsal was proximally splint-like (#334) and would have supported two phalanges (#335), as also occurs in *Camptosaurus dispar* (Carpenter and Galton 2018, fig. 26GG). In *Tenontosaurus tilletti* (Forster 1990, fig. 22A), *Eousdrysaurus nanohallucis* (Escaso, pers. comm.), *Talenkauen santacrucensis* (Rozadilla et al. 2019, fig. S7E) and *Anabisetia saldiviai* (Cambiaso 2007, fig.

120B) the proximal articular head of the first metatarsal was expanded and not splint-like. The second metatarsal of *Muttaburrasaurus langdoni* (Herne et al. 2018, fig. 32O), the Vegagete rhabdodontid and *Tenontosaurus tilletti* (Dieudonné et al. 2016, fig. 15C, E) are similar in that they equal or exceed the total breadth of their third metatarsal (#327). In camptosaurids and dryosaurids, for example, the second metatarsal is much reduced with respect to the third (Carpenter and Galton 2018, fig. 26GG, JJ ; Galton 1981, fig. 15F). It is even more drastically reduced in the lineage of gondwanan ornithopods leading to elasmarians (e.g. *Anabisetia saldiviai*, Cambiaso 2007, fig. 120B). Whichever their earlier phylogenetic origins, the divergence by the Late Jurassic between rhabdodontomorphs and other basal iguanodonts should have led the former to progressively lose their numerous, closely packed teeth characterizing all iguanodonts, and progressively aquire more slowly-growing and larger blade-like teeth (Godefroit et al. 2017 ; Dieudonné and Torcida Hernández-Baldor, 2019).

Institutional abbreviations. CM, Carnegie Museum of Natural History, Pittsburgh, PA.; IVPP, Institute of Vertebrate Paleontology and Paleoanthropology, Beijing, China; LRF, Australian Opal Centre, Lightning Ridge, New South Wales, Australia ; MDS, Museo de Dinosaurios de Salas de los Infantes, Burgos, Spain ; QM, Queensland Museum, Brisbane, Queensland, Australia; SAM, Iziko South African Museum, Cape Town ; UBB, Catedra de Geologie, Facultatea de Biologie şi Geologie, Universitatea din Babes-Bolyai, Cluj-Napoca.

Systematic paleontology

DINOSAURIA Owen, 1842

ORNITHISCHIA Seeley, 1887

NEORNITHISCHIA Cooper, 1985

CERAPODA Sereno, 1986

ORNITHOPODA Marsh, 1881 sensu Butler et al. 2008

IGUANODONTIA Dollo, 1888

RHABDODONTOMORPHA Dieudonné, Tortosa, Torcida Fernández-Baldor, Canudo, Díaz-Martínez, 2016

Etymology: From the genus of the first representative of this clade *Rhabdodon priscus* and "-morpha" the suffix indicating an ancient variant or morph for this clade.

Phylogenetic definition: Rhabdodontomorpha is phylogenetically defined as a node-based taxon consisting of the most inclusive clade containing *Rhabdodon priscus* MATHERON, 1869 and *Muttaburrasaurus langdoni* BARTHOLOMAI AND MOLNAR, 1981. Rhabdodontomorpha currently includes *F. dhimbangunmal*, *Mochlodon suessi*, *M. vorosi*, *Muttaburrasaurus langdoni*, *Rhabdodon priscus*, *R. septimanicus*, *Zalmoxes robustus* and *Z. shqiperorum*.

Diagnosis: Rhabdodontomorpha is redefined by the combination of the following synapomorphies : dorsal margin of ilium sigmoidal from a dorsal view with the postacetabular process deflected medialward (2), dorsal margin of ilium thickenned from the level above the ischiac peduncle anteriorly (3), ischiac peduncle of ilium anteroposteriorly elongated (4), brevis shelf consisting in a very smooth, dorsally convex ridge that is only visible from a medial view (5). One more cranial feature – i.e. the suture between the supraoccipital and opisthotics being nearly vertical – likely constitutes an additional synapomorphy for the group, although it is uncertain and not explicitly stated for *Muttaburrasaurus langdoni* (Bartholomai and Molnar 1981). A smooth and shallow *trochanteris* fossa on the proximal extremity of the femur and a distomedial femoral condyle that is higher than the distolateral condyle are likely plesiomorphic for Rhabdodontormopha.

Rhabdodontidae Weishampel, Jianu, Csiki & Norman, 2003

Etymology: From the genus of the first representative of this clade *Rhabdodon priscus* and and "-idae" the suffix indicating a family-level for the clade.

Phylogenetic definition: The most recent common ancestor of *Zalmoxes robustus*, *Rhabdodon priscus*, the Vegagete ornithopod and all the descendants of this common ancestor. Note that Dieudonné et al. (2016) diagnosed the Vegagete ornithopod as the most basal rhabdodontid, but used the phylogenetic definition of 'Weishampel et al. (2003) sensu Sereno (2005)'. Such formulation is equivocal, as these authors use both a node-based and a stem-based taxon respectively. Defining Rhabdodontidae as stem-based would make this family not mutually exclusive with Rhabdodontomorpha. We therefore redefine Rhabdodontidae as a node-based taxon, as did previously Weishampel et al. (2003). However, we also include the Vegagete ornithopod within the family because it possesses all of the diagnostic features for that clade.

Diagnosis : Rhabdodontidae is defined by the combination of the following synapomorphies (see phylogenetic analysis): 1) a humerus with a flat proximal anterior surface, i.e. devoid of any bicipital sulcus, 2) a humerus with a concave lateral border between the head and the deltopectoral crest in anteroposterior view, 3) an ulna with a relatively large olecranon process.

Conclusion

Ornithischian were an important and flourishing clade of herbivorous dinosaurs. Yet, their phylogeny has always suffered from incomplete taxonomic sampling and many of its OTUs were represented by incomplete skeletal remains. This work shows that apparenly insoluble phylogenies such as that of Ornithischians could be improved by revising and increasing simultaneously character and taxonomic sampling, notably paying particular attention to the most problematic and incomplete taxa. We provide another revised datamatrix for ornithischians with particular focus on the origins of Marginocephalia and basal iguanodonts. We increase the character support of Marginocephalia thanks to the integration of the datamatrix of Xu et al. (2006) to a wholy revised dataset stemming from Butler et al. (2008 *et seq.*). We resolve the 'Heterodontosauridae' as an unnatural paraphyletic lineage at the base of Pachycephalosauria, thus considerably reducing the ghot lineage of this clade. Ornithopod origins is a long-standing problem to dinosaur paleontologists. Their Middle to Late Jurassic origin was conditionned by the apparition of their earliest relative which are mostly represented by the derived basal iguanodonts. The finding of heterodontosaurinae as basal members of Marginocephalia pulls the ornithopod origins back to the early Jurassic. This leaves much more time for ornithopod to evolve and diversifiy into the impressive array of forms that thrived throughout the Cretaceous. This also reinforce the concept that basal ornithopods suffer from an incomplete fossil record. Basal iguanodontian evolution is reanalized based on character comparisons. Gondwanan ornithopods leading to the South-American clade Elasmaria would be much closer to *Eousdryosaurus nanohallucis*, a basal iguanodont form which is also akin to Late Jurassic dryosaurids. Besides, we reinforce the monophyly of the node-based clade Rhabdodontomorpha. Yet, the origin of this clade is still mysterious. Our resulting tree topology places them as more basal than elasmarian but in a slightly more derived position than *Tenontosaurus*. We suspect that such basal positionning

could be biased by the incompleteness of their preserved skeletal elements, combined with possible homoplastic evolution. We show that rhabdodontormorphs bear interesting affinities to basal ankylopollexians such as *Camptosaurus aphanoecetes*, which still keep incompletely fused distal carpals. This work could have never been achieved without the more recent and detailed taxonomic works that came to light in the past few years. The phylogenetic relationships here recovered are not aimed to be unchangeable or unalterable. They will certainly be challenged by subsequent works and the discovery of new taxa.

Acknowledgements

We are grateful to Catherine Forster, Phil Senter, Matthew Herne, Fernando Escaso for their helpful answers to questions concerning material in their care. We specially thank Matthew Herne and Fidel Torcida Fernández-Baldor for sharing some crucial and important photos. To all the people who helped directly or indirectly, and who provided unconditionnal support, help and accomodation facilities through the redaction of this paper (Ferrán and Alba, Cope and Silvia, Fidel, Geoffroy and his family, first author's family). Financial support has been partially provided by the Spanish Ministerio de Ciencia e Innovación and the European Regional Development Fund (CGL2017-85038-P), by the Agencia Nacional de Promoción Científica y Técnica (PICT 2016-0491), by the Universidad Nacional de Río Negro (PI 40-A-737).

Bibliography

Andrzejewski KA, Winkler DA and Jacobs LL. 2019. A new basal ornithopod (Dinosauria : Ornithischia) from the Early Cretaceous of Texas. PLoS ONE, 14, 1–44.

Bakker RT, Sullivan RM, Porter V, Larson P and Saulsbury SJ. 2006. *Dracorex hogwartsia*, n. gen. n. sp., a spiked, flat-headed pachycephalosaurid dionsaur from the Upper Cretaceous Hell Creek Formation of South Dakota. New Mexico Museum of Natural History and Science Bulletin, 35, 331–45.

Barrett PM, Butler RJ and Knoll F. 2005. Small-bodied ornithischians dinosaurs from the Middle Jurassic of Sichuan, China. Journal of Vertebrate Paleontology, 25, 823–34.

Barrett PM, Butler RJ, Twitchett RJ and Hutt S. 2011. New material of *Valdosaurus canaliculatus* (Ornithischia, Ornithopoda) from the Lower Cretaceous of southern England. Special Papers in Palaeontology, 86, 131–163.

Barrett PM, and Maidment SCR. 2011. The locomotor musculature of basal ornithischian dinosaurs. Journal of Vertebrate Paleontology, 31, 1265–391.

Bartholomai A and Molnar RE. 1981. *Muttaburrasaurus*, a new iguanodontid (Ornithischia: Ornithopoda) dinosaur from the Lower Cretaceous of Queensland. Memoirs of the Queensland Museum, 20, 319–49.

Bell PR, Brougham T, Herne MC, Frauenfelder T and Smith ET. 2019. *Fostoria dhimbangunmal*, gen. et sp. nov., a new iguanodontian (Dinosauria, Ornithopoda) from the mid-Cretaceous of Lightning Ridge, New South Wales, Australia. Journal of Vertebrate Paleontology, 39 : e1564757.

Boyd CA. 2014. The cranial anatomy of the neornithischian dinosaur *Thescelosaurus neglectus*. PeerJ, 2 : e669.

Boyd CA. 2015. The systematic relationships and biogeographic history of ornithischian dinosaurs. PeerJ, 3, 1–62.

Brown B and Schlaikjer EM. 1940. The structure and relationships of *Protoceratops*. Annals of the New York Academy of Sciences, 40, 133–266.

Brown B and Schlaikjer EM. 1943. A study of the troödont dinosaurs, with the description of a new genus and four new species. Bulletin of the American Museum of Natural History, 82, 115–150.

Brown CM, Evans DC, Ryan MJ and Russell AP. 2013. New data on the diversity and abundance of small-bodied ornithopods (Dinosauria, Ornithischia) from the Belly River Group (Campanian) of Alberta. Journal of Vertebrate Paleontology, 33, 495–520.

Butler RJ, Porro LB, Galton PM and Chiappe LM. 2012. Anatomy and Cranial Functional Morphology of the Small-Bodied Dinosaur *Fruitadens haagarorum* from the Upper Jurassic of the USA. PLoS ONE, 7 : e31556.

Butler RJ and Sullivan RM. 2009. The phylogenetic position of the ornithischian dinosaur *Stenopelix valdensis* from the Lower Cretaceous of Germany and the early fossil record of Pachycephalosauria. Acta Palaeontologica Polonica, 54, 21–34.

Butler RJ, Sullivan RM, Upchurch P and Norman DB. 2008. The phylogeny of the ornithischian dinosaurs. Journal of Systematic Palaeontology, 6, 1–40.

Butler RJ and Zhao, Q. 2009. The small-bodied ornithischian dinosaurs *Micropachycephalosaurus hongtuyanensis* and *Wannanosaurus yansiensis* from the late Cretaceous of China. Cretaceous Research, 30, 63–77.

Calvo J, Porfiri J and Novas F. 2007. Discovery of a new ornithopod dinosaur from the Portezuelo Formation (Upper Cretaceous), Neuquén, Patagonia, Argentina. Arquivos Do Museu Nacional, 65, 471–83.

Cambiaso AV. 2007. Los ornitópodos e iguanodontes basales (Dinosauria, Ornithischia) del Cretácico de Argentina y Antártida [The ornithopods and basal iguanodonts (Dinosauria, Ornithischia) from the Cretaceous of Argentina and the Antarctic]. Unpublished PhD thesis, Universidad de Buenos Aires, Facultad de Ciencias Exactas y Naturales, 410 pp. Spanish.

Carpenter K and Galton PM. 2018. A photo documentation of bipedal ornithischian dinosaurs from the Upper Jurassic Morrison Formation, USA. Geology of the Intermountain West, 5, 167–207.

Carpenter K and Lamanna MC. 2015. The braincase assigned to the ornithopod dinosaur Uteodon McDonald, 2011, reassigned to *Dryosaurus* Marsh, 1894 : implications for iguanodontian morphology and taxonomy. Annals of Carnegie Museum, 83, 149–65.

Carpenter K and Wilson Y. 2008. A new species of *Camptosaurus* (Ornithopoda: Dinosauria) from the Morrison formation (Upper Jurassic) of Dinosaur National Monument, Utah, and biomechanical analysis of its forelimb. Annals of Carnegie Museum, 76, 227–63.

Charig AJ. 1972. The evolution of the archosaur pelvis and hindlimb: an explanation in functional terms. 121–155. In Joysey KA and Kemp TS, editors. Studies in vertebrate evolution: essays presented to Dr. F. R. Parrington, F.R.S., Oliver and Boyd, Edinburgh, 284pp.

Cincotta A, Pestchevitskaya EB, Sinitsa SM, Markevich VS, Debaille V, Reshetova SA, Mashchuk IM, Frolov AO, Gerdes A, Yans J, Godefroit P. 2019. The rise of feathered dinosaurs : *Kulindadromeus zabaikalicus*, the oldest dinosaur with 'feather-like' structures. PeerJ, 7 :e6239.

Cohen KM, Finney SC, Gibbard PL and Fan J-X. 2013, updated. The ICS International Chronostratigraphic Chart. Episode 36, 199-204.

Cooper MR. 1985. A revision of the ornithischian dinosaur *Kangnasaurus coetzeei* Haughton, with a classification of the Ornithischia. Annals of the South African Museum, 95, 281-317.

Coria RA and Calvo JO. 2002. A new Iguanodontian Ornithopod from Neuquen Basin, Patagonia, Argentina. Journal of Vertebrate Paleontology, 22, 503–9.

Coria RA and Salgado L. 1996. A basal iguanodontian (Ornithischia, Ornithopoda) from the Late Cretaceous of South America. Journal of Vertebrate Paleontology, 16, 445–57.

Cruzado-Caballero P, Gasca JM, Filippi LS, Cerda I, Garrido AC. 2019. A new ornithopod dinosaur from the Santonian of Northern Patagonia (Rincón de los Sauces, Argentina), Cretaceous Research, 98, 211-29.

Dieudonne P-E, Tortosa T, Torcida Fernandez Baldor F, Canudo JI and Diaz-Martinez I. 2016. An unexpected early rhabdodontid from Europe (Lower Cretaceous of Salas de los Infantes, Burgos Province, Spain) and a Re- Examination of basal iguanodontian relationships. PLoS ONE, 11 : e0156251.

Dieudonne P-E, Torcida Fernandez Baldor, F. 2019. Unrelated ornithopods with similar tooth morphology in the vicinity of Salas de los Infantes (Burgos Province, Spain): an intriguing case-study, VIII Jornadas sobre Paleontología de Dinosaurios, Salas de los Infantes, España, 53-56.

Dodson P, Madsen JH and Jr. 1981. On the Sternum of *Camptosaurus*. Journal of Paleontology, 55, 109-112.

Dollo L. 1888. Iguanodontidae et Camptonotidae [Iguanodontidae and Camptonotidae]. Comptes rendus de l'Académie des sciences de Paris, 106, 775–7. French.

Dong Z and Azuma Y. 1997. On A Primitive Neoceratopsian from the Early Cretaceous of China. Sino-Japanese Silk Road Dinosaur Expedition. China Ocean Press, Beijing, 68–89.

Escaso F, Ortega F, Dantas P, Malafaia E, Silva B, Gasulla JM, Mocho P, Narvaez I, Sanz JL. 2014. A new dryosaurid ornithopod (Dinosauria, Ornithischia) from the Late Jurassic of Portugal. Journal of Vertebrate Paleontology, 34, 1102–12.

Felsenstein J. 1978. Cases in which parsimony or compatibility methods will be positively misleading. Systematic zoology, 27, 401-10.

Felsenstein J. 2004. Inferring phylogenies. Sunderland, Massachusetts: Sinauer associates, Inc. 664 pp.

Forster CA. 1990. The postcranial skeleton of the ornithopod dinosaur *Tenontosaurus tilletti*. Journal of Vertebrate Paleontology, 10, 273–94.

Galton PM. 1974a. The ornithischian dinosaur *Hypsilophodon* from the Wealden of the Isle of Wight. Bulletin of the British Museum. Natural History. Geology Series, 25, 1–152.

Galton PM. 1974b. Notes on Thescelosaurus, a conservative ornithopod dinosaur from the Upper Cretaceous of North America, with comments on ornithopod classification. Journal of Paleontology, 1974b, 1048–67.

Galton PM. 1978. Fabrosauridae, the basal family of ornithischian dinosaurs (Reptilia: Ornithopoda). Paläontologische Zeitschrift, 52, 138.

Galton PM. 1981. *Dryosaurus*, a hypsilophodontid dinosaur from the Upper Jurassic of North America and Africa; postcranial skeleton. Palaeontologische Zeitschrift, 55, 271–312.

Galton PM. 1983. The cranial anatomy of *Dryosaurus*, a hypsilophodontid dinosaur from the Upper Jurassic of North America and East Africa, with a review of hypsilophodontids from the Upper Jurassic of North America. Geologica et Palaeontologica, 17, 207–43.

Galton PM. 2014. Notes on the postcranial anatomy of the heterodontosaurid dinosaur *Heterodontosaurus tucki*, a basal ornithischian from the Lower Jurassic of South Africa, Revue de Paléobiologie, 33, 97–141.

Galton PM and Taquet P. 1982. *Valdosaurus*, a hypsilophodontid dinosaur from the Lower Cretaceous of Europe and Africa, Geobios, 15, 147-59.

Gasca JM, Canudo J-I, and Moreno Azanza M. 2014. On the diversity of Iberian iguanodont dinosaurs : New fossils from the lower Barremian, Teruel province, Spain. Cretaceous Research, 50, 264–72.

Gilmore CW. 1909. Osteology of the Jurassic reptile *Camptosaurus*, with a revision of the species of the genus, and description of two new species. Proceedings of the United States National Museum, 36, 197–332.

Gilmore CW. 1924. On Troodon validus, an Orthopodous Dinosaur from the Belly River Cretaceous of Alberta, Canada. University of Alberta Press, 1, 1–58.

Godefroit P, Codrea V and Weishampel DB. 2009. Osteology of *Zalmoxes shqiperorum* (Dinosauria, Ornithopoda), based on new specimens from the Upper Cretaceous of Nalat-Vad (Romania). Geodiversitas, 31, 525–53.

Godefroit P, Garcia G, Gomez B, Stein K, Cincotta A, Lefevre U, Valentin X. 2017. Extreme tooth enlargement in a new Late Cretaceous rhabdodontid dinosaur from Southern France. Scientific Reports, 7, 1–9.

Godefroit P, Sinitsa SM, Dhouailly D, Bolotsky YL, Sizov AV, Mcnamara ME, Benton MJ, Spagna P. 2014. A Jurassic ornithischian dinosaur from Siberia with both feathers and scales. Science, 345, 451–55.

Goloboff P, Farris JS, Nixon K. 2008. TNT, a free program for phylogenetic analysis. Cladistic, 24, 774–86.

Hailu Y and Dodson P. 2004. Basal Ceratopsia. 478-93. In Weishampel DB, Dodson P and Osmolska H, editors. The Dinosauria, 2nd edn. University of California Press, Berkeley, 861 pp.

Han F-L, Barrett PM, Butler RJ and Xu X. 2012. Postcranial anatomy of *Jeholosaurus shangyuanensis* (Dinosauria, Ornithischia) from the Lower Cretaceous Yixian Formation of China. Journal of Vertebrate Paleontology, 32, 1370–95.

Han F-L, Forster CA, Clark JM and Xu X. 2015. Cranial anatomy of *Yinlong downsi* (Ornithischia : Ceratopsia) from the Upper Jurassic Shishugou Formation of Xinjiang, China, 36, e1029579.

Han F-L, Forster CA, Xu X and Clark JM. 2018. Postcranial anatomy of *Yinlong downsi* (Dinosauria : Ceratopsia) from the Upper Jurassic Shishugou Formation of China and the phylogeny of basal ornithischians. Journal of Systematic Palaeontology, 16, 1159–87.

Herne MC. 2014. Anatomy, systematics and phylogenetic relationships of the Early Cretaceous ornithopod dinosaurs of the Australian-Antarctic rift system. Unpublished PhD thesis, The University of Queensland, Brisbane, 335 pp.

Herne MC, Nair JP, Evans AR and Tait AM. 2019. New small-bodied ornithopods (Dinosauria, Neornithischia) from the Early Cretaceous Wonthaggi Formation (Strzelecki Group) of the Australian-Antarctic rift system, with revision of *Qantassaurus intrepidus*. Journal of Paleontology, 93, 543-584.

Herne MC, Tait AM, Weisbecker V, Hall M, Nair JP, Cleeland M and Salisbury SW. 2018. A new small-bodied ornithopod (Dinosauria, Ornithischia) from a deep, high-energy Early Cretaceous river of the Australian–Antarctic rift system. PeerJ, 5, e4113.

Hou L. 1977. A primitive pachycephalosaurid from the Cretaceous of Anhui, China, *Wannanosaurus yansiensis* gen. et sp. nov. Vertebrata PalAsiatica, 15, 198–202.

Horner JN, Weishampel DB, Forster CA. 2004. Hadrosauridae. 438-63. In Weishampel DB, Dodson P and Osmolska H, editors. The Dinosauria, 2nd edn. University of California Press, Berkeley, 861 pp.

Janensch W. 1955. Der Ornithopod *Dysalotosaurus* der Tendaguruschichten [The ornithopod *Dysalotosaurus* from the Tendaguru]. Palaeontographica, Suppl. 7, 1955, 105–76. German.

Liyong J, Jun C, Shuqin Z, Butler RJ and Godefroit P. 2010. Cranial anatomy of the small ornithischian dinosaur *Changchunsaurus parvus* from the Quantou Formation (Cretaceous, Aptian-Cenomanian) of Jilin Province, northeastern China. Journal of Vertebrate Paleontology, 30, 196–214.

Madzia D, Boyd CA, Mazuch M. 2018. A basal ornithopod dinosaur from the Cenomanian of the Czech Republic. Journal of Systematic Palaeontology, 16, 967-79.

Madzia D, Jagt JWM, Mulder EWA. 2020. Osteology, phylogenetic affinities and taxonomic status of the enigmatic late Maastrichtian ornithopod taxon *Orthomerus dolloi* (Dinosauria, Ornithischia), Cretaceous Research, 108, https://doi.org/10.1016/j.cretres.2019.104334.

Makovicky PJ, Kilbourne BM, Sadleir RW and Norell MA. 2011. A new basal ornithopod (Dinosauria, Ornithischia) from the Late Cretaceous of Mongolia. Journal of Vertebrate Paleontology, 31, 626–40.

Marsh OC. 1881. Principal characters of American Jurassic dinosaurs. American Journal of Science, 21, 417–23.

Maryanska T and Osmolska H. 1974. Pachycephalosauria, a New Suborder of Ornithischian Dinosaurs. Palaeontologia Polonica, 30, 45–102.

Maryanska T and Osmolska H. 1985. On ornithischian phylogeny. Palaeontologica Polonica, 30, 137-50.

Mateus O and Antunes MT. 2001. *Draconyx loureiroi*, a new camptosauridae (Dinosauria, Ornithopoda) from the Late Jurassic of Lourinha, Portugal. Annales de Paléontologie, 87, 61–73.

Mcdonald AT, Kirkland JI, Deblieux DD, Madsen SK, Cavin J, Milner ARC and Panzarin L. 2010. New basal iguanodonts from the cedar mountain formation of utah and the evolution of thumb-spiked dinosaurs. PLoS ONE, 5.

Nopcsa FB. 1925. Dinosaurierreste aus siebenbürgen. IV. Die Wirbelsaule von *Rhabdodon* und *Orthomerus*. Palaeontologica Hungarica, 1, 273-316.

Norman DB. 1980. On the ornithischian dinosaur *Iguanodon bernissartensis* from the Lower Cretaceous of Bernissart (Belgium). Mémoires de l'Institut Royal des Sciences Naturelles de Belgique, 178, 1-105.

Norman DB. 2004. Basal Iguanodontia. 413–37. In Weishampel DB, Dodson P and Osmolska H, editors. The Dinosauria, 2nd edn. University of California Press, Berkeley, 861 pp.

Norman DB, Crompton AW, Butler RJ, Porro LB and Charig AJ. 2011. The Lower Jurassic ornithischian dinosaur *Heterodontosaurus tucki* Crompton and Charig, 1962 : cranial anatomy, functional morphology, taxonomy, and relationships. Zoological Journal of the Linnean Society, 163, 182–276.

Norman DB, Sues H-D, Witmer LM, Coria RA. 2004. Basal Ornithopoda. 393-437. In Weishampel DB, Dodson P and Osmolska H, editors. The Dinosauria, 2nd edn. University of California Press, Berkeley, 861 pp.

Osborn HF. 1924. *Psittacosaurus* and *Protiguanodon*: two lower Cretaceous iguanodonts from Mongolia. American Museum Novitates, 127, 1–16.

Ösi A, Prondvai E, Butler R and Weishampel DB. 2012. Phylogeny, Histology and Inferred Body Size Evolution in a New Rhabdodontid Dinosaur from the Late Cretaceous of Hungary. PLoS ONE, 7.

Owen R. 1842. Report on British fossil reptiles, part. II. Report of the British Association for the Advancement of Science, 11.

Owen R. 1858. Monograph on the fossil Reptilia of the Wealden and Purbeck Formations. Part V. Lacertilia. Monographs of the Palaeontographical Society, 12, 31–9.

Peng G. 1992. Jurassic ornithopod *Agilisaurus louderbacki* (Ornithopoda: Fabrosauridae) from Zigong, Sichuan, China. Vertebrata PalAsiatica, 30, 39–53.

Perle A, Maryanska T and Osmolska H. 1982. *Goyocephale lattimorei* gen. et sp. n., a new flat-headed pachycephalosaur (Ornithischia, Dinosauria) from the Upper Cretaceous of Mongolia. Acta Palaeontologica Polonica, 27, 8–132.

Pincemaille-Quillevere M, Buffetaut E, Quillevere F. 2006. Description ostéologique de l'arrière-crâne de *Rhabdodon* (Dinosauria, Euornithopoda) et implications phylogénétiques, Bulletin de la Société géologique de France, 177, 97-104.

Pol D, Rauhut OWM and Becerra M. 2011. A Middle Jurassic heterodontosaurid dinosaur from Patagonia and the evolution of heterodontosaurids. Naturwissenschaften, 98, 369–79.

Rozadilla S, Agnolin FL, Novas FE, Aranciaga Rolando AM, Matias JM, Lirio JM and Isasi MP. 2016. A new ornithopod (Dinosauria, Ornithischia) from the Upper Cretaceous of Antarctica and its palaeobiogeographical implications. Cretaceous Research, 57, 311–24.

Rozadilla S, Agnolin FL, Novas FE. 2019. Osteology of the Patagonian ornithopod *Talenkauen santacrucensis* (Dinosauria, Ornithischia). Journal of Systematic Paleontology, 17, 1-47.

Ruiz-Omeñaca JI, Pereda Suberbiola X and Galton PM. 2007. *Callovosaurus leedsi*, the earliest dryosaurid dinosaur (Ornithischia: Euornithopoda) from the Middle Jurassic of England. 1-16. In Carpenter K, editor. Horns and Beaks: Ceratopsian and ornithopod dinosaurs, Indiana University Press.

Salgado L, Canudo JI, Garrido AC, Moreno-Azanza M, Martinez LCA, Coria RA and Gasca JM. 2017. A new primitive neornithischian dinosaur from the Jurassic of Patagonia with gut contents. Nature Publishing Group, 7, 1–10.

Salgado L, Coria RA and Heredia SE. 1997. New materials of *Gasparinisaura cincosaltensis* (Ornithischia, Ornithopoda) from the Upper Cretaceous of Argentina. Journal of Paleontology, 71, 933–40.

Santa Luca AP. 1980. The postcranial skeleton of *Heterodontosaurus tucki* (Reptilia, Ornithischia) from the Stormberg of South Africa. Annals of the South African Museum. 79, 159-211.

Scheetz RD. 1999. Osteology of *Orodromeus malelai* and the phylogeny of basal ornithopod dinosaurs. Unpublished PhD thesis, Montana State University, Bozeman, 186 pp.

Schmidt-Lebuhn A. 2016. TNT script for the Templeton Test. 10.13140/RG.2.1.3484.9522. See. https://www.researchgate.net/publication/306055781, also available at : https://www.anbg.gov.au/cpbr/tools/templetontest.tnt [both accessed 2020 Mar 03].

Seeley HG. 1887. On the classification of the fossil animals commonly named Dinosauria. Proceedings of the Royal Society of London, 43, 165–71.

Senter P. 2007. Analysis of forelimb function in basal ceratopsians. Journal of Zoology, 273, 305–14.

Sereno PC. 1984. The phylogeny of the Ornithischia : a reappraisal. 219-26. In Reif W and Westphal F, editors. Third Symposium on Mesozoic Terrestrial Ecosystems, Short Papers. Attempto Verlag, Tübingen University Press.

Sereno PC. 1986. Phylogeny of the bird-hipped dinosaurs (Order Ornithischia). National Geographic Research 2, 234-56.

Sereno PC. 1991. *Lesothosaurus*, "Fabrosaurids," and the early evolution of Ornithischia. Journal of Vertebrate Paleontology, 11, 168–97.

Sereno PC. 1993. The pectoral girdle and forelimb of the basal theropod *Herrerasaurus ischigualastensis*. Journal of Vertebrate Paleontology, 13, 425–50.

Sereno PC. 1998. A rationale for phylogenetic definitions with application to higher-level taxonomy of Dinosauria. Neues Jabrbuch für Geologie and Paläontologie Abhandlungen, 210, 41-83.

Sereno PC. 2000. The fossil record, systematics and evolution of pachycephalosaurs and ceratopsians from Asia. 480–516. In Benton MJ, Shishkin MA, Unwin DM, and Kurochkin

EN, editors. The Age of Dinosaurs in Russia and Mongolia, Cambridge University Press, Cambridge.

Sereno PC. 2010. Taxonomy, Cranial Morphology, and Relationships of Parrot-Beaked Dinosaurs (Ceratopsia: *Psittacosaurus*). 219-26. In Ryan MJ, Chinnery-Allgeier BJ and Eberth DA, editors. New perspectives on horned dinosaurs: the Royal Tyrrell Museum Ceratopsian Symposium, Indiana University Press, 656 pp.

Sereno PC. 2012. Taxonomy, morphology, masticatory function and phylogeny of heterodontosaurid dinosaurs, 226, 1–225.

Sereno PC and Novas FE. 1993. The skull and neck of the basal theropod *Herrerasaurus ischigualastensis*. Journal of Vertebrate Paleontology, 13, 451–76.

Snively E and Theodor JM. 2011. Common Functional Correlates of Head-Strike Behavior in the Pachycephalosaur *Stegoceras validum* (Ornithischia, Dinosauria) and Combative Artiodactyls. PLoS ONE, 6 : e21422.

Sues H-D and Galton PM. 1987. Anatomy and Classification of the North American Pachycephalosauria (Dinosauria: Ornithischia). Palaeontographica Abteilung A, 198, 1–40.

Sues H-D and Norman DB. 1990. Hypsilophodontidae, *Tenontosaurus* and Dryosauridae. 498-509. In Weishampel DB, Dodson P and Osmolska H, editors. The Dinosauria, 1st edn. University of California Press, Berkeley.

Templeton A. 1983. Phylogenetic inference from restriction endonuclease cleavage site maps with particular reference to the evolution of humans and the apes. Evolution, 37, 221-44.

Tennant J. 2013. Osteology of a near-complete skeleton of *Tenontosaurus tilletti* (Dinosauria: Ornithopoda) from the Cloverly Formation, Montana, USA [master's thesis]. University of Manchester, Manchester, 195 pp.

Thomas DA. 2015. The cranial anatomy of *Tenontosaurus tilletti* Ostrom, 1970 (Dinosauria, Ornithopoda). Palaeontologia Electronica, 18, 1–99.

Vickaryous MK, Maryanska T and Weishampel DB. 2004. Ankylosauria. 363–92. Weishampel DB, Dodson P and Osmolska H, editors. The Dinosauria, 2nd edn. University of California Press, Berkeley, 861 pp.

Weishampel DB and Heinrich RE. 1992. Systematics of hypsilophodontidae and basal Iguanodontia (dinosauria : Ornithopoda). Historical Biology : An International Journal of Paleobiology, 6, 159-84.

Weishampel DB, Jianu C-M, Csiki Z, and Norman DB. 2003. Osteology and phylogeny of *Zalmoxes* (n. g.), an unusual Euornithopod dinosaur from the latest Cretaceous of Romania. Journal of Systematic Palaeontology, 1, 65.

Wiens JJ. 2005. Can Incomplete Taxa Rescue Phylogenetic Analyses from Long-Branch Attraction ? Systematic Biology, 54, 731-42.

Winkler DA, Murry PA and Jacobs LL. 1997. A new species of *Tenontosaurus* (Dinosauria; Ornithopoda) from the Early Cretaceous of Texas. Journal of Vertebrate Paleontology, 17, 330–48.

Xu X, Makovicky PJ, Wang X, Norell MA and You H. 2002. A ceratopsian dinosaur from China and the early evolution of Ceratopsia. Nature, 416, 314–17.

Xu X, Forster CA, Clark JM and Mo J. 2006. A basal ceratopsian with transitional features from the Late Jurassic of northwestern China. Proceedings of the Royal Society of London, Series B. 273, 2135–40.

You H-L and Dodson P. 2003. Redescription of neoceratopsian dinosaur *Archaeoceratops* and early evolution of Neoceratopsia. Acta Palaeontologica Polonica, 48, 261–72.

You H-L and Dodson P. 2004. Basal Ceratopsia. 478–93. In Weishampel DB, Dodson P and Osmolska H, editors. The Dinosauria, 2nd edn. University of California Press, Berkeley, 861 pp.

You H-L, Tanoue K and Dodson P. 2008. New data on cranial anatomy of the ceratopsian dinosaur *Psittacosaurus major*. Acta Palaeontologica Polonica, 53, 183–96.

Zhao X, Cheng Z and Xu X. 1999. The earliest ceratopsian from the Tuchengzi Formation of Liaoning, China. Journal of Vertebrate Paleontology, 19, 681–91.

Zheng X-T, You H-L, Xu X and Dong Z-M. 2009. An Early Cretaceous heterodontosaurid dinosaur with filamentous integumentary structures. Nature, 458, 333–36.

SUPPORTING INFORMATION

Additional Supporting Information can be found in the online version of this article:

Supplemental material 1 – Characters list.

Supplemental material 2 – Excel file of the full character-taxon matrix used in this study.

Supplemental material 3 – Comments on changes made from the raw datamatrix of Dieudonné et al. (2016).

Supplemental material 4 – Nexus file of the full datamatrix.

Supplemental material 5 – Nexus file of the datamatrix without *Yandusaurus hongheensis*.

Supplemental material 6 – Table of clades names, definitions and supporting characters.

Supplemental material 7 – Choice of the reference tree and phylogenetic hypotheses.

Figure 1 : 50% Majority Rule Consensus calibrated over the chronostratigraphic timescale of Cohen *et al.* (2013, updated version), showing relationships among non-ornithopodan ornithischians. The analysis was run under equally-weighted parsimony with the removal of *Fruitadens haagarorum*. Bootstrap values are reported below each node whenever these are superior to 50%.

Figure 2 : 50% Majority Rule Consensus calibrated over the chronostratigraphic timescale of Cohen *et al.* (2013, updated version), showing relationships within Ornithopoda. The analysis was run under equally-weighted parsimony with the removal of *Fruitadens haagarorum*. Bootstrap values are reported below each node whenever these are superior to 50%.

Figure 3 : Rhabdodontomorphans features. A-C : right ilium QM F6140 of *Muttaburrasaurus langdoni* in A, lateral; B, medial (with close-up of postacetabular process); C, dorsal views. D-E: left (UBB NVZ1-17) and right (UBB NVZ1-16) ilium of *Zalmoxes shqiperorum* in D, medial (reversed to right) ; E, dorsal views. F, right femur MDS-VG, 135 of the Vegagete rhabdodontid in distal view. G, right femur LRF 3050.V of *Fostoria dhimbangunmal* in distal view. A proceeds from Bartholomai & Molnar (1981, fig. 8C). B and C are line-drawing outlines made-up from photos of *Muttaburrasaurus'* ilium kindly provided by Matthew Herne. D and E proceed from Godefroit *et al.* (2009, fig. 18B, C). F is a distal view of the largest distal femur of the Vegagete ornithopod (cf. same bone in posterior view in Dieudonné *et al.* 2016a, fig. 8C). G proceeds from Bell *et al.* (2019, fig. 8E). Abbreviations : bs, brevis shelf ; eg, extensor groove ; ifg, iliofibularis groove ; ip, ischiac peduncle ; pp, pubic peduncle. Characters numbers are referred with their state in parentheses. We precise that state 2 of character #309 occurs in F and G as lh (lateral width) divided by wd (distal width) is inferior to 40%. Scales bars are 15 cm (A-C), 5 cm (D, E and G), and 5 mm (F).

Supplemental material 1 - Characters list.

Characters marked with an asterisk indicate that comments and modifications of these characters are referred to and detailed in supplemental material 2. Those characters went rescored for specific taxa and/or reformulated partly or wholy. Each newly added or modified character as well as each modification on specific taxonomic scoring is signaled in the Excel file datamatrix as cells written in red font with light brown background color (supplemental material 3).

Cranial skeleton

1(*). Skull, rostral-quadrate length relative to the body length: 10 % (0), 13 % or more (1) (Xu et al. 2006 #1; Ösi et al. 2012 #2).

2(*). Skull, preorbital region, percentage out of the total skull length from the rostrum to the quadrate: equal or more than 40% (0), much less than 40% (1) (Xu et al. 2006 #21; Ösi et al. 2012 #1).

3(*). Skull, position of maximum widening of the skull: beneath the jugal–postorbital bar (0), posteriorly, beneath the infratemporal fenestra (1) (modified from Ösi et al. 2012 #37, Xu et al. 2006 #2).

4. Lower margin of the infratemporal fenestra with respect to the lower margin of the orbit: level or higher (0), lower (1) (new character).

5(*). Infratemporal fenestra size: small, much smaller than the orbit (0) or large, subequal or larger than the orbit (1) (Xu et al. 2006 #87).

6(*). Skull, widening of the skull across the jugals, chord from frontal orbital margin to extremity of jugal is more than minimum interorbital width: absent (0), present, skull has a triangular shape in dorsal view (1) (Ösi et al. 2012 #36).

7. Skull, cortical remodeling of surface of dermal bone: absent (0), present (1) (Ösi et al. 2012 #89).

8(*). Rostral bone (neomorphic bone anterior to premaxilla): absent (0), present (1) (Xu et al. 2006 #3; Ösi et al. 2012 #3).

9. Rostral ventral process: absent (0) or present (1) (modified from Xu et al. 2006 #4).

10(*). Rostral, shape of anterior face: round, convex (0) or sharply keeled (1) (Ösi et al. 2012 #4; Xu et al. 2006 #5).

11. Rostral bone, ventrolateral processes: rudimentary (0), well-developed (1) (Ösi et al. 2012 #5).

12. Snout, anterior margin shape: sloped posterodorsally, snout shallow (0) or more vertical anterior margin, snout deep (1) (Xu et al. 2006 #52).

13(*). Premaxilla, anterior and dorsal surface: lacks rugosities (0), bears distinct rugose surface (1) (Brown et al., 2013 #136).

14(*). Premaxilla, ventral inflection: absent, oral margin even with ventral margin of maxilla (0), present, oral margin projects farther ventrally than ventral margin of maxilla (1) (modified from Xu et al. 2006 #37; McDonald et al. 2010 #30; Ösi et al. 2012 #9).

15(*). Premaxilla, denticles on oral margin: absent (0), present (1) (modified from Weishampel et al., 2003 #7; McDonald et al. 2010 #33).

16(*). Premaxilla, edentulous anterior region: absent, first premaxillary tooth is positioned adjacent to the symphysis (0), present: if any, the first premaxillary tooth is inset the width of one or more crowns (1) (rephrased from Ösi et al. 2012 #6).

17(*). Premaxilla, posterolateral process: does not contact lacrimal (0), contacts the lacrimal, excludes maxilla–nasal contact (1) (Xu et al. 2006 #34; Ösi et al. 2012 #7).

18. Premaxilla, ventral (or oral) margin: narial portion of the body of the premaxilla slopes steeply from the external naris to the oral margin (0), ventral premaxilla flares laterally to form a partial floor of the narial fossa (1) (Ösi et al. 2012 #8).

19. Premaxilla, premaxillary foramen: absent (0), present (1) (Ösi et al. 2012 #10).

20. Premaxilla, premaxillary palate: strongly arched, forming a deep, concave palate (0), horizontal or only gently arched (1) (Xu et al. 2006 #6; Ösi et al. 2012 #11).

21(*). Premaxillae: unfused (0), fused (1) (Brown et al. 2013 #124).

22(*). Premaxilla, external naris size: small, entirely overlies the premaxilla (0), enlarged, extends posteriorly to overlie the maxilla (1) (modified from McDonald et al. 2010 #38; Ösi et al. 2012 #18).

23(*). Premaxillary internarial bar : present, reaches the nasal (0), incomplete or absent (1) (modified from Ösi et al. 2012 #12; Boyd 2015 #11).

24(*). Premaxilla, position of the ventral margin of external nares: below the ventral margin of the orbits (0), above the ventral margin of the orbits (1) (Ösi et al. 2012 #17; Xu et al. 2006 #22).

25(*). Premaxilla, narial fossa surrounding external nares on lateral surface of premaxilla, position of ventral margin of fossa relative to the ventral margin of the premaxilla: closely approaches the ventral margin of the premaxilla (0), separated by a broad flat margin from the ventral margin of the premaxilla (1) (Ösi et al. 2012 #16).

26(*). Maximum length of external nares less than 15% basal skull length (0), maximum length of external nares greater than 15% basal skull length (1) (Boyd 2015 #88).

27(*). Premaxilla-maxilla contact, fossa-like depression positioned on the premaxilla–maxilla boundary: absent (0), present (1) (Ösi et al. 2012 #13).

28(*). Premaxilla-maxilla diastema: weak to absent, maxillary teeth continue to anterior end of maxilla (0), present, substantial diastema of at least one crown length between maxillary and premaxillary teeth (1) (Ösi et al. 2012 #14).

29(*). Premaxilla-vomer, ventral contact: present (0), absent, excluded by midline contact between maxillae (1) (rephrased from Ösi et al. 2012 #84; Xu et al. 2006 #9).

30(*). Premaxilla-prefrontal contact: absent (0) or present (1) (Xu et al. 2006 #23).

31(*). Maxilla, prominent anterolateral boss articulates with the medial premaxilla: absent (0), present (1) (Ösi et al. 2012 #24).

32(*). Maxilla, at least a small prolongation that bulges out in front of the anterior edge of the maxillary ascending process (not considering the ventral premaxillary process): absent (0), present (1) (Ösi et al. 2012 #25).

33(*). Maxilla, buccal emargination: absent (0), present (1) (Ösi et al. 2012 #26).

34(*). Maxilla, eminence on the rim of the buccal emargination of the maxilla near the junction with the jugal: absent (0), present (1) (Ösi et al. 2012 #27; Xu et al. 2006 #24).

35(*). External antorbital fenestra, shape (regardless of position): triangular (0), oval or circular (1) (modified from Ösi et al. 2012 #22).

36(*). Antorbital fenestra, position of the posterior part with respect to the orbit: passes below the orbit (0), next to or anterior to the orbit (1) (new character).

37(*). External antorbital fenestra, exclusion of the jugal from the posteroventral margin by lacrimal–maxilla contact: absent (0), present (1) (Ösi et al. 2012 #34; Xu et al. 2006 #79).

38(*). External antorbital fenestra, maximum diameter: 60% or more of orbital diameter (0), approximately 50% of orbital diameter (1) or very small or absent (2) (modified from Xu et al. 2006 #38).

39(*). Internal antorbital fenestra, length relative to skull length: large, generally at least 15 % (0), very much reduced, less than 10% (1), or absent (2) (modified from Ösi et al. 2012 #20).

40(*). Antorbital fenestra, position: level or higher than the orbit (0), anteroventral to the orbit (1) (modified from Xu et al. 2006 #77).

41(*). Prominent horizontal ridge under the antorbital fossa: absent (0) or present (1) (Xu et al. 2006 #78).

42(*). Nasals, depression present along sutural line of the bones: absent (0), present (1) (modified from Ösi et al. 2012 #19; Xu et al. 2006 #82).

43(*). Frontal, contacts orbit: along more than 25% of total frontal length (0), less than 25% (1), excluded from orbital margin (2) (modified from Butler et al. 2011; Brown et al. 2013 #24).

44(*). Frontal, ratio of frontal length to nasal length: greater than 120% (0), between 120% and 60% (1) or less than 60% (2) (Brown et al. 2013 #25).

45(*). Frontals, each one are short and broad (0), narrow and elongate (at least twice as long as wide) (1) (reformulated from Ösi et al. 2012 #64).

46(*). Frontals arching over orbit from lateral view: present (0), absent, frontals dorsally flattened over orbit (1) (Boyd 2015 #65).

47(*). Lacrimal-jugal contact: jugal doesn't, or barely touches lacrimal (0), jugal meets lacrimal with more contact (1) (modified from Brown et al. 2013 #50).

48. Lacrimal proportions: anteroposteriorly long, the posterior branch expands posteroventrally to form a slight portion of the anteroventral orbital margin (0), anteroposteriorly short, the posterior branch is not expanding posteroventrally (1) (new character).

49(*). Lacrimal-nasal contact: present (0), absent (1) (new character).

50(*). Accessory ossification(s) in the orbit (palpebral/supraorbital): absent (0), present (1) (Ösi et al. 2012 #29; Xu et al. 2006 #68).

51. Palpebral/supraorbital: free, projects into orbit from contact with lacrimal/prefrontal (0), incorporated into orbital margin (1) (Ösi et al. 2012 #30).

52(*). Palpebral, shape in dorsal view: rod-shaped (0), plate-like with wide base (1) (Ösi et al. 2012 #31).

53. Palpebral/supraorbital, number: one (0), two (1) or three (2) (Ösi et al. 2012 #32).

54(*). Supraorbital(s) horizontal extension across the orbit (wether fused or not to the orbital margin) : contact the postorbital posteriorly (0), does not contact the postorbital, but crosses at least half of the orbit (1), crosses less than half of the orbit (2) (modified from Boyd 2015 #25).

55(*). Lower margin of the orbit circular (0), lower margin of the orbit subrectangular (1) (Boyd 2015 #95).

56(*). Depression on lateral surface of postorbital, : absent, the lateral surface is devoid of any pronounced depression, and varies from smoothly concave to smoothly convex over the whole postorbital anteroposteriorly (0); present and well-demarcated, opens posteriorly toward infratemporal fenestra (1); present on the anterior side toward the orbit (2) (modified from Xu et al. 2006 #86; Pol et al. 2011 #229).

57(*). Squamosal process of postorbital relative to the jugal process: much shorter (0) or subequal or longer (1) (Xu et al. 2006 #83).

58(*). Postorbital: inverted 'L'-shaped (0), triangular and plate like with normal expansion of squamosal process (1), triangular and plate-like with a very short squamosal process (2) (modified from Xu et al. 2006 #11).

59(*). Postorbital-squamosal tubercle row: absent (0) or present (1) (Xu et al. 2006 #49).

60(*). Postorbital participation to the lower temporal opening: present (0), postorbital excluded from margin (1) (reformulated from Xu et al. 2006 #12).

61(*). Postorbital-parietal contact: absent (0), very narrow (1), broad (2) (modified from Ösi et al. 2012 #51).

62(*). Distinctive indentation on posterior cranial midline between the parietals: present (0) or absent (1) (Xu et al. 2006 #25).

63(*). Parietal sagittal crest: narrow shelf or sharply defined crest (0) or broad, essentially absent (1) (Xu et al. 2006 #102).

64. Parietal fenestration: absent (0) or present (1) (Xu et al. 2006 #71).

65. Parietal, location of posterior margin relative to squamosal: anterior to (0) or level with or posterior to (1) that of squamosal (Xu et al. 2006 #60).

66(*). Parietal, posterior margin relative to rest of skull: below or level with the anterior skull roof (0) higher than the anterior skull roof (1) (modified from Xu et al. 2006 #61).

Homalocephale calathocercos and *Hexinlusaurus multidens* were corrected and coded (1).

67(*). Squamosal-Quadratojugal contact: present, between dorsal process of quadratojugal and descending process of the squamosal (0), absent (1) (Ösi et al. 2012 #52).

68(*). Supratemporal fenestra length relative to the basal skull length (BSL): short, fenestrae are less than 25% BSL (0), elongated, more than 25% BSL (1) (Ösi et al. 2012 #66; Xu et al. 2006 #58).

69(*). Squamosal with significant overhang lateral to the descending process and quadrate: absent (0) or present (1) (Xu et al. 2006 #84).

70(*). Distance between the squamosal-quadrate articulation and a point on the dorsal surface of the squamosal aligned with the upper axis of the quadrate shaft: close (0), away from the main body of the squamosal, on a distinct and robust ventral process (1) (rephrased from Xu et al. 2006 #100).

71(*). Squamosal prequadratic process: present, covers the anterodorsal part of the proximal quadrate shaft (0); absent (1) (new character).

72(*). Parietosquamosal shelf, posteromedial process of squamosal: does not overhang the occipital region (0); overhang the occipital region, forms at least a slight dorsal horizontal shelf (1); consists of a vertically oriented sheet of bone (2) (modified from Ösi et al. 2012 #68, Xu et al. 2006 #45).

73(*). Postorbital-squamosal tubercle/node row: absent (0), present (1) (Ösi et al. 2012 #72).

74(*). Postorbital-squamosal tubercle row, enlarged tubercle row on the posterior squamosal: absent (0), present (1) (Ösi et al. 2012 #73).

75. Postorbital-squamosal bar, morphology of the ventral junction with the jugal process of postorbital: smoothly concave and large (0); narrow “T-shaped”, sharply angled (1) (new character).

76(*). Squamosal, morphology of postorbital process dorsal to *M. adductor mandibulae externus* origin site: gently convex (0), mediolaterally compressed and blade-like (1) (McDonald et al., 2010 #65).

77(*). Jugal with prominent ventral flange: absent (0) or present (1) (Xu et al. 2006 #69).

78. Jugal anterior process: shallow and tapered (0) or expanded dorsoventrally (1) (Xu et al. 2006 #55).

79(*). Jugal wing (formed by quadratojugal and jugal), height that contact the quadrate: greater than 20% quadrate height (0), less than 20% (1) (new character).

80(*). Jugal wing, degree of anteroposterior overlap of the quadrate shaft (not considering the pterygoid wing): complete, reaches the posterior border of quadrate (0), almost complete, cover more than 50% of quadrate length (1), partial, cover much less than 50% of quadrate length (2) (modified from Brown et al., 2013 #1).

81(*). Jugal, ventral extent of the wing formed by the jugal and quadratojugal ends: at or near distal condyles of quadrate (0), above distal condyles (1), well above the distal condyles (2) (Brown et al. 2013 #9; Ösi et al. 2012 #54).

82(*). Jugal, articulation with quadrate: jugal fails to articulate with quadrate (0), jugal articulates with quadrate (1) (Brown et al. 2013 #14).

83(*). Posterior maxillary process on the medial side of the jugal: straight to modestly arched medially (0), anteromedially projected and arched (1) (modified from Boyd 2015 #39).

84. Jugal, ectopterygoid articular facet on medial view: consists of a deep groove (0), rounded scar (1) (Brown et al. 2013 #47).

85(*). Jugal anterior ramus: dorsoventrally deeper than mediolaterally broad (0), broader than deep (1) (Boyd 2015 #32).

86(*). Jugal, morphology of portion of maxillary process that overlaps maxilla: tapers at anterior ends of maxillary and lacrimal contacts, with slightly convex ventral margin and slightly concave dorsal margin (0), subrectangular with parallel dorsal and ventral margins (1) (modified from: McDonald et al. 2010 #54; Ösi et al. 2012 #35).

87(*). No boss present on lateral surface of the jugal (0), presence of a boss or horn on the lateral surface of the jugal (1) (modified from Boyd 2015 #38).

88(*). Jugal ornamentation: absent (0), or present, nodular (1) (modified from Ösi et al. 2012 #41; Xu et al. 2006 #81).

89(*). Jugal-postorbital bar, anteroposterior width relative to that of the infratemporal fenestra: less expanded (0), equally expanded (1), or anteroposteriorly broader than the infratemporal fenestra (2) (modified from Ösi et al. 2012 #42).

90(*). Jugal-postorbital joint: elongate scarf joint (0), short butt joint (1) (Ösi et al. 2012 #43).

91(*). Jugal, form of postorbital process: not expanded dorsally (0), dorsal portion of postorbital process expanded posteriorly (1) (Ösi et al. 2012 #44).

92(*). Jugal, posterior ramus forking: absent (0), present, incision between processes vary from narrow to more than 45° (1) (Pol et al. 2011 #46; modified from Ösi et al. 2012 #46).

93(*). Jugal, posterior ramus: forms anterior and ventral margin of infratemporal fenestra (0), forms part of posterior margin, expands towards squamosal (1) (Ösi et al. 2012 #47).

94(*). Jugal-squamosal contact: absent, separated by postorbital (0) or present (1) (Xu et al. 2006 #72).

95(*). Jugal–quadratojugal contact: overlapping (0), tongue-and-groove (1) (Ösi et al. 2012 #48).

96(*). Jugal (or jugal–epijugal), ridge dividing the lateral surface of the jugal into two planes: absent (0), present (1) (Ösi et al. 2012 #38).

97(*). Quadratojugal, shape: inverted L-shaped, with elongate anterior and ventral processes (0), subrectangular with long axis vertical, short, deep anterior process (1), horizontal T-shaped, with sharp angle between the anterior and dorsal processes (2) (modified from Ösi et al. 2012 #53).

98(*). Paraquadratic/quadratojugal foramen, pierces the quadratojugal: absent (0), present (1) (modified from Weishampel et al., 2003 #17; McDonald et al., 2010 #58).

99(*). Paraquadratic/quadratojugal foramen size: small and/or narrow if dorsoventrally tall (0) large (1) (modified from Xu et al. 2006 #40).

100(*). Paraquadratic/quadratojugal foramen or notch, location: opens between quadratojugal and quadrate, notches the anterior margin of the quadrate (0), opens inside the quadratojugal (1) (modified from Ösi et al. 2012 #60).

101(*). Quadrate foramen location and orientation of the openning: posteriorly onto the posterolateral aspect of quadrate shaft (0), on lateral aspect of quadrate or quadratojugal (1) (Xu et al. 2006 #39).

102(*). Body of the quadrate leans posteriorly (0), body of quadrate oriented vertically (1), body of quadrate leans anteriorly (2) (Boyd 2015 #47).

103(*). Quadrate, prominent oval fossa on pterygoid ramus: absent (0), present (1) (Ösi et al. 2012 #57).

104(*). Quadrate, mandibular articulation: quadrate condyles subequal in size (0), medial condyle is larger than lateral condyle (1), lateral condyle is larger than medial (2) (Ösi et al. 2012 #63).

105(*). Laterosphenoid, socket for the head: occurs along frontal-postorbital suture (0), only in postorbital (1) (modified from Brown et al. 2013 #21).

106(*). Post-temporal foramen position: at the boundary between the parietals/squamosals and the paroccipital process (0), entirely within the opisthotic (1), positioned entirely within the squamosal (2) (modified from Pol et al. 2011 #77; Boyd 2015 #103).

107. Opisthotic, presence of a 'Y-shaped' indentation on the dorsal edge for the passage of the post-temporal foramen: absent (0), present (1) (reformulated from Brown et al. 2013 #127).

108(*). Prootic, position of the foramen for the trigeminal nerve (V): notches the posteroventral edge of the laterosphenoid at the boundary with the prootic (0), nearly or completely enclosed in prootic (1) (modified from Brown et al., 2013 #76).

109(*). Prootic-basisphenoid plate: absent (0), present (1) (Ösi et al. 2012 #81).

110(*). Supraoccipital, contribution to dorsal margin of the foramen magnum: forms entire dorsal margin of foramen magnum (0), exoccipital with medial process that restricts the contribution of the supraoccipital (1), the exoccipital join medially and excludes totally the supraoccipital from the dorsal margin of the foramen magnum (2) (modified from Ösi et al. 2012 #78; ordered character).

111(*). Supraoccipital: nuchal crest is present (0) or absent (1) (Brown et al. 2013 #68).

112(*). Supraoccipital (SO), anteroposterior inclination and sutural contact with the opisthotics (OP) from a posterior view: the SO is obliquely inclined anteroposteriorly, the sutural contact with the OP is diagonal from the top laterally to the foramen magnum ventromedially (0), the SO completely roofs the endocranial cavity, it overlains the OP and its sutural contact with the OP is horizontal from a posterior view (1), the SO is held almost vertically and sutures nearly vertically with the adjacent opisthotics (2) (new character).

113(*). Paroccipital processes (Exoccipital-Opisthotic complex): extend laterally and transit smoothly toward a slight dorsoventral expansion distally (0), distal end pendent, sharply deflects ventrally (1) (modified from Xu et al. 2006 #94; McDonald et al., 2010 #72 ; Ösi et al. 2012 #75)

114(*). Paroccipital processes, proportions: short and deep (height ≥ 1/2 length) (0), elongate and narrow (1) (Xu et al. 2006 #35; Ösi et al. 2012 #76).

115(*). Basioccipital, contribution to the border of the *foramen magnum*: *foramen magnum* occupies less than 50% of occipital condyle or is completely excluded from it by the exoccipitals (0), more than 50% of occipital condyle (1) (modified from Ösi et al. 2012 #79; Brown et al. 2013 #71).

116(*). Basioccipital, ventral margin of occipital condyle: forms a neck before a being posteroventrally expanded (0), smooth and continuous, devoid of ventral neck (1) (rephrased from McDonald et al. 2010 #74).

117(*). Basioccipital, anteroposteriorly directed groove extending along ventral surface: absent (0), present (1) (McDonald et al. 2010 #75).

118(*). Basioccipital, median ridge extending along ventral surface: absent (0), present (1) (reformulated from Xu et al. 2006 #95; McDonald et al. 2010 #76; Brown et al. 2013 #73).

119(*). Basioccipital, anteroventral part: produces an elongated process that is "locked" between the basal tubera of the basisphenoid (0), forms a broadly concavo-convex contact with the basisphenoid, or is completely restricted to the posterior aspect of the basal tubera (1) (new character).

120(*). Basioccipital, basal tubera: extend much farther ventrally than the basisphenoid/parasphenoid plate (0), level (1) (reformulated from Brown et al. 2013 #74).

121(*). Basioccipital, basal tubera: level with the base of the basioccipital condyle (0), form a massive buttress which extends much lower than the base of the basioccipital condyle (1) (reformulated from Ösi et al. 2012 #82).

122(*). Angle between the base of the braincase (i.e. the axis formed by the occipital condyle and basisphenoid) and long axis of the braincase : less than 35 degrees (0), equal or more than 35 degrees (1) (reformulated from Boyd 2015 #98).

123(*). Basisphenoid, basipterygoid processes articular facet orientation: anteroventral and/or anterolateral (0), ventral (1), posteroventral (2) (modified from Xu et al. 2006 #14; Ösi et al. 2012 #83).

124(*). Notch between posteroventral edge of basisphenoid and base of basipterygoid process: deep (0) or notch shallow with base of basipterygoid process close to basioccipital tubera (1) (Xu et al. 2006 #15).

125(*). Basisphenoid, length relative to basioccipital length: longer or subequal (0), shorter than basioccipital (1) (Ösi et al. 2012 #80).

126(*). Pterygoid, contact with its counterpart: absent, the basicranium is mostly exposed in ventral view, (0) present, the basicranium is mostly obscured in ventral view by an interpterygoid contact formed by the palatal and/or quadrate rami (1) (modified from Xu et al. 2006 #98).

127. Palatal keel, dorsoventrally deep (deeper than 50% of snout depth) median palatal keel formed of the vomers, pterygoids and palatines: absent (0), present (1) (Ösi et al. 2012 #85).

128(*). Pterygoid-maxilla contact, at posterior end of tooth row: absent (0), present (1) (Ösi et al. 2012 #87).

129(*). Pterygoid participation to the pterygo-palatine fenestra: present (0), absent, the ectopterygoid prevents the pterygoid from participating to the pterygo-palatine fenestra (1) (new character).

130(*). Lower jaw, length of post-coronoid elements (from the dorsal border of the coronoid-surangular suture) relative to the total length of the lower jaw: more than 35 (0), 25-35% (1) (modified from Brown et al. 2013 #62; Boyd 2015, #83).

131(*). Predentary: absent (0), present (1) (Ösi et al. 2012 #90).

132(*). Predentary, size and position: short and the posterior extremity is posteriorly set, the predentary oppose only the first half of the premaxilla (0), short, the posterior border is anteriorly set, all but the posterodorsal corner of the predentary is positioned anterior to the

last premaxillary tooth (1), roughly equal in length to the premaxilla, premaxillary teeth only oppose predentary all along (2), (modified from Ösi et al. 2012 #91).

133(*). Predentary, shape: rounded tip (0), pointed tip (1), (Ösi et al. 2012 #92).

134(*). Predentary, grooves on either side of midline on anterior surface, extending ventrolaterally to dorsomedially: absent (0), present (1) (McDonald et al. 2010 #6).

135(*). Predentary, oral margin: relatively smooth (0), denticulate (1) (Ösi et al. 2012 #93).

136(*). Predentary, tip of in lateral view: does not project above the main body (0), strongly upturned relative to main body (1) (Xu et al. 2006 #33; Ösi et al. 2012 #94).

137(*). Predentary, ventral process: single (0), bilobate (1) (Ösi et al. 2012 #95).

138(*). Predentary, ventral process: present, well-developed (0), very reduced or absent (1) (Ösi et al. 2012 #96).

139. Predentary length of lateral processes relative to the ventral process: short (0), long, more than half the length of the ventral process (1) (rephrased from Xu et al. 2006 #93).

140(*). Dentary, ratio of dentary height (just anterior to the rising coronoid process) divided by length of dentary: between 15-20% (0), 20-35% (1) (Brown et al. 2013 #63).

141(*). Dentary, symphysis: V-shaped (0), spout-shaped (1) (Ösi et al. 2012 #97).

142(*). Dentary, position of the anterior tip: positioned high (0), mid height (1), near lower margin of dentary (2), below lower margin (3) (modified from: Ösi et al. 2012 #98; Brown et al. 2013 #51).

143(*). Dentary, morphology of ventral margin of anterior ramus leading to the predentary articulation: straight with an anterior break in slope leading to the tip of the predentary process (0), inflected ventrally before reaching the predentary articulation and symphysis (1), curves in a regular and continuous way dorsally toward the symphysis and predentary articulation (2) (modified from McDonald et al. 2010 #16).

144(*). Dentary, tooth row (and edentulous anterior portion) in lateral view: straight (0), anterior end downturned (1) (Ösi et al. 2012 #98).

145(*). Dentary, dorsal and ventral margins before their locking into the predentary: converge anteriorly (0), subparallel (1), deepen anteriorly (2) (modified from McDonald et al., 2010 #15; Ösi et al. 2012 #99).

146(*). Dentary, ventral flange: absent (0), present (1) (Ösi et al. 2012 #100).

147(*). Dentary, orientation of tooth row relative to lateral surface of dentary: convergent anteriorly and posteriorly, bowed medially at mid-length, the tooth row ends anterior and aligned to the coronoid process (0), convergent anteriorly and divergent posteriorly so that the tooth row ends anterior to the coronoid and medial to its longitudinal axis (1), the dentary tooth row ends posteromedially to the coronoid (2) (modified from Xu et al. 2006 #17; McDonald et al. 2010 #12 and Ösi et al. 2012 #103).

148(*). Dentary, coronoid process: absent or weak, posterodorsally oblique, depth of mandible at coronoid is less than 150% depth of mandible beneath tooth row (0), well-developed, distinctly elevated, depth of mandible at coronoid is more than 150% depth of mandible beneath tooth row (1) (Pol et al. 2011 #101).

149. Dentary, the posterolateral surface bears a profound circular depression: absent (0), present (1) (modified from Ösi et al. 2012 #230).

150(*). Dentary, number of dentary teeth: 10 or fewer (0), 11–13 (1), 14–17 (2), more than 18 (3) (modified from Weishampel et al. 2003: #30; Butler et al. 2011; Ösi et al. 2012 #228; ordered character).

151(*). Coronoid, swells ventrolaterally until below the dentary tooth row: abent (0), present (1) (new character).

152. Surangular lateral surface: flat to weakly convex (0) or with pronounced laterally convex curvature (1) (Xu et al. 2006 #32).

153(*). Ridge or process on lateral surface of surangular, anterior to jaw suture: incipient or absent (0); anteroposteriorly extended ridge (1); dorsally directed finger-like process or strongly bulging boss (2) (reformulated from Ösi et al. 2012 #106, reintegrated).

154(*). External mandibular fenestra, situated on dentary-surangular-angular boundary: present (0), absent (1) (Xu et al. 2006 #41; Ösi et al. 2012 #104).

155. Retroarticular process: long, subequal to or exceeding the length of the glenoid (0), rudimentary or absent (1) (reformulated from Xu et al. 2006 #29; Ösi et al. 2012 #107).

156(*). Dentary-angular, node-like ornamentation: absent (0), present (1) (Ösi et al. 2012 #108; Xu et al. 2006 #88).

157(*). Dorsoventral extension of the angular at the level of the coronoid process: forms less than half of the dorsoventral height of the mandibular ramus (0); forms half or more of the height of the mandibular ramus, but remains below the dentary tooth row (1), reach the dorsal extent of the mandibular ramus or is higher (2) (modified from Pol et al. 2011 #230).

158(*). Jaw, level of jaw joint: level with tooth row, or weakly depressed ventrally (0), strongly depressed ventrally, more than 40% of the height of the quadrate is below the level of the maxillary occlusal margin (1) (modified from Xu et al. 2006 #36; Ösi et al. 2012 #109).

159(*). Premaxillary teeth: more than three (0), ≤ three (1), absent, premaxilla edentulous (2) (modified from Xu et al. 2006 #18; Ösi et al. 2012 #111).

160(*). Premaxillary (non-caniniform) tooth crown orientations in lateral view: recurved (0) or straight (1) (reformulated from Xu et al. 2006 #74).

161(*). Premaxillary teeth, crown mesiodistal expansion above root: absent, no distinction between root and crown is observable (0), crown is moderately expanded above root (1) (reformulated from Ösi et al. 2012 #113).

162(*). Premaxillary teeth, shape: transversely compressed (0), bulbous, strongly convex labially (1) (modified from Xu et al. 2006 #66).

163(*). Premaxillary teeth, posterior increase in size (breadth and/or height) : absent, all premaxillary teeth are subequal in size and not significantly broader than the succeeding maxillary teeth (0), premaxillary teeth increase in breadth and height posteriorly, and the most posterior tooth is larger than succeeding maxillary teeth (1) (modified from Ösi et al. 2012 #114; Xu et al. 2006 #73).

164(*). Premaxillary tooth row and anterior portion of maxillary tooth row: aligned with each other (0), maxillary teeth are inset the width of one or more crowns from the premaxillary teeth (1) (new character, derived from Han et al.2018 #31).

165(*). Teeth, crown mesiodistal expansion above root in cheek teeth: very weak to absent (0), present (1) (Ösi et al. 2012 #129).

166(*). Teeth, close-packing and quicker replacement eliminating spaces between alveolar border and crowns of adjacent functional teeth: absent (0), present (1) (Xu et al. 2006 #103; Ösi et al. 2012 #131).

167(*). Teeth, wear facets on teeth: absent or sporadically developed (0), systematic development of wear facets along the entire tooth row (1) (Ösi et al. 2012 #222).

168(*). Maxillary/dentary teeth, position of maximum apicobasal crown height in tooth rows: anterior portion of tooth row (0), central portion of tooth rows (1), posterior portion of tooth rows (2) (Ösi et al. 2012 #130).

169. Maxillary/dentary teeth, marginal ornamentations: fine serrations set at right angles to the margin of the tooth (0), coarse serrations (denticles) angle upwards at 45 degrees from the margin of the tooth (1) (Ösi et al. 2012 #116).

170(*). Maxillary/dentary teeth, enamel symmetrical (0), asymmetrical (1) (Ösi et al. 2012 #117). Enamel is told to be asymmetrically distributed on the dentary teeth of *Kulindadromeus zabaikalicus* (Godefroit et al. 2014, supplementary material, p. 7). *K. zabaikalicus* was corrected and coded (1).

171(*). Maxillary teeth, number and morphology of secondary/accessory ridges on labial surface of crown: no secondary ridges, only accessory ridges or swellings arising from marginal denticles (0), a few parallel and apicobasally extending secondary and accessory ridges (1), multiple parallel and apicobasally extending secondary and accessory ridges so that entire labial surface is corrugated (2) (modified from Pol et al. 2011 #118).

172. Maxillary/dentary teeth crown from a labial view, mesiodistal borders extend into a prominent mesial and distal bounding ridge and terminate in an apical denticle: absent (0), present (1) (modified from Xu et al. 2006 #76).

173(*). Maxillary/dentary teeth, at least weakly developed labiolingual expansion of the crown ('cingulum') above the root: absent (0), present (1) (modified from Ösi et al. 2012 #123).

174(*). Maxillary/dentary teeth, interdental space: non-packed teeth (0), lack of space between adjacent teeth up through the occlusional margin (1), overlapping of adjacent crowns with an overlapping "*en échelon*" pattern (2) (modified from: Xu et al. 2006 #103; McDonald et al., 2010 #88; Ösi et al. 2012 #128; Brown et al., 2013 #31).

175(*). Maxillary/dentary alveolar foramina ('special foramina') medial to tooth rows: present (0), absent (1) (Ösi et al. 2012 #126).

176(*). Maxillary teeth, crown shape: lingually concave (0), lingually convex (1) (Brown et al., 2013 #37).

177(*). Maxillary and dentary tooth crowns, apicobasal height: high, ratio of crown height / maximum mesiodistal width ≥ 1.5 (0); low, ratio < 1.5 (1) (modified from Pol et al. 2011 #228).

178(*). Maxillary and dentary teeth, cingulum height and crown shape: cingulum low and crown triangular (0), cingulum moderately high and crown spade-like or triangular (1), or cingulum high and diamond-shaped crowns (2) (modified from Xu et al. 2006 #75; Pol et al. 2011 #115; Brown et al. 2013 #41 and #60).

179(*). Maxillary teeth, apical ridge or swelling position, centrally placed (0), posteriorly set (1) (modified from Brown et al. 2013 #38).

180(*). Maxillary tooth crown, mesiodistal edges: diverging from the root (0), chisel-shaped with parallel sides (1) (modified from Xu et al. 2006 #75).

181(*). Maxillary teeth, relative prominence of the primary ridge on labial surface of crown: primary and secondary ridges absent or weakly developped from the apex of the crown (0), outstanding in comparison to other secondary ridges (1), completely undistinguishable from at least a few other secondary ridges in (2) (modified from McDonald et al. 2010 #92, Ösi et al. 2012 #120).

182. Maxillary teeth, root shape: straight (0), curved (1) (Brown et al. 2013 #33; Boyd 2015 #119).

183(*). Dentary dentition, heterodonty: no substantial heterodonty is present in dentary dentition (0), single, enlarged, caniform anterior dentary tooth (1) (Ösi et al. 2012 #124).

184. Dentary teeth, peg-like tooth located anteriorly within dentary lacks denticles, strongly reduced in size: absent (0), present (1) (Ösi et al. 2012 #125).

185(*). Dentary teeth, intercrown spaces: present (0), absent (1) (McDonald et al. 2010 #80).

186(*). Dentary teeth, apical ridge position: anteriorly or centrally positioned (0), posteriorly positioned (1) (Brown et al. 2013 #52).

187. Dentary teeth, number of ridges reaching the base of the crown: fewer than 10 (0), more than 10, and often more than 17 (1) (rephrased from Weishampel et al. 2003 #32; Ösi et al. 2012 #229).

188(*). Dentary teeth, shape and prominence of the primary ridge on lingual surface of the crown: absent, there is a smooth swelling instead of a primary ridge (0), the primary ridge is mesiodistally as thin as the secondary ridges and varyingly deep labiolingually (1), the primary ridge largely oversizes secondary ridges in both height and width, and also oversizes all the maxillary teeth ridges (2) (modified from Ösi et al. 2012 #121).

189(*). Dentary teeth, number and morphology of secondary and/or accessory ridges on lingual surface of the crown: no secondary ridges, faint accessory ridges arising from marginal denticles (0), multiple parallel and evenly-spaced secondary ridges on either side of the central ridge, such that entire lingual surface is corrugated (1), a few parallel and well defined secondary ridges with multiple faint accessory ridges arising from marginal denticles (2) (modified from McDonald et al., 2010 #87).

190(*). Ridges present on both the labial and lingual sides of dentary crowns (0), ridges mostly limited to the lingual side of dentary crowns and very faint to absent on the labial side (1) (modified from Boyd 2015 #124).

191. Dentary teeth, root shape in cross-section: round (0), oval (1), squared (2) (modified from Brown et al. 2013 #58).

192(*). Dentary tooth roots straight in anterior or posterior view all along the row (0), dentary tooth roots curved in anterior or posterior view (1) (modified from Boyd 2015 #135).

Axial skeleton:

193(*). Cervical vertebrae, shape of postzygapophyses: posterodorsally arched and higher dorsoventrally (0), dorsally flat and dorsoventrally low (1) (modified from Cambiaso, 2007 #59; Han et al. 2018, #235).

194(*). Cervical vertebrae, heightenning of neural spines along the series: remains low and triangular all along, more than three times as long as high in posterior cervicals (0), reach a substancial height posteriorly, less than twice as long as they are tall (1) (modified from Han et al. 2018 #236).

195(*). Axis neural spine: anteroposteriorly short (0), long, extends caudally to overlap more than half of the total length of C3 cervical centrum (1) (modified from Xu et al. 2006 #30).

196(*). Postaxial cervical vertebrae, epipophyses on the postzygapophyses somewhere within the neck: present (0), absent (1) (modified from Ösi et al. 2012 #133, Rozadilla et al. 2016 #234).

197(*). Cervical vertebrae (4-9), form of central surfaces: amphicoelous (0), at least slightly opisthocoelous (1) (Ösi et al. 2012 #134).

198(*). Ventral surface of the cervical vertebrae rounded (0), presence of a broad, flattened keel on the ventral surface of the cervical vertebrae (1), presence of a sharp ventral keel on the ventral surface of the cervical vertebrae (2) (Boyd 2015 #143 ; Rozadilla et al. 2016 #237).

199(*). Anterior cervical centra less than 1.5 times longer than tall (0), length of anterior cervical centra equal or greater than 1.5 times longer than tall (1) (Boyd 2015 #144).

200(*). Cervical vertebrae, evolution of central length throughout the series: central length remains approximately the same or decrease posteriorly (0), increase posteriorly (1).

201(*). Cervical vertebrae, number: 7/8 (0), 9 (1), 10 or more (2) (Ösi et al. 2012 #135).

202(*). Dorsal vertebrae, number: 12–13 (0), 14-15 (1), 16 or more (2) (modified from Ösi et al. 2012 #137; ordered character).

203(*). Dorsal vertebrae, neural spine: anteriorly positioned or centered over the dorsal centrum (0), start projecting farther posteriorly than their own centra at some point within the dorsal vertebral series (1) (modified from Brown et al. 2013 #78).

204(*). Sacrum composed of three or fewer fused vertebral centra (0), sacrum composed of between four and five fused vertebral centra (1), sacrum composed of six fused vertebral centra (2), sacrum composed of seven or more fused vertebra centra (3) (modified from Xu et al. 2006 #104; Boyd 2015 #148).

205(*). Sacral vertebrae, neural spines height: less than 2 times the height of the centrum (0), neural spines between 2 and 2,5 times the height of the centrum (1), greater than 2,5 times (2) (Brown et al. 2013 #82).

206(*). Sacrum, accessory articulation with pubis: pubis does not articulate with the sacrum (0), pubis supported by sacral rib (1), pubis supported by sacral centrum (2) (modified from: Ösi et al. 2012 #139; Brown et al. 2013 #84).

207(*). Ischiac peduncle of the ilium is not supported by a sacral rib (0), ischiac peduncle of the ilium supported by a sacral rib (1) (Boyd 2015 #190).

208(*). Proximal caudal vertebrae, neural spines position: caudal neural spines positioned over centrum (0), project backward beyond own centrum to an angle of more than 50° over the horizontal (1), project backward to an angle of less than 50° over the horizontal (2) (modified from Brown et al. 2013 #88).

209(*). Anterior caudal vertebrae, neural spines: height (from above the prezygapophyses) the same or up to 50% taller than the centrum (0), more than 50% taller than the centrum (1) (Ösi et al. 2012 #142).

210. Dorsal ribs, transition between a near vertical orientation of the *tuberculum* and *capitulum* to a horizontal orientation: occurs within ribs 2-4 (0), 5-6 (1), 6-8 (2) (Brown et al. 2013 #79).

211(*). Anterior dorsal ribs, distal portions of the shaft in cross-section: circular or oval (0), highly laterally compressed with concave lateral and rugose posterior surfaces (1) (Brown et al. 2013 #135).

212(*). Dorsal ribs, distal anteroposterior thickening: absent (0), present (1) (new character).

213(*). Ossified epaxial tendons along dorsal and sacral vertebrae: absent (0), present (1) (new character).

214. Partial ossification of the sternal segments of the cranial dorsal ribs absent (0), present (1) (Boyd 2015 #157; Ösi et al. 2012 #145).

215(*). Proximal caudal ribs, location: borne on centrum (0), on neurocentral suture (1), on neural arch (2) (modified from Brown et al. 2013 #85).

216(*). Caudal ribs, longest rib position: the first caudal vertebra bears longest rib (0), longest rib posterior to the first (1) (Brown et al. 2013 #87).

217(*). Distal caudal chevrons shape: rod-shaped, often with slight distal expansion (0), strongly asymmetrically expanded distally (1) (rephrased from Ösi et al. 2012 #144).

218(*). Ossified epaxial/hypaxial tendons along caudal vertebrae: absent (0), present (1) (modified from Ösi et al. 2012 #216 and #217; Brown et al. 2013 #86).

219. Ossified epaxial tendons (back or tail), arrangement: longitudinally arranged (0), Basket-like arrangement of fusiform tendons in caudal region (1), double-layered lattice (2). (modified from Ösi et al. 2012 #218).

Appendicular skeleton:

220. Ossified clavicles: absent (0), present (1) (Ösi et al. 2012 #147).

221(*). Scapula-Humerus, proportions: scapula longer or subequal to the humerus (0), humerus substantially longer than the scapula (1) (Ösi et al. 2012 #149).

222(*). Scapula, blade-shape: strongly expanded distally (0), weakly expanded, near parallel-sided (1) (Ösi et al. 2012 #152).

223(*). Scapula, scapular blade length relative to minimum width: relatively short and broad, length is 5-8 times minimum width (0), elongate and strap-like, length is at least 9 times the minimum width (1) (Ösi et al. 2012 #150).

224(*). Scapula, acromion shape: weakly developped or absent (0), well-expanded anteriorly, spine-like (1) (reformulated from Ösi et al. 2012 #151).

225(*). Scapula, acromion process proximal extent: low, almost reaches the coracoid anterodorsally (0), high, elevated with respect to the coracoid (1) (new character).

226(*). Scapula, angle formed by the medial borders of the 'supra-glenoid' process: acute, less than 75° (0), more than 75° (1) (modified and derived from Xu et al. 2006 #20; Dieudonné et al. 2016a #191).

227(*). Scapula, posterior edge of the supra-glenoid process: smoothly deflects posteroventrally with respect to the ventral edge of the scapular shaft (0), sharply deflects posteroventrally with respect to the ventral edge of the scapular shaft (1) (new character, derived from Dieudonné et al. 2016a #191).

228(*). Coracoid, height divided by length (considering an horizontal inclination of the scapulocoracoid, and by omitting the "extra-height" entailed by the sternal process with respect to the infraglenoid corner): between 70% and 120% (0) equal or greater than 120% (1) (modified from Brown et al. 2013 #90).

229(*). Coracoid, coracoid foramen position from a lateral view: enclosed within coracoid (0), open along coracoid-scapula suture (1) (rephrased from Brown et al. 2013 #91).

230. Coracoid, development of the sternal process: short and broad (0), extremely elongated and narrow (ratio greater than 0.80) (1) (Weishampel et al. 2003: # 44; Ösi et al. 2012 #231).

231(*). Sternal plates, shape: absent (0), kidney-shaped or semi-lunate (1), shafted or hatchet-shaped (rod-like posterolateral process, expanded anteromedial end) (2), of right-angle triangle with broad medial contact for collateral sternal (3) (rephrased and modified from Ösi et al. 2012 #148).

232(*). Humerus, length relative to femoral length: more than 60% (0), less than 60% (1) (Ösi et al. 2012 #153).

233(*). Humerus, appearance of the anterior surface in proximal view: a varyingly developed flexor bicipital sulcus is visible (0), the anterior surface is straight to smoothly convex, no bicipital sulcus visible (1) (Dieudonné et al. 2016a #197).

234. Humerus, proximal end in anterior/posterior view, lateral border between head and deltopectoral crest: straight or gently convex (0), concave (1) (Ösi et al. 2012 #232).

235(*). Humerus, proximal head separated from prominent medial tubercle on proximal surface by a shallow median groove: absent (0), present (1) (modified from Ösi et al. 2012 #223).

236(*). Humerus, deltopectoral crest: well developped, projecting at a distinct angle from the shaft (0), low and rounded (1), almost imperceptible (2) (modified from Xu et al. 2006 #42; Ösi et al. 2012 #154).

237(*). Humerus, deltopectoral crest shape: distal margin rounded and merges gradually with the lateral margin of the humeral shaft (0), distal margin angular and merges abruptly with the lateral margin of the humeral shaft (1) (modified from Weishampel et al. 1993 #37; McDonald et al., 2010 #103).

238(*). Humerus, proximolateral margin with respect to the main axis of the shaft in anteroposterior view: straight, aligned with the distolateral margin (0), medially bowed (1) (modified from Ösi et al. 2012 #155).

239(*). Humerus, proximal shaft curvature from a lateral view: proximal portion is aligned with distal portion of the shaft (0), proximal portion of the humeral shaft is bent backward relative to the distal portion (1) (new character).

240(*). Humerus, anterior coronoid fossa from a distal view: more deeply incised (0), widely open and shallow (1) (new character).

241(*). Humerus, posterior olecranon fossa from a distal view: present (0), forms only a weak depression or is totally absent (1) (new character).

242(*). Ulna, olecranon process: low (0), moderately developed (1), high (2) (Butler et al. 2011; Brown et al. 2013 #93).

243. Ulna, distal end: directed ventrally in medial or lateral view (0), curves gently posteriorly in medial or lateral view (1) (Ösi et al. 2012 #233).

244 (*). Radius, distal end: subspherical to ovate (0), anteroposteriorly expanded, with its medial surface sub-parallel to closely juxtaposed to the ulna (1), mediolaterally more expanded than the ulna, the radius expands distally at right angle from the ulna and does not cross over it (2) (new character).

245(*). Carpus, fusion: unfused (0), fused (1) (Brown et al. 2013 #97).

246(*). Ulnare, cushion-like and proximodistally compressed in dorsoventral view: absent (0), present (1) (new character).

247(*). Ulnare: articulates distally *via* the distal carpal 4: with the third metacarpal (0), mostly with the fourth metacarpal (1) (new character).

248(*). Metacarpals, block-like proximal ends: absent (0), present (1) (Ösi et al. 2012 #157).

249. Metacarpals I and V: substantially shorter in length than metacarpal III (0), subequal in length to metacarpal III (1) (Ösi et al. 2012 #158).

250(*). Metacarpal I greater than 50% the length of metacarpal II (0), metacarpal I less than 50% the length of metacarpal II (1) (Boyd 2015 #174).

251(*). Metacarpal/manual phalanges, extensor pits on the dorsal surface of the distal end: absent or poorly developed (0), deep, well-developed (1) (Ösi et al. 2012 #162).

252. First finger phalanx of digit I, length relative to the first finger phalanx of digit III: significantly longer (0), subequal or shorter (1) (new character).

253. First finger phalanx of digit II, length relative to the first finger phalanx of digit III: significantly longer (0), subequal or shorter (1) (new character).

254(*). Penultimate phalanx of fingers II and III: shorter than or subequal to first phalanx (0), longer than the first phalanx (1) (modified from Ösi et al. 2012 #159).

255(*). Manual digit III, number of phalanges: 4 (0), 3 or fewer (1) (Ösi et al. 2012 #160).

256(*). Manual unguals, strongly recurved with prominent flexor tubercle: absent (0), present (1) (Ösi et al. 2012 #163).

257(*). Ilium length taken from the tip of the preacetabular process to the tip of the postacetabular process (measured on a straight line with a ruler): shorter than (0), or longer than (1) 90% of the femur length (modified from Xu et al. 2006 #90).

258. Ilium postacetabular process from a lateral view: much deeper than (0) or subequal to (1) that of the preacetabular process (rephrased from Xu et al. 2006 #91).

259(*). Ilium, preacetabular process shape and length: short, tab-shaped, distal end is posterior to pubic peduncle (0), elongate, strap-shaped, distal end is anterior to pubic peduncle (1) (Ösi et al. 2012 #165).

260(*). Ilium, preacetabular process length relative to the ilium length: less than 50% (0), more than 50% (1) (Ösi et al. 2012 #166).

261(*). Ilium, preacetabular process curvature from a lateral view: no distinct break in slope, dorsal surface varies from straight to smoothly convex all along (0), the downward break in slope located above the pubic peduncle (1), the downward break in slope starting well anterior to the pubic peduncle (2) (new character).

262(*). Ilium, outline of dorsal margin from a dorsal view: postacetabular process straight until above the acetabulum, and the preacetabular process subtly to moderately deflected from midline laterally (0), the dorsal margin forms a regular and continuous curve from the postacetabular process to the preacetabular process, with the medial side convex all along and the preacetabular process well deflected laterally (1), sigmoidal: the preacetabular process is well deflected laterally, and the postacetabular process curves toward the medial side posteriorly (2), straight all along (3) (modified from Xu et al. 2006 #50; Ösi et al. 2012 #167).

263(*). Ilium, preacetabular process expands mediolaterally towards its distal end in dorsal view: absent (0), present (1) (Ösi et al. 2012 #169).

264(*). Ilium, medioventral acetabular flange, partially closing the acetabulum: present (0), absent (1) (Ösi et al. 2012 #175).

265(*). Ilium, supra-acetabular ‘crest’ or ‘flange’ on the dorsolateral part of the acetabulum: present (0), absent (1) (modified from Ösi et al. 2012 #176).

266(*). Ilium, postacetabular process orientation from a lateral view: posteriorly directed (0), curves posterodorsally with both its dorsal and ventral margins (1) (McDonald et al. 2010 #114; Ösi et al. 2012 #170).

267(*). Ilium, morphology of dorsal margin at the level of the acetabulum: smooth, almost no modification of dorsal margin (0), well thickened above the ischiac peduncle onward (1), thickened above the pubic peduncle onward (2) (modified from McDonald et al. 2010 #112; Ösi et al. 2012 #168; Dieudonné et al. 2016a #222).

268. Ilium, laterally-bulging everted rim on the dorsal margin above the acetabulum: absent (0), present (1) (McDonald et al. 2010 #112; splitted from Dieudonné et al. 2016a #222).

269(*). Ilium, dorsal surface of postacetabular process until the origin of *M. iliocaudalis* from a lateral view: smoothly convex with a posterior break in slope (0), the postacetabular blade looks strongly quadrangular-shaped (1), tapers with no break in slope for the attachment of *M. iliocaudalis* (2) (modified from McDonald et al. 2010 #113; Dieudonné et al. 2016a #223).

270(*). Ilium, brevis shelf and fossa: faces ventrolaterally and shelf is near vertical and creates a deep postacetabular portion anteriorly (0), fossa faces ventrally for most of its length and is less visible from a lateral view (1), the brevis shelf consists in a small and smooth ridge that is only visible from a medial view (2) (reformulated from Ösi et al. 2012 #173; Dieudonné et al. 2016a #224).

271(*). Ilium, brevis shelf and fossa, transverse width: narrow (0); very broad and expanding in width towards its caudal margin such that it appears triangular in dorsal or ventral view (1) (McDonald, 2012 #132).

272(*). Ilium, length of the postacetabular process relative to the total ilium length: 20% or less (0), 25-35% (1), more than 35% (2) (Ösi et al. 2012 #174).

273(*). Ilium, pubic peduncle: elongate and robust (0), ventrally projected, elongate and strap-like (1), often reduced in size, anteriorly projected so its distal tip is higher than the ventral extent of the ischial peduncle (2) (modified from Ösi et al. 2012 #178).

274(*). Ilium, ischiac peduncle: projects ventrally (0), broadly swollen, projects ventrolaterally (1) (Butler et al. 2011; Ösi et al. 2012 #177).

275(*). Ilium, ischiac peduncle: anteroposteriorly short (0), massive and anteroposteriorly long (1) (new character).

276(*). Ilium, acetabulum: normal to high (0), low (1) (reformulated after Boyd 2015 #182).

277. Pubis, massive and dorsolaterally rotated body obscuring the obturator foramen in lateral view: absent (0), present (1) (Ösi et al. 2012 #191).

278(*). Pubis, orientation: anteroventral (0), rotated posteroventrally to lie alongside the ischium (opisthopubic) (1) (Ösi et al. 2012 #186).

279. Pubis, prepubic process: absent (0), present (1) (Ösi et al. 2012 #192).

280(*). Pubis, prepubic process shape in its distal extremity: compressed mediolaterally, dorsoventral height exceeds mediolateral width (0), rod-like, mediolateral width exceeds dorsoventral height (1), dorsoventrally compressed (2) (modified from: Butler et al. 2011; Ösi et al. 2012 #193).

281(*). Pubis, prepubic process length: stub-like and poorly developed, extends only a short distance anterior to the pubic peduncle of the ilium (0), elongated into distinct anterior process, but does not extend beyond the distal end of the preacetabular process of ilium (1), elongate and extending up to the level or beyond the distal end of preacetabular process of ilium (2) (modified from Xu et al. 2006 #43, #106; Ösi et al. 2012 #194, #195).

282(*). Pubis, angle between prepubic process and distal postpubic shaft : less than 130 degrees (0) ; greater than 130 degrees but less than 170° (1) ; aligned along the same plane (2) (modified from Boyd 2015 #196).

283(*). Pubis, pubic symphysis: elongate or at least present distally on a significant part of the pubic blade (0), much reduced or absent (1) (modified from Xu et al. 2006 #47; Ösi et al. 2012 #196).

284(*). Pubis, shape of the postpubis shaft in cross-section: blade-shaped (0), rod-shaped (1) (Ösi et al. 2012 #187).

285(*). Pubis, length of postpubis shaft relative to ischium length: approximately equal (0), extends for around half the length (1), very short to absent (2) (modified from: McDonald et al., 2010 #117 ; Ösi et al. 2012 #188, #189).

286(*). Ischium, pubic peduncle shape: transversely compressed (0), dorsoventrally compressed and mediolaterally thick (1) (reformulated from Ösi et al. 2012 #179).

287(*). Ischium, pubic peduncle breadth from a lateromedial view: larger than or subequal to that of the iliac peduncle (0); much smaller than that of the iliac peduncle (1) (modified from Gasca et al. 2014 #3; Boyd 2015 #200).

288(*). Ischium, orientation of the proximal main axis of the shaft and angle with respect to the pubic peduncle: falls between the iliac and pubic peduncles main axis, angle inferior to 140° (0), falls between the iliac and pubic peduncles main axis, angle widely open and superior to 140° (1), falls in the same axis of that of the pubic peduncle (2) (modified from Gasca et al. 2014 #1).

289. Ischium, curvature of the acetabular margin in lateral view: gentle, defines a wide acetabular recess (0), marked, defines a narrow acetabular recess (1) (Gasca et al. 2014 #4).

290(*). Ischium, angle formed by the iliac peduncle and the proximal long axis: superior to 120° (0), equal or inferior to 120° (1) (modified from Gasca et al. 2014 #5).

291(*). Ischium, tab-shaped obturator process: absent, lacks an obturator process (0), present and placed 60% down the shaft of ischium (1), placed within the first proximal half of the shaft (2) (modified from: Xu et al. 2006 #44; Ösi et al. 2012 #184; Brown et al. 2013 #102).

292(*). Ischium, shaft in cross-section: compressed mediolaterally (0), subcircular and bar-like (1) (Ösi et al. 2012 #181).

293(*). Ischium, symphysis length: median symphysis with the opposing blade along at least 50% of its length (0), symphysis only presents distally (1) (Ösi et al. 2012 #185).

294(*). Femur, shape in medial/lateral view: bowed anteriorly along length (0), straight (1) (McDonald et al. 2010 #121; Ösi et al. 2012 #197).

295. Femur, femoral head: arises from a well-constricted neck (0), arises from a shallow and thick, unconstricted neck (1) (new character).

296(*). Femur, femoral head: confluent with greater trochanter, *fossa trochanteris* consists in a smooth and shallow groove (0), *fossa trochanteris* is modified into distinct constriction separating head and greater trochanter (1) (rephrased from Ösi et al. 2012 #198).

297(*). Femur, anterior extension of the greater trochanter beyond the femoral head: almost inexistent (0), shortly expanded and thick anteriorly (1), moderately to very elongated (2) (modified from Rozadilla et al. 2016 #231).

298(*). Anterior trochanter, level with respect to the greater trochanter: well below (0), from moderately below to slightly below the level of the greater trochanter (1) level or higher (2) (modified from: Boyd 2015 #215; Ösi et al. 2012 #200).

299(*). Anterior trochanter of femur in proximal view: positioned anterior to greater trochanter (0), possess a beveled posterior surface (anteromedial to posterolateral in direction), so that it appears positioned somewhat anterolateral to the greater trochanter (1), L-shaped anterior trochanter with very thin edges bordering both anterior and lateral sides of the greater trochanter (2) (modified from Boyd 2015 #216).

300(*). Posterolateral edge of the greater trochanter : globular and rounded (0), triangular, the lateral edge of the greater trochanter is globally flatenned (1) (reformulated from Boyd 2015 #213).

301. Femur, fourth trochanter shape: low eminence or absent (0), straight ridge (1), pendent (2) (modified from: Butler et al. 2011; Ösi et al. 2012 #201).

302(*). Femur, fourth trochanter position: located entirely on proximal half of femur (0) or positioned at mid-length, or distal to mid-length (1) (Ösi et al. 2012 #202).

303(*). Femur, pendent fourth trochanter, rod-like with subparallel anterior and posterior surfaces: absent (0), present (1) (Ösi et al. 2012 #224).

304(*). Femur, location of insertion scar of *M. caudifemoralis longus*: extends from fourth trochanter onto medial surface of femoral shaft (0), widely separated from fourth trochanter, restricted to medial surface of femoral shaft (1) (McDonald et al., 2010 #125).

305(*). Femur, anterior (extensor) intercondylar groove: absent (0), shallow and wide open through with sides that diverge from each other cranially (1), deep and narrow open through with parallel sides (2) (modified from McDonald et al. 2010 #127; Ösi et al. 2012 #203).

306(*). Femur, posterior (flexor) intercondylar groove: fully open (0), medial condyle inflated laterally, partially covers opening of flexor groove (1) (modified from Butler et al. 2011; Ösi et al. 2012 #204).

307(*). Femur, posterolateral condyle position and size in ventral view: positioned relatively laterally and slightly narrower in width than the medial condyle (0), strongly inset medially, reduced in width relative to medial condyle (1) (modified from Ösi et al. 2012 #205).

308. Femur, cranial expansion of medial condyle: equal to, or less than lateral condyle (0), protrudes cranially to lateral condyle, and continues onto the cranial surface as a diaphyseal ridge to cranial trochanter (1) (Herne, 2014 #233).

309(*). Femur proportions in distal view by taking the iliofibularis groove as a reference point whenever possible or the posterior intercondylar groove in all other cases: maximum anteroposterior length of the distolateral condyle (without considering the posterolateral condylid) out of distal width: ≥ 50% (0), between 40 and 50% (1), < 40% (2).

310(*). Tibia, lateral fibular condyle from an anteroposterior view: gradually and merges with the shaft distally (0), defines an abrupt overhanging buttress with sub-horizontal ventral margin above the shaft (1).

311(*). Tibia, cnemial crest from a proximal view: straight, faces anteriorly (0), strongly bent laterally (1) (new character).

312. Tibia, distal shape: subquadrate, posterolateral process not substantially developed (0), elongate posterolateral process, backing fibula (1) (Ösi et al. 2012 #206).

313. Tibia, maximum expansion of distal end relative to proximal: distal end is considerably less expanded than proximal (0), maximum expansion of distal end is subequal or larger than that of proximal end (1) (rephrased from Ösi et al. 2012 #227).

314(*). Fibula, proximal head: moderately expanded at both sides (0), features a major anterior expansion of its anteroproximal corner (1) (new character).

315. Fibula, shaft in cross-section: elliptical or round (0), D-shaped (1) (Brown et al. 2013 #115).

316(*). Fibula, distal end is strongly reduced and splint-like: absent (0), present (1) (Ösi et al. 2012 #225).

317(*). Astragalus/calcaneum, indistinguishable and fused to one another: absent (0), present (1) (Ösi et al. 2012 #226).

318(*). Astragalus, anterior process: moderate to high, from tooth-like to wide anteriorly (0), low to absent (1) (modified from Brown et al. 2013 #118).

319(*). Astragalus, posterior side size: low (0), high (1) (Brown et al., 2013 #117).

320(*). Astragalus, fibular facet on the lateral margin of the proximal surface: large (0), reduced to small articulation or absent (1) (rephrased from Ösi et al. 2012 #207).

321(*). Calcaneum, tibial articular surface from a lateral view: facet for tibia absent (0), facet for tibia present and subequal in length to that for the fibula (1), facet for tibia longer than the

facet for the fibula, and the posteroventral part of the calcaneum is elongated into a distinct caudal process (2) (modified from Ösi et al. 2012 #208, Rozadilla et al. 2016 #236).

322(*). Calcaneum, angle between the edge separating the tibial and fibular articular facets, and the lateral border of the calcaneum on the posterior side: greater than 110 degrees (0), less than 110 degrees (1) (modified from Brown et al. 2013 #119).

323(*). Medial distal tarsal, shape: blocky in dorsal view (0), thin and rectangular (1), round (2) (Brown et al., 2013 #120).

324(*). Medial distal tarsal: articulates distally with metatarsal III only (0), articulates distally with metatarsals II and III (1) (Ösi et al. 2012 #209).

325(*). Lateral distal tarsal, shape in dorsoventral view: square (0), kidney-shaped (1), sub-triangular (2) (modified from Brown et al. 2013 #122).

326(*). Metatarsal II/metatarsal III, morphology of the contact in proximal view: continuous, flat to smoothly concave anteroposteriorly (0), metatarsal II forms a lateral step over a proximal outgrowth on the ventro-medial side of the metatarsal III (1) (Dieudonné et al. 2016a #277).

327(*). Metatarsal II, width of proximal articular surface at mid dorsoplantar height (at the level of its lateral “step” whenever present): inferior to 75% the maximum width of MT III (0), exceeds 75%, but is still below 100% of MT III maximum width (1), equals or exceeds 100% the maximum width of MT III (2) (new character).

328(*).Metatarsal III, dominance of proximal articular surface, width of MT III largely exceeds width of metatarsal IV (by omitting the eventual posteromedial process of MT IV and associated caudolateral notch on MT III): absent (0), present (1) (rephrased and modified from Rozadilla et al. 2016 #232).

329(*). Metatarsal III and IV proximal contact, dorsolateral notch on the proximolateral surface of MT III for eventual dorsomedial overlap of metatarsal IV: absent (0), present (1) (new character).

330(*). Metatarsal IV, proximal extremity: sends a prominent posteromedial process toward MT III, which is eventually hosted within a deep caudolateral notch on MT III: absent (0); present (1) (rephrased from McDonald, 2012 #134; Dieudonné et al. 2016a #278).

331(*). Metatarsal III and IV, proximal contact: tightly adpressed, no notch is observed posteriorly between them (0), conspicuous concavity to either, or both, the posterolateral side of metatarsal III and the posteromedial side of metatarsal IV which can eventually host the fifth metatarsal (1) (Dieudonné et al. 2016a #279).

332. Metatarsal V, length relative to that of metatarsal III: more than 50% (0), less than 25% (1) (Ösi et al. 2012 #213).

333. Metatarsal V: bears digits (0), lacks digits (1) (Ösi et al. 2012 #214).

334(*). Metatarsal I, proximal surface: developped into a distinct articular surface (0), proximally splint-like or devoid of any articular surface (1) (new character).

335(*). Pedal digit I, number of pedal phalanges on the first metatarsal: two phalanges (0), bears only one ungueal or does not bear digits at all (1) (modified from Ösi et al. 2012 #211; Brown et al., 2013 #123).

336(*). Pedal digit I, configuration: the first metatarsal is well-developed, distal end of last phalanx projects beyond the distal end of metatarsal II (0), metatarsal I reduced or absent, end of phalanx I-1 not extending beyond the end of metatarsal II (1) (modified from Ösi et al. 2012 #211).

337. Pedal unguals, shape: tapering, narrow pointed, claw-like (0), wide, blunt, hoof-like (1) (Ösi et al. 2012 #215; Xu et al. 2006 #105).

Dermal skeleton

338. Mandibular osteoderm: absent (0), present (1) (Ösi et al. 2012 #110).

339. Dermal osteoderms, parasagittal row on the dorsum of the body: absent (0), present (1) (Ösi et al. 2012 #219).

340. Dermal osteoderms, lateral row of keeled dermal osteoderms on the dorsum of the body: absent (0), present (1) (Ösi et al. 2012 #220).

341. Dermal osteoderms, U-shaped cervical/pectoral collars composed of contiguous keeled osteoderms: absent (0), present (1) (Ösi et al. 2012 #221).

New numerotation	-	1	2	3	4	5	6	7	8
Dieudonné *et al.* 2016 n°	-	1	2	3	-	-	4	5	6
References (*)	-	O2	O1	O37	new	X87	O36	O89	O3
Herrerasaurus_ischigualastensis	0	0	0	0	1	0	0	0	0
Abrictosaurus_consors	0	0	1	?	?	?	0	0	0
Agilisaurus_louderbacki	0	0	0	1	1	0	0	0	0
Anabisetia_saldiviai	0	?	?	?	?	?	?	?	?
Ankylosauria	0	0	0	?	1	?	0	1	0
Archaeoceratops_oshimai	0	1	0	1	0	0	0	0	1
Camptosaurus_aphanoecetes	0	?	?	?	?	?	?	?	?
Camptosaurus_dispar	0	0	0	0	0	0	0	0	0
Changchunsaurus_parvus	0	0	0	?	1	0	0	0	0
Chaoyangsaurus_youngi	0	?	1	1	?	1	1	0	1
Convolosaurus_marri	0	0	0	0	?	?	0	0	0
Dryosaurus	0	0	0	0	0	0	0	0	0
Dysalotosaurus_lettowvorbecki	0	?	0	?	0	?	0	0	0
Echinodon_becklesii	0	?	?	?	?	?	?	?	0
Emausaurus_ernstii	0	?	0	0	1	0	0	1	0
Eocursor_parvus	0	0	?	?	?	?	?	?	?
Eousdryosaurus_nanohallucis	0	?	?	?	?	?	?	?	?
Fostoria_dhimbangunmal	0	?	?	?	?	?	?	?	?
Fruitadens_haagarorum	0	?	?	?	?	?	?	?	0
Gasparinisaura_cincosaltensis	0	0	0	?	1	0	0	0	?
Goyocephale_lattimorei	0	?	1	?	?	?	0	0	0
Haya_griva	0	?	0	?	1	?	0	0	0
Heterodontosaurus_tucki	0	0	1	0	0	0	0	0	0
Hexinlusaurus_multidens	0	0	1	0	0	0	0	0	0
Homalocephale_calathocercos	0	?	?	1	0	0	0	0	0
Hypsilophodon_foxii	0	0	0	0	0	0	0	0	0
Iguanodon_bernissartensis	0	0	0	0	1	0	0	0	0
Isaberrysaura_mollensis	0	?	0	0	1	0	0	0	?
Jeholosaurus_shangyuanensis	0	?	0	0	1	0	0	0	0
Kangnasaurus_coetzeei	0	?	?	?	?	?	?	?	?
Koreanosaurus_boseongensis	0	?	?	?	?	?	?	?	?
Kulindadromeus_zabaikalicus	0	?	?	?	0	0	?	0	?
Lesothosaurus_diagnosticus	0	0	0	0	0	0	0	0	0
Laquintasaura_venezuelae	0	?	?	?	?	?	?	?	?
Liaoceratops_yanzigouensis	0	?	0	1	1	0	0	0	1
Lycorhinus_angustidens	0	?	?	?	?	?	?	?	?
Macrogryphosaurus_gondwanicus	0	?	?	?	?	?	?	?	?
Mahuidacursor_lipanglef	0	?	?	?	?	?	?	?	?
Mochlodon_suessi	0	?	?	?	?	?	?	?	?
Mochlodon_vorosi	0	?	?	?	?	?	?	?	?
Morrosaurus_antarcticus	0	?	?	?	?	?	?	?	?
Muttaburrasaurus_langdoni	0	?	?	0	0	?	?	?	?
Nanosaurus_agilis	0	?	?	?	?	?	?	?	?
Orodromeus_makelai	0	0	0	?	?	?	0	0	0
Pachycephalosaurus_wyomingensis	0	?	0	1	0	0	0	0	0
Parksosaurus_warreni	0	0	0	?	1	0	0	0	?
Prenocephale_prenes	0	?	1	1	0	0	0	0	0

Psittacosaurus_mongoliensis	0	1	1	1	1	1	1	0	1
Psittacosaurus_major	0	?	1	1	1	1	1	0	1
Rhabdodon_priscus	0	?	?	?	?	?	?	?	?
Rhabdodon_sp1	0	?	?	?	?	?	?	?	?
Scelidosaurus_harrisonii	0	0	0	0	1	0	0	1	0
Scutellosaurus_lawleri	0	0	?	?	?	?	0	1	0
Stegoceras_validum	0	?	1	1	0	0	0	0	0
Stegosauria	0	0	0	0	0	?	0	0	0
Stenopelix_valdensis	0	?	?	?	?	?	?	?	?
Talenkauen_santacrucensis	0	0	?	?	?	?	?	0	0
Tenontosaurus_dossi	0	0	0	0	0	?	0	0	0
Tenontosaurus_tilletti	0	0	0	0	0	0	0	0	0
Thescelosaurus_neglectus	0	0	0	0	0	0	0	0	0
Thescelosaurus_assiniboiensis	0	?	?	?	?	?	?	?	?
Tianyulong_confuciusi	0	0	0	?	?	?	?	?	0
Valdosaurus_canaliculatus	0	?	?	?	?	?	?	?	?
Vegagete_ornithopod	0	?	?	?	?	?	?	?	?
Wannanosaurus_yansiensis	0	?	?	?	?	?	0	0	?
Yandusaurus_hongheensis	0	?	?	?	?	?	0	0	?
Yueosaurus_tiantaiensis	0	?	?	?	?	?	?	?	?
Yinlong_downsi	0	1	1	1	1	1	1	0	1
Zalmoxes_robustus	0	0	0	?	0	?	0	0	0
Zalmoxes_shqiperorum	0	0	?	?	0	?	0	0	?
Zephyrosaurus_schaffi	0	?	?	?	0	?	0	0	0

(*) Explanation for line of references	First letters of First authors' names and their corresponding datamatrix	
References are listed as the concatenation of the first letter of the first author's name with the character number from his datamatrix. Those letters correspond to the papers cited in this table.	Bd =	Boyd (2015)
	Br =	Brown *et al.* (2013)
	C =	Cambiaso (2007)
	D =	Dieudonné *et al.* (2016)
	G =	Gasca *et al.* (2014)
	H =	Han *et al.* (2018)
	He =	Herne (2014)
	MD =	McDonald *et al.* (2010)
	O =	Ösi *et al.* (2012)
	P =	Pol *et al.* (2011)
	R =	Rozadilla *et al.* (2016)
	X =	Xu *et al.* (2006)

9	10	11	12	13	14	15	16	17	18	19	20	21	22	23	24	25
-	7	8	-	9	10	11	12	13	14	16	17	18	19	20	21	22
X4	O4X5	O5	X52	Br136	37MD	MD33	O6	X34O7	O8	O10	X6O11	Br124	O18	12Bd1	22O1	O16
-	-	-	0	0	0	0	0	0	0	0	0	0	0	0	1	1
-	-	-	0	?	1	?	1	?	0	1	?	?	0	0	0	0
-	-	-	0	0	0	0	1	0	0	1	1	0	0	0	0	0
?	?	?	?	?	?	?	?	?	?	?	?	?	?	?	?	?
-	-	-	0	?	?	?	1	0	0	1	1	?	0	?	0	0
1	1	1	0	?	0	?	1	0	0	1	0	?	0	0	0	1
?	?	?	?	?	?	?	?	?	?	?	?	?	?	?	?	?
-	-	-	0	0	1	1	1	1	1	0	1	0	1	?	0	0
-	-	-	0	1	0	0	1	0	0	1	1	1	0	0	0	0
?	0	0	1	?	0	?	1	?	0	?	0	?	0	?	1	1
-	-	-	1	1	1	0	1	0	0	1	1	0	0	0	0	0
-	-	-	0	0	1	0	1	1	1	0	1	0	1	0	0	0
-	-	-	0	0	?	0	1	1	1	0	1	0	1	0	0	0
-	-	-	?	?	1	?	?	?	0	?	1	?	?	?	?	0
-	-	-	0	?	0	?	?	0	0	?	1	?	0	?	0	0
?	?	?	?	?	?	?	?	?	?	?	?	?	?	?	?	?
?	?	?	?	?	?	?	?	?	?	?	?	?	?	?	?	?
?	?	?	?	?	?	?	?	?	?	?	?	?	?	?	?	?
-	-	-	?	?	?	?	1	?	0	?	1	?	?	?	?	?
?	?	?	?	?	?	?	?	?	?	?	?	0	?	?	?	?
-	-	-	0	?	0	0	?	?	0	?	?	0	0	1	0	0
-	-	-	0	0	0	0	1	0	0	1	?	0	0	0	1	0
-	-	-	0	0	1	?	1	1	0	1	1	0	0	0	0	0
-	-	-	0	?	?	?	?	0	?	?	?	?	0	?	?	?
-	-	-	?	?	?	?	?	?	?	?	?	?	?	?	?	?
-	-	-	0	1	1	0	1	0	0	1	1	0	0	0	0	0
-	-	-	0	0	1	1	1	1	1	0	1	0	1	?	0	0
?	?	?	0	?	0	?	?	0	0	?	?	?	0	?	?	?
-	-	-	0	1	0	0	1	1	0	1	1	?	0	0	0	0
?	?	?	?	?	?	?	?	?	?	?	?	?	?	?	?	?
?	?	?	?	?	?	?	?	?	?	?	?	?	?	?	?	?
-	-	-	?	?	?	?	?	1	?	?	?	?	?	?	?	?
-	-	-	0	0	0	0	1	0	0	1	1	0	0	?	0	0
?	?	?	?	?	?	?	1	?	?	?	?	?	?	?	?	?
1	0	1	0	?	0	?	1	?	0	1	0	?	0	0	0	1
?	?	?	0	?	?	?	?	?	?	?	?	?	?	?	?	?
?	?	?	?	?	?	?	?	?	?	?	?	?	?	?	?	?
?	?	?	?	?	?	?	?	?	?	?	?	?	?	?	?	?
?	?	?	?	?	?	?	?	?	?	?	?	?	?	?	?	?
?	?	?	?	?	?	?	?	?	?	?	?	?	?	?	?	?
?	?	?	?	?	?	?	?	?	?	?	?	?	?	?	?	?
?	?	?	?	?	?	?	?	1	?	?	?	?	0	?	?	?
?	?	?	?	?	?	?	?	?	?	?	?	0	?	?	?	?
-	-	-	?	1	0	0	1	0	0	1	1	0	0	0	0	0
0	-	-	0	1	0	?	?	0	?	?	?	?	?	0	0	?
?	?	?	0	?	?	?	?	0	?	?	?	?	?	?	?	?
0	-	-	0	?	1	0	1	0	0	1	1	0	0	0	0	0

0	0	0	1	?	0	0	1	1	0	1	0	0	0	0	1	1
0	0	0	1	0	0	0	1	1	0	1	0	0	0	0	1	1
?	?	?	?	?	?	?	?	?	?	?	?	?	?	?	?	?
?	?	?	?	?	?	?	?	?	?	?	?	?	?	?	?	?
-	-	-	0	?	?	?	1	0	0	?	?	?	?	0	?	?
-	-	-	0	0	?	0	?	?	0	1	1	0	?	0	0	0
0	-	-	0	1	1	0	1	0	0	?	1	0	0	0	0	0
-	-	-	0	?	0	?	1	0	0	1	1	?	0	?	0	0
?	?	?	?	?	?	?	?	?	?	?	?	?	?	?	?	?
-	-	-	0	?	0	0	1	0	1	?	1	?	1	0	0	0
-	-	-	0	0	1	0	1	1	1	0	1	0	1	0	0	0
-	-	-	0	?	1	0	1	1	1	0	1	0	1	?	0	0
-	-	-	0	1	0	0	1	0	0	1	1	?	0	0	0	0
?	?	?	?	?	?	?	?	?	?	?	?	?	?	?	?	?
-	-	-	0	?	1	?	1	1	0	?	?	?	0	0	0	0
?	?	?	?	?	?	?	?	?	?	?	?	?	?	?	?	?
?	?	?	0	?	?	0	?	?	0	?	?	?	?	?	?	?
?	?	?	?	?	?	?	?	?	?	?	?	?	?	?	?	?
?	?	?	?	?	?	?	?	?	?	?	?	?	?	?	?	?
?	?	?	?	?	?	?	?	?	?	?	?	?	?	?	?	?
1	0	1	0	?	0	?	1	1	0	1	0	0	0	1	0	0
-	-	-	0	1	0	0	1	0	0	0	1	0	0	0	1	0
?	?	?	?	?	?	?	?	?	?	?	?	?	?	?	?	?
-	-	-	0	1	0	0	1	?	0	1	1	1	0	0	0	0

26	27	28	29	30	31	32	33	34	35	36	37	38	39	40	41	42
23	25	26	28	-	29	-	31	32	34	-	35	-	36	-	-	38
Bd88	O13	O14	X9O84	X23	O24	O25	O26	)27X2⁴	O22	new	O34	X38	O20	X77	X78	)19X8⁴
0	0	0	?	0	0	0	0	0	1	1	0	0	0	0	0	1
?	0	1	?	?	?	0	1	0	0	0	0	0	1	1	1	?
0	0	0	?	0	?	0	1	0	0	1	0	1	1	0	0	1
?	?	?	?	?	?	?	1	?	?	?	?	?	?	?	?	?
?	0	0	0	?	0	1	1	0	?	?	?	?	1	?	?	0
0	0	0	?	0	?	0	1	1	0	0	0	1	1	1	0	0
?	?	?	?	?	?	?	?	?	?	?	?	?	?	?	?	?
1	0	?	0	1	0	1	1	0	0	1	0	2	1	0	0	0
0	1	1	0	0	?	0	1	0	0	1	?	?	1	0	0	1
?	0	0	?	?	?	?	1	1	?	?	?	?	1	?	0	?
0	0	0	0	0	0	0	1	0	1	1	1	2	1	0	1	0
1	0	?	0	1	0	1	1	0	1	1	0	2	1	1	0	0
1	0	?	0	1	0	1	1	0	0	1	1	2	1	1	0	0
?	?	?	?	?	?	?	1	?	?	?	?	?	?	?	1	?
?	0	0	?	0	0	1	0	0	0	0	0	0	1	0	0	?
?	?	?	?	?	?	?	?	?	?	?	?	?	?	?	?	?
?	?	?	?	?	?	?	?	?	?	?	?	?	?	?	?	?
?	?	?	?	?	?	?	?	?	?	?	?	?	?	?	?	?
?	?	1	?	?	0	?	1	?	?	?	?	?	?	?	?	?
?	?	?	?	?	?	1	1	0	1	1	1	2	1	0	0	?
0	0	1	1	0	0	0	1	0	?	?	?	?	?	?	?	1
0	1	0	?	0	0	0	1	0	0	1	1	1	1	0	0	1
0	0	1	1	1	0	0	1	0	0	0	0	0	1	1	1	1
?	?	?	?	0	?	0	1	0	0	0	1	1	1	0	0	1
?	?	?	?	?	?	?	1	0	?	?	?	?	2	?	?	?
0	1	0	0	0	0	0	1	0	1	1	1	2	1	0	0	?
1	0	?	0	1	0	1	1	0	0	1	1	2	1	0	0	0
?	0	0	?	0	0	1	1	0	0	0	0	0	?	0	0	1
0	1	0	1	0	?	0	1	0	0	0	1	1	1	0	0	1
?	?	?	?	?	?	?	?	?	?	?	?	?	?	?	?	?
?	?	?	?	?	?	?	?	?	?	?	?	?	?	?	?	?
?	?	?	?	0	0	0	?	?	1	1	1	0	1	0	1	?
?	0	0	0	0	0	0	0	0	0	0	0	0	1	0	0	1
?	?	?	?	?	?	?	0	?	0	?	?	?	1	?	?	?
0	0	0	1	1	?	0	1	1	0	0	0	1	1	1	0	1
?	0	1	?	?	?	0	1	0	0	?	?	?	1	?	?	?
?	?	?	?	?	?	?	?	?	?	?	?	?	?	?	?	?
?	?	?	?	?	?	?	?	?	?	?	?	?	?	?	?	?
?	?	?	?	?	?	?	?	?	?	?	?	?	?	?	?	?
?	?	?	?	?	?	?	?	?	?	?	?	?	?	?	?	?
?	?	?	?	?	?	?	?	?	?	?	?	?	?	?	?	?
?	?	?	?	1	?	1	1	?	?	?	?	?	1	0	?	?
?	?	?	?	?	?	?	?	?	?	?	?	?	?	?	?	?
?	1	0	0	0	1	1	1	0	1	1	0	2	1	0	0	?
?	?	?	?	0	0	?	1	0	?	?	0	1	2	1	0	?
0	?	0	?	0	?	1	1	0	1	1	1	2	1	0	0	0
0	?	1	1	0	0	0	1	0	1	1	0	1	1	1	0	1

0	0	0	1	1	0	1	1	1	-	-	-	?	1	-	0	1
0	0	0	1	1	0	1	1	1	-	-	-	2	?	-	0	?
?	?	?	?	?	?	?	?	?	?	?	?	?	?	?	?	?
?	?	?	?	?	?	?	?	?	?	?	?	?	?	?	?	?
?	?	0	?	0	0	?	0	0	0	0	0	0	1	0	0	0
?	?	?	?	?	?	?	?	0	?	?	?	?	?	?	?	?
0	0	1	1	0	0	0	1	0	?	1	0	1	2	1	0	1
?	[0 1]	0	0	0	0	1	1	0	?	?	0	0	1	0	?	0
?	?	?	?	0	?	?	?	?	?	?	?	?	?	?	?	?
?	0	0	?	?	0	1	1	0	1	1	?	?	1	?	0	?
0	0	0	0	0	0	1	1	0	1	1	1	2	1	1	0	0
1	0	?	0	0	0	1	1	0	1	1	1	2	1	1	0	0
0	1	0	0	0	0	1	1	0	1	1	1	1	1	1	0	0
?	?	?	?	?	?	?	?	?	?	?	?	?	?	?	?	?
0	0	1	?	0	?	0	1	0	?	1	0	0	1	1	1	?
?	?	?	?	?	?	?	?	?	?	?	?	?	?	?	?	?
?	?	?	?	?	?	?	?	?	?	?	?	?	?	?	?	?
?	?	?	?	?	?	?	?	?	?	?	?	?	?	?	?	?
?	?	?	?	?	0	0	1	0	0	?	?	?	1	?	0	?
?	?	?	?	?	?	?	?	?	?	?	?	?	?	?	?	?
0	0	0	?	0	?	0	1	0	0	0	0	2	1	1	0	1
0	0	?	?	?	0	1	1	0	1	1	?	2	1	?	0	?
?	?	?	?	?	?	?	?	?	?	?	?	?	?	?	?	?
?	?	0	?	?	1	0	1	0	?	?	?	?	1	0	0	?

43	44	45	46	47	48	49	50	51	52	53	54	55	56	57	58	59
39	40	41	42	43	-	-	44	45	46	47	48	49	-	-	-	-
Br24	Br25	O64	Bd65	Br50	new	new	O29	O30	O31	O32	Bd25	Bd95	86P22	X83	X11	X49
0	2	0	?	1	1	0	0	-	-	-	-	0	0	0	0	0
?	?	?	?	?	0	?	1	0	0	0	?	?	?	?	?	?
0	1	0	0	0	1	0	1	0	1	1	0	0	0	0	0	0
?	?	?	?	?	?	?	?	?	?	?	?	?	?	?	?	?
?	?	0	?	?	?	?	1	1	?	2	0	?	?	0	2	?
?	2	0	?	1	0	1	1	0	1	0	1	?	0	1	1	0
?	?	?	?	?	?	?	?	?	?	?	?	?	?	?	?	?
1	1	0	1	1	1	1	1	0	0	0	1	0	0	1	0	0
?	?	?	?	1	0	0	1	0	?	0	?	0	0	1	0	0
?	?	?	?	?	?	?	?	?	?	?	?	?	?	?	?	?
1	?	0	0	0	1	0	1	0	0	1	0	1	?	1	1	0
0	1	0	0	1	0	1	1	0	0	0	0	0	?	0	0	0
0	1	0	0	1	0	1	1	0	0	0	1	0	?	1	0	0
?	?	?	?	?	?	?	?	?	?	?	?	?	?	?	?	?
0	1	0	?	?	?	?	1	0	1	0	1	?	?	0	2	0
?	?	?	?	?	?	?	?	?	?	?	?	?	?	?	?	?
?	?	?	?	?	?	?	?	?	?	?	?	?	?	?	?	?
1	?	0	1	?	?	?	?	?	?	?	?	?	?	?	?	?
?	?	?	?	?	?	?	?	?	?	?	?	?	?	?	?	?
0	?	?	0	1	1	?	1	0	0	0	1	0	?	1	1	0
2	1	0	-	?	?	?	1	1	-	1	0	?	?	?	?	1
0	?	1	1	?	1	0	1	0	0	1	1	0	0	1	1	0
0	1	0	0	1	0	0	1	0	0	0	1	0	1	1	0	0
?	?	0	0	0	0	1	1	0	0	0	1	0	1	0	1	0
2	?	0	?	?	0	?	1	1	-	1	0	0	?	0	0	1
0	1	1	0	0	0	0	1	0	0	0	1	0	0	1	0	0
1	1	0	1	1	0	1	1	0	0	1	0	0	0	1	1	0
?	?	0	?	?	0	0	1	1	0	1	0	?	0	?	?	?
0	?	1	?	1	0	0	1	0	0	0	1	0	0	1	1	0
?	?	?	?	?	?	?	?	?	?	?	?	?	?	?	?	?
?	?	?	?	?	?	?	?	?	?	?	?	?	?	?	?	?
0	2	0	0	0	1	0	1	0	?	0	1	0	?	0	1	0
0	0	0	0	1	0	0	1	0	0	0	1	0	0	0	0	0
?	?	1	?	?	?	?	?	?	?	?	?	?	?	?	?	?
?	1	0	?	1	0	1	?	?	?	?	?	?	?	1	1	0
?	?	?	?	?	?	?	?	?	?	?	?	?	?	?	?	?
?	?	?	?	?	?	?	?	?	?	?	?	?	?	?	?	?
?	?	?	?	?	?	?	?	?	?	?	?	?	?	?	?	?
?	?	?	?	?	?	?	?	?	?	?	?	?	?	?	?	?
?	?	?	?	?	?	?	?	?	?	?	?	?	1	1	1	?
?	?	?	?	?	?	?	?	?	?	?	?	?	?	?	?	?
1	?	0	1	1	?	?	?	?	?	?	?	?	?	1	?	0
?	?	?	?	?	?	?	?	?	?	?	?	?	?	?	?	?
0	?	1	?	1	1	0	1	0	?	0	1	0	0	?	1	0
2	?	0	-	?	?	?	1	1	-	?	0	0	0	?	-	1
0	1	?	?	1	0	?	1	0	?	0	?	0	?	?	?	0
2	?	0	-	1	0	1	1	1	-	1	0	0	2	1	-	1

0	0	0	1	1	0	1	1	0	1	0	2	0	1	?	0	0
0	0	0	1	1	0	1	1	0	1	0	2	0	?	1	0	0
?	?	?	?	?	?	?	?	?	?	?	?	?	?	?	?	?
?	?	?	?	?	?	?	?	?	?	?	?	?	?	?	?	?
2	?	0	-	?	?	1	1	1	?	2	0	?	0	0	2	0
?	?	1	?	?	?	?	?	?	?	?	?	?	?	?	?	?
2	?	0	-	1	1	1	1	1	-	1	0	0	2	1	-	1
2	2	0	?	?	0	0	1	1	?	2	0	0	0	0	2	0
?	?	?	?	?	?	?	?	?	?	?	?	?	?	?	?	?
?	?	?	?	?	?	?	?	?	?	?	?	?	?	?	?	?
0	1	0	1	1	1	0	1	0	0	0	1	1	1	1	1	0
0	1	0	1	1	1	0	1	0	1	0	1	1	1	1	1	0
1	1	0	1	1	0	0	1	0	1	1	0	0	1	1	1	0
1	?	?	1	?	?	?	1	0	1	?	?	?	?	?	?	0
?	?	?	?	1	0	0	?	?	?	?	?	0	?	?	?	?
?	?	?	?	?	?	?	?	?	?	?	?	?	?	?	?	?
?	?	?	?	?	1	?	?	?	?	?	?	?	?	?	?	?
?	?	?	?	?	?	?	1	1	?	?	0	?	?	0	0	1
0	1	?	?	?	?	?	?	?	?	?	?	?	?	?	?	?
?	?	?	?	?	?	?	?	?	?	?	?	?	?	?	?	?
0	0	0	0	1	0	0	1	0	0	0	2	0	0	1	0	1
1	?	0	1	?	1	0	?	?	?	?	?	?	1	?	1	0
?	?	0	1	1	?	?	?	?	?	?	?	?	1	1	1	0
0	?	1	1	?	?	?	1	0	1	0	1	0	?	?	1	?

60	61	62	63	64	65	66	67	68	69	70	71	72	73	74	75	76
-	51	-	-	-	-	-	52	53	-	-	-	54	55	56		57
X12	O51	X25	X102	X71	X60	X61	O52	)66X5{	X84	X100	new	{45O6{	O72	O73	new	MD65
0	1	0	1	0	0	0	0	0	0	0	0	0	0	-	0	0
?	?	?	?	?	?	?	?	?	?	?	?	?	?	?	?	?
0	1	1	0	0	0	0	?	0	0	0	1	0	0	-	0	?
?	?	?	?	?	?	?	?	?	?	?	?	?	?	?	?	?
0	1	1	1	0	0	0	?	?	?	?	?	0	0	-	0	?
0	?	?	?	?	?	1	?	1	1	1	0	2	1	0	0	1
?	?	?	?	?	?	?	?	?	?	?	?	?	?	?	?	?
0	1	1	0	0	0	0	1	0	0	0	0	0	0	-	0	0
0	?	?	?	?	?	?	1	?	?	0	0	?	0	-	0	0
?	?	?	?	?	?	?	?	?	?	?	?	?	?	?	?	?
0	1	?	0	?	?	0	1	0	?	0	0	0	0	0	0	?
0	1	0	1	0	0	0	1	0	0	0	0	0	0	-	0	0
0	1	0	1	0	0	0	1	0	0	0	0	0	0	-	0	0
?	?	?	?	?	?	?	?	?	?	?	?	?	?	?	?	?
0	0	1	?	0	0	0	?	0	?	0	0	0	0	-	0	?
?	?	0	1	0	0	?	?	?	?	?	?	?	?	?	?	?
?	?	?	?	?	?	?	?	?	?	?	?	?	?	?	?	?
?	?	1	0	0	0	0	?	?	?	?	?	?	?	?	?	?
?	?	?	?	?	?	?	?	?	?	?	?	?	?	?	?	?
0	?	?	0	0	0	0	0	0	0	0	0	?	0	-	0	0
0	1	1	1	0	0	?	?	0	1	?	?	1	1	1	?	0
0	1	?	0	0	0	0	1	0	0	0	0	0	0	-	0	?
0	?	0	0	0	0	0	0	0	1	1	0	1	0	-	0	0
0	1	1	0	0	0	1	?	0	0	0	0	0	0	-	0	0
0	2	1	1	0	0	1	1	0	1	1	0	1	1	1	0	0
0	1	1	0	0	0	0	1	0	0	0	0	0	0	-	0	0
0	1	1	0	0	0	0	1	0	0	0	0	0	0	-	0	0
?	0	?	?	?	?	?	1	0	?	?	?	?	0	-	0	?
0	1	1	0	0	0	0	1	0	0	0	0	0	0	-	0	0
?	?	?	?	?	?	?	?	?	?	?	?	?	?	?	?	?
?	?	?	?	?	?	?	?	?	?	?	?	?	?	?	?	?
0	0	?	1	0	0	?	1	0	?	0	0	0	0	-	0	?
0	1	1	1	0	0	0	0	0	0	0	0	0	0	-	0	0
0	?	?	?	?	?	?	?	?	?	?	?	0	?	?	1	?
1	0	1	0	1	1	1	1	1	1	1	?	2	1	0	0	1
?	?	?	?	?	?	?	?	?	?	?	?	?	?	?	?	?
?	?	?	?	?	?	?	?	?	?	?	?	?	?	?	?	?
?	?	?	?	?	?	?	?	?	?	?	?	?	?	?	?	?
?	?	?	?	?	?	?	?	?	?	?	?	?	?	?	?	?
?	?	?	?	?	?	?	?	?	?	?	?	?	?	?	0	?
?	?	?	?	?	?	?	?	?	?	?	?	?	?	?	?	?
0	?	1	0	0	0	0	?	0	?	?	?	?	?	?	?	?
?	?	?	?	?	?	?	?	?	?	?	?	?	?	?	?	?
0	1	?	0	0	0	0	1	0	0	0	0	0	0	-	0	?
0	2	1	1	0	?	0	1	0	?	1	1	1	1	1	0	0
0	?	?	?	?	?	?	?	0	?	?	?	0	?	?	?	?
0	2	1	1	0	0	0	1	0	1	1	0	1	1	1	0	0

0	1	0	0	0	1	1	1	0	?	0	0	2	0	-	1	?
0	1	0	0	0	1	1	1	1	1	0	0	2	0	-	1	?
?	?	?	?	?	?	?	?	?	?	?	?	?	?	?	?	?
?	?	?	?	?	?	?	?	?	?	?	?	?	?	?	?	?
0	0	1	1	?	0	1	?	0	0	?	?	0	0	-	0	?
?	?	?	?	?	?	?	?	0	?	?	?	?	?	?	?	?
0	2	1	1	0	0	0	1	0	1	1	1	1	1	1	0	0
0	0	1	1	0	0	0	1	0	0	0	?	0	0	-	0	0
?	?	?	?	?	?	?	?	?	?	?	?	?	?	?	?	?
?	?	?	?	?	?	?	?	?	?	?	?	?	?	?	?	?
0	1	0	0	0	0	0	1	0	0	0	0	0	0	-	0	0
0	1	0	0	0	0	0	1	0	0	0	0	0	0	-	0	0
0	1	[0 1]	0	0	0	0	1	0	0	0	0	0	0	-	0	0
0	1	?	?	?	?	?	?	?	?	0	0	0	0	-	?	0
?	?	?	?	?	?	?	?	?	?	?	?	?	?	?	?	?
?	?	?	?	?	?	?	?	?	?	?	?	?	?	?	?	?
?	?	?	?	?	?	?	?	?	?	?	?	?	?	?	?	?
0	?	?	?	?	?	0	?	0	1	1	0	1	1	1	0	0
?	?	?	?	?	?	?	?	?	?	?	?	?	?	?	?	?
?	?	?	?	?	?	?	?	?	?	?	?	?	?	?	?	?
0	0	0	0	0	0	1	?	1	1	1	0	1	1	0	0	?
0	0	?	0	0	0	0	1	0	0	1	0	2	0	-	0	1
0	?	?	0	0	0	0	1	0	0	1	0	2	0	-	0	1
?	?	?	?	?	?	?	?	0	?	?	?	?	0	-	?	?

77	78	79	80	81	82	83	84	85	86	87	88	89	90	91	92	93
-	-	-	58	59	60	61	62	63	64	65	66	67	68	69	71	72
X69	X55	new	Br1	3r9O5	Br14	Bd39	Br47	Bd32	MD54	Bd38	)41X8	O42	O43	O44	'46O4	O47
0	1	?	1	0	0	?	?	0	0	0	0	0	0	0	1	0
?	?	?	0	2	?	?	?	0	?	?	?	?	?	?	?	?
0	0	?	0	?	0	?	?	?	0	0	0	0	0	0	0	0
?	?	?	?	?	?	?	?	?	?	?	?	?	?	?	?	?
?	?	?	?	?	?	?	?	?	?	?	?	1	1	0	0	0
0	0	0	0	1	0	?	?	0	0	?	1	2	0	1	0	0
?	?	?	?	?	?	?	?	?	?	?	?	?	?	?	?	?
1	0	0	1	2	0	0	1	?	0	0	0	0	0	0	0	1
0	0	0	0	1	0	?	?	0	0	1	1	0	?	?	1	0
0	1	?	0	1	0	1	?	?	0	1	1	?	?	?	1	0
0	0	0	?	1	?	?	?	0	0	0	0	?	0	0	0	0
0	0	0	2	1	1	0	0	0	0	0	0	0	0	0	0	1
0	0	1	2	2	1	0	0	0	0	0	0	0	0	0	0	1
?	?	?	?	?	?	?	?	?	?	?	?	?	?	?	?	?
?	0	?	0	0	?	?	?	1	?	0	0	0	0	0	1	0
?	?	?	?	?	?	?	?	?	?	?	?	?	?	?	?	?
?	?	?	?	?	?	?	?	?	?	?	?	?	?	?	?	?
?	?	?	?	?	?	?	?	?	?	?	?	?	?	?	?	?
?	?	?	?	?	?	?	?	?	?	?	?	?	?	?	?	?
0	0	1	1	2	0	?	?	0	0	0	?	0	0	0	0	0
0	0	?	?	?	?	?	?	?	?	0	1	?	1	0	0	0
0	0	?	0	1	0	?	?	0	0	0	0	0	0	0	1	0
1	0	1	0	2	0	0	?	0	0	1	0	0	0	0	1	0
0	0	0	1	0	1	?	?	0	0	0	0	1	0	0	0	1
0	0	0	1	0	0	0	?	0	0	0	1	1	1	0	0	0
0	0	0	1	1	0	0	?	0	0	0	0	0	0	0	0	0
0	0	0	2	2	0	1	1	?	0	0	0	0	0	0	0	1
0	0	1	?	?	0	1	?	1	1	0	0	0	0	0	0	0
0	0	?	0	1	0	?	?	0	0	1	1	0	0	0	1	0
?	?	?	?	?	?	?	?	?	?	?	?	?	?	?	?	?
?	?	?	?	?	?	?	?	?	?	?	?	?	?	?	?	?
0	0	0	?	0	1	?	?	?	?	0	0	0	0	0	0	0
0	0	0	0	0	0	0	?	0	0	0	0	0	0	0	1	0
?	?	?	?	?	?	?	?	?	?	?	?	0	0	?	?	?
1	0	0	0	1	0	1	?	0	0	0	1	2	0	1	0	0
?	?	?	?	?	?	?	?	?	?	?	?	?	?	?	?	?
?	?	?	?	?	?	?	?	?	?	?	?	?	?	?	?	?
?	?	?	?	?	?	?	?	?	?	?	?	?	?	?	?	?
?	?	?	?	?	?	?	?	?	?	?	?	?	?	?	?	?
?	?	?	?	?	?	?	?	?	?	?	?	?	?	?	?	?
?	?	?	?	?	?	?	?	?	?	?	?	?	?	?	?	?
0	0	0	2	2	0	?	?	0	1	0	0	?	0	?	0	1
?	?	?	?	?	?	?	?	?	?	?	?	?	?	?	?	?
?	0	1	1	1	0	0	0	0	1	1	0	0	0	0	0	0
0	0	0	1	0	1	?	?	?	0	0	1	2	1	0	0	0
?	0	1	1	2	0	?	?	0	?	0	?	0	0	0	0	0
0	0	0	1	0	1	0	?	0	0	0	1	2	1	0	0	0

1	1	0	0	1	0	1	?	0	0	1	0	0	0	0	1	0
1	1	0	0	1	0	1	?	0	0	1	0	0	0	0	1	0
?	?	?	?	?	?	?	?	?	?	?	?	?	?	?	?	?
?	?	?	?	?	?	?	?	?	?	?	?	?	?	?	?	?
0	0	0	0	1	?	0	?	1	0	0	0	1	0	0	1	0
0	0	?	?	?	?	?	?	1	1	0	0	0	0	0	1	0
0	0	0	0	0	1	0	?	0	0	0	1	2	1	0	0	0
0	0	0	0	1	?	?	?	?	?	0	0	0	0	0	0	0
?	?	?	?	?	?	?	?	?	?	?	?	?	?	?	?	?
?	?	?	?	?	?	?	?	?	0	?	?	?	?	?	?	?
?	0	0	2	1	0	?	?	0	?	0	?	0	0	0	0	0
0	0	0	2	1	0	0	?	0	0	0	0	0	0	0	0	0
0	0	0	1	1	0	?	0	0	0	0	0	0	0	0	0	0
?	?	?	?	?	?	?	?	?	?	0	0	?	?	?	?	?
0	?	?	?	?	?	?	?	0	?	0	?	?	?	?	?	?
?	?	?	?	?	?	?	?	?	?	?	?	?	?	?	?	?
?	?	?	?	?	?	?	?	?	?	?	?	?	?	?	?	?
0	0	?	?	?	?	?	0	0	1	0	1	?	1	0	?	?
?	?	0	1	?	0	?	?	?	0	0	0	0	0	0	0	0
?	?	?	?	?	?	?	?	?	?	?	?	?	?	?	?	?
0	1	?	0	1	?	1	?	0	0	0	1	0	0	1	1	0
0	0	0	1	?	0	0	?	0	1	0	0	0	?	0	0	1
0	0	?	?	?	?	?	0	0	1	0	0	?	?	?	0	1
0	0	0	1	?	0	0	0	0	1	1	0	0	0	0	?	0

94	95	96	97	98	99	100	101	102	103	104	105	106	107	108	109	110
-	74	75	76	78	-	83	-	79	82	84	85	92	86	87	88	89
X72	O48	O38	O53	MD58	X40	O60	X39	Bd47	O57	O63	Br21	J103P	Br127	Br76	O81	O78
0	0	0	2	1	0	0	0	2	0	1	?	0	?	?	0	0
?	?	?	0	?	?	?	?	?	?	?	?	?	?	?	?	?
0	0	0	1	0	-	-	-	0	1	1	0	?	?	?	0	0
?	?	?	?	?	?	?	?	?	?	?	?	?	?	?	?	?
0	0	0	1	?	0	0	?	?	0	1	?	?	?	?	0	0
0	0	1	1	0	-	0	?	0	?	2	?	?	?	?	?	0
?	?	?	?	?	?	?	?	?	?	?	?	?	?	?	?	?
0	0	0	0	0	1	0	1	?	0	0	0	0	-	0	0	1
0	0	0	1	0	-	-	-	0	0	0	?	?	?	?	?	0
?	0	0	1	0	-	0	?	?	?	2	?	?	?	?	?	?
0	0	0	1	1	?	1	1	0	0	0	?	?	?	?	0	1
0	0	0	1	0	1	0	1	1	?	2	0	0	0	1	0	2
0	0	0	1	?	1	0	1	1	?	2	?	0	0	1	0	1
?	?	?	?	?	?	?	?	?	?	?	?	?	?	?	?	?
0	0	0	1	?	?	0	?	?	?	?	?	?	?	?	?	?
?	?	?	?	?	?	?	?	?	?	?	?	?	?	?	1	?
?	?	?	?	?	?	?	?	?	?	?	?	?	?	?	?	?
?	?	?	?	?	?	?	?	?	1	2	?	?	?	?	?	?
?	?	?	?	?	?	?	?	?	?	?	?	?	?	?	?	?
0	0	0	2	1	0	?	1	0	?	?	?	1	-	?	?	0
?	?	0	?	?	?	?	?	?	?	?	?	?	?	?	?	?
0	0	0	1	1	0	1	1	0	0	?	?	1	-	?	0	0
0	0	0	0	1	0	0	0	0	0	2	0	0	0	0	1	0
0	0	0	1	0	-	-	-	1	?	?	?	?	?	?	?	0
0	0	0	1	?	?	0	?	0	0	0	0	?	?	?	1	0
0	0	0	1	1	1	1	1	0	0	2	0	1	-	0	0	0
0	0	0	1	0	1	0	1	1	0	0	?	0	0	0	0	2
0	0	0	1	?	?	?	?	?	?	?	?	?	?	?	?	?
0	0	0	1	1	1	1	1	0	?	0	0	0	?	?	?	?
?	?	?	?	?	?	?	?	?	?	?	?	?	?	?	?	?
?	?	?	?	?	?	?	?	?	?	?	?	?	?	?	?	?
0	0	0	1	1	0	1	1	0	?	?	?	?	?	?	?	?
0	0	0	1	0	-	-	-	0	0	1	0	1	-	0	0	0
?	?	0	?	?	?	?	?	?	0	1	?	?	?	?	?	?
1	0	1	1	0	-	0	0	0	0	2	?	1	-	?	0	0
?	?	?	?	?	?	?	?	?	?	?	?	?	?	?	?	?
?	?	?	?	?	?	?	?	?	?	?	?	?	?	?	?	?
?	?	?	?	?	?	?	?	?	?	?	?	?	?	?	?	?
?	?	?	?	?	?	?	?	?	?	?	?	?	?	?	?	?
?	?	?	?	?	?	?	?	?	0	2	?	?	?	?	?	?
?	?	?	?	?	?	?	?	?	?	?	?	?	?	?	?	?
0	?	?	1	0	1	0	1	1	?	?	?	?	?	?	?	1
?	?	?	?	?	?	?	?	?	?	?	?	?	?	?	?	?
0	0	0	1	0	-	-	-	0	?	2	1	0	?	0	0	0
0	?	0	1	?	?	?	?	0	0	?	0	?	?	0	?	2
0	?	0	2	?	?	?	?	0	1	?	?	?	?	0	?	?
0	0	0	1	1	?	?	?	0	?	0	0	?	?	0	1	1

0	?	0	1	?	?	?	?	0	?	0	?	?	?	?	?	?
0	1	0	1	0	-	-	-	0	?	0	?	?	?	?	0	0
?	?	?	?	?	?	?	?	?	?	?	?	?	?	?	?	?
?	?	?	?	?	?	?	?	?	?	?	?	?	?	?	?	?
0	0	0	1	?	?	0	?	?	0	1	?	?	?	?	0	0
0	0	0	?	?	?	?	?	?	?	1	?	?	?	?	?	?
0	0	0	1	1	0	0	0	0	?	0	0	?	?	?	1	0
0	0	0	1	?	?	0	?	0	1	1	?	?	?	?	0	0
?	?	?	?	?	?	?	?	?	?	?	?	?	?	?	?	?
?	?	?	?	?	?	?	?	?	?	?	?	?	?	?	?	?
0	1	0	1	1	0	1	1	0	?	0	0	?	0	0	?	2
0	1	0	1	1	0	1	1	0	?	0	0	0	0	0	0	2
0	1	0	1	1	0	1	1	0	1	0	0	0	1	1	0	1
?	?	?	?	?	?	?	?	?	?	?	0	0	1	0	?	1
?	?	?	?	?	?	?	?	?	?	2	?	?	?	?	?	?
?	?	?	?	?	?	?	?	?	?	?	?	?	?	?	?	?
?	?	?	?	?	?	?	?	?	?	?	?	?	?	1	?	?
0	0	0	?	?	?	?	?	?	?	?	?	?	?	?	?	?
?	?	0	?	?	?	?	?	0	1	?	?	?	?	?	?	?
?	?	?	?	?	?	?	?	?	?	?	?	?	?	?	?	?
0	1	1	1	0	0	0	0	1	?	2	0	1	-	?	0	0
0	1	0	1	0	?	?	?	1	0	2	1	2	-	?	?	1
0	1	0	1	?	?	?	?	?	0	2	1	2	-	?	?	?
0	?	0	?	?	?	?	?	0	?	0	0	1	-	1	0	0

	111	112	113	114	115	116	117	118	119	120	121	122	123	124	125	126	127
	-	-	90	91	93	94	95	97	-	99	100	101	102	-	103	-	104
	Br68	new	75MD7	O76	79Br7	MD74	MD75	Md76E	new	Br74	O82	Bd98	14O83	X15	O80	X98	O85
	?	0	0	0	0	0	0	?	0	?	0	?	0	0	?	1	0
	?	?	?	?	?	?	?	?	?	?	?	?	?	?	?	?	?
	?	?	1	0	?	?	?	?	1	?	0	?	?	?	0	?	0
	?	?	?	?	?	0	0	1	1	1	?	?	?	?	?	?	?
	?	?	0	0	?	?	?	?	?	?	0	?	1	?	1	1	1
	?	?	0	1	0	0	?	?	?	?	?	?	?	1	?	?	0
	?	?	?	?	?	?	?	?	?	?	?	?	?	?	?	?	?
	0	0	1	0	0	0	1	1	0	1	0	1	2	0	0	?	0
	?	?	?	?	?	0	0	?	0	?	0	?	0	0	0	1	0
	?	?	?	?	?	?	?	?	?	?	?	?	?	?	?	?	0
	0	1	1	0	0	?	?	?	?	?	1	?	?	?	?	?	0
	0	0	1	0	1	0	0	0	0	0	0	1	1	0	0	0	0
	0	0	1	0	1	0	?	0	1	1	0	1	1	0	0	?	0
	?	?	?	?	?	?	?	?	?	?	?	?	?	?	?	?	?
	?	?	?	?	?	?	?	?	?	?	0	?	1	0	0	?	?
	0	?	?	?	?	?	?	?	?	?	?	?	0	0	?	?	?
	?	?	?	?	?	?	?	?	?	?	?	?	?	?	?	?	?
	0	2	0	?	?	?	?	?	?	?	?	?	?	?	?	?	?
	?	?	?	?	?	?	?	?	?	?	?	?	?	?	?	?	?
	0	0	0	0	?	0	?	?	?	?	?	?	?	?	?	?	?
	?	?	1	0	0	0	0	1	0	1	0	?	?	?	?	?	?
	?	?	0	0	1	0	0	1	?	?	0	?	1	0	0	?	0
	0	0	1	0	?	0	0	?	1	1	0	0	0	0	0	1	0
	0	0	1	?	?	0	?	?	?	?	?	?	?	?	?	?	?
	0	?	1	0	1	0	?	?	?	?	1	?	?	0	?	1	0
	0	0	0	0	1	0	0	1	1	1	0	1	1	0	0	0	0
	0	0	?	0	0	0	1	0	1	0	0	?	2	?	0	0	0
	?	?	?	?	?	?	?	?	?	?	?	?	?	?	?	?	?
	?	?	0	0	?	0	?	1	1	?	?	?	1	0	0	1	?
	?	?	?	?	?	?	?	?	?	?	?	?	?	?	?	?	?
	?	?	?	?	?	?	?	?	?	?	?	?	?	?	?	?	?
	?	?	?	?	?	?	?	?	?	?	?	?	?	?	?	?	?
	0	0	0	0	0	0	?	1	1	?	0	?	1	0	0	1	0
	?	?	0	0	?	?	?	?	?	?	0	?	?	?	?	?	?
	?	?	0	1	0	0	0	1	1	?	?	?	?	1	0	1	0
	?	?	?	?	?	?	?	?	?	?	?	?	?	?	?	?	?
	?	?	?	?	?	?	?	?	?	?	?	?	?	?	?	?	?
	?	?	?	?	?	?	?	?	?	?	?	?	?	?	?	?	?
	?	?	?	?	?	?	?	?	?	?	?	?	?	?	?	?	?
	?	?	?	?	?	?	?	?	?	?	?	?	?	?	?	?	?
	?	2	0	?	0	0	?	?	?	?	?	?	?	?	?	?	?
	?	?	?	?	?	?	?	?	?	?	?	?	?	?	?	?	?
	1	0	0	0	1	?	?	1	1	1	1	?	1	0	0	?	?
	?	?	?	0	?	0	?	1	?	?	?	?	?	?	?	1	0
	?	?	?	?	?	?	?	?	?	?	0	?	?	?	?	?	?
	?	0	1	0	0	0	?	1	0	?	?	?	?	?	?	1	0

0	?	0	1	1	?	?	?	?	?	?	?	?	?	?	?	?
0	?	0	1	1	0	?	?	1	1	0	1	0	?	0	1	0
?	?	?	?	?	?	?	?	?	?	?	?	?	?	?	?	?
?	?	?	?	?	?	?	?	?	?	?	?	?	?	?	?	?
?	?	?	0	?	?	?	?	?	?	0	?	1	?	1	?	1
?	?	?	?	?	?	?	?	?	?	?	?	?	?	?	?	?
0	?	1	0	0	0	?	1	0	1	0	0	1	0	?	1	0
?	0	[0 1]	0	?	?	?	?	1	1	0	0	1	0	1	1	1
?	?	?	?	?	?	?	?	?	?	?	?	?	?	?	?	?
?	?	?	?	?	?	?	?	?	?	?	?	?	?	?	?	?
?	1	1	0	0	0	?	?	?	0	1	1	?	0	?	?	0
0	1	1	0	0	0	0	1	1	0	1	1	1	0	0	0	0
1	1	1	0	0	0	0	1	1	0	0	1	1	0	0	0	?
1	1	?	?	0	?	?	1	1	?	1	?	1	0	?	?	?
?	?	?	?	?	?	?	?	?	?	?	?	?	?	?	?	?
?	?	?	?	?	?	?	?	?	?	?	?	?	?	?	?	?
?	2	?	?	?	?	?	?	?	?	?	?	?	?	?	?	?
?	?	?	?	?	?	?	?	?	?	?	?	?	?	?	?	?
?	?	?	?	?	?	?	?	?	?	?	?	?	?	?	?	?
?	?	?	?	?	?	?	?	?	?	?	?	?	?	?	?	?
0	?	?	1	1	0	0	1	1	1	1	?	2	1	0	1	?
?	2	?	0	0	1	0	0	1	0	1	?	1	1	0	?	?
0	2	?	?	?	1	0	0	1	?	1	?	1	?	0	?	?
0	0	1	0	?	0	0	1	1	1	1	1	1	0	0	?	?

128	129	130	131	132	133	134	135	136	137	138	139	140	141	142	143	144
105	-	106	107	108	109	110	111	112	113	114	-	115	116	117	118	119
O87	new	62Bd8	O90	O91	O92	MD6	O93	33O94	O95	O96	X93	Br63	O97	Br51	MD16	O98
0	0	0	0	-	-	-	-	-	-	-	-	0	-	-	?	0
?	?	?	1	2	?	?	0	0	?	1	0	?	0	?	0	0
0	?	1	1	1	1	0	0	0	?	0	0	?	1	?	1	0
?	?	?	?	?	?	?	?	?	?	?	?	?	?	?	?	0
0	?	?	1	0	0	?	0	0	?	1	?	?	1	?	?	1
?	?	1	1	2	1	?	0	1	1	0	0	1	1	0	2	0
?	?	?	?	?	?	?	?	?	?	?	?	1	1	2	0	1
0	?	1	1	2	0	1	1	0	1	0	1	1	1	2	1	0
0	1	1	1	2	1	1	0	1	1	0	0	1	1	1	1	0
?	?	0	1	2	1	?	0	1	1	0	?	1	1	?	?	0
?	?	?	1	2	0	?	0	0	0	0	0	1	1	1	1	0
0	?	0	1	2	0	?	1	0	?	0	1	1	1	1	0	1
0	?	0	1	2	0	1	1	0	1	0	1	1	1	1	0	1
?	?	?	1	?	?	?	?	?	?	?	?	?	0	0	0	0
?	?	?	?	?	?	?	?	?	?	?	?	?	1	?	?	1
?	?	1	?	?	?	?	?	?	?	?	?	?	1	0	0	0
?	?	?	?	?	?	?	?	?	?	?	?	?	?	?	?	?
?	?	?	?	?	?	?	?	?	?	?	?	?	?	?	?	?
?	?	?	?	?	?	?	?	?	?	?	?	?	0	?	?	0
?	?	1	?	?	?	?	?	?	?	?	?	1	?	2	0	?
0	?	?	?	1	?	?	?	?	?	?	?	1	0	0	0	0
0	?	1	1	2	1	1	0	?	1	0	0	1	1	1	1	0
0	?	1	1	2	1	0	0	0	0	1	0	1	0	0	0	0
?	?	?	?	?	?	?	?	?	?	?	?	?	?	?	?	?
?	1	?	?	?	?	?	?	?	?	?	?	?	?	?	?	?
0	0	1	1	2	1	0	0	0	?	0	1	1	1	1	1	0
0	0	1	1	2	0	1	1	0	1	0	1	1	1	3	1	0
?	?	?	1	1	?	?	?	?	?	0	0	?	?	?	?	?
?	?	1	1	2	1	1	0	0	0	0	0	1	1	1	2	0
?	?	?	?	?	?	?	?	?	?	?	?	?	?	?	?	?
?	?	?	?	?	?	?	?	?	?	?	?	?	?	?	?	?
?	?	?	1	?	?	?	?	?	?	?	?	?	?	?	?	0
0	0	0	1	0	0	0	0	0	0	0	0	0	1	0	0	0
?	?	?	?	?	?	?	?	?	?	?	?	?	?	?	?	?
1	1	1	1	2	0	0	0	1	0	0	0	1	1	0	0	0
?	?	?	?	?	?	?	?	?	?	?	?	?	?	?	?	?
?	?	?	?	?	?	?	?	?	?	?	?	?	?	?	?	?
?	?	?	?	?	?	?	?	?	?	?	?	?	?	?	?	?
?	?	?	1	?	?	?	?	?	?	?	?	1	1	1	2	0
?	?	?	1	?	?	?	?	?	?	?	?	1	1	0	2	0
?	?	?	?	?	?	?	?	?	?	?	?	?	?	?	?	?
?	?	?	?	?	?	?	?	?	?	?	?	?	?	?	?	?
?	?	?	?	?	?	?	?	?	?	?	?	1	?	1	?	0
?	?	1	1	?	?	?	?	0	?	0	?	1	1	1	1	0
0	0	?	?	?	?	?	?	?	?	?	?	?	?	?	?	?
?	?	1	?	?	?	?	?	?	?	?	?	1	?	?	?	0
0	0	?	?	?	?	?	?	?	?	?	?	?	?	?	?	?

?	?	?	1	1	0	0	0	0	1	0	0	1	?	1	2	0
1	?	0	1	1	0	0	0	0	?	0	0	1	?	0	2	0
?	?	?	?	?	?	?	?	?	?	?	?	1	?	1	1	1
?	?	?	?	?	?	?	?	?	?	?	?	1	?	2	1	1
?	?	1	?	?	?	?	?	?	?	?	?	?	1	?	?	?
?	?	?	?	?	?	?	?	?	?	?	?	0	?	0	0	0
0	0	1	?	1	?	?	?	?	?	?	?	1	0	?	0	0
0	?	1	1	1	0	0	0	0	0	0	1	1	1	0	0	1
?	?	?	?	?	?	?	?	?	?	?	?	?	?	?	?	?
?	?	?	1	2	1	?	1	?	1	0	1	1	1	1	?	1
0	?	1	1	2	0	1	1	0	1	0	1	1	1	2	?	?
0	0	1	1	2	0	1	1	0	1	0	1	1	1	2	1	1
?	1	1	1	2	1	?	0	0	1	0	1	1	1	2	0	1
?	?	?	?	?	?	?	?	?	?	?	?	?	?	?	?	?
?	?	1	1	1	?	?	0	0	0	1	0	?	?	?	0	0
?	?	?	?	?	?	?	?	?	?	?	?	?	?	?	?	?
?	?	?	?	?	?	?	?	?	?	?	?	?	?	?	?	?
?	?	1	1	?	1	0	0	0	0	1	?	1	0	0	0	0
?	?	?	?	?	?	?	?	?	?	?	?	?	?	?	?	?
?	?	?	?	?	?	?	?	?	?	?	?	?	?	?	?	?
?	1	0	1	0	1	0	0	0	1	0	0	?	1	0	2	0
?	?	1	1	2	0	0	0	0	1	0	1	1	1	1	2	0
?	?	?	1	2	0	0	0	0	?	?	?	1	1	1	2	0
?	?	?	?	?	?	?	?	?	?	?	?	1	?	?	?	?

	145	146	147	148	149	150	151	152	153	154	155	156	157	158	159	160	161
	120	121	122	123	127	126	-	-	-	128	129	130	-	131	132	-	133
	MD15	O100	O12O1	P101	O230	O228	new	X32	O106	41O10	29O10	88O10	P230	109X3	18O11	X74	66O11
	0	0	?	0	0	2	?	0	0	0	0	0	1	0	0	0	0
	2	0	?	0	0	2	?	?	?	0	0	0	?	?	1	1	0
	1	0	?	1	0	3	0	0	0	0	0	0	1	0	0	0	1
	?	0	1	1	?	?	?	?	?	?	?	?	?	?	?	?	?
	0	0	?	0	?	?	?	?	0	1	0	0	?	0	0	?	1
	1	0	2	1	0	?	0	1	1	0	1	0	2	0	1	1	1
	2	0	0	1	?	2	0	?	?	?	?	?	?	?	?	?	?
	2	0	1	1	0	2	0	0	0	1	0	0	0	1	2	-	-
	1	0	1	1	0	2	0	0	0	1	0	0	1	1	0	?	1
	1	0	0	1	0	?	?	0	0	0	1	0	2	0	1	1	1
	0	0	1	1	0	[0 1]	0	?	2	0	0	0	?	1	0	1	1
	1	0	0	1	0	2	0	0	2	1	0	0	0	1	2	-	-
	1	0	0	1	0	1	0	0	0	1	0	0	0	1	2	-	-
	0	0	0	0	?	1	1	?	?	?	?	?	?	?	1	0	1
	?	0	?	0	?	3	?	0	1	0	0	0	1	0	0	?	1
	1	0	0	0	0	?	0	0	1	0	0	0	1	0	?	?	?
	?	?	?	?	?	?	?	?	?	?	?	?	?	?	?	?	?
	?	?	?	?	?	?	?	?	?	?	?	?	?	?	?	?	?
	0	0	?	?	?	1	?	?	?	?	?	?	?	?	1	0	1
	0	0	?	1	0	1	0	0	0	1	0	0	0	1	?	?	?
	0	0	0	0	0	2	?	0	?	0	?	1	?	0	1	0	1
	1	0	?	1	0	2	?	0	0	1	0	0	1	1	0	0	1
	2	0	0	1	0	1	0	0	0	0	0	0	2	1	1	1	0
	?	?	0	1	0	3	?	?	?	?	?	?	?	?	?	?	?
	?	?	?	?	?	?	?	?	?	?	?	?	?	0	?	?	?
	0	0	0	1	0	2	0	0	0	1	0	0	0	1	0	1	1
	2	0	2	1	0	3	0	0	0	1	0	0	0	1	2	-	-
	?	?	?	?	?	?	?	?	?	?	?	?	?	0	0	0	1
	1	0	?	1	0	?	0	0	0	1	0	0	1	1	0	0	1
	?	?	?	?	?	?	?	?	?	?	?	?	?	?	?	?	?
	?	?	?	?	?	?	?	?	?	?	?	?	?	?	?	?	?
	?	0	?	0	0	3	0	?	?	1	0	0	0	0	?	0	?
	1	0	0	0	0	3	0	0	1	0	0	0	1	0	0	0	1
	?	?	?	?	?	?	?	?	?	?	?	?	?	?	0	?	1
	1	1	2	1	0	0	0	1	0	0	1	1	2	0	1	1	1
	?	?	?	?	?	1	?	?	?	0	?	?	?	?	0	0	0
	?	?	?	?	?	?	?	?	?	?	?	?	?	?	?	?	?
	?	?	?	?	?	?	?	?	?	?	?	?	?	?	?	?	?
	1	0	1	1	1	0	0	?	?	?	?	0	?	?	?	?	?
	1	0	1	1	1	0	0	?	?	1	?	?	?	?	?	?	?
	?	?	?	?	?	?	?	?	?	?	?	?	?	?	?	?	?
	?	?	?	?	?	?	0	0	2	1	0	0	?	1	?	?	?
	?	0	0	?	?	?	?	?	?	?	?	0	?	?	0	?	?
	1	0	?	1	0	?	?	0	0	1	0	0	1	?	0	?	1
	?	?	?	?	?	?	?	?	?	?	?	?	?	1	?	?	?
	0	0	?	1	0	3	0	0	?	?	?	0	?	1	?	?	?
	?	?	?	?	?	?	?	?	?	?	?	?	?	0	1	?	?

1	1	1	1	0	1	0	0	0	0	0	0	1	1	2	-	-
1	1	1	1	0	0	0	0	0	0	0	0	1	1	2	-	-
1	?	1	1	0	0	?	?	?	?	?	0	?	?	?	?	?
1	0	?	?	?	0	?	0	?	?	0	0	?	?	?	?	?
?	0	?	0	0	3	?	?	1	1	0	0	1	0	0	?	?
0	0	?	0	?	3	?	?	1	?	?	0	?	?	0	?	?
0	0	0	1	0	2	1	0	?	1	0	1	2	1	1	0	1
0	0	?	0	0	3	?	0	0	1	0	0	0	0	[0 1]	-	-
?	?	?	?	?	?	?	?	?	?	?	?	?	?	?	?	?
0	0	1	1	?	?	?	?	2	?	?	0	?	1	1	1	1
1	0	?	1	0	1	0	0	2	?	0	0	0	1	1	?	?
1	0	1	1	0	1	0	0	2	1	0	0	0	1	2	-	?
1	0	1	1	0	3	0	0	2	1	0	0	1	1	0	0	1
?	?	?	?	?	?	?	?	?	?	?	?	?	?	?	?	?
0	0	?	1	0	?	?	?	0	0	?	0	2	0	1	?	?
?	?	?	?	?	?	?	?	?	?	?	?	?	?	?	?	?
1	?	0	?	1	?	?	?	?	?	?	?	?	?	1	1	0
0	0	0	0	0	1	1	0	0	1	0	0	?	?	?	?	?
?	?	?	?	?	?	?	?	?	?	?	?	?	?	?	?	?
?	?	?	?	?	?	?	?	?	?	?	?	?	?	?	?	?
1	0	0	1	0	2	0	0	0	0	1	0	2	0	1	1	1
1	0	1	1	0	0	0	0	0	1	0	0	0	1	2	-	?
1	0	1	1	0	0	0	0	0	1	?	0	?	?	?	?	?
?	?	?	?	?	?	?	0	?	?	?	?	?	1	0	0	1

162	163	164	165	166	167	168	169	170	171	172	173	174	175	176	177	178
-	134	-	135	136	137	138	139	140	141	-	143	144	145	146	-	147
X66	73O11	new	O129	.03O13	O222	O130	O116	O117	P118	X76	O123	D88O1	O126	Br37	P228	115Br4
0	0	0	0	0	0	0	0	0	0	0	1	0	1	1	0	-
0	0	?	0	0	1	1	1	?	?	?	0	1	?	?	0	-
1	1	0	0	0	1	1	1	0	0	1	0	1	0	?	0	2
?	?	?	1	?	?	?	1	?	[1 2]	0	1	?	?	1	1	2
?	0	0	1	0	[0 1]	1	1	0	0	0	1	?	0	?	1	?
1	0	1	?	0	1	1	1	?	2	0	0	1	0	?	?	?
?	?	?	1	1	1	?	1	1	?	0	1	?	0	?	0	2
-	?	?	1	1	1	1	1	1	1	0	1	1	0	1	0	2
1	0	?	1	0	1	1	1	0	0	1	1	2	0	?	1	1
1	0	?	0	0	1	1	1	1	0	1	0	1	0	1	?	?
1	0	?	1	0	1	1	1	1	2	0	1	2	0	1	1	1
-	-	?	1	1	1	1	1	1	1	0	1	1	0	1	0	2
-	-	?	1	1	1	1	1	1	1	0	1	1	0	?	0	2
0	1	0	1	0	0	1	1	0	0	1	1	0	0	?	1	1
?	0	0	1	0	0	1	1	0	0	1	?	?	0	?	1	?
?	?	?	1	0	0	1	1	?	0	1	1	?	0	?	1	?
?	?	?	?	?	?	?	?	?	?	?	?	?	?	?	?	?
?	?	?	?	?	?	?	?	?	?	?	?	?	?	?	?	?
0	0	0	1	0	0	1	1	0	0	1	1	0	0	?	1	1
?	?	?	1	0	?	1	1	1	2	?	1	1	?	?	?	2
0	1	0	1	0	1	?	1	?	[0 2]	0	1	?	?	?	1	0
1	0	0	1	0	1	1	1	0	0	?	?	2	0	?	1	1
0	1	1	0	0	1	1	1	1	0	1	0	1	1	?	0	-
?	?	?	1	0	0	1	1	0	1	1	0	0	0	?	0	2
?	?	?	1	0	1	?	1	?	?	?	?	?	?	1	1	?
0	0	1	1	0	1	1	1	1	2	0	1	2	0	1	1	1
-	-	?	1	1	1	1	1	1	1	1	1	1	0	1	0	2
0	0	?	1	?	0	?	1	0	0	0	1	?	?	?	0	0
1	0	1	1	0	?	1	1	?	?	1	1	2	0	?	1	1
?	?	?	?	?	?	?	?	?	2	0	?	?	?	?	1	2
?	?	?	?	?	?	?	?	?	?	?	?	?	?	?	?	?
?	?	?	1	0	?	1	1	1	?	?	1	2	0	?	1	2
1	0	0	1	0	1	1	1	0	0	0	1	0	0	0	1	0
?	?	?	1	?	0	?	1	0	2	0	1	?	0	?	0	0
1	0	1	?	0	1	1	1	1	2	0	0	1	0	?	?	?
?	1	?	1	0	1	1	1	?	0	1	1	?	1	?	0	?
?	?	?	?	?	?	?	?	?	?	?	?	?	?	?	?	?
?	?	?	?	?	?	?	?	?	?	?	?	?	?	?	?	?
?	?	?	1	?	?	?	1	?	2	0	1	?	?	1	1	1
?	?	?	1	0	1	1	1	1	2	0	1	?	0	1	1	1
?	?	?	?	?	?	?	?	?	?	?	?	?	?	?	?	?
?	?	?	?	?	1	?	1	?	2	0	1	2	0	?	1	2
?	?	?	1	0	?	?	1	1	0	1	1	0	?	0	1	0
?	0	?	1	0	1	1	1	0	1	0	1	2	0	?	1	0
?	?	?	1	0	?	?	?	?	2	0	1	1	?	1	1	1
?	?	?	1	0	1	1	1	1	2	?	1	2	0	?	?	?
?	1	0	?	0	1	?	?	0	2	?	?	0	?	1	?	?

-	-	1	0	0	1	1	1	1	0	?	0	?	0	?	?	1
-	-	1	0	0	1	1	1	1	0	0	0	1	0	?	0	1
?	?	?	1	0	1	?	?	?	?	?	?	?	0	1	?	?
?	?	?	1	0	1	?	?	1	2	0	1	?	?	1	1	1
?	0	?	1	0	1	1	1	0	0	1	1	?	0	?	1	0
?	0	?	1	0	0	1	1	0	0	1	1	0	0	0	1	0
0	0	0	1	0	1	?	1	0	[0 1]	0	1	0	?	1	1	0
-	-	?	1	0	0	1	1	0	0	0	1	0	0	0	1	?
?	?	?	?	?	?	?	?	?	?	?	?	?	?	?	?	?
?	?	?	1	1	?	1	1	1	2	0	1	2	?	?	0	2
?	?	?	1	?	1	1	1	1	2	?	1	2	0	?	?	?
?	?	?	1	1	1	1	1	1	2	0	1	2	0	1	0	2
1	0	1	1	0	1	1	1	0	2	0	1	2	0	1	1	0
?	?	?	?	?	?	?	?	?	?	?	?	?	?	?	?	?
?	1	?	1	0	0	2	?	?	0	1	1	0	?	?	1	1
?	?	?	?	?	?	?	?	?	?	?	?	?	?	?	?	?
0	0	?	1	0	1	?	1	1	2	0	1	2	?	1	1	1
?	?	?	1	0	0	1	1	?	?	0	1	?	?	?	1	?
?	?	?	1	0	1	1	1	1	2	1	0	2	?	?	?	?
?	?	?	?	?	?	?	?	?	?	?	?	?	?	?	?	?
1	1	1	0	0	?	1	1	?	0	1	0	?	?	?	0	1
?	?	?	1	0	1	1	1	1	2	0	1	2	0	1	1	1
?	?	?	1	0	1	1	1	1	2	0	1	?	0	?	?	?
?	0	?	1	0	1	1	1	1	2	0	0	2	0	1	1	1

	179	180	181	182	183	184	185	186	187	188	189	190	191	192	193	194	195
	148	-	150	151	152	153	154	156	157	158	159	160	161	162	-	-	-
	Br38	X75	O92O1	33Bd1	O124	O125	MD80	Br52	O229	O121	MD87	Bd124	Br58	Bd135	59H23	H236	X30
	-	?	-	?	0	0	0	-	?	-	?	?	?	?	1	1	0
	?	1	?	?	0	1	?	?	0	?	?	?	?	?	0	?	?
	1	0	0	?	1	0	1	?	0	0	0	?	?	?	?	?	?
	1	0	1	?	?	?	?	0	?	1	2	?	?	?	1	0	?
	-	0	?	?	0	0	?	?	?	?	?	?	?	?	?	?	?
	?	?	?	?	0	0	1	?	?	?	2	?	?	?	?	?	?
	?	?	?	?	0	0	1	0	0	1	2	?	?	1	1	0	0
	1	0	1	1	0	0	1	1	0	1	2	1	2	1	0	0	0
	?	0	0	?	0	0	1	0	0	0	0	?	?	?	0	1	1
	?	0	?	?	0	0	?	?	?	?	?	?	?	?	0	0	0
	1	0	1	?	0	0	?	0	0	1	2	0	?	?	?	1	0
	1	0	1	1	0	0	1	0	0	1	2	1	1	1	1	0	0
	?	0	1	?	0	0	1	0	0	1	2	1	1	1	1	1	0
	0	0	?	?	0	?	?	?	0	0	?	?	?	?	?	?	?
	?	0	?	?	0	0	?	?	0	?	?	?	?	?	?	?	?
	?	0	?	?	0	?	?	?	0	?	?	?	?	0	0	?	?
	?	?	?	?	?	?	?	?	?	?	?	?	?	?	?	?	?
	?	?	?	?	?	?	?	?	?	?	?	?	?	?	?	?	?
	?	0	?	?	1	1	?	?	?	0	?	?	?	?	?	?	?
	1	0	1	?	0	0	?	?	?	?	?	?	?	?	0	0	0
	?	0	1	?	1	0	?	0	0	0	0	?	?	?	?	?	?
	?	0	0	?	0	0	?	?	?	0	0	?	?	?	0	1	0
	0	1	1	?	1	1	1	0	0	2	0	0	1	0	0	1	1
	?	0	2	?	?	0	1	?	0	1	0	0	?	?	0	1	0
	?	?	?	?	?	?	?	?	?	?	?	?	?	?	?	?	?
	1	0	1	0	0	0	1	0	0	1	2	1	0	1	0	1	0
	1	1	1	1	0	0	1	1	0	1	2	1	2	1	0	1	0
	-	0	?	?	?	?	?	?	?	0	?	?	?	?	?	?	?
	?	0	0	?	0	0	1	?	?	0	?	?	?	?	0	1	1
	0	0	1	?	?	?	?	?	?	2	?	?	?	?	?	?	?
	?	?	?	?	?	?	?	?	?	?	?	?	?	?	0	?	?
	?	0	?	?	0	0	1	?	0	0	0	?	?	?	?	?	?
	1	0	0	0	0	0	0	0	0	0	?	0	0	0	0	?	0
	?	0	?	?	?	?	?	?	?	0	?	?	?	?	?	?	0
	?	?	?	?	0	0	1	0	0	1	2	?	?	?	?	?	?
	0	0	?	?	?	?	?	?	0	0	?	?	?	?	?	?	?
	?	?	?	?	?	?	?	?	?	?	?	?	?	?	1	0	?
	?	?	?	?	?	?	?	?	?	?	?	?	?	?	1	0	?
	1	0	2	?	0	0	?	0	1	2	2	0	0	?	?	?	?
	1	0	2	?	0	0	?	0	1	2	1	0	?	?	?	?	?
	?	?	?	?	?	?	?	?	?	?	?	?	?	?	?	?	?
	1	0	?	?	?	?	?	0	?	?	?	?	?	?	0	?	?
	1	0	2	0	?	?	0	0	?	1	0	0	0	0	0	1	?
	0	0	?	0	0	0	1	0	0	0	0	0	0	0	1	0	0
	0	0	?	?	?	?	?	?	?	?	?	?	?	?	0	1	?
	1	0	2	1	0	0	1	0	0	1	1	0	0	1	?	?	?
	?	?	?	?	?	?	?	?	?	?	?	?	?	?	?	?	?

?	?	?	?	0	0	?	0	0	2	0	?	?	?	?	1	1
0	1	0	?	0	?	1	0	0	2	0	?	?	?	?	?	?
?	?	?	?	0	0	1	0	1	2	1	?	?	?	?	?	?
?	0	2	0	0	0	1	0	1	2	1	?	?	?	?	?	?
?	0	?	?	0	0	?	?	0	0	0	?	?	?	?	?	?
0	0	0	?	?	0	0	0	0	0	0	?	0	0	?	?	?
0	0	1	?	1	0	1	0	0	0	0	0	?	?	?	?	?
-	0	?	?	0	0	?	?	?	?	?	?	?	?	1	0	0
?	?	?	?	?	?	?	?	?	?	?	?	?	?	?	?	?
1	0	1	?	0	?	1	?	?	2	1	?	?	?	1	0	0
?	0	?	1	0	0	1	0	0	?	?	1	2	1	0	1	0
1	?	2	1	0	0	1	0	0	2	2	1	2	1	0	1	0
1	0	2	0	0	0	1	0	0	1	?	0	1	0	0	1	?
?	?	?	?	?	?	?	?	?	?	?	?	?	?	?	?	?
0	0	1	?	1	0	?	?	0	?	?	?	?	?	?	1	?
?	?	?	?	?	?	?	?	?	?	?	?	?	?	?	?	?
1	0	2	0	0	0	?	0	0	2	2	1	1	1	?	?	?
?	?	?	?	?	?	0	0	0	?	0	?	0	0	?	?	?
1	0	0	?	?	?	?	?	?	1	?	0	?	?	0	1	?
?	?	?	?	?	?	?	?	?	?	?	?	?	?	0	1	?
-	1	0	?	0	0	1	?	?	0	?	?	?	?	0	1	1
1	0	2	0	0	0	1	0	1	2	1	?	?	1	0	?	0
?	0	?	?	0	0	1	0	1	2	1	0	?	1	?	?	?
1	0	2	0	0	?	?	0	?	1	1	0	0	0	?	?	?

196	197	198	199	200	201	202	203	204	205	206	207	208	209	210	211	212
163	164	165	166	-	167	168	169	170	171	173	174	175	176	177	178	-
l33R2:	O134	143R2	Bd144	new	O135	O137	Br78	04Bd1	Br82	Br84	Bd190	Br88	O142	Br79	Br135	new
0	0	?	1	0	2	1	0	0	0	0	0	0	0	?	?	?
1	?	?	?	?	?	?	?	1	?	?	?	?	?	?	?	?
1	0	?	?	?	1	1	?	1	?	0	1	?	0	?	?	?
0	?	2	1	?	?	?	?	?	?	?	?	2	?	?	?	?
1	0	?	?	?	0	?	?	?	?	?	?	?	0	?	?	?
?	?	?	?	?	?	0	?	2	?	1	?	?	?	?	?	0
1	1	2	1	1	1	2	1	1	0	0	1	1	1	1	1	1
1	1	1	1	1	1	1	1	?	2	0	1	1	1	0	0	?
1	0	1	0	0	1	1	?	?	?	?	?	?	?	?	1	0
1	0	?	0	0	?	?	?	?	?	?	?	?	?	?	?	?
1	1	2	1	0	1	1	?	2	1	1	?	1	1	?	?	0
1	1	1	1	1	1	1	?	2	?	0	1	2	1	1	0	0
1	1	1	?	0	1	1	1	2	?	1	1	2	1	?	?	0
?	?	?	?	?	?	?	?	?	?	?	?	?	?	?	?	?
?	?	?	?	?	?	?	?	?	?	?	?	?	?	?	?	?
?	0	?	?	0	?	?	?	1	?	?	?	?	?	?	?	?
?	?	?	?	?	?	?	?	?	?	?	1	1	1	?	?	?
?	0	?	1	?	?	?	1	?	?	?	?	?	?	?	?	0
?	0	?	1	0	?	?	?	2	?	?	?	0	1	?	?	?
?	0	1	1	?	?	?	?	2	0	1	1	[0 1]	?	?	?	?
?	?	?	?	?	?	?	?	1	?	?	?	?	?	?	?	?
1	0	?	0	0	1	1	0	2	0	2	?	1	0	?	1	0
0	0	1	1	0	1	0	0	1	1	?	?	0	1	0	0	0
1	0	1	1	0	1	1	?	1	?	0	1	?	0	?	?	0
?	?	?	?	?	?	?	0	2	?	0	1	0	1	?	0	0
1	0	?	0	0	1	1	0	2	0	1	1	1	1	0	?	0
1	1	?	1	0	2	2	1	?	2	1	1	1	1	2	0	0
?	?	?	?	?	?	?	?	?	?	?	?	?	?	?	?	?
0	0	1	0	0	1	?	0	2	0	?	1	1	0	?	?	?
?	?	2	?	?	?	?	?	?	?	?	?	?	?	?	?	?
?	0	2	1	?	?	?	0	?	0	?	1	?	?	?	?	?
?	?	?	?	?	?	?	?	?	?	?	?	0	0	?	?	?
0	0	?	1	?	?	1	?	?	?	0	0	0	0	?	?	?
?	?	?	?	?	?	?	?	?	?	?	?	?	?	?	?	?
?	?	?	?	?	?	?	?	?	?	?	?	?	?	?	?	?
?	?	?	?	?	?	?	?	?	?	?	?	?	?	?	?	?
0	0	2	1	1	2	1	0	2	0	0	1	?	?	?	1	1
?	0	2	1	1	?	?	?	?	?	?	?	?	?	1	1	1
?	?	?	?	?	?	?	?	?	?	?	?	?	?	?	?	?
?	?	?	?	?	?	?	?	?	?	?	?	?	?	?	?	?
?	?	?	?	?	?	?	?	?	?	?	?	?	?	?	?	?
0	1	?	?	?	1	?	?	2	?	0	?	?	?	?	?	?
?	0	1	0	0	?	1	0	2	0	0	1	1	1	?	?	1
1	0	2	1	0	1	1	0	3	0	2	1	1	0	0	0	?
?	?	?	?	0	?	?	?	?	?	?	?	?	?	?	?	?
?	?	?	1	?	?	2	0	?	?	0	1	1	?	?	0	0
?	?	?	?	?	?	?	?	?	?	?	1	?	?	?	?	0

1	0	?	?	0	1	0	?	2	?	0	0	1	?	?	?	0
?	?	?	?	?	1	?	?	3	?	?	?	?	?	?	?	?
?	?	?	?	?	?	?	1	?	?	?	?	1	?	?	?	?
?	1	?	?	?	?	?	1	?	?	?	?	1	?	?	1	0
0	0	?	?	?	0	2	?	?	?	0	?	?	0	?	?	0
?	0	1	1	0	1	1	?	1	?	?	?	?	?	?	0	0
?	?	?	?	?	?	?	?	?	?	?	?	0	1	?	0	0
1	0	?	1	0	[0 1 2][0 1 2]		?	?	?	?	?	?	1	?	?	0
?	?	?	?	?	?	?	?	?	?	?	?	?	?	?	?	0
0	0	2	1	1	1	2	0	?	?	?	?	?	?	?	1	1
0	1	?	?	0	2	?	?	2	1	?	?	0	1	?	?	?
0	1	?	1	0	2	2	1	2	1	1	1	0	1	1	0	0
1	0	1	1	0	1	2	1	2	0	1	1	1	1	?	1	1
?	?	?	?	?	?	?	?	?	?	?	1	1	?	?	?	1
?	?	?	?	?	?	?	?	?	?	?	?	?	?	?	?	?
?	1	1	1	?	?	?	0	?	?	?	?	2	1	?	?	?
?	0	?	1	?	?	?	?	?	?	?	?	?	?	?	?	?
?	0	2	0	?	?	?	?	?	?	?	?	?	?	?	?	?
?	0	?	?	?	?	?	0	?	?	?	?	1	?	?	?	0
?	0	2	1	0	?	?	1	?	?	?	?	1	1	?	?	0
1	0	?	0	0	1	0	?	2	?	0	?	1	0	?	?	0
0	1	1	0	1	?	?	1	3	1	0	?	1	1	?	1	0
?	?	?	0	?	?	?	?	3	?	?	1	?	?	?	?	?
?	?	2	1	?	?	?	0	?	?	2	?	1	?	0	0	?

213	214	215	216	217	218	219	220	221	222	223	224	225	226	227	228	229
-	179	180	181	182	183	184	186	187	188	189	190	-	191	-	192	193
new	Bd157	Br85	Br87	O144	6/217!	O218	O147	O149	O152	O150	O151	new	20D19	new	Br90	Br91
0	0	?	0	0	0	?	?	?	1	1	1	?	1	0	?	0
1	?	?	?	?	?	?	?	0	1	?	1	?	?	?	?	?
1	0	1	?	0	0	0	0	1	0	0	1	1	1	1	?	0
?	?	2	?	0	1	0	?	0	0	0	1	0	1	1	1	0
?	?	?	?	0	1	0	0	0	1	0	?	?	?	?	?	?
?	?	?	?	0	?	0	?	?	?	?	?	?	?	?	?	?
1	?	2	?	?	0	-	0	0	0	0	1	0	0	0	1	0
1	0	1	1	[0 1]	0	-	0	0	0	0	1	0	0	1	1	1
1	0	?	?	?	?	0	?	?	0	0	?	?	?	?	0	0
?	?	?	?	?	?	?	?	?	?	?	0	0	1	1	?	?
1	0	1	1	1	1	0	0	0	0	0	0	0	1	1	0	0
1	0	2	0	0	?	0	0	0	0	0	0	0	1	1	1	1
1	0	2	1	0	1	0	0	0	0	0	0	0	1	1	1	1
?	?	?	?	?	?	?	?	?	?	?	?	?	?	?	?	?
?	?	?	?	?	?	?	?	?	?	?	?	?	?	?	?	?
?	?	?	?	?	?	?	?	0	0	0	1	1	0	1	?	?
1	?	2	1	?	1	0	?	?	?	?	?	?	?	?	?	?
?	?	2	?	?	?	?	?	?	?	?	1	0	1	1	?	?
?	?	?	?	?	?	?	?	?	?	?	?	?	?	?	?	?
1	?	1	0	1	1	0	0	?	0	?	0	0	1	0	1	0
?	?	?	?	?	1	1	?	?	?	?	?	?	?	?	?	?
1	0	0	1	0	0	0	0	0	0	0	1	0	0	1	1	1
1	0	0	0	0	0	0	0	0	1	1	1	0	1	0	0	?
1	0	?	?	0	0	0	0	1	0	0	0	0	1	1	?	?
?	?	1	?	0	1	1	?	?	?	?	?	?	?	?	?	?
1	1	1	1	0	1	0	0	0	0	0	1	0	1	1	1	1
1	0	1	1	0	1	2	0	0	0	0	1	1	0	1	0	1
?	?	?	?	?	?	0	?	?	?	?	?	?	?	?	?	?
1	?	?	?	0	0	0	?	1	1	0	1	0	?	0	?	?
?	?	?	?	?	?	?	?	?	?	?	?	?	?	?	?	?
0	0	?	?	?	?	-	?	0	0	0	1	0	1	1	0	0
?	?	?	?	?	0	?	?	1	1	0	1	0	1	0	?	?
1	?	?	?	?	1	0	?	0	0	0	0	1	1	0	0	0
?	?	?	?	0	?	?	?	?	0	0	0	1	?	?	?	?
?	?	?	?	?	?	?	?	?	?	?	?	?	?	?	?	?
?	?	?	?	?	?	?	?	?	?	?	?	?	?	?	?	?
1	1	2	?	1	?	?	?	?	?	?	?	?	?	?	?	?
1	?	?	?	?	?	?	0	0	0	0	1	0	1	0	0	0
?	?	?	?	?	?	?	?	?	?	?	?	?	?	?	?	?
?	?	?	?	?	?	?	?	?	?	?	0	?	1	0	0	0
?	?	?	?	?	?	?	?	?	?	?	?	?	?	?	?	?
?	?	?	?	?	?	?	?	?	0	?	1	?	1	0	1	1
1	1	1	?	0	?	0	0	0	0	0	1	0	0	?	0	0
1	?	1	0	0	0	0	0	0	0	0	1	0	1	1	0	0
?	?	?	?	?	?	?	?	?	?	?	?	?	?	?	?	?
1	1	1	0	1	1	0	?	0	0	0	0	0	1	0	0	0
?	?	?	?	?	1	1	?	?	?	?	?	?	?	?	?	?

1	0	?	?	0	1	0	1	0	1	0	0	1	1	1	0	?
?	?	?	?	?	?	?	?	?	?	?	?	?	?	?	?	?
?	?	0	?	?	?	?	?	?	?	?	?	?	?	?	?	?
?	?	0	?	?	?	?	?	?	0	0	1	0	1	0	0	0
?	0	?	?	0	?	0	0	0	0	0	?	?	?	?	?	?
?	?	?	?	?	?	?	?	?	?	?	0	0	1	0	0	0
?	?	?	?	0	1	1	?	0	1	1	1	0	0	1	1	0
?	?	?	?	0	[0 1]	0	0	0	1	0	0	0	1	0	0	?
?	?	?	?	0	0	0	?	?	1	?	?	?	?	?	?	?
1	?	?	?	?	?	0	0	1	0	0	1	0	0	1	1	0
1	0	1	?	0	1	0	0	0	0	0	0	0	0	1	0	0
1	0	1	?	0	1	0	0	0	0	0	0	0	0	1	0	0
?	1	?	1	0	1	0	0	0	0	0	1	0	0	1	1	0
?	?	?	?	?	?	?	?	?	?	?	?	?	?	?	?	?
?	?	?	?	?	1	0	?	?	1	?	1	0	?	?	0	0
1	?	2	?	1	1	?	?	?	?	?	?	?	?	?	?	?
?	?	2	?	?	?	?	?	?	?	?	?	?	1	0	?	0
?	?	?	?	?	?	?	?	?	?	?	?	?	?	?	?	?
?	?	1	?	?	?	?	?	0	0	0	0	?	?	?	1	0
0	?	1	?	0	0	-	?	0	0	0	?	0	1	1	?	?
1	?	1	?	0	0	?	?	0	[0 1]	1	[0 1]	1	1	1	?	?
?	?	1	?	0	?	?	?	?	0	0	0	0	1	0	1	0
?	?	1	?	?	1	?	?	?	1	1	0	0	1	1	1	0
?	?	1	?	?	?	?	?	?	?	?	?	?	?	?	?	0

230	231	232	233	234	235	236	237	238	239	240	241	242	243	244	245	246
194	195	196	197	198	199	200	201	202	-	-	-	203	204	-	205	-
O231	O148	O153	D197	O232	O223	42O15	MD103	O155	new	new	new	Br93	O233	new	Br97	new
?	?	0	0	?	0	0	?	?	?	?	?	2	0	0	0	0
?	?	0	?	?	?	0	?	0	?	?	?	?	?	?	?	0
0	?	1	0	0	0	0	?	1	?	?	?	0	0	2	?	?
0	?	0	0	0	0	2	0	1	0	1	0	2	0	1	0	?
?	1	0	?	?	0	0	?	0	0	0	0	?	?	?	?	?
?	?	?	?	?	?	?	?	?	?	?	?	?	?	?	?	?
0	?	0	0	0	0	1	0	0	1	0	0	2	0	0	0	1
0	1	0	0	0	0	0	1	[0 1]	1	0	0	1	0	0	1	1
0	1	?	0	0	0	0	1	?	1	?	?	?	?	?	?	?
?	?	?	?	?	?	?	?	?	?	?	?	?	?	?	?	?
0	?	0	?	1	0	0	1	1	0	0	0	2	0	0	0	0
0	1	0	0	0	0	1	0	0	1	0	0	0	0	0	1	0
0	1	0	0	0	0	1	0	0	1	0	0	1	0	0	?	?
?	?	?	?	?	?	?	?	?	?	?	?	?	?	?	?	?
?	?	?	?	?	?	?	?	?	?	?	?	?	?	?	?	?
?	?	0	?	0	0	0	?	1	?	0	0	?	?	?	?	?
?	?	?	?	?	?	?	?	?	?	?	?	?	?	?	?	?
?	?	?	?	?	?	1	0	1	?	?	?	?	?	1	?	?
?	?	0	?	0	1	0	?	0	1	0	1	?	?	?	?	?
0	?	?	0	0	0	0	1	0	0	1	0	0	?	?	?	?
?	2	1	?	0	0	1	0	1	1	?	1	0	?	?	?	?
0	1	0	?	0	0	0	1	?	1	?	?	1	?	?	?	?
0	?	0	?	0	1	0	1	0	1	0	1	2	0	2	0	0
0	?	0	?	0	0	0	1	1	0	0	0	?	0	0	?	?
?	2	?	?	?	?	?	?	?	?	?	?	?	?	?	?	?
0	1	0	0	0	0	0	1	0	1	0	0	1	0	0	0	0
0	2	0	0	0	0	0	0	1	?	0	0	2	0	?	1	1
?	?	?	?	?	?	?	?	?	?	?	?	?	?	?	?	?
?	?	0	0	?	?	0	1	1	?	0	0	?	?	?	?	?
?	?	?	?	?	?	?	?	?	?	?	?	?	?	?	?	?
1	1	?	0	0	0	0	0	1	?	0	0	2	?	?	?	?
?	?	?	?	0	0	0	1	1	?	?	0	0	0	?	?	?
0	?	0	0	0	0	0	0	0	1	0	0	0	0	0	0	?
?	?	?	?	?	?	?	?	?	?	?	?	?	?	?	?	?
?	?	?	?	?	?	?	?	?	?	?	?	?	?	?	?	?
?	?	?	?	?	?	?	?	?	?	?	?	?	?	?	?	?
?	3	?	?	?	?	?	?	?	?	?	?	?	?	?	?	?
0	3	?	0	0	0	2	0	1	0	1	0	0	1	1	0	0
?	?	?	?	?	?	?	?	?	?	?	?	?	?	1	?	?
1	?	?	1	1	0	0	1	?	0	?	?	2	1	?	?	?
?	?	?	?	?	?	?	?	?	?	?	?	?	?	?	?	?
?	?	?	0	0	0	1	0	1	1	?	0	0	?	1	0	1
0	1	0	?	0	0	0	0	?	1	0	0	0	?	?	0	?
0	1	?	0	0	0	0	1	0	1	0	0	2	0	0	0	0
?	?	?	?	?	?	?	?	?	?	?	?	?	?	?	?	?
0	1	0	?	?	?	0	0	?	?	?	?	2	?	0	?	?
?	?	?	?	?	?	?	?	?	?	?	?	?	?	?	?	?

1																	
2	0	?	0	?	0	0	0	1	1	1	?	0	0	0	?	0	0
3	?	?	?	?	?	?	?	?	?	?	?	?	?	?	?	?	?
4	?	?	?	?	?	?	?	?	?	?	?	?	?	?	1	?	?
5	0	?	?	?	?	?	?	?	?	?	?	?	?	?	1	?	?
6	0	?	0	?	0	0	0	?	?	?	?	0	2	0	?	?	?
7	0	?	0	?	0	0	0	0	1	?	?	0	0	?	?	0	?
8	0	?	1	?	0	0	2	0	0	1	?	1	2	0	2	?	?
9	?	?	0	?	?	0	0	1	0	0	0	0	?	?	2	?	?
10	?	?	?	?	?	?	?	?	?	?	?	?	?	?	?	?	?
11	0	?	0	0	0	?	2	0	1	1	0	0	?	?	1	?	?
12	0	1	0	?	0	0	0	1	1	?	0	0	1	0	1	0	?
13	0	1	0	0	0	0	0	1	1	1	0	0	1	0	1	0	0
14	0	0	0	0	0	0	1	0	?	1	0	0	0	0	0	0	0
15	?	?	?	?	?	?	?	?	?	?	?	?	?	?	?	?	?
16	0	?	0	?	?	?	0	?	?	1	?	?	2	?	2	?	?
17	?	?	?	?	?	?	?	?	?	?	?	?	?	?	?	?	?
18	?	?	?	1	1	0	?	?	?	?	1	0	2	?	?	?	?
19	?	?	1	?	0	0	1	0	1	1	?	1	?	?	?	?	?
20	0	?	?	?	0	0	0	?	1	?	0	0	0	?	?	0	?
21	?	?	?	?	?	?	0	?	?	?	0	0	?	?	?	?	?
22	?	?	0	?	?	?	0	1	1	1	0	0	2	?	0	?	0
23	?	?	?	1	1	0	0	1	1	?	0	2	1	1	?	?	
24	1	?	?	1	1	0	0	1	1	?	?	?	2	?	?	?	?
25	?	?	?	?	?	?	?	?	?	?	?	?	0	?	?	?	?
26																	
27																	
28																	
29																	
30																	
31																	
32																	
33																	
34																	
35																	
36																	
37																	
38																	
39																	
40																	
41																	
42																	
43																	
44																	
45																	
46																	
47																	
48																	
49																	
50																	
51																	
52																	
53																	
54																	
55																	
56																	
57																	
58																	
59																	
60																	

247	248	249	250	251	252	253	254	255	256	257	258	259	260	261	262	263
-	206	207	208	209	-	-	211	213	214	-	-	215	216	-	217	219
new	O157	O158	Bd174	O162	new	new	O159	O160	O163	X90	X91	O165	O166	new	50O16	O169
0	1	0	0	1	0	1	0	0	1	?	0	0	0	0	?	0
0	1	0	?	1	0	?	?	?	?	1	1	1	0	0	?	0
?	?	?	0	?	?	?	?	?	?	0	0	1	0	0	?	0
?	0	0	?	0	?	0	0	?	0	1	1	1	1	2	1	0
?	0	1	?	0	?	?	0	1	0	1	1	1	1	1	?	0
?	?	?	?	?	?	?	?	?	?	?	0	1	0	0	1	0
0	0	0	1	0	1	1	0	1	0	?	0	1	0	1	1	0
1	0	0	1	0	1	1	0	1	0	1	0	1	0	[0 1]	?	0
?	?	?	?	?	?	?	?	?	?	?	?	?	?	?	?	?
?	?	?	?	?	?	?	?	?	?	?	?	?	?	?	?	?
0	0	0	0	0	1	0	0	0	0	?	?	1	0	0	?	0
1	?	?	0	?	1	1	?	?	?	?	1	1	0	2	1	0
?	?	?	?	?	?	?	?	?	?	0	1	1	0	2	1	0
?	?	?	?	?	?	?	?	?	?	?	?	?	?	?	?	?
?	0	1	?	?	?	?	?	?	?	?	?	?	?	?	?	?
?	?	0	?	1	?	?	?	?	?	?	0	1	?	0	?	0
?	?	?	?	?	?	?	?	?	?	0	1	1	0	0	1	0
?	?	?	?	?	?	?	?	?	?	?	?	?	?	?	?	?
?	?	?	?	?	?	?	?	?	?	?	?	?	?	?	?	?
?	?	?	?	?	?	1	?	1	?	0	0	1	0	0	1	0
?	?	?	?	?	?	?	?	?	?	?	?	1	0	?	0	1
?	0	0	0	0	?	?	?	?	?	1	0	1	0	0	?	0
0	1	0	0	1	0	0	1	0	1	1	1	1	0	0	0	1
?	0	0	0	0	1	0	0	0	0	0	0	1	0	1	3	0
?	?	?	?	?	?	?	?	?	?	1	1	1	0	0	2	1
?	0	0	0	0	1	?	0	0	0	?	0	1	0	0	0	0
1	0	0	1	0	0	1	0	1	0	1	0	1	0	1	?	0
?	?	?	?	?	?	?	?	?	?	?	?	1	0	?	?	0
?	?	?	?	?	?	?	?	?	?	1	0	1	0	0	1	0
?	?	?	?	?	?	?	?	?	?	?	?	?	?	?	?	?
?	?	?	?	?	?	?	?	?	?	?	?	?	?	?	?	?
?	?	?	?	?	?	?	?	?	?	0	1	1	0	1	?	?
?	0	0	0	0	?	1	0	?	0	0	0	1	0	0	0	0
?	?	?	?	?	?	?	?	?	?	?	?	1	?	?	?	0
?	?	?	?	?	?	?	?	?	?	?	?	?	?	?	?	?
?	?	?	?	?	?	?	?	?	?	?	?	?	?	?	?	?
?	?	?	?	?	?	?	?	?	?	?	?	1	?	2	1	?
?	0	0	0	0	?	?	?	?	?	?	?	?	?	?	?	?
?	?	?	?	?	?	?	?	?	?	?	?	?	?	?	?	?
?	?	?	?	?	?	?	?	?	?	?	?	?	?	?	?	?
?	?	?	?	?	?	?	?	?	?	?	?	?	?	?	?	?
?	0	?	?	0	?	?	?	?	?	?	1	1	0	1	2	?
?	?	?	0	?	?	?	?	?	?	1	0	1	0	0	?	0
1	0	0	?	0	?	1	0	0	0	0	1	1	0	1	1	0
?	?	?	?	?	?	?	?	?	?	?	?	?	?	?	?	?
?	?	?	?	?	?	?	?	?	?	1	0	1	0	0	?	0
?	?	?	?	?	?	?	?	?	?	1	?	?	?	?	?	1

0	0	0	0	0	1	1	0	0	0	1	1	1	0	0	?	0
?	?	?	?	?	?	?	?	?	?	?	?	?	?	?	3	0
?	?	?	?	?	?	?	?	?	?	?	?	?	?	?	?	?
?	?	?	?	?	?	?	?	?	?	?	?	?	?	?	?	?
?	?	?	?	?	?	?	?	?	?	1	0	1	1	1	?	0
?	0	0	?	0	?	?	?	?	0	?	?	1	?	?	?	0
?	?	?	?	?	?	?	?	?	?	?	1	1	0	0	2	1
?	0	1	?	0	?	?	0	1	0	1	1	1	1	0	?	0
?	?	?	?	?	?	?	?	?	?	1	1	1	0	0	0	0
?	?	?	?	?	?	?	?	?	?	0	0	1	0	2	?	0
?	0	0	?	0	?	?	?	?	0	0	0	1	0	2	1	0
1	0	0	0	0	1	1	0	1	0	0	0	1	0	1	3	0
1	0	0	0	0	0	0	0	0	0	0	0	1	0	1	1	0
?	?	?	?	?	?	?	?	?	?	0	0	?	?	1	1	0
?	1	?	?	1	0	0	1	0	1	?	?	?	?	?	?	?
?	?	?	?	?	?	?	?	?	?	1	1	1	1	2	?	0
?	?	?	?	?	?	?	?	?	?	?	?	?	?	?	?	?
?	?	?	?	?	?	?	?	?	?	?	?	1	?	?	?	?
?	?	?	?	?	?	?	?	?	?	?	?	?	?	?	?	?
?	?	?	?	?	?	?	?	?	?	?	?	?	?	?	?	?
?	0	?	0	?	1	0	?	?	0	1	1	1	0	0	3	0
?	?	?	?	?	?	?	?	?	?	?	0	1	0	0	2	1
?	?	?	?	?	?	?	?	?	?	?	0	1	0	1	2	1
?	?	?	?	?	?	?	?	?	?	?	?	?	?	?	?	?

264	265	266	267	268	269	270	271	272	273	274	275	276	277	278	279	280
226	220	221	222	-	223	224	-	225	227	228	-	229	230	231	232	233
O175	O176	MD114	2O168	MD112	MD113	O173	Md132	O174	O178	O177	new	Bd182	O191	O186	O192	O193
0	0	0	1	0	0	0	0	1	0	0	0	0	0	0	0	-
?	?	0	?	0	0	1	?	1	1	0	0	?	?	?	?	?
0	0	0	0	0	0	0	0	1	2	0	0	0	0	1	1	0
1	1	0	0	?	0	1	1	1	2	1	1	0	0	1	1	0
0	0	0	?	?	?	0	?	0	0	0	?	1	1	1	1	0
1	1	0	0	0	0	1	0	2	2	1	0	0	0	1	1	2
1	1	1	0	0	1	1	1	1	1	1	0	1	0	1	1	0
1	1	0	?	0	0	1	?	1	2	1	1	1	0	1	1	0
1	?	?	?	?	?	1	0	?	?	1	?	?	?	?	?	?
?	?	?	?	?	?	?	?	?	?	?	?	?	?	?	?	?
1	1	1	0	0	?	0	0	1	2	1	0	0	0	1	1	0
1	1	1	0	0	1	0	1	1	2	1	0	0	0	1	1	0
1	1	1	0	0	1	0	1	1	2	1	0	0	0	1	1	?
?	?	?	?	?	?	?	?	?	?	?	?	?	?	?	?	?
?	?	?	?	?	?	?	?	?	?	?	?	?	?	?	?	?
0	0	0	?	?	0	1	0	1	0	0	0	0	0	1	1	0
1	1	1	0	0	1	0	1	1	2	1	0	0	?	?	?	?
?	?	?	?	?	?	?	?	?	?	?	?	?	?	?	?	?
?	?	?	?	?	?	?	0	?	?	?	?	?	?	?	?	?
1	1	1	0	0	1	1	0	1	2	1	0	0	0	1	1	1
1	1	?	2	0	?	1	0	2	?	?	?	?	?	?	?	?
1	1	0	0	0	?	0	0	2	2	0	0	0	0	1	1	1
1	1	0	0	0	0	1	0	1	1	0	0	0	0	1	1	0
0	1	0	0	0	0	1	0	1	2	0	0	0	0	1	1	1
1	1	0	2	0	0	1	0	2	2	1	0	0	0	1	1	0
1	1	0	0	0	0	0	0	2	2	1	0	0	0	1	1	1
1	1	0	2	1	0	1	?	1	2	1	1	1	0	1	1	0
?	?	?	?	?	?	?	?	?	?	?	?	?	?	?	?	?
1	1	0	0	0	0	1	0	1	2	1	0	0	0	1	1	?
?	?	?	?	?	?	?	?	?	?	?	?	?	?	?	?	?
1	1	?	0	?	?	?	0	?	?	?	0	0	?	?	?	?
1	1	0	0	?	0	1	0	2	2	0	0	0	0	1	1	1
0	0	0	0	0	0	0	0	1	0	0	0	0	0	1	1	0
0	0	0	?	0	?	0	0	?	0	0	0	?	0	1	1	?
?	?	?	?	?	?	?	?	?	?	?	?	?	?	?	?	?
?	?	?	?	?	?	?	?	?	?	?	?	?	?	?	?	?
1	1	1	0	0	?	1	0	?	2	1	0	0	0	1	1	0
?	?	?	?	?	?	?	?	?	?	?	?	?	?	?	?	?
?	?	?	?	?	?	?	?	?	?	?	?	?	?	?	?	?
?	?	?	?	?	?	?	?	?	?	?	?	?	?	?	?	?
?	?	?	?	?	?	?	?	?	?	?	?	?	?	?	?	?
0	1	?	1	?	?	2	0	0	2	1	1	1	0	1	1	1
?	1	0	0	0	0	0	1	1	1	1	0	0	0	1	1	1
1	1	0	0	0	0	1	0	2	2	1	0	0	0	1	1	1
?	?	?	?	?	?	?	?	?	?	?	?	?	?	?	?	?
?	1	0	0	?	0	?	?	?	?	?	?	?	0	1	1	1
?	?	?	2	0	?	?	?	?	?	?	?	?	?	?	?	?

1	1	0	0	0	0	?	0	2	2	1	0	0	0	1	1	2
?	?	?	?	0	?	?	0	?	?	1	?	?	?	1	?	?
?	?	?	?	?	?	?	?	?	?	?	?	?	?	?	?	?
?	?	?	?	?	?	?	?	?	?	1	?	?	0	1	1	0
0	0	0	?	?	0	0	?	0	0	0	?	1	1	1	1	0
?	0	0	?	?	0	?	?	1	?	?	?	0	0	1	1	0
1	1	0	2	0	0	?	0	2	2	0	0	0	?	?	?	?
0	0	0	?	?	0	0	0	0	0	0	0	1	[0 1]	1	1	0
1	1	0	0	0	0	1	0	1	1	0	0	0	0	1	1	2
1	1	1	?	?	1	1	?	1	2	1	0	0	0	?	1	0
1	1	1	?	?	1	1	0	1	2	1	0	0	0	1	1	0
1	1	1	0	0	1	0	0	1	2	1	0	0	0	1	1	0
1	1	1	?	0	1	0	0	1	2	1	0	0	0	1	1	1
?	1	?	?	0	1	0	?	?	?	1	0	0	?	?	1	1
?	?	?	?	?	?	?	?	?	?	?	?	?	?	1	?	?
?	1	1	?	0	1	?	1	1	2	1	0	0	0	1	1	0
?	?	0	?	?	2	?	?	?	?	?	?	?	?	?	?	?
?	1	?	?	?	?	?	?	?	?	?	?	?	?	?	?	?
?	?	?	?	?	?	?	?	?	?	?	?	?	?	?	?	?
?	?	?	?	?	?	?	?	?	?	?	?	?	?	1	?	?
1	1	0	0	0	0	1	0	1	?	0	0	0	0	1	1	2
1	1	0	1	1	2	2	0	1	2	1	1	1	?	?	?	?
1	1	0	1	1	2	2	0	1	2	1	1	1	?	1	1	1
?	?	?	?	?	?	?	?	?	?	?	?	?	?	?	?	?

281	282	283	284	285	286	287	288	289	290	291	292	293	294	295	296	297
34/23	236	237	238	239	240	241	-	-	-	243	245	247	248	-	249	-
O6O19	Bd196	47O19	O187	O188	O179	3Bd20	G1	G4	G5	O184B	O181	O185	O197	new	O198	R231
-	-	0	0	0	0	0	0	0	0	0	1	0	0	0	0	0
?	?	?	?	?	?	?	?	?	?	?	?	?	0	?	?	0
1	?	?	1	0	0	0	0	0	0	2	0	0	0	?	0	?
2	1	1	1	0	0	0	1	0	0	2	0	1	0	0	1	2
0	?	?	1	1	1	-	0	-	0	0	0	1	1	1	0	?
1	2	1	1	2	?	?	?	?	?	0	0	1	?	0	1	?
2	0	1	1	0	0	0	0	0	0	2	1	1	0	0	0	1
2	0	1	1	0	0	0	0	0	0	2	1	1	0	0	?	?
?	?	?	?	?	?	?	?	?	?	?	?	?	?	0	1	2
?	?	?	?	?	?	?	?	?	?	?	?	?	?	?	?	?
2	1	1	1	0	0	0	0	0	0	1	0	1	0	0	1	?
2	0	1	1	0	0	0	0	0	0	2	1	1	0	0	1	1
2	0	1	1	0	0	0	0	1	0	2	1	1	0	0	1	1
?	?	?	?	?	?	?	?	?	?	?	?	?	?	?	?	?
?	?	?	?	?	?	?	?	?	?	?	?	?	?	?	?	?
0	0	?	1	0	0	0	0	0	0	0	0	0	0	0	0	?
?	?	?	?	?	?	?	?	?	?	?	?	?	0	0	1	2
?	?	?	?	?	0	?	?	?	0	2	0	1	1	0	?	?
?	?	?	?	?	?	?	?	?	?	?	?	?	0	0	0	1
2	1	1	1	0	0	0	0	0	0	2	0	1	0	0	1	2
?	?	?	?	?	?	?	?	?	?	?	?	?	?	?	?	?
2	1	1	1	0	0	?	0	0	0	2	0	?	0	0	1	?
0	2	1	1	0	0	0	2	0	1	0	0	1	0	?	0	1
2	1	1	1	0	0	0	0	0	0	?	0	1	0	0	0	?
2	?	1	1	1	1	0	2	1	1	?	1	1	0	1	1	?
2	0	1	1	0	0	0	0	0	0	2	0	1	0	0	1	0
2	0	1	1	1	0	0	0	0	0	2	1	1	1	0	0	?
?	?	?	?	?	?	?	?	?	?	?	?	?	?	?	?	?
?	1	1	1	0	0	0	0	0	0	2	0	0	0	0	1	2
?	?	?	?	?	?	?	?	?	?	?	?	?	0	?	1	2
?	?	?	?	?	0	1	0	0	0	?	?	?	0	0	1	?
?	1	?	1	0	0	1	1	0	0	2	0	0	0	0	1	?
0	1	0	1	0	0	0	0	0	0	1	0	1	0	1	0	0
0	?	?	1	?	0	?	0	0	-	1	0	0	?	0	0	?
?	?	?	?	?	?	?	?	?	?	?	?	?	?	?	?	?
?	?	?	?	?	?	?	?	?	?	?	?	?	?	?	?	?
2	1	1	1	0	0	0	0	0	0	?	0	1	?	?	?	?
?	?	?	?	?	?	?	?	?	?	?	?	?	?	?	?	?
?	?	?	?	?	?	?	?	?	?	?	?	?	0	?	?	?
?	?	?	?	?	?	?	?	?	?	?	?	?	0	1	0	1
?	?	?	?	?	?	?	?	?	?	?	?	?	?	0	1	2
?	1	?	?	?	0	?	?	?	?	?	?	?	?	0	0	0
2	1	1	1	0	0	0	0	0	0	2	0	1	0	0	1	0
2	1	1	1	0	0	0	0	0	0	2	0	1	0	0	1	2
?	?	?	?	?	?	?	?	?	?	?	?	?	?	?	?	?
2	?	1	1	?	0	0	0	0	0	1	0	1	0	0	1	?
?	?	?	?	?	?	?	2	?	?	0	?	?	0	1	?	?

1	2	1	1	2	?	1	2	0	0	0	0	0	0	?	?	?
?	?	?	?	?	?	?	?	?	?	?	?	?	?	?	?	?
?	?	?	?	?	?	?	?	?	?	?	?	?	?	1	1	1
?	?	?	?	?	0	1	1	0	0	2	0	?	1	1	1	?
0	?	?	1	0	?	0	0	0	0	0	0	0	0	1	0	?
?	1	?	1	0	1	0	?	1	?	0	0	0	0	0	0	0
?	?	?	?	?	?	0	2	1	1	0	1	1	0	1	?	?
1	1	0	1	0	0	0	0	0	0	0	0	1	1	1	0	?
1	?	1	1	?	0	?	2	0	0	0	0	0	0	?	1	?
2	?	1	?	?	?	?	?	?	?	?	0	?	?	?	?	?
2	?	1	1	0	0	0	0	0	0	2	0	1	0	0	0	?
2	0	1	1	1	0	1	0	0	0	2	0	1	1	0	0	1
2	1	1	1	0	?	0	0	0	0	2	0	1	0	0	1	?
?	?	?	?	?	?	?	?	?	?	?	?	?	?	0	?	1
?	?	1	1	1	?	?	?	?	?	0	0	?	0	?	?	?
2	0	1	1	?	0	?	1	?	1	2	0	1	0	0	1	1
?	?	?	?	?	?	?	?	?	?	?	?	?	?	0	0	1
?	?	?	?	?	?	?	?	?	?	?	?	?	0	?	?	?
?	?	?	?	?	?	?	?	?	?	2	?	?	?	?	?	0
?	?	1	1	0	?	?	?	?	?	?	?	?	0	?	?	?
1	2	1	1	2	?	1	2	0	0	0	?	0	0	0	?	1
?	?	?	?	?	?	1	1	0	0	0	1	1	1	1	1	1
2	1	?	?	?	?	1	1	0	?	0	0	1	1	1	1	?
?	?	?	?	?	?	?	?	?	?	?	?	?	?	?	?	?

298	299	300	301	302	303	304	305	306	307	308	309	310	311	312	313	314
250	251	252	253	254	255	256	258	259	260	261	-	-	-	264	265	-
O200	Bd216	Bd213	O201	O202	O224	MD125	MD127	O204	O205	He233	new	new	new	O206	O227	new
0	0	0	1	0	?	0	0	0	0	0	0	0	1	0	0	0
1	?	?	2	0	1	?	0	?	?	?	?	?	?	1	?	?
0	?	?	2	0	0	0	0	0	0	0	?	0	?	1	1	?
2	1	0	2	0	0	1	1	1	1	1	1	1	0	1	?	0
?	?	?	0	1	?	?	?	0	0	?	?	0	?	1	1	?
1	?	?	?	?	?	?	?	?	?	?	?	?	?	1	?	?
[1 2]	1	1	2	0	0	0	2	1	1	1	1	0	1	1	1	1
1	1	?	2	1	0	0	2	1	1	0	1	0	1	1	1	1
1	1	1	?	?	0	?	0	?	?	?	?	0	0	1	?	0
?	?	?	?	?	?	?	?	?	?	?	?	?	?	?	?	?
1	?	?	2	0	0	1	?	0	0	?	1	0	0	1	1	0
2	0	1	2	0	0	1	2	1	1	0	0	1	1	1	1	0
2	1	1	2	0	0	1	[1 2]	1	1	0	0	1	?	1	1	0
?	?	?	?	?	?	?	?	?	?	?	?	?	?	?	?	?
?	?	?	?	?	?	?	?	?	?	?	?	?	?	?	?	?
0	0	?	2	0	0	?	0	0	0	?	0	0	1	1	1	0
2	0	1	?	0	?	1	1	?	1	?	?	1	0	1	1	0
?	?	?	?	?	?	0	1	1	1	1	2	?	?	1	?	0
1	1	1	2	0	1	?	0	0	0	?	0	0	1	1	0	0
1	1	0	2	0	0	?	0	0	0	0	0	1	0	1	1	?
?	?	?	?	?	?	?	?	?	?	?	?	?	?	1	?	?
1	?	?	2	0	0	0	0	0	0	?	?	?	?	1	1	?
1	1	1	2	0	1	?	0	0	0	?	0	0	1	1	0	1
0	0	1	2	0	0	1	0	0	0	?	0	0	0	1	1	0
?	?	?	1	0	0	?	1	0	?	0	?	?	?	1	?	?
1	0	1	2	0	0	0	0	0	0	0	0	0	1	1	1	0
1	1	?	1	1	0	0	2	1	1	0	0	1	1	1	1	1
?	?	?	?	?	?	?	?	?	?	?	?	?	?	?	?	?
1	?	1	2	0	0	0	0	0	0	0	0	1	0	1	1	0
1	2	0	?	0	?	1	1	1	1	1	1	1	0	1	1	?
1	1	1	2	0	1	?	0	0	1	0	1	?	1	1	1	?
?	?	?	2	0	0	?	?	?	?	0	?	?	1	1	1	?
0	0	?	2	0	0	0	0	0	0	0	0	0	0	1	1	0
0	?	?	2	0	0	?	?	0	1	?	1	?	?	1	1	?
?	?	?	?	?	?	?	?	?	?	?	?	?	?	?	?	?
?	?	?	?	?	?	?	?	?	?	?	?	?	?	?	?	?
?	?	?	?	?	?	?	?	?	?	?	?	?	?	?	?	?
?	?	?	?	?	?	?	?	?	?	?	?	?	?	?	?	?
?	?	?	1	?	?	0	?	?	?	?	?	?	?	?	?	?
1	1	?	1	0	0	0	?	?	1	?	?	0	0	1	1	?
1	2	0	?	?	?	?	1	1	1	?	1	?	0	?	?	0
1	1	1	2	0	0	?	1	1	1	1	1	?	?	1	1	0
1	1	1	2	0	0	0	0	0	0	0	0	1	?	1	1	0
?	0	1	2	0	0	0	0	1	1	0	0	1	1	1	?	0
?	?	?	?	?	?	?	?	?	?	?	?	?	?	?	?	?
1	1	1	2	1	0	?	?	?	?	?	?	0	1	1	1	0
?	?	?	?	?	?	?	1	?	?	?	?	?	?	?	?	?

1	?	?	2	0	0	?	?	0	0	?	?	?	?	1	1	0
?	?	?	?	?	?	?	?	?	?	?	?	?	?	?	?	?
?	1	?	?	0	?	0	1	0	1	1	?	?	?	?	?	?
?	1	?	1	0	0	0	1	0	1	1	?	?	0	1	?	0
0	0	?	2	1	0	?	0	0	0	?	?	0	?	1	1	0
0	0	0	2	0	0	?	0	0	0	?	?	0	?	1	1	0
?	?	?	1	0	0	?	1	?	?	0	?	0	?	1	1	0
?	?	?	0	1	?	?	?	0	0	?	2	0	0	1	1	0
1	?	?	?	?	?	?	?	?	?	?	?	?	?	1	1	0
1	1	?	2	0	0	?	?	?	?	?	?	1	0	1	?	0
1	1	?	2	1	0	?	?	1	1	?	?	1	?	1	1	?
1	1	1	2	1	0	0	1	1	1	0	1	1	0	1	1	1
1	1	1	2	1	0	?	1	?	0	?	?	?	1	1	1	0
1	1	1	?	1	?	0	1	1	?	1	0	?	1	1	?	0
?	?	?	?	?	?	?	?	0	0	?	?	0	?	1	?	0
2	1	1	2	0	0	1	2	1	1	0	0	1	0	1	1	0
1	1	1	?	?	?	0	1	0	1	1	2	0	0	1	1	?
?	?	?	?	0	0	?	?	?	?	?	?	?	0	1	0	?
?	?	?	?	?	?	?	0	0	0	?	0	?	0	?	?	0
?	1	1	2	0	0	1	?	?	?	?	?	?	?	1	?	?
?	1	?	2	0	[0 1]	?	0	?	?	?	0	0	?	?	?	0
1	1	1	1	1	0	0	1	0	1	1	2	?	?	1	1	0
1	?	1	1	1	0	0	1	0	1	?	2	0	0	1	1	0
?	?	?	?	?	?	?	?	?	?	?	?	?	?	?	?	?

315	316	317	318	319	320	321	322	323	324	325	326	327	328	329	330	331
266	267	268	269	270	271	272	273	274	275	276	277	-	-	-	278	279
Br115	O225	O226	Br118	Br117	O207	208R2:	Br119	Br120	O209	Br122	D277	new	R232	new	D278	D279
0	0	0	?	0	0	0	?	?	0	2	0	1	0	0	0	0
?	1	?	?	?	?	?	?	?	?	?	?	?	?	?	?	?
?	0	0	?	?	1	1	?	?	0	?	?	?	0	?	?	?
?	?	0	1	1	1	2	?	2	?	?	1	0	1	1	1	?
?	0	?	?	?	1	?	?	?	?	?	?	?	?	?	?	?
?	?	0	0	0	1	1	0	?	1	?	0	1	0	1	0	0
?	0	0	1	1	1	?	?	?	?	?	1	?	?	0	0	0
0	0	0	1	1	1	?	0	2	0	?	?	0	1	1	1	?
?	0	0	?	?	?	1	?	?	?	?	?	?	?	?	?	?
?	?	?	?	?	?	?	?	?	?	?	?	?	?	?	?	?
?	0	0	1	0	1	1	?	?	1	?	0	2	0	0	0	0
?	0	0	1	1	1	2	1	1	1	1	1	0	1	1	1	0
?	0	0	1	1	1	2	1	1	?	1	0	0	1	1	1	0
?	?	?	?	?	?	?	?	?	?	?	?	?	?	?	?	?
?	?	?	?	?	?	?	?	?	?	?	?	?	?	?	?	?
?	0	?	?	?	?	?	?	?	?	?	0	1	0	0	?	?
1	0	0	1	1	1	2	1	1	?	1	0	0	0	1	0	1
?	?	?	?	?	?	?	?	?	?	?	?	?	?	?	?	?
?	1	1	?	0	1	2	?	?	?	?	?	?	?	?	?	?
0	0	0	1	0	1	2	?	2	1	1	0	0	1	1	1	1
?	?	?	?	?	?	?	?	?	1	2	0	1	0	1	0	0
?	0	0	?	?	1	?	?	?	1	?	?	?	?	?	?	0
?	1	1	?	0	?	?	?	0	1	2	?	?	?	?	?	0
?	0	0	?	0	1	1	?	?	1	?	?	1	0	0	0	0
?	1	0	0	0	1	?	?	?	1	?	?	?	?	?	?	?
0	0	0	0	0	1	1	0	1	1	1	0	0	0	0	0	0
0	0	0	1	1	1	1	0	?	0	1	1	1	0	1	0	0
?	?	?	?	?	?	?	?	?	?	?	?	?	?	?	?	?
?	0	0	0	0	1	1	?	?	1	?	?	?	?	?	?	0
?	?	0	?	?	?	2	?	?	?	?	0	0	1	1	1	1
?	0	?	?	?	?	?	?	?	?	?	?	?	?	?	?	?
?	?	?	?	?	?	?	?	?	?	?	0	?	?	?	?	?
?	0	0	0	?	1	?	0	?	0	?	?	?	?	?	?	?
?	?	0	?	?	0	?	?	?	?	?	?	?	?	?	?	?
?	?	?	?	?	?	?	?	?	?	?	?	?	?	?	?	?
?	?	?	?	?	?	?	?	?	?	?	?	?	?	?	?	?
?	?	?	?	?	?	?	?	?	?	?	?	?	?	?	?	?
?	?	?	?	?	?	?	?	?	?	?	?	?	?	?	?	?
?	?	?	?	?	?	?	?	?	?	?	?	?	?	?	?	?
?	?	?	?	?	?	?	?	?	?	?	?	?	?	?	?	?
1	?	?	?	?	?	?	?	2	?	?	0	0	1	0	1	0
?	0	0	1	0	1	?	0	2	0	?	?	2	?	0	?	1
?	0	0	0	0	1	1	?	1	1	1	0	1	0	0	0	0
1	0	1	0	1	?	1	0	1	1	0	0	?	?	0	0	?
?	?	?	?	?	?	?	?	?	?	?	?	?	?	?	?	?
0	0	0	0	0	?	?	?	?	?	0	?	2	?	?	0	0
?	?	?	?	?	?	?	?	?	?	?	?	?	?	?	?	?

?	0	0	?	?	?	1	?	?	0	?	?	?	?	?	?	?
?	?	?	?	?	?	?	?	?	?	?	?	?	?	?	?	?
?	?	?	?	?	?	?	?	?	?	?	?	?	?	?	?	?
0	?	?	?	?	?	?	?	?	?	?	?	?	?	?	?	?
?	0	0	?	?	1	?	?	?	0	?	?	?	?	?	?	?
?	0	0	?	?	?	?	?	?	?	?	?	?	?	?	?	?
?	1	?	?	?	?	?	?	?	?	?	0	?	?	?	?	?
?	0	0	1	0	1	0	1	?	?	?	0	0	0	0	0	0
?	0	0	?	?	?	?	?	?	?	?	?	?	?	?	?	?
?	0	?	1	1	1	2	1	?	?	?	?	1	0	?	1	0
0	0	0	1	0	1	?	?	1	?	0	?	?	?	?	?	?
0	0	0	1	0	1	1	1	1	1	0	1	2	0	0	0	0
?	0	0	?	0	1	1	0	?	1	?	?	?	?	?	?	0
?	?	0	?	0	?	1	?	?	?	?	0	1	0	1	1	0
?	1	?	?	?	?	?	?	?	?	?	?	?	?	?	?	?
0	0	0	0	0	?	2	1	?	?	?	0	0	1	1	1	0
?	0	0	1	0	1	2	1	?	?	?	1	1	0	0	0	1
?	1	?	?	?	?	?	?	?	?	?	?	?	?	?	?	?
0	?	?	?	?	?	?	?	1	?	?	?	?	?	?	?	?
1	0	0	1	?	?	?	?	?	?	?	?	?	?	?	?	?
?	0	0	?	0	?	?	?	?	0	1	?	?	?	?	?	?
?	0	0	1	?	1	?	?	?	?	?	?	?	?	?	?	?
?	0	0	?	?	1	?	?	?	?	?	?	?	0	?	?	?
1	?	1	?	0	?	?	0	1	?	0	?	?	?	?	?	?

332	333	334	335	336	337	338	339	340	341
280	281	-	282	283	284	285	286	287	288
O213	O214	new	11Br1	O211	O215	O110	O219	O220	O221
0	0	0	0	0	0	0	0	0	0
1	1	1	?	1	0	0	0	0	0
1	1	0	0	1	0	0	0	0	0
1	1	0	0	1	0	0	0	0	0
1	1	?	?	1	1	1	1	1	1
1	1	0	0	1	0	0	0	0	0
?	?	?	?	?	?	0	0	0	0
1	1	1	0	0	0	0	0	0	0
?	?	1	0	1	0	0	0	0	0
?	?	?	?	?	?	0	?	?	?
1	1	0	0	0	0	0	0	0	0
1	1	?	0	1	0	0	0	0	0
1	1	1	?	?	0	0	0	0	0
?	?	?	?	?	?	?	?	?	?
?	?	?	?	?	0	0	1	1	?
?	?	?	?	?	?	0	0	0	0
?	?	0	1	1	0	0	0	0	0
?	?	?	0	?	?	?	?	?	?
?	?	?	?	?	?	?	?	?	?
1	1	0	1	1	0	0	0	0	0
?	?	?	?	?	0	0	0	0	0
?	?	1	0	0	0	0	0	0	0
1	1	1	0	1	0	0	0	0	0
1	1	0	?	1	0	0	0	0	0
?	?	?	?	?	?	?	0	0	0
1	1	0	0	0	0	0	0	0	0
1	1	1	1	1	0	0	0	0	0
?	?	?	?	?	?	?	0	?	?
?	?	1	0	1	0	0	0	0	0
?	?	?	?	?	?	?	?	?	?
?	?	?	?	?	?	?	0	0	0
?	?	0	0	0	0	0	0	0	0
1	1	1	0	1	0	0	0	0	0
?	?	?	?	?	0	?	?	?	?
?	?	?	?	?	?	0	?	?	?
?	?	?	?	?	?	?	?	?	?
?	?	?	?	?	?	?	?	?	?
?	?	?	?	?	?	?	?	?	?
?	?	?	?	?	?	0	?	?	?
?	?	?	?	?	?	?	?	?	?
?	?	?	?	?	?	?	?	?	?
?	?	?	0	?	?	?	0	0	0
1	1	1	0	1	0	0	0	0	0
1	1	1	0	0	0	0	0	0	0
?	?	?	?	?	?	?	?	?	?
1	1	1	0	0	0	0	0	0	0
?	?	?	?	?	?	?	?	?	?

1	1	?	0	0	0	0	0	0	0
?	?	?	?	?	?	?	?	?	?
?	?	?	?	?	0	0	0	0	0
?	1	?	[0 1]	?	0	0	0	0	0
1	1	?	?	0	1	1	1	1	1
?	?	?	0	?	0	0	1	1	0
?	?	1	0	1	0	?	?	?	?
1	1	?	1	1	1	0	1	1	0
1	1	?	?	0	0	?	0	0	0
?	1	0	?	0	0	0	0	0	0
1	1	0	0	0	0	0	0	0	0
1	1	0	0	0	0	0	0	0	0
1	1	1	0	0	0	0	0	0	0
1	1	?	0	0	?	?	?	?	?
?	?	?	?	1	0	0	0	0	0
-	-	-	1	1	0	0	0	0	0
1	1	1	0	0	0	0	0	0	0
?	?	?	?	?	?	0	?	?	?
?	?	?	0	?	0	?	?	?	?
?	?	?	?	?	0	?	0	0	0
?	?	?	?	0	0	0	0	0	0
?	?	?	?	?	?	0	0	0	0
?	?	?	?	?	?	0	0	0	0
?	?	?	0	?	?	?	?	?	?

Supplemental material 3 – Comments on changes made from the raw datamatrix of Dieudonné et al. (2016*a*).

Supplemental material 3.1 – Corresponding comments on characters called with an asterisk on supplemental material 1. Most of these comments refer to changes on character definition and scorings, but some of them are simple observations. Note that the "unapplicable" character states were marked as hyphens and often not considered as actual modifications whenever they just replaced previous question marks.

Cranial skeleton

1(*). Skull, rostral-quadrate length relative to the body length: 10 % (0), 13 % or more (1) (Xu et al. 2006 #1; Ösi et al. 2012 #2).

Dryosaurus was corrected and coded (0) after Galton (1983 pl. 4).

2(*). Skull, preorbital region, percentage out of the total skull length from the rostrum to the quadrate: equal or more than 40% (0), much less than 40% (1) (Xu et al. 2006 #21; Ösi et al. 2012 #1).

The preorbital skull length of *Heterodontosaurus tucki* (Norman et al. 2011, fig.1A), *Abrictosaurus consors* (Sereno 2012, fig. 34) is less than 40% of the total skull length. The preorbital skull length of *Hexinlusaurus multidens* is also much less than 40% in all probabilities given the general outline of its snout, although the anteriormost tip of the premaxilla is absent (He and Cai 1984, fig. 3). The skull roof of *Goyocephale lattimorei* shows the location of its orbits (Perle et al. 1982, pl. 41), with the preorbital skull length forming clearly less than 40% of the total skull length. The same occurs for the skull of *Stegoceras validum* (Maryanska and Osmolska 1974, fig. 1-A1). By contrast, *Pachycephalosaurus wyomingensis* differs in having a preorbital skull length forming slightly

more than 40% of its skull length (Horner and Goodwin 2009, fig. 2B). *H. tucki*, *A. consors*, *H. multidens*, *G. lattimorei* were corrected and coded (1).

3(*). Skull, position of maximum widening of the skull: beneath the jugal–postorbital bar (0), posteriorly, beneath the infratemporal fenestra (1) (modified from Ösi et al. 2012 #37, Xu et al. 2006 #2).

The maximum widening of the skull of *Herrerasaurus ischigualastensis* (Sereno and Novas 1993, fig. 1C), *Scelidosaurus harrisoni* (Owen 1861, pl. 6), *Emausaurus ernsti* (Haubold 1990, fig. 2), *Isaberrysaura mollensis* (Salgado et al. 2017, fig. 2A, B), *Lesothosaurus diagnosticus* (Sereno 1991, fig. 11B), *Heterodontosaurus tucki* (Norman et al. 2011, fig. 3A), *Hexinlusaurus multidens* (He and Cai 1984, fig. 3), *Agilisaurus louderbacki* (Peng 1992, fig. 1B), *Thescelosaurus neglectus* (Boyd 2014, fig. 3), *Hypsilophodon foxii* (Galton 1974*a*, cf. fig. 6A), *Muttaburrasaurus langdoni* (Bartholomai and Molnar, 1981, fig. 1B), *Dryosaurus altus* (Galton 1983, fig. 2B), *Camptosaurus dispar* (Gilmore 1909, fig. 3) and *Tenontosaurus dossi* (Andrzejewski et al. 2019 #37) is located beneath the jugal-postorbital bar. Among the Asian clade, the skull width of *Jeholosaurus shangyuanensis* (Barrett and Han, 2009, fig. 1A) is held constant from the jugal chord to the squamosals. This condition seems to be similar in *Haya griva*, although unfortunately the skull is deformed (Makovicky et al. 2011, fig. 1E). In *Changchunsaurus parvus* this character is not available (Butler et al. 2011, fig. 1). By contrast, the maximum widening of the skull of *Chaoyangsaurus youngi* (Zhao et al. 1999, see fig. 2B), *Yinlong downsi* (Han et al. 2015, cf. fig. 4B), *Psittacosaurus mongoliensis* (Osborn 1923), *Homalocephale calathocercos*, (Maryanska and Osmolska 1974, fig. 1-D3) is located posteriorly, beneath their infratemporal fenestra. *H. ischigualastensis*, *S. harrisonii*, *E. ernsti*, *I. mollensis*, *L. diagnosticus*, *H. tucki*, *H. multidens*, *A. louderbacki*, *T. neglectus*, *M. langdoni*, *D. altus*, *C. dispar*, *T. dossi* and *J. shangyuanensis* were corrected and coded (0). *C.*

youngi, *Y. downsi*, Psittacosauridae, *H. calathocercos* were corrected and coded (1). *H. griva* was corrected and coded with a question mark.

5(*). Infratemporal fenestra size: small, much smaller than the orbit (0) or large, subequal or larger than the orbit (1) (Xu et al. 2006 #87).

In *Chaoyangosaurus youngi*, the infratemporal fenestra is incomplete (Zhao et al. 1999), so its character state was recoded as a question mark. *Heterodontosaurus tucki* (Norman et al. 2011) has an infratemporal fenestra that is not as large as its orbit. Note that in the ankylopollexians *Camptosaurus dispar* (Gilmore 1909, fig. 2) and *Iguanodon bernissartensis* (Norman 1980, fig. 2), the orbit is quite small so the infratemporal fenestra is subequal to larger than the orbit. *H. tucki* was corrected with character state (0). Both *C. dispar* and *I. bernissartensis* were coded with character state (1).

6(*). Skull, widening of the skull across the jugals, chord from frontal orbital margin to extremity of jugal is more than minimum interorbital width: absent (0), present, skull has a triangular shape in dorsal view (1) (Ösi et al. 2012 #36).

in *Archaeoceraops oshimai* (You and Dodson 2003, fig. 1E) and *Liaoceratops yanzigouensis* (Xu et al. 2002, fig. 2B), the jugal doesn't look lateromedially expanded so the dorsal width between the frontal orbital margin and outer jugal margin doesn't exceed the interorbital width. In *Chaoyangsaurus youngi* (Zhao et al. 1999) the frontals are not preserved but the jugals are greatly expanded lateromedially. *A. oshimai, L. yanzigouensis* were corrected and coded (0). *C. youngi* was left coded (1).

8(*). Rostral bone (neomorphic bone anterior to premaxilla): absent (0), present (1) (Xu et al. 2006 #3; Ösi et al. 2012 #3).

10(*). Rostral, shape of anterior face: round, convex (0) or sharply keeled (1) (Ösi et al. 2012 #4; Xu et al. 2006 #5).

The anterior face of the rostral is convex in *Liaoceratops yanzigouensis* (Xu et al. 2002, fig. 2A) so this taxon was corrected and coded with character state (0).

13(*). Premaxilla, anterior and dorsal surface: lacks rugosities (0), bears distinct rugose surface (1) (Brown et al., 2013 #136).

The rostral surface of the premaxilla is not rugose in *Y. downsi* (Han et al. 2015, fig. 2A, 3A, 5A). The premaxilla of *Zalmoxes robustus* is told to be laterally ridged and pitted (Weishampel et al. 2003). Note that the premaxillae of *Stegoceras validum* (Sues and Galton 1987, p.6) and *Pachycephalosaurus wyomingensis* (Brown and Schlaikjer 1943, pl. 38) bear rugosities, but that of *P. major* doesn't (You et al. 2008). *P. major* was newly coded (0). *Y. downsi* was corrected and coded (0). *Z. robustus* was corrected and coded (1).

14(*). Premaxilla, ventral inflection: absent, oral margin even with ventral margin of maxilla (0), present, oral margin projects farther ventrally than ventral margin of maxilla (1) (modified from Xu et al. 2006 #37; McDonald et al. 2010 #30; Ösi et al. 2012 #9).

In the pachycephalosaurs *Stegoceras validum* (Brown and Schlaikjer 1943, pl. 44; Maryanska and Osmolska 1974, fig. 1A), *Prenocephale prenes* (Maryanska and Osmolska 1974, fig. 1A), and in heterodontosaurids such as *Echinodon becklesii* (Sereno 2012, fig. 19B) the premaxillae appear ventrally deflected. By contrat, although the premaxilla looks downwardly bending in *Goyocephale lattimorei* (Perle et al. 1992, pl. 42, fig. 5) they are roughly level with the maxilla. In the adult of *Pachycephalosaurus wyomingensis*, the premaxillaries are missing (Brown and Schlaikjer 1943, p. 133), but in the juvenile specimen the premaxillaries appear level with the maxillaries (Bakker et al. 2006, fig. 2). In ceratopsids, the premaxilla doesn't project farther ventrally than the maxilla (e.g. *Yinlong downsi*, Han et al. 2015; *Chaoyangosaurus youngi*, Zhao et al. 1999). *G. lattimorei*, *Chaoyangosaurus youngi*, *Liaoceratops yanzigouensis*, *Archaeoceratops oshimai* were corrected and coded (0).

15(*). Premaxilla, denticles on oral margin: absent (0), present (1) (modified from Weishampel et al., 2003 #7; McDonald et al. 2010 #33).

Denticles are absent on the oral margin of the premaxilla of both *Psittacosaurus major* and *P. mongoliensis* (You et al. 2008, fig. 1B; Sereno 2010, fig. 2.7). Both were newly coded (0).

16(*). Premaxilla, edentulous anterior region: absent, first premaxillary tooth is positioned adjacent to the symphysis (0), present: if any, the first premaxillary tooth is inset the width of one or more crowns (1) (rephrased from Ösi et al. 2012 #6).

According to Winkler et al. (1997) and Andrzejewski et al. (2019 #6), *Tenontosaurus dossi* was corrected and coded (1).

17(*). Premaxilla, posterolateral process: does not contact lacrimal (0), contacts the lacrimal, excludes maxilla–nasal contact (1) (Xu et al. 2006 #34; Ösi et al. 2012 #7).

The lacrimal of basal genasaurian (e.g. *Scelidosaurus harrisoni*, Owen 1861), basal neornithischians (*Hexinlusaurus multidens*, Barrett et al. 2005; *Agilisaurus louderbacki*, Peng 1992), *Haya griva* (Makovicky et al. 2011), and pachycephalosaurs (e.g. *Stegoceras validum*, Maryanska and Osmolska 1974, fig. A1; *Pachycephalosaurus wyomingensis*, Brown and Schlaikjer 1943, p.134) does not contact the postero-lateral process of premaxilla. Heterodontosaurids and psittacosaurs (Sereno 2010, fig. 2.3, 2.7), *Yinlong downsi* (Xu et al. 2006 #34; Han et al. 2015, fig. 8B) share the presence of a premaxilla-lacrimal contact. In *Yinlong downsi*, some figures don't show a premaxilla-lacrimal contact (Han et al. 2015, fig. 3), but in the latter case this could be due to breakage of the anterior lacrimal branch. In *Liaoceratops yanzigouensis* the posterolateral premaxillary process was coded as providing contact with the lacrimal (Xu et al. 2006 #34). The posterolateral premaxillary branch does contact the prefrontal (Xu et al. 2002) but there is no clear, obvious indication for a premaxilla-lacrimal contact from the figures. Such character could not be inferred for *Abrictosaurus consors* given the bad state of preservation of its skull (Sereno 2012, fig. 34,

35). Information on this character is lacking in *Goyocephale lattimorei* (Perle et al. 1982). Let's remark that in *Jeholosaurus shangyuanensis* the contact appears in the most adult forms (Han et al. 2012). In *Haya griva* (Makovicky et al. 2011) and *Changchunsaurus parvus* (Liyong et al. 2010, fig. 3A) there is no contact between the posterolateral process of the premaxilla and the lacrimal. This lack of contact also occurs in the North American form *Thescelosaurus neglectus* (e.g. Brown et al. 2013, fig. 15), and in the European one *Hypsilophodon foxii* (Galton 1974*a*). In the elasmarian *Talenkauen santacrucensis* it can also be assessed that the premaxillary could'nt have contacted the lacrimal posteriorly (Novas et al. 2004, fig. 2A), because of the shortness of the posterior premaxillary process. *Muttaburrasaurus langdoni* was corrected by Bell et al. (2019) as possessing a premaxilla/lacrimal contact. *C. parvus* was corrected and coded (0). *M. langdoni* was corrected and coded (1) instead of (0). *A. consors*, *G. lattimorei* and *L. yanzigouensis* were corrected and coded with a question mark.

21(*). Premaxillae: unfused (0), fused (1) (Brown et al. 2013 #124).

In *Yinlong downsi*, the premaxillae suture is visible (Han et al. 2015, fig. 5). The premaxillae fail to contact with each other in *Psittacosaurus major* (You et al. 2008, p. 185) and *P. mongoliensis* (Sereno 2010, fig. 2.7A). *Y. downsi*, *P. major* and *P. mongoliensis* were corrected and coded (0).

22(*). Premaxilla, external naris size: small, entirely overlies the premaxilla (0), enlarged, extends posteriorly to overlie the maxilla (1) (modified from McDonald et al. 2010 #38; Ösi et al. 2012 #18).

Talenkauen santacrucensis was previously coded as having a narial fossa nto extending posteriorly over the maxilla. However, its narial opening is clearly expanded posteriorly, and a quick observation of the posteromedial slit-like opening for the anterior maxillary process shows that it would have overlied the maxilla (Rozadilla et al. 2019, fig. 2D). T.

santacrucensis was corrected and coded (1). *Muttaburrasaurus langdoni* was corrected by Bell et al. (2019) as having an external naris entirely overlying the premaxilla. We follow Bell et al. (2019) and correct and code *M. langdoni* (0) instead of (1).

23(*). Premaxillary internarial bar : present, reaches the nasal (0), incomplete or absent (1) (modified from Ösi et al. 2012 #12; Boyd 2015 #11).

Goyocephale lattimorei wasn't described for the presence or absence of premaxillary internarial bar, although the figures clearly depict such absence in an apparently unbroken premaxilla (Perle et al. 1982, pl. 41, fig. 3, pl. 42, fig. 5). In *Kulindadromeus zabaikalicus* (Godefroit et al. 2014, fig. S4B), the presence or absence of premaxillary internarial bar cannot be inferred. You et al. (2008, p. 185, fig. 1B) and Sereno (2010, fig. 2.7) describe a lack of mutual contact between the right and left premaxillae in *Psittacosaurus major* and *P. mongoliensis* because of the intervenning rostral bone. Notwithstanding one can clearly observe that in both taxa each premaxilla reaches to contact the nasal internarial bar at least ventrally. Therefore, a short premaxillary branch does contact the nasal above the narial fossa. *Muttaburrasaurus langdoni* is not known for this character (Bell et al. 2019 #20). *Goyocephale lattimorei* was corrected and coded (1). *P. major* and *P. mongoliensis* were newly coded (0). *M. langdoni* and *K. zabaikalicus* were corrected and coded with a question mark.

24(*). Premaxilla, position of the ventral margin of external nares: below the ventral margin of the orbits (0), above the ventral margin of the orbits (1) (Ösi et al. 2012 #17; Xu et al. 2006 #22).

Muttaburrasaurus langdoni is not known for this character (Bell et al. 2019 #21) so it was corrected and coded with a question mark instead of (0) previously.

25(*). Premaxilla, narial fossa surrounding external nares on lateral surface of premaxilla, position of ventral margin of fossa relative to the ventral margin of the premaxilla: closely approaches

the ventral margin of the premaxilla (0), separated by a broad flat margin from the ventral margin of the premaxilla (1) (Ösi et al. 2012 #16).

Liaoceratops yanzigouensis (Xu et al. 2002) and *Archaeoceratops oshimai* (You and Doson, 2003) were corrected and coded (1). *Haya griva* (Makovicky et al. 2011) was corrected and coded (0).

26(*). Maximum length of external nares less than 15% basal skull length (0), maximum length of external nares greater than 15% basal skull length (1) (Boyd 2015 #88).

As in most other ornithopods, and in spite of bad crushing of its skull, the maximum length of external nares was found to be much less than 15% of the total skull length in *Parksosaurus warreni* (Galton 1973). Maximum length of external nares is less than 15% the total skull length in *Psittacosaurus mongoliensis* (Sereno 2010, fig. 2.7) and *Psittacosaurus major* (You et al. 2008, fig. 1B). *P. warreni* was corrected and coded (0). *P. mongoliensis* and *P. major* were newly coded (0).

27(*). Premaxilla-maxilla contact, fossa-like depression positioned on the premaxilla–maxilla boundary: absent (0), present (1) (Ösi et al. 2012 #13).

No depression between premaxilla and maxilla is observable in *Yinlong downsi* (Han et al. 2015, e.g. fig. 2A). No fossa-like depression is oberved between the premaxilla and maxilla of *Convolosaurus marri* either (Andrzejewski et al. 2019, fig. 7). *Y. downsi* and *C. marri* were corrected and coded (0).

28(*). Premaxilla-maxilla diastema: weak to absent, maxillary teeth continue to anterior end of maxilla (0), present, substantial diastema of at least one crown length between maxillary and premaxillary teeth (1) (Ösi et al. 2012 #14).

A premaxilla-maxilla diastema is absent in *Archaeoceratops oshimai* (You and Dodson 2003, fig. 1), *Liaoceratops yanzigouensis* (Xu et al. 2002, fig. 1). There is no indication for a diastema in *Zephyrosaurus schaffi* and the small posterior depression of the premaxilla

probably served for the anterolateral boss of the maxilla (Sues 1980, p.55). In *Hypsilophodon foxii* (Galton 1974*a*, fig. 3), *Haya griva* (Makovicky et al. 2011, fig. 1B), *Thescelosaurus neglectus* (Boyd 2014, fig. 1), *Parksosaurus warreni* (Galton 1973, fig. 1), *Tenontosaurus tilletti* (Thomas 2015, fig. 2), *Tenontosaurus dossi* (Winkler et al. 1997, fig. 3), *Talenkauen santacrucensis* (Cambiaso 2007, by fitting premaxilla and maxilla from fig. 7, 8), the premaxilla-maxilla diastema is weakly developped to totally absent. *Convolosaurus marri* (Andrzejewski et al. 2019, fig. 7) is as most other ornithopods in that the space between the anteriormost maxillary tooth and the premaxilla is too small for being regarded as a "true" diastema. In *Psittacosaurus mongoliensis* (Sereno 2010, fig. 2.7A) and *Psittacosaurus major* (You et al. 2008, fig. 1B), a very weak gap is present between the maxilla and premaxilla, but it is not substancially significant. In *Gasparinisaura cincosaltensis* (Coria and Salgado 1996, fig. 2) and *Kulindadromeus zabaikalicus* (Godefroit *et al*. 2014, fig. S4), any absence of premaxilla-maxilla diastema couldn't be safely inferred from the preserved material. *H. foxii*, *H. griva*, *T. neglectus*, *P. warreni*, *T. tilletti*, *T. dossi*, *T. santacrucensis*, *C. marri*, *P. mongoliensis* and *P. major A. oshimai*, *L. yanzigouensis* and *Z. schaffi* were corrected and coded (0). *G. cincosaltensis* and *K. zabaikalicus* were corrected and coded with a question mark.

29(*). Premaxilla-vomer, ventral contact: present (0), absent, excluded by midline contact between maxillae (1) (rephrased from Ösi et al. 2012 #84; Xu et al. 2006 #9).

Prenocephale prenes, *Stegoceras validus* and *Goyocephale lattimorei* (Mayanska and Osmolska, 1974, fig. 1A3, 1C3; Perle et al. 1982, p. 118) do actually have an intermaxillary contact in front of the vomers. Norman et al. (2011, p. 204) states that in *Heterodontosaurus tucki*, "the anterior processes of the maxillae meet in the midline and probably receive the rostral tips of the fused vomers". The interpretative sagittal reconstruction of the ventral premaxillary palate clearly shows that the maxillae met with each other and the vomers

interlocked behind the intermaxillary joint (Norman et al. 2011, fig. 10: "mxs"). The premaxillary-vomeral contact could exist in *Yinlong downsi*, although we interpret that the actual joint suture of the anterior diamond-shaped vomeral head might also be obscured from a ventral view as in *H. tucki* (Han et al. 2015, p. 11, 12). The vomers largely contact the premaxillae anteriorly in *Tenontosaurus tilletti* (Thomas 2015, fig. 6), *Tenontosaurus dossi* (Winkler et al. 1997, fig. 2-4; Andrzejewski et al. 2019 #84), *Thescelosaurus necglectus* (Boyd 2014, fig. 5C), *Lesothosaurus diagnosticus* (Sereno 1991, fig. 12D). In *Orodromeus makelai*, Scheetz (1999, p.30) declares that "[The rostral end of the vomers] joins the anterior ramus of the maxilla into the posterior end of the premaxilla, over the palate", so we deduce that an intermaxillary contact was absent. *T. tilletti*, *T. neglectus* and *O. makelai*, *L. diagnosticus* were corrected and coded (0). *Y. downsi* was corrected and coded (1).

30(*). Premaxilla-prefrontal contact: absent (0) or present (1) (Xu et al. 2006 #23).

The premaxillaries of *Dryosaurus altus* (Galton 1983, fig. 2A), *Dysalotosaurus lettowvorbecki* (Janensch 1955, fig. 1A), *Camptosaurus dispar* (Gilmore 1909, fig. 2) and *Iguanodon bernissartensis* (Norman 1980, fig. 2) contact the prefrontal: they were coded (1) contra Xu et al. (2006 #23). According to Norman et al. (2011) and Sereno (2012, p. 94), the posterolateral process of premaxilla of *Heterodontosaurus tucki* would insert between the lacrimal and prefrontal. Therefore *H. tucki* was coded (1). This differs from what is observed in another heterodontosaurid: *Tianyulong confuciusi*, which lateral process of premaxilla extends far away in direction of the prefrontal but doesn't properly reach it (Zheng et al. 2009, fig. 1D). Worth of note is that *Psittacosaurus mongoliensis* has a premaxilla contacting the prefrontal (Sereno et al. 1988, fig. 5), as *Liaoceratops yanzigouensis* (Xu et al. 2002). By contrast, *Yinlong downsi* (Han et al. 2015), *Stenopelix valdensis* (Butler and Zhao 2009) and pachycephalosaurs (e.g. *Prenocephale prenes* or *Stegoceras validum*, Maryanska and Osmolska 1974) do not feature a premaxillary-prefrontal contact.

31(*). Maxilla, prominent anterolateral boss articulates with the medial premaxilla: absent (0), present (1) (Ösi et al. 2012 #24).

The maxillary anterolateral boss of *Thescelosaurus neglectus* described by Boyd (2014, cf. fig. 5A) and *Talenkauen santacrucensis* (Novas et al. 2004, fig. 2A) is far from looking as prominent as in *Zephyrosaurus schaffi* (Sues 1980, cf. fig. 3) or *Orodromeus makelai* (Scheetz 1999, cf. fig. 5). No anterolateral boss appears in the maxilla of *Kulindadromeus zabaikalicus* (INREC K4/42, Godefroit et al. 2014, fig. S4D). As a whole, this character strengthens the distinctiveness of the *Orodromeus*+*Zephyrosaurus* clade. *T. neglectus*, *T. santacrucensis* and *K. zabaikalicus* were corrected and coded (0).

32(*). Maxilla, at least a small prolongation that bulges out in front of the anterior edge of the maxillary ascending process (not considering the ventral premaxillary process): absent (0), present (1) (Ösi et al. 2012 #25).

Psittacosaurus major and *Psittacosaurus mongoliensis* (Sereno 2010, fig. 2.3, 2.7) differ from other ceratopsians in having their maxillae bulging at some height in front of the anterior ascending process of maxilla. We disagree with Andrzejewski et al. (2019) and keep character state (1) for *Tenontosaurus dossi*: a break in slope in front of the anterior ascending maxillary process could be observed in figure 3B of Winkler et al. (1997).

33(*). Maxilla, buccal emargination: absent (0), present (1) (Ösi et al. 2012 #26).

Lesothosaurus diagnosticus is told to have no maxillary buccal emargination (Porro et al. 2015, p. 11). In *Scelidosaurus harrisonii*, Owen (1861*b*) desribes a longitudinal ridge which separates the lateral side of the maxillary 'into an upper and lower facet'. He adds : 'there is a lower and slighter longitudinal prominence of the maxillary along the outer alveolar plate'. However, no proper buccal emargination was described. In *Emausaurus ernsti* (Haubold 1990) there appears to be no buccal emargination as well. The maxillary tooth row of *Kulindadromeus zabaikalicus* is told to be bordered dorsally by a salient crest, although there

would be no 'true buccal emargination' (Godefroit et al. 2014, supplementary material). The interpretation of the presence or absence of such a feature in *K. zabaikalicus* is hindered by the squashed nature of the skull. *L. diagnosticus*, *S. harrisonii*, *E. ernsti* were corrected and coded (0). *S. lawleri* and *K. zabaikalicus* were corrected and coded with a question mark.

34(*). Maxilla, eminence on the rim of the buccal emargination of the maxilla near the junction with the jugal: absent (0), present (1) (Ösi et al. 2012 #27; Xu et al. 2006 #24).

In *Isaberrysaura mollensis* (Salgado et al. 2017), the buccal maxillary rim is not eminent. By contrast, the buccal emargination of the maxilla near the junction with the jugal is much pronounced in *Archaeoceratops oshimai* (You and Dodson 2003). *I. mollensis* was corrected and coded (0). *A. oshimai* was corrected and coded (1).

35(*). External antorbital fenestra, shape (regardless of position): triangular (0), oval or circular (1) (modified from Ösi et al. 2012 #22).

In *Hypsilophodon foxii* (Galton 1974*a*, fig. 3), *Orodromeus makelai* (Scheetz 1999, fig. 4), *T. santacrucensis* (Cambiaso 2007, fig. 8A), *Convolosaurus marri* (Andrzejewski et al. 2019) and *Kulindadromeus zabaikalicus* (Godefroit et al. 2014, fig. 1C), the antorbital fenestra is rounded and subcircular. The antorbital fenestra of *Scelidosaurus harrisonii* looks basally elongated with both an acute posterodorsal and posteroventral corner (Owen 1861, pl. 4). In *Yinlong downsi* the antorbital fossa appears triangular in outline, except that the anterior process of jugal overlaps the posterior corner of the antorbital fenestra, thus giving it a more rounded aspect (Han et al. 2015, fig. 2A). In psittacosaurs, the antorbital fenestra disappeared (Sereno 2000). Witin the "Asian clade", *Haya griva*, *Jeholosaurus shangyuanensis* and *Changchunsaurus parvus* have a triangular antorbital fenestra (Makovicky et al. 2011, fig. 1A; Barrett and Han, 2009, fig. 5A, F; Liyong et al. 2010, fig. 1 respectively). In the dryomorphans *Dysalotosaurus lettowvorbecki* (Janensch 1955, fig. 1), *Camptosaurus dispar* (Gilmore 1909, fig. 2), *Iguanodon bernissartensis* (Norman 1980, fig. 2), but not *Dryosaurus*

(Galton 1983, fig. 5A), the external antorbital fenestra is posteriorly much thinner, so it also appears subtriangular. In *Tianyulong confuciusi* (Sereno 2012, fig. 23) and *Stegosaurus stenops* (Gilmore 1914, pl. 5), the real contour of this antorbital fenestra is not well delineated. *Y. downsi* was corrected and coded (0) as also occurs for other ceratopsians. *C. parvus*, *D. lettowvorbecki*, *C. dispar*, *I. berissartensis* and *S. harrisonii* were corrected and coded (0). *C. marri*, *H. foxii*, *T. santacrucensis*, *K. zabaikalicus* were corrected and coded (1). Psittacosaurs were corrected and coded with a hyphen (non-applicable state) for all characters dealing with the antorbital fenestra. *T. confuciusi* and Stegosauria were corrected and coded with a question mark.

36(*). Antorbital fenestra, position of the posterior part with respect to the orbit: passes below the orbit (0), next to or anterior to the orbit (1) (new character).

In *Tianyulong confuciusi* (Sereno 2012, fig. 21), the jugal seems to wraps around the orbit anteriorly, so the antorbital fenestra should be much more anteriorly located with respect to it. The real contour of this antorbital fenestra is not well delineated (Sereno 2012, fig. 23). The relative position of the antorbital fenestra was never really discussed in pachycephalosaurs. The only taxon for which it appears clearly is *Prenocephale prenes* (Sullivan 2006, fig. 6), which displays an anteriorly located, rounded antorbital fenestra. The cranial density map of *Stegoceras validum* (Snively and Theodor 2011, fig. 1C) reveals that the antorbital fossa of *Stegoceras validum* was situated well anterior to the orbit. *Haya griva* (Makovicky et al. 2011, fig. 1A) differs from *Jeholosaurus shangyuanensis* (Barrett and Han, 2009, fig. 5A) and *Changchunsaurus parvus* (Liyong et al. 2010) in having an anteriorly located antorbital fenestra. Barrett et al. (2005) also use this character – amongst others – to distinguish between *Hexinlusaurus multidens* and *Agilisaurus louderbacki*: the first has an antorbital fenestra underlying the orbit, and the latter has an antorbital fenestra much more anteriorly located.

37(*). External antorbital fenestra, exclusion of the jugal from the posteroventral margin by lacrimal–maxilla contact: absent (0), present (1) (Ösi et al. 2012 #34; Xu et al. 2006 #79).

The antorbital fenestra of *Iguanodon bernissartensis* is separated from the anterior branch of the jugal (Norman 1980, fig. 2) so this taxon was recoded (1). We follow Bell et al. (2019 #35) who corrected and coded *Muttaburrasaurus langdoni* and coded it with a question mark, instead of (1) previously.

38(*). External antorbital fenestra, maximum diameter: 60% or more of orbital diameter (0), approximately 50% of orbital diameter (1) or very small or absent (2) (modified from Xu et al. 2006 #38).

In *Kulindadromeus zabaikalicus*, the external antorbital fenestra is very large and makes rhoughly 60% of the orbit length (Godefroit et al. 2014, fig. 1B). The skull reconstruction of *Abrictosaurus consors* shows a relatively large antorbital fossa (Sereno 2012, fig. 34, 35. Despite this taxon doesn't preserve its orbit, the global skull length is appreciable and the antorbital fossa would have been as large as for *Heterodontosaurus tucki* (Sereno 2012, fig. 57, 58). In *Archaeoceratops oshimai* (You and Dodson 2003, fig. 1A) and *Liaoceratops yanzigouensis* (You et al. 2007, fig. 1E) the antorbital length is roughly half that of the orbit, whereas in *Yinlong downsi* (Han et al. 2018, fig. 2) the antorbital length is much less than half that of orbit. In *Hexinlusaurus multidens* (He and Cai 1984, fig. 3), the antorbital fossa length approaches half of the orbital length (14.8mm. /32.3mm. = 46%), this taxon was therefore coded (1). The same occurs for *Agilisaurus louderbacki* (Peng 1992, fig. 1A). In *Haya griva* (Makovicky et al. 2011, fig. 1A) and *Jeholosaurus shangyuanensis* (Barrett and Han, 2009, fig. 5A) the external antorbital fenestra is roughly half the orbital length. In *Changchunsaurus parvus*, however, the external border of this fenestra is uncertain (Liyong et al. 2010) so this taxon was coded with a question mark. In the "elasmarian" *Parksosaurus warreni* (Galton 1973, fig. 1; Weishampel et al. 2003 #3), and *Gasparinisaura cincosaltensis* (Coria and

Salgado 1996, fig. 2B; Weishampel et al. 2003 #3) the antorbital fenestra accounts for much less than half of the orbit, but this is curiously not the case for *Thescelosaurus neglectus* (Boyd 2014) which keeps a larger antorbital fenestra. The former two taxa were therefore coded (2) and the latter was coded (1). The antorbital fossa is also very small in *Orodromeus makelai* (Scheetz 1999, fig. 3) and *Hypsilophodon foxii* (Galton 1974*a*, fig. 4) so these taxa were coded (2).

39(*). Internal antorbital fenestra, length relative to skull length: large, generally at least 15 % (0), very much reduced, less than 10% (1), or absent (2) (modified from Ösi et al. 2012 #20).

An internal antorbital fenestra is present in *Kulindadromeus zabaikalicus* (Godefroit et al. 2014, fig. 1B). According to Maryanska and Osmolska (1974), and to the exception of *Prenocephale prenes*, the pachycephalosaurs *Homalocephale calathocercos*, *Pachycephalosaurus wyomingensis*, and *Stegoceras validum* all lack an antorbital foramen. This feature is not known in *Goyocephale lattimorei* (Perle et al. 1982). *K. zabaikalicus* was corrected and coded (1). *H. calathocercos* was corrected and coded (2). *G. lattimorei* was corrected and coded with a question mark.

40(*). Antorbital fenestra, position: level or higher than the orbit (0), anteroventral to the orbit (1) (modified from Xu et al. 2006 #77).

In the pachycephalosaurs *Pachycephalosaurus wyomingensis*, *Stegoceras validum* (Brown and Schlaikjer 1943, pl. 38 and 44 respectively), *Prenocephale prenes* (Sullivan 2006, fig. 6A) the antorbital fenestra is situated ventrally with respect to the orbit. In basal ornithopods such as *Zephyrosaurus schaffi* (Sues 1980, fig. 16), *Orodromeus makelai* (Scheetz, fig. 3), *Hexinlusaurus multidens* (He and Cai 1984, fig. 3), the basal height of the antorbital fossa is level with that of the orbit. These taxa are therefore coded (0). In *Muttaburrasaurus langdoni* the antorbital fenestra appears at least at the same level as the orbit anteriorly (Molnar 1996, fig. 5), as also occurs for its congeneric species from Dunluce (Molnar 1996, fig. 7B).The

lacrimals of *Dysalotosaurus lettowvorbecki* (Janensh, 1955, pl. 10.7A) and of *Dryosaurus altus* (Galton 1983, fig. 3O-P, pl. 1.1) are reminiscent of the primitive condition and show an antorbital fossa which is located below the ventral margin of the orbit. In *Tenontosaurus dossi* (Winkler et al. 1997, fig. 3) and *Tenontosaurus tilletti* (Thomas 2015) the external antorbital fossa is ventrally deflected, so these taxa were coded (1).

41(*). Prominent horizontal ridge under the antorbital fossa: absent (0) or present (1) (Xu et al. 2006 #78).

Sereno (2012, p. 102) states that in *Heterdontosaurus tucki*, "the ventral border of the external antorbital fenestra is straight, relatively sharp edged, and strongly everted, as in all heterodontosaurids preserving this region of the maxilla". The heterodontosaurid *Echinodon becklesii* was confirmed to bear such rim ventral to its antorbital fenestra as well in spite of previous considerations (Sereno 2012). Therefore, *H. tucki*, *Manidens condoriensis*, *Abrictosaurus consors*, *Lycorhinus angustidens*, *Tianyulong confuciusi*, *Echinodon becklesii* could safely be coded (1) for this character. A "salient crest" is reported above the maxillary tooth row of *Kulindadromeus zabaikalicus* (Godefroit et al. 2014, supplementary material).

42(*). Nasals, depression present along sutural line of the bones: absent (0), present (1) (modified from Ösi et al. 2012 #19; Xu et al. 2006 #82).

In *Thescelosaurus neglectus,* Boyd (2014, see fig.3) states that 'there is no evidence of a midline depression on the nasals'. Concerning *Lesothosaurus diagnosticus*, Porro et al. (2015) stand that 'in transverse section each nasal is dorsally arched, so that the midline contact between them lies in a shallow depression that extends along the top of the snout'. Liyong et al. (2010) report a shallow median depression along the nasals of *Changchunsaurus parvus*. Following Osborn (1923, fig. 2C), *Psittacosaurus mongoliensis* should also be corrected and coded (1). Pachycephalosaurs were previously coded (0) for this character. However, (Perle et al. 1982, p. 121) state that "the medial part of the cranial roof in *G. lattimorei* is slightly

depressed along the frontals and posterior part of the nasals […]". The same slight median depression is described in *Stegoceras validum* (Gilmore 1924, p. 15; Brown and Shlaikjer, 1943, pl. 44) as well as in *Prenocephale prenes* (Maryanska and Osmolska 1974, p.54). This feature should be viewed as homologous to the other taxa median nasals depression. *Hypsilophodon foxii* was never described to bear an elliptical fossa between its nasals, and no figure supports this statement (Galton 1974*a*). The same happens with *Orodromeus makelai* (Scheetz 1999) which only preserves a crushed nasal (MOR 473) with no further information available. *T. neglectus* was corrected and coded (0). *L. diagnosticus*, *C. parvus*, Psittacosauridae, *G. lattimorei* were corrected and coded (1). *H. foxii* and *O. makelai* were corrected and coded with a question mark.

43(*). Frontal, contacts orbit: along more than 25% of total frontal length (0), less than 25% (1), excluded from orbital margin (2) (modified from Butler et al. 2011; Brown et al. 2013 #24).

Psittacosaurus mongoliensis (Sereno 2010, fig. 1.11) and *Psittacosaurus major* (You et al. 2008, fig. 1A) have their frontal contacting with the orbit for more than 25% of their length. *P. mongoliensis* and *P. major* were newly coded (0). By contrast, pachycephalosaurs are well known for having their frontals excluded from the orbital margin because of their supraorbital bones (e.g. Maryanska and Osmolska 1974). *Stegoceras validum* (Gilmore 1924), *Prenocephale prenes*, *Homalocephale calathocercos* (Maryanska and Osmolska 1974), *Goyocephale lattimorei* (Perle et al. 1982) and *Pachycephalosaurus wyomingensis* (Brown and Shlaikjer, 1943) were all coded (2).

44(*). Frontal, ratio of frontal length to nasal length: greater than 120% (0), between 120% and 60% (1) or less than 60% (2) (Brown et al. 2013 #25).

In *Goyocephale lattimorei* the sutures between the parietal and the frontal are still visible and make at most between 120% and 60% of nasal length (Perle et al. 1982, pl. 41-1A). The ratio of frontal length to nasal length is greater than 120% in *Psittacosaurus major* (You et al.

2008, fig. 1A) and *Psittacosaurus mongoliensis* (Sereno 2010, fig. 2.11). In *Yinlong downsi*, the frontals are much longer than the nasals (Han et al. 2015, fig. 4), which is very different from what is observed in more derived ceratopsians such as *Archaeoceratops oshimai* (Dong and Azuma 1997, fig. 2) or *Liaoceratops yanzigouensis* (Xu et al. 2002, fig. 1C). In *Emausaurus ernsti* the ratio of frontal length to nasal length is between 120% and 60% (Haubold 1990, fig. 2). *Kulindadromeus zabaikalicus* lacks the anterior tip of its nasals, yet the frontals length is less than 60% that of the preserved portion of the nasals (Godefroit et al. 2014, fig. 1B). In *Stegosaurus stenops*, the frontals are very short with respect to the nasals (cf. Marsh 1887, pl. 6-1). *P. major* and *P. mongoliensis* were newly coded (0). *Y. downsi* was corrected and coded (0). *G. lattimorei* and *E. ernsti* was corrected and coded (1). Stegosauria was corrected and coded (2).

45(*). Frontals, each one are short and broad (0), narrow and elongate (at least twice as long as wide) (1) (reformulated from Ösi et al. 2012 #64).

In *Convolosaurus marri* (Andrzejewski et al. 2019, fig. 9D) the frontals are only slightly narrower as they are long. *C. marri* was corrected and coded (0).

46(*). Frontals arching over orbit from lateral view: present (0), absent, frontals dorsally flattened over orbit (1) (Boyd 2015 #65).

Frontals appear to be plate-like above the orbital margin in Psittacosaurids (*P. major*, You et al. 2008, fig. 1B; *P. mongoliensis*, Sereno 2010, fig. 2.7). This feature is not accessible for *Nanosaurus agilis* (Carpenter and Galton 2018). In *Orodromeus makelai*, the only information concerning this character comes from a frontal from the juvenile skull in lateral view (Scheetz 1999, fig. 3). No description allows to infer that the frontal was arched over the orbit in the adult specimen. In *Jeholosaurus shangyuanensis*, the frontals from the adult specimen are poorly preserved and can't be seen from a lateral view (Barrett and Han, 2009).

P. major, *P. mongoliensis* were newly coded (1). *N. agilis*, *O. makelai* and *J. shangyuanensis* were corrected and coded with a question mark.

47(*). Lacrimal-jugal contact: jugal doesn't, or barely touches lacrimal (0), jugal meets lacrimal with more contact (1) (modified from Brown et al. 2013 #50).

The "butt-joint" contact was judged too difficult to characterize within the large variety of possible jugallacrimal contacts. Therefore this character state was merely removed. In *Hexinlusaurus multidens*, the maxillary process of the jugal barely touches the lacrimal (He and Cai 1984). In *Yandusaurus hongheensis*, the lacrimal-jugal contact is not preserved (He and Cai 1984). As in *Convolosaurus marri* (Andrzejewski et al. 2019, fig. 6-7), the jugal of *Hypsilophodon foxii* (Galton 1974*a*, fig. 3) only barely touches the lacrimal. In *Manidens condorensis* (Pol et al. 2011, fig. 2B) the maxillary process of the jugal is overlapped by the maxilla anteriorly, so it would have been excluded from contact with the lacrimal. However, in *Heterodontosaurus tucki* (Norman et al. 2011) and *Tianyulong confuciusi* (Zheng *et al*. 2009), the lacrimal appears well sutured to the jugal. The anterior process of jugal is well sutured to the lacrimal in psittacosaurs (*P. major*, You et al. 2008, fig. 1B; *P. mongoliensis*, Sereno 2010, fig. 2.7). *H. multidens* and *H. foxii* were corrected and coded (0). *O. makelai*, *T. neglectus*, *I. bernissartensis* were corrected and coded (1). *P. major*, *P. mongoliensis* were newly coded (1). *Y. hongheensis* was corrected and coded with a question mark.

49(*). Lacrimal-nasal contact: present (0), absent (1) (new character).

A naso-lacrimal contact is present in *Heterodontosaurus tucki* (Norman et al. 2011, fig. 4, although not described), *Tianyulong confuciusi* (Zheng et al. 2009, fig. 1C, D), *Archaeoceratops oshimai* (You and Dodson 2003, fig. 1A, p. 263, although this view is contradicted by Han et al. 2015, p. 14). Xu et al. (2006 #34) coded for the presence of a premaxilla-lacrimal contact in *Yinlong downsi*. If a premaxilla-lacrimal contact did exist (Han et al. 2015, fig. 8B), the anterior lacrimal branch would have necessarily contacted with the

nasal as well. However, Han et al. (2015, p. 14) states that the lacrimal does not contact the nasal in *Yinlong downsi*. We however regard such contact as present on account of sutural contacts preserved in IVPP V18636 (Han et al. 2015, fig. 8). A lacrimal-nasal contact is also observable in IVPP V14530 (Han et al. 2015, fig. 3), although in this specimen the anterior lacrimal branch of the left and right sides should have been broken. The lacrimal fails to meet the nasal in psittacosaurids (e.g. You et al. 2008, fig. 1B), and in the pachycephalosaurs *Prenocephale prenes* and *Stegoceras validum* (Maryanska and Osmolska 1974, fig. 1A1, C1). In *Liaoceratops yanzigouensis* the prefrontal-premaxilla contact would have prevented the nasolacrimal contact (Xu et al. 2002). However, in other derived neoceratopsians the nasal do also contact with the lacrimal (You and Dodson 2003; Han et al. 2015, p. 14). Let's note that a naso-lacrimal contact should be plesiomorphic for Marginocephalia, as it is also present in the neornithischian *Agilisaurus louderbacki* (Peng 1992, fig. 1A) and in early ornithopods such as *Jeholosaurus shangyuanensis* (Barrett and Han, 2009). The lacrimal of *Hexinlusaurus multidens* fails to contact the nasals because of the posterior expansion of the maxilla (He and Cai 1984, fig. 3). In dryomorphans (*Camptosaurus dispar*, Gilmore 1909, fig. 2; *Dryosaurus altus*, Galton 1983, fig. 2; *Dysalotosaurus lettowvorbecki*, Galton 1983, fig. 5C; *Iguanodon bernissartensis*, Norman 1980, fig. 2) the lacrimal is excluded from contact with the nasal, and contacts the posterior premaxillary process. This is in clear contrast with what occurs in *Tenontosaurus tilletti* (Thomas 2015), *Thescelosaurus neglectus* (Brown et al. 2013; Boyd 2014), *Zalmoxes robustus* (Weishampel et al. 2003) where the lacrimal contacts the nasals and the posterior premaxillary process doesn't reach the lacrimal. Unfortunately, no information concerning such contact is available for *Muttaburrasaurus langdoni* (Bartholomai and Molnar, 1981). Interestingly, *Hypsilophodon foxii* (Galton 1974*a*, fig. 4A) and *Orodromeus makelai* (Scheetz 1999, fig. 4) display intermediate features in these respects among ornithopods. They have a lacrimal which still contacts with the nasal, and an elongated

posterior premaxillary process. However, the posterior premaxillary process wouldn't reach the lacrimal posteriorly, or at least, this feature is neither described nor clearly figured in *H. foxii* (Galton 1974*a*, fig. 7A). Sereno (1991) states that in three specimen of *Lesothosaurus diagnosticus*, the lacrimal makes a short contact with the nasal (BMNH R8501, RUB23, R11956). We therefore coded (0) for this taxon.

50(*). Accessory ossification(s) in the orbit (palpebral/supraorbital): absent (0), present (1) (Ösi et al. 2012 #29; Xu et al. 2006 #68).

Contra Xu et al. (2006) scorings, the supraorbitals bones I and II that make the dorsal margin of the orbit in pachycephalosaurs should be considered as homologous to the palpebral and supraorbital of other ornithischians (Coombs 1972).

52(*). Palpebral, shape in dorsal view: rod-shaped (0), plate-like with wide base (1) (Ösi et al. 2012 #31).

The palpebral (or supraorbital) of *Thescelosaurus neglectus* (Boyd 2014, fig. 17B) and *Tenontosaurus tilletti*, Thomas (2015, p. 33) is dorsoventrally flattened. In *Orodromeus makelai,* "the supraorbital is slightly wider transversely than it is vertically, with a sharp lateral edge" (Scheetz 1999 p. 17). However, the supraorbital is too small to assess more firmly for a plate-like shaped palpebral. *T. neglectus* and *T. tilletti* were corrected and coded with character state (1). *O. makelai* was corrected and coded with a question mark.

54(*). Supraorbital(s) horizontal extension across the orbit (wether fused or not to the orbital margin) : contact the postorbital posteriorly (0), does not contact the postorbital, but crosses at least half of the orbit (1), crosses less than half of the orbit (2) (modified from Boyd 2015 #25).

All pachycephalosaurs for which a skull is preserved (Maryanska and Osmolska 1974, fig. 1), ankylosaurs (see *Pinacosaurus grangeri*, in Maidment and Porro 2010), *Stegosaurus stenops* (Marsh 1887), *Isaberrysaura mollensis* (Salgado et al. 2017), *Scelidosaurus harrisonii* (Owen

1861) have supraorbitals bones crossing their whole orbit. In *Abrictosaurus consors*, the supraorbital bones are incomplete (Sereno 2012, fig. 34B). Pachycephalosaurs, Ankylosauria, *S. stenops*, *I. mollensis*, *S. harrisonii* were corrected and coded with character state (0). *A. consors* was corrected and coded with a question mark.

55(*). Lower margin of the orbit circular (0), lower margin of the orbit subrectangular (1) (Boyd 2015 #95).

The lower orbital margin of psittacosaurids (*P. mongoliensis*, Osborn 1923 fig. 2A and *P. major*, You et al. 2008, fig. 1B) is circular. Note that in *Convolosaurus marri* (Andrzejewski et al. 2019, fig. 8) the straight posterior edge of the lacrimal gives the orbit a subrectangular aspect. In *Zalmoxes robustus*, the area for contact with the lacrimal is not preserved (Weishampel et al. 2003). In *Zalmoxes shqiperorum*, the jugal anterior process is slightly curved upward with a concave dorsal surface (Godefroit et al. 2009, fig. 3), but the lacrimal is not preserved. In *Muttaburrasaurus langdoni*, the lacrimal is not sufficiently well preserved (Bartholomai and Molnar, 1981). Psittacosaurs were corrected and coded (0). Both *Zalmoxes* species, and *M. langdoni* were corrected and coded with a question mark.

56(*). Depression on lateral surface of postorbital, : absent, the lateral surface is devoid of any pronounced depression, and varies from smoothly concave to smoothly convex over the whole postorbital anteroposteriorly (0); present and well-demarcated, opens posteriorly toward infratemporal fenestra (1); present on the anterior side toward the orbit (2) (modified from Xu et al. 2006 #86; Pol et al. 2011 #229).

Xu et al. 2006 (#86) recognized the presence of a flange crossing the lateral surface of the postorbital in *Yinlong downsi* and *Heterodontosaurus tucki*, which demarcates some lateral concavity. However, Han et al. (2015) only distinguished the presence of such flange on one side of a single skull of *Yinglong downsi*, so they dismissed this character as diagnostic to this taxon. Furthermore, Han et al. (2015, p. 15) describe the postorbital of *Yinlong downsi* as

laterally flat to smoothly concave, so any homology with the postorbital of *H. tucki* doesn't hold. The postorbital of *Archaeoceratops oshimai* was described as plate-like, and appears to be broadly and smoothly concave anteroposteriorly (You and Dodson 2003, fig. 1A, p. 264). A lateral concavity of the postorbital (Pol et al. 2011 #229) is found under a variety of forms within Ornithischia. In the Asian ornithopods *Jeholosaurus shangyuanensis* (Barrett and Han, 2009), *Changchunsaurus parvus* (Liyong et al. 2010) the lateral surface of the postorbital is only very smoothly concave anteroposteriorly so we consider it as plate-like. The postorbitals of *Scelidosaurus harrisonii* (Owen 1861, pl. 4, 5), *Stegosaurus stenops* (Gilmore 1914, pl. 5), *Lesothosaurus diagnosticus* (Porro et al. 2015, p. 17), *Agilisaurus louderbacki* (Barrett et al. 2005), *Hypsilophodon foxii* (Galton 1974*a*), *Orodromeus makelai* (Scheetz 1999, fig. 7E), *Haya griva* (Makovicky et al. 2011, fig. 1B), do not feature a marked lateral depression, but are rather flat to smoothly convex laterally. Within Ankylopollexia, the postorbital of *Camptosaurus dispar* (Gilmore 1909, fig. 2, p. 212) and *Iguanodon bernissartensis* (Norman 1980, fig. 2, 3, p 22) does not seem to feature any lateral cavity either. In *Hexinlusaurus multidens* (Barrett et al. 2005, fig. 1D), the cavity is pronounced and covers most of the lateral surface of the postorbital. As to what regards pachycephalosaurs, Gilmore (1924, p. 17) described the postorbital of *Stegoceras validum* as follow: "the lateral edge [of the postorbital] is slightly raised, more especially at the anterior end, thus forming behind it a shallow, longitudinal depression, which becomes more pronounced as it passes forward above the orbit". Such depression is well visible on the anterior part of the postorbital and continues onto the postfrontal anteriorly above the orbits in *S. validum* (Gilmore 1924, pl. 1; Brown and Schlaikjer 1943, pl. 44.2) and *Prenocephale prenes* (Sullivan 2006, fig. 6A). It appears absent in *Pachycephalosaurus wyomingensis* (Brown and Schlaikjer 1943, pl. 38). In heterodontosaurids such as *H. tucki* (Norman et al. 2011, fig. 4A) or *M. condoriensis* (Pol et al. 2011, fig. 1G), the concavity is found on the posterior part of the postorbital and is

bordered anteriorly by a rim. In *Psittacosaurus mongoliensis*, the jugal and squamosal branches are very thin, and a conspicuous posterodorsal concavity borders the infratemporal fenestra (Sereno 2000, fig. 25.5). In *Psittacosaurus major* (You et al. 2008, fig. 1B), the lateral aspect of the postorbital appears to feature some concavity, but this is only hardly suggested from the figures. In the ornithopods *Thescelosaurus neglectus* (Boyd 2014, fig. 7C), *Tenontosaurus tilletti* (Thomas 2015, fig. 26), *Tenontosaurus dossi* (Winkler et al. 1997, fig. 3A), *Zalmoxes robustus* (Weishampel et al. 2003, fig. 8A), *Zalmoxes shqiperorum* (Godefroit et al. 2009, fig. 7B), *Mochlodon vorosi* (Ösi et al. 2012, fig. 2I), the lateral concavity (presumably for the insertion of the adductor jaw musculature) is found toward the posterior infratemporal region of the postorbital. *Zephyrosaurus schaffi* likely presents a posterior concavity, although this is only suggested from a drawing (Sues 1980, fig. 7C). *S. harrisonii*, *S. stenops* (for Stegosauria), *A. louderbacki*, *Y. downsi*, *A. oshimai*, *H. foxii*, *J. shangyuanensis*, *O. makelai*, *C. dispar* and *I. bernissartensis* (for Ankylopollexia) were corrected and coded (0). *P. mongoliensis* (for Psittacosauridae), *H. multidens*, *T. neglectus*, *T. tilletti* and *T. dossi*, *Z. robustus* and *Z. shqiperorum* (for Rhabdodontidae), were corrected and coded (1).

57(*). Squamosal process of postorbital relative to the jugal process: much shorter (0) or subequal or longer (1) (Xu et al. 2006 #83).

A longer jugal process of postorbital is observed in *Herrerasaurus ischigualastensis* (Sereno and Novas 1993, fig. 1A), *Lesothosaurus diagnosticus* (Sereno 1991, fig. 12A), and every tyreophoran (*Scelidosaurus harrisonii,* Owen 1861, pl. 5; *Emausaurus ernstii*, Haubold 1990, fig. 2; *Stegosaurus stenops*, Marsh 1887, pl. 6; the ankylosaur *Pinacosaurus grangeri*, Maidment and Porro 2010, fig. 4E), so character state (0) must be plesiomorphic to ornithischians. In *Wannanosaurus yansiensis* (Butler and Zhao 2009, fig. 6C) the squamosal process of postorbital is shorter than the jugal process. In derived pachycephalosaurs,

definition of this character is difficulted by the backward inclination of the infratemporal opening, and by the fusion of the supraorbitals dorsally to the postorbital. We define the dorsal limit of the postorbital jugal branch, as the point level with the upper border of the infratemporal fenestra. This upper border should be as high as possible, so that the distance between it and the last supraorbital is as short as possible. In such case, *Tylocephale gilmorei* and *Homalocephale calathocercos* (Maryanska and Osmolska 1974, fig. 1B, D) have clearly a taller jugal branch. By contrast, such feature is much more problematical in *Stegoceras validum* and *Prenocephale prenes* (Maryanska and Osmolska 1974, fig. 1A, C), where the postorbital is inclined anteroposteriorly. The latter two taxa were coded has bearing subequal jugal and squamosal branches. *Hexinlusaurus multidens* (He and Cai 1984) and *Agilisaurus louderbacki* (Peng 1992) also retain the pleiosmorphic character state of a longer jugal branch on their postorbital. The jugal process of *Dryosaurus altus* is longer than the squamosal process (Galton 1983, fig. 5B), but not in *Dysalotosaurus lettowvorbecki* (Janensch, fig. 1A), where they are subequals. In the rhabdodontids *Zalmoxes shqiperorum* (Godefroit et al. 2009, fig. 7B), *Z. robustus* (Weishampel et al. 2003, fig. 8C-E) and *Mochlodon vorosi* (Ösi et al. 2012, fig. 2K), the jugal process of postorbital is almost unexpanded ventrally. *Z. shqiperorum* and *M. vorosi* were coded (1). In *Z. robustus*, the squamosal process is broken (Weishampel et al. 2003) so this taxon could not be coded for this character.

58(*). Postorbital: inverted ‘L’-shaped (0), triangular and plate like with normal expansion of squamosal process (1), triangular and plate-like with a very short squamosal process (2) (modified from Xu et al. 2006 #11).

The postorbital shape of *Homalocephale calathocercos* and that of *Tylocephale gilmorei* could still be considered as looking as an “inverted-L” (Maryanska and Osmolska 1974, fig. 1D). *H. calathocercos* was coded (0) instead of the previous non-applicable state. Other pachycephalosaurs such as *Stegoceras validum*, *Prenocephale prenes*, *Pachycephalosaurus*

wyomingensis have a plate-like postorbital which is not triangular in outline (Maryanska and Osmolska 1974): they were left coded with a dash-line. Derived ceratopsians such as *Liaoceratops yanzigouensis* (Xu et al. 2002) and *Archaeoceratops oshimai* (You and Dodson 2003) are not the only taxa which feature a triangular and plate-like postorbital. The squamosal and jugal branches of postorbital are nearly aligned to each other and form a triangular plate with the anterior branch, in a number of other ornithischians. These include: *Haya griva* (Makovicky et al. 2011, fig. 1B), *Changchunsaurus parvus* (Liyong et al. 2010, fig. 1), *Jeholosaurus shangyuanensis* (Barrett and Han, 2009, fig. 3A), *Orodromeus makelai* (Scheetz 1999, fig. 7E), *Zephyrosaurus schaffi* (Sues 1980, p. 59), *Kulindadromeus zabaikalicus* (Godefroit et al. 2014, fig. 1B), *Gasparinisaura cincosaltensis* (Coria and Salgado 1996, fig. 2), *Thescelosaurus neglectus* (Boyd 2014, fig. 2), *Hexinlusaurus multidens* (He and Cai 1984, fig. 3), *Mochlodon vorosi* (Ösi et al. 2012, fig. 2), *Zalmoxes robustus* (Weishampel et al. 2003, fig. 8-C, D), *Zalmoxes shqiperorum* (Godefroit et al. 2009, fig. 7), *Tenontosaurus tilletti* (Thomas 2015, fig. 2), *Tenontosaurus dossi* (Winkler et al. 1997, fig. 4), *Iguanodon bernissartensis* (Norman 1980, fig. 2). This part of the skull is incomplete in *Parksosaurus warreni* (Parks 1926, pl. 1) and damaged in *Muttaburrasaurus langdoni* (Bartholomai and Molnar, 1981). In *Camptosaurus dispar* (Gilmore 1909, fig. 2), *Hypsilophodon foxii* (Galton 1974*a*, fig. 4A), *Dryosaurus altus* and *Dysalotosaurus lettowvorbecki* (Galton 1981, fig. 5A, C), the jugal and squamosal branch of postorbital form a conspicuous arch so that both are nearly oriented at right angle with each another at their extremity. Within Tyreophora (*Stegosaurus stenops*, *Scelidosaurus harrisonii*, *Emausaurus ernstii*, *Pinacosaurus grangeri*, see Marsh 1887, pl. 6; Owen 1861, pl. 5; Haubold 1990, fig. 2; Maidment and Porro 2010, fig. 4E respectively) the postorbital ressembles a “plate-shape” and the squamosal process of the postorbital is very short and/or dorsally inclined.

Contrary to other ornithopods, *C. dispar*, *H. foxii*, *Dryosaurus*, *D. lettowvorbecki* were left coded (0). *H. griva*, *C. parvus*, *J. shangyuanensis*, *O. makelai*, *Z. schaffi*, *G. cincosaltensis*, *T. neglectus*, *H. multidens*, *M. vorosi*, *Z. robustus*, *Z. shqiperorum*, *T. tilletti*, *T. dossi*, *I. bernissartensis* were corrected and coded (1). *S. stenops*, *S. harrisonii*, *E. ernstii*, Ankylosauria were corrected and coded (2). *P. warreni* and *M. langdoni* were corrected and coded with a question mark.

59(*). Postorbital-squamosal tubercle row: absent (0) or present (1) (Xu et al. 2006 #49).

No description and no figuration of any postorbital-squamosal tubercle row is given for *Liaoceratops yanzigouensis* (Xu et al. 2002). We corrected and coded this taxon with character state (0).

60(*). Postorbital participation to the lower temporal opening: present (0), postorbital excluded from margin (1) (reformulated from Xu et al. 2006 #12).

In *Archaeoceratops oshimai* (You and Dodson 2003, cf. fig. 1B), the postorbital is not completely excluded from participation to the infratemporal fenestra. Thus, this taxon was corrected and coded (0).

61(*). Postorbital-parietal contact: absent (0), very narrow (1), broad (2) (modified from Ösi et al. 2012 #51).

In *Zalmoxes robustus* (Weishampel et al. 2003, fig. 8C) a contact between postorbital and parietal is absent but in *Muttaburrasaurus langdoni* there have been different, opposite interpretations of this character (Bartholomai and Molnar, 1981, fig. 1B, Bell et al. 2019, fig. 4E). *Convolosaurus marri* displays a well-preserved contact between its postorbital and parietal (Andrzejewski et al. 2019, fig. 9C, D). *C. marri* was corrected and coded (1). *M. langdoni* was corrected and coded with a question mark.

62(*). Distinctive indentation on posterior cranial midline between the parietals: present (0) or absent (1) (Xu et al. 2006 #25).

The crania vary from a thin posterior indentation to a wider, more linear posterior concavity or even to a straight or convex posterior surface. We decided here to code only with character state (0) for the cases where an acute posterior indentation was present, and (1) for the rest of cases. In *Heterodontosaurus tucki* (Norman et al. 2011, fig. 12), *Yinlong downsi* (Han et al. 2015, fig. 4B), *Psittacosaurus mongoliensis* (Sereno 1992, cf. fig. 15.2), and in *Psittacosaurus major* (You et al. 2008, fig. 1A2) a distinctive, acute posterior indentation in the midline between the parietals is observed, so these taxa were coded (0). In *Thescelosaurus neglectus*, the posterior midline of the parietal is widely open, but with a sort of an acute 100° indentation posteriorly (Boyd 2014, fig. 3). This differs with the more regularly concave surfaces seen in the parietals of other ornithopods, like for example *H. foxii* (Galton 1974*a*, fig. 5B) or *Jeholosaurus shangyuanensis* (Barret and Han, 2009, fig. 2A). *Thescelosaurus neglectus* was coded [0 1] because of its intermediate condition, whereas *H. foxii* and *J. shangyuanensis* were coded (1). In *Haya griva*, the posterior side is somewhat concave posteriorly, but we could not observe in details wether there was an acute indentation or not (Makovicky et al. 2011, fig. 1E). Within Iguanodontia, the parietals are very narrow posteriorly, and a posterior indentation is observed in *Tenontosaurus tilletti* (Thomas 2015, fig. 5), *T. dossi* (Winkler et al. 1997, fig. 5), *Dryosaurus* and *Dysalotosaurus lettowvorbecki* (Galton 1983, fig. 5A, C), but the parietal is no more indented in the ankylopollexian *Camptosaurus dispar* (Gilmore 1909, fig. 3) and *Iguanodon bernissartensis* (Norman 1980, fig. 3). The basal iguanodontian *Muttaburrasaurus langdoni* lacks a posterior indentation on its parietal (Bartholomai and Molnar, 1981, fig. 2B). Such indentation is also absent in *Eocursor parvus* (Butler 2010) and pachycephalosaurs (Maryanska and Osmolska 1974, fig. 1). *E. parvus* was corrected and coded (0).

63(*). Parietal sagittal crest: narrow shelf or sharply defined crest (0) or broad, essentially absent (1) (Xu et al. 2006 #102).

The dorsal part of the parietal seems to be flattened as a plesiomorphic condition. Actually, In *Herrerasaurus ischigualastensis* (Sereno and Novas 1993), *Eocursor parvus* (Butler 2010), *Stegosaurus ungulatus* (Galton 2001, fig. 5.1.A), *Stegosaurus stenops* (Marsh 1887, fig. 1.3), *Scelidosaurus harrisonii* (Owen 1861, pl. 6), *Lesothosaurus diagnosticus* (Sereno 1991, fig. 11), the dorsal midline of the parietal looks largely flattened. In *Kulindadromeus zabaikalicus*, the lack of sharp sagittal crest on the parietal was related to a possible juvenile stage (Godefroit et al. 2014, supplementary material). However, in absence of any comparative material, and due to the globally wide parietal of *K. zabaikalicus*, we still consider this character as globaly phylogenetically informative. In *Hexinlusaurus multidens*, the parietals form "an extremely weak crest" which "attenuates anteriorly" (He and Cai 1984). Pachycephalosaurs also bear a dorsally broader and flattened sagital crest of parietal (Perle *et al.* 1982; Maryanska and Osmolska 1974). Other ornithopods (e.g. *Agilisaurus louderbacki*, Peng 1992; *Hyspilophodon foxii*, Galton 1974*a*; *Thescelosaurus neglectus*, Boyd 2014), heterodontosaurids (e.g. *Heterodontosaurus tucki*, Norman et al. 2011) or even ceratopsians (e.g. *Yinlong downsi*, Han et al. 2015) display a sharper midline crest.

66(*). Parietal, posterior margin relative to rest of skull: below or level with the anterior skull roof (0) higher than the anterior skull roof (1) (modified from Xu et al. 2006 #61).

In dome-headed pachycephalosaurs, the frontoparietal looks much higher than both the front and the rear of the skull (Maryanska and Osmolska 1974, fig. 1). In flat-headed pachycephalosaurs like *Homalocephale calathocercos*, the posterior border of the parietal is clearly higher than the frontals, with no central doming (Maryanska and Osmolska 1974, fig. 1D). The same occurs in *Hexinlusaurus multidens*, in which the parietal increases in height posteriorly, until the posteriormost border (He and Cai 1984, fig. 3).

Homalocephale calathocercos and *Hexinlusaurus multidens* were corrected and coded (1).

67(*). Squamosal-Quadratojugal contact: present, between dorsal process of quadratojugal and descending process of the squamosal (0), absent (1) (Ösi et al. 2012 #52).

In *Yinlong downsi*, the dorsal end of the quadratojugal is always missing (Han et al. 2015). In *Scelidosaurus harrisonii*, there is no clear indication as to wether the quadratojugal contacted the squamosal or not (Owen 1861, pl. 4), and in *Emausaurus ernsti* (Haubold 1990, fig. 2) we do not have this information at all. *Y. downsi*, *S. harrisonii*, *E. ernsti* were corrected and coded a question mark.

68(*). Supratemporal fenestra length relative to the basal skull length (BSL): short, fenestrae are less than 25% BSL (0), elongated, more than 25% BSL (1) (Ösi et al. 2012 #66; Xu et al. 2006 #58).

In *Isaberrysaura mollensis* (Salgado et al. 2017, see fig. 2B) the supratemporal fenestra makes less than 25% of basal skull length. Contra Xu et al. (2006 #58), the supratemporal fenestra appears to make slightly less than 25% of the total skull length in *Psittacosaurus mongoliensis* (Osborn 1923, fig. 2C), as well as in *Heterodontosaurus tucki* (e.g. Norman et al. 2011, fig. 12). By contrast, in *Psittacosaurus major* (You et al. 2008, fig. 1A1) and more derived ceratopsians, the supratemporal fenestra makes more than 25% of the basal skull length. The cranial material attributed to *Eocursor parvus* (Butler 2010) does not allow to code for this taxon so it was corrected and coded with a question mark. *I. mollensis*, *H. tucki* were corrected and coded (0). Psittacosaurids were corrected and coded as being polymorphic for this character.

69(*). Squamosal with significant overhang lateral to the descending process and quadrate: absent (0) or present (1) (Xu et al. 2006 #84).

There is no significant overhang of the squamosal lateral to the quadrate descending process in the pachycephalosaur *Tylocephale gilmorei* (Maryanska and Osmolka, 1974, fig. 1B4) but this taxon was not coded in this data matrix. There is a slight to moderate overhang in

Stegoceras validum, *Prenocephale prenes*, *Homalocephale calathocercos* (Maryanska and Osmolka, 1974, fig. 1A4, C4, D4), *Goyocephale lattimorei* (Perle et al. 1982, pl. 42.1), *Wannanosaurus yansiensis* (IVPP V 4447, Butler and Zhao 2009, fig. 5B). The squamosals of *Psittacosaurus major* (You et al. 2008, fig. 1B), *Yinlong downsi* (Han et al. 2015, fig. 3A, 5A), *Heterodontosaurus tucki* (Norman et al. 2011, appendix 3A, 4A-B) clearly feature a dorsolateral rim as well. The skull of *Psittacosaurus mongoliensis* was so far only figured by line drawings (Osborn 1923, fig. 2A; Sereno 2000, fig. 25.5; Sereno 2010, fig. 2.7). The presence of a lateral overhang is difficult to assess on the squamosal of this taxon, although it might have been present (Osborn 1923, fig. 2A). *H. tucki* was corrected and coded (1). *P. mongoliensis* was corrected and coded with a question mark.

70(*). Distance between the squamosal-quadrate articulation and a point on the dorsal surface of the squamosal aligned with the upper axis of the quadrate shaft: close (0), away from the main body of the squamosal, on a distinct and robust ventral process (1) (rephrased from Xu et al. 2006 #100).

In *Psittacosaurus major* (You et al. 2008, fig. 1B) and *Psittacosaurus mongoliensis* (Sereno 2010, fig. 2.7) the squamosal-quadrate articulation lies close to the main body of the squamosal. In *Heterodontosaurus tucki* (e.g. Norman et al. 2011, fig. 5A), the squamosal appears more enlarged ventrally with a well developped posterior process which caps the proximal head of the quadrate posteriorly. In the rhabdodontids for which a squamosal is known (i.e. *Zalmoxes robustus*, Weishampel et al. 2003, fig. 9; *Zalmoxes shqiperorum*, Godefroit et al. 2009, fig. 4) this bone is widely expanded ventrally. The squamosal is also tall above its articulation with the quadrate in *Tenontosaurus* (*T. tilletti*, Thomas 2015, fig. 2; *T. dossi*, Winkler et al. 1997, fig. 4), dryosaurids (*Dryosaurus*, *D. lettowvorbecki*, Galton 1983, fig. 5A and 5C respectively), *C. dispar* (Gilmore 1909, fig. 2), but such overhang is anteriorly located with respect to the dorsal squamosal surface on the alignment with the upper quadrate

shaft. *P. mongoliensis* was corrected and coded (0). *H. tucki*, *Z. robustus* and *Z. shqiperorum* were corrected and coded (1).

71(*). Squamosal prequadratic process: present, covers the anterodorsal part of the proximal quadrate shaft (0); absent (1) (new character).

H. foxii (Galton 1974*a*), *L. diagnosticus* (Sereno 1991, fig. 7A), *H. tucki* (Norman et al. 2011, fig. 1), *Yinlong downsi* (Han et al. 2015, fig. 2B), *Hexinlusaurus multidens* (He and Cai 1984, fig. 3) and most other ornithischians have a descending process of their squamosal that caps to varying degrees the proximal head of the quadrate anteriorly. In *Archaeoceratops oshimai* the squamosal anterior capping of the quadrate is very small, but it is still present (You and Dodson 2003, fig. 1). In *Liaoceratops yanzigouensis*, Xu et al. (2002, p.315) tells that "a long posterodorsal process of the jugal reaches the squamosal and forms most of the anterior and dorsal border of the infratemporal fenestra". This feature may be present and may indicate that the squamosal could have capped the proximal head of the quadrate anteriorly, but is not visible on the figures (Xu et al. 2002, fig. 1). This taxon was therefore kept as unknown for this character. In *Agilisaurus louderbacki* (Peng 1992, fig. 1A), as well as convergently in some pachycephalosaurs: *Stegoceras validum* (Gilmore 1924, fig. 1), *Tylocephale gilmorei* (Maryanska and Osmolska 1974, fig. B1) and both the juveniles and adults of *Pachycephalosaurus wyomingensis* (Bakker et al. 2006, fig. 4A, Horner and Goodwin 2009, fig. 3B respectively) the squamosal doesn't cap the anterodorsal part of the quadrate. By change, there is an anterior descending process above the dorsal part of the quadrate in the other pachycephalosaurs: *Wannanosaurus yansiensis* (Butler and Zhao 2009, fig. 6G), *Homalocephale calathocercos* and *Prenocephale prenes* (Maryanska and Osmolska, fig. 1C1-D1 respectively) so this may be the plesiomorphic condition for Pachycephalosauria.

72(*). Parietosquamosal shelf, posteromedial process of squamosal: does not overhang the occipital region (0); overhang the occipital region, forms at least a slight dorsal horizontal

shelf (1); consists of a vertically oriented sheet of bone (2) (modified from Ösi et al. 2012 #68, Xu et al. 2006 #45).

The parietosquamosal shelf varies considerably in shape within Marginocephalia. Actually, within ceratopsids, the squamosal of *Archaeoceratops oshimai* is well expanded lateromedially, but has the form of a vertical strap of bone which is medioventrally deflected (You and Dodson 2003). In *Liaoceratops yanzigouensis* as well as in the psittacosaurids *Psittacosaurus mongoliensis* and *Psittacosaurus major* the medial squamosal process forms a vertical sheet of bone from a dorsal view and keeps a dorsal alignement with the parietal (cf. Xu et al. 2002, fig. 1C; Osborn 1923, fig. 2C; Sereno, 2007, fig. 1 respectively). *Yinlong downsi* (e.g. Han et al. 2015, fig. 4) contrasts markedly from all other ceratopsids in having its squamosal forming a kind of "dorsal horizontal roof" posterolaterally. The medial process of the squamosal then thins medially toward the parietal. In pachycephalosaurs, the parietosquamosal forms a more or less expanded shelf anteroposteriorly and overhangs the occipital region (see also Butler and Zhao 2009, p.71). The squamosal is stoutly sutured to the frontoparietal and is aligned dorsally with the posterodorsal surface of the parietal (e.g. *Stegoceras validum*, Gilmore 1924, pl. 2 and 4; *Wannanosaurus yansiensis*, Butler and Zhao 2009, fig. 5D; *Homalocephale calathocercos* and *Prenocephale prenes*, Maryanska and Osmolska 1974, fig. 1C4, 1D4 respectively). Note that a slight posterior overhang of squamosal - which is not a consequence of the posterior wrapping of the proximal cotylus of quadrate - also exists in heterodontosaurids for which the posterior skull roof is preserved, i.e. in *Heterodontosaurus tucki* (Sereno 2012, fig. 93) and *Manidens comodorensis* (Pol et al. 2011, fig. 2A, B). In the rhabdodontids *Z. robustus* (Weishampel et al. 2003, fig. 9D) and *Z. shqiperorum* (Godefroit et al. 2009, fig. 4B), the parietal process of the squamosal forms a "ridge-bound facet" for contact with the parietal. This feature is convergently found in ceratopsids. The squamosals of *Zephyrosaurus schaffi* (Sues 1980) and *Eocursor parvus*

(Butler et al. 2007) are not preserved, that of *Isaberrysaura mollensis* (Salgado et al. 2017) is present but unsufficiently preserved, the medial process of squamosal of *Changchunsaurus parvus* is not exposed (Liyong et al. 2010) and the medial process of squamosal of *Gasparinisaura cincosaltensis* (Coria and Salgado 1996) is not figured nor described for this character. After modification of this character definition, pachycephalosaurs, *Yinlong downsi* and *Heterodontosaurus tucki* were coded (1), the ceratopsids *Archaeoceratops oshimai* and *Liaoceratops yanzigouensis* as well as the rhabdodontids *Z. robustus* and *Z. shqiperorum* were coded (2). *Fostoria dhimbangunmal* was corrected and coded with a question mark. All other taxa for which this feature was available could be coded (0). *Z. schaffi*, *E. parvus*, *I. mollensis*, *C. parvus* and *G. cincosaltensis* were corrected and coded with a question mark.

73(*). Postorbital-squamosal tubercle/node row: absent (0), present (1) (Ösi et al. 2012 #72).

Han et al. (2015) describe the presence of a low nodular ornamentation onto the postorbital-squamosal bar of *Yinlong downsi*, and also observe a similar series of nodes in *Archaeoceratops oshimai* (You and Dodson 2003, e.g. fig. 1A) and *Liaoceratops yanzigouensis* (Xu et al. 2002, fig. 1). Therefore, *A. oshimai* and *L. yanzigouensis* were corrected and coded (1) for this character.

74(*). Postorbital-squamosal tubercle row, enlarged tubercle row on the posterior squamosal: absent (0), present (1) (Ösi et al. 2012 #73).

Butler and Zhao (2009) report that in *Wannanosaurus yansiensis*, "two larger posterolaterally directed nodes are present on the posterolateral corner of the right squamosal". There is no indication for a node enlargement toward the posterior side of the squamosal-postorbital bar in ceratopsids (Han et al. 2015; You and Dodson 2003, fig. 1A; Xu et al. 2002, fig. 1). *Y. downsi* was corrected and coded (0). *W. yansiensis* was corrected and coded (1).

76(*). Squamosal, morphology of postorbital process dorsal to *M. adductor mandibulae externus* origin site: gently convex (0), mediolaterally compressed and blade-like (1) (McDonald et al., 2010 #65).

The anterior squamosal process of *Hexinlusaurus multidens* looks "bar-like" and very little expanded in both dorsoventral and mediolateral directions (He and Cai 1984, fig. 3), so it may not look blade-like. The anterior squamosal process is not mediolaterally compressed, but rather large and dorsally convex in *Dryosaurus* (Galton 1983, fig. 2), *Dysalotosaurus lettowvorbecki* (Janensch 1955, fig. 1B), *Tenontosaurus tilletti* (Thomas 2015, fig. 5) and *Tenontosaurus dossi* (Winkler et al. 1997, fig. 5), *Thescelosaurus neglectus* (Boyd 2014, fig. 3) and *Thescelosaurus assiniboiensis* (Brown et al. 2011, fig. 6A). By contrast, the anterior squamosal process looks clearly mediolaterally compressed in *Archaeoceratops oshimai* and *Liaoceratops yanzigouensis* (You and Dodson 2003, fig. 1E and Xu et al. 2002, fig. 2B respectively). The dorsal morphology of the anterior squamosal process in *Agilisaurus louderbacki* is hardly discernible, and appears relatively short anteroposteriorly (Peng 1992, fig. 1B). In *Orodromeus makelai* (Scheetz 1999), no figure or description allows to firmly assess this character state. *H. multidens*, *Dryosaurus*, *D. lettowvorbecki*, *T. tilletti*, *T. dossi*, *T. neglectus*, *T. assiniboiensis* were corrected and coded (0). Pending revision, *A. louderbacki* and *O. makelai* were corrected and coded with a question mark.

77(*). Jugal with prominent ventral flange: absent (0) or present (1) (Xu et al. 2006 #69).

In *Liaoceratops yanzigouensis* (Xu et al. 2002, fig. 1B) and psittacosaurids (*P. major*, Sereno, 2007; *P. mongoliensis*, Osborn 1923; *Hongshanosaurus houi*, You et al. 2003) the jugal forms a prominent ventral process in front of the quadratojugal. Within Heterodontosauridae, a tongue-shaped, transversely compressed flange projects postero-ventrally from the ventral margin of the jugal in *Heterodontosaurus tucki* and *Manidens condoriensis* (Norman et al. 2011; Sereno 2012, p.219). In the pachycephalosaur *Wannanosaurus yansiensis* (Butler and

Zhao 2009, fig. 6A, B) and the basal ceratopsians *Yinlong downsi* (Han et al. 2015), *Archaeoceratops oshimai* (You and Dodson 2003) and *Chaoyangosaurus youngi* (Zhao et al. 1999), the jugal doesn't prolongates into a distinct ventral flange, although in other ceratopsians, a jugal crest is present and projects posteriorly in the horizontal plane. The jugal of *Camptosaurus dispar* (Gilmore 1909, fig. 2) differs from that of all other basal iguanodonts in that it possesses a ventral flange, so that it was recoded (1).

79(*). Jugal wing (formed by quadratojugal and jugal), height that contact the quadrate: greater than 20% quadrate height (0), less than 20% (1) (new character).

In *Heterodontosaurus tucki* (Norman et al. 2011, fig. 1B), *Hexinlusaurus multidens* (He and Cai 1984, fig. 3), *Thescelosaurus neglectus* (cf. NCSM 15728, Boyd 2014, fig. 1), *Zephyrosaurus schaffi* (Sues 1980, fig. 8), the total overlap of the jugal wing on the quadrate makes more than 20% of the total quadrate height. Although the quadrate of *Muttaburrasaurus langdoni* is not complete proximally, the jugal wing is dorsoventrally tall and overlaps the quadrate on a very significant portion (Bartholomai and Molnar, 1981, fig. 1A). In *Parksosaurus warreni* (Galton 1973, fig. 1A), *Orodromeus makelai* (Scheetz 1999, fig. 1, 2), *Gasparinisaura cincosaltensis* (Coria and Salgado 1996, fig. 2), the jugal wing contacts the quadrate on much less than 20% of the total quadrate height.

80(*). Jugal wing, degree of anteroposterior overlap of the quadrate shaft (not considering the pterygoid wing): complete, reaches the posterior border of quadrate (0), almost complete, cover more than 50% of quadrate length (1), partial, cover much less than 50% of quadrate length (2) (modified from Brown et al., 2013 #1).

In *Herrerasaurus ischigualastensis* (Sereno and Novas 1993, fig. 1A), a large part of the quadrate is covered by the quadratojugal. In *Emausaurus ernstii* (Haubold 1990, fig. 2), *Scelidosaurus harrisonii* (Owen 1861, pl. 5), *Stegosaurus stenops* (Gimore, 1914, pl. 5), *Agilisaurus louderbacki* (Peng 1992, fig. 1A), *Abrictosaurus consors* (Sereno 2012, fig. 31),

Heterodontosaurus tucki (Norman et al. 2011, fig; 1), *Yinlong downsi* (Han et al. 2015, fig. 2), *Psittacosaurus major* and *Psittacosaurus mongoliensis* (Sereno 2010, fig. 2.3, 2.7), *Chaoyangsaurus youngi* (Zhao et al. 1999), *Archaeoceratops oshimai* (You and Dodson 2003), *Liaoceratops yanzigouensis* (Xu et al. 2002), *Jeholosaurus shangyuanensis* (Han et al. 2012, fig. 5A), *Changchunsaurus parvus* (Liyong et al. 2010, fig. 1B), *Haya griva* (Makovicky et al. 2011, fig. 1B), *Lesothosaurus diagnosticus* (Sereno 1991, fig. 12A), *Stegoceras validum* (Maryanska and Osmolska 1974, fig. A1), the quadrate is overlapped by the quadratojugal for its whole anteroposteriorlength. In *Hexinlusaurus multidens* (Barrett et al. 2005, fig. 1A), *Gasparinisaura cincosaltensis* (Coria and Salgado 1996, fig. 2), *Thescelosaurus neglectus* (Boyd 2014, fig. 1A), the posterior branch of quadratojugal extends over an important portion of the total quadrate length. In *Kulindadromeus zabaikalicus*, the quadrate is reported as anteroposteriorly slender and no mention is made of the degree of quadrate overlap by the jugal wing. Notwithstanding, such overlap could have been important by judging from the photographs (Godefroit et al. 2014, fig. S4A). In *Muttaburrasaurus langdoni* (Herne 2014, fig. 5.30), *Tenontosaurus tilletti* (Thomas 2015, fig. 2), *Tenontosaurus dossi* (Winkler et al. 1997, fig. 4), *Dryosaurus* (Galton 1983, fig. 2), *Dysalotosaurus lettowvorbecki* (Janensch 1955, fig. 1), *Iguanodon bernissartensis* (Norman 1980, fig. 2), the quadratojugal covers less than half of the total quadrate length. Owing to the implementation of the first state of character, taxa that were previously coded (1) are now coded (2). Taxa that were previously coded (0) are now coded (1), except for the following ones which are left and/or corrected with the newly formulated character state (0): *E. ernstii*, *S. harrisonii*, *L. diagnosticus*, *S. validum*, *A. louderbacki*, *A. consors*, *H. tucki*, *Y. downsi*, *P. major*, *P. mongoliensis*, *J. shangyuanensis*, *C. parvus*, *H. griva*, *C. youngi*, *L. yanzigouensis*, *A. oshimai*.

81(*). Jugal, ventral extent of the wing formed by the jugal and quadratojugal ends: at or near distal condyles of quadrate (0), above distal condyles (1), well above the distal condyles (2) (Brown et al. 2013 #9; Ösi et al. 2012 #54).

In *Herrerasaurus ischigualastensis* (Sereno and Novas 1993, fig. 1A, B), *Lesothosaurus diagnosticus* (Sereno 1991, fig. 12A; Porro et al. 2015, fig. 2A) and *Emausaurus ernsti* (Haubold 1990, fig. 2), *Hexinlusaurus multidens* (He and Cai 1984, fig. 3), the ventral extent of the jugal wing (considering its prolongation formed by the quadratojugal) ends almost level with the distal quadrate condyles. *Scelidosaurus harrisonii* (Owen 1861, pl. 4) and *Stegosaurus stenops* (Marsh 1887, pl. 6) however, differ in having a marked step between the ventral extent of the jugal wing and the distal quadrate condyles. In the ceratopsians *Yinlong downsi* (Han et al. 2015, fig. 2), *Psittacosaurus mongoliensis* (Osborn 1923, fig. 2B) and *Psittacosaurus major* (Sereno et al. 2007, fig. 1A) the jugal wing ends a step higher than the distal condyles of the quadrate, as occurs in other ceratopsians - e.g. *Liaoceratops yanzigouensis* (Xu et al. 2002) and *Archaeoceratops oshimai* (You and Dodson 2003). This is also the case in the basal ornithopod *Orodromeus makelai* (Scheetz 1999, fig. 2, 3), *Hypsilophodon foxii* (Galton 1974*a*, fig. 3) and in *Dryosaurus* (Galton 1983, pl. 1-1). In *Zephyrosaurus schaffi* (Sues 1980) there is no possibility to correctly infer this character. In *Hexinlusaurus multidens* (He and Cai 1984, fig. 3), the ventral border of the jugal is straight and lowers in a continuous manner until it gets lower than the maxillary tooth row, as do occur in pachycephalosaurs (e.g. Maryanska and Osmolska 1974, fig. 1). Unfortunately, *H. multidens* doesn't preserve its distal quadrate condyles. In the heterodontosaurids *Heterodontosaurus tucki* (e.g. Norman et al. 2011, fig. 5A), *Abrictosaurus consors* (Sereno 2012, fig. 31B) the ventral extent of the jugal wing ends well above the distal condyles of the quadrate. This is also congruent with what occurs in the heterodontosaurid *Manidens condorensis* (Sereno 2012, fig. 81B). In *Tenontosaurus tilletti* (Thomas 2015) and

Tenontosaurus dossi (Winkler et al. 1997, fig. 3, 4; contra Andrzejewski et al. 2019 #54) the jugal wings ends markedly higher than the distal quadrate condyles. This is similar to the condition seen in *Convolosaurus marri* (Andrzejewski et al. 2019, fig. 8A), in which the distal quadrate condyles appear in articulation with the surangular and articular, with the quadratojugal articulating markedly higher in front of it. *H. ischigualastensis*, *E. ernsti* and *H. multidens* were corrected and coded (0). Y. *downsi*, *P. mongoliensis*, *P. major*, *O. makelai*, *H. foxii*, *Dryosaurus*, *C. marri*, *T. tilletti* and *T. dossi* were corrected and coded (1). *H. tucki*, *A. consors* were corrected and coded (2). *Z. schaffi* was corrected and coded with a question mark.

82(*). Jugal, articulation with quadrate: jugal fails to articulate with quadrate (0), jugal articulates with quadrate (1) (Brown et al. 2013 #14).

Hexinlusaurus multidens (He and Cai 1984, fig. 3), *Kulindadromeus zabaikalicus* (Godefroit et al. 2014, fig. S4A, B) as well as all pachycephalosaurs to the exception of *H. calathocercos* (Maryanska and Osmolska 1974, fig. 1) feature a ventral contact between the jugal and the quadrate. In psittacosaurs, the jugal fails to articulate directly with the quadrate (*P. mongoliensis*, *P. major*, Osborn 1923, fig. 2A and Sereno et al. 2007, fig. 1A respectively). Within Iguanodontia, the jugal contacts with the quadrate in Dryosauridae exclusively (*D. altus* and *D. lettowvorbecki*, Galton 1983, fig. 5A, C). The jugal fails to articulate with the quadrate in *Camptosaurus dispar* (Gilmore 1909, fig. 2), *Tenontosaurus tilletti* (Thomas 2015, fig. 2) and *Tenontosaurus dossi* (Winkler et al. 1997, fig. 4). Psittacosaurs, *C. dispar*, *T. tilletti*, *T. dossi* were corrected and coded (0).

83(*). Posterior maxillary process on the medial side of the jugal: straight to modestly arched medially (0), anteromedially projected and arched (1) (modified from Boyd 2015 #39).

In *Heterodontosaurus tucki* (Norman et al. 2011, fig. 13), *Scelidosaurus harrisonii* (Owen 1861, pl. 4), *Lesothosaurus diagnosticus* (Porro et al. 2015, fig. 2G-H), *Hypsilophodon foxii*

(Galton 1974*a*, fig. 5B-C), *Zalmoxes robustus* (Weishampel et al. 2003, fig. 4B, D), *Tenontosautus tilletti* (Thomas 2015, fig. 6), *Dryosaurus* (Galton 1983, fig. 2), *Dysalotosaurus lettowvorbecki* (Janensh, 1955, fig. 1B), the jugal anterior ramus is regularly and modestly arched. The maxillary process on the medial side of the jugal is posterolaterally arched in *Yinlong downsi* (Han et al. 2015, fig. 18). This also occurs in other ceratopsians such as *Liaoceratops yanzigouensis* (Xu et al. 2002, fig. 1D). *H. tucki*, *S. harrisonii*, *L. diagnosticus*, *T. tilletti*, Z. *robustus*, *Dryosaurus*, *D. lettowvorbecki* were corrected and coded (0). *Y. downsi* was corrected and coded (1).

85(*). Jugal anterior ramus: dorsoventrally deeper than mediolaterally broad (0), broader than deep (1) (Boyd 2015 #32).

Psittacosaurus mongoliensis and *Psittacosaurus major* bear a dorsoventrally deep anterior ramus of jugal (Osborn 1923 and Sereno et al. 2007 respectively). In *Isaberrysaura mollensis*, the anterior ramus of jugal is relatively broad and very little expanded dorsoventrally (Salgado et al. 2017, fig. 2). *P. mongoliensis* and *P. major* were corrected and coded (0). *I. mollensis* was corrected and coded (1).

86(*). Jugal, morphology of portion of maxillary process that overlaps maxilla: tapers at anterior ends of maxillary and lacrimal contacts, with slightly convex ventral margin and slightly concave dorsal margin (0), subrectangular with parallel dorsal and ventral margins (1) (modified from: McDonald et al. 2010 #54; Ösi et al. 2012 #35).

The relative dorsoventral expansion of the anterior jugal process with respect to the posterior jugal process (character states 2 and 3) was already dealt with in Xu et al. (2006 #55). Character states (2) and (3) were therefore omitted and were reconsidered in the light of character states (0) and (1) only. The jugal of *Scutellosaurus lawleri* (Rosenbaum and Padian, 2000, fig1.A, B) and *Isaberrysaura mollensis* (Salgado et al. 2017, fig. 2C, D) bear subparallels superior and inferior borders. In the mature skull of *Orodromeus makelai*

(Scheetz 1999, fig; 4) the anterior process of jugal also seems to have a subrectangular outline with subparallels dorsal and ventral margins. Note that, contrary to more derived pachycephalosaurs, but similarly to *Zephyrosaurus schaffi* and *Orodromeus makelai*, the anterior jugal ramus of *Wannanosaurus yansiensis* is also subrectangular with parallels dorsal and ventral margins (cf. Butler and Zhao 2009, fig. 6A). In *Scelidosaurus harrisonii* (Owen 1861, pl. 5), *Yinlong downsi* (Han et al. 2015, fig. 2, 3), *Psittacosaurus mongoliensis* (Sereno 2010, fig. 2.7), *Psittacosaurus major* (You et al. 2008, fig. 2.3) the anterior ramus of the jugal tapers anteriorly. *S. harrisonii*, Y. *downsi*, *P. mongoliensis* and *P. major* were recoded (0). *S. lawleri*, *I. mollensis*, *O. malelai* were corrected and coded (1).

87(*). No boss present on lateral surface of the jugal (0), presence of a boss or horn on the lateral surface of the jugal (1) (modified from Boyd 2015 #38).

Yandusaurus hongheensis (He and Cai 1984, fig. 23), *Scelidosaurus harrisonii* (Owen 1861, pl. 4), *Emausaurus ernsti* (Haubold 1990, fig. 2), *Lesothosaurus diagnosticus* (Sereno 1991), *Liaoceratops yanzigouensis* (You et al. 2007), *Yinlong downsi* (Xu et al. 2006 ; Han et al. 2015) all lack a jugal boss. By contrast, *Psittacosaurus mongoliensis* appears to have a large and prominent jugal horn (Osborn 1923), and a boss also appears to be present in *Chaoyangosaurus youngi* (Zhao et al. 1999). Sereno (2012, p. 219) states that a jugal horn is present in both *Heterodontosaurus tucki* and *Manidens condoriensis*, Note that *Tianyulong confuciusi* differs from these two heterodontosaurids in not possessing any jugal horn (Sereno 2012, p. 55). *Y. hongheensis*, *S. harrisonii*, *E. ernsti*, *L. diagnosticus*, *L. yanzigouensis*, *Y. downsi* were corrected and coded (0). Psittacosauridae, *C. youngi*, *H. tucki* were corrected and coded (1).

88(*). Jugal ornamentation: absent (0), or present, nodular (1) (modified from Ösi et al. 2012 #41; Xu et al. 2006 #81).

A nodular ornamentation of the jugal is present in *Jeholosaurus shangyuanensis* (Barrett and Han, 2009) and *Changchunsaurus parvus* (Zan et al. 2005). Barrett and Han (2009) state that 'nodular ornamentation is also present in some ceratopsians', citing among others *Archaeoceratops oshimai* (IVPP V11114: You and Dodson 2003), *Chaoyangosaurus youngi* (IGCAGS V371: Zhao et al. 1999), *Yinlong downsi* (Xu et al. 2006). The nodular ornamentation is well expanded along the jugal-postorbital bar in pachycephalosaurs (Maryanska and Osmólska 1974; Sues and Galton 1987; Butler and Zhao 2009). Barrett and Han (2009) add that, contrary to those above cited taxa, *Orodromeus makelai* and *Zephyrosaurus schaffi* lack such nodular ornamentation, although the external surface of their jugal is striated (see also Sues 1980, see also fig. 8A ; Scheetz 1999 respectively). No striation nor any ornamentation of any type is present in *Thescelosaurus neglectus* (Boyd 2014) or *Thescelosaurus assiniboiensis* (Brown et al. 2011). A 'rugose horn' is told to be present in the heterodontosaurids *Manidens condorensis* and *Heterodontosaurus tucki* (Sereno 2012, p. 219). Though, such 'rugose' surface would still be unornamented and rather smooth (Liyong et al. 2010, p.207). Pending further examination of this character we considered that the striation of the jugal was not equivalent to a nodular ornamentation.

89(*). Jugal-postorbital bar, anteroposterior width relative to that of the infratemporal fenestra: less expanded (0), equally expanded (1), or anteroposteriorly broader than the infratemporal fenestra (2) (modified from Ösi et al. 2012 #42).

Note that *Hexinlusaurus multidens* (He and Cai 1984, fig. 3) and *H. calathocercos* (Maryanska and Osmolska 1974, fig. 1D) have a well expanded postorbital bar which forms the same anteroposterior length as the infratemporal fenestra. In *Wannanosaurus yansiensis* (Butler and Zhao 2009) the posterior process of the jugal is broken. Given the state of preservation of the *Convolosaurus marri* skull (Andrzejewski et al. 2019), it is not possible to safely infer the scoring of this taxon between state (0) or state (1). *H. multidens* and *H.*

calathocercos were corrected and coded (1). *C. marri* and *W. yansiensis* were corrected and coded with a question mark.

90(*). Jugal-postorbital joint: elongate scarf joint (0), short butt joint (1) (Ösi et al. 2012 #43).

In *H. tucki*, the postorbital-jugal joint structure should have been somewhat obscured from a lateral view. Norman et al. (2011, p. 203) describe the postorbital-jugal suture as follow: "The ventral portion of the postorbital is robust and curves anteriorly toward its distal end as it forms an extensive scarf-jointed suture with the ascending process of the jugal". *H. tucki* was therefore corrected and coded (0).

91(*). Jugal, form of postorbital process: not expanded dorsally (0), dorsal portion of postorbital process expanded posteriorly (1) (Ösi et al. 2012 #44).

In *Parksosaurus warreni* (Galton 1973, fig. 1) as well as in *Haya griva* (Makovicky et al. 2011, fig. 1B) the dorsal portion of the postorbital process is not expanded posteriorly. In *Yinlong downsi* (e.g. Han et al. 2015, fig. 2) the dorsal portion of the postorbital process is slightly offset posteriorly. *P. warreni* and *H. griva* were corrected and coded (0). *Y. downsi* was corrected and coded (1).

92(*). Jugal, posterior ramus forking: absent (0), present, incision between processes vary from narrow to more than 45° (1) (Pol et al. 2011 #46; modified from Ösi et al. 2012 #46).

A posterior forking of the jugal wing of *Heterodontosaurus tucki* (Norman, 2011, fig. 1) is clearly visible, although only the dorsal ramus of such forking contacts with the quadratojugal. There is no posterior forking in the jugal wings of *Goyocephale lattimorei* (Perle et al. 1982, pl. 42-4). There is a posterior forking in the jugal wings of *Yinlong downsi* (Han et al. 2015, fig. 2A, B), as also occurs in *P. mongoliensis* (Osborn 1923, fig. 2B) and *P. major* (Sereno et al. 2007, fig. 1). The junction between the jugal and the quadratojugal is undulating in *Chaoyangosaurus youngi* (Zhao et al. 1999, fig. 2A) so this taxon was also considered to bear a forked jugal wing. The posterior process of the jugal in *Wannanosaurus*

yansiensis is reported to be broken (Butler and Zhao 2009). *G. lattimorei* were corrected and coded (0). *H. tucki*, *Y. downsi* and *C. youngi* were corrected and coded (1). *W. yansiensis* was corrected and coded with a question mark.

93(*). Jugal, posterior ramus: forms anterior and ventral margin of infratemporal fenestra (0), forms part of posterior margin, expands towards squamosal (1) (Ösi et al. 2012 #47).

The jugal posterior ramus forms only the anterior and ventral margins of the infratemporal fenestra in *Goyocephale lattimorei* (Perle et al. 1982, pl. 42-4), and it also forms the posterior margin of such fenestra in *Hexinlusaurus multidens* (He and Cai 1984, fig. 3). The posterior process of the jugal in *Wannanosaurus yansiensis* is reported as broken (Butler and Zhao 2009). *G. lattimorei* was corrected and coded (0). *H. multidens* was corrected and coded (1). *W. yansiensis* was corrected and coded with a question mark.

94(*). Jugal-squamosal contact: absent, separated by postorbital (0) or present (1) (Xu et al. 2006 #72).

In *Archaeoceratops oshimai* (You and Dodson 2003) the contact between the squamosal and the jugal ascending process is not completely made, so this taxon was corrected and coded (0).

95(*). Jugal–quadratojugal contact: overlapping (0), tongue-and-groove (1) (Ösi et al. 2012 #48).

The "tongue-and-groove" kind of quadratojugal-jugal contact (character state 1) exists in a variety of forms. In *Tenontosaurus tilletti*, the quadratojugal inserts ventrally between the medial and lateral tabs of the posterior jugal process, within a "tongue and groove" articulation (Thomas 2015, p. 36-37). What's more, the posteroventral border of the jugal wing deflects medially with respect to the quadratojugal (Thomas 2015, fig. 2). In *Thescelosaurus neglectus*, the jugal-quadratojugal joint appears to be complex. Boyd (2014, p. 22) describes the anteroventral corner of its quadratojugal as bearing a dorsovenrally extending groove for contact with the jugal anteriorly. This would cause the posterior process

of the jugal to insert medial to the quadratojugal. In *Yinlong downsi* (Han et al. 2015), the quadratojugal lies dorsomedial to the jugal posterior process, i.e. into a medially flanked horizontal groove of the jugal. In *Psittacosaurus major*, the jugal wing forms two small posteroventral prongs into which the quadratojugal slots (You et al. 2008). *Thescelosaurus neglectus, Yinlong downsi*, *P. major* were therefore corrected and coded (1). Given the variety of morphologies of the quadratojugal-jugal joint, a detailed first-hand examination of this character in more taxa could bring more valuable information in the future.

96(*). Jugal (or jugal–epijugal), ridge dividing the lateral surface of the jugal into two planes: absent (0), present (1) (Ösi et al. 2012 #38).

No epijugal ridge is described or figured for *Psittacosaurus major* (Sereno et al. 2007; You et al. 2008) and *Psittacosaurus mongoliensis* (Osborn 1923). These two taxa were corrected and coded (0) for this character.

97(*). Quadratojugal, shape: inverted L-shaped, with elongate anterior and ventral processes (0), subrectangular with long axis vertical, short, deep anterior process (1), horizontal T-shaped, with sharp angle between the anterior and dorsal processes (2) (modified from Ösi et al. 2012 #53).

The quadratojugal of *H. tucki* and *A. consors* are clearly "inverted L-shaped" with an elongated anterior process (Norman et al. 2011, fig. 1; Sereno 2012, fig. 34, respectively). In both *Parksosaurus warreni* (Galton 1973, fig. 1, 5) and *Gasparinisaura cincosaltensis* (Coria and Salgado 1996, fig. 2), the quadratojugal has the shape of an horizontal "T" with a sharply defined posterodorsal process. The outgroup taxon *H. ishigualastensis* (Sereno and Novas 1993, fig. 1A) has a quadratojugal with elongated and sharply angled anterior and posterodorsal processes, with no posteroventral process. *H. tucki* and *A. consors* were corrected and coded (0). *H. ischigualastensis*, *P. warreni* and *G. cincosaltensis* were corrected and coded (2).

98(*). Paraquadratic/quadratojugal foramen, pierces the quadratojugal: absent (0), present (1) (modified from Weishampel et al., 2003 #17; McDonald et al., 2010 #58).

Heterodontosaurus tucki (Norman et al. 2011, p. 198), *Herrerasaurus ischigualastensis* (Sereno and Novas 1993) all bear a quadratojugal foramen. Han et al. (2015) state that there is no quadratojugal foramen in the lateral aspect of the quadratojugal of *Yinlong downsi*, although a fossa is present posterodorsally at the junction between the quadrate and the quadratojugal. *Agilisaurus louderbacki* (Peng 1992) and *Hexinlusaurus multidens* (He and Cai 1984) are told to lack a quadratojugal foramen. In *Changchunsaurus parvus*, Liyong et al. (2010, p. 208) state that a quadratojugal foramen is absent. In *Muttaburrasaurus langdoni* (Bartholomai and Molnar, 1981, p. 324), the quadratojugal/paraquadratic foramen is located at the junction between the quadrate and quadratojugal and hence, it does not pierce the quadratojugal *per se*. A paraquadratic foramen opens onto the quadrate of *Dryosaurus* (Galton 1983, fig. 2A) and *Camptosaurus dispar* (Carpenter and Lamanna 2015, fig. 13G-H), although this is no indication for the possible piercing of their quadratojugal. In *Dryosaurus*, the paraquadratic foramen notches the junction between the quadratojugal and quadrate, so the quadratojugal is devoid of any foramen (Galton 1983, p. 213, pl. 1.1, 1.3). Similarly the quadratojugals of *Camptosaurus dispar* (Gilmore 1909, pl. 8), *Iguanodon bernissartensis* (Norman 1980, fig. 12), but also *Zalmoxes robustus* (Weishampel et al. 2003, fig. 6C, D) are also devoid of any foramen. This condition is unknown in *Dysalotosaurus lettowvorbecki* (Janensch 1955). *H. tucki*, *H. ischigualastensis* were corrected and coded (1). *I. bernissartensis*, *M. langdoni Y. downsi*, *H. multidens* and *C. parvus* were corrected and coded (0). *D. lettowvorbecki* was corrected and coded with a question mark.

99(*). Paraquadratic/quadratojugal foramen size: small and/or narrow if dorsoventrally tall (0) large (1) (modified from Xu et al. 2006 #40).

It seems that the plesiomorphic condition is a small, rounded quadratojugal foramen, lodged between the quadrate and the quadratojugal and openning in posterior direction (cf. *Herrerasaurus ischigualastensis*, Sereno and Novas 1993, fig. 1G). In *Stegoceras validum*, the quadratojugal foramen is circular in shape and could be considered as being small in size (Sues and Galton 1987, fig. 1B). In *Heterodontosaurus tucki*, the quadratojugal foramen is dorsoventrally elongated, but mediolaterally narrow (Norman et al. 2011, fig. 14). In *Tenontosaurus tilletti* (Thomas 2015, fig. 2), *Tenontosaurus dossi* (Winkler et al. 1997, fig. 4), and *Thescelosaurus neglectus* (Boyd 2014, fig. 1), the quadratojugal foramen is small. In *Haya griva* (Makovicky et al. 2011, fig. 1) the quadratojugal foramen is well delineated onto the lateral aspect of this bone, but is still relatively small. By contrast, in *Iguanodon bernissartensis* (Norman 1980, fig. 2), *Dryosaurus* and *Dysalotosaurus lettowvorbecki* (Galton 1983, fig. 5A, C), the "quadratojugal" foramen is large, and opens laterally onto the anterior side of the quadrate.

100(*). Paraquadratic/quadratojugal foramen or notch, location: opens between quadratojugal and quadrate, notches the anterior margin of the quadrate (0), opens inside the quadratojugal (1) (modified from Ösi et al. 2012 #60).

In *Iguanodon bernissartensis* (Norman 1980, fig. 2), *Dryosaurus* and *Dysalotosaurus lettowvorbecki* (Galton 1983, fig. 5A, C) but also *Camptosaurus dispar* (Carpenter and Lamanna 2015, fig. 13G-H), the paraquadratic/quadratojugal foramen is large and opens laterally onto the anterior side of the quadrate. The presence of a paraquadratic/quadratojugal foramen is likely but unknown in *Zalmoxes shqiperorum* (Godefroit et al. 2009), *Zalmoxes robustus* (Weishampel et al. 2003) and for *Parksosaurus warreni* (Galton 1973). In *Kulindadromeus zabaikalicus* (Godefroit et al. 2014) and *Haya griva* (Makovicky et al. 2011) the quadratojugal foramen opens inside the same bone. *D. altus*, *D. lettowvorbecki*, *C. dispar* and *I. bernissartensis* were corrected and coded (0). *K. zabaikalicus* and *Haya griva* were

corrected and coded (1). *Z. shqiperorum* and *P. warreni* were corrected and coded with a question mark.

101(*). Quadrate foramen location and orientation of the openning: posteriorly onto the posterolateral aspect of quadrate shaft (0), on lateral aspect of quadrate or quadratojugal (1) (Xu et al. 2006 #39).

In *Stegoceras validum* (Sues and Galton 1987), *Heterodontosaurus tucki* (Norman et al. 2011, fig. 14, p. 198), the quadratojugal foramen is located at the boundary between the quadrate and the quadratojugal and opens posteriorly. In *Yinlong downsi*, Han et al. (2015) state that there is no quadratojugal foramen on the lateral side of the quadratojugal, but that a fossa is present posterodorsally between the quadrate and quadratojugal. Such fossa is visible and figured in the posterior aspect and in that same location (Han et al. 2015, fig. 9B). The quadratojugal foramen opens posteriorly between the quadrate and quadratojugal in *Liaoceratops yanzigouensis* (Xu et al. 2002) so this taxon was corrected and coded (0).

102(*). Body of the quadrate leans posteriorly (0), body of quadrate oriented vertically (1), body of quadrate leans anteriorly (2) (Boyd 2015 #47).

In *Psittacosaurus major* (You et al. 2008, fig. 1B) and *Psittacosaurus mongoliensis* (Osborn 1923, fig. 2A), *Tenontosautus tilletti* (Thomas 2015, fig. 1) and *Tenontosaurus dossi* (Winkler et al. 1997, fig. 2A) the quadrate is leant posteriorly. In *Hexinlusaurus multidens*, by change, the quadrate os told to be nearly vertical (He and Cai 1984, p. 7). The quadrate shaft is also vertical in *Iguanodon bernissartensis* (Norman 1980, fig. 2). Psittacosauridae, *T. tilletti* and *T. dossi* were corrected and coded (0). *H. multidens* and *I. bernissartensis* were corrected and coded (1).

103(*). Quadrate, prominent oval fossa on pterygoid ramus: absent (0), present (1) (Ösi et al. 2012 #57).

In *Parksosaurus warreni*, the pterygoid ramus of quadrate is reported to bear a faint depression (Parks 1926 ; Galton 1973), supposedly for the insertion of the quadratojugal. A wide depression is also reported in *Yandusaurus hongheensis* (He and Cai 1984). An ovoid fossa, located laterally near the posterior border of the pterygoid ramus of quadrate, was reported by Boyd (2014) for *Thescelosaurus neglectus*. Boyd (2014) further coments that such fossa is also present in *Zephyrosaurus schaffi* (Sues 1980), *Jeholosaurus shangyuanensis* (Barrett and Han, 2009), *Orodromeus makelai* (Scheetz 1999), *Parksosaurus warreni* (Galton 1973) and *Dysalotosaurus lettowvorbecki* (Norman et al. 2004). However, for what concerns *Z. schaffi*, *O. makelai*, *J. shangyuanensis*, *D. lettowvorbecki* no explicit mention or figure of an oval fossa on the posterolateral side of the pterygoid ramus was made (Sues 1980 ; Scheetz 1999 ; Barrett and Han, 2009 ; Galton 1983 ; Norman et al. 2004). The same occurs for *Dryosaurus* (Galton 1983), *Tenontosaurus tilletti* (Thomas 2015), *Tenontosaurus dossi* (Winkler et al. 1997) for which there is no information concerning this character. Although not reported, a shallow fossa-like depression seems to be present onto the posterolateral surface of the pterygoid wing of quadrate in *Fostoria dhimbangunmal* (Bell et al. 2019, fig. 2A, B). *F. dhimbangunmal*, *T. neglectus*, *P. warreni*, and *Y. hongheensis* were corrected and coded (1). *Z. schaffi*, *O. makelai*, *Dryosaurus*, *D. lettowvorbecki*, *J. shangyuanensis*, *T. tilletti*, *T. dossi* were therefore corrected and coded with a question mark.

104(*). Quadrate, mandibular articulation: quadrate condyles subequal in size (0), medial condyle is larger than lateral condyle (1), lateral condyle is larger than medial (2) (Ösi et al. 2012 #63).

Lesothosaurus diagnosticus bears a more ventrally projected medial condyle of quadrate distally (Porro et al. 2015, fig. 6G). Barrett and Han (2009) describe the distal quadrate condyles of *Jeholosaurus shanguyanensis* as being slightly more ventrally projected medially than laterally. However, in the matrix of Han et al. (2012, #63), the distal quadrate condyles

of *Jeholosaurus shangyuanensis* are coded as being subequal in size. In *Changchunsaurus parvus* (Liyong et al. 2010), the distal condyles of the quadrate are also reported to be "approximatively subequal in size". The distal quadrate condyles of the *Psittacosaurus mongoliensis* (Osborn 1923, fig. 2D) and *Psittacosaurus major* (You et al. 2008, fig. 2C1) appear to be level to one another. In *Thescelosaurus neglectus* (Boyd 2014), the distal condyles of the quadrate are told to be slightly asymmetrical with the lateral one being further ventrally extended than the medial one. However, the same author also affirms that both distal condyles are not much separated from each other (Boyd 2014, fig. 4, 8C-D). *Hypsilophodon foxii* (Galton 1974*a*, fig. 7B), *Orodromeus makelai* (Scheetz 1999, p. 24, 25), *Dysalotosaurus lettowvorbecki* (Janensch 1955, fig. 8A) and *Dryosaurus* (Galton 1983, pl. 1.3) have a distolateral quadrate condyle that is larger and more expanded distally than the distomedial one. In *Fostoria dhimbangunmal*, the lateral condyle of quadrate is "only slightly smaller than the medial condyle" (Bell et al. 2019, p. 3-4), but the figures support the idea that the lateral condyle is much larger than the medial one (Bell et al. 2019, fig. 2A, F). In *Haya griva* (Makovicky et al. 2011) the skull appears to have suffered some distortion so the character state could not be assessed. In *Parksosaurus warreni* (Parks 1926, pl. 1) the distal quadrate condyles are not preserved. *P. major* and *P. mongoliensis* were corrected and coded (0). *L. diagnosticus* was corrected and coded (1). *D. lettowvorbecki*, *Dryosaurus*, *F. dhimbangunmal*, *O. makelai* and *H. foxii* were corrected and coded (2). *H. griva*, *P. warreni* were corrected and coded with a question mark.

105(*). Laterosphenoid, socket for the head: occurs along frontal-postorbital suture (0), only in postorbital (1) (modified from Brown et al. 2013 #21).

In *Zalmoxes shqiperorum*, Godefroit et al. (2009, p. 533) say that the laterosphenoid articulated onto the postorbital exclusively, at the junction between the squamosal process, the jugal process and the anterior plate. Note that the anterodorsal head of the laterosphenoid also

contacted the postorbital exclusively in *Orodromeus makelai* (Scheetz 1999, p. 20), which is similar to what occurs in *Z. robustus* (Weishampel et al. 2003) and *Z. shqiperorum* (Godefroit et al. 2009). The dorsal head of the laterosphenoid contacted the frontal-postorbital suture in *Hypsilophodon foxii* (Galton 1974*a*), *Zephyrosaurus schaffi* (Sues 1980), *Agilisaurus louderbacki* (Barrett et al. 2005), *Jeholosaurus shangyuanensis* (Barrett and Han, 2009), *Tenontosaurus tilletti* (Thomas 2015, p. 35 and fig. 21), *Thescelosaurus assiniboiensis* and *Thescelosaurus neglectus* (Boyd 2014). For what concerns *Heterodontosaurus tucki* (Norman et al. 2011, p. 202) and *Yinlong downsi* (Han et al. 2015, p. 15), the anterodorsal head of the laterosphenoid is told to have contacted respectively the frontal-postorbital suture, and the postorbital process of the frontal. *H. tucki*, *Y. downsi*, *A. louderbacki*, *J. shangyuanensis*, *T. tilletti*, *T. neglectus* were corrected and coded (0). *Z. shqiperorum* was corrected and coded (1).

106(*). Post-temporal foramen position: at the boundary between the parietals/squamosals and the paroccipital process (0), entirely within the opisthotic (1), positioned entirely within the squamosal (2) (modified from Pol et al. 2011 #77; Boyd 2015 #103).

Dryosaurus, Dysalotosaurus lettowvorbecki (Galton 1983, fig. 1B, 3H), *Tenontosaurus tilletti* (Thomas 2015, fig. 1), *Camptosaurus dispar* (Carpenter and Lamanna 2015, fig. 7E) and *Orodromeus makelai* (Scheetz 1999, p. 28) present a post-temporal fossa located at the boundary between the paroccipital process and the squamosal. In *Iguanodon bernissartensis* (Norman 1980, fig. 6B), the post-temporal foramen notches the dorso-lateral margin of the supraoccipital at the boundary with the squamosal. We consider such position to be homologous with a post-temporal foramen notching the dorsal margin of the opisthotics. In *Tenontosaurus dossi*, the post-temporal foramen is reported to be at the junction between the squamosal and parietal, literally, in a position “dorsomedial to the squamosal bosses at the junction with the parietals” (Winkler et al. 1997, p.335). This condition of a post-temporal

foramen located dorsal to the boundary between the paroccipital process and the squamosal is a very unusual. In *Heterodontosaurus tucki* (Norman et al. 2011, fig. 14), the post-temporal fenestra is located at the limit between the supraoccipital and the parietal, and this limit is at the same level with, but medial to the suture between the paroccipital process and the squamosal. This position is momentaneously considered as homologous to that of a post-temporal foramen located at the boundary between the paroccipital process and the squamosal (not as in Pol et al. 2011 #77). *H. tucki*, *Dryosaurus*, *D. lettowvorbecki*, *I. bernissartensis*, *T. tilletti*, *C. dispar*, *O. makelai* were corrected and coded (0). The homology for the position of the post-temporal foramen position in *T. dossi* is dubious, so it was corrected and coded with a question mark. Every taxon that wasn't coded as having the posttemporal foramen at the limit between the opisthotic and the parietal/squamosal in previous character was corrected and coded as non-applicable for this character.

108(*). Prootic, position of the foramen for the trigeminal nerve (V): notches the posteroventral edge of the laterosphenoid at the boundary with the prootic (0), nearly or completely enclosed in prootic (1) (modified from Brown et al., 2013 #76).

Concerning the laterosphenoid of *Orodromeus makelai*, Scheetz (1999, p. 29) affirms that 'a depression occurs anterior to the trigeminal nerve (V) of the prootic which it borders'. We interpret this as meaning that the trigeminal nerve produces a depression on the posteroventral edge of the laterosphenoid in this taxon. In *Tenontosaurus tilletti*, the cranial nerve V notches the posterior edge of the laterosphenoid at the boundary with the prootic (Thomas 2015, fig. 35). In the Vegagete rhabdodontid, the posteroventral edge of the laterosphenoid is straight (Dieudonné et al. 2016a, fig. 3C, D). Therefore, wether the trigeminal passed at the boundary between the prootic and laterosphenoid or it was completely enclosed within the prootic, it didn't notch the laterosphenoid. In *Camptosaurus dispar*, the trigeminal foramen of the so-immature specimen DMNH 50131 is completely enclosed within the prootic (Carpenter and

Lamanna 2015, fig. 7B), and the trigeminal foramen of USNM V 5473 notches the inferoposterior corner of the laterosphenoid (Gilmore 1909, fig. 5; Carpenter and Galton 2018, fig. 21G). *O. makelai* and *T. tilletti* were corrected and coded (0). The Vegagete ornithopod was corrected and coded (1).

109(*). Prootic-basisphenoid plate: absent (0), present (1) (Ösi et al. 2012 #81).

The presence of a developped basisphenoid sheet was reported in *Heterodontosaurus tucki* (Norman et al. 2011 #81, from Butler et al. 2008 #81), *Eocursor parvus* (Butler 2010), and pachycephalosaurs (Maryanska and Osmolska 1974, see discussion of the prootic and basisphenoid, p. 65-66). In *H. tucki*, such sheet was called the "basisphenoid flange". In *E. parvus* it was reported as the "preoptic pendant". Such "plate" runs through the entire lateral surface of the basisphenoid from the junction with the prootic below cranial nerve (V) posterodorsally, to the lateral surface of the basipterygoid processes anteroventrally. A similar flange exists in *Hypsilophodon foxii*, but it is less prominent, shorter, and crosses both the prootic and a small portion of the basisphenoid (Galton 1974*a*, fig. 4B). Such plate could not be observed and were not described in the basal ceratopsians *Yinlong downsi*, Han et al. (2015, fig. 19D) and *Psittacosaurus major* (You et al. 2008). *Y. downsi* was corrected and coded (0) for this character. *E. parvus* and *H. tucki* were corrected and coded (1) for this character.

110(*). Supraoccipital, contribution to dorsal margin of the foramen magnum: forms entire dorsal margin of foramen magnum (0), exoccipital with medial process that restricts the contribution of the supraoccipital (1), the exoccipital join medially and excludes totally the supraoccipital from the dorsal margin of the foramen magnum (2) (modified from Ösi et al. 2012 #78; ordered character).

The dorsal contribution of the supraoccipital to the dorsal margin of the foramen magnum is partly reduced by the opisthotics in *Camptosaurus dispar* (Gilmore 1909, fig. 4) and

Dysalotosaurus lettowvorbecki (Galton 1983, fig. 3H; Hübner and Rauhut 2010, fig. 2C) but yet, it is still overwhelming. *Dryosaurus* was reported by Carpenter and Lamanna (2015, fig. 4E) to have its supraoccipital completely excluded from the dorsal margin of the foramen magnum. In *Zalmoxes robustus*, the ventral portion of the supraoccipital is laterally reduced, which should be caused by a ventromedial protrusion of the opisthotics (Weishampel et al. 2003, fig. 10B). The unnamed *Rhabdodon* species described by Pincemaille-Quilleveré et al. (2006, fig. 2) and *Muttaburrasaurus langdoni* (Bartholomai and Molnar, 1981, fig. 1C, 2B) presents the same condition. *Iguanodon bernissartensis* (Norman 1980), *Tenontosaurus tilletti* (Thomas 2015), *Tenontosaurus dossi* (Winkler et al. 1997, fig. 8) bear an exoccipital bar which excludes the supraoccipital from contact with the dorsal margin of the foramen magnum. In *Yinlong downsi*, the supraoccipital participates largely in the dorsal margin of the foramen magnum (Han et al. 2015, fig. 20). Consequently to the inclusion of character state (2), *Dryosaurus*, *I. bernissartensis*, *T. tilletti* and *T. dossi* were corrected and coded (2). *Z. robustus* and *M. langdoni* were corrected and coded (1). *Y. downsi* was corrected and coded (0).

111(*). Supraoccipital: nuchal crest is present (0) or absent (1) (Brown et al. 2013 #68).

A nuchal crest is absent in *Thescelosaurus neglectus* (Boyd 2014, p. 46), *Orodromeus makelai* (Scheetz 1999, p. 27), but it is present in other taxa as *Eocursor parvus*, *Lesothosaurus diagnosticus*, *Gasparinisaura cincosaltensis*, and *Tenontosaurus*. A nuchal crest – sometimes called "supraoccipital ridge" or "septum" – is actually observed in *Tenontosaurus tilletti* (see Thomas 2015, fig. 38), *Zalmoxes shqiperorum* (Godefroit et al. 2009), *Yinlong downsi* (Han et al. 2015), *Psittacosaurus mongoliensis* (Osborn 1923), *Psittacosaurus major* (You et al. 2008). *E. parvus*, *Z. shqiperorum*, *Y. downsi*, *P. mongoliensis* and *P. major* were corrected and/or newly coded (0).

112(*). Supraoccipital (SO), anteroposterior inclination and sutural contact with the opisthotics (OP) from a posterior view: the SO is obliquely inclined anteroposteriorly, the sutural contact with the OP is diagonal from the top laterally to the foramen magnum ventromedially (0), the SO completely roofs the endocranial cavity, it overlains the OP and its sutural contact with the OP is horizontal from a posterior view (1), the SO is held almost vertically and sutures nearly vertically with the adjacent opisthotics (2) (new character).

In *Thescelosaurus assiniboiensis* (Brown et al. 2011, fig. 11B), *Thescelosaurus neglectus* (Boyd 2014, fig. 4, 11A), and *Tenontosaurus tilletti* (Thomas 2015, fig. 1, 37), the supraoccipital is completely on top of the opisthotics, and the sutural contact between these bone is horizontal. In *Tenontosaurus dossi*, the supraoccipital is slightly inclined anteroposteriorly, though it has the shaped of an "inverted T" as in *T. tilletti* (Thomas 2015) and completely overlaps the opisthotics from a posterior view (Winkler et al. 1997, fig. 6C, 7B). What's more, Winkler et al. (1997, p. 335) make the following observation: "An anterior process of the supraoccipital […] extends from the lambdoidal crest, beneath the squamosal, and anteriorly onto the dorsolateral wall of the braincase, ventral to the parietal and dorsal to the prootic. A large supraoccipital that contributes significantly to the lateral wall of the braincase appears to be primitive relative to most iguanodontians and hadrosaurids (Norman and Weishampel, 1990; Sereno 1991)". We therefore coded (1) for *T. dossi*. In *Zephyrosaurus schaffi* the left lateral reconstruction of the braincase shows an almost horizontal supraoccipital (Sues 1980, fig. 11). However, the supraoccipital is indented within the opsithotics from a posterior view (Sues 1980, fig. 12B). Owing to these observations, we coded this taxon with the primitive character state (0). The dryomorphans largely differ from *Thescelosaurus* and *Tenontosaurus* in this character. For example, the supraoccipital of *Dryosaurus* is visible on a quite large extent from a dorsal view (Galton 1983, fig. 3B), and its sutural surfaces with the opisthotics are diagonally inclined (Galton 1983, fig. 1B, 3B). This

means that the *Dryosaurus altus*' supraoccipital must have been inclined anteroposteriorly. In *Dysalotosaurus lettowvorbecki*, the condition is in exactly the same, with the supraoccipital being inclined anteroposteriorly and joining the parietal anterodorsally (Janensch 1955, fig. 1b, 2a, 4). *Iguanodon bernissartensis* apparently preserves the same character state: "the supraoccipital is restored as a broad symmetrical bone, inclined forward and upward beneath the parietal" (Norman 1980, p. 16, fig. 6B). In *Hypsilophodon foxii* (Galton 1974*a*, fig. 4B), the supraoccipital is completely overlapped by the parietal, but it is clear that it is obliquely inclined anteroposteriorly, with diagonal edges for sutural contact with the opisthotics (Galton 1974*a*, fig. 8). In *Prenocephale prenes*, Maryanska and Osmolska (1974, p.63) make the following observation: "The supraoccipital forms the narrow portion of the roof of the medulla oblonga and anteriorly it expands and bounds the inner ear cavity posteromedially". Basing on this description, we coded *P. prenes* with character state (0).

113(*). Paroccipital processes (Exoccipital-Opisthotic complex): extend laterally and transit smoothly toward a slight dorsoventral expansion distally (0), distal end pendent, sharply deflects ventrally (1) (modified from Xu et al. 2006 #94; McDonald et al., 2010 #72 ; Ösi et al. 2012 #75)

In *Psittacosaurus mongoliensis* (Osborn 1923, fig. 2D) and *Psittacosaurus major* (You et al. 2008, fig. 2C2), the paroccipital processes are long and strap-like, and only slightly dorsoventrally expanded distally. The only heterodontosaurid for which the paroccipital processes are preserved is *Heterodontosaurus tucki*. Norman et al. (2011, p. 243) observe that *H. tucki* display paroccipital processes which are distally pendant and unusually deep for an early ornithischian. The same condition occurs in pachycephalosaurids (see also Maryanska and Osmolska 1974). The skull of *Agilisaurus louderbacki* was never illustrated from a posterior view (Peng 1992, 1997, Barrett et al. 2005). Peng (1992, p. 2) describes *A. louderbacki* as having thin exoccipitals, that "extend ventrally to form the angularly shaped

paroccipital process. Psittacosauridae was corrected and coded (0). *H. calathocercos*, *G. lattimorei*, *H. tucki* and *A. louderbacki* were corrected and coded (1).

114(*). Paroccipital processes, proportions: short and deep (height ≥ 1/2 length) (0), elongate and narrow (1) (Xu et al. 2006 #35; Ösi et al. 2012 #76).

Yinlong downsi (Xu et al. 2006, sup. material 1B), *Psittacosaurus mongoliensis* (Osborn 1923, fig. 2D) and *Psittacosaurus major* (You et al. 2008, fig. 2C2) display long and narrow paroccipital processes. *Y. downsi*, P. *mongoliensis* and *P. major* were corrected and coded (1).

115(*). Basioccipital, contribution to the border of the *foramen magnum*: *foramen magnum* occupies less than 50% of occipital condyle or is completely excluded from it by the exoccipitals (0), more than 50% of occipital condyle (1) (modified from Ösi et al. 2012 #79; Brown et al. 2013 #71).

The character codings were modified because the proportions of basioccipital contribution to the foramen magnum are almost always above 30%, and could even reach ≈ 80% of the total basioccipital condyle width in some instances. The outgroup taxon *Herrerasaurus ischigualastensis* displays a relatively small basioccipital condyle contribution to the foramen magnum (≈ 18.2%, Sereno and Novas 1993, fig. 1G): the basioccipital condyle is in fact mostly constituted by the exoccipitals/opithotics laterally. In most of the cases, basal ornithischians show a basioccipital contribution to the foramen magnum of 50% or less of its total width. This was globally the case for pachycephalosaurids such as *Goyocephale lattimorei* (27.3%, Perle et al. 1982, pl. 41.2A), *Stegoceras validum* (≈ 43,8%, Maryanska and Osmolska 1974, fig. 1A4) and *Prenocephale prenes* (≈ 43,8%, Maryanska and Osmolska 1974, fig. 1C4), but not *Homalocephale calathocercos* (≈ 57.1%, Maryanska and Osmolska 1974, fig. 1D4); *L. diagnosticus* (≈ 47.2%, Sereno 1991, fig. 12C) and *H. multidens* (≈ 41.2%, He and Cai 1984, fig. 3); the ornithopods *T. neglectus* (≈ 42.1%, Boyd 2014, fig. 4) and basal iguanodontians *T. dossi* (≈ 36.8%, Winkler et al. 1997, fig. 8) and *T. tilletti* (≈ 49.2%, Thomas

2015, fig. 1); the elasmarian *A. saldiviai* (≈ 42%, Cambiaso 2007, fig. 98C'). Rhabdodontomorphans such as *M. langdoni* (≈ 36%, Bartholomai and Molnar, 1981, fig. 1C) and *Z. robustus* (≈ 37%, Weishampel et al. 2003, fig. 11) stand out as having a relatively narrow participation of the foramen magnum to the total basioccipital width. As Bell et al. (2019) pointed out, the skull of *G. cincosaltensis* is laterally deformed so it is not really possible to infer its state for this character. Some ornithopods such as *H. foxii* (≈ 67%, Galton 1974, fig. 8), *T. assiniboiensis* (≈ 58%, Brown et al. 2011, fig. 11B), *O. makelai* (≈ 82%, Scheetz 1999, fig. 9A), *H. griva* (≈ 56%, Makovicky et al. 2011, fig. 1C) show a wide contribution of their foramen magnum to their total respective basioccipital width. This is also the case for ceratopsians: *P. major* (≈ 51%, You et al. 2008, fig. 2C1), *P. mongoliensis* (≈ 54%, Osborn 1923, fig. 2D), *A. oshimai* (≈ 57.9%, You and Dodson 2003, fig. 1F), *Y. downsi* (> 65%, Han et al. 2015, fig. 9) and dryosaurids: *D. lettowvorbecki* (≈ 52.4%, Galton 1983, fig. 3H), *Dryosaurus altus* (≈ 54% Galton 1983, fig. 1B). The basioccipital condyle contribution to the foramen magnum is small in the ankylopollexians *Iguanodon bernissartensis* (<30%, Norman 1980, fig. 4B) and *C. dispar* (46,8%, Gilmore 1909, fig. 4), but this is because the lateral walls formed by the exoccipitals/opisthotics are thin and medially displaced from the lateral borders of the basioccipital condyles. In *Dryosaurus* (Galton 1983, fig. 1B) the basioccipital condyle portion which contributes to the foramen magnum is wider, and the lateral walls formed by the exoccipitals/opisthotics are also thin and medially displaced. In *A. oshimai* (You and Dodson 2003) and *L. yanzigouensis* (Xu et al. 2002) the exoccipital almost or completely exclude the basioccipital from the foramen magnum. These two taxa recoded (0) because of the new character definition since that of Ösi et al. (2012 #79).

116(*). Basioccipital, ventral margin of occipital condyle: forms a neck before a being posteroventrally expanded (0), smooth and continuous, devoid of ventral neck (1) (rephrased from McDonald et al. 2010 #74).

The basioccipital condyle of *Yinlong downsi* (Han et al. 2015, fig. 19D) is posteroventrally directed. Therefore, *Y. downsi* was corrected and coded (0).

117(*). Basioccipital, anteroposteriorly directed groove extending along ventral surface: absent (0), present (1) (McDonald et al. 2010 #75).

There is no ventral groove along the basioccipital of *Yinlong downsi* (Han et al. 2015, fig. 19E). Similarly, Weishampel et al. (2003) do not report any anteroposteriorly directed groove along the ventral surface of *Zalmoxes robustus* basioccipial. *Y. downsi* and *Z. robustus* were corrected and coded (0).

118(*). Basioccipital, median ridge extending along ventral surface: absent (0), present (1) (reformulated from Xu et al. 2006 #95; McDonald et al. 2010 #76; Brown et al. 2013 #73).

The basioccipital of *Zalmoxes robustus* (Weishampel et al. 2003) is described as forming a "narrower hemicylindrical column" anteriorly, but no median ridge is alluded to so far. *Lesothosaurus diagnosticus* (Porro et al. 2015), *Yinlong downsi* (Han et al. 2015, fig. 18B), *Hypsilophodon foxii* (Galton 1974*a*, fig. 6A), *Tenontosaurus tilletti* (Thomas 2015, fig. 6) *Thescelosaurus neglectus* (Boyd 2014, fig. 11D), *Orodromeus makelai* (Scheetz 1999, p. 31) and *Zephyrosaurus schaffi* (Sues 1980, fig. 15A) all are described to bear a median tubercle, ridge or keel in the antero-inferior part of the basioccipital. The pachycephalosaurs *Stegoceras validum* (Sues and Galton 1987, p. 9), *Prenocephale prenes* and *Pachycephalosaurus wyomingensis* (Maryanska and Osmolska 1974, p. 64) all bear a median keel along the anteroventral part of the basioccipital. *Goyocephale lattimorei* is told to have a similar basioccipital as that of other pachycephalosaurs (Perle et al. 1982). The presence of a median keel may therefore be plesiomorphic at least for Cerapoda. *Nanosaurus agilis* was never

described for such cranial material (Carpenter and Galton 2018, fig. 11). No information could be extracted on this character in *Parksosaurus warreni* (Galton 1973) either. *Z. robustus* was corrected and coded (0). *L. diagnosticus*, *Y. downsi*, *G. lattimorei*, *H. foxii*, *T. tilletti*, *T. neglectus*, *O. makelai*, *Z. schaffi* were corrected and coded (1). *N. agilis* and *P. warreni* were corrected and coded with a question mark.

119(*). Basioccipital, anteroventral part: produces an elongated process that is "locked" between the basal tubera of the basisphenoid (0), forms a broadly concavo-convex contact with the basisphenoid, or is completely restricted to the posterior aspect of the basal tubera (1) (new character).

In *Stegoceras validum* (Gilmore 1924), *Prenocephale prenes* (Maryanska and Osmolska 1974, p. 64), *Herrerasaurus ischigualastensis* (Sereno and Novas 1993), the basioccipital is tightly locked anteriorly and form the central portion between the basal tubera of the basisphenoid. Despite no detailed description was provided, *Goyocephale lattimorei* was told to have a similar basioccipital as that of other pachycephalosaurs (Perle et al. 1982, pl. 41.2C). Note that in *Heterodontosaurus tucki*, transverse reconstruction of the braincase shows that the basioccipital would protrude between the basal tubera anteriorly (Norman et al. 2011, p. 207, fig. 11). However, a ventral view of the braincase of *H. tucki* shows no protrusion of the basioccipital between the basal tubera (Norman et al. 2011, fig. 13). Accounting for what is figured and observable, *H. tucki* was coded (1). In *Agilisaurus louderbacki* (Peng 1992), the basioccipital is told to be fused anteriorly with the "basipterygoid": Peng (1992) may have here referred to the basisphenoid. Furthermore, the "basipterygoid" is told to extend laterally into smooth and rounded ridges (which we interpret as the basal tubera), and that an anterior basipterygoid process is poorly developped. We deduce from this description that the basioccipital was offset posteriorly from the basisphenoid and its basal tubera. *Camptosaurus dispar* (Gilmore 1909, p. 206, 208;

Carpenter and Lamanna 2015, fig. 7D) and *Dryosaurus* (Carpenter and Lamanna 2015, fig. 4E) are unique in that their basioccipital bear a tongue-like anterior prolongation which inserts between the basal tubera of the basisphenoid.

120(*). Basioccipital, basal tubera: extend much farther ventrally than the basisphenoid/parasphenoid plate (0), level (1) (reformulated from Brown et al. 2013 #74).

In *Heterodontosaurus tucki* (Norman, 2011, fig. 2), *Goyocephale lattimorei* (Perle et al. 1982, pl. 41.2A-C, pl. 42.2), *Stegoceras validum* (Snively and Theodor 2011, fig. 5B), *Stegosaurus stenops* (Gilmore 1914, pl. 8), *Yinlong downsi* (Han et al. 2015, fig. 19D), *Psittacosaurus major* (You et al. 2008, fig. 2A), *Hypsilophodon foxii* (Galton 1974*a*, fig. 5A), *Zephyrosaurus schaffi* (Sues 1980, fig. 10), *Anabisetia saldiviai* (Coria and Calvo 2002, fig. 4), *Dysalotosaurus lettowvorbecki* (Janensch 1955, pl. 9.1A), *Camptosaurus dispar* (Gilmore 1909, fig. 5), the basal tubera are roughly level with the parasphenoid. In *Orodromeus makelai* (Scheetz 1999, fig. 9), the complete basicranium was not figured. However, the parasphenoid is told to extend below the orbit, and by comparing figures 4 and 9 of Scheetz (1999), we could safely infer that the basal tubera should have been level with the anterior extension of the basisphenoid and parasphenoid. This codification was already made anteriorly, which confirm our interpretation of this character. By contrast, in *Thescelosaurus neglectus* (Boyd 2014, fig. 11), *Tenontosaurus tilletti* (Thomas 2015, fig. 36), the basal tubera are situated much lower with respect to the basisphenoid/parasphenoid. In *Zalmoxes robustus* (Weishampel et al. 2003, fig. 11D-E) the anterodorsal shift of the basipterygoid processes clearly shows that the anterior basisphenoid/parasphenoid should have been situated higher than the basal tubera. In *T. assiniboiensis* (Brown et al. 2011, fig. 11G), and *Zalmoxes shqiperorum* (Godefroit et al. 2009, fig. 8) the basisphenoid/parasphenoid plate is not preserved so this character is difficult to infer without first-hand examination. In *Iguanodon bernissartensis*, the parasphenoid is projected anterodorsally (Norman 1980, fig. 9) in a way

not observed in more basal ornithopods: this induces that the basal tubera are located well below posteriorly. *Y. downsi,* Psittacosauridae*, H. tucki*, *H. foxii* and *D. lettowvorbecki* were corrected and coded (1). *T. tilletti*, *T. neglectus* were corrected and newly coded (0). *T. assiniboiensis* and *Z. shqiperorum* were corrected and coded with a question mark.

121(*). Basioccipital, basal tubera: level with the base of the basioccipital condyle (0), form a massive buttress which extends much lower than the base of the basioccipital condyle (1) (reformulated from Ösi et al. 2012 #82).

In *Psittacosaurus major* (You et al. 2008, fig. 2A), *Thescelosaurus neglectus* (Boyd 2014, fig. 11B), *Hypsilophodon foxii* (Galton 1974*a*), *Dryosaurus* (Galton 1983), *Dysalotosaurus lettowvorbecki* (Janensch 1955, pl. 9.1A), *Anabisetia saldiviai* (Coria and Calvo 2002, fig. 4), the ventral extremity of the basal tubera are roughly level with that of the occipital condyle. In *Changchunsaurus parvus* (Liyong et al. 2010, fig. 6CA), a ventral close-up of the braincase strongly suggests that the basal tubera aren't much ventrally extending either. In *Goyocephale lattimorei*, the basal tubera are roughly level with the basioccipital condyle (Perle et al. 1982, pl. 42-2). This is coherent with what is also observed in *Stegoceras validum* (Snively and Theodor 2011, fig. 5B). In *Homalocephale calathocercos* (Maryanska and Osmolska 1974) the basal tubera are told to be much ventrally expanded, so pending further confirmation we left this taxon coded (1). In *Zalmoxes robustus* (Weishampel et al. 2003, fig. 11D-E), *Zalmoxes shqiperorum* (Godefroit et al. 2009, fig. 8), *Zephyrosaurus schaffi* (Sues 1980, fig. 10), *Orodromeus makelai* (Scheetz 1999, fig. 9), *Tenontosaurus tilletti* (Thomas 2015, fig. 35), *Tenontosaurus dossi* (Winkler et al. 1997, fig. 7), *Thescelosaurus assiniboiensis* (Brown et al. 2011, fig. 11), *Convolosaurus marri* (Andrzejewski et al. 2019, fig. 10A, B) the basal tubera form a massive, ventrally extending buttress with respect to the occipital condyle. This feature was neither described nor figured in *Jeholosaurus shangyuanensis* (Barret and Han, 2009), *Haya griva* (Makovicky et al. 2011), *Eocursor parvus* (Butler 2010, fig. 4),

Liaoceratops yanzigouensis (Xu et al. 2002), *Archaeoceratops oshimai* (Dong and Azuma 1997) and not available in *Chaoyangosaurus youngi* (Zhao et al. 1999). *G. lattimorei* was corrected and coded (0). *Z. robustus*, *Z. shqiperorum*, *Z. schaffi*, *O. makelai*, *C. marri*, *T. tilletti*, *T. dossi* were corrected and coded (1). *J. shangyuanensis*, *H. griva*, *E. parvus*, *L. yanzigouensis*, *A. oshimai*, *C. youngi* were corrected and coded with a question mark.

122(*). Angle between the base of the braincase (i.e. the axis formed by the occipital condyle and basisphenoid) and long axis of the braincase : less than 35 degrees (0), equal or more than 35 degrees (1) (reformulated from Boyd 2015 #98).

Contra previous condifications of this character (Weishampel and Heinrich 1992 #16), it seems that the primitive condition for this character is an angle between the base and long axis of the braincase which is largely inferior to 35°. This is the case for *Heterodontosaurus tucki* (Norman et al. 2011, fig. 11), *Stegoceras validum* (Snively and Theodor 2011, fig. 5B), or *Stegosaurus stenops* (Galton 2001, fig. 5.8). Ornithopods are apparently all bearing the condition of a higer angle between the base and long axis of their braincase. This is notably the case for *Hypsilophodon foxii* (Galton 1974*a*, fig. 4), *Zephyrosaurus schaffi* (Sues 1980, fig. 11), *Thescelosaurus neglectus* (Boyd 2014, fig. 11A). Such character is difficultly identificable in *Orodromeus makelai* (Scheetz 1999, fig. 9). Much interestingly, the basal ceratopsian *Psittacosaurus major* displays a steeply inclined braincase long axis (You et al. 2008, fig. 2A2), which markedly differ from what is observed in the pachycephalosaur *Stegoceras validum* (Snively and Theodor 2011, fig. 5B). *H. tucki* was corrected and coded (0). *H. foxii*, *Z. schaffi*, *T. neglectus* were corrected and coded (1). *O. makelai* was corrected and coded with a question mark.

123(*). Basisphenoid, basipterygoid processes articular facet orientation: anteroventral and/or anterolateral (0), ventral (1), posteroventral (2) (modified from Xu et al. 2006 #14; Ösi et al. 2012 #83).

The basipterygoid processes are anteroventrally directed in *Herrerasaurus ischigualastensis* (Sereno and Novas 1993), *Eocursor parvus* (Butler 2010) and *Heterodontosaurus tucki* (Norman et al. 2011). In many ornithischians, the basipterygoids processes are anteroventrally projected, but end in a abrupt vertical plane anteriorly. This is notably the case of *Stegosaurus stenops* (Gilmore 1914, p. 30), *Emausaurus ernsti* (Haubold 1990, fig. 3), the Ankylosaur *Pawpawsaurus campbelli* (Paulina-Carabajal et al. 2016, fig. 3A, B), *Lesothosaurus diagnosticus* (Porro et al. 2015, fig. 9I), *Orodromeus makelai* (Scheetz 1999, fig. 9). In *Jeholosaurus shangyuanensis* (Barrett and Han, 2009) and *Haya griva* (Makovicky et al. 2011, fig. 1D) the basipterygoid processes are told to be slightly rostroventrally oriented. These processes are more pronouncedly oriented rostroventrally in *Changchunsaurus parvus* (Liyong et al. 2010, fig. 6A). In *Yinlong downsi*, the basipterygoid processes are oriented caudoventrally (Han et al. 2015, cf. fig. 19D). The basipterygoid processes of basal neoceratopsians such as *Liaoceratops yanzigouensis* (Xu et al. 2002) and *Archaeoceratops oshimai* (Dong and Azuma 1997 ; You and Dodson 2003) were largely obscured ventrally by the central plate of the pterygoids. However in *Psittacosaurus major* a fracture allows us to see that the basipterygoid processes were anteroventrally directed (You et al. 2008, p. 191, fig. 2A). Maryanska and Osmolska (1974, p. 66, pl. 25-2A) state that the basisphenoid of *Prenocephale prenes* and pachycephalosaurs in general send a pair of thick basipterygoid process anteroventrally, but such affirmation is hard to assess from the provided figures. From currently known material, pachycephalosaurs display ventrally to slightly posteroventrally directed basipterygoid processes (*Goyocephale lattimorei*, Perle et al. 1982, pl. 41-2 ; *Stegoceras validum*, Snively and Theodor 2011, fig. 1B). The basipterygoid processes of *Convolosaurus marri* are represented by a ‘separate piece’ of right basipterygoid, but aren’t figured (Andrzejewski et al. 2019, p. 14). *L. diagnosticus*, *E. ernsti*, Ankylosauria, Stegosauria, *O. makelai*, *J. shangyuanensis*, *H. griva* were corrected and coded (1). *Y. downsi*

was corrected and coded (2). *C. marri*, *L. yanzigouensi*, *A. oshimai*, *H. calathocercos* were corrected and coded with a question mark.

124(*). Notch between posteroventral edge of basisphenoid and base of basipterygoid process: deep (0) or notch shallow with base of basipterygoid process close to basioccipital tubera (1) (Xu et al. 2006 #15).

Yinlong downsi was corrected and newly coded (1) based on figure 19D of Han et al. (2018). As far as we know, there is no sufficiently detailed published information concerning the skull of *Psittacosaurus mongoliensis*, so we corrected and coded a question mark for this taxon, instead of (0) previously. In *Psittacosaurus major* (You et al. 2008) the basipterygoid processes are told to form a thikenned ridge stuck to the base of the quadrate medially. However, we could not observe this on the figure (You et al. 2008, fig. 1C) so we temporarily coded a question mark for this taxon as well for this taxon. In *Zalmoxes robustus* (Weishampel et al. 2003, fig. 11D), the basipterygoid processes are also very close to the basal tubera.

125(*). Basisphenoid, length relative to basioccipital length: longer or subequal (0), shorter than basioccipital (1) (Ösi et al. 2012 #80).

Only a portion of the basisphenoid is preserved in *Convolosaurus marri* (Andrzejewski et al. 2019). The anterior part of the basisphenoid is hidden from a ventral view by the pterygoids in pachycephalosaurs (Maryanska and Osmolska 1974). *C. marri* and *Homalocephale calathocercos* were corrected and coded with a question mark.

126(*). Pterygoid, contact with its counterpart: absent, the basicranium is mostly exposed in ventral view, (0) present, the basicranium is mostly obscured in ventral view by an interpterygoid contact formed by the palatal and/or quadrate rami (1) (modified from Xu et al. 2006 #98).

It seems that an anterior contact between the pterygoids is a primitive condition for ornithischians as this occurs for *Herrerasaurus ischigualastensis* (Novas 1994, fig. 7D). In

Heterodontosaurus tucki, the pterygoids were close to each other, and more particularly so anteriorly, so the basisphenoid was still visible posteriorly. They were probably linked to each other by connective tissue (Norman et al. 2011). In *Yinlong downsi* (Han et al. 2015, p. 22, fig. 18), "the pterygoid contact on the midline at the point where the three plate-like rami (palatine, maxillary, quadrate) converge", which leaves the basisphenoid visible from a ventral view. In *Psittacosaurus major* (You et al. 2008), the pterygoids are also much expanded and contact each other on their anterior part, leaving the basisphenoid visible in ventral view. In *Liaoceratops yanzigouensis*, the pterygoid are extensively contacting with each other anteriorly, and the possibility to view the basisphenoid from a ventral view is not discussed (Xu et al. 2002, see fig. 1D). Within the "Asian clade", the same interpterygoid contact also happens in front of the basisphenoid, in *Changchunsaurus parvus* (Liyong et al. 2010, fig. 6B) and *Jeholosaurus shangyuanensis* (Barrett and Han, 2009, fig. 2B). Pachycephalosaurs differ in that their pterygoids fully contact each other posteriorly, so the basisphenoid is fully obscured posteriorly, and there is a narrow interpterygoid vacuity anteriorly (Maryanska and Osmolska 1974). In *Stegosaurus stenops* (Gilmore 1914, pl. 7) and *Lesothosaurus diagnosticus* (Sereno 1991) the pterygoids also contact each other on their posterior portion, but the basisphenoid is fully visible behind from a ventral view. Owing to the important difference observed between *H. tucki* and other taxa for which the pterygoid are clearly not contacting, with a more vertical orientation, *H. tucki* was corrected and coded (1). *C. parvus* and *J. shanguyanensis* were corrected and/or newly coded (1).

128(*). Pterygoid-maxilla contact, at posterior end of tooth row: absent (0), present (1) (Ösi et al. 2012 #87).

Haya griva (Makovicky et al. 2011, cf. fig. 1D and p. 630), *Chaoyangosaurus youngi* (Zhao et al. 1999, p. 689) and *Scelidosaurus harrisonii* (Owen 1861) were incorrectly coded as bearing a pterygoid-maxillary contact: it is absent in the former, and it is impossible to infer

for the latter two. A very small contact between the pterygoid and the maxilla is described for *P. major* (You et al. 2008), as well as in *L. yanzigouensis* (Han et al. 2018 #138). *C. youngi* and *S. harrisonii* were corrected and coded with a question mark. *H. griva* was corrected and coded (0). *L. yanzigouensis* was corrected and coded (1).

129(*). Pterygoid participation to the pterygo-palatine fenestra: present (0), absent, the ectopterygoid prevents the pterygoid from participating to the pterygo-palatine fenestra (1) (new character).

In basal ceratopsians (e.g. Han et al. 2015, fig. 18B; Xu et al. 2002, fig. 1D), the pachycephalosaur *Homalocephale calathocercos* (Maryanska and Osmolska 1974, fig. 1D3), and cerapods such as *Haya griva* (Makovicky et al. 2011), and *Thescelosaurus neglectus* (Boyd 2014), the ectopterygoid widely contributes to the pterygo-palatine fenestra so the pterygoid is excluded from its margin. In *Changchunsaurus parvus*, a small "postpalatine" foramen that lies in contact with the ectopterygoid, pterygoid and palatine is described (Liyong et al. 2010, p. 208). However, and as deduced from the photograph (Liyong et al. 2010, fig. 6B), the ectopterygoid appears much expanded anteriorly so that the pterygoid doesn't contact the postpalatine foramen. Some pachycephalosaurs such as *Stegoceras validum* and *Prenocephale prenes* feature a reversed condition with respect to their marginocephalian ancestor in having a pterygoid that contributes to the pterygo-palatine fenestra (Gilmore 1924, pl. 5; Maryanska and Osmolska 1974, fig. 1A3, 1C3). In *Heterodontosaurus tucki*, the palatine branch of the pterygoid is poorly preserved and no specific mention of the pterygo-palatine fenestra is made except that the palatine branch of the pterygoid would be laterally sutured to the ectopterygoid (Norman et al. 2011, p. 208). Norman et al. (2011, fig. 13) provide a conjectural reconstruction of the skull in ventral view, where the pterygoid participates in the pterygo-palatine fenestra. However, the right side of SAM-PK-K1332 (Norman et al. 2011, appendix 5.A) seems to feature a pterygo-palatine

fenestra enclosed by the ectopterygoid and palatine. This is not that clear on the left side of the same skull.

130(*). Lower jaw, length of post-coronoid elements (from the dorsal border of the coronoid-surangular suture) relative to the total length of the lower jaw: more than 35 (0), 25-35% (1) (modified from Brown et al. 2013 #62; Boyd 2015, #83).

The post-coronoid elements of the lower jaw of *Psittacosaurus major* (You et al. 2008, fig. 4) make more than 35% of the total lower jaw length. The post-coronoid elements of the lower jaw of *Eocursor parvus* (Butler et al. 2007, fig. 2A), *Heterodontosaurus tucki* (Norman et al. 2011), *Scelidosaurus harrisonii* (Owen 1861, pl. 5), *Gasparinisaura cincosaltensis* (Coria and Calvo, 1996, fig. 2A), *Orodromeus makelai* (Scheetz 1999, fig. 4), *Tenontosaurus tilletti* (Thomas 2015, fig. 51), *Tenontosaurus dossi* (Winkler et al. 1997, fig. 10) make up 35% or less than the total length of the lower jaw. *P. major* and *Auroella* were corrected and coded (0). E. *parvus*, *H. tucki*, *S. harrisonii*, *G. cincosaltensis*, *O. makelai*, *T. tilletti*, *T. dossi* were corrected and coded (1).

131(*). Predentary: absent (0), present (1) (Ösi et al. 2012 #90).

The predentary of *Isaberrysaura mollensis* (Salgado et al. 2017, fig. 2C), and *Wannanosaurus yansiensis* (Hou 1977, fig. 1) is preserved. The predentary of *Kulindadromeus zabaikalicus* is not (Godefroit et al. 2014, fig. 1B, C). *I. mollensis* and *W. yansiensis* were corrected and coded (1). *K. zabaikalicus* was corrected and coded with a question mark.

132(*). Predentary, size and position: short and the posterior extremity is posteriorly set, the predentary oppose only the first half of the premaxilla (0), short, the posterior border is anteriorly set, all but the posterodorsal corner of the predentary is positioned anterior to the last premaxillary tooth (1), roughly equal in length to the premaxilla, premaxillary teeth only oppose predentary all along (2), (modified from Ösi et al. 2012 #91).

The predentary of *Isaberrysaura mollensis* (Salgado et al. 2017, fig. 2C) clearly opposes the anterior extremity of the premaxilla. In *Stegosaurus stenops* (Marsh 1887, pl. 6) the predentary is short but its posterior border starts in a relative anterior position. An anteriorly placed predentary is described for *Tianyulong confuciusi* (Sereno 2012, fig. 22, p. 55) and is clearly visible in *Agilisaurus louderbacki* (Peng 1992, fig. 1A). While describing *Goyocephale lattimorei*, Perle et al. (1982, p. 119) state that "The third premaxillary caniniform extended lateral to the anterior tip of the dentary". This means undoubtedly that, despite of not being preserved, the predentary was anteriorly located with respect to the last premaxillary tooth. The predentary is also unpreserved in *Stegoceras validum*, but the facets on its symphyseal end indicates that it did exist on the anterior tip of the dentary (Sues and Galton 1987, fig. 3), and that it was very short (Gilmore 1924). In addition, the relation between the lower jaw and the skull (e.g. Brown and Slaikjer, 1943, pl. 44) clearly indicates that the last premaxillary tooth would have been posteriorly located with respect to the proximal articulation of the predentary. The predentary of *Psittacosaurus mongoliensis* (Osborn 1923, fig. 2A; Sereno 2010, fig. 2.7) and *Psittacosaurus major* (You et al. 2008, fig. 2A1 and 4A1 assembled together) is much anteriorly offset so it almost only covers the oral margin of the rostral bone. The oral margin of the predentary of *Convolosaurus marri* is described as being the same length as the premaxilla, and likely oppose the whole premaxilla as well (Andrzejewski et al. 2019, fig. 6, 7). The predentary is not preserved in the tyreophorans *Emausaurus ernsti* (Haubold 1990) and *Scelidosaurus harrisoni* (Owen 1861). *C. marri* was corrected and coded (2). Stegosauria, *I. mollensis*, Psittacosauridae, *S. validum*, *Goyocephale lattimorei*, *A. louderbacki*, *T. confuciusi* were corrected and coded (1). *S. harrisonii* and *E. ernsti* were corrected and coded with a question mark.

133(*). Predentary, shape: rounded tip (0), pointed tip (1), (Ösi et al. 2012 #92).

The predentary of *Psittacosaurus major* (You et al. 2008; Sereno 2010) and *Psittacosaurus mongoliensis* (Sereno 2010) has a rounded tip. The predentary of *Heterodontosaurus tucki* (Norman et al. 2011) as well as that of *Wannanosaurus yansiensis* (Hou 1977) is described as "triangular" and looks relatively pointed. *P. major* and *P. mongoliensis* were corrected and coded (0). *Heterodontosaurus tucki* and *Wannanosaurus yansiensis* were corrected and coded (1).

134(*). Predentary, grooves on either side of midline on anterior surface, extending ventrolaterally to dorsomedially: absent (0), present (1) (McDonald et al. 2010 #6).

The predentary of *Yinlong downsi* (Han et al. 2015), *Heterodontosaurus tucki* (Norman et al. 2011), *Psittacosaurus mongoliensis* (Sereno 2010, fig. 2.7), *Psittacosaurus major* (You et al. 2008, fig. 4A), *Agilisaurus louderbacki* (Peng 1992) lack a lateral groove. The predentary of *Haya griva* (IGM/100-2017, Han et al. 2018, sup. info 3, illustration for character #153) displays a lateral groove. *Y. downsi*, *H. tucki*, *A. louderbacki* were corrected and coded (0). *H. griva* was corrected and coded (1).

135(*). Predentary, oral margin: relatively smooth (0), denticulate (1) (Ösi et al. 2012 #93).

The original predentary of *Wannanosaurus yansiensis* featured a smooth oral margin before it was lost (Hou 1977). *Talenkauen santacrucensis* has been reported to bear a denticulate oral margin of predentary (Cambiaso 2007, fig. 14C, D). *W. yansiensis* was corrected and coded (0). *T. santacrucensis* was corrected and coded (1).

136(*). Predentary, tip of in lateral view: does not project above the main body (0), strongly upturned relative to main body (1) (Xu et al. 2006 #33; Ösi et al. 2012 #94).

W. yansiensis (Hou 1977) was corrected and coded (0).

137(*). Predentary, ventral process: single (0), bilobate (1) (Ösi et al. 2012 #95).

Zhao et al. (1999, p. 683) tell that in *Chaoyangosaurus youngi*, "grooves on the surface of the symphysis suggest that the predentary sends a rather long ventral process under the full length

of the symphysis and two short lateral processes". Psittacosaurs are told to bear a remnant of the bifid ventral process of the predentary, as also occurs for neornithischians (Sereno 2010, p. 26). This feature is explicitly referred to a young individual of *Psittacosaurus mongoliensis* (Sereno 2010, p. 51). In ornithopods such as *Tenontosaurus tilletti* (Thomas 2015, fig. 48.4), the ventral process of the predentary is stout but bilobate. In *Tenontosaurus dossi* (Winkler et al. 1997), the ventral process of predentary is reported as bearing a weak indent. In *Wannanosaurus yansiensis* (Hou 1977) and *Tianyulong confuciusi* (Sereno 2012) the predentary is described as "extremely short", so it is almost devoid of ventral process. In *Heterodontosaurus tucki*, the ventral process is clearly unilobate (Norman, 2011, fig. 3B). Galton (1974*a*) indicates the presence of only one predentary for *Hypsilophodon foxii*, which actually lacks the extremity of the ventral process (Galton 1974*a*, fig. 11). In *Agilisaurus louderbacki* (Peng 1992, 1997; Barrett et al. 2005), there is no indication to firmly assess the presence of a bilobate or unilobate ventral process of predentary. *C. youngi* was corrected and coded (1). *P. mongoliensis* was coded (1) for this character, contra previous codification (0) for Psittacosauridae. *T. tilletti* and *T. dossi* were corrected and coded (1). *W. yansiensis*, *T. confuciusi* and *H. tucki* were corrected and coded (0). *H. foxii* and *A. louderbacki* were corrected and coded with a question mark.

138(*). Predentary, ventral process: present, well-developed (0), very reduced or absent (1) (Ösi et al. 2012 #96).

The predentary of *Wannanosaurus yansiensis* is now lost, but was figured by Hou (1977, fig. 1) as short, blocky and wedge-shaped bone, dorsally upturned and not reaching the anteroventral tip of the dentary. This is very similar to the predentary of *Tianyulong confucuisi* which is described by Sereno (2012, p. 55) as short and lacking any ventral process. In *Agilisaurus louderbacki* (Peng 1992), the predentary is cone-shaped and dorsally directed, but it covers the whole dorsoventral extent of the dentary symphysis anteriorly. The

predentary of *Isaberrysaura mollensis* (Salgado et al. 2017, fig. 2C) is considered as preserved and showing a moderate ventral process. *I. mollensis* and *Aurorella* were corrected and coded (0). The heterodontosaurid *Tianyulong confuciusi* (Sereno 2012) and the pachycephalosaur *Wannanosaurus yansiensis* (Hou 1977) were corrected and coded (1) for this character.

140(*). Dentary, ratio of dentary height (just anterior to the rising coronoid process) divided by length of dentary: between 15-20% (0), 20-35% (1) (Brown et al. 2013 #63).

In *Nanosaurus agilis*, the ratio of dentary height to length is slightly superior to 20% in the largest dentary (SMA 0006, Carpenter and Galton 2018, fig. 7J). No dentary is available for *Yandusaurus hongheensis* (He and Cai 1984). Psittacosaurids (Sereno 2010) and *Talenkauen santacrucensis* (Cambiaso 2007, fig. 15A, B) bear a relatively stout dentary. *Iguanodon bernissartensis* bears an elongated but deep dentary (Norman 1980, fig. 2). *N. agilis, P. mongoliensis*, *P. major*, *T. santacrucensis* and *I. bernissartensis* were corrected and coded (1) for this character. *Y. hongheensis* was corrected and coded with a question mark

141(*). Dentary, symphysis: V-shaped (0), spout-shaped (1) (Ösi et al. 2012 #97).

The unexpanded distal end of the dentary in *Herrerasaurus ischigualastensis* (Sereno and Novas 1993, fig. 2F, 4) doesn't look similar in any manner to the strongly buttressed v-shaped symphysis observed in *Heterodontosaurus tucki* (Norman et al. 2011, appendix 6.D). The shape of the dentary symphysis could not be safely inferred on *Kulindadromeus zabaikalicus* from the informations available (Godefroit et al. 2014, fig. S4F). This part of the skull is unknown for *Hexinlusaurus multidens* (He and Cai 1984). *K. zabaikalicus* and *H. multidens* were corrected and coded a question mark. *H. ischigualastensis* was corrected and coded as non-applicable for this character, as its dentary symphysis is neither v-shaped, nor spout-shaped.

142(*). Dentary, position of the anterior tip: positioned high (0), mid height (1), near lower margin of dentary (2), below lower margin (3) (modified from: Ösi et al. 2012 #98; Brown et al. 2013 #51).

The anterior tip of the dentary is located near the lower margin of the mandible in *Thescelosaurus neglectus* (Boyd 2014, fig. 1), *Gasparinisaura cincosaltensis* (Coria and Salgado 1996, fig. 2) and *Camptosaurus dispar* (Gilmore 1909, fig. 2). Contra previous codifications, the anterior tip of the dentary is not located near its lower margin in *Dryosaurus* (Galton 1983, fig. 2A) and *Dysalotosaurus lettowvorbecki* (Janensh, 1955, fig. 1A), but rather at mid-height. Contra previous codifications, the anterior tip of the dentary is not located near its lower margin in *Dryosaurus* (Galton 1983, fig. 2A) and *Dysalotosaurus lettowvorbecki* (Janensh, 1955, fig. 1A), but rather at mid-height. The anterior tip is located at rhoughly mid-height in *Hypsilophodon foxii* (Galton 1974*a*, fig. 10A), *Talenkauen santacrucensis* (Cambiaso 2007, fig. 15A, B), *Haya griva* (Makovicky et al. 2011, fig. 1A), *Jeholosaurus shangyuanensis* (Barrett and Han, 2009, fig. 6), *Changchunsaurus parvus* (Liyong et al. 2010, fig. 1), *Psittacosaurus mongoliensis* (Sereno 2010, fig. 2.14). Though it appears quite low, the anterior tip of the dentary is higher in *Zalmoxes* genera than in other taxa that were coded with character state (2): we consider that the anterior tip is located at mid-height in *Zalmoxes robustus* (Weishampel et al. 2003, fig. 12E, F) and *Zalmoxes shqiperorum* (Godefroit et al. 2009, fig. 9B, D). The anterior tip of dentary is rhoughly located at mid-hight in *Mochlodon suessi* (Sachs and Hornung 2005, fig. 2.1-2), *Rhabdodon priscus* (Matheron 1869, pl. 3-2A), and is very highly situated in *Mochlodon vorosi* (Ösi et al. 2012, fig. 2F). *Rhabdodon* sp1 from Vitrolles has an unusually low tip, lying near the lower margin of the dentary (Pincemaille-Quilleveré 2002, fig. 3). The anterior tip of dentary is highly situated in *Echinodon becklesii* (Sereno 2012, Fig. 15-18). In *Eocursor parvus*, the anterior extremity is thin and poorly defined, but the anterior tip for the predentary should be highly situated

(Butler 2010, fig. 5). The anterior tip of dentary is located relatively high in *Psittacosaurus major* (You et al. 2008, fig. 4), *Yinlong downsi* (Han et al. 2015, fig. 3), and more derived ceratopsians (cf. Xu et al. 2002; You and Dodson 2003). The dentary is unpreserved in *Yandusaurus hongheensis* (He and Cai 1984). *T. neglectus*, *C. dispar*, *G. cincosaltensis*, *Rhabdodon* sp1 were corrected and coded (2). *Dryosaurus*, *D. lettowvorbecki*, *H. foxii*, *T. santacrucensis*, *H. griva*, *J. shangyuanensis*, *C. parvus*, *P. mongoliensis*, *Z. robustus*, *Z. shqiperorum*, *M. suessi* and *R. priscus* were corrected and coded (1). *E. becklesii*, *E. parvus*, *P. major* and *Y. downsi* were corrected and coded (0). *Y. hongheensis* was corrected and coded with a question mark.

143(*). Dentary, morphology of ventral margin of anterior ramus leading to the predentary articulation: straight with an anterior break in slope leading to the tip of the predentary process (0), inflected ventrally before reaching the predentary articulation and symphysis (1), curves in a regular and continuous way dorsally toward the symphysis and predentary articulation (2) (modified from McDonald et al. 2010 #16).

In *Psittacosaurus major* and *Psittacosaurus mongoliensis* (Sereno 2010, fig. 2.3A, 2.7), *Yinlong downsi* (Han et al. 2015, fig. 3), *Archaeoceratops oshimai* (You and Dodson 2003, fig. 1) the anteroventral margin of the dentary smoothly curves upward to the anterior dentary symphysis, without any break in slope. Such a smooth curving toward the anterior tip of dentary is also observed in the adult skull of *Jeholosaurus shangyuanensis* (Barrett and Han, 2009, fig. 5A). It is not observed in the other two members of the Asian clade: *Haya griva* (Makovicky et al. 2011, fig. 1A) and *Changchunsaurus parvus* (Liyong et al. 2010, fig. 1) in which the dentary forms a distinct ventral inflection before rising again to the anterior tip. The lower margin of the dentary is also inflected downward in *Agilisaurus louderbacki* (Peng 1992, fig. 1A), *Tenontosaurus tilletti* (Thomas 2015, fig. 47), *Hypsilophodon foxii* (Galton 1974*a*, fig. 10A, C), In *Eocursor parvus* (Butler 2010, fig. 5), *Echinodon becklesi* (Sereno

2012, fig. 16-18), *Abrictosaurus consors* (Sereno 2012, fig. 34), *Tianyulong confuciusi* (Sereno 2012, fig. 22, 23), the lower margin of the dentary is straight anteriorly. The dentary is broken ventral to the mexkelian groove in *Talenkauen santacrucensis* (Rozadilla et al. 2019, fig. 9, p. 11). This character is unknown in *T. dossi* (cf. Winkler et al. 1997) and *H. Multidens* (He and Cai 1984). *J. shangyuanensis*, *P. mongoliensis, P. major*, *Y. downsi* were corrected and coded (2). *H. griva*, *C. parvus*, *A. louderbacki*, *T. tilletti*, *T. santacrucensis* and *H. foxii* were corrected and coded (1). *E. parvus, E. becklesi*, *A. consors*, *T. confuciusi* were corrected and coded (0). *T. santacrucensis*, *T. dossi* and *H. Multidens* were corrected and coded with a question mark.

144(*). Dentary, tooth row (and edentulous anterior portion) in lateral view: straight (0), anterior end downturned (1) (Ösi et al. 2012 #98).

The edentulous anterior portion of the dentary isn't downwardly sloping in *Nanosaurus agilis* (Carpenter and Galton 2018, fig. 7A-K). A downward curve of the oral margin of the dentary is observed in *Talenkauen santacrucensis* (Cambiaso 2007, fig. 15A, B), *Tenontosaurus tilletti* (Thomas 2015, fig. 47, 51), *Dysalotosaurus lettowvorbecki* (Janensch 1955, fig. 11), *Rhabdodon* sp1. (Pincemaille-Quilleveré 2002, fig. 2), *Rhabdodon priscus* (Matheron 1869, pl. 3.2A) before it connects to the predentary. It also appears to be the case, although to a lesser extent, for *Dryosaurus altus* (Galton 1983, pl. 1.1, 1.15) and *Thescelosaurus neglectus* (Boyd 2014, fig. 1). This information is not available and/or difficult to infer for *Scelidosaurus harrisonii* (Owen 1861, pl. 4), *Isaberrysaura mollensis* (Salgado et al. 2017, fig. 2C), *Hexinlusaurus multidens* (He and Cai 1984), *Kulindadromeus zabaikalicus* (Godefroit et al. 2014, supplementary material), *Tenontosaurus dossi* (Winkler et al. 1997), and *Gasparinisaura cincosaltensis* (Coria and Calvo, 1996, fig. 1). In the latter taxon, the predentary is not preserved so we could not safely infer to how extent the downward curve of the dentary was capped by the predentary. *N. agilis* was corrected and coded (0). *T.*

santacrucensis, *T. tilletti*, *R.* sp1, *R. priscus*, *Dryosaurus*, *D. lettowvorbecki*, *T. neglectus* were corrected and coded (1). *S. harrisonii*, *H. multidens*, *K. zabaikalicus*, *T. dossi*, *G. cincosaltensis* were corrected and coded with a question mark.

145(*). Dentary, dorsal and ventral margins before their locking into the predentary: converge anteriorly (0), subparallel (1), deepen anteriorly (2) (modified from McDonald et al., 2010 #15; Ösi et al. 2012 #99).

In *Camptosaurus dispar* (Gilmore 1909, fig. 2) and *Iguanodon bernissartensis* (Norman 1980, fig. 2) the anteroventral "chin-like" projection induces a dorsoventral deepening of the dentary. In heterodontosaurids such as *Abrictosaurus consors* (Sereno 2012, fig. 5A), *Heterodontosaurus tucki* (Norman, 2011), the dentary deepens anteriorly, at a level below the caniniform tooth. *Fruitadens haagarorum* (Sereno 2012, fig. 9A), *Echinodon becklesii* (Sereno 2012, fig. 19B) and *Tianyulong confuciusi* (Sereno 2012, fig. 22) differ from the above-cited heterodontosaurids in having the ventral margin of their mandible margin swinging upward before contacting with the predentary, with dorsoventral margins that converge anteriorly. Let's remark that such dorsoventral thinning of the dentary ramus must not be necessarily interpreted as that of the anterior tip being locked into the upper and lower processes of the predentary. In *Eocursor parvus* (Butler 2010, fig. 5), *Lesothosaurus diagnosticus* (Sereno 1991, fig. 13G), *Agilisaurus louderbacki* (Peng 1992, fig. 1A), *Thescelosaurus neglectus* (Boyd 2014, fig. 1), *Jeholosaurus shangyuanensis* (Barrett and Han, 2009, fig. 5A), *Changchunsaurus parvus* (Liyong et al. 2010, fig. 1), *Haya griva* (Makovicky et al. 2011, fig. 1A), *Orodromeus makelai* (Scheetz 1999, Fig. 10), *Psittacosaurus mongoliensis* (Ryan et al. 2010, fig. 2.14), *Psittacosaurus major* (You et al. 2008, fig. 4), *Chaoyangosaurus youngi* (Zhao et al. 1999, fig. 2A), *Yinlong downsi* (Han et al. 2015, fig. 2A), *Archaeoceratops oshimai* (You and Dodson 2003, fig. 1), *Liaoceratops yanzigouensis* (Xu et al. 2002, fig. 2C), the dorsal and ventral margins of the dentary are sub-

parallels. In *Gasparinisaura cincosaltensis* (Coria and Calvo, 1996, fig. 1) the dorsal and ventral margins of the dentary converge anteriorly. Such information is unavailable for *Hexinlusaurus multidens* (He and Cai 1984). *F. haagarorum*, *E. becklesii*, *T. confuciusi*, *G. cincosaltensis* were corrected and coded (0). *E. parvus*, *L. diagnosticus*, *A. louderbacki*, *T. neglectus*, *J. shangyuanensis*, *C. parvus*, *H. griva*, *O. makelai* and all ceratopsians from this data-matrix were corrected and coded (1). *C. dispar*, *I. bernissartensis*, *A. consors* and *H. tucki* were corrected and coded (2). *H. multidens* was corrected and coded with a question mark.

146(*). Dentary, ventral flange: absent (0), present (1) (Ösi et al. 2012 #100).

Hexinlusaurus multidens (He and Cai 1984) is unknown for this character. *H. multidens* was corrected and coded with a question mark.

147(*). Dentary, orientation of tooth row relative to lateral surface of dentary: convergent anteriorly and posteriorly, bowed medially at mid-length, the tooth row ends anterior and aligned to the coronoid process (0), convergent anteriorly and divergent posteriorly so that the tooth row ends anterior to the coronoid and medial to its longitudinal axis (1), the dentary tooth row ends posteromedially to the coronoid (2) (modified from Xu et al. 2006 #17; McDonald et al. 2010 #12 and Ösi et al. 2012 #103).

In *Wannanosaurus yansiensis* (Butler and Zhao 2009, fig. 7B), the dentary tooth row is reported as straight, and ends anterior and slightly medial to the coronoid eminence. Owing to the hardly discernible medial deflection, we considered it as level with the coronoid process as also occurs for other pachycephalosaurs, like *Goyocephale lattimorei* (Perle et al. 1982, pl. 43-1B). The dentary tooth row of *Eocursor parvus* is reported to compare favorably to that of *Lesothosaurus diagnosticus* (Butler 2010), so it was only very slightly medially deflected. The dentary tooth row ends anterior and in line with the coronoid in *Nanosaurus agilis* (Carpenter and Galton 2018, p. 173). In *Changchunsaurus parvus* (Liyong et al. 2010, fig.

4F), *Camptosaurus dispar* (Gilmore 1909, fig. 8.2), *Thescelosaurus neglectus* (Boyd 2014, fig. 14C), *Tenontosaurus tilletti* (Thomas 2015, fig. 57), *Talenkauen santacrucensis* (Cambiaso 2007, fig. 15C), *Anabisetia saldiviai* (Coria and Calvo 2002, fig. 3C, F; Cambiaso 2007, fig. 95) the dentary tooth row ends anterior to the coronoid and deflects medially to its longitudinal axis. In *Dryosaurus altus* (Carpenter and Galton 2018, fig. 28W) and *Dysalotosaurus lettowvorbecki* (Janensch 1955, pl. 11.3C) the dentary tooth row converges again posterolaterally toward the coronoid and ends anterior to it. Such character could not be determined in *Jeholosaurus shangyuanensis* (Barrett and Han, 2009) and *Haya griva* (Makovicky et al. 2011). In the basal ceratopsians *Yinlong downsi* (Han et al. 2015, p. 23, fig. 20C) and *Chaoyangsaurus youngi* (Tanoue et al. 2010, fig. 16.1A) the dentary tooth row is strongly concave labially and ends anterior and level with the coronoid process. In *Psittacosaurus mongoliensis* (Sereno 2010, fig. 2.7C) and *Psittacosaurus major* (You et al. 2008, fig. 4B) the dentary tooth row deflects medially, though it still ends anterior to the coronoid process. In more derived ceratopsians such as *Archaeoceratops oshimai* (Tanoue et al. 2010, fig. 16.3F) or *Liaoceratops yanzigouensis* (Tanoue et al. 2010, fig. 16.4H-J) the dentary tooth row ends clearly medial to the coronoid. This also occurs convergently in *Iguanodon bernissartensis* (Norman 1980, pl. 4). *E. parvus*, *G. lattimorei*, *Y. downsi*, *C. youngi*, *Dryosaurus* and *D. lettowvorbecki* were corrected and coded (0). *C. dispar*, *T. tilletti*, A. *saldiviai*, and *T. santacrucensis*, *T. neglectus* were corrected and coded (1). *L. yanzigouensis*, *A. oshimai*, *I. bernissartensis* were corrected and coded (2). *J. shangyuanensis* and *H. griva* are unknown for this character so they were corrected and coded with a question mark.

148(*). Dentary, coronoid process: absent or weak, posterodorsally oblique, depth of mandible at coronoid is less than 150% depth of mandible beneath tooth row (0), well-developed,

distinctly elevated, depth of mandible at coronoid is more than 150% depth of mandible beneath tooth row (1) (Pol et al. 2011 #101).

In *Stegosaurus stenops* (Gilmore 1914, pl. 8) as in other tyreophorans, the coronoid process is very low. In *Kulindadromeus zabaikalicus*, a mandible depth of 150% that of the dentary at the level of the coronoid would mean that the coronoid process would have rised up to the lower margin of the orbit (Godefroit et al. 2014, cf. fig. S4A): which isn't conceivable. Therefore, the mandible depth at the coronoid should have been well under 150% the height of the mandible beneath tooth row. The coronoid process of some pachycephalosaurs, such as *Wannanosaurus yansiensis* (Butler and Zhao 2009, fig. 7A), *Goyocephale lattimorei* (Perle et al. 1982, pl. 43.1C-F) is very low. That of *Stegoceras validum* is, by contrast, high (Gilmore 1924, pl. 6.1). Among heterodontosaurids, this character is also variable. In *Heterodontosaurus tucki*, the height of the coronoid process makes 150% the height of the mandible (Norman, 2011). In *Abrictosaurus consors* (Sereno 2012, fig. 34) and *Echinodon becklesii* (Sereno 2012, fig. 19B) the height of the coronoid makes respectively 130% and 138% the height of the dentary. In *Tianyulong confuciusi* (Sereno 2012, fig. 21) the posterior lower jaw is badly damaged so this character could not be inferred. *S. stenops*, *K. zabaikalicus*, *G. lattimorei*, *W. yansiensis, A. consors*, *E. becklesii*, *S. stenops* were corrected and coded (0).

150(*). Dentary, number of dentary teeth: 10 or fewer (0), 11–13 (1), 14–17 (2), more than 18 (3) (modified from Weishampel et al. 2003: #30; Butler et al. 2011; Ösi et al. 2012 #228; ordered character).

Sereno (2012, fig. 9A, 19B, 58) reconstructs 11 teeth for *Fruitadens haagarorum*, *Echinodon becklesii*, and *Heterodontosaurus tucki*. Butler and Zhao (2009) also estimate a total of 11 dentary teeth for *Wannanosaurus yansiensis*. *Goyocephale lattimorei* (Perle et al. 1982) counts 18 dentary teeth, and *Stegoceras validum* (Sues and Galton 1987) records 17 dentary

teeth alveoli. In the unnamed rhabdodontid from Vegagete (Dieudonné et al. 2016a), the dentary tooth count is much lesser than 10. In *Psittacosaurus major*, the dentary tooth count is 10 (You et al. 2008, p. 194), and in *Psittacosaurus mongoliensis*, it is 12 (Sereno 2010, fig. 2.7). 14 dentary teeth are counted on a complete dentary of *Yinlong downsi* (Han et al. 2015, fig. 20C). Derived ceratopsians bear fewer than 10 dentary teeth (e.g. *Liaoceratops yanzigouensis*, You et al. 2007, fig. 2). The number of dentary teeth cannot be determined in *Tianyulong confuciusi* (Sereno 2012, p. 56). The Vegagete ornithopod was corrected and coded (0). *F. haagarorum* and *E. becklesii* were corrected and coded (1). *P. major* was newly coded (0), and *P. mongoliensis* was newly coded (1). *Y. downsi* was corrected and coded (2). *Tianyulong confuciusi* was corrected and coded with a question mark.

151(*). Coronoid, swells ventrolaterally until below the dentary tooth row: abent (0), present (1) (new character).

The coronoid projects below the dentary tooth row in *Echinodon becklesii* (Sereno 2012, fig. 19B), *Stegoceras validum* (Sues and Galton 1987, fig. 3A) and *Wannanosaurus yansiensis* (Butler and Zhao 2009, fig. 7A). We consider this character as unknown for *Tianyulong confuciusi* (Sereno 2012, fig. 21) as the deep coronoid ramus appears broken anteriorly, and the dentary tooth row may be partly hidden by the jugal posteriorly. It is neither figured nor described for *Abrictosaurus confuciusi* (Sereno 2012).

153(*). Ridge or process on lateral surface of surangular, anterior to jaw suture: incipient or absent (0); anteroposteriorly extended ridge (1); dorsally directed finger-like process or strongly bulging boss (2) (reformulated from Ösi et al. 2012 #106, reintegrated).

This character was unduely omitted in Dieudonné et al. (2016a) but we reintegrate it here. A dorsally directed process is similarly much developped in *Talenkauen santacrucensis* (Cambiaso 2007, fig. 16). The holotype of *Dryosaurus elderae* (CM 3392, Carpenter and Galton 2018, fig. 28V) features a posteriorly offset but prominent process on its surangular.

This character seems unaccessible in *Dryosaurus altus* (DMNH 9001, Carpenter and Galton 2018, fig. 28BB). Note that *Dysalotosaurus lettowvorbecki* (Galton 1983, pl. 4.6) features a smooth dorsal bulge on its surangular, but this does not correspond to the markedly projecting process or boss that is considered for this character. According to Winkler et al. (1997) and Andrzejewski et al. (2019), *Tenontosaurus dossi* was corrected and coded (2). *T. santacrucensis* and *Dryosaurus* were also corrected and coded (2).

154(*). External mandibular fenestra, situated on dentary-surangular-angular boundary: present (0), absent (1) (Xu et al. 2006 #41; Ösi et al. 2012 #104).

A remnant of such external mandibular fenestra is present in the *Liaoceratops yanzigouensis* specimen described by Xu et al. (2002, fig. 1B), and such fenestra is present and much larger in the specimen described by You et al. (2007, fig. 1A, B). Such fenestra is present in *Agilisaurus louderbacki* at the boundary between the angular and the surangular (cf. Barrett and Han, 2005, fig. 5A), *Chaoyangsaurus youngi* (Zhao et al. 1999, fig. 2A), *Psittcosaurus mongoliensis* (Ryan et al. 2010, fig. 2.7), and *Psittacosaurus major* (You et al. 2008, fig. 4A). *Lycorhinus angustidens* is cited by Sereno (2012, p. 55) as bearing an external mandibular fenestra. An external mandibular fenestra wasn't described for *A. oshimai* (You and Dodson 2003, fig. 1A) or *Goyocephale lattimorei* (Perle et al. 1982, pl. 43C), but we suggest it was present in those taxa based on figure observations. The external mandibular fenestra appears absent in *Stegosaurus stenops* (Gilmore 1914, pl. 5). Andrzejewski et al. (2019, fig. 4) describe the presence of a small foramen at the boundary between the surangular and dentary of *Convolosaurus marri*. *A. louderbacki, A. oshimai*, *L. yanzigouensis*, *C. youngi*, *P. major* and *P. mongoliensis*, *L. angustidens*, *G. lattimorei*, *C. marri* were corrected and coded (0). *S. stenops* was corrected and coded (1). was corrected and coded with a question mark.

156(*). Dentary-angular, node-like ornamentation: absent (0), present (1) (Ösi et al. 2012 #108; Xu et al. 2006 #88).

No ornamentation is visible on the lateral aspect of the dentary and angular of *Yinlong downsi* (Han et al. 2015, fig. 15H), *Chaoyangsaurus youngi* (Zhao et al. 1999, fig. 2A), *Archaeoceratops oshimai* (You and Dodson 2003, fig. 1A, B). The Vegagete rhabdodontid (Dieudonné et al. 2016a), *Hexinlusaurus multidens* (He and Cai 1984) as well as *Echinodon becklesii* (e.g. Sereno 2012) do not preserve any sufficient posterior portion of their lower jaw so that they could be coded with enough confidence. *Y. downsi*, *C. youngi*, *A. oshimai* were corrected and coded (0). The Vegagete rhabdodontid, *H. Multidens*, *E. becklesii* were corrected and coded with a question mark.

157(*). Dorsoventral extension of the angular at the level of the coronoid process: forms less than half of the dorsoventral height of the mandibular ramus (0); forms half or more of the height of the mandibular ramus, but remains below the dentary tooth row (1), reach the dorsal extent of the mandibular ramus or is higher (2) (modified from Pol et al. 2011 #230).

Pol et al. (2011) coded character #230 only for *Herrerasaurus ischigualastensis*, *Pisanosaurus mertii*, *Euparkeria capensis*, *Lesothosaurus diagnosticus*, *Eocursor parvus*, *Heterodontosaurus tucki*, *Manidens condoriensis*, *Tianyulong confuciusi*. Among these, only *H. tucki* and *M. condoriensis* were coded as sharing the exclusive character of an angular being taller than half the height of the mandibular ramus. However, such character appears much more widespread within ornithischians. The angular of *Herrerasaurus ischigualastensis* is roughly half the height of the mandible (Sereno and Novas 1993, fig. 1A, B). The heterodontosaurids *Heterodontosaurus tucki* (Norman et al. 2011, fig. 16) and *Manidens condoriensis* (Pol et al. 2011, fig. 2D), *Tianyulong confuciusi* (Zheng et al. 2009, fig. 1C), the ceratopsian *Chaoyangsaurus youngi* (Zhao et al. 1999, fig. 2A), *Archaeoceratops oshimai* (You and Dodson 2003, fig. 1A, C), *Liaoceratops yanzigouensis* (You et al. 2007, fig. 2A, B), the pachycephalosaur *Stegoceras validum* (Gilmore 1924, pl. 1) all have an angular that arises to the level of the mandibular ramus. In *Yinlong downsi*, the angular reaches the upper

mandibular margin in the left side of IVPP V14530, IVPP V18636 and IVPP V18686 (Han et al. 2015, fig. 3, 8A, 11A respectively), but not on the right side of IVPP V14530 (Han et al. 2015, fig. 2). The amount of evidence plaids in favor of regarding *Y. downsi* as bearing a dorsoventrally tall angular as the aforementionned taxa. A small dorsal fragment of angular is preserved in *Abrictosaurus consors*, and lies to a level lower than half of the height of the mandible (Sereno 2012, fig. 34A). However it could have been disarticulated so it is not possible to safely infer its original position lateral to the surangular. The angular of *Agilisaurus louderbacki* (Barrett et al. 2005, fig. 5A), *Psittacosaurus mongoliensis* (Sereno 2000, fig. 25.5) and *Psittacosaurus major* (You et al. 2008, fig. 4A2) is taller than half the height of the mandibular ramus but doesn't reach the upper margin of the mandibular ramus. The same is true for all other taxa previously coded as having a tall angular arising to more than half of the mandibular ramus such as *Lesothosaurus diagnosticus* (Sereno 1991, fig. 13F) or *Eocursor parvus* (Butler 2010, fig. 5A). The angular also forms a significant part (half or more) of the mandible height in *Jeholosaurus shangyuanensis* (Barrett and Han, 2009, fig. 6), *Thescelosaurus neglectus* (Boyd 2014, fig. 1), *Orodromeus makelai* (Scheetz 1999, fig. 4). Ornithopods such as *Hypsilophodon foxii* (Galton 1974*a*, fig. 10A), *Tenontosaurus tilletti* (Thomas 2015, fig. 46), *Tenontosaurus dossi* (Winkler et al. 1997, fig. 10C), *Dysalotosaurus lettowvorbecki* (Galton 1983, fig. 3T), *Dryosaurus altus* (Galton 1983, pl. 1.4), *Camptosaurus dispar* (Gilmore 1909, fig. 2) all feature an angular that is less than half the height of the mandible at the level of the coronoid process. In *Zalmoxes robustus*, the angular is not preserved but the surangular shows a much flattened insertion area for the angular (Weishampel et al. 2003, fig. 12J). *S. stenops* (for Stegosauria), *H. foxii*, *T. tilletti*, *T. dossi, Dryosaurus, D. lettowvorbecki, C. dispar* (for Ankylopollexia), *Z. robustus* (for Rhabdodontidae) were corrected and coded (0). *H. ischigualastensis*, *E. parvus*, *L. diagnosticus*, *S. harrisonii*, *E. ernstii*, *A. louderbacki*, the psittacosaurids *P major* and *P.*

mongoliensis, *A. louderbacki*, *O. makelai*, *J. shanguyanensis*, *T. neglectus* were corrected and coded (1). *A. oshimai, L. yanzigouensis*, *C. youngi*, *Y. downsi, T. confuciusi*, *H. tucki, S. validum,* were corrected and coded (2).

158(*). Jaw, level of jaw joint: level with tooth row, or weakly depressed ventrally (0), strongly depressed ventrally, more than 40% of the height of the quadrate is below the level of the maxillary occlusal margin (1) (modified from Xu et al. 2006 #36; Ösi et al. 2012 #109).

The jaw joint articulation is very much depressed ventrally in *Zephyrosaurus schaffi* (Sues 1980, fig. 9C), *Parksosaurus warreni* (Galton 1973, fig. 1), *Thescelosaurus neglectus* (Boyd 2014, fig. 1), *Tenontosaurus tilletti* (Thomas 2015, fig. 2) and *Tenontosaurus dossi* (Winkler et al. 1997, fig. 10D-F), *Convolosaurus marri* (Andrzejewski et al. 2019, fig. 8A), *Dysalotosaurus lettowvorbecki* (Galton 1983, fig. 3T), *Dryosaurus altus* (Galton 1983, pl. 4-5, 6). *Talenkauen santacrucensis* (Cambiaso 2007, fig. 15, 16), *Muttaburrasaurus langdoni* (Bartholomai and Molnar, 1981, fig. 1A), *Zalmoxes robustus* (Weishampel et al. 2003, fig. 12E, H), *Haya griva* (Makovicky et al. 2011, fig. 1A), *Changchunsaurus parvus* (Liyong et al. 2010, fig. 1A), *Jeholosaurus shangyuanensis* (Barrett and Han, 2009, fig. 5A), *Psittacosaurus mongoliensis* (Sereno 2010, fig. 2.7), *Psittacosaurus major* (You et al. 2008, fig. 4). The jaw joint articulation of *Isaberrysaura mollensis* (Salgado et al. 2017, fig. 2C) is relatively high. *Agilisaurus louderbacki* (Peng 1992, fig. 1A) has a highly situated jaw joint because of a highly positionned glenoid. The level of the jaw joint in *Tianyulong confuciusi* appears to be level with the maxillary tooth row owing to a strong uplift of the lower jaw posteriorly. This position is higher than in any other heterodontosaurids (Sereno 2012, fig. 9C). *Goyocephale lattimorei* (Perle et al. 1982, pl. 43-1C-F), *Prenocephale prenes* and *Homalocephale calathocercos* (Maryanska and Osmolska 1974, fig. 1C, D respectively) is only weakly depressed. By contrast, *Stegoceras validum* (Sues and Galton 1987, fig. 3) and *Pachycephalosaurus wyomingensis* (Maryanska and Osmolska 1974, fig. 1E) display a much

more ventrally depressed jaw joint. Available material does not allow us to know the state of this character for *Wannanosaurus yansiensis* (Butler and Zhao 2009, fig. 7, p. 72) and *Zalmoxes shqiperorum* (Godefroit et al. 2009, fig. 9) which lack their articular and prearticular, *Hexinlusaurus multidens* which do not preserves its lower jaw (He and Cai 1984, fig. 3), *Orodromeus makelai* for which only the juvenile skull is available (Scheetz 1999, fig. 3). *I. mollensis* was corrected and coded (0). *P. warreni*, *Z. schaffi*, *T. neglectus*, *T. tilletti*, *T. dossi*, *Dryosaurus*, *D. lettowvorbecki*, *T. santacrucensis*, *M. langdoni*, *Z. robustus*, *H. griva*, *C. parvus*, *J. shangyuanensis*, *P. mongoliensis*, *P. major*, *P. wyomingensis* and *S. validum* were corrected and coded (1). *W. yansiensis*, Z. *shqiperorum*, *H. multidens*, *O. makelai* were corrected and coded with a question mark.

159(*). Premaxillary teeth: more than three (0), ≤ three (1), absent, premaxilla edentulous (2) (modified from Xu et al. 2006 #18; Ösi et al. 2012 #111).

This character was modified to account for an arbitrary threshold of three premaxillary teeth when premaxillary teeth are present. Marginocephalians are primitively all presenting three premaxillary teeth, whereas most ornithopods keep having more than three premaxillary teeth. Every taxa previously coded for the presence of premaxillary teeth were now corrected and splitted between character state (0) and (1). Taxa previously coded as lacking premaxillary teeth were coded with character state (2). Note that *Talenkauen santacrucensis* bears two alveoli on the oral margin of its premaxilla (Rozadilla et al. 2019, p. 13). This taxon therefore bears two premaxillary teeth, and was here coded (1) following the new character definition. Less than three premaxillary teeth are also observed in *Tenontosaurus dossi* (Winkler et al. 1997) and the Vegagete ornithopod (pers. obs.). *Nanosaurus agilis* likely bears more than 4 premaxillary teeth (Carpenter and Galton 2018, fig. 11B). *Kulindadromeus zabaikalicus* bears at least 3 premaxillary teeth, but it is impossible to infer wether there were more in the current

state of knowledge. *N. agilis* was corrected and coded (0) instead of its previously unknown state. *K. zabaikalicus* was corrected and coded with a question mark.

160(*). Premaxillary (non-caniniform) tooth crown orientations in lateral view: recurved (0) or straight (1) (reformulated from Xu et al. 2006 #74).

Premaxillary teeth of *Goyocephale lattimorei* (Perle et al. 1982, pl. 42-6A-B) and *Stegoceras validum* (Gilmore 1924, pl. 1) are recurved backward. The same occurs for heterodontosaurids such as *Fruitadens haagarorum* (Butler et al. 2012, fig. 1), *Echinodon becklesii* (Sereno 2012, p. 43), *Lycorhinus angustidens* (Sereno 2012, fig. 80, p141) and basal ornithischians such as *Lesothosaurus diagnosticus* (Sereno 1991, p. 187), *Isaberrysaura mollensis* (Salgado et al. 2017, fig. 2E). In other heterodontosaurids such as *Heterodontosaurus tucki* (Norman et al. 2011, fig. 20) or *Abrictosaurus consors* (Sereno 2012, fig. 32, p. 74), non-caniniform premaxillary crowns are straighter, and thinner from a lateral view. The premaxillary crown of *Hypsilophodon foxii* (Galton 1974*a*, fig. 13), *Talenkauen santacrucensis* (Cambiaso 2007, fig. 17A), as well as that the Vegagete rhabdodontid (Dieudonné et al. 2016a, before it broke, its smooth distal curvature was anteriorly directed) are not posteriorly recurved. By contrast, those of *Zephyrosaurus schaffi* (Sues 1980, fig. 2), *Thescelosaurus neglectus* (Boyd 2014, fig. 18A), *Jeholosaurus shangyuanensis* (Barrett and Han, 2009, p. 50), *Haya griva* (Makovicky et al. 2011, fig. 1B) are at least slightly recurved backward to their distal tip. *H. tucki*, *A. consors* were corrected and coded (1) for this character.

161(*). Premaxillary teeth, crown mesiodistal expansion above root: absent, no distinction between root and crown is observable (0), crown is moderately expanded above root (1) (reformulated from Ösi et al. 2012 #113).

Unlike other heterodontosaurids, *Echinodon becklesii* and *Fruitadens haagarorum* have premaxillary teeth that are expanded above their root (Owen 1858, pl. 8.1; Butler et al. 2012,

p. 6). *Talenkauen santacrucensis* preserves only one premaxillary crown that is mesiodistally expanded above its root (Cambiaso 2007, fig. 17A). *Tianyulong confuciusi* only preserves one caniniform premaxillary tooth (Sereno 2012), so the state of character for this taxon was considered as unknown. *Scelidosaurus harrisonii* does not preserve any premaxillary tooth (Owen 1861).

E. becklesii and *T. santacrucensis* were corrected and coded (1) for this character. *L. venezuelae*, *T. confuciusi*, and *S. harrisonii* were corrected and coded with a question mark.

162(*). Premaxillary teeth, shape: transversely compressed (0), bulbous, strongly convex labially (1) (modified from Xu et al. 2006 #66).

Premaxillary crowns are strongly convex labially in *Lesothosaurus diagnosticus* (Porro et al. 2015, fig. 3), *Thescelosaurus neglectus* (Boyd 2014, fig. 18A), *Haya griva* (Makovicky et al. 2011, p. 631), *Jeholosaurus shangyuanensis* (Barrett and Han, 2009, p. 50) and ceratopsians. Most of the premaxillary teeth of *Changchunsaurus pavus* (Liyong et al. 2010, p. 211) were damaged but the few teeth that could be described were compared favorably with those of basal cerapodan (above-cited), all of which have laterally bulging crowns. This character is not described for *Agilisaurus louderbacki*, but its premaxillary teeth appear strongly convex labially (Barrett et al. 2005, fig. 3A). *L. diagnosticus, T. neglectus*, *H. griva*, *J. shangyuanensis*, *C. parvus*, *A. louderbacki* were corrected and coded (1).

163(*). Premaxillary teeth, posterior increase in size (breadth and/or height) : absent, all premaxillary teeth are subequal in size and not significantly broader than the succeeding maxillary teeth (0), premaxillary teeth increase in breadth and height posteriorly, and the most posterior tooth is larger than succeeding maxillary teeth (1) (modified from Ösi et al. 2012 #114; Xu et al. 2006 #73).

The premaxillary teeth are significantly broader than subsequent maxillary teeth in *Agilisaurus louderbacki* (Barrett et al. 2005, fig. 3A), *Yinlong downsi* (Han et al. 2015, fig.

11A), *Lycorhinus angustidens* (Sereno 2012, fig. 76A), *Tianyulong confuciusi* (Sereno 2012, Fig. 22). The posterior premaxillary tooth of *Goyocephale lattimorei* (Perle et al. 1982, pl. 42.9) and *Prenocephale prenes* (Maryanska and Osmolska 1974, fig. 1C1) is caniniform and significantly enlarged. *Stegoceras validum* (Gilmore 1924, pl. 1) does not have significantly enlarged premaxillary teeth with respect to their succeeding maxillary teeth. *Abrictosaurus consors* (Sereno 2012, fig. 9A, 19, 35, p. 177) and *Fruitadens haagarorum* (Butler et al. 2012, p. 5) differ from other heterodontosaurids in not having posteriorly enlarged premaxillary teeth. The first and third premaxillary teeth of *Echinodon becklesii* have been broken since they were first represented by Owen (1861*a*), yet the last premaxillary tooth of this taxon is clearly caniniform (Galton 1978, fig. 1A). *A. consors* and *F. haagarorum* were corrected and coded (0). *G. lattimorei*, *T. confuciusi*, *E. becklesii*, *L. angustidens*, *Y. downsi* and *A. louderbacki* were corrected and coded (1).

164(*). Premaxillary tooth row and anterior portion of maxillary tooth row: aligned with each other (0), maxillary teeth are inset the width of one or more crowns from the premaxillary teeth (1) (new character, derived from Han et al.2018 #31).

Archaeoceratops oshimai and *Liaoceratops yanzigouensis* (Han et al. 2018, figure in characters #30(1) and #142), *Yinlong downsi* (Han et al. 2015, fig. 7A, B) and *Heterodontosaurus tucki* (Norman et al. 2011, fig. S5A) feature laterally offset premaxillary teeth with respect to the anterior portion of their maxillary row. In *Psittacosaurus major* and *Psittacosaurus mongoliensis* the anterior maxillary tooth row is clearly inset medially with respect to their edentulous premaxillary wall (You et al. 2008, fig. 1C1; Sereno 2010, fig. 2.19F). In *Jeholosaurus shanguyanensis*, a ventral skull view shows that laterally salient premaxillary teeth are visible from a ventral view (Barrett and Han, 2009, fig. 7B, D), which indicates that the maxillary tooth row was medially inset with respect to the premaxillary tooth row. The same condition also occurs in *Haya griva* (Norell and Barta 2016, fig. 3),

Hypsilophodon foxii (Galton 1974*a*, fig. 6A) and *Thescelosaurus neglectus* (Boyd 2014, fig. 2). Contrary to the above-mentionned *A. oshimai*, *L. yanzigouensis*, *Y. downsi* and *H. tucki* and ornithopods, the anterior maxillary tooth rows of *Fruitadens haagarorum* (Butler et al. 2012, fig. 7C, D) and *Echinodon beclklesii* (Sereno 2012, fig. 12, 13) aren't inset from the outer maxillary margin but rather lie close to it. The premaxilla does not broaden posteriorly, so the premaxillary teeth would have been in straight alignment with the maxillary row. The same also occurs in pachycephalosaurs *Stegoceras validum*, *Prenocephale prenes* (Maryanska and Osmolska 1974, fig. 1A3, C3) and *Goyocephale lattimorei* (Perle et al. 1982, pl. 41.3). *Agilisaurus louderbacki* (Han et al. 2018, illustration of character #197(0)) and *Lesothosaurus diagnosticus* (Sereno 1991, fig. 2B) appear to retain the plesiomorphic ornithischian condition of premaxillary teeth aligned with the maxillary tooth row.

165(*). Teeth, crown mesiodistal expansion above root in cheek teeth: very weak to absent (0), present (1) (Ösi et al. 2012 #129).

Crowns are very weakly expanded above the tooth roots in *Agilisaurus louderbacki* (Peng 1992, p. 6), *Psittacosaurus major* (Sereno 2010, fig. 2.6A), *Psittacosaurus mongoliensis* (Sereno 2010, fig. 2.14), *Yinlong downsi* (Han et al. 2015, fig. 20B), *Chaoyangsaurus youngi* (Zhao et al. 1999, fig. 3). Mesiodistal edges of *Abrictosaurus consors* maxillary teeth are nearly parallel-sided (Sereno 2012, fig. 33), as for *Heterodontosaurus tucki* (e.g. Sereno 2012, fig. 93). The shape of cheek crowns aren't sufficiently described nor illustrated so that we could satisfactorily code for this character in *Archaeoceratops oshimai* (Dong and Azuma 1997; You and Dodson 2003) or *Liaoceratops yanzigouensis* (Xu et al. 2002; You et al. 2007). *A. consors*, A. *louderbacki*, *P. major*, *P. mongoliensis*, *Y. downsi*, *C. youngi* were corrected and coded (0) for this character. *A. oshimai* and *L. yanzigouensis* were corrected and coded with a question mark.

166(*). Teeth, close-packing and quicker replacement eliminating spaces between alveolar border and crowns of adjacent functional teeth: absent (0), present (1) (Xu et al. 2006 #103; Ösi et al. 2012 #131).

Dentary teeth of *Nanosaurus agilis* are widely spaced (Carpenter and Galton 2018). In *Heterodontosaurus tucki*, teeth are closely packed but waves of tooth replacement are scarce, and no tooth intervenes between the alveolar border and the adjacent functional teeth (e.g. Norman et al. 2011, fig. 2A). In addition, there are very few examples of active tooth replacement in *Heterodontosaurus tucki* (Norman et al. 2011, p. 219). *Tenontosaurus tilletti* (Thomas 2015, fig. 52), *Dryosaurus* (Galton 1983, fig. 3Y, Z), *Dysalotosaurus lettowvorbecki* (Janensch 1955, fig. 12) all present distinct waves of actively replacing teeth. We remark that although less teeth per toot family are present in this taxon, dentary teeth of *Talenkauen santacrucensis* (Rozadilla et al. 2019, fig. 9) appear to have had a relatively high tooth eruption rate, with no space left between adjacent functional teeth and their alveolar border. *Tenontosaurus dossi* is not described for this character (Winkler et al. 1997). *H. tucki* was corrected and coded (0). *T. santacrucensis*, *T. tilletti*, *Dryosaurus*, *D. lettowvorbecki* were corrected and coded (1) for this character. *T. dossi* was corrected and coded with a question mark.

167(*). Teeth, wear facets on teeth: absent or sporadically developed (0), systematic development of wear facets along the entire tooth row (1) (Ösi et al. 2012 #222).

Echinodon becklesii and *Fruitadens haagarorum* (Butler et al. 2012, p. 12), *Wannanosaurus hongtuyanensis* (Butler and Zhao 2009, p. 72), *Hexinlusaurus multidens* (Barrett et al. 2005, p. 826) were reported to lack systematic wear development. *Isaberrysaura mollensis* shows weak or non-existent wear-facets (Salgado et al. 2017, p. 5). The maxillary and dentary teeth of *Scelidosaurus harrisonii* are occluding with each other all along (Owen 1861), so any concrete information about a continuous or discontinuous development of wear facet should

be taken with caution unless actual first-hand observation is made. The tooth wear of *Haya griva* is not described, but figures show that it was quite much developped along the entire dentary tooth row (Makovicky et al. 2011, fig. 1A). *E. becklesii*, *I. mollensis* were corrected and coded (0). *H. griva* was corrected and coded (1). *S. harrisonii* was corrected and coded with a question mark.

168(*). Maxillary/dentary teeth, position of maximum apicobasal crown height in tooth rows: anterior portion of tooth row (0), central portion of tooth rows (1), posterior portion of tooth rows (2) (Ösi et al. 2012 #130).

This character is not described for *Homalocephale calathocercos* (Maryanska and Osmolska 1974, p. 57). *H. calathocercos* was corrected and coded with a question mark.

170(*). Maxillary/dentary teeth, enamel symmetrical (0), asymmetrical (1) (Ösi et al. 2012 #117).

Enamel is told to be asymmetrically distributed on the dentary teeth of *Kulindadromeus zabaikalicus* (Godefroit et al. 2014, supplementary material, p. 7). *K. zabaikalicus* was corrected and coded (1).

Maxillary teeth of *Prenocephale prenes* (Maryanska and Osmolska 1974, p. 54) and *Stegoceras validum* (Sues and Galton 1987, p. 11) are reported to be enameled on both sides. Although we could doubt wether such enamel was actually thicker on one side or on another (and this is certainly almost always the case), we interpret this statement as indicating the presence of significantly thick enamel on both the labio-lingual sides of dentary and maxillary teeth respectively. *Echinodon becklesii* and *Fruitadens haagarorum* (Butler et al. 2012, p. 12) feature symmetrical enamel distribution. *Heterodontosaurus tucki* (Norman et al. 2011, p. 212) differs in possessing asymmetrical enamel distribution. *Hexinlusaurus multidens* and *Changchunsaurus parvus* (Liyong et al. 2010) are reported to bear symmetrical enamel on their maxillary tooth crowns, in contrast to *Yandusaurus hongheensis* (He and Cai 1984). Enamel is told to be asymmetrically distributed on the dentary teeth of *Kulindadromeus*

zabaikalicus (Godefroit et al. 2014, supplementary material, p. 7). The teeth of *Talenkauen santacrucensis* (Cambiaso 2007, p. 51), *Haya griva* (Makovicky et al. 2011, p. 631) are also covered with an asymmetrical distribution of enamel. *T. santacrucensis* and *K. zabaikalicus* were corrected and coded (1). We follow Bell et al. (2019 #140) in correcting and coding *Muttaburrasaurus langdoni* with a question mark, instead of (1) previously.

171(*). Maxillary teeth, number and morphology of secondary/accessory ridges on labial surface of crown: no secondary ridges, only accessory ridges or swellings arising from marginal denticles (0), a few parallel and apicobasally extending secondary and accessory ridges (1), multiple parallel and apicobasally extending secondary and accessory ridges so that entire labial surface is corrugated (2) (modified from Pol et al. 2011 #118).

Scoring the presence of secondary swellings is made difficult as there are a number of taxa which maxillary teeth potentially bear secondary swellings, but which teeth are poorly preserved or figured (e.g. Scheetz 1999; Godefroit et al. 2014). Moreover, secondary swellings are sometimes more apicobasally developped than terciary ridges (c.f. the secondary "swellings" in the maxillary teeth of *Nanosaurus agilis*, Carpenter and Galton 2018, fig. 4), and sometimes not. We modified this character to consider the presence of both secondary/terciary ridges independently of wether these ridges looked more like ridges or swellings. The maxillary teeth of *Eocursor parvus* (Butler 2010, fig. 5C), *Scelidosaurus harrisonii* (Owen 1861, pl. 5), *Scutellosaurus lawleri* (Colbert 1981, fig. 9E), *Emausaurus ernsti* (Haubold 1990, fig. 10B), ankylosaurs (Mallon and Anderson 2014, fig. 1), *Stegosaurus ungulatus* (Gilmore 1914, fig. 11), *Lesothosaurus diagnosticus* (Sereno 1991, fig. 4A) lack secondary ridges. No "distinctly raised ridges" are present on the teeth of *Fruitadens haagarorum* (Butler et al. 2012), *Heterodontosaurus tucki* (Norman et al. 2011, fig. 32B), *Echinodon becklesii* (Sereno 2012, fig. 14), *Tianyulong confuciusi* (Sereno 2012, fig. 24), *Lycorhinus angustidens* (Sereno 2012, fig. 77C). Similarly, in basal ceratopsians the

labial ridges on maxillary teeth are poorly developped and hardly goes beyond the size of simple terciary ridges or swellings (e.g. *Psittacosaurus major*, Sereno 2010, fig. 2.6A; *Psittacosaurus mongoliensis*, Sereno et al. 1988, fig. 7A; *Yinlong downsi*, Han et al. 2015, fig. 20B, 21E; *Chaoyangsaurus youngi*, Zhao et al. 1999, fig. 4B). By contrast, the cheek teeth of *Archaeoceratops oshimai* and *Liaoceratops yanzigouensis* are described as bearing numerous secondary labial ridges (You and Dodson 2003; You et al. 2007). In *Goyocephale lattimorei*, Perle et al. (1982, p. 119) say that the maxillary teeth have apicobasally extending ridges, although these do not all reach the base of the crown. In *Prenocephale prenes*, Maryanska and Osmolska 1974, p. 54) describe maxillary teeth which secondary ridges all reach the base of the crown. In *Pachycephalosaurus wyomingensis* (Brown and Schlaikjer 1943, pl.40-1) the secondary ridges do not reach the base of the crown. In *Stegoceras validum* (Sues and Galton 1987, fig. 4C) a few apicobasal ridges are present in only a few maxillary teeth, and most of the crown surface is not covered by any ridges at all. Unfortunately, no description of those ridges was provided for *Homalocephale calathocercos* (Maryanska and Osmolska 1974, p. 57), and no maxillary teeth are preserved in *Wannanosaurus yansiensis* (Butler and Zhao 2009). There appears to be no secondary ridges corrugating the labial surface of *Agilisaurus louderbacki* maxillary teeth (Barrett et al. 2005, fig. 2B). Very few ridges teeth cover the apicobasal height of the maxillary crown in *Orodromeus makelai* (Scheetz 1999, fig. 6A). In *Anabisetia saldiviai* maxillary teeth are heterodont (Herne et al. 2019): some feature a conspicuous primary ridge with no secondary ridges, other feature numerous secondary ridges of varying apicobasal extension (Cambiaso 2007, fig. 96). Maxillary teeth of *Yandusaurus hongheensis* (He and Cai 1984, P. 46) and *Parksosaurus warreni* (Galton 1973, fig. 4) are covered labially with numerous secondary ridges that all reach the base of their crown. We could not figure out wether secondary ridges reached the base of the crown or not in *Jeholosaurus shangyuanensis* (Barrett and Han, 2009, p. 50). *E. parvus*, *S. harrisonii*, *S.*

lawleri, *E. ernsti*, Ankylosauria, Stegosauria, *L. diagnosticus*, the heterodontosaurids *H. tucki, L. angustidens*, *F. haagarorum*, *E. becklesii*, *T. confuciusi*, the basal ceratopsians *Y. downsi*, *C. youngi* and psittacosaurids, *A. louderbacki* were also corrected and coded (0). *O. makelai* was corrected and coded (1). *A. oshimai*, *Y. hongheensis*, *P. warreni* were corrected and coded (2). *A. saldiviai* was corrected and coded [1 2]. *G. lattimorei* was corrected and coded [0 2] and *S. validum* was corrected and coded [0 1]. *W. yansiensis, H. calathocercos*, *J. shangyuanensis* were corrected and coded with a question mark.

173(*). Maxillary/dentary teeth, at least weakly developed labiolingual expansion of the crown ('cingulum') above the root: absent (0), present (1) (modified from Ösi et al. 2012 #123).

In *Scelidosaurus harrisoni*, the crowns are told to "bulge outwards" and a smooth cingulum is visible (Owen 1861, cf. p. 13, pl. 4). In *Scutellosaurus lawleri*, the maxillary teeth are "expanded at their bases" (Colbert 1981, p. 12, fig. 9). A smooth cingulum is also visible in *Laquintasaura venezuelae* (Barrett et al. 2014, see p.2 and fig. S2), *Isaberrysaura mollensis* Salgado et al. 2017, fig. 2F-G), *Stegosaurus stenops* (Gilmore 1914, p. 44), *Eocursor parvus* (Butler 2010, fig. 5C). In the basal neornithischians *Hexinlusaurus multidens* (He and Cai 1984, p. 12) and *Yandusaurus hongheensis* (He and Cai 1984, fig. 22, p. 47) both maxillary and mandibular teeth have at most a very weak cingulum. In *Heterodontosaurus tucki*, the cingulum is unexistent as also occurs in *Manidens condoriensis* and *Abrictosaurus consors* (Sereno 2012 #10), but also ceratopsians. By contrast, other heterodontosaurids display a more developped cingulum (e.g. *Lycorhinus angustidens*, *Echinodon becklesii*, *Tianyulong confuciusi*, *Fruitadens haagarorum*, see Sereno 2012, #10). *Talenkauen santacrucensis* (Cambiaso 2007), *Mochlodon suessi* (Sachs and Hornung 2005), *Mochlodon vorosi* (Ösi et al. 2012), *Zalmoxes robustus* (Weishampel et al. 2003), *Zalmoxes shqiperorum* (Godefroit et al. 2009), *Tenontosaurus dossi* (Winkler et al. 1997), *Tenontosaurus tilletti* (Thomas 2015, p. 76), *Convolosaurus marri* (Andrzejewski et al. 2019, fig. 11A), *Dryosaurus altus* and

Dysalotosaurus lettowvorbecki (Carpenter and Galton 2018, fig. 28), *Camptosaurus dispar* (Gilmore 1909, fig. 7, 8), *Iguanodon bernissartensis* (Norman 1980, fig. 18, 20) all do possess a basal cingulum. *Homalocephale calathocercos* (Maryanska and Osmolska 1974, p. 57), *Haya griva* (Makovicky et al. 2011, p. 631), *Rhabdodon priscus* (Matheron 1869) are not described for this character. *A. louderbacki* and *A. consors* were corrected and coded (0). *T. santacrucensis*, *M. suessi*, *M. vorosi*, *Z. robustus, Z. shqiperorum*, *T. dossi*, *T. tilletti*, *C. marri*, *Dryosaurus*, *D. lettowvorbecki*, *C. dispar*, *I. bernissartensis* were corrected and coded (1). *H. calathocercos*, *H. griva*, *R. priscus* were corrected and coded with a question mark.

174(*). Maxillary/dentary teeth, interdental space: non-packed teeth (0), lack of space between adjacent teeth up through the occlusional margin (1), overlapping of adjacent crowns with an overlapping "*en échelon*" pattern (2) (modified from: Xu et al. 2006 #103; McDonald et al., 2010 #88; Ösi et al. 2012 #128; Brown et al., 2013 #31).

Maxillary teeth of *Stegosaurus stenops* (Gilmore 1914, fig. 12), *Lesothosaurus diagnosticus* (Sereno 1991, fig. 12A), *Stegoceras validum* (Sues and Galton 1987, fig. 4C, D) are unpacked. In *Prenocephale prenes,* Maryanska and Osmolska (1974, p. 55) argue that 'although the maxillary teeth are very densely arranged they overlap each other only very slightly', so interdental space may not be completely concealed. In *Pachycephalosaurus wyomingensis*, Brown and Schlaikjer (1943, p. 139) describes maxillary teeth that are obliquely oriented and which overlap each other in an "*échelon*" manner. Although they differ between each other in many respects, the maxillary teeth of *Agilisaurus louderbacki* and *Hexinlusaurus multidens* are closely packed up-through their occlusional margins withouth overlapping each other (Barrett et al. 2005, fig. 2). The heterodontosaurids *Abrictosaurus consors* and *Heterodontosaurus tucki* (Sereno 2012, fig. 31, 40-42 respectively), as well as all ceratopsians plesiomorphically (e.g. *Yinlong downsi*, Han et al. 2015, fig. 20B; *Psittacosaurus major*, You et al. 2008, fig. 5A) share the presence of tall, non-overlapping maxillary teeth

that are closely packed together until their occlusional margin. Maxillary teeth of dryomorphans such as *Dryosaurus* (Galton 1983, pl. 3-1), *Dysalotosaurus lettowvorbecki* (Janensch 1955, fig. ; Carpenter and Galton 2018, fig. 28EE), *Camptosaurus dispar* (Gilmore 1909, fig. 7; Carpenter and Galton 2018, fig. 20A-E), *Iguanodon bernissartensis* (Norman 1980, fig. 20), were never described as organized "*en échelon*". They rather appear to be organized in distinct rows of teeth that belong to different generations. Gilmore (1909, p. 224, fig. 7, 8, 10) states about *C. dispar* teeth in general that "all of the maxillae and dentaries examined show a great irregularity of the functional row". Maxillary teeth of *Yandusaurus hongheensis* (He and Cai 1984, fig. 25), *Kulindadromeus zabaikalicus* (Godefroit et al. 2014, fig. S4), *Hypsilophodon foxii* (Galton 1974*a*), *Zephyrosaurus schaffi* (Sues 1980, fig. 4), *Orodromeus makelai* (Scheetz 1999, p. 15), *Talenkauen santacrucensis* (Cambiaso 2007, p. 50), *Thescelosaurus neglectus* (Boyd 2014, p. 59, fig. 18), *Parksosaurus warreni* (Galton 1973). *Changchunsaurus parvus* (Liyong et al. 2010, fig. 10), *Jeholosaurus shangyuanensis* (Barrett and Han, 2009, fig. 1D), *Muttaburrasaurus langdoni* (Bartholomai and Molnar, 1981), *Zalmoxes robustus* (Weishampel et al. 2003, fig. 4D) and *Convolosaurus marri* (Andrzejewski et al. 2019) are arranged "*en échelon*". Similarly, in *Tenontosaurus tilletti*, the occlusal surface of dentary and maxillary teeth are told to be rotated 45° with respect to the long axis of the tooth row (Thomas 2015, p. 77). Maxillary teeth of *T. tilletti* compare favorably to those of its congeneric *T. dossi* (Winkler et al. 1997). The posterior maxillary fragment of the Vegagete ornithopod (Dieudonné et al. 2016a, fig. 2B1, B2) also displays imbricated teeth. In *Haya griva*, Makovicky et al. (2011, fig. 1A) do not describe such arrangement, but it could be clearly observed from the figures. This character is unknown for *Anabisetia saldiviai* (Coria and Calvo 2002; Cambiaso 2007) and is not described for *Gasparinisaura cincosaltensis* (Coria and Salgado 1996; Cambiaso 2007). However, in the latter taxon it seems that maxillary teeth are closely adpressed until their occlusional margin,

whithout overlapping each other (Coria and Salgado 1996, fig. 2). *A. consors,* psittacosaurids, *G. cincosaltensis* were corrected and coded (1). *Y. hongheensis*, *K. zabaikalicus*, *C. parvus*, *J. shangyuanensis*, *H. griva*, *H. foxii*, *Z. schaffi*, *O. makelai*, *T. santacrucensis*, *T. tilletti*, *T. dossi*, *T. neglectus*, *P. warreni*, *M. langdoni*, *Z. robustus*, *C. marri* and the Vegagete ornithopod were corrected and coded (2). *A. saldiviai* was corrected and coded with a question mark.

175(*). Maxillary/dentary alveolar foramina ('special foramina') medial to tooth rows: present (0), absent (1) (Ösi et al. 2012 #126).

A line of nutrient foramina along the ventromedial part of the mandible is reported in *Kulindadromeus zabaikalicus* (Godefroit et al. 2014, supplementary material p. 6). *K. zabaikalicus* was corrected and coded (0).

176(*). Maxillary teeth, crown shape: lingually concave (0), lingually convex (1) (Brown et al., 2013 #37).

The maxillary teeth of *Thescelosaurus neglectus* (Boyd 2014, p. 60) are lingually convex. Anterior and posterior maxillary crowns of *Nanosaurus agilis* appear to be lingually flat (Bakker et al. 1990, fig. 10). *N. agilis* was previously coded (0) so we considered that the flat or concave lingual side of maxillary crowns was comparable, and fitted in the same character state. The convex or concave nature of the lingual side of maxillary crowns was not described for *Orodromeus makelai* (Scheetz 1999) and *Parksosaurus warreni* (Galton 1973). *T. neglectus* was corrected and coded (1). *O. makelai* and *P. warreni* were corrected and coded with a question mark.

177(*). Maxillary and dentary tooth crowns, apicobasal height: high, ratio of crown height / maximum mesiodistal width ≥ 1.5 (0); low, ratio < 1.5 (1) (modified from Pol et al. 2011 #228).

We modified this character to consider the teeth from any position within a single tooth row. We assumed that the differences in tooth proportions that might be observed within the tooth row of single species did never vary in such a manner that those from the middle of the row would fall within a different category of proportions as those from the anterior or posterior extremity. Those proportions are implicitly meant to be measured from unabraded teeth so that there is no risk to underestimate the original crown height and to mistakenly put it within the lower size-category. Maxillary crowns of *Agilisaurus louderbacki* (Barrett et al. 2005, fig. 2B) are more than 1.5 time higher than wide. Much of the teeth from *Yinlong downsi* appear in an advanced abraded state, but the least abraded ones appear to fall largely within the tall category (Han et al. 2015, fig. 21E). The same occurs for *Psittacosaurus major* (Sereno 2010, fig. 2.6A). Teeth of *Anabisetia saldiviai* (Cambiaso 2007, fig. 96), *Jeholosaurus shangyuanensis* (Barrett and Han, 2009, fig. 1D), *Orodromeus makelai* (Scheetz, fig. 6) fall within the low crown category. Teeth of *Tenontosaurus tilletti* (Thomas 2015, fig. 23, 52) are dryomorphe-like and fall just above the low crown category. The posteriormost, posteriorly inclined dentary crown of *Talenkauen santacrucensis* seems little abraded and has a height to width ratio exceeding 1.5 (Rozadilla et al. 2019, fig. 9B). Teeth of *Gasparinisaura cincosaltensis* (Coria and Salgado 1996) seem to vary randomly and independently of their position within the row, but this might be because all of the teeth are well-abraded at the same level along the occlusal plane. *A. louderbacki*, *Y. downsi*, psittacosaurs, *T. santacrucensis*, *T. tilletti* were corrected and coded (0). *A. saldiviai*, *J. shangyuanensis*, *O. malelai* were corrected and coded (1). *G. cincosaltensis* was corrected and coded with a question mark.

178(*). Maxillary and dentary teeth, cingulum height and crown shape: cingulum low and crown triangular (0), cingulum moderately high and crown spade-like or triangular (1), or cingulum high and diamond-shaped crowns (2) (modified from Xu et al. 2006 #75; Pol et al. 2011 #115; Brown et al. 2013 #41 and #60).

It seems logical that unabraded crowns should always be preferred while coding for a character dealing with crown shape. The blade-like teeth referred to in character state (0) of Pol et al. (2011, #115) may correspond to any kind of maxillary teeth while considering abraded teeth. One feature may help distinguish between triangular teeth and low spade-like teeth, whichever their abrasion state. Triangular crowns use to have very low and open cingula, so their apices rise in a steep manner from the crown base. Blade-like teeth should be recognized because of their relatively taller cingulum, and not necessarily for the shape of their crown apex which is often found in an abraded state. High diamond-shaped crowns have proportionally taller cingula and a taller crown apex, so its overall height/width ratio is more elevated than any other type of crown. Moreover, the angle formed by their cingular vertex is much sharper. As in other tyreophorans, the dentary teeth of *Scelidosaurus harrisonii* (Owen 1861, pl. 6.2) bear a very low cingulum and are clearly triangular-shaped. Teeth of psittacosaurids are blade-like and feature a moderately tall cingulum (e.g. *P. major* and *P. mongoliensis* Sereno 2010, fig. 2.6, 2.14). In several heterodontosaurids such as *Manidens condoriensis*, *Pegomastax africanus*, *Abrictosaurus consors*, *Heterodontosaurus tucki*, 'the crown is poorly differenciated from the root transversely and mesiodistally' (Sereno 2012 #10, p. 218). These taxa were therefore corrected and coded with as non-applicable for this character with its current definition. By contrast, other heterodontosaurids would feature a more distinct cingulum (Sereno 2012 #10, p. 218). Actually, *E. becklesii* (e.g. Sereno 2012, fig. 12), *Fruitadens haagarorum* (Butler et al. 2012), *Tianyulong confuciusi* (Sereno 2012, fig. 22), feature triangular-shaped maxillary crowns with a moderately tall cingulum. The maxillary teeth of *L. angustidens* seem different because their cingulum is much verticalized and would have been quite tall (Sereno 2012, fig. 77C). Unfortunately all of the teeth from *L. angustidens* were worn out so even the cingula are not complete apicobasally. The crowns apew of the neornithischians *Hexinlusaurus multidens* and *Agilisaurus louderbacki* (Barrett et

al. 2005, fig. 2A, 2B) are triangular, and also feature a weak and tall cingulum. He and Cai (1984, p. 47) alledge that teeth of *Yandusaurus hongheensis* lack a distinctive cingulum. Because the neornithischian *H. multidens* and *A. louderbacki* may be similar, we did not code for this taxon pending better-quality photographs from its maxillary teeth. The teeth of *Kulindadromeus zabaikalicus* (Godefroit et al. 2014, fig. S4E) are spade-like although they also bear a high cingulum. Similarly, the upper and lower teeth of *Thescelosaurus neglectus* (Boyd 2014, fig. 19), orodromiines (Brown et al. 2013, fig. 11) and *Orodromeus makelai* (Scheetz 1999, fig. 6) are triangular-shaped with a very low cingulum. The following ornithopods feature a moderately high cingulum with a more obtuse cingular vertex and spade-like crowns: *Hypsilophodon foxii* (Galton 2009, fig. 2), *Changchunsaurus parvus*, Liyong et al. (2010, fig. 8A), *Haya griva* (Makovicky et al. 2011, fig. 1A, B), *Jeholosaurus shangyuanensis* (Barrett and Han, 2009, fig. 1D), *Mochlodon suessi* (Sachs and Hornung 2005, fig. 2.4, 2.6), *Mochlodon vorosi* (Ösi et al. 2012, fig. 4A, D, F), *Rhabdodon* sp1 (Pincemaille-Quilleveré 2002, fig. 5), the Vegagete ornithopod (Dieudonné et al. 2016a), *Zalmoxes robustus* (Weishampel et al. 2003), *Zephyrosaurus schaffi* (Sues 1980, fig. 3-4). Coria and Salgado (1996) affirm that the maxillary teeth of *Gasparinisaura cincosaltensis* are diamond-shaped, but Cambiaso (2007) also affirms that they are also relatively low. Herne (2014, fig. 5.28) shows a photograph of the maxillary teeth of *G. cincosaltensis*, which look diamond-shaped though quite much abraded. In *Kangnasaurus coetzeei* (Cooper 1985, fig. 3A) the tooth bears a much verticalized and tall cingulum, so we may consider the tooth as diamond-shaped. The teeth of *Anabisetia saldiviai* (Cambiaso 2007, fig. 96C), *Talenkauen santacrucensis* (Cambiaso 2007, fig. 139A, B) and *Tenontosaurus tilletti* (Thomas 2015, fig. 23) are relatively wide but have much verticalized mesial and distal cingula so we may consider their teeth as more “diamond-shaped”. The teeth of *Parksosaurus warreni* are not sufficiently described nor figured to establish with clarity the character scoring for this taxon

(Parks 1926; Galton 1973). Only poor illustrations of *Muttaburrasaurus langdoni* teeth were provided to date (Bartholomai and Molnar, 1981, plate 2.D), but this taxon was corrected and coded as bearing tall, diamond-shaped teeth by Bell et al. (2019 #147). *S. harrisonii* was corrected and coded (0). *E. becklesii*, *F. haagarorum*, *T. confuciusi*, psittacosaurids were corrected and coded (1) and *A. consors*, *H. tucki* were corrected and coded as non-applicable. *H. foxii*, *A. saldiviai, T. santacrucensis*, *T. tilletti*, *C. parvus*, *H. griva*, *J. shangyuanensis*, *M. suessi*, *M. vorosi*, *M. langdoni*, *R.* sp1, the Vegagete ornithopod, *Z. robustus*, *Z. schaffi* were also corrected and coded (1). Taxa previously coded for having high diamond-shaped crowns were passed to character state (2). With the redefinition of this character, we further correct and code *H. multidens*, *A. louderbacki*, *K. zabaikalicus*, *G. cincosaltensis*, *K. coetzeei*, *A. saldiviai*, *T. santacrucensis*, *T. tilletti* and *M. langdoni* (following Bell et al. 2019 #147) with character state (2). *P. warreni* and *Y. hongheensis* were corrected and coded with a question mark pending further reexamination or obtention of higher quality photographs.

179(*). Maxillary teeth, apical ridge or swelling position, centrally placed (0), posteriorly set (1) (modified from Brown et al. 2013 #38).

Talenkauen santacrucensis (Cambiaso 2007, fig. 17C), *Anabisetia saldiviai* (Cambiaso 2007, p. 204), *Zephyrosaurus schaffi* (Sues 1980, fig. 5A) and the Vegagete ornithopod (Dieudonné et al. 2016a, fig. 4B1) all feature maxillary teeth with a more posteriorly set primary ridge. In *Psittacosaurus major* (You et al. 2008, fig. 5A) the primary ridge is centrally placed. In some taxa the maxillary teeth bear no conspicuous central ridge or swelling: this is the case of *Yinlong downsi* (Han et al. 2015, p. 25), ankylosaurs (Mallon and Anderson 2014, fig. 1), Stegosaurs (Gilmore 1914, fig. 11, 12) and *Isaberrysaura mollensis* (Salgado et al. 2017, fig. 2F, G). *Echinodon becklesi* (Sereno 2012, fig. 12, 14), *Tianyulong confuciusi* (Sereno 2012, fig. 24A, B), *Lycorhinus angustidens* (Sereno 2012, fig. 77) all feature maxillary teeth with centrally placed swelling labially. *T. santacrucensis*, *A. saldiviai*, *Z. schaffi*, the Vegagete

ornithopod were corrected and coded (1). Psittacosaurs, *E. becklesi*, *T. confuciusi*, *L. angustidens* were corrected and coded (0). *Y. downsi*, Stegosaurs, ankylosaurs, *I. mollensis* were corrected and coded as non-applicable for this character

180(*). Maxillary tooth crown, mesiodistal edges: diverging from the root (0), chisel-shaped with parallel sides (1) (modified from Xu et al. 2006 #75).

The ovate crowns were formerly coded as character state (2) for psittacosaurs and neoceratopsians. This characteristic was considered as non-mutually exclusive with the chisel nature of the crowns (character state 1), so character state (2) was removed

181(*). Maxillary teeth, relative prominence of the primary ridge on labial surface of crown: primary and secondary ridges absent or weakly developped from the apex of the crown (0), outstanding in comparison to other secondary ridges (1), completely undistinguishable from at least a few other secondary ridges in (2) (modified from McDonald et al. 2010 #92, Ösi et al. 2012 #120).

Lesothosaurus diagnosticus (Sereno 1991, fig. 4A), *Agilisaurus louderbacki* (Barrett et al. 2005, fig. 2B), *Yandusaurus hongheensis* (He and Cai 1984, p. 47), *Jeholosaurus shangyuanensis* (Barrett and Han, 2009, fig. 1D, p. 50), *Haya griva* (Makovicky et al. 2011, p. 631), *Changchunsaurus parvus* (Liyong et al. 2010, fig. 10A), *Yinlong downsi* (Han et al. 2015, p. 25), *Scutellosaurus lawleri* (Colbert 1981, fig. 9E) have no visible primary ridge on their maxillary crown, although they eventually feature a smooth central swelling. In *Stegoceras validum* (Sues and Galton 1987, fig. 4C) and *Tianyulong confuciusi* (Sereno 2012, fig. 24A) a central ridge is visible on the labial side and reaches the apex of the crown. A weak central ridge is also dcescribed for *Goyocephale lattimorei* (Perle et al. 1982, p. 119). In *Psittacosaurus major* (Sereno 2010, fig. 2.6A), the presupposed primary ridge aren't distinguishable from other secondary ridges. We rather consider that there was neither primary nor secondary ridges in this taxon, but solely strong and tubular terciary ridges that

prolongate from the apical denticles down for the first half of the labial crown surface. *Anabisetia saldiviai* (Coria and Calvo 2002, fig. 2; Cambiaso 2007, fig. 96A, C), *Talenkauen santacrucensis* (Cambiaso 2007, fig. 17C), *Camptosaurus dispar* (Gilmore 1909, fig. 7), *Dryosaurus altus* (Galton 1983, fig. 28DD), *Dysalotosaurus lettowvorbecki* (Carpenter and Galton 2018, fig. 28EE), *Gasparinisaura cincosaltensis* (Herne 2014, fig. 5.32), *Heterodontosaurus tucki* (Norman et al. 2011, fig. 22), *Hypsilophodon foxii* (Galton 2009, fig. 2J, K, Q, R, Z), *Iguanodon bernissartensis* (Norman 1980, fig. 20), all have an outstanding primary ridge with respect to secondary ridges. Andrzejewski et al. (2019, p. 16) states that there is no prominent primary ridge on the maxillary teeth of *Convolosaurus marri*. However a primary ridge is clearly visible as more prominent in their figure 11. We assumed that the maxillary tooth SMU 72316 (Andrzejewski et al. 2019, fig. 11) was representative of the maxillary dentition of *C. marri*. *Yandusaurus hongheensis* (He and Cai 1984, p. 46-47), *Hexinlusaurus multidens* (Barrett et al. 2005, fig. 2A, p. 825), *Nanosaurus agilis* (Bakker et al. 1990, p. 9; Carpenter and Galton 2018, fig. 10G), *Mochlodon suessi* (Sachs and Hornung 2005, fig. 2.6), *Mochlodon vorosi* (Ösi et al. 2012, fig. 4D, F), *Parksosaurus warreni* (Parks 1926, fig. 1), *Rhabdodon* sp. from Vitrolles (Pincemaille-Quilleveré 2002, fig. 5), *Tenontosaurus tilletti* (Thomas 2015, fig. 23.1), *Thescelosaurus neglectus* (Boyd 2014, fig. 19), the Vegagete ornithopod (Dieudonné et al. 2016a, fig. 4B1), *Zalmoxes robustus* (Weishampel et al. 2003, fig. 13A, D), *Zephyrosaurus schaffi* (Sues 1980, fig. 5A), all bear a primary ridge on their maxillary tooth which relative thickness is hardly or not distinguishable at all from that of secondary ridges. In *Muttaburrasaurus langdoni*, the labial side of maxillary crow displays “finely and evenly ornamented” subparallels ridges, but no primary ridge is reported (Bartholomai and Molnar, 1981, p. 326). Bell et al. (2019 #149) corrected and coded *Muttaburrasaurus langdoni* as bearing a more prominent primary ridge on the labial side. However, given the slight difference between character states (1) and (2) on this

character, and the absence of clear photographs of its teeth, we are currently unable to code *M. langdoni* appropriately. *L. diagnosticus*, *A. louderbacki*, *Y. hongheensis*, *J. shangyanensis*, *H. griva*, *C. parvus*, *Y. downsi*, *S. lawleri*, Psittacosauridae were corrected and coded (0). *T. confuciusi*, *C. marri*, *A. saldiviai*, *T. santacrucensis*, *C. dispar*, *Dryosaurus*, *D. lettowvorbecki*, *G. cincosaltensis*, *H. tucki*, *H. foxii*, *I. bernissartensis* were corrected and coded (1). *Y. hongheensis*, *H. multidens*, *N. agilis*, *M. suessi*, *M. vorosi*, *P. warreni*, the Vitrolles *Rhabdodon* sp., *T. tilletti*, *T. neglectus*, the Vegagete ornithopod, *Z. robustus*, *Z. schaffi* were corrected and coded (2). *M. langdoni* was temporarily corrected and coded with a question mark (instead of (1) previously under the current definition).

183(*). Dentary dentition, heterodonty: no substantial heterodonty is present in dentary dentition (0), single, enlarged, caniform anterior dentary tooth (1) (Ösi et al. 2012 #124).

The relative mesiodistal enlargement of the anterior dentary crown above its root was seen as irrelevant in the analysis with respect to the presence of an enlarged caniform dentary tooth anteriorly. Character state (2) dealing with the presence of a caniform dentary tooth with enlarged crown base was therefore removed. In *Goyocephale lattimorei*, the first mandibular tooth is caniform and enlarged with respect to all other mandibular teeth (Perle et al. 1982, pl. 42: fig. 9). It also looks recurved backward with its crenulation being only in its posterior side (Perle et al. 1982, pl. 42: fig. 9b). The anteriormost dentary tooth is also enlarged in *Stegoceras validum*, although smaller than in heterodontosaurids and pachycephalosaurs (Sues and Galton 1987, fig. 3). *A. louderbacki* was corrected and coded (1) instead of its previous character state (2).

185(*). Dentary teeth, intercrown spaces: present (0), absent (1) (McDonald et al. 2010 #80).

There is an intercrown space or “interdental vacuity” between dentary teeth of *Nanosaurus agilis* (Carpenter and Galton 2018, fig. 7A-K) and the primitive pachycephalosaur *Wannanosaurus yansiensis* (Hou 1977), but no intercrown space between the dentary teeth of

Agilisaurus louderbacki (Peng 1992, fig. 2B), *Psittacosaurus major* (You et al. 2008, fig. 4), *Yinlong downsi* (Han et al. 2015, fig. 20C), *Hypsilophodon foxii* (Galton 2009, fig. 3A-C), and *Heterodontosaurus tucki* (e.g. Norman et al. 2011). *N. agilis* and *W. yansiensis* were corrected and coded (0). *A. louderbacki*, *Y. downsi, H. foxii* and *H. tucki* were corrected and coded (1). *P. major* was newly coded (1).

186(*). Dentary teeth, apical ridge position: anteriorly or centrally positioned (0), posteriorly positioned (1) (Brown et al. 2013 #52).

The apical ridge/ swelling is centrally positioned in the dentary teeth of *Psittacosaurus major* (You et al. 2008, fig. 5B) and *Psittacosaurus mongoliensis* (Osborn 1923, fig. 4). Bell et al. (2019 #156) corrected and coded *Dryosaurus altus* and *Dysalotosaurus lettowvorbecki* as bearing a centrally placed apical ridge on their dentary teeth, an observation with which we concur (cf. Galton 1983, fig. 4). Note that the same is also true for the dentary teeth of *Camptosaurus aphanoecetes*, as opposed to *Camptosaurus dispar* in which the apical ridge is more posteriorly set (Gilmore 1909, fig. 8.2; Carpenter and Wilson 2008, fig. 5A-B). Nothing could be said to what regard the position of the primary ridge on the dentary teeth of *Jeholosaurus shangyuanensis* (Barrett and Han, 2009, p. 50). *P. major* and *P. mongoliensis* were newly coded (0). *Dryosaurus* and *D. lettovorbecki* were corrected and coded (0). *J. shangyuanensis* was corrected and coded with a question mark.

188(*). Dentary teeth, shape and prominence of the primary ridge on lingual surface of the crown: absent, there is a smooth swelling instead of a primary ridge (0), the primary ridge is mesiodistally as thin as the secondary ridges and varyingly deep labiolingually (1), the primary ridge largely oversizes secondary ridges in both height and width, and also oversizes all the maxillary teeth ridges (2) (modified from Ösi et al. 2012 #121).

Anabisetia saldiviai and *Gasparinisaura cincosaltensis* were corrected and coded as bearing a prominent primary ridge by Bell et al. (2019 #158). However we remark that dentary teeth are

obscured in *G. cincosaltensis* (Coria and Salgado 1996). In *Anabisetia saldiviai* a primary ridge would actually be present, and it seems not to have oversized other ridges in mesiodistal width (Coria and Calvo 2002, cf. fig. 3B and 3E). Dentary teeth are also obscured in *Chaoyangsaurus youngi* (Zhao et al. 1999). Dentary crowns of *Yinlong downsi* lack primary and secondary ridges (Han et al. 2015, p. 25). As members of Dryomorpha, *Dryosaurus altus*, *Camptosaurus dispar*, *Dysalotosaurus lettowvorbecki* (Carpenter and Galton 2018, fig. 4, 28DD-EE) lack a distinctly prominent primary central ridge on their dentary teeth. The dentary teeth of *Talenkauen santacrucensis* bear a strong central ridge which is much larger than the secondary ridges, and also larger than the primary ridge of maxillary teeth (Rozadilla et al. 2019, p. 14, fig. 11). In *Tenontosaurus tilletti*, there are much fewer secondary ridges but the primary ridge is also very large (Thomas 2015, fig. 47). SAM-PK-2732 was previously referred to a maxillary tooth from *Kangnasaurus coetzeei* (Haughton 1915, p. 19, fig. 1). It is rather referable to a dentary tooth owing to its strong central ridge (Herne 2014, fig. 5.40). The primary ridge of *Hypsilophodon foxii* dentary teeth were described as large, and feature a prominent central spike in their worn crowns (Galton 2009, p. 21). However, figures show that dentary teeth from *Hypsilophodon foxii* are rather narrow mesiodistally (Galton 2009, fig. 2T, 3G-M; Tennant 2013, fig. 39A). *A. saldiviai* was corrected and coded (1). We corrected and coded *G. cincosaltensis* and *C. youngi* with a question mark.

189(*). Dentary teeth, number and morphology of secondary and/or accessory ridges on lingual surface of the crown: no secondary ridges, faint accessory ridges arising from marginal denticles (0), multiple parallel and evenly-spaced secondary ridges on either side of the central ridge, such that entire lingual surface is corrugated (1), a few parallel and well defined secondary ridges with multiple faint accessory ridges arising from marginal denticles (2) (modified from McDonald et al., 2010 #87).

The Vegagete ornithopod (Dieudonné et al. 2016a, fig. 4E1), *Mochlodon suessi* (Sachs and Hornung 2005) and the Laño rhabdodontid (Pereda and Sanz, 1999) share the apomorphy of dentary teeth with very few secondary ridges on either side of the primary ridge. *Hypsilophodon foxii* (Galton 2009, fig. 2U, V, W), *Tenontosaurus tilletti* (Thomas 2015, fig. 23.2) have few secondary ridges around the primary ridge. The dentary teeth of *Anabisetia saldiviai* were reported to bear more or less seven secondary ridges (Cambiaso 2007, p. 204). *Parksosaurus warreni* (Galton 1973, p. 11, 14), *Talenkauen santacrucensis* (Cambiaso 2007, fig. 17E), *Zephyrosaurus schaffi* (1980, fig. 5) have multiple secondary ridges that are evenly spaced. This character could not be safely inferred for *Thescelosaurus neglectus* from the provided descriptions (Boyd 2014, p. 61-62). *T. santacrucensis*, *P. warreni*, *Z. schaffi* were corrected and coded (1). *M. suessi*, *H. foxii*, *T. tilletti* were corrected and coded (2).

190(*). Ridges present on both the labial and lingual sides of dentary crowns (0), ridges mostly limited to the lingual side of dentary crowns and very faint to absent on the labial side (1) (modified from Boyd 2015 #124).

Ridges seem to be present on both sides of dentary crowns in *Heterodontosaurus tucki* (Norman et al. 2011, fig. 25A, B). *Mochlodon suessi* (Sachs and Hornung 2005, fig. 2.5), *Mochlodon vorosi* (Ösi et al. 2012, fig. 4B) share dentary teeth with very faint ridges on the labial side of the unworn crown surfaces of their dentary teeth. This is also the case in some teeth of the Vegagete ornithopod, although those labial ridges are fainter and not systematically developped (Dieudonné et al. 2016a, fig. 4E2, pers. obs.). *H. tucki*, *M. suessi* and *M. vorosi* were corrected and coded (0). The Vegagete rhabdodontid was corrected and coded (1).

192(*). Dentary tooth roots straight in anterior or posterior view all along the row (0), dentary tooth roots curved in anterior or posterior view (1) (modified from Boyd 2015 #135).

We modified the definition of this character to account for the possible variability in dentary tooth root curvature within a single tooth row. This is what actually happens in the Vegagete rhabodontid, where the outward curvature of the dentary teeth roots is more pronounced in the middle of the row (Dieudonné et al. 2016a, fig. 2C3). We corrected and coded the Vegagete ornithopod (1).

Axial skeleton:

193(*). Cervical vertebrae, shape of postzygapophyses: posterodorsally arched and higher dorsoventrally (0), dorsally flat and dorsoventrally low (1) (modified from Cambiaso 2007 #59; Han et al. 2018, #235).

This character was completely recoded based on bibliography. The postzygapophyses of *Camptosaurus aphanoecetes* (Carpenter and Wilson 2008, fig. 7A), *Mahuidacursor lipanglef* (Cruzado-Caballero et al. 2019), *Anabisetia saldiviai* (Cambiaso 2007, fig. 100B, C), *Talenkauen santacrucensis* (Cambiaso 2007, fig. 19-20), *Macrogryphosaurus gondwanicus* (Calvo et al. 2007, fig. 1), *Convolosaurus marri* (Andrzejewski et al. 2019, fig. 13B), *Orodromeus makelai* (Scheetz 1999, fig. 11A), *Dysalotosaurus lettowvorbecki* (Janensch 1955, pl. 12.4-10), *Dryosaurus altus* (Carpenter and Galton 2018, fig. 29D) are dorsally flat, dorsoventrally low and project posteriorly in a straight manner. This differs from the more upward posterior inclination, dorsally arched and somewhat higher postygapophyses found in the cervical of *Camptosaurus dispar* (Carpenter and Wilson 2008, fig. 7C), *Zalmoxes robustus* (Weishampel et al. 2003, fig. 15C, G), *Muttaburrasaurus langdoni* (Molnar 1996), *Iguanodon bernissartensis* (Norman 1980, fig. 22), *Tenontosaurus tilletti* (Forster 1990, fig. 1), *Tenontosaurus dossi* (Winkler et al. 1997, fig. 12B), *Thescelosaurus neglectus* (Galton 1974*b*, pl. 3.3), *Gasparinisaura cincosaltensis* (Cambiaso 2007, fig. 56A), *Hypsilophodon foxii* (Galton 1974*a*, fig. 19) and more basal neornithischians such as *Abrictosaurus consors*

(cervicals C5 and C6, Sereno 2012, p. 77-78), *Heterodontosaurus tucki* and *Jeholosaurus shangyuanensis* (cf. Han et al. 2018, figures of characters #231 and #235A respectively), *Changchunsaurus parvus* (Butler et al. 2011, fig. 2B), *Haya griva* (Makovicky et al. 2011, fig. 3B), *Hexinlusaurus multidens* (He and Cai 1984, fig. 6) or *Nanosaurus agilis* (Carpenter and Galton 2018, fig. 12D). The postzygapophyses of *Chaoyangsaurus youngi* are tall and point strictly posteriorly, however they are also dorsoventrally thicker which was retained as the principal argument to code this taxon (0), as for its closest ancestors (Zhao et al. 1999, fig. 5C). The postzygapophyses of basal ornithischians such as *Lesothosaurus diagnosticus* (Baron et al. 2016, fig. 2, p. 6-7) are also posterodorsally inclined and arched.

194(*). Cervical vertebrae, heightenning of neural spines along the series: remains low and triangular all along, more than three times as long as high in posterior cervicals (0), reach a substancial height posteriorly, less than twice as long as they are tall (1) (modified from Han et al. 2018 #236).

This character was completely recoded based on bibliography. The posterior cervical neural spines remain low in *Mahuidacursor lipanglef* (Cruzado-Caballero et al. 2019). Similarly, the posteriormost cervicals neural spines of *Dryosaurus altus* (Carpenter and Galton 2018, fig. 29B), *Camptosaurus dispar* (Gilmore 1909, fig. 14; Galton 1974*b*, p. 1052; Carpenter and Galton 2018, fig. 22A, B), *Gasparinisaura cincosaltensis* (Coria and Salgado 1996; Cambiaso 2007, fig. 56A), *Orodromeus makelai* (Scheetz 1999, fig. 12A), *Talenkauen santacrucencis* (Rozadilla et al. 2019, fig. 13C, D), *Macrogryphosaurus gondwanicus* (Calvo et al. 2007, fig. 3), and the seventh and eighth neural spines of *Anabisetia saldiviai* (Cambiaso 2007, p. 215, fig. 99) are low, triangular and relatively undeveloped. Posterior cervical neural spines are comparatively very low in *Stegosaurus stenops* (Maidment et al. 2015, fig 12, 13), *Chaoyangsaurus youngi* (Butler and Zhao 2009, p. 687). Cervical neural spines gain substancial height in the posterior cervicals of *Tenontosaurus tilletti* (Forster 1990, fig. 1),

Hypsilophodon foxii (Galton 1974*a*, fig. 19), *Thescelosaurus neglectus* (Galton 1974*b*, pl. 3.3), *Dysalotosaurus lettowvorbecki* (Janensch 1955, pl. 12.10). In *Muttaburrasaurus langdoni*, the neural spine is weak in cervical five and gets slightly stronger from cervical five posteriorly (Bartholomai and Molnar, 1981, p. 327); however they weren't figured so any assessment of their relative length to height ratio is for now impossible. Weishampel et al. (2003, p. 83) suggest that the posterior cervical neural spines of *Zalmoxes robustus* were as tall as those of the anterior dorsal vertebrae, although they are preserved solely at their base.

195(*). Axis neural spine: anteroposteriorly short (0), long, extends caudally to overlap more than half of the total length of C3 cervical centrum (1) (modified from Xu et al. 2006 #30).

In *Manidens condorensis* (Pol et al. 2011, fig. 1E) and *Haya griva* (Mackovicky et al. 2012, fig. 3B), the axial neural spine is elongated though it appears much vertically held. In *Heterodontosaurus tucki* (Galton 2014, fig. 5A, B), and *Yinlong downsi* (Han et al. 2018, p. 1162) the axis neural spine is very elongated and extends posteriorly to half or more of the third cervical centrum length. A posteriorly extending axial neural spine also occurs in *Psittacosaurus sibiricus* (Averianov et al. 2006, fig. 12G), *Jeholosaurus shangyuanensis* (Han et al. 2012, fig. 1A), *Changchunsaurus parvus* (Butler et al. 2011, fig. 2A). Xu et al. (2006 #30) coded *Psittacosaurus mongoliensis* with character state (0), and Osborn (1924, fig. 2) drew a general outline of the skeleton of *P. mongoliensis*, with a much elongated axis neural spine, but more detailed description or photographs are lacking. In absence of more recent contradicting informations, we kept regarding *P. mongoliensis* as bearing a posteriorly elongated axis neural arch. The axis neural arch looks more foreshortened in *Chaoyangsaurus youngi* (Zhao et al. 1999, fig. 5B). *Y. downsi* was corrected and coded (1).

196(*). Postaxial cervical vertebrae, epipophyses on the postzygapophyses somewhere within the neck: present (0), absent (1) (modified from Ösi et al. 2012 #133, Rozadilla et al. 2016 #234).

We modify this character to code for the presence of postzygapophyseal epipophyses somewhere within the neck instead of just on anterior cervical vertebrae. Therefore, any taxa having an incomplete neck should be coded with a question mark as there could still be some epipophyses over the lacking postzygapophyses. Calvo et al. (2007) noted that the presence of epipophyses on the postzygapophyses of anterior cervical and declared it as exclusive to *Talenkauen* and *Macrogryphosaurus*. Weishampel et al. (2003, p. 83, fig. 15C, G) state that in *Zalmoxes robustus* "a slight shelf, supported by a slight vertical buttress, connects the pre and postzygapophyses and form an incipient neural platform". Such a shelf might actually correspond to an epipophyse. In *Muttaburrasaurus langdoni*, Bartholomai and Molnar (1981, p. 327) state that "in cervical 6, a strong ridge is present running from the middle of the dorsomesial surface of the postzygapophysis towards the neural spine". Such ridge might be attributable to a postzygapophyeal epipophysis as well. Forster (1990, p. 276) notes that in *Tenontosaurus tilletti*, "a high ridge, terminating in a short, caudally projected spine, extends down the dorsal surface of the postzygapophyses of C3 through C7". We also interpret such a ridge as an epipophyse. Their presence was indeed already coded in character #133 from Ösi et al. (2012) in both *Tenontosaurus tilletti* and *Tenontosaurus dossi*. Han et al.(2018, p. 1162) report that epipophyses were absent in *Yinlong downsi*, contrary to what occurs in *Heterodontosaurus tucki* and *Lesothosaurus diagnosticus*. Epipophyses seem also absent in the cervicals of *Chaoyangsaurus youngi* (Zhao et al. 1999, fig. 5) and *Abrictosaurus consors* (Sereno 2012, p. 77). *Z. robustus* and *M. langdoni* were corrected and coded (0) (Bell et al. 2019 #163 corrected and coded *M. langdoni* with a question mark for this character instead of (1) previously). *Y. downsi, C. youngi* and *A. consors* were corrected and coded (1).

197(*). Cervical vertebrae (4-9), form of central surfaces: amphicoelous (0), at least slightly opisthocoelous (1) (Ösi et al. 2012 #134).

Isolated posterior cervical vertebrae from *Yinlong downsi* revealed to be amphiplatian (Han et al. 2018, p. 1162). One cervical vertebra of *Rhabdodon priscus* was described by Lapparent (1947, pl. 2.1, cited in Pincemaille-Quilelveré, 2002, p. 48) as opisthocoelous, but Pincemaille-Quilleveré (2002, p. 48) says that its state of preservation is unsufficient so that this could be clearly affirmed. *Rhabdodon* sp1 from Vitrolles features opisthocoelous cervical vertebrae (Pincemaille-Quilleveré 2002, p. 48). *Y. downsi* was corrected and coded (0). *R.* sp1 was corrected and coded (1).

198(*). Ventral surface of the cervical vertebrae rounded (0), presence of a broad, flattened keel on the ventral surface of the cervical vertebrae (1), presence of a sharp ventral keel on the ventral surface of the cervical vertebrae (2) (Boyd 2015 #143 ; Rozadilla et al. 2016 #237).

The ventral surface of the cervical vertebrae of *Anabisetia saldiviai* (Cambiaso 2007, fig. 100D'), *Talenkauen santacrucensis* (Rozadilla et al. 2019, fig. 13B) and *Macrogryphosaurus gondwanicus* (Calvo et al. 2007, p. 473) are sharply keeled. A ventral keel is told to be well developped posteriorly to the third cervical in *Muttaburrasaurus langdoni* (Bartholomai and Molnar, 1981, p. 327). However the relative sharpness of such a keel cannot be acertained without being properly figured. The axial and post-axial cervical centra of *Camptosaurus aphanoecetes* are ventrally keeled, whereas those of *Camptosaurus dispar* are more rounded (Carpenter and Wilson 2008, p. 236-237). Zheng et al. (2012, p. 210) states that the ventral surfaces of the cervical centra are more strongly keeled in *Yueosaurus tiantaiensis* than in *Hypsilophodon foxii* (Galton 1974*a*), *Thescelosaurus neglectus* (Gilmore 1915), and *Zalmoxes robustus* (Weishampel et al. 2003). *C. dispar* was corrected an coded (1). *Y. tiantaiensis*, *A. saldiviai*, *T. santacrucensis* and *M. gondwanicus* were corrected and coded (2). *M. langdoni* was corrected and coded with a question mark.

199(*). Anterior cervical centra less than 1.5 times longer than tall (0), length of anterior cervical centra equal or greater than 1.5 times longer than tall (1) (Boyd 2015 #144).

Note that the length to height ratio of cervical centra usually decreases posteriorly. Anterior cervical centra of *Lesothosaurus diagnosticus* (Baron et al. 2016, fig. 2), *Fruitadens haagarorum* (Carpenter and Galton 2018, fig. 5J), *Heterodontosaurus tucki* (Galton 2014, p. 105), *Hexinlusaurus multidens* (He and Cai 1984, fig. 6), *Yueosaurus tiantaiensis* (Zheng et al. 2012, fig. 2), *Tenontosaurus tilletti* (Forster 1990, fig. 1), *Thescelosaurus neglectus* (Galton 1974*b*, pl. 2-1A), *Orodromeus makelai* (Scheetz 1999, fig. 11A), *Zephyrosaurus schaffi* (Sues 1980, fig. 18B), *Anabisetia saldiviai* (Cambiaso 2007, fig. 99A-C), *Iguanodon bernissartensis* (Norman 1980, fig. 22) are elongate and low (more than 1.5 times longer than tall). Anterior cervical centra are relatively short in *Yinlong downsi* (Han et al. 2018, fig. 1C). The axis of *Tenontosaurus dossi* is much concave ventrally, and other cervical centra are hardly measurable from a lateral view (Winkler et al. 1997, fig. 12A, B). *Y. downsi* was corrected and coded (0). *L. diagnosticus, F. haagarorum, H. tucki, H. multidens*, *Y. tiantaiensis, T. tilletti*, *T. neglectus*, *O. makelai*, *Z. schaffi, A. saldiviai, Anabisetia saldiviai I. bernissartensis* were corrected and coded (1). *T. dossi* was corrected and coded with a question mark.

200(*). Cervical vertebrae, evolution of central length throughout the series: central length remains approximately the same or decrease posteriorly (0), increase posteriorly (1).

Dryomorphs such as *Dryosaurus altus* (Carpenter and Galton 2018, fig. 29D), *Camptosaurus dispar* (Carpenter and Galton 2018, fig. 22A) feature a posterior increase in cervical centrum length. The same is also true for *Camptosaurus aphanoecetes*, also the latter taxon also feature a posterior decrease from the mid-series toward the dorsals vertebrae (Carpenter and Wilon, 2008, fig. 6A). In *Valdosaurus canaliculatus*, the posterior cervical centrum BELUM K17051 (Barrett *et al*. 2011, fig. 2B) is quite elongate so - although this could not be ruled out - it could represents the resultant of a continuous posterior lengthenning of cervical centra. The cervical centra of *Iguanodon bernissartensis* (Norman 1980, fig. 22) and *Dysalotosaurus*

lettowvorbecki (Janensch 1955, pl. 12.4-10) contrast in remaining of fairly similar lengths. The elasmarian *Talenkauen santacrucensis* (Rozadilla et al. 2019, fig. 12, 13), *Macrogryphosaurus gondwanicus*, but also *Mahuidacursor lipanglef* (Cruzado-Caballero et al. 2019) share the character of posteriorly elongating cervical centra, except for their very last one. *Gasparinisaura cincosaltensis* (Coria and Salgado 1996; Cambiaso 2007, p. 136) was told to have its two posteriormost cervical centra shorter than its axis, but was figured in Cambiaso (2007, p. 275) in the opposite way. At any case its cervical series is quite incomplete so any pattern could not be safely deduced. On what regards *Zalmoxes robsustus*, Weishampel et al. (2003, BMNH R.3809: fig. 15) did not provide a cervical series satisfying enough so that we could code for this character. There should be a slight increase between the anteriormost two and posteriormost three, but there also seems to be a slight decrease in length amongst themselves in a separate way (BMNH R.3809, Weishampel et al. 2003, fig. 15). Nocpsa (1925, R.3841: pl. 4.1A, 1C) figures an anterior cervical series with a clear posterior lengthening. In the heterodontosaurids *Fruitadens haagarorum* (Carpenter and Galton 2018, fig. 5J, L), *Heterodontosaurus tucki* (Galton 2014, fig. 4A) the cervical centra decrease in length posteriorly. A marked decrease is also observed between individually preserved cervical centra four and nine of *Pachycephalosaurus wyomingensis* (Bakker et al. 2006, fig. 10B, 11B). Cervical centra of *Nanosaurus agilis* (Carpenter and Galton 2018, fig. 12D), *Thescelosaurus neglectus* (Galton 1974*b*, pl. 3.3), *Orodromeus makelai* (Scheetz 1999, fig. 11A, 12A), *Tenontosaurus tilletti* (Forster 1990, fig. 1), *Hypsilophodon foxii* (Galton 1974*a*, fig. 19), *Convolosaurus marri* (Andrzejewski et al. 2019, fig. 13B), *Jeholosaurus shangyuanensis* (Han et al. 2012, fig. 1C), *Haya griva* (Makovicky et al. 2011, fig. 3B), *Changchunsaurus parvus* (Butler et al. 2011, fig. 2A) remain of overall similar lengths all along.

201(*). Cervical vertebrae, number: 7/8 (0), 9 (1), 10 or more (2) (Ösi et al. 2012 #135).

Macrogryphosaurus gondwanicus present 10 cervical vertebrae due to the cervicalization of an anterior dorsal vertebra (Rozadilla et al. 2020). Note that *Psittacosaurus mongoliensis* was reported to bear 6 cervical centra by Osborn (1924). You and Dodson (2004, p. 487) report 8 to 9 cervical vertebrae in *P. mongoliensis* and *P. sinensis*, basing on the position of the parapophysis over the neurocentral suture. Sereno et al. (2007, Table 1) measures the dimensions of 9 cervical centra for both *P. mongoliensis* and *P. major*. *Yinlong downsi* is reported to have 9 cervical vertebrae (Han et al. 2018, fig. 1E). Bell et al. (2019 #167) corrected and coded a question mark for *Muttaburrasaurus langdoni*. However, Bartholomai and Molnar (1981, p. 326) stated that 9 cervical vertebrae were present. *P. mongoliensis*, *P. major* and *Y. downsi* were corrected and coded (1). In absence of other contradicting element, we left *M. langdoni* coded (1). *M. gondwanicus* was corrected and coded (2).

202(*). Dorsal vertebrae, number: 12–13 (0), 14-15 (1), 16 or more (2) (modified from Ösi et al. 2012 #137; ordered character).

Here we group a dorsal vertebral count of 14 and 15 altogether into character state (1), as no character state was previously designed for a count of 14 dorsal vertebrae. 13 dorsal vertebrae were reported in *Yinlong downsi* (IVPP V18636, Han et al. 2018, fig. 2A). *Y. downsi* was corrected and coded (0).

203(*). Dorsal vertebrae, neural spine: anteriorly positioned or centered over the dorsal centrum (0), start projecting farther posteriorly than their own centra at some point within the dorsal vertebral series (1) (modified from Brown et al. 2013 #78).

We note that usually, dorsal neural spines start projecting further posteriorly than their own centra posteriorly along the dorsal series. Therefore, anterior dorsal vertebrae with posteriorly projecting neural spines could be coded (1), but taxa which solely preserve their anterior dorsal vertebrae might not be coded. In *Thescelosaurus neglectus* (Galton 1974*b*, pl. 2.5) the neural spines project farther posteriorly to the posterior central surface in posterior dorsal

vertebrae. In *Thescelosaurus assiniboiensis* (Brown et al. 2011, fig. 13) the dorsal neural spines are broken, so such character could not be inferred. In *Dryosaurus altus* (Galton 1981, fig. 2O) the eleventh or twelth dorsal neural spine appears not to project farther posteriorly to the posterior central surface, but we would require to see more posterior dorsal spines to correctly infer this character in this taxon. In *Dysalotosaurus lettowvorbecki*, the neural spines of the last two dorsals project farther posteriorly from the posterior dorsal centra (Janensch 1955, fig. 23). In *Talenkauen santacrucensis* (Rozadilla et al. 2019, fig. 14A, D) and *Macrogryphosaurus gondwanicus* (Calvo et al. 2007, fig. 4B) the posterior dorsal vertebrae maintain a n upright neural arch. In *Kulindadromeus zabaikalicus*, the dorsal neural arch does not appear to be very much expanded posteriorly to the posterior central surface (INREC 3/112, Godefroit et al. 2014, fig. S5A). However, only this dorsal vertebra could be observed from a lateral view so we might remain cautious and left this taxon uncoded for this character. In *Heterodontosaurus tucki* (Galton 2014, fig. 4B) the dorsal neural spines do not project further beyond the posterior central surface in the dorsal series. *T. neglectus* and *D. lettowvorbecki* were corrected and coded (1). *H. tucki*, *T. santacrucensis* and *M. gondwanicus* were corrected and coded (0). *T. assiniboiensis*, *Dryosaurus* and *K. zabaikalicus* were corrected and coded with a question mark.

204(*). Sacrum composed of three or fewer fused vertebral centra (0), sacrum composed of between four and five fused vertebral centra (1), sacrum composed of six fused vertebral centra (2), sacrum composed of seven or more fused vertebra centra (3) (modified from Xu et al. 2006 #104; Boyd 2015 #148).

Thescelosaurus neglectus was reported to bear five fused sacral vertebrae (Gilmore 1915), with the first two sacral fused intervertebrally by the same sacral rib. However Sternberg (1940) describes a specimen of *Thescelosaurus* bearing 6 sacral centra and attributes it to a new species, namely *T. edmontonensis*. Galton (1974b) refutes the attribution of the latter to a

new species, *T edmontonensis* should be thus considered as a subjective junior synonym of *T. neglectus*. *Hypsilophodon foxii* is represented by both pentapleural and hexapleural specimens (Galton 1974*a*), and this seems to also have happened for *Thescelosaurus neglectus*. There are seven sacral vertebrae in *Psittacosaurus major*, as compared to six in other psittacosaurids species (Sereno et al. 2007, p. 277). Six sacral vertebrae are present in *Yinlong downsi* (Han et al. 2018), *Archaeoceratops oshimai* (You and Dodson 2003) and *Homalocephale calathocercos* (Maryanska and Osmolska 1974). Four sacrals only were counted for *Goyocephale lattimorei* (Perle et al. 1982). Sereno (2012, p. 125, 126) observes 13 dorsal and 5 sacral vertebrae in *Heterodontosaurus tucki*. Bell et al. (2019 #170) corrected and coded *Muttaburrasaurus langdoni* with a question mark. However, Bartholomai and Molnar (1981, p. 329) counted 6 sacral rib insertions onto its ilium and deduced the presence of six sacral vertebrae, a conclusion with which we also concur (pers. obs.). *P. major* was corrected and coded (3). *Y. downsi* and *P. mongoliensis* were corrected and coded (2). Pending a better revision of the distribution of this character, and as was done for *H. foxii*, we chose to code *T. neglectus* for its maximum reported number of sacral vertebrae. *T. neglectus* was therefore corrected and coded (2). *H. tucki* was corrected and coded (1).

205(*). Sacral vertebrae, neural spines height: less than 2 times the height of the centrum (0), neural spines between 2 and 2,5 times the height of the centrum (1), greater than 2,5 times (2) (Brown et al. 2013 #82).

In *Macrogryphosaurus gondwanicus* (Calvo et al. 2007, fig. 9B, pers. obs.), the sacral neural spines are less than two times the proper height of their centra. In *Heterodontosaurus tucki*, the sacral neural spines appear to be about 2 times as high as their proper centra (Galton 2014, fig. 4C). In *Dryosaurus altus*, there is no way to infer the relative height of the sacral neural spines (Galton 1981, Shepherd et al. 1977, fig. 1P). In *Convolosaurus marri*, the sacral neural spines are told to be more than twice the height of their centra, and we infer from last sacral

centrum (SMU 72316, Andrzejewski et al. 2019, fig. 15A) that those sacral neural spines wouldn't have exceeded 2.5 times their own centrum height. *H. tucki* and *C. marri* were corrected and coded (1). *M. gondwanicus* was corrected and coded (0). *Dryosaurus* was corrected and coded with a question mark.

206(*). Sacrum, accessory articulation with pubis: pubis does not articulate with the sacrum (0), pubis supported by sacral rib (1), pubis supported by sacral centrum (2) (modified from: Ösi et al. 2012 #139; Brown et al. 2013 #84).

Every sacral rib contacts the ilium within a sacral "yoke" in *Zalmoxes robustus* (Weishampel et al. 2003) so any contact between a sacral rib or centrum with the pubis is impossible. Sacral ribs are inserted along a medial horizontal plane of the ilium in *Muttaburrasaurus langdoni* (Bartholomai and Molnar, 1981, fig. 8C and pers. obs., contra Bell et al. 2019 #173) so it seems highly improbable that any other sacral rib had bifurcated to contact with the pubis. In *Macrogryphosaurus gondwanicus*, the pubis does not articulate with the sacrum (Calvo et al. 2007, fig. 9B). In *Yinlong downsi*, the pubis wasn't described to contact anything else but the ilium itself (Han et al. 2018, p. 1175). Similarly, all sacral ribs form an exclusive contact with the ilium in *Psittacosaurus mongoliensis* (Osbron, 1924, fig. 9). The pubis is supported by sacral ribs in *Archaeoceratops oshimai* (You and Dodson 2003, p. 267). *Z. robustus*, *M. gondwanicus*, *Y. downsi* and *P. mongoliensis* were corrected and coded (0).

207(*). Ischiac peduncle of the ilium is not supported by a sacral rib (0), ischiac peduncle of the ilium supported by a sacral rib (1) (Boyd 2015 #190).

The ischiac peduncle of ilium is not supported by a sacral rib in *Psittacosaurus mongoliensis* (Osborn 1924, fig. 9). *P. mongoliensis* was corrected and coded (0).

208(*). Proximal caudal vertebrae, neural spines position: caudal neural spines positioned over centrum (0), project backward beyond own centrum to an angle of more than 50° over the

horizontal (1), project backward to an angle of less than 50° over the horizontal (2) (modified from Brown et al. 2013 #88).

We note that the caudal spines always tend to bend more posteriorly conforming we get more posteriorly in the tail (e.g. *Tenontosaurus tilletti*, Forster 1990, fig. 5B). Thus, we modified the character definition to deal only with the more proximal caudal vertebrae. In *Tenontosaurus tilletti* (Forster 1990, fig. 5B) and *Tenontosaurus dossi* (Winkler et al. 1997, fig. 14C), the proximal caudal neural spines do not project further posteriorly with respect to their own centrum, and hardly project further posteriorly in more posterior caudal vertebrae. In *Homalocephale calathocercos* (Maryanska and Osmolska 1974, pl. 28.2) and *Stegoceras validum* (Gilmore 1924, pl. 12.2-3) the caudal neural spines do not project posteriorly to their centra at all. This is also similar to what occurs in *Heterodontosaurus tucki* (Galton 2014, fig. 7I-J), *Fruitadens haagarorum* (Carpenter and Galton 2018, fig. 5V) but also in both of the above-mentionned *Tenontosaurus* species. In *Yinlong downsi* (Han et al. 2018, p. 1166) the proximal caudal neural spines project posteriorly to an angle of about 60°. All reconstructions of the tail of *Psittacosaurus mongoliensis* (=*Protiguanodon mongoliense*) given by Osborn (1924) point to caudal neural spines strongly projecting posteriorly. Along with You and Dodson (2003, p. 265) the caudal spines of *Archaeoceratops oshimai* are tall and "only slightly inclined posteriorly". In absence of clear figure we could not code for this character for the moment. Whilst most ornithopods as *Hypsilophodon foxii* (≈70°, Galton 1974*a*, fig. 28), *Nanosaurus agilis* (≈61°, Galton and Jensen 1973, fig. 2G), *Eousdryosaurus nanohallucis* (≈ 58°, Escaso et al. 2014, fig. 2), *Camptosaurus dispar* and *Camptosaurus aphanoecetes* (≈ 58°, Carpenter and Galton 2018, fig. 22I, J respectively) feature proximal caudal neural spine only moderately inclined posteriorly, a specific cluster of taxa groups *Dryosaurus altus* (≈44.6°, Galton 1981, fig. 5O), *Dysalotosaurus lettowvorbecki* (from ≈47° to ≈32° in the first proximal caudals, Janensch 1955, pl. 13.4-6), *Anabisetia saldiviai*

(arctangeant of neural spine height to length ≈33° in MCF-PVPH-75, Cambiaso, 2007, fig. 105A, A'), *Valdosaurus canaliculatus* (≈23°, Barrett 2016, fig. 3), and *Diluvicursor pickeringi* (≈25°, Herne et al. 2018, fig. 9A) as having proximal caudal neural spines drastically inclined posteriorly, i.e. to less than 50° from the horizontal. The degree of posterior inclination of the proximal caudal neural spines is not known at any precision in *Gasparinisaura cincosaltensis* (Cambiaso 2007, fig. 60A). Only one distal caudal vertebra is preserved in *Koreanosaurus boseongensis* (Huh et al. 2010) so this character is unknown for this taxon. *F. haagarorum, T. tilletti* and *T. dossi* were corrected and coded (0). *Y. downsi* and Psittacosaurs (for *P. mongoliensis*) were corrected and coded (1). *A. saldiviai*, *Dryosaurus*, *D. lettowvorbecki*, *V. canaliculatus* were corrected and coded (2). *G. cincosaltensis* was corrected and coded as polymorphic (1, 2) until more precise observations could be made. *K. boseongensis* was corrected and coded with a question mark.

209(*). Anterior caudal vertebrae, neural spines: height (from above the prezygapophyses) the same or up to 50% taller than the centrum (0), more than 50% taller than the centrum (1) (Ösi et al. 2012 #142).

The height of the first neural spines is less than half the height of their centra in *Yinlong downsi* (Han et al. 2018, p. 8). The height of the first caudal neural spines is more than 150% the height of their centra in *Yueosaurus tiantaiensis* (Zheng et al. 2012, fig. 3), *Nanosaurus agilis* (Galton and Jensen 1973, fig. 2G), *Hypsilophodon foxii* (Galton 1974*a*, fig. 28C), *Fruitadens haagarorum* (Carpenter and Galton 2018, fig. 5V), *Heterodontosaurus tucki* (Galton 2014, fig. 7I-J), *Homalocephale calathocercos* (Maryanska and Osmolska 1974, pl. 28.2) and *Stegoceras validum* (Gilmore 1924, pl. 12.2-3). *Y. tiantaiensis*, *N. agilis*, *H. foxii*, *F. haagarorum*, *H. tucki* and *H. calathocercos* were corrected and coded (1). *Y. downsi* was corrected and coded (0).

211(*). Anterior dorsal ribs, distal portions of the shaft in cross-section: circular or oval (0), highly laterally compressed with concave lateral and rugose posterior surfaces (1) (Brown et al. 2013 #135).

Dorsal ribs of *Talenkauen santacrucensis* (Rozadilla et al. 2019, p. 20, fig. 16A-B), *Changchunsaurus parvus* (Butler et al. 2011, p. 673), *Haya griva* (Makovicky et al. 2011, p. 633) are described as transversely compressed. The anterior dorsal ribs of *Zalmoxes robustus* are anteriorly thickened and rounded and posteriorly narrow so they acquire a "T-shaped" proximal cross-section, they then become more mediolaterally compressed toward their distal end (Weishampel et al. 2003, p. 86). All the preserved ribs from the here termed *Rhabdodon* sp1 from Vitrolles (posterior dorsals and cervical ribs) are characterized by being typically mediolaterally compressed (Pincemaille-Quilleveré 2002, p. 53). By contrast, Forster (1990, p. 277) describes the dorsal ribs of *Tenontosaurus tilletti* as tapering distally for ribs 1 and 2, but as ending as thick rugose tips for the following ones. In *Fostoria dhimbangunmal,* Bell et al. (2019, p. 12) the dorsal ribs end-up as being "blade-like", but there was no mention of wether this occurred from a mediolateral or anteroposterior compression. The more proximal dorsal rib shaft was told to be anteroposteriorly compressed. It is still possible that such anteroposterior compression resulted from a twist of an originally mediolaterally compressed blade or not. Preserved dorsal ribs of *Homalocephale calathocercos* are described as "rod-like" (Maryanska and Osmolska 1974, p. 58). Dorsal ribs of *Stegoceras validum* don't look especially compressed mediolaterally either (Gilmore 1924, pl. 13.4; see also Maryanska and Osmolska 1974, p. 94 to avoid the confusion between tendons and ribs made by the former author). *T. tilletti* was corrected and coded (0). *C. parvus*, *H. griva*, *T. santacrucensis*, *Z. robustus* and *R.* sp1 were corrected and coded (1). *F. dhimbangunmal* was corrected and coded with a question mark.

212(*). Dorsal ribs, distal anteroposterior thickening: absent (0), present (1) (new character).

A distal anteroposterior thickening of dorsal ribs is visible in *Mahuidacursor lipanglef* (Cruzado-Caballero et al. 2019), *Talenkauen santacrucensis* (Rozadilla et al. 2019, fig. 16B, 17A), *Macrogryphosaurus gondwanicus* (Calvo et al. 2007, fig. 10), *Thescelosaurus neglectus* (Gilmore 1915, pl. 79), *Thescelosaurus assiniboiensis* (Brown et al. 2011, fig. 16), *Camptosaurus aphanoecetes* (Carpenter and Wilson 2008, fig. 42), *Nanosaurus agilis* (Galton and Jensen 1973, pl. 1). It is absent in *Tenontosaurus tilletti* (Tennant 2013, fig. 12A) and other cerapods.

213(*). Ossified epaxial tendons along dorsal and sacral vertebrae: absent (0), present (1) (new character).

There appears to be no ossified tendons along the whole vertebral column of *Herrerasaurus ischigualastensis* (Novas 1994), and that of the neornithischian *Yueosaurus tiantaiensis* (Zheng et al. 2012, fig. 2). *Koreanosaurus boseongensis* (Huh et al. 2010, fig. 5) stands out because of its lack of ossified tendons along its back, and was described only for a single distal caudal vertebra (Huh et al. 2010, fig. 8). Although the absence of ossified tendons on its tail would be unlikely, this cannot be assessed with the material at hands. We created this character to account for the absence of epaxial tendons on the back of Y. *tiantaiensis* and *K. boseongensis*.

215(*). Proximal caudal ribs, location: borne on centrum (0), on neurocentral suture (1), on neural arch (2) (modified from Brown et al. 2013 #85).

This character was modified to consider only the proximal caudal centra, as the origin of the transverse processes could vary within the tail of some taxa. In *Yueosaurus tiantaiensis* (Zheng et al. 2012, fig. 2B, 3G), the caudal transverse processes seem to be borne on the neurocentral suture. *Yinlong downsi* "the facet for the transverse process indicates they were born primarily on the neural arch, but that their ventral aspect articulates with the centrum." (Han et al. 2018, p. 7). Provided that the transverse processes of *Y. downsi* still contacted the

centrum, and that no other basal ceratopsian are available for this information on this data-matrix, we considered that *Y. downsi* preserved the plesiomorphic state of transverse processes borne on the limit between the centrum and the neural spine. The transverse processes of the proximal caudals in *Valdosaurus canaliculatus* (Barrett 2016, fig. 3C) and *Macrogryphosaurus gondanicus* (Rozadilla et al. 2020, fig. 9C) are clearly borne onto their neural arches, i.e. above the neurocentral suture. Note that the transverse processes of the proximal caudal centra of *Camptosaurus aphanoecetes* are born on the neural arch (Carpenter and Wilson 2008, fig. 14), as in dryosaurids (Galton 1981), *Fostoria dhimbangunmal* (Bell et al. 2019), and the Vegagete rhabdodontid (MDS-VG, 72, 101, Dieudonné et al. 2016a, fig. 5I). Caudal ribs appear to be borne on the neurocentral suture in *Homalocephale calathocercos* (Maryanska and Osmolska 1974, fig. 4D-E). *Y. tiantaiensis*, *Y. downsi*, *H. calathocercos* were corrected and coded (1). The Vegagete rhabdodontid and *M. gondwanicus* were corrected and coded (2).

216(*). Caudal ribs, longest rib position: the first caudal vertebra bears longest rib (0), longest rib posterior to the first (1) (Brown et al. 2013 #87).

The caudal transverse processes are told to be narrow in *Tenontosaurus tilletti* (Forster 1990, p. 278) however there is no indication as to wether the first caudal ribs were actually longer or shorter than the succeeding ones. *T. tilletti* was corrected and coded with a question mark.

217(*). Distal caudal chevrons shape: rod-shaped, often with slight distal expansion (0), strongly asymmetrically expanded distally (1) (rephrased from Ösi et al. 2012 #144).

The few preserved chevrons of *Yinlong downsi* are slightly expanded distally, but their distal anteroposterior width do not exceed their height (Han et al. 2018, fig. 4G). Chevrons aren't asymmetrically expanded in *Anabisetia saldiviai* (Cambiaso 2007, p. 227). By contrast, they look strongly asymmetrically developped distally in *Convolosaurus marri* (Andrzejewski et al. 2019, fig. 17A, B). Distal caudal chevrons of *Camptosaurus dispar* are keeled and bear

distally expanding "knife-like ends", but not its anterior caudals (Gilmore 1909, fig. 19, 20, p. 245). In *Eousdryosaurus nanohallucis*, only the proximal caudal chevrons are preserved and are unexpanded distally (Escaso et al. 2014, fig. 2). In *Valdosaurus canaliculatus*, the mid-caudal chevrons from the twelth bacward are well expanded and triangular-shaped (Barrett 2016, fig. 4A). Any putative variation of their distal symmetry in more distal caudals is unknown. *Y. downsi*, *A. saldiviai* were corrected and coded (0). *C. marri* was corrected and coded (1). *C. dispar* was corrected and coded as polymorphic (0, 1).

218(*). Ossified epaxial/hypaxial tendons along caudal vertebrae: absent (0), present (1) (modified from Ösi et al. 2012 #216 and #217; Brown et al. 2013 #86).

We modified the definition of this character to code for the presence or absence of ossified epaxial/hypaxial tendons along the tail only. Note that epaxial and hypaxial tendons are usually found at the same time along the tail. The outgroup taxon *Herrerasaurus ischigualastensis* (Novas 1994), and the neornithischian *Yueosaurus tiantaiensis* (Zheng et al. 2012) purportedly lack ossified tendons along their whole vertebral column. Many basal neornithischians have ossified tendons along their back and lack them along their tail. This is the case of *Agilisaurus louderbacki* (Peng 1992, p. 8), *Hexinlusaurus multidens* (He and Cai 1984, p. 25), *Orodromeus makelai* (Scheetz 1999, p. 47), *Jeholosaurus shangyuanensis* (Han et al. 2012, p. 1380), *Haya griva* (Makovicky et al. 2011, p. 633), *Stenopelix valdensis* (Butler and Sullivan 2009, p. 31) and the basal ceratopsian *Yinlong downsi* (Han et al. 2018, p. 9). We remark that no ossified tendons were reported along the caudal series of *Stegosaurus stenops* (Maidment et al. 2015), *Camptosaurus dispar* or *Camptosaurus aphanoecetes* (Gilmore 1909; Carpenter and Wilson 2008). Within Heterodontosauridae, *Heterodontosaurus tucki* lacks ossified tendons along its tail, but not *Tianyulong confuciusi* (Galton 2014, p. 135; Zheng et al. 2009, fig. 1A). *Nanosaurus agilis* (Galton and Jensen 1973, pl. 2) was drawn some ossified tendons along its back, but the presence of tendons along its tail isn't documented. Very little

material is known of the tail of *Talenkauen santacrucensis* (Cambiaso 2007, fig. 24). The presence of ossified tendons along the tail of *Dryosaurus altus* (Galton 1981) and *Camptosaurus dispar* (Gilmore 1909, p. 246), *Changchunsaurus parvus* (Butler et al. 2011) and *Archaeoceratops oshimai* (Dong and Azuma 1997; You and Dodson 2003) is not determined. The presence of tendons is not known for *Scelidosaurus harrisonii* (Owen 1861; Newman 1968) and *Isaberrysaura mollensis* (Salgado et al. 2017). *Eocursor parvus* (Butler 2010), *Scutellosaurus lawleri* (Colbert 1981), *Zalmoxes robustus* (Weishampel et al. 2003) and *Rhabdodon* sp. from Vitrolles (Pincemaille-Quilleveré 2002) were reported to bear ossified tendons, but their exact location is unknown. *A. louderbacki*, *O. makelai*, *J. shangyuanensis*, *H. griva*, *H. tucki*, *Z. robustus*, *R.* sp1 (Vitrolles), *S. valdensis* and *Y. downsi*, *C. dispar* were corrected and coded (0). *E. parvus*, *I. mollensis*, *S. lawleri*, *S. harrisonii*, *N. agilis*, *C. parvus*, *T. santacrucensis*, *Dryosaurus*, *C. dispar*, *A. oshimai*, were corrected and coded with a question mark. Any taxa lacking tendons along their tail should be corrected and coded as non-applicable for the following character dealing with the arrangement of the epaxial tendons along the tail.

Appendicular skeleton:

221(*). Scapula-Humerus, proportions: scapula longer or subequal to the humerus (0), humerus substantially longer than the scapula (1) (Ösi et al. 2012 #149).

The scapula of *Yueosaurus tiantaiensis* (Zheng et al. 2012, fig. 2), *Stegoceras validum* (Gilmore 1924, pl. 9-1, 2), *Yinlong downsi* (Han et al. 2018, p. 10) is substantialy longer than its humerus, contrary to *Agilisaurus louderbacki* (Peng 1992, fig. 3, 4) and *Hexinlunsaurus multidens* (He and Cai 1984, fig. 15). Any estimation of the relation of scapula to humerus length in *Jeholosaurus shangyuanensis* is not allowed, as the scapula of this taxon is incomplete distally and both bones are of comparable length (Han et al. 2012, fig. 2, 8). In

Talenkauen santacrucencis (Rozadilla et al. 2019, fig. 18, 20), *Jeholosaurus shangyuanensis* (Han et al. 2012, IVPP V15719, fig. 2A, 8), *Agilisaurus louderbacki* (Peng 1992, fig. 3, 4), *Hexinlusaurus multidens* (He and Cai 1984, fig. 15B, D), *Kulindadromeus zabaikalicus* (Godefroit et al. 2014, fig. S6A) the humerus is markedly longer than the scapula. However, we note that this is not the case for a close relative to *J. shangyuanensis*: *Haya griva* (Makovicky et al. 2011, fig. 4A). *T. santacrucensis* and *J. shangyuanensis* were corrected and coded (1). *Y. tiantaiensis*, *Y. downsi*, were corrected and coded (0). *J. shangyuanensis* was corrected and coded with a question mark.

222(*). Scapula, blade-shape: strongly expanded distally (0), weakly expanded, near parallel-sided (1) (Ösi et al. 2012 #152).

The distal scapular blades of *Heterodontosaurus tucki* (Galton 2014, fig. 2A-B), *Abrictosaurus consors* (Sereno 2012, p. 78), *Tianyulong confuciusi* (Zheng et al. 2009, supp. info. p.5, Sereno 2012, p. 65), *Psittacosaurus mongoliensis* (Senter 2007, fig. 3J), *Stegoceras validum* (Gilmore 1924, pl. 9.1), *Kulindadromeus zabaikalicus* (Godefroit et al. 2014, fig. S6A) are very weakly expanded distally. *Yinlong downsi* appears polymorphic for this character as two similarly-sized scapulae are either expanded or unexpanded distally (IVPP V18678 and IVPP V18684, Han et al. 2018, fig. 5B-C). Bell et al. (2019 #188) modified the character coding of *Muttaburrasaurus langdoni* from (0) to (1). However, Bartholomai and Molnar (1981, p. 330, fig. 5A) state that the scapulae of *M. langdoni* are distally expanded, which is also confirmed from the figures. *H. tucki*, *A. consors*, *T. confuciusi*, *P. mongoliensis*, *S. validum*, *K. zabaikalicus*, were corrected and coded (1). *Y. downsi* was corrected and coded as polymorphic (0, 1) for this character.

223(*). Scapula, scapular blade length relative to minimum width: relatively short and broad, length is 5-8 times minimum width (0), elongate and strap-like, length is at least 9 times the minimum width (1) (Ösi et al. 2012 #150).

The scapula of *Yinlong downsi* (Han et al. 2017, fig. 5B, C) is almost 9 times as long as its minimum width. The scapular length is unknown in *Muttaburrasaurus langdoni* (Bartholomai and Molnar, 1981, fig. 5A; Bell et al. 2019 #189). *Y. downsi* was corrected and coded (1). *M. langdoni* was corrected and coded with a question mark.

224(*). Scapula, acromion shape: weakly developped or absent (0), well-expanded anteriorly, spine-like (1) (reformulated from Ösi et al. 2012 #151).

In *Lesothosaurus diagnosticus* (Barrett et al. 2016, fig. 5A), *Scutellosaurus lawleri* (Rosembaum and Padian, 2001, fig. 4A), *Stegosaurus stenops* (Maidment et al. 2015, fig. 66), *Hexinlusaurus multidens* (He and Cai 1984, fig. 15A, B1), *Chaoyangsaurus youngi* (Zhao et al. 1999, fig. 6A, B) the acromion process is undevelopped. A totally absent acromion appears to be apomorphic for the rhabdodontids (*Z. robustus* and *Z. shqiperorum*, cf. Weishampel et al. 2003; *Mochlodon vorosi*, cf. Ösi et al. 2012, fig. 6D). Within early ceratopsians the relative development of the acromial process appears to be polymorphic. In *Yinlong downsi*, for example, the acromion process appears well developped in IVPP V18678 and IVPP V18684, but not in IVPP V14530 (Han et al. 2018, fig. 5A-C). *Psittacosaurus mongoliensis* (Senter 2007, fig. 3J) doesn't bear any spike-like acromial process, but *Psittacosaurus neimongoliensis* does (Senter 2007, fig. 3A). The acromial process of *Tenontosaurus dossi* is very weakly developped (Winkler et al. 1997, fig. 16A), so we do not follow the correction brought by Andrzejewski et al. (2019 #151). The acromial process is slightly more developped in *Convolosaurus marri* (Andrzejewski et al. 2019, fig. 18A, B). In *Muttaburrasaurus langdoni*, Bell et al. (2019 #190) regarded the presence of a developped acromial process as impossible to determine probably because of its incompleteness, but it appears well developped as figured by Bartholomai and Molnar (1981, fig. 5). *Jeholosaurus shangyuanensis* (Han et al. 2012, fig. 2A), *Haya griva* (Makovicky et al. 2011, fig. 3A), *Camptosaurus dispar* (Gilmore 1909, fig. 23) and *Rhabdodon* sp. from Vitrolles (Pincemaille-

Quillevere, 2002, fig. 13) bear a well developped acromial process. This character varies through the ontogeny of *Hypsilophodon foxii* (Galton 1974), with the development of a more acute acromial process in adults individuals. We could not assess the presence of a well developped acromial process for *Scelidosaurus harrisonii* from the available literature. The acromion process of *Changchunsaurus parvus* (Butler et al. 2011) and *Yueosaurus tiantaiensis* (Zheng et al. 2012) is reported as broken. *L. diagnosticus*, *S. lawleri*, Stegosauria, *H. multidens*, *Y. hongheensis*, *C. youngi* and *M. vorosi*, *C. marri* were corrected and coded (0). *Y. downsi* and Psittacosauridae were newly coded as polymorphic [0 1]. *S. harrisonii, C. parvus* and *Y. tiantaiensis* were corrected and coded with a question mark. *J. shangyuanensis*, *C. dispar*, *Rhabdodon* sp. from Vitrolles ("sp1"), *M. langdoni* were corrected and coded (1).

225(*). Scapula, acromion process proximal extent: low, almost reaches the coracoid anterodorsally (0), high, elevated with respect to the coracoid (1) (new character).

N.B.: In the basal ceratopsians *Psittacosaurus mongoliensis*, *Psittacosaurus neimongoliensis* and *Yinlong downsi* (Senter 2007; Han et al. 2018), the anterodorsal tip of the acromial process is distally placed and widely separated from the coracoid.

226(*). Scapula, angle formed by the medial borders of the 'supra-glenoid' process: acute, less than 75° (0), more than 75° (1) (modified and derived from Xu et al. 2006 #20; Dieudonné et al. 2016a #191).

This character was reformulated to specify that the medial borders of the supra-glenoid process are to be considered, and not the lateral ones which shape the lateral edge of the glenoid fossa. The supra-glenoid borders of scapula are rather acute in *Talenkauen santacrucensis* (Cambiaso 2007, fig. 26) and *Thescelosaurus neglectus* (Gilmore 1915, fig. 10). They are rather obtuse in *Yinlong downsi* (Han et al. 2018, fig. 5B), *Yueosaurus tiantaiensis* (Zheng et al. 2012, fig. 4A-E), *Scutellosaurus lawleri* (Rosembaum and Padian 2000, fig. 4A), Psittacosauridae (Senter 2007, fig. 3), *Orodromeus makelai* (Scheetz 1999, fig.

19B), *Koreanosaurus boseongensis* (Huh et al. 2010, fig. 9B, C), *Hypsilophodon foxii* (Galton 1974*a*, e.g fig. 35A, B), *Hexinlusaurus multidens* (He and Cai 1984, fig. 15A, B), *Dryosaurus altus* (Galton 1981, fig. 6A) and *Dysalotosaurus lettowvorbecki* (Janensch 1955, fig. 31), *Anabisetia saldiviai* (Cambiaso 2007, fig. 108), *Agilisaurus louderbacki* (Peng 1992, fig. 3), *Herrerasaurus ischigualastensis* (Sereno 1993, fig. 2A). In *Fostoria dhimbangunmal*, the angle formed by the medial borders of the supraglenoid process fall just at or slightly above 75° in smaller individuals and much over 75° in larger ones (Bell et al. 2019, fig. 5). With the new formulation of this character that considers a character state boundary of 75°, *T. santacrucensis* and *T. neglectus* were corrected and coded (0). *Y. downsi*, *Y. tiantaiensis*, *S. lawleri*, *P. mongoliensis*, *O. makelai*, *K. boseongensis*, *H. foxii*, *H. multidens*, *D. altus*, *D. lettowvorbecki*, *F. dhimbangunmal*, A. *saldiviai*, *A. louderbacki*, *H. ischigualastensis* were corrected and coded (1).

227(*). Scapula, posterior edge of the supra-glenoid process: smoothly deflects posteroventrally with respect to the ventral edge of the scapular shaft (0), sharply deflects posteroventrally with respect to the ventral edge of the scapular shaft (1) (new character, derived from Dieudonné et al. 2016a #191).

Amongst rhabdodontomorphs, *Z. shqiperorum* is an exception in that it has a proximo-posterior edge of scapula almost completely shifted to the horizontal posteriorly (cf. Weishampel et al. 2003, fig. 28).

228(*). Coracoid, height divided by length (considering an horizontal inclination of the scapulocoracoid, and by omitting the “extra-height” entailed by the sternal process with respect to the infraglenoid corner): between 70% and 120% (0) equal or greater than 120% (1) (modified from Brown et al. 2013 #90).

The coracoid height largely exceeds its length in *Haya griva* (Makovicky et al. 2011, fig. 4A), *Yandusaurus hongheensis* (He and Cai 1984, fig. 28B), *Thescelosaurus neglectus* (Gilmore

1915, fig. 10; Galton 1974*b*, fig. 2H), *Hypsilophodon foxii* (Galton 1974*a*, fig. 34A, 35B), *Dysalotosaurus lettowvorbecki* (Janensch 1955, fig. 32), *Dryosaurus altus* (Galton 1981, fig. 6A), *Camptosaurus dispar* (Gilmore 1909, fig. 24), *Zalmoxes robustus* (Weishampel et al. 2003, fig. 19A), *Zalmoxes shqiperorum* (Godefroit et al. 2009, fig. 15D-E), *Anabisetia saldiviai* (Cambiaso 2007, fig. 61A''), *Gasparinisaura cincosaltensis* (Cambiaso 2007, fig. 134A), *Talenkauen santacrucensis* (Cambiaso 2007, fig. 27, 134B). The condition is similar in the Vegagete ornithopod, although the preserved coracoid is broken posterodorsally, and belongs to the smallest individual (Dieudonné et al. 2016a, fig. 6B). In *Muttaburrasaurus langdoni*, Bartholomai and Molnar (1981, fig. 5, p. 330) describe a coracoid which is apparently small, short and deep. This means that the preserved part of the coracoid is very short and dorsoventrally expanded. In *Rhabdodon* sp. from Vitrolles (here termed "sp1") the coracoid height is about 80% of its length (Pincemaille-Quilleveré 2002, fig. 13). In *Tenontosaurus tilletti* (Forster 1990, fig. 8), *Convolosaurus marri* (Andrzejewski et al. 2019, fig. 18D-E), *Orodromeus makelai* (Cambiaso 2007, fig. 134D), *Changchunsaurus parvus* (Butler et al. 2011, fig. 4A), *Koreanosaurus boseongensis* (Huh et al. 2010, fig. 9A), *Tianyulng confuciusi* (Sereno 2012, p. 65), *Iguanodon bernissartensis* (Norman 1980, fig. 53A) the coracoid height makes from 100% to less than 120% of its proper length. In *Agilisaurus louderbacki*, Peng (1992, p. 9, fig. 3) states that the coracoid is nearly square. It probably doesn't appear so because of its medial curvature. We leave this taxon uncoded pending further verification. In *Stegoceras validum* (Gilmore 1924, p. 33, pl. 9.3) the coracoid is told to lack much of its anterior and inferior margins. In *Psittacosaurus mongoliensis* (Senter 2007, fig. 3J) the coracoid is longer than tall. In *Jeholosaurus shangyuanensis* (Han et al. 2012, p. 1380) the coracoid margins are broken so it is not possible to infer its proportions. *Zephyrosaurus schaffi* was previously coded as having a coracoid with rhoughly subequal height and length, but it was never formally described nor figured (Sues 1980). *H. griva, Y.*

hongheensis, *T. neglectus*, *H. foxii*, *D. lettowvorbecki*, *Dryosaurus*, *C. dispar*, *Z. robustus*, *Z. shqiperorum*, *A. saldiviai*, G. *cincosaltensis*, *T. santacrucensis*. *M. langdoni* were corrected and coded (1). *R.* sp1, *C. parvus*, *T. confuciusi,* Psittacosaurs (as *P. mongoliensis*) were corrected and coded (0). *Aurorella* was corrected and coded (0) given the change in character definition. *J. shangyuanensis* and *Z. schaffi* were corrected and coded with a question mark.

229(*). Coracoid, coracoid foramen position from a lateral view: enclosed within coracoid (0), open along coracoid-scapula suture (1) (rephrased from Brown et al. 2013 #91).

The coracoid foramen appears enclosed within the coracoid in *Tianyulong confuciusi* (Zheng et al. 2009, supp. info. p. 5). It is also enclosed laterally within the coracoid in *Talenkauen santacrucensis* (Rozadilla et al. 2019, p. 24), *Anabisetia saldiviai* (Cambiaso 2007, fig. 108A-B). Note that whilst the coracoid foramen appears to open laterally along the coracoid-scapual suture in *Camptosaurus dispar* (Gilmore 1909, fig. 24) it is well offset from that suture lateral view in *Camptosaurus aphanoecetes* (Carpenter and Wilson 2008, fig. 16A). *T. confuciusi*, *T. santacrucensis, A. saldiviai* were corrected and coded (0).

231(*). Sternal plates, shape: absent (0), kidney-shaped or semi-lunate (1), shafted or hatchet-shaped (rod-like posterolateral process, expanded anteromedial end) (2), of right-angle triangle with broad medial contact for collateral sternal (3) (rephrased and modified from Ösi et al. 2012 #148).

The sternal of *Heterodontosaurus tucki* appears to be hatched-shaped in being expanded and bilobate to one side and elongate to the other side, as in *Homalocephale calathocercos* (Maryanska and Osmolska 1974, pl. 30.1). In *H. tucki* the expanded, bilobate side would be posterior (Galton 2014, fig. 5F) and the exact contour of the sternal is unclear anteriorly. *H. tucki* was left uncoded for this character pending further verifications. The sternal plates of *Tenontosaurus tilletti* and *Tenontosaurus dossi* (Winkler et al. 1997, p. 339) as well as those of *Camptosaurus dispar* (Dodson and Madsen 1981, fig. 1B; Carpenter and Galton 2018, fig.

23N) are semi-lunate. A lunate sternal was also reported on "*Tenontosaurus*" by Dodson and Madsen (1981). The sternal plates of *Macrogryphosaurus gondwanicus* (Calvo et al. 2007, fig. 6), *Mahuidacursor lipanglef* (Cruzado-Caballero et al. 2019) have the shape of a right-angle triangle with their posterolateral process supporting a broad posteriorly expanding plate. This posteriorly expanding plate is right angled posteromedially and makes a broad medial contact with the collateral sternal. The sternals of *Iguanodon bernissartensis* are hatched-shaped with a long posterolaterally extending rod-like process, and an anteromedially short semi-lunate process (Norman 1980, fig. 56). *C. dispar* was corrected and coded (1). *M. gondwanicus* was corrected and coded (3).

232(*). Humerus, length relative to femoral length: more than 60% (0), less than 60% (1) (Ösi et al. 2012 #153).

In *Yinlong downsi* (Han et al. 2018, p. 1168) and *Tianyulong confuciusi* (Zheng et al. 2009, supp. info.) the ratio of humerus length to femur length equals or exceeds 60%. In *Stegoceras validum* (Gilmore 1924, pl. 9.2, 11.1) the ratio of humerus length to femur length is as in other pachycephalosaurs well under 60%. *Y. downsi* and *T. confuciusi* were corrected and coded (0).

233(*). Humerus, appearance of the anterior surface in proximal view: a varyingly developed flexor bicipital sulcus is visible (0), the anterior surface is straight to smoothly convex, no bicipital sulcus visible (1) (Dieudonné et al. 2016a #197).

In *Fostoria dhimbangunmal*, only the mid-diaphysis fragment of humerus is preserved (LRF 350.S, Bell et al. 2019, fig. 6D-F). It is therefore impossible to infer the presence or absence of a bicipital sulcus on its proximal extremity. *F. dhimbangunmal* was corrected and coded with a question mark.

235(*). Humerus, proximal head separated from prominent medial tubercle on proximal surface by a shallow median groove: absent (0), present (1) (modified from Ösi et al. 2012 #223).

It is highly improbable that the groove which separates the medial proximal tubercle from the humeral head is homologous between heterodontosaurids (e.g. *F. haagarorum* and *H. tucki*, Galton 2014, fig. 9N-R and 9H-M respectively) and *Herrerasaurus ischigualastensis* (Sereno 1993, fig. 3). Actually, in *F. haagarorum* and *H. tucki*, the proximal humeral groove is almost unconspicuous from an antero-posterior view (Galton 2014, fig. 9O, L) and is located right on the middle of the humeral shaft (Galton 2014, fig. 9R, I), whereas in *H. ischigualastensis* that groove is deep and offset to the medialmost part of the humeral shaft (Sereno 1993, fig. 3). Therefore, any similar coding between heterodontosaurids and *H. ischigualastensis* for this character might be inadequate. For this reason this character was modified to more precisely deal with the presence or absence of a weak anteroposteriorly extending median groove between the medial tubercle and the humeral head. *H. ischigualastensis* was corrected and coded (0) for this character.

236(*). Humerus, deltopectoral crest: well developped, projecting at a distinct angle from the shaft (0), low and rounded (1), almost imperceptible (2) (modified from Xu et al. 2006 #42; Ösi et al. 2012 #154).

The deltopectoral crest of *Yinlong downsi* is well pronounced (Han et al. 2018, fig. 6A, C). In *Muttaburrasaurus langdoni* is it described as a weak, distally rounded thickenning (Bartholomai and Molnar, 1981, p. 331). The same condition also occurs in *Fostoria dhimbangunmal* (Bell et al. 2019, fig. 6D-F), *Dryosaurus altus* (Galton 1981, fig. 7E-F), *Dysalotosaurus lettowvorbecki* (Galton 1981, fig. 8A, C, G, J), *Thescelosaurus neglectus* (Galton 1974*b*, fig. 2A). The deltopectoral crest is imperceptible in *Anabisetia saldiviai* (Cambiaso 2007, fig. 30), *Talenkauen santacrucensis* (Cambiaso 2007, fig. 28), *Notohyspilophodon comodorensis* (Ibiricu et al. 2014, fig. 7A). The nature of the deltopectoral crest distal merging is neither decribed nor figured for *Yandusaurus hongheensis* (He and Cai 1984, fig. 28C, p. 55). *A. saldiviai*, *T. santacrucensis* were corrected and newly

coded (2). *M. langdoni*, *F. dhimbangunmal, Dryosaurus*, *D. lett*owvorbecki and *T. neglectus* were corrected and coded (1). *Y. downsi* was corrected and coded (0). *Y. hongheensis* was corrected and coded with a question mark.

237(*). Humerus, deltopectoral crest shape: distal margin rounded and merges gradually with the lateral margin of the humeral shaft (0), distal margin angular and merges abruptly with the lateral margin of the humeral shaft (1) (modified from Weishampel et al. 1993 #37; McDonald et al., 2010 #103).

The deltopectoral crest is unpreserved in the Vegagete ornithopod (Dieudonné et al. 2016). The distal merging of the deltopectoral crest cannot be deduced from the available information in *Agilisaurus louderbacki* (Peng 1992, p. 8). The deltopectoral crest merges abruptly with the lateral margin of the humeral shaft in *Hexinlusaurus multidens* (He and Cai 1984, fig. 15D3), *Yinlong downsi* (Han et al. 2018, fig. 6A, C), *Hypsilophodon foxii* (Galton 1974*a*, fig. 38A, C), *Camptosaurus dispar* (Carpenter and Wilson 2008, fig. 20G). Note that such a feature appears to vary within camptosaurids as *C. aphanoecetes* features a very low deltopectoral crest (Carpenter and Wilson, fig. 19C). The Vegagete ornithopod and *A. louderbacki* were corrected and coded with a question mark. *H. multidens*, *Y. downsi, H. foxii* and *C. dispar* and were corrected and coded (1).

238(*). Humerus, proximolateral margin with respect to the main axis of the shaft in anteroposterior view: straight, aligned with the distolateral margin (0), medially bowed (1) (modified from Ösi et al. 2012 #155).

The proximal humeral shaft is medially bowed in *Yinlong downsi* (Han et al. 2018, fig. 6A, C), *Goyocephale lattimorei* (Perle et al. 1982, pl. 43.4A, C), *Wannanosaurus yansiensis* (Butler and Zhao 2009, fig. 8C, D), *Psittacosaurus mongoliensis* (Senter 2007, fig. 3K, M), *Zalmoxes robustus* (Weishampel et al. 2003, fig. 20A) and *Zalmoxes shqiperorum* (Godefroit et al. 2009, fig. 16), *Convolosaurus marri* (Andrzejewski et al. 2019, fig. 18F), *Fostoria*

dhimbangunmal (Bell et al. 2019, fig. 6D, F), and *Muttaburrasaurus langdoni* (Bartholomai and Molnar, 1981, fig. 6A, C; contra Bell et al. 2019 #202). In *Camptosaurus dispar*, the degree of proximomedial bending of the humeral shaft appears to vary depending on the individuals (cf. Carpenter and Wilson 2008, fig. 20C, E, F). In *Lesothosaurus diagnosticus* (Thulborn 1972, fig. 7A, B), *Orodromeus makelai* (Scheetz 1999, fig. 21A), *Gasparinisaura cincosaltensis* (Coria and Salgado 1996, fig. 6A), *Hypsilophodon foxii* (Galton 1974*a*, fig. 38D, 39D), *Dryosaurus altus* (Galton 1981, fig. 7C, D), *Dysalotosaurus lettowvorbecki* (Galton 1981, fig. 9A), the heterodontosaurids *Heterodontosaurus tucki* (Galton 2014, fig. 9L) and *Abrictosaurus consors* (Galton 2014, fig. 9O, Q), the ankylosaur *Crichtonsaurus benxiensis* (Junchang et al. 2007, pl. 3.G, H) and *Stegosaurus stenops* (Maidment et al. 2015, fig. 67A, B), the proximolateral border of the humeral shaft does not bend with respect to the distolateral one but rather follows the same straight line. Whether the proximal humerus of *Herrerasaurus ischigualastensis* was medially bent or not cannot be safely inferred from the preserved humeral fragment (Sereno 1993, fig. 3A, B). The proximal humeral extremity of *Yueosaurus tiantaiensis* is missing (Zheng et al. 2012). The humerus of *Scelidosaurus harrisonii* (Owen 1863, pl. 3), *Tianyulong confuciusi* (Zheng et al. 2009, supp. info. p. 5; Sereno 2012) and *Haya griva* (Makovicky et al. 2011, fig. 4A) are not available from an anteroposterior view and weren't described for this feature. In *Thescelosaurus neglectus*, the humerus is only available from sketches, and both a straight and curved proximolateral humeral surfaces were figured (Galton 1974*b*, fig. 2B, D, I). Because of the new character definition, all taxa previously coded (0) were corrected and coded (1), except for Ankylosauria, *Stegosaurus stenops*, *L. diagnosticus*, *O. makelai, G. cincosaltensis, H. foxii*, *Dryosaurus*, *D. lettowvorbecki*, *H. tucki*, *A. consors* which were left coded (0). *O. makelai* was corrected and coded (0). *Y. downsi*, *C. marri, F. dhimbangunmal* and *M. langdoni* were corrected and coded (1). *C. dispar* was corrected and coded as polymorphic with character

states [0, 1]. *H. ischigualastensis*, *S. harrisonii, T. confuciusi, H. griva, Y. tiantaiensis* and *T. neglectus* were corrected and coded with a question mark.

239(*). Humerus, proximal shaft curvature from a lateral view: proximal portion is aligned with distal portion of the shaft (0), proximal portion of the humeral shaft is bent backward relative to the distal portion (1) (new character).

Galton and Jensen (1973, p. 150) noticed that this character was subject to changes throughout ontogeny in some taxa, with the posterior flexure of the proximal humeral shaft occurring in older individuals. Heterodontosaurids (*Tianyulong confuciusi*, Zheng et al. 2009, fig. 1A; *Heterodontosaurus tucki* and *Fruitadens haagarorum*, Galton 2014, fig. 9K, N respectively), pachycephalosaurs (*Wannanosaurus yansiensis,* Butler and Zhao, fig. 8C; *Stegoceras validum*, Sues and Galton 1987, p. 21; *Goyocephale lattimorei*, Perle et al. 1982, pl. 43.4B), basal ceratopsians (*Yinlong downsi*, Han et al. 2017, fig. 6C; *Psittacosaurus mongoliensis*, Osborn 1924, fig. 5). *Psittacosaurus sibiricus*, Averianov et al. 2006, fig. 18B, D), the Asian ornithopods *Changchunsaurus parvus* (Butler et al. fig. 11, fig. 4E), *Haya griva* (Makovicky et al. 2011, fig. 4), and the basal ornithischian *Lesothosaurus diagnosticus* (Thulborn 1972, fig. 7C) all show a posteriorly shifted proximal extremity of humerus. The humerus shaft is also posteriorly shifted proximally in ornithopods such as *Orodromeus makelai* (Scheetz 1999, fig. 21B), *Hypsilophodon foxii* (Galton 1974*a*, fig. 38A, C), and dryosaurids (*Dryosaurus altus*, Galton 1981, fig. 6D and 7E, F; *Dysalotosaurus lettowvorbecki*, Galton 1981, fig. 8A, C, G), and also but more weakly so in *Othnielosaurus rex* (Galton and Jensen 1973, fig. 3B, Carpenter and Galton 2018, fig. 14C), *Camptosaurus dispar* (Carpenter and Galton 2018, fig. 23R), *Talenkauen santacrucensis* (Cambiaso 2007, fig. 28B), *Tenontosaurus tilletti* (Forster 1990, fig. 10D), *Thescelosaurus neglectus* (Galton 1974*b*, fig. 2A, C), *Muttaburrasaurus langdoni* (Bartholomai and Molnar, 1981, fig. 6D), and *Zalmoxes robustus* (Weishampel et al. 2003, fig. 20B). Without consideration of the

posteriorly projecting humeral head, the humeri of a few ornithopods such as *Notohypsilophodon comodorensis* (Cambiaso 2007, fig. 84B), *Anabisetia saldiviai* (Cambiaso 2007, fig. 109B), *Gasparinisaura cincosaltensis* (Cambiaso 2007, fig. 62B), *Convolosaurus marri* (Andrzejewski et al. 2019, fig. 18G), *Mahuidacursor lipanglef* (Cruzado-Caballero et al. 2019), *Mochlodon vorosi* (Ösi et al. 2012, fig. 6I) is straight from a mediolateral view. The humerus of *Stegosaurus stenops* (Maidment et al. 2015, fig. 67C, D) and *Chuanqilong chaoyangensis* (Han et al. 2014, fig. 5C) appears also straight from a mediolateral view. The basal ankylopollexian *Camptosaurus dispar* (Carpenter and Wilson 2008, fig. 20G) shows a straight humeral shaft from a lateral view, this should be a reversal within Dryomorpha.

240(*). Humerus, anterior coronoid fossa from a distal view: more deeply incised (0), widely open and shallow (1) (new character).

We note that the deepening of the coronoid fossa might be under ontogenetic control in some taxa, and increase markedly for larger individuals (e.g. *Hypsilophodon foxii*, Galton 1974*a*, fig. 38F, 39F). The coronoid fossa is deeply incised – i.e. with both radial and ulnar condyle delimiting its anteromedial and anterolateral edges – in *Fruitadens haagarorum* and *Heterodontosaurus tucki* (Galton 2014, fig. 9S, J respectively), *Thescelosaurus neglectus* (Galton 1974*b*, fig. 2F), *Hypsilophodon foxii* (Galton 1974a, fig. 38F), *Convolosaurus marri* (Andrzejewski et al. 2019, p. 25), *Tenontosaurus tilletti* (Forster 1990, fig. 10A), *Talenkauen santacrucensis* (Rozadilla et al. 2019, fig. 20F), *Dysalotosaurus lettowvorbecki* (Galton 1981, fig. 8F, I). The coronoid fossa is as shallow as the olecranon fossa but also very narrow in *Dryosaurus altus* (Galton 1981, fig. 7B). The distal coronoid fossa is quite wide but also deep in *Camptosaurus aphanoecetes* (Carpenter and Wilson 2008, fig. 19F). A few gondwanan ornithopods feature a widely open and shallow coronoid fossa, such as *Gasparinisaura cincosaltensis* (Cambiaso 2007, fig. 63F), *Notohypsilophodon comodorensis* (Cambiaso 2007,

fig. 84E), *Anabisetia saldiviai* (Cambiaso 2007, fig. 109E), *Mahuidacursor lipanglef* (Cruzado-Caballero et al. 2019), and the Vegagete rhabdodontid (pers. obs.).

241(*). Humerus, posterior olecranon fossa from a distal view: present (0), forms only a weak depression or is totally absent (1) (new character).

We noticed that *Fruitadens haagarorum* and *Heterodontosaurus tucki* (Galton 2014, fig. 9S, J respectively) both lack a posterior olecranon fossa. It is particularly striking that such olecranon fossa was also reported to be weak or absent in *Stegoceras validum* (Gilmore 1924, pl. 9.2, p. 34) and *Goyocephale lattimorei* (Perle et al. 1982, pl. 43.4A). In *Wannanosaurus yansiensis*, both the olecranon and coronoid fossae are told to be shallow, although as figured from a posterior view the olecranon fossa looks only weakly depressed (Butler and Zhao 2009, fig. 8D), which is in marked contrast with all other taxa that have a pronounced olecranon fossa.

242(*). Ulna, olecranon process: low (0), moderately developed (1), high (2) (Butler et al. 2011; Brown et al. 2013 #93).

The proximal olecranon process of ulna is told to be a slightly inflated in *Agilisaurus louderbacki* (Peng 1992, p. 9, fig. 4). In *Psittacosaurus mongoliensis* (Senter 2007, fig. 5F), *Gasparinisaura cincosaltensis* (Salgado et al. 1997, fig. 6) the olecranon process is rather poorly developped. By contrast, it is well developped in *Yinlong downsi* (Han et al. 2018, fig. 7A). In *Muttaburrasaurus langdoni*, Bartholomai and Molnar (1981, p. 331) report that the proximal olecranal process is partly broken but was “probably not extensive”. In *Scelidosaurus harrisonii* (Owen 1863, pl. 3), *Orodromeus makelai* (Scheetz 1999, fig. 22B), *Anabisetia saldiviai* (Cambiaso 2007, fig. 110D), *Stegoceras validum* (Gilmore 1924, pl. 9.4), *Tianyulong confuciusi* (Sereno 2012, P. 55) the olecranon process of the ulna appears well developped. Parks (1926, p. 24) describes a proximal olecranon process that is much expanded for *Parksosaurus warreni*. In *Koreanosaurus boseongensis* (Huh et al. 2010, fig.

13) the ulnar olecranon process is well developped, although the anterior crest sweeps upward anteriorly which gives the wrong impression that the olecranon process is somewhat lower. *A. louderbacki*, *P. mongoliensis*, *G. cincosaltensis* and *M. langdoni* (in agreement with Bell et al. 2019) were corrected and coded (0). *S. harrisonii*, *Y. downsi*, *T. confuciusi*, *O. makelai*, *K. boseongensis, P. warreni, A. saldiviai* were corrected and coded (2).

244 (*). Radius, distal end: subspherical to ovate (0), anteroposteriorly expanded, with its medial surface sub-parallel to closely juxtaposed to the ulna (1), mediolaterally more expanded than the ulna, the radius expands distally at right angle from the ulna and does not cross over it (2) (new character).

Plesiomorphically, the distal extremity of the radius appears subspherical to ovale. It is the case for *Herrerasaurus ischigualastensis* (Sereno 1993, p. 432), *Lesothosaurus diagnosticus* (Thulborn 1972, fig. 7K). The distal end of radius is also ovoid to elliptical in *Hexinlusaurus multidens* (He and Cai 1984, p. 30), *Yinlong downsi* (Han et al. 2018, fig. 7G), *Hypsilophodon foxii* (Galton 1974*a*, fig. 40F), *Orodromeus makelai* (Scheetz 1999, fig. 22H), *Thescelosaurus neglectus* (Galton 1974*b*, fig. 2N). In *Parksosaurus warreni*, the radius is told to be slender, rod-like, and little expanded at either ends (Parks 1926, p. 25), so *P. warreni* is considered to bear a distally ovoid radius. In *Dysalotosaurus lettowvorbecki* (Galton 1981, fig. 8M) the distal end of the radius is subspherical and, despite of being flat for its distal contact with the ulna, it remains unexpanded along the direction of that contact. In *Dryosaurus altus* the global condition is the same, though there is only a very small expansion on one side (Galton 1981, fig. 7Q). The radius of *Camptosaurus dispar* (Gilmore 1909, p. 251) is described as very slightly expanded distally and rhoughly subcrescentic in outline from a distal view. In *Tenontosaurus tilletti* (Forster 1990, fig. 12A), the distal end of radius appears clearly anteroposteriorly enlarged, and mediolaterally narrower. The radius of *T. dossi* is described as being identical to that of its congeneric *T. tilletti* (Winkler et al. 1997, p. 339). In *Anabisetia*

saldiviai (Cambiaso 2007, fig. 110F) and *Talenkauen santacrucensis* (Cambiaso 2007, fig. 30E), the distal end of the radius is tear-drop-shaped, and bears a concave lateral surface for a contact with the ulna. In *Zalmoxes robustus*, the distal end of the radius has a slightly but distinctly enlarged distal extremity, which bears a "shallow flattened area" for contact with the ulna (Weishampel et al. 2003, fig. 21A, B). In other rhabdodontids the distalmost extremity of the radius is incomplete (i.e. *Rhabdodon* sp. from Vitrolles, Pincemaille-Quilleveré 2002, fig. 14; *Mochlodon suessi*, Sachs and Hornung 2005, fig. 4), but the shaft morphology indicates that the distal extremity was craniocaudally expanded and mediolaterally narrow. Sachs and Hornung (2005) further mention that the flattened side of the radius would have contacted the ulna distally. Following De Lapparent (1947, cited in Sachs and Hornung 2005, p. 422), the radius of *Rhabdodon priscus* would be also much similar. In *Muttaburrasaurus langdoni*, Bartholomai and Molnar (1981, fig. 7 and p. 331) describe a radius which long axis is directed anteroposteriorly, and which proximal extremity was more circular than the distal extremity. In *Fostoria dhimbangunmal,* the distal end of the radius is mediolaterally compressed and slightly expanded anteroposteriorly (Bell et al. 2019, p. 7). The tyreophoran *Stegosaurus stenops* markedly differs from the afor-mentionned cases, as it possesses a distally wide and craniocaudally flatenned radius (Maidment et al. 2015, fig. 69F). In some taxa, the radius could not be seen in distal view. Notwithstanding, it appears clearly that the radius was mediolaterally wider than the ulna from an anteroposterior view. The radius of heterodontosaurids: *Heterodontosaurus tucki* (Galton 2014, fig. 11A), *Tianyulong confuciusi* (Sereno 2012, fig. 27), and that of the pachycephalosaur *Stegoceras validum* (Gilmore 1924, fig. 11C, D) appear to be laterally expanded with respect to the ulna, with little to no contact with the latter bone. Note that in *Abrictosaurus consors* the ulna and radius are mutually as expanded from a dorsal view, the slenderness of the latter could not be asserted, and the absence of mutual contact between both distally could not be totally ensured

(Sereno 2012, fig. 36). Similarly to heterodontosaurids, the radius of *Agilisaurus louderbacki* (Peng 1992, p. 9) is described as being "broad and flat". It looks more mediolaterally expanded than the ulna from an anterior view (Peng 1992, fig. 4). Owing to either approximativeness of the descriptions, figures, or to preservation drawbacks, no coding could be provided for the radii of *A. consor*s (Sereno 2012, fig. 36), *Haya griva* (Makovicky et al. 2011, p. 634), *Iguanodon bernissartensis* (Norman 1980, fig. 58), *Gasparinisaura cincosaltensis* (Salgado et al. 1997; Cambiaso 2007).

245(*). Carpus, fusion: unfused (0), fused (1) (Brown et al. 2013 #97).

Note that in *Camptosaurus aphanoecetes*, the first metacarpal is fused to the radiale although a trace of suture is still visible, and the reste of carpals elements are not fused with each other (Carpenter and Wilson 2008, fig. 23A). This contrasts with the manus of *Camptosaurus dispar* in which all carpal elements are in a much more advanced state of fusion (Carpenter and Wilson 2008, fig. 23B). The carpal bones appear unfused in *Psittacosaurus mongoliensis* (Senter 2007, fig. 5E-F). *P. mongoliensis* was newly coded (0) for this character.

246(*). Ulnare, cushion-like and proximodistally compressed in dorsoventral view: absent (0), present (1) (new character).

In *Dryosaurus altus* (Galton 1981, fig. 6J, K), *Tenontosaurus tilletti* (Forster 1990, fig. 13B) the ulnare is as anteroposteriorly expanded as the intermedium. In *Iguanodon bernissartensis* (Norman 1980, fig. 60A), *Camptosaurus aphanoecetes* and *Camptosaurus dispar* (Carpenter and Wilson 2008, fig. 22A, 23A-B) the intermedium is anteroposteriorly shorter and cushion-shaped. Bartholomaoi and Molnar (1981, p. 332) further reports a "cuchion-shaped" ulnare for *Muttaburrasaurus langdoni*.

247(*). Ulnare: articulates distally *via* the distal carpal 4: with the third metacarpal (0), mostly with the fourth metacarpal (1) (new character).

In *Orodromeus makelai* (Scheetz 1999, fig. 23), *Thescelosaurus neglectus* (Gilmore 1915, fig. 11), *Psittacosaurus mongoliensis* (Senter 2007, fig. 5F), *Tenontosaurus tilletti* (Forster 1990, p. 284; Tennant 2013, fig. 23), *Camptosaurus dispar* (Carpenter and Wilson 2008, fig. 23B), *Iguanodon bernissartensis* (Norman 1980, fig. 60A), *Dryosaurus altus* (Galton 1981, fig. 6I) the ulnare covers mostly the fourth metacarpal but hardly any part of the third metacarpal. This is not the case for *Camptosaurus aphanoecetes* (Carpenter and Wilson 2008, fig. 23A), *Convolosaurus marri* (Andrzejewski et al. 2019, fig. 20), *Heterodontosaurus tucki* (Sereno 2012, fig. 67C; Galton 2014, fig. 11A), *Abrictosaurus consors* (Sereno 2012, fig. 36). Cambiaso (2007, fig. 65) figured a left hand of *Gasparinisaura cincosaltensis*, with the carpals consisting only of the ulnare and radiale. However, we suggest from the figure that the "ulnare" element would in fact be composed of three elements: the intermedium medially, the true ulnare laterally, and an additional distal carpal more distally. The actual outline of each of those elements is doubtful unless more precise first-hand observation is done, although it appears that the ulnare would have covered only the proximal fourth metacarpal. In *Hypsilophodon foxii*, a seam of carbonaceous material traverses through the ulnare of the preserved left manus (R 196, Galton 1974*a*, p. 80), so although it appears to covers a small part of the proximal metacarpal III, its exact shape and extension should not be inferred unless a closer observation is made first-hand. In *Mahuidacursor lipanglef* the ulnare is not expressedly mentioned, but it might correspond to the rectangular bone beneath the distal extremity of ulna (Cruzado-Caballero et al. 2019, fig. 9D). Because of the overall widespread trait of an ulnare covering the fourth but not the third metacarpal, and because the right hand of *M. lipanglef* is incomplete, we shed doubt on the actual distribution of the metacarpals in this taxon and suggest that the first metacarpal would in fact have been missing, so the most lateral ones be the fourth and the fifth metacarpals, rather than the fourth and the third one. Yet, we keep this taxon uncoded pending further verification.

248(*). Metacarpals, block-like proximal ends: absent (0), present (1) (Ösi et al. 2012 #157).

In *Yinlong downsi*, the metacarpals are proximally wider than dorsoventrally tall (Han et al. 2018, p. 1171). By contrast, the proximal metacarpals of *Tianyulong confuciusi* are block-like (Galton 2014, p. 117). *Y. downsi* was corrected and coded (0). *T. confuciusi* was corrected and coded (1).

250(*). Metacarpal I greater than 50% the length of metacarpal II (0), metacarpal I less than 50% the length of metacarpal II (1) (Boyd 2015 #174).

In *Psittacosaurus mongoliensis* (Senter 2007, fig. 5E, F) and *Yinlong downsi* (Han et al. 2018, fig. 8C), the first metacarpal is greater tan 50% the length of metacarpal II. *P. mongoliensis* was newly coded (0). *Y. downsi* was corrected and coded (0).

251(*). Metacarpal/manual phalanges, extensor pits on the dorsal surface of the distal end: absent or poorly developed (0), deep, well-developed (1) (Ösi et al. 2012 #162).

Han et al. (2018, p. 1171) state that the manual phalanges of *Yinlong downsi* bear a distal sulcus between theirs distomedial and distolateral condyles (presumably, anteriorly located, although this was not clearly explicited). Some extensor ligament pits might be present onto the anterodistal surface of some metacarpals and manual phalanges (Han et al. 2018, fig. 8B, C) though the same authors coded it as absent in this taxon (Han et al. 2018 #291). We await first-hand observation of the hand of *Y. downsi* to confirm its actual presence or absence. Following Galton (2014, p. 117) the non-ungueal phalanges of *Tianyulong confuciusi* bear distal extensor pits as also occurs for other heterodontosaurids. *T. confuciusi* was corrected and coded (1). Bell et al. (2019 #209) corrected and coded *Muttaburrasaurus langdoni* with character state (0), with which we concur in absence of other contradicting information.

254(*). Penultimate phalanx of fingers II and III: shorter than or subequal to first phalanx (0), longer than the first phalanx (1) (modified from Ösi et al. 2012 #159).

In *Herrerasaurus ischigualastensis* (Sereno 1993, fig. 13 and 15), the penultimate phalanx of fingers II and III are not longer but similarly-sized for digit II and shorter for digit III with respect to the first phalanx of each of those two digits respectively. In *Eocursor parvus*, the manus is highly incomplete and the fingers could not be properly diagnosed from a digit or another (Butler 2010, fig. 12). In *Tianyulong confuciusi*, the penultimate phalange of digit III is longer than the first one, and there is only two phalanges on digit II (Sereno 2012, fig. 26). *H. ischigualastensis* was corrected and coded (0). *T. confuciusi* was corrected and coded (1). *E. parvus* was corrected and coded with a question mark.

255(*). Manual digit III, number of phalanges: 4 (0), 3 or fewer (1) (Ösi et al. 2012 #160).

There are four phalanges on digit III in *Tianyulong confuciusi* (Sereno 2012, fig. 27). *Gasparinisaura cincosaltensis* bears only three manual phalanges on its third finger, which argues in favor of this taxon being closer to basal iguanodontians (Cambiaso 2007, fig. 65). *T. confuciusi* was corrected and coded (0). *G. cincosaltensis* was corrected and coded (1).

256(*). Manual unguals, strongly recurved with prominent flexor tubercle: absent (0), present (1) (Ösi et al. 2012 #163).

The manual ungual phalanges are strongly recurved in *Tianyulong confuciusi* (Sereno 2012, fig. 27). *T. confuciusi* was therefore corrected and coded (1).

257(*). Ilium length taken from the tip of the preacetabular process to the tip of the postacetabular process (measured on a straight line with a ruler): shorter than (0), or longer than (1) 90% of the femur length (modified from Xu et al. 2006 #90).

In *Camptosaurus aphanoecetes* the ilium would make-up rhoughly 82% of the total femur length from measures taken on the figures (CM 11337, Carpenter and Wilson 2008, fig. 24A, 30B), but this is contradicted by the reconstruction of the same specimen (Carpenter and Wilson 2008, fig. 4C). In *Nanosaurus agilis* (YPM VP 1882, Carpenter and Galton 2018, fig. 8B), *Camptosaurus dispar* (Gilmore 1909, pl. 19; Carpenter and Galton 2018, fig. 19G),

Iguanodon bernissartensis (IRSNB 1534, Norman 1980, fig. 64, 68), *Jeholosaurus shangyuanensis* (IVPP V15939, Han et al. 2012, fig. 9A, D, fig. 10I-L), *Haya griva* (IGM 100/2015, Makovicky et al. 2011, fig. 3A), *Parksosaurus warreni* (Parks 1926, fig. 9, 12), *Anabisetia saldiviai* (MCF-PVPH-76, Cambiaso 2007, fig. 112, 116A-D'), *Valdosaurus canaliculatus* (Barrett 2016, fig. 8, 9A), *Abrictosaurus consors* (NHMUK RU B54, Galton 2014, fig. 7K, 13I), *Heterodontosaurus tucki* (SAM-PK-K-1332, Galton 2014, fig. 12A), *Homalocephale calathocercos* (SPS 100/51, Maryanska and Osmolska 1974, pl. 29.1, 31.1), *Prenocephale prenes* (MgD-I/104 Maryanska and Osmolska 1974, pl. 25.3a, 31.2), *Psittacosaurus mongoliensis* (Osborn 1924, fig. 4), *Yinlong downsi* (IVPP V18637 Han et al. 2018, fig. 11A, 12E) and *Stenopelix valdensis* (Butler and Sullivan 2009, fig. 1A) the ilium is longer than 90% the total length of the femur. Considering the preacetabular process curvature within the measure of ilium length would make it longer than 100% of the total femur length in *H. tucki*. The ilium was already longer than 100% the total femur length in *A. consors* and *Y. downsi* with the ruler. In *Stegoceras validum* (Gilmore 1924) the measurement table gives a relation superior to 90%, but measures performed directly on the photographs give a result below 90%. *S. validum* was therefore left uncoded. Owen (1863) reports that the femur of *Scelidosaurus harrisonii* is one foot and four inches, which represents 16 inches. The ilium lacks a small portion of its anterior and posterior extremities and its preserved portion makes 18 inches. Therefore, the ratio of iliac to femoral length is higher than 90% in this taxon. The ilium is also much longer than 90% of the femoral length in *S. stenops* (Maidment et al. 2015, fig. 31, 72) and the ankylosaur *Crichtonsaurus benxiensis* (Junchang et al. 2007, pl. 3B-C, pl. 5C-D). In *Lesothosaurus diagnosticus* (Thulborn 1972, cf. estimated lengths taken from the measurement table for the smaller individual), *Agilisaurus louderbacki* (Peng 1992, fig. 5, 6A), *Hexinlusaurus multidens* (He and Cai 1984, fig. 17B, 18C), *Kulindadromeus zabaikalicus* (INREC K3, Godefroit et al. 2014, fig. S7A, D), *Dryosaurus*

altus (AMNH 834, Galton 1981, fig. 10A, 15S), *Talenkauen santacrucensis* (MPM10001, Cambiaso 2007, fig. 31, 34) and *Thescelosaurus assiniboiensis* (RSNP 1225.1, Brown et al. 2011, fig. 18, 20) the ilium is much shorter than 90% the length of the femur. In *Tenontosaurus tilletti* (AMNH 3040, Forster 1990, fig. 15, 19), *T. dossi* (FWMSH 93B1 and B2, Winkler et al. 1997, fig. 18A, D), *Orodromeus makelai* (MOR 623, Scheetz 1999, fig. 24, 27), *Gasparinisaura cincosaltensis* (MUCPv-208, Coria and Salgado 1996, fig. 7, 8A-D), *Dysalotosaurus lettowvorbecki* (UT 1495, Galton 1981, fig. 11K, 14A), the ilium is slightly shorter than 90% of the ilium length. Gilmore (1915, pl. 49) provided a line-drawing of *Thescelosaurus neglectus* which gives an ilium that makes about 90% the femur length, but Galton (1974b, fig. 4) provides another one in which the ilium length is less than 90% the length of the femur. Overall we considered this sufficient to code *T. neglectus* as having an iliac length up to 90% the length of the femur. (0). *Camptosaurus dispar* has an ilium slightly longer than 90% of its total femoral length (Gilmore 1909, pl. 19).

259(*). Ilium, preacetabular process shape and length: short, tab-shaped, distal end is posterior to pubic peduncle (0), elongate, strap-shaped, distal end is anterior to pubic peduncle (1) (Ösi et al. 2012 #165).

We follow Bell et al. (2019 #215) in correcting and coding (1) for *Muttaburrasaurus langdoni*.

260(*). Ilium, preacetabular process length relative to the ilium length: less than 50% (0), more than 50% (1) (Ösi et al. 2012 #166).

In *Scutellosaurus lawleri* (Rosembaum and Padian 2000), the anterior process of ilium would have been quite long but the rest of the iliac body is absent. Therefore this taxon was corrected and coded with a question mark. In *Scelidosaurus harrisonii* (Charig 1972, fig. 2), the anterior process of the ilium is more than half of the whole iliac length. This taxon was

therefore corrected and coded (1). We follow Bell et al. (2019 #216) in correcting and coding (0) for *Muttaburrasaurus langdoni*.

261(*). Ilium, preacetabular process curvature from a lateral view: no distinct break in slope, dorsal surface varies from straight to smoothly convex all along (0), the downward break in slope located above the pubic peduncle (1), the downward break in slope starting well anterior to the pubic peduncle (2) (new character).

Anabisetia saldiviai (Cambiaso 2007, fig. 112), *Valdosaurus canaliculatus* (Barrett 2016, fig. 8), *Talenkauen santacrucensis* (Rozadilla et al. 2019, fig. 21A), *Macrogryphosaurus gondwanicus* (Calvo et al. 2007, fig. 9B), *Dryosaurus altus* and *Dysalotosaurus lettowvorbecki* (Galton 1981, fig. 10A, 11A, C, J) exclusively share by their preacetabular process of ilium being bent downward with an anterior break in slope situated anterior to their iliac pubic peduncle. By contrast, *Camptosaurus aphanoecetes* (Carpenter and Galton 2018, fig. 25I), *Muttaburrasaurus langdoni* (Bartholomai and Molnar, 1981, fig. 8A), *Iguanodon bernissartensis* (Norman 1980, fig. 64), *Zalmoxes shqiperorum* (Godefroit et al. 2009, fig. 13, 18), *Thescelosaurus neglectus* (Galton 1974*b*, fig. 3N), *Tenontosaurus tilletti* (Tennant 2013, fig. 25) all have an ilium which preacetabular process has a downward curve which posterior apex is located right above the pubic peduncle. *Tenontosaurus dossi* (Winkler et al. 1997, fig. 18A) differs from its congeneric in having a preacetabular process curvature which apex is more offset anteriorly. In *Camptosaurus dispar* the preacetabular curve is poorly defined and almost straight so the exact location of the break in slope is undefined (Carpenter and Galton, fig. 25C, J), except for the smaller specimen AMNH FARB 6120 (Carpenter and Galton, fig. 25F) in which the break in slope occurs right above the pubic peduncle. In *Zalmoxes robustus* (Weishampel et al. 2003, fig. 22A, B) the preacetabular process follow the same downward curve as the dorsally convex iliac margin, so the location of the downward break in slope could not be pinpointed.

262(*). Ilium, outline of dorsal margin from a dorsal view: postacetabular process straight until above the acetabulum, and the preacetabular process subtly to moderately deflected from midline laterally (0), the dorsal margin forms a regular and continuous curve from the postacetabular process to the preacetabular process, with the medial side convex all along and the preacetabular process well deflected laterally (1), sigmoidal: the preacetabular process is well deflected laterally, and the postacetabular process curves toward the medial side posteriorly (2), straight all along (3) (modified from Xu et al. 2006 #50; Ösi et al. 2012 #167). In *Goyocephale lattimorei* (Perle et al. 1982, pl. 45.5-6) and *Heterodontosaurus tucki* (Galton 2014, fig. 7A), the dorsal margin of the postacetabular process is straight and the preacetabular process is deflected laterally. In *Homalocephale calathocercos* (Maryanska and Osmolska 1974, pl. 29.1C) and *Stegoceras validum* (Gilmore 1924, pl. 10.1) the dorsal outline of the ilium is sigmoidal. In *Yinlong downsi* (Han et al. 2018, fig. 11C), *Psittacosaurus major* (Sereno et al. 2007, fig. 3), *Hexinlusaurus multidens* (He and Cai 1984, p. 31), and *Tenontosaurus tilletti* (Forster 1990, fig. 15), the ilium appears straight all along. In *Stenopelix valdensis* the dorsal margin of the ilium is apparently straight from a lateral view, although it is also described as bearing a subtle lateral deflection of its preacetabular process (Butler and Sullivan 2009, fig. 3A, p. 29). In *Archaeoceratops oshimai* (You and Dodson 2003, fig. 2) the dorsal margin of the ilium is different from that of other more basal ceratopsians in that its preacetabular and postacetabular portions are rather straight but they are laterally oriented and sharply deflect from each other at a level right above the acetabulum. In *Macrogryphosaurus gondwanicus*, the ilium is curved all along and broadly concave laterally (Calvo et al. 2007, fig. 9). In *Eocursor parvus*, the relative lateral deflection of the preacetabular process is not formally described (Butler 2010, p. 670). In *Agilisaurus louderbacki*, the dorsal iliac margin is reported as laterally concave anteroposteriorly (Peng 1992), but this was not substanciated by any figure. In *Isaberrysaura mollensis* (Salgado et al.

2017) the mediolateral curvature of the dorsal iliac margin is neither described nor figured. In *Herrerasaurus ischigualastensis*, the dorsal outline of the ilium is unlike that of any other ornithischians so it does not correspond to any of the above-cited character states (Novas 1994, fig. 3B). *G. lattimorei, H. calathocercos* and *H. tucki* were corrected and coded (0). *A. oshimai* and *M. gondwanicus* were corrected and coded (1). *H. calathocercos* was corrected and coded (2). *Y. downsi*, *P. major*, *H. multidens, T. tilletti* were corrected and newly coded (3). *H. ischigualastensis*, *E. parvus*, *I. mollensis* and *A. louderbacki* were corrected and coded with a question mark.

263(*). Ilium, preacetabular process expands mediolaterally towards its distal end in dorsal view: absent (0), present (1) (Ösi et al. 2012 #169).

Heterodontosaurus tucki differs from *Abrictosaurus consors* in that the anterior end of its preacetabular process ends in a lobe-shaped expansion (Sereno 2012, p. 81). The anterior end of preacetabular process is unexpanded in *Stenopelix valdensis* (Butler and Sullivan 2009, fig. 1A) and *Yinlong downsi* (Han et al. 2018, fig. 9B, 11C). The anterior end of preacetabular process is transversely expanded in *Zalmoxes robustus* (Weishampel et al. 2003, fig. 22A-C) and *Z. shqiperorum* (Godefroit et al. 2009, fig. 18C). This character could not be coded for *Wannanosaurus yansiensis* under the current state of knowledge (Hou 1977; Butler and Zhao 2009). *S. valdensis* and *Y. downsi* were corrected and coded (0). *H. tucki*, *Z. robustus* and *Z. shqiperorum* were corrected and coded (1). *W. yansiensis* was corrected and coded with a question mark.

264(*). Ilium, medioventral acetabular flange, partially closing the acetabulum: present (0), absent (1) (Ösi et al. 2012 #175).

A medial ventral flange partially closes the acetabulum in *Eocursor parvus* (Butler 2010, p. 654). *Muttaburrasaurus langdoni* (Bartholomai and Molnar, 1981, p. 333; Dieudonné et al. 2016b, fig. 2A) features a medioventral flange on the upper border of its acetabulum. There is

no medioventral acetabular flange in *Macrogryphosaurus gondwanicus* (Calvo et al. 2007, fig. 9B). This feature is not described for *Nanosaurus agilis* (Galton and Jensen 1973). *M. gondwanicus* was corrected and coded (1). *E. parvus* and *M. langdoni* were corrected and coded (0). *N. agilis* was corrected and coded with a question mark.

265(*). Ilium, supra-acetabular 'crest' or 'flange' on the dorsolateral part of the acetabulum: present (0), absent (1) (modified from Ösi et al. 2012 #176).

No supraacetabular flange is observable in *Nanosaurus agilis* (Galton and Jensen 1973; Carpenter and Galton 2018, fig. 15) and *Macrogryphosaurus gondanicus* (Calvo et al. 2007, fig. 9B). *Jeholosaurus shangyuanensis* was coded as bearing a dorsolateral supra-acetabular flange (Han et al. 2012), but the same authors declare that it is very discrete, as attested by the figures (Han et al. 2012, fig. 9A). *Muttaburrasaurus langdoni* wasn't described as presenting a dorsolateral flange roofing its acetabulum and apparently lacks it (Bartholomai and Molnar, 1981, p. 333). *Isaberrysaura mollensis* (Salgado et al. 2017, fig. 3) does not preserve the acetabular part of its ilium. *N. agilis* was corrected and coded (0). *J. shangyuanensis*, *M. langdoni*, *N. agilis* and *M. gondanicus* were corrected and coded (1). *I. mollensis* was corrected and coded with a question mark.

266(*). Ilium, postacetabular process orientation from a lateral view: posteriorly directed (0), curves posterodorsally with both its dorsal and ventral margins (1) (McDonald et al. 2010 #114; Ösi et al. 2012 #170).

As plesiomorphically found within Ornithischia, *Abrictosaurus consors* and *Heterodontosaurus tucki* (Galton 2014, fig. 7K-L, 12A-B), *Nanosaurus agilis* (Carpenter and Galton 2018, fig. 15E), *Hypsilophodon foxii* (Galton 1974*a*, fig. 48A, 51B) feature no dorsal kink above their postacetabular process. Ankylopollexians such as *Camptosaurus dispar* (Carpenter and Galton 2018, fig. 24C-D) and *Iguanodon bernissartensis* (Norman 1980, fig. 63-64) feature a very weak dorsal postacetabular kink, but it is too weak so that it could be

really coded (0). When discarding any contribution of the ventromedial brevis shelf to the overall postacetabular process outline, the postacetabular process rises upward with both ventral and dorsal margins in dryosaurids (Galton 1981, fig. 10A, 11A). *Camptosaurus aphanoecetes* (CM 11337, Carpenter and Wilson 2008, fig. 24A), both *Tenontosaurus* species (Forster 1990; Winkler et al. 1997), *Talenkauen santacrucensis* (Cambiaso 2007, fig. 36), *Gasparinisaura cincosaltensis* (Cambiaso 2007, fig. 68), *Thescelosaurus neglectus* (Galton 1974*b*, pl. 2.5), *Thescelosaurus assiniboiensis* (Brown et al. 2011, fig. 18A), *Convolosaurus marri* (Andrzejewski et al. 2019, fig. 21), *Macrogryphosaurus gondwanicus* (although its postacetabular process is incomplete, Calvo et al. 2007, fig. 9B) all feature a dorsal kink of their postacetabular process. Although a dorsal "kink" seems to be present, the very dorsal margin of postacetabular process is missing in *Muttaburrasaurus langdoni* (cf. Bartholomai and Molnar, 1981, fig. 8A). There is no dorsal kink in rhabdodontids (except in UBB SPZ2, one ilium of *Zalmoxes shqiperorum* that differs from other ilia of the same species in this respect, cf. Godefroit et al. 2009, fig. 13), and *Anabisetia saldiviai* (Cambiaso 2007, fig. 112). We note however that although the latter two taxa might not be coded as presenting a dorsal "kink", the dorsal margin of their ilia is thinkenned above their postacetabular process. We propose that such thikenning might result from some lateral eversion or compression of an ancestrally present dorsal kink, although this explanation might be difficult to rule out. *T. snatacrucensis*, *M. gondwanicus*, *Dryosaurus*, *D. lettowvorbecki* and *G. cincosaltensis* were corrected and coded (1). *M. langdoni* was corrected and coded with a question mark.

267(*). Ilium, morphology of dorsal margin at the level of the acetabulum: smooth, almost no modification of dorsal margin (0), well thickened above the ischial peduncle onward (1), thickened above the pubic peduncle onward (2) (modified from McDonald et al. 2010 #112; Ösi et al. 2012 #168; Dieudonné et al. 2016a #222).

The difference between the presence or absence of a smooth laterally bulging eminence on the dorsal margin of the ilium, at the level of the ischial peduncle, was judged too tenuous to be characterized with sufficient confidence. The dorsal margin of the ilium isn't expanded in *Psittacosaurus mongoliensis* (Osborn 1924), *Stenopelix valdensis* (Butler and Sullivan 2009, fig. 1A) and *Yinlong downsi* (Han et al. 2018, fig. 10B). The dorsal margin of ilium starts to expand mediolaterally from the level above the pubic peduncle onward in the pachycephalosaurs *Goyocephale lattimorei* (Perle et al. 1982, pl. 44.2-3), *Prenocephale prenes* and *Homalocephale calathocercos* (Maryanska and Osmolska 1974, pl. 25.3A, 29.1C respectively), and *Stegoceras validum* (Gilmore 1924, pl. 10.4). *Anabisetia saldiviai* (Cambiaso 2007, fig. 113B), *Dryosaurus altus* and *Dysalotosaurus lettowvorbecki* (Galton 1981, fig. 10J and 4E, H respectively) were considered to bear a dorsally unthickenned margin of ilium at the level of the ischial peduncle. Gilmore (1909, p. 256) describes the dorsal margin of the iliac blade of *Camptosaurus dispar* as being characteristic of the genus and "rounded and thickened transversely". However, a dorsal illustration of the ilium of *C. dispar* was not provided. On the other hand, the dorsal margin of the iliac blade of *Camptosaurus aphanoecetes* (Carpenter and Wilson 2008, fig. 13A) appears thin all along. The dorsal margin of the ilium of *Herrerasaurus ischigualastensis* is reported to thicken in both anterior and posterior extremities, and it is still apparently thick at the level above the ischial peduncle (Novas 1994, fig. 3B). Following the new formulation of this character, *A. saldiviai*, *Dryosaurus* and *D. lettowvorbecki* (Galton 1981, fig. 10J and 4E, H respectively), but also *P. mongoliensis, S. valdensis* and *Y. downsi* were corrected and coded (0). The dorsally everted rim featured by the rhabdodontids *Zalmoxes robustus* and *Z. shqiperorum* was not considered here, so these two taxa were corrected and coded (1). *G. lattimorei, P. prenes, H. calathocercos, S. validum* were corrected and coded (2). *C. dispar* was corrected

and coded with a question mark. Other taxa previously coded with character state (2) and (3) were newly coded (1) and (2) respectively.

269(*). Ilium, dorsal surface of postacetabular process until the origin of *M. iliocaudalis* from a lateral view: smoothly convex with a posterior break in slope (0), the postacetabular blade looks strongly quadrangular-shaped (1), tapers with no break in slope for the attachment of *M. iliocaudalis* (2) (modified from McDonald et al. 2010 #113; Dieudonné et al. 2016a #223).

We removed the adjective describing a "concave" dorsal postacetabular margin, as it is not mutually exclusive with the quadrangular nature of the postacetabular process and the concave dorsal border was already dealt with in an already mentionned character above. In *Scelidosaurus harrisonii* (Charig 1972, fig. 2), *Scutellosaurus lawleri* (Colbert 1981, fig. 23) the dorsal surface of the ilium is relatively straight and forms a posteriorly convex slope. The postacetabular process of *Dysalotosaurus lettowvorbecki* is strongly quadrangular-shaped (Janensch 1955, fig. 37A) as that of other dryosaurids such as *Dryosaurus altus* (Galton 1981, fig. 10A, L), but also as *Tenontosaurus tilletti* and *T. dossi* (Forster 1990, fig. 15; Winkler et al. 1997, fig. 18A), *Thescelosaurus neglectus* and *T. assiniboiensis* (Galton 1974*b*, pl.2-5; Brown et al. 2011, fig. 18A), *Talenkauen santacrucensis* (Cambiaso 2007, fig. 31) and *Gasparinisaura cincosaltensis* (Cambiaso 2007: see MUCPv-208 on fig. 67A; MCS-Pv111 on fig. 68). This feature is absent in *Camptosaurus dispar* (Carpenter and Wilson 2008, fig. 24B-D) and *Iguanodon bernissartensis* (Verdu et al. 2017, fig. 10). In *Zalmoxes shqiperorum* (Godefroit et al. 2009, fig. 18B) and *Zalmoxes robustus* (Weishampel et al. 2003, fig. 22A-B) the postacetabular process tapers posteriorly with its dorsoventral margins converging smoothly in a tip, but there is no dorsal concavity. In the Vegagete ornithopod, the postacetabular process of ilium ends in a kind of posteriorly tapering "node" (Dieudonné et al. 2016a, fig. 7A), In *Muttaburrasaurus langdoni* the postacetabular process likely tapers posteriorly but its exact nature is unknown as it misses portion of its dorsal margin (Fig. 3A,

Bartholomai and Molnar, 1981, fig. 8B). This character is not described or figured for *Goyocephale lattimorei* (Perle et al. 1982). The Vegagete ornithopod was corrected and coded (2). *Dryosaurus, D. lettowvorbecki*, *T. tilletti*, *T. dossi*, *T. neglectus* were corrected and coded (1). *S. harrisonii*, *G. lattimorei* and *M. langdoni* were corrected and coded with a question mark.

270(*). Ilium, brevis shelf and fossa: faces ventrolaterally and shelf is near vertical and creates a deep postacetabular portion anteriorly (0), fossa faces ventrally for most of its length and is less visible from a lateral view (1), the brevis shelf consists in a small and smooth ridge that is only visible from a medial view (2) (reformulated from Ösi et al. 2012 #173; Dieudonné et al. 2016a #224).

No mention of post-acetabular brevis shelf is made for the ilia of *Zalmoxes robustus* and *Z. shqiperorum*, and if present it would only have been a very small ridge (cf. Weishampel et al. 2003; Godefroit et al. 2009). The same seems to occur in *Muttaburrasaurus langdoni* (see Dieudonné et al. 2016b, fig. 2A), where the brevis shelf would have been almost absent (Herne, personal communication; Bartholomai and Molnar, 1981, fig. 8A). The brevis shelf is visible from a lateral view and mostly faces ventrolaterally in *Dryosaurus altus* (Galton 1981, fig. 10A), *Dysalotosaurus lettowvorbecki* (Janensch 1955, fig. 37A), *Tenontosaurus tilletti* (Forster 1990, fig. 15), *Convolosaurus marri* (Andrzejewski et al. 2019, fig. 15A), *Thescelosaurus assiniboiensis* (Brown et al. 2011, fig. 18A), *Haya griva* (Makovicky et al. 2011, fig. 3) and *Nanosaurus agilis* (Carpenter and Galton 2018, fig. 15E, H). This also seems to be true for *Hyspilophodon foxii* (Galton 1974*a*, fig. 46A) and *Thescelosaurus neglectus* (Galton 1974*b*, fig. 3N; Brown et al. 2011, p. 1178). In *Macrogryphosaurus gondwanicus* the brevis shelf faces ventrally so it remains invisible from a lateral view (Calvo et al. 2007, fig. 9B). "There is no trace of vertical brevis shelf" in *Koreanosaurus boseongensis*, but that doesn't allow us to know wether there was actually a brevis shelf or not (Huh et al. 2010, p.

16). *Dryosaurus*, *D. lettowvorbecki*, *T. tilletti, C. marri, T. assiniboiensis, T. neglectus, H.griva, H. foxii* and *N. agilis* were corrected and coded (0). *M. gondwanicus* was corrected and coded (1). *K. boseongensis* was corrected and coded with a question mark.

271(*). Ilium, brevis shelf and fossa, transverse width: narrow (0); very broad and expanding in width towards its caudal margin such that it appears triangular in dorsal or ventral view (1) (McDonald 2012 #132).

A large, triangular brevis shelf is present in *Anabisetia saldiviai* (Cambiaso 2007, fig. 113B, C). The brevis shelf is moderately wide and triangular in *Nanosaurus agilis* (Galton and Jensen 1973, fig. 2H; Carpenter and Galton 2018, fig. 15E). The same might also occur in *Camptosaurus dispar* as in *Camptosaurus aphanoecetes* (Carpenter and Galton 2018, fig. 25), and also in *Iguanodon bernissartensis* (Norman 1980; Verdu et al. 2017) but we aren't aware of any figure that can support this assumption. *N. agilis* and *A. saldiviai* were corrected and coded (1) for this character. *C. dispar* and *I. bernissartensis* were corrected and coded with a question mark.

272(*). Ilium, length of the postacetabular process relative to the total ilium length: 20% or less (0), 25-35% (1), more than 35% (2) (Ösi et al. 2012 #174).

Though it appears slightly incomplete posteriorly, we could safely infer that the postacetabular blade of *Muttaburrasaurus langdoni* was very short (Bartholomai and Molnar, 1981; Dieudonné et al. 2016b, fig. 2A). The postacetabular blade of the ilium of *Yinlong downsi* is about 30% of the total ilium length (Han et al. 2018, fig. 9). *M. langdoni* was corrected and coded (0). *Y. downsi* was corrected and coded (1).

273(*). Ilium, pubic peduncle: elongate and robust (0), ventrally projected, elongate and strap-like (1), often reduced in size, anteriorly projected so its distal tip is higher than the ventral extent of the ischial peduncle (2) (modified from Ösi et al. 2012 #178).

Character state (1) was added to deal with the elongated but slender, ventrally projected pubic peduncles of ilium. Previous character state (1) was turned to character state (2). Heterodontosaurids bear an elongate but thin and strap-like pubic peduncle of ilium that is ventrally directed (cf. *Abrictosaurus consors* and *Heterodontosaurus tucki* Galton 2014, fig. 7L and 12 respectively). The same occurs in *Psittacosaurus mongoliensis* (Osborn 1924, fig. 8), *Stenopelix valdensis* (Butler and Sullivan 2009, fig. 2), *Yinlong downsi* (Han et al. 2018, fig. 9A), and also in the Late Jurassic cerapod *Nanosaurus agilis* (Carpenter and Galton 2018, fig. 15E). In pachycephalosaurs the pubic peduncle of ilium is elongate but it does not reach the level of the ischiac peduncle in *Homalocephale calathocercos* (Maryanska and Osmolska 1974, pl. 29), and it is more robust and anteroventrally projected in *Stegoceras validum* (Gilmore 1924, pl. 10). In *Archaeoceratops oshimai* (You and Dodson 2003, fig. 3B, D), *Haya griva* (Makovicky et al. 2011, fig. 3) and *Kulindadromeus zabaikalicus* (Godefroit et al. 2014, fig. S7A) the pubic peduncle is moderately elongated but also anteriorly projected so it appears dorsoventrally shorter than the ischiac peduncle. This character is unavailable for *Isaberrysaura mollensis* (Salgado et al. 2017). Every taxa that were previously coded (1) were turned to character state (2) because of the change in character definition. *H. tucki*, *A. consors*, *P. mongoliensis*, *S. valdensis*, *Y. downsi*, *N. agilis* were corrected and coded with the new character state (1). *Aurorella, K. zabaikalicus* and *H. griva* were corrected and coded (2). *I. mollensis* was corrected and coded with a question mark.

274(*). Ilium, ischiac peduncle: projects ventrally (0), broadly swollen, projects ventrolaterally (1) (Butler et al. 2011; Ösi et al. 2012 #177).

In *Thescelosaurus neglectus*, the ischial peduncle is described as a “heavy swelling” (Gilmore 1915, p. 608). *Thescelosaurus assiniboiensis* also features a large, laterally projected ischial peduncle of ilium (Brown et al. 2011, fig. 18C). The ischial peduncle is described as “enormous and lenticular” in *Zalmoxes robustus* (Weishampel et al. 2003, p. 90) and swells

"rapidly posteriorly and laterally" in *Muttaburrasaurus langdoni* (Bartholomai and Molnar, 1981, p. 333). This is also the case for *Talenkauen santacrucensis* (Rozadilla et al. 2019, pers. obs.). In *Stegoceras validum*, the lateral swelling of the ischial peduncle was described as straight up and down laterally, and appears undistinguishable from a dorsal view in the figures (Gilmore 1924, pl. 10.1). This differs from the smooth lateral bulging of the ischial peduncle seen in *Homalocephale calathocercos* (Maryanska and Osmolska 1974, pl. 29.1C). In *Psittacosaurus major* (Sereno, 2007, fig. 3) and *Psittacosaurus mongoliensis* (Osborn 1924, fig. 9), the ischial peduncle is ventrolaterally directed so it also appears laterally swelling. In *Koreanosaurus boseongensis*, the ischial peduncle was described as "ventrolaterally projected". However, it doesn't seem to swell laterally as seen from a lateral view (Huh et al. 2010, fig. 15A). We await that further verification in made first-hand on this taxon before coding for it. The ischial peduncle is – as far as we are concerned – not preserved in *Isaberrysaura mollensis* (Salgado et al. 2017). *T. neglectus*, *T. assiniboiensis*, *T. santacrucensis*, *Z. robustus* and *M. langdoni* were corrected and coded (1). The psittacosaurs *P. major* and *P. mongoliensis* were coded (1). *I. mollensis* and *K. boseongensis* were corrected and coded with a question mark.

275(*). Ilium, ischial peduncle: anteroposteriorly short (0), massive and anteroposteriorly long (1) (new character).

The ischial peduncle of ilium is anteroposteriorly expanded in *Zalmoxes shqiperorum* (Godefroit et al. 2009, fig. 13C, Fig. 3), *Zalmoxes robustus* (Weishampel et al. 2003, fig. 22A) and *Muttaburrasaurus langdoni* (Dieudonné et al. 2016b, fig. 1.2A, Fig. 3). Although to a somewhat lesser extent, the ischiac peduncle of ilium also looks "thick" and anteroposteriorly expanded in *Anabisetia saldiviai* (Coria and Calvo 2002, fig. 6).

276(*). Ilium, acetabulum: normal to high (0), low (1) (reformulated after Boyd 2015 #182).

Tenontosaurus dossi (Winkler et al. 1997, fig. 18A) and *Tenontosaurus tilletti* (Forster 1990, fig. 15), *Agilisaurus louderbacki* (Peng 1992, fig. 5), *Dryosaurus altus* (Galton 1981, fig. 10A, L) and *Dysalotosaurus lettowvorbecki* (Janensch 1955, fig. 37) all have a high acetabular region. The ilia of *Scelidosaurus harrisonii*, *Stegosaurus* and *Ankylosaurus* (Charig 1972, fig. 2, 7A, 7B respectively) feature a very low acetabulum, contrary to the basal tyreophoran *Scutellosaurus lawleri* (Colbert 1981, fig. 21). The acetabulum is normal to high in *Archaeoceratops oshimai* (You and Dodson 2003, fig. 3B, D), *Psittacosaurus mongoliensis* (Osborn 1924, fig. 9) and also *Koreanosaurus boseongensis* (Huh et al. 2010, fig. 15A). The acetabulum of *Muttaburrasaurus langdoni* is dorsoventrally low, even by making abstraction of the thin medial crest on its anterodorsal extremity (cf. Dieudonné et al. 2016b, fig. 2A). *K. boseongensis*, *T. dossi*, *T. tilletti*, *A. louderbacki*, *Dryosaurus*, *D. lettowvorbecki* were corrected and coded (0). *P. mongoliensis* was newly coded (0). *M. langdoni* was corrected and coded (1).

278(*). Pubis, orientation: anteroventral (0), rotated posteroventrally to lie alongside the ischium (opisthopubic) (1) (Ösi et al. 2012 #186).

No postpubis was preserved in *Talenkauen santacrucensis* (Rozadilla et al. 2019) so although an opisthopubic condition is certain for being an ornithischian, this taxon was corrected and coded with a question mark.

280(*). Pubis, prepubic process shape in its distal extremity: compressed mediolaterally, dorsoventral height exceeds mediolateral width (0), rod-like, mediolateral width exceeds dorsoventral height (1), dorsoventrally compressed (2) (modified from: Butler et al. 2011; Ösi et al. 2012 #193).

The prepubic process of *Homalocephale calathocercos* is described as dorsoventrally flattened proximally but mediolaterally compressed and dorsoventrally expanded distally (Maryanska and Osmolska 1974, p. 91). *H. calathocercos* was corrected and coded (0).

281(*). Pubis, prepubic process length: stub-like and poorly developed, extends only a short distance anterior to the pubic peduncle of the ilium (0), elongated into distinct anterior process, but does not extend beyond the distal end of the preacetabular process of ilium (1), elongate and extending up to the level or beyond the distal end of preacetabular process of ilium (2) (modified from Xu et al. 2006 #43, #106; Ösi et al. 2012 #194, #195).

We started up coding this new character as follow. Every character coded (0) for character #234 of Ösi et al. (2012) deal with the short stub-like prepubic process and were again coded (0) here. Every character coded (1) for character #235 of Ösi et al. (2012) deal with the elongate prepubic process and were recoded (2). Whenever characters #234 and #235 or both were found with a question mark, such question mark was reported. The remaining characters correspond to taxa with a moderately elongate prepubic process but which does not reach the preacetabular process of ilium: these were coded (1). Note that in *Agilisaurus louderbacki* (Barrett et al. 2005, fig. 4B) the prepubic process is developped byt does not extend farther beyond the preacetabular process of ilium. This condition is similar to that of other ceratopsians. In *Stenopelix valdensis* the prepubic process is short so that is shouldn't have oversize the preacetabular process of ilium (cf. articulated specimen in Butler and Zhao 2009, fig. 1). In *Macrogryphosaurus gondwanicus* the prepubic process was calculated to oversize the preacetabular process of ilium (Calvo et al. 2007, fig. 9, 12). This is similar to the condition found in *Valdosaurus canaliculatus* (Barrett 2016) and Anabisetia saldiviai (Cambiaso 2007, fig. 112). *S. valdensis* was corrected and coded (1). *M. gondwanicus* was corrected and coded (2).

282(*). Pubis, angle between prepubic process and distal postpubic shaft : less than 130 degrees (0) ; greater than 130 degrees but less than 170° (1) ; aligned along the same plane (2) (modified from Boyd 2015 #196).

The character was modified so that there is the same boundary - fixed to 130° - for the taxa with a lower or greater angle between the prepubic process and the pubic shaft. Character states (0) and (1) were reversed. Finally, a new character state was added to deal with the aligned prepubic process and pubic shaft of ceratopsians. In *Muttaburrasaurus langdoni* (Bartholomai and Molnar, 1981, fig. 8A), *Zalmoxes shqiperorum* (Godefroit et al. 2009, fig. 8E), *Macrogryphosaurus gondwanicus* (Calvo et al. 2007, fig. 12; Rozadilla et al. 2020, fig. 11), the angle between the prepubic process and pubic shaft is very open and angles to more than 130°. In the basal ceratopsians *Archaeoceratops oshimai* (Dong and Azuma 1997, fig. 7), *Yinlong downsi* (Xu et al. 2006) and *Psittacosaurus mongoliensis* (Osborn 1924, fig. 8), the prepubic process and pubic shaft are aligned on the same plane. The same also occurs between the stub-like prepubic process and pubic shaft of *Heterodontosaurus tucki* (e.g. Galton 2014, fig. 12). In *Eocursor parvus*, the prepubic process and pubic shaft are set to an angle of 40° to one another (Butler 2010, p. 671). *E. parvus* was corrected and coded (0). *M. langdoni* and *M. gondwnanicus* were corrected and coded (1). *Y. downsi* and *H. tucki* were corrected and coded (2).

283(*). Pubis, pubic symphysis: elongate or at least present distally on a significant part of the pubic blade (0), much reduced or absent (1) (modified from Xu et al. 2006 #47; Ösi et al. 2012 #196).

A pubic symphysis is distally present in *Lesothosaurus diagnosticus* (Sereno 1991, fig. 9E, F) and stegosaurs such as *Stegosaurus stenops* (Maidment et al. 2015, fig. 71). Contrary to what was coded in Xu et al. (2006 #47), heterodontosaurids are devoid of an elongate distal pubic symphysis. *Tianyulong confuciusi* lacks such symphysis (Zheng et al. 2009, supp. info. p. 5) and in *Heterodontosaurus tucki* it was either absent, or restricted to the distalmost end of the pubic shaft (Galton 2014, p. 119). The eventual pubic symphysis was not described for *Agilisaurus louderbacki* (Peng 1992, 1997; Butler et al. 2005), it is hidden in *Scutellosaurus*

lawleri (Carpenter et al. 2013, p. 4) and this bone remains entirely unknown in *Scelidosaurus harrisonii* (Owen 1863; Thulborn 1977). The presence of a pubic symphysis in *Eocursor parvus* is likely although it could not be ascertained (Butler 2010, p. 671). As far as we know, it was not described either in ankylosaurs, some of which were even devoid of a pubis (Carpenter et al. 2013). *L. diagnosticus* and *S. stenops* were corrected and coded (0). *A. louderbacki, S. lawleri*, *S. harrisonii,* Ankylosauria and *E. parvus* were corrected and coded with a question mark.

284(*). Pubis, shape of the postpubis shaft in cross-section: blade-shaped (0), rod-shaped (1) (Ösi et al. 2012 #187).

No postpubis was preserved in *Talenkauen santacrucensis* (Rozadilla et al. 2019) so this taxon was corrected and coded with a question mark.

285(*). Pubis, length of postpubis shaft relative to ischium length: approximately equal (0), extends for around half the length (1), very short to absent (2) (modified from: McDonald et al., 2010 #117 ; Ösi et al. 2012 #188, #189).

The postpubic shaft is relatively elongated in *Camptosaurus dispar* and *Camptosaurus aphanoecetes* so, although incomplete distally, it might have formed more than half the length of the ischium (Carpenter and Wilson 2008, fig. 34A, B). The postpubic shaft is very short in *Archaeoceratops oshimai* (Dong and Azuma 1997, fig. 7), and also less than half the length of the pubis shaft in *Yinlong downsi* (Han et al. 2018, p. 1175). The pubis of *Stenopelix valdensis* was slender but its exact length cannot be inferred (Butler and Zhao 2009, p. 28). *C. dispar* was corrected and coded (0). *A. oshimai* and *Y. downsi* were corrected and coded (2). *S. valdensis* was corrected and coded with a question mark.

286(*). Ischium, pubic peduncle shape: transversely compressed (0), dorsoventrally compressed and mediolaterally thick (1) (reformulated from Ösi et al. 2012 #179).

There is no mention for an either transversely or dorsoventrally compressed pubic peduncle of ischum in *Scelidosaurus* in its related literature (Owen 1861; Charig 1972). The ischia of *Dryosaurus altus* and *Dysalotosaurus lettowvorbecki* (Shepherd et al. 1977; Galton 1981), *Camptosaurus dispar* (Carpenter and Wilson 2008), Rhabdodon sp.1 (Pincemaille-Quilleveré 2002, p. 59) are mediolaterally compressed. The pubic peduncle of ischium is reported as a "narrow flat blade" in *Iguanodon bernissartensis* (Norman 1980). The proximal blade of the ischium seems mediolaterally thick in *Scutellosaurus lawleri* (Rosembaum and Padian 2000, fig. 3). No ischium is preserved in *Isaberrysaura mollensis* (Salgado et al. 2017). The proximal ishium of *Archaeoceratops oshimai* is reported as preserved but isn't described nor figured (Dong and Azuma 1997, p. 80, fig. 7). *S. lawleri* was corrected and coded (1). *Dryosaurus*, *D. lettowvorbecki*, *C. dispar*, *Rhabdodon* sp1. and *I. bernissartensis* were corrected and coded (0). *I. mollensis*, *A. oshimai* were corrected and coded with a question mark.

287(*). Ischium, pubic peduncle breadth from a lateromedial view: larger than or subequal to that of the iliac peduncle (0); much smaller than that of the iliac peduncle (1) (modified from Gasca et al. 2014 #3; Boyd 2015 #200).

In *Dysalotosaurus lettowvorbecki*, the pubic peduncle of ischium is larger and sometimes subequal in breadth to the iliac peduncle (e.g. Janensch 1955, fig. 39 and pl. 13; Galton 1981, fig. 12A-G). This double condition was retained to form the modified character state (0). Character state (1) now solely code for a smaller pubic peduncle with respect to the iliac one. In *Macrogryphosaurus gondwanicus* the pubic peduncle appears very broad (Calvo et al. 2007, fig. 10.12) so it appears slightly larger than the iliac peduncle. The pubic and iliac peduncles look subequal in *Anabisetia saldiviai* (e.g. Coria and Calvo 2002, fig. 6). The iliac peduncle is smaller than the pubic peduncle in *Scelidosaurus harrisonii* (Carpenter et al. 2013, fig. 3). *Tenontosaurus tilletti* (Forster 1990, fig. 18C) appears to bear a smaller pubic

peduncle of ischium. This character appears to vary within the genus *Camptosaurus*. The iliac peduncle of ischium is larger than the pubic peduncle in *C. aphanoecetes* and *C. dispar* (Gilmore 1909, pl. 16; Carpenter and Wilson 2008, fig. 27, 28, 29A, B), except in *C. browni* where they are subequal (Carpenter and Wilson 2008, fig. 28D). In rhabdodontids such as *Zalmoxes robustus* (Weishampel et al. 2003, fig. 22D) and *Zalmoxes shqiperorum* (Godefroit et al. 2009, fig. 18E), the iliac peduncle of ischium appears broadly expanded anteroposteriorly to support the large ischial peduncle of ilium. Such difference is also extreme in the *Rhabdodon* species from Vitrolles (Pincemaille-Quilleveré 2002, fig. 17). The pubic peduncle of ischium is unknown in *Muttaburrasaurus langdoni* (Bartolomai and Molnar, 1981). The iliac peduncle is broader than the pubic peduncle in *Psittacosaurus sibiricus* (Averianov et al. 2006, fig. 20H, I), *Psittacosaurus mongoliensis* (Osborn 1924, fig. 7), *Yinlong downsi* (Han et al. 2018, fig. 11E, G). The iliac and pubic peduncles of the pachycephalosaurs *Stegoceras validum* (Gilmore 1924, pl. 10.3) and *Homalocephale calathocercos* (Maryanska and Osmolska 1974, fig. 5-A4) are subequal in widths. The proximal head of ischium is unknown in *Archaeoceratops oshimai* (You and Dodson 2003). To conform the new character definition, *Scutellosaurus lawleri* (Colbert 1981, fig. 22), *I. bernissartensis* (see Norman 1980, fig. 64), *S. stenops* (Maidment *et al*. 2015, fig. 70), *Anabisetia saldiviai* (Cambiaso 2007, fig. 115A), *Gasparinisaura cincosaltensis* (Coria and Salgado 1996, fig. 7), *Parksosaurus warreni* (Parks 1926, fig. 10), *Tenontosaurus dossi* (Winkler et al. 1997, fig. 18B), *M. gondwanicus*, *C. dispar* were corrected and coded (0). *S. harrisonii* was corrected and coded (0). *P. mongoliensis* and *Yinlong downsi* were corrected and newly coded (1). *A. oshimai* was corrected and coded with a question mark.

288(*). Ischium, orientation of the proximal main axis of the shaft and angle with respect to the pubic peduncle: falls between the iliac and pubic peduncles main axis, angle inferior to 140° (0), falls between the iliac and pubic peduncles main axis, angle widely open and superior to

140° (1), falls in the same axis of that of the pubic peduncle (2) (modified from Gasca et al. 2014 #1).

This character was modified to include an intermediary state between the sharply angled pubic peduncle of ischium and proximal main axis (0), and an ischial shaft falling straight in the same axis as the pubic peduncle (2). The angle formed by the proximal part of the ischial shaft and its pubic peduncle is widely open in rhabdodontids (*Zalmoxes robustus* and *Zalmoxes shqiperorum*, Weishampel et al. 2003, fig. 22D, 31; *Rhabdodon* sp1., Pincemaille-Quilleveré et al. 2002, fig. 17), *Anabisetia saldiviai* (Cambiaso 2007, fig. 112) and *Valdosaurus canaliculatus* (Barrett 2016, fig. 8A) although forming less than 180° with each other. *A. saldiviai* was corrected and coded (1).

290(*). Ischium, angle formed by the iliac peduncle and the proximal long axis: superior to 120° (0), equal or inferior to 120° (1) (modified from Gasca et al. 2014 #5).

In *Herrerasaurus ischigualastensis* (Novas 1994, fig. 5A) and every ornithischian except *Heterodontosaurus tucki* (Galton 2014, fig. 12F, G) and pachycephalosaurs (*H. calathocercos*, Maryanska and Osmolska 1974, pl. 29; *S. validum*, Gilmore 1924, pl. 10.3), the angle formed by the iliac process of ischium and the proximal main axis of ischium is markedly more than 120°. In the heterodontosaurid *M. condoriensis* (Pol et al. 2011, fig. 1), this angle seems to be equal to 120°, although because of the small size of the image such interpretation is difficult.

291(*). Ischium, tab-shaped obturator process: absent, lacks an obturator process (0), present and placed 60% down the shaft of ischium (1), placed within the first proximal half of the shaft (2) (modified from: Xu et al. 2006 #44; Ösi et al. 2012 #184; Brown et al. 2013 #102).

The obturator process would arise from a broadly expanded flange in juveniles to a more tab-like structure in adult individuals of *L. diagnosticus* (Baron et al. 2016). An obturator process is absent in *Eocursor parvus* (Butler 2010, fig. 13F, 14E), *Heterodontosaurus tucki* and

Tianyulong confuciusi (Galton 2014). An obturator process is lacking in *Prenocephale prenes* (Maryanzka and Osmolska, 1974, pl. 25.3B) and *Stegoceras validum* (Sues and Galton 1987). The ischial shaft is not complete in *H. calathocercos* (Maryanzka and Osmolska, 1974, pl. 29). It is absent in basal ceratopsians such as *Psittacosaurus mongoliensis* (Osborn 1924), *Archaeoceratops oshimai* (not described, Dong and Azuma 1997, fig. 7). It was considered as absent if in the form of a broad flange like in *Yinlong downsi* (Han et al. 2018, p. 16, fig. 11E, G). It is present proximally in *Jeholosaurus shangyuanensis* (Han et al. 2012), *Hypsilophodon foxii* (Galton 1974*a*), *Gasparinisaura cincosaltensis* (despite the ischial shaft is incomplete distally, cf. Cambiaso 2007), *Kulindadromeus zabaikalicus* (Godefroit et al. 2014, fig. S7C). *J. shangyuanensis*, *H. foxii*, *G. cincosaltensis*, *K. zabaikalicus* were corrected and coded (2). Given the new character definition, *F. dhimbangunmal* was corrected and coded (2) instead of the former character state (3). *Lesothosaurus diagnosticus* was corrected and coded (1). *P. prenes* was corrected and coded (0), and *H. calathocercos* was corrected and coded with a question mark.

292(*). Ischium, shaft in cross-section: compressed mediolaterally (0), subcircular and bar-like (1) (Ösi et al. 2012 #181).

The ischial shaft of *Zalmoxes robustus* is subcircular (Weishampel et al. 2003, fig. 22D, E) but that of *Zalmoxes shqiperorum* is reported as mediolaterally flatenned (Godefroit et al. 2009, p. 542). The ischial shaft is mediolaterally flatenned in *Talenkauen santacrucensis* (Rozadilla et al. 2019, fig. 22H, M). The ischial shaft is also ‘angularly rounded’ in *Stegoceras validum* (Gilmore 1924, p. 36) and uncompressed mediolaterally. In *Homalocephale calathocercos*, the ischial shaft is described as very slender, and slightly expanded distally with a flat ventrolateral side (Maryanska and Osmolska 1974, p. 91). On account of its slender nature and bar-like appearance for most of its length (Maryanska and Osmolska 1974, pl. 30.2), *H. calathocercos* was considered as bearing a subcircular ischial

shaft. Note that the ischium of *Tianyulong confuciusi* looks very slender and bar-like before its distal extremity (Zheng et al. 2009, supp. info. p. 5), although it was described as lateromedially flatenned (Sereno 2012, p. 67; Galton 2014, p. 119). *Z. shqiperorum* and *T. santacrucensis* were corrected and coded (0). *H. calathocercos* was corrected and coded (1).

293(*). Ischium, symphysis length: median symphysis with the opposing blade along at least 50% of its length (0), symphysis only presents distally (1) (Ösi et al. 2012 #185).

Scelidosaurus harrisonii (Carpenter et al. 2013, p. 7), *Laquintasaura venezuelae* (Barrett et al. 2014, fig. 1F) and *Psitacosaurus mongoliensis* (Osborn 1924, p. 7) feature a long midline ischial symphysis. In *Yinlong downsi*, 'the ischial shaft is deepest where the ventral expansion forms a flange that marks the proximal contact between contralateral ischia' (Han et al. 2018, fig. 11E). This feature was also observed in *Stenopelix valdensis*, in which the ischial flange arise at mid-shaft with a distinct curvature (Butler and Sullivan 2009; Han et al. 2018, p. 1174). It is therefore much likely that such flange also marked the sutural contact with the contralateral ischium in *S. valdensis*. In *Kulindadromeus zabaikalicus*, a similar change in the ischial curvature might also indicate the start of a sutural contact with the contralateral ischium (Godefroit et al. 2014, fig. S7C). In *Heterodontosaurus tucki*, the ischial shafts are not closely applied to one another, except possibly toward their distal end, although interestingly the ischial shaft has a more extensive mutual suture in *Manidens condorensis* (Galton 2014, p. 119). In *Tianyulong confuciusi*, both ischia look closely applied to one another (Zheng et al. 2009, supp. info. p. 5), but the length of any possible mutual suture wasn't described and cannot be inferred. *S. harrisonii, L. venezuelae, P. mongoliensis, Y. downsi*, *S. valdensis* and *K. zabaikalicus* were corrected and coded (0). *H. tucki* was corrected and coded (1).

294(*). Femur, shape in medial/lateral view: bowed anteriorly along length (0), straight (1) (McDonald et al. 2010 #121; Ösi et al. 2012 #197).

Note that Winkler et al. (1997) do neither mention nor figure the femur of *Tenontosaurus dossi* in medial or lateral view, so we don't follow Andrzejewski et al. (2019 #197) in coding this taxon (0). Bell et al. (2019, p. 9) argue that the femur of *Fostoria dhimbangunmal* was dorsoventrally crushed, although there is no *a priori* reason to believe that as both medial and lateral posterodistal condyles are present and well developped (Bell et al. 2019, fig. 8A, E). *F. dhimbangunmal* was corrected and coded (1).

296(*). Femur, femoral head: confluent with greater trochanter, *fossa trochanteris* consists in a smooth and shallow groove (0), *fossa trochanteris* is modified into distinct constriction separating head and greater trochanter (1) (rephrased from Ösi et al. 2012 #198).

The fossa trochanteris is smooth and shallow in *Tenontosaurus tilletti* (Forster 1990, fig. 19A) and Tenontosaurus dossi (Winkler et al. 1997, fig. 18D). This character could not be safely inferred for *Talenkauen santacrucensis* owing to its mediolateral crushing (Rozadilla et al. 2019, fig. 23). *T. tilletti* and *T. dossi* were corrected and coded (0). *T. santacrucensis* was corrected and coded with a question mark.

297(*). Femur, anterior extension of the greater trochanter beyond the femoral head: almost inexistent (0), shortly expanded and thick anteriorly (1), moderately to very elongated (2) (modified from Rozadilla et al. 2016 #231).

In *Homalocephale calathocercos* (Maryanska and Osmolska 1974, fig. 5C1), the greater trochanter is widely expanded anterolaterally. This is similar to the condition observed in the Asian Clade (represented by *Jeholosaurus shangyuanensis*: Han et al. 2012, fig. 10G, and *Changchunsaurus parvus*: Butler et al. 2011, fig. 6C), *Orodromeus makelai*, *Kangnasaurus coetzeei*, *Morrosaurus antarcticus*, *Anabisetia saldiviae*, *Gasparinisaura cincosaltensis* (see Rozadilla et al. 2016, fig. 3). *Fruitadens haagarorum* (Carpenter and Galton 2018, fig. 5GG), *Heterodontosaurus tucki* (Galton 2014, fig. 13D), *Yinlong downsi* (Han et al. 2018, fig. 12G), *Thescelosaurus assiniboiensis* (Brown et al. 2011, fig. 20E) bear a shortly expanded and thick

greater trochanter. With the new definition of this character, *F. haagarorum*, *H. tucki*, *Y. downsi*, T. *assiniboiensis* were corrected and coded (1). *H. calathocercos*, *J. shangyuanensis*, *C. parvus*, *O. makelai*, *K. coetzeei*, *M. antarcticus*, *A. saldiviai*, *G. cincosaltensis* were corrected and coded (2).

298(*). Anterior trochanter, level with respect to the greater trochanter: well below (0), from moderately below to slightly below the level of the greater trochanter (1) level or higher (2) (modified from: Boyd 2015 #215; Ösi et al. 2012 #200).

Primitive ornithischians such as *Scutellosaurus lawleri* (Colbert 1981), *Hexinlusaurus multidens* (He and Cai 1984, fig. 18C), *Agilisaurus louderbacki* (Peng 1992, fig. 6) feature a neatly lowered lesser trochanter. In *Psittacosaurus mongoliensis*, the lesser trochanter ends slightly below the greater trochanter (Osborn 1924, fig. 4). *Fruitadens haagarorum* (Butler et al. 2009, fig. 2G, H), *Heterodontosaurus tucki* (Galton 2014, fig. 12A, C), *Jeholosaurus shangyuanensis* (Han et al. 2012, fig. 10), *Koreanosaurus boseongensis* (Huh et al. 2010, fig. 16B), *Yinlong downsi* (Han et al. 2018, fig. 12A, C, E), *Nanosaurus agilis* (Galton and Jensen 1973, fig. 5A), *Haya griva* (Makovicky et al. 2011, fig. 5B), *Morrosaurus antarcticus* (Rozadilla et al. 2016, fig. 2A), *Camptosaurus dispar* (Gilmore 1909, fig. 33), *Iguanodon bernissartensis* (Verdu et al. 2017, fig. 13), the Vegagete ornithopod (Dieudonné et al. 2016a, fig. 8A2), *Zalmoxes shqiperorum* (Godefroit et al. 2009, fig. 19D), *Zalmoxes robustus* (Weishampel et al. 2003, fig. 23D), *Thescelosaurus assiniboiensis* (Brown et al. 2011, fig. 20), *Dryosaurus altus* (Galton 1981, fig. 13A), *Tenontosaurus tilletti* (Forster 1990, fig. 19B), *Gasparinisaura cincosaltensis* (Cambiaso 2007, fig. 70B), *Muttaburrasaurus langdoni* (Bartholomai and Molnar, fig. 9D) all feature a lesser trochanter wich rises from moderately below to almost level with the greater trochanter. The anterior lesser trochanter of *Anabisetia saldiviai* (Coria and Calvo 2002, fig. 7), *Valdosaurus canaliculatus* (Barrett et al. 2011, fig. 6), *Dysalotosaurus lettowvorbecki* (Janensch 1955, pl. 14-2; Galton 1981, fig. 14A, C, G, I)

and *Dryosaurus altus* (Galton 1981, fig. 13C) reaches the upper level of the fourth trochanter. *Homalocephale calathocercos* lacks its greater and lesser trochanters (Maryanska and Osmolska 1974, p. 91). In *Thescelosaurus neglectus* the lesser trochanter appears to be either slightly lower or level with the greater trochanter depending on the view and drawings (Gilmore 1915, fig. 12, 14), so we could not code for this taxon. *A. saldiviai* and *Dryosaurus* were corrected and coded (2). *H. griva*, *J. shangyuanensis*, *G. cincosaltensis*, *F. haagarorum*, *H. tucki*, *K. boseongensis*, *N. agilis*, *C. dispar*, *I. bernissartensis*, *A. saldiviai*, *G. cincosaltensis*, *M. antarcticus*, the Vegagete ornithopod, *Z. robustus* and *Z. shqiperorum* were corrected and coded (1). *P. mongoliensis* was newly coded (1). *H. calathocercos* was corrected and coded with a question mark.

299(*). Anterior trochanter of femur in proximal view: positioned anterior to greater trochanter (0), possess a beveled posterior surface (anteromedial to posterolateral in direction), so that it appears positioned somewhat anterolateral to the greater trochanter (1), L-shaped anterior trochanter with very thin edges bordering both anterior and lateral sides of the greater trochanter (2) (modified from Boyd 2015 #216).

In *Haya griva* (Mackoviky *et al*. 2011, fig. 5B) and *Jeholosaurus shangyuanensis* (Han et al. 2012, fig. 10G), the lesser trochanter appears to be "L-shaped" around the lateral and anterior surfaces of the greater trochanter. However, unfortunately, in *Haya griva*, the proximal view is unavailable and in *Jeholosaurus shangyuanensis*, the exact proximal outline of the femur is unclear. Because of these reasons we decided not to code the latter two taxa. *Rhabdodon priscus* (Matheron 1869, pl. 5-14) possesses a lesser trochanter positionned anterior and somewhat lateral to its greater trochanter. This character is not described for *Agilisaurus louderbacki* (Peng 1992). *R. priscus* was corrected and coded (1). *A. louderbacki* was corrected and coded with a question mark.

300(*). Posterolateral edge of the greater trochanter : globular and rounded (0), triangular, the lateral edge of the greater trochanter is globally flatenned (1) (reformulated from Boyd 2015 #213).

The lateral surface of the greater trochanter is flat in *Yueosaurus tiantaiensis* (Zheng et al. 2012, fig. 5A). The lateral side of the greater trochanter of *Agilisaurus louderbacki* was told to be 'unevenly concave and convex' (Peng 1992), so the exact state of character is unknown for this taxon. The posterolateral edge of the greater trochanter appears definitely globular and rounded in *Gasparinisaura cincosaltensis* as in *Anabisetia saldiviai* (Cambiaso 2007, fig. 116E, E'), *Morrosaurus antarcticus* (Rozadilla et al. 2016, fig. 2E), and *Kangnasaurus coetzeei* (Cooper 1985, fig. 17). *Y. tiantaiensis* was corrected and coded (1). *G. cincosaltensis* was corrected and coded (0). *A. louderbacki* was corrected and coded with a question mark.

302(*). Femur, fourth trochanter position: located entirely on proximal half of femur (0) or positioned at mid-length, or distal to mid-length (1) (Ösi et al. 2012 #202).

The fourth trochanter is located on the proximal half of the femoral shaft in *Talenkauen santacrucensis* (Rozadilla et al. 2019, fig. 23B, C). *T. santacrucensis* was corrected and coded (0).

303(*). Femur, pendent fourth trochanter, rod-like with subparallel anterior and posterior surfaces: absent (0), present (1) (Ösi et al. 2012 #224).

In *Yinlong downsi*, the fourth trochanter is strongly pendant with subparallel anterior and posterior surfaces in IVPP V14530 and IVPP V18679, and it is pendant though more club-shaped in IVPP V18684 (Han et al. 2018, fig. 12B, C, E). In *Koreanosaurus boseongensis*, the fourth trochanter is very thin and hook-shaped (Huh et al. 2010, fig. 16B). Note that the fourth trochanter of *Haya griva* (Makovicky et al. 2011, fig. 5A-D) also has a hook-shaped appearance but it is much more massive and its distal end is more triangular-shaped. *Y.*

downsi was corrected and coded as polymorphic with character states (0) and (1). *K. boseongensis* was corrected and coded (1).

304(*). Femur, location of insertion scar of *M. caudifemoralis longus*: extends from fourth trochanter onto medial surface of femoral shaft (0), widely separated from fourth trochanter, restricted to medial surface of femoral shaft (1) (McDonald et al., 2010 #125).

We note a striking resemblance between the camptosaurid *Draconyx loureori* (Mateus and Antunes 2001, fig. 6; Galton 2009, fig. 6P), *Eousdryosaurus nanohallucis* (Escaso et al. 2014, fig. 4A), dryosaurids and *Anabisetia saldiviai* (Coria and Calvo 2002) in that they share a medial *caudifemoralis* muscle scar positionned far away anteriorly from the fourth trochanter. However, such anteriorly offset muscle scar on the medial surface of the femur was not found in camptosaurids such as *C. dispar* or *C. aphanoecetes* (Carpenter and Wilson 2008; Galton 2009). *A. saldiviai* was corrected and coded (1).

305(*). Femur, anterior (extensor) intercondylar groove: absent (0), shallow and wide open through with sides that diverge from each other cranially (1), deep and narrow open through with parallel sides (2) (modified from McDonald et al. 2010 #127; Ösi et al. 2012 #203).

We modified the character to include the cases in which there is no extensor groove on the distal part of femur. There is no extensor groove in *Yinlong downsi* (Han et al. 2018, fig. 12J), *Orodromeus makelai* (Scheetz 1999, fig. 28C), *Nanosaurus agilis* (Galton and Jensen, fig. 5A). By contrast, the pachycephalosaurs *Homalocephale calathocercos* and *Prenocephale prenes* (Maryanska and Osmolska, 9174, pl. 31-1A, 2A respectively), *Thescelosaurus neglectus* (Gilmore 1915, p. 604), *Anabisetia saldiviai* (Cambiaso 2007, fig. 116F), *Morrosaurus antarcticus* (Rozadilla et al. 2016, fig. 2G), *Muttaburrasaurus langdoni* (Bartholomai and Molnar, 1981, fig. 9G), *Kangnasaurus coetzeei* (Cooper 1985, fig. 16), *Rhabdodon priscus* (Matheron 1869, pl. 5-3A), *Rhabdodon* sp. from Vitrolles (Pincemaille-Quilleveré 2002, p. 61, fig. 18.2), *Zalmoxes robustus*, *Zalmoxes shqiperorum* and the

Vegagete ornithopod (Dieudonné et al. 2016a, fig. 16A, B, D respectively) all display a shallow extensor groove on the distal part of their femur. The extensor through in the femur of *Tenontosaurus tilletti* is described as broad and shallow as well, although it appears a more profound distally than in above-cited taxa (Forster 1990, p. 287, fig. 19). *Fostoria dhimbangunmal* (Bell et al. 2019, fig. 8E) and *Muttaburrasaurus langdoni* (Molnar 1996, fig. 11) possess a relatively deep and wide anterior intercondylar groove on their distal femur, which differ from characteristically deep and narrow anterior groove of camptosaurids (Gilmore 1909, p. 260; Carpenter and Wilson 2008), *Iguanodon bernissartensis* (Norman 1980, fig. 68) and *Dryosaurus altus* (Galton 1981, fig. 13B). The deepness and narrowness of the anterior intercondylar groove appears to vary depending on the specimens in *Dysalotosaurus lettowvorbecki* (Galton 1981, fig. 14F, L) so we corrected and coded this taxon as polymorphic (1, 2). *Y. downsi*, *O. makelai*, *N. agilis* were corrected and coded (0). *T. neglectus*, *A. saldiviai*, *M. antarcticus*, *M. langdoni*, *K. coetzeei*, *R. priscus*, *R.* sp1 (Vitrolles), *Z. robustus*, *Z. shqiperorum*, the Vegagete ornithopod and *F. dhimbangunmal* were corrected and coded (1). *C. dispar*, *I. bernissartensis*, *Dryosaurus*, *D. lettowvorbecki* were corrected and coded (2).

306(*). Femur, posterior (flexor) intercondylar groove: fully open (0), medial condyle inflated laterally, partially covers opening of flexor groove (1) (modified from Butler et al. 2011; Ösi et al. 2012 #204).

Orodromeus makelai features the derived trait of a medial condyle medially inflated covering the posterior popliteal groove (Scheetz 1999, fig. 28C). *O. makelai* was corrected and coded (1). *Thescelosaurus neglectus* (Gilmore 1915) was corrected and coded with a question mark for this character.

307(*). Femur, posterolateral condyle position and size in ventral view: positioned relatively laterally and slightly narrower in width than the medial condyle (0), strongly inset medially, reduced in width relative to medial condyle (1) (modified from Ösi et al. 2012 #205).

The posterolateral condylid is relatively wide but strongly inset medially in *Orodromeus makelai* (Scheetz 1999, fig. 28C). *O. makelai* was corrected and coded (1) instead of its previous polymorphic state which in fact corresponded to an unknown character state in this case.

309(*). Femur proportions in distal view by taking the iliofibularis groove as a reference point whenever possible or the posterior intercondylar groove in all other cases: maximum anteroposterior length of the distolateral condyle (without considering the posterolateral condylid) out of distal width: ≥ 50% (0), between 40 and 50% (1), < 40% (2).

N.B. taxa for which the distolateral condylid was not medially inset were still coded as long as the anterior limit of the distolateral condylid could be demarcated in some way. Whenever this could not be achieved, the anterior edge of the posterior intercondylar groove was used as a reference for measuring the distolateral anteroposterior length (e.g. in *F. haagarorum*, Carpenter and Galton 2018, fig. 5KK). Distal proportions of the femur in rhabdodontids are about ≈ 35% in *Z. robustus* (Dieudonné et al. 2016a, fig. 16A), ≈ 37% in *Z. shqiperorum* (Brusatte et al. 2017, fig. 6F), ≈ 37% in the Vegagete ornithopod (MDS-VG, 132, 134 and 135, Dieudonné et al. 2016a, 8D2, 16D and pers. obs.). *F. dhimbangunmal* (≈ 37%, Bell et al. 2019, fig. 8E) share with rhabdodontids its extremely wide and anteroposteriorly short distal proportions of femur. By contrast, *M. langdoni* (≈ 41% along with Bartholomai and Molnar, 1981, fig. 9G), *T. tilletti* (≈ 42%, Forster 1990, fig. 19), *C. dispar* (≈ 46.6%, Galton 2009, fig. 12H), *M. antarcticus* (≈ 42.9%, Rozadilla et al. 2016, fig. 2G), *A. saldiviai* (between ≈ 47.4% and ≈ 42.3%, Cambiaso 2007, fig. 116F, F'), *K. coetzeei* (Cooper 1985, fig. 16), *C. marri* (Andrzejewski et al. 2019, fig. 23E), *K. boseongensis* (Huh et al. 2010, fig. 16C) have

length/width proportions superior to 40% but never more than 50%. Many ornithopods, marginocephalians and more phylogenetically nested ornithischians have distal femoral proportions superior to 50%. We could cite the dryomorphs *D. altus* (≈ 52%, Galton 1981, fig. 13B), *D. lettowvorbecki* (between ≈ 53% and ≈ 61% Galton 1981, fig. 14F, L), *V. canaliculatus* (≈ 54.6%, Barrett et al. 2011, pl. 1.6, 1.12), *I. bernissartensis* (≈ 72%, Norman 1980, fig. 58). Amongst other cerapods, we might cite *G. cincosaltensis* (≈ 58.3%, Salgado et al. 1997, fig. 4.6), *N. comodorensis* (≈ 51.4%, Cambiaso 2007, fig. 87E'), *H. foxii* (> 58%, Galton 1974*a*, fig. 54F; Herne 2014, fig. 9.38), *O. makelai* (≈ 51.5%, Scheetz 1999, fig. 28C), *T. assiniboiensis* (≈ 50%, Brown et al. 2011, fig. 20F), *H. tucki* (≈ 71%, Galton 2014, fig. 13G), *F. haagarorum* (≈ 69%, Carpenter and Galton 2018, fig. 5KK), *Y. downsi* (≈ 58.5%, Han et al. 2018, fig. 12J), *J. shangyuanensis* (≈ 60%, Herne 2014, fig. 9.38), *N. agilis* (≈ 55%, Galton and Jensen 1973, fig. 5A), *H. multidens* and *Y. hongheensis* (≈ 96.7% and ≈ 61.4%, He and Cai 1984, fig. 18C, 29A respectively). Such a high ratio could also be measured in the basal ornithischian *L. diagnosticus* (≈ 58%, Thulborn 1972, fig. 10), *E. parvus* (≈ 62.5%, Butler 2010, fig. 15F) and in the outgroup taxon *H. ischigualastensis* (≈ 75%, Novas 1994, fig. 7F). *L. venezuelae* (≈ 41% Barrett et al. 2014, fig. 1G) and *S. stenops* (very wide proportions, cf. Maidment et al. 2015, fig. 72F, L) are exceptions amongst basal ornithischians.

310(*). Tibia, lateral fibular condyle from an anteroposterior view: gradually and merges with the shaft distally (0), defines an abrupt overhanging buttress with sub-horizontal ventral margin above the shaft (1).

Tenontosaurus tilletti (Forster 1990, fig. 20A), dryosaurids (Janensch 1955, pl. 14.3B; Galton 1981, fig. 16F; Barrett et al. 2011, fig. 7A; Escaso et al. 2014, fig. 4K), *Iguanodon bernissartensis* (Norman 1980, fig. 69A), but also *Orodromeus makelai* (Scheetz 1999, fig. 29A), *Gasparinisaura cincosaltensis* (Salgado et al. 1997, fig. 4.7) and *Talenkauen*

santacrucensis (Cambiaso 2007, fig. 35C-D), *Anabisetia saldiviai* (Cambiaso 2007, fig. 117A, C), *Jeholosaurus shangyuanensis* (Han et al. 2012, fig. 11K-L), *Nanosaurus agilis* (SMA 006 which should be a left tibia, cf. Carpenter and Galton 2018, fig. 16O) all have their tibial fibular condyle forming an abrupt lateral buttress above the shaft. An overhanging fibular butress seems to be present in *Muttaburrasaurus langdoni* although closer photograph would be better to determine this more precisely (Bartholomai and Molnar, 1981, fig. 10). *Camptosaurus dispar* and *Camptosaurus aphanoecetes* (Galton 2009, fig. 12O; Carpenter and Galton 2018, fig. 26Q, V) differ from the above-mentionned taxa in that their outer fibular condyle merges gradually with the tibial shaft distally. In rhabdodontids, the outer fibular condyle also appears to merge gradually with the shaft distally (e.g. *Zalmoxes shqiperorum*, Brusatte et al. 2017, fig. 18B, D; the Vegagete rhabdodontid, Dieudonné et al. 2016a, fig. 9A1, B1).

311(*). Tibia, cnemial crest from a proximal view: straight, faces anteriorly (0), strongly bent laterally (1) (new character).

Hypsilophodon foxii (Galton 1974*a*, fig. 56E), *Orodromeus makelai* (Scheetz 1999, fig. 29C), *Thescelosaurus assiniboiensis* (Brown et al. 2011, fig. 21D, E), *Thescelosaurus neglectus* (Galton 1974*b*, fig. 3A), *Dryosaurus altus* (Galton 1981, fig. 16E), *Nanosaurus agilis* (Galton and Jensen 1973, fig. 5B-C), *Camptosaurus aphanoecetes* (Carpenter and Wilson 2008, fig. 31E) all share the presence of a strongly laterally turned cnemial crest, which appear to contrast with all other ornithopods which bear a rather straight, anteriorly facing cnemial crest. In *Parksosaurus warreni*, the precnemial crest is well excavated for the reception of the fibular head and well visible from a posterior view (Parks 1926, fig. 13, p. 32); it is also forms a strong lateral expansion from an anterior view which strongly suggests that it was confluent with the cnemial crest itself. The posterior inner condyle is also visible from an anterior view, which further adds to the former idea that the proximal head of tibia is in fact strongly bent

anterolaterally (Parks 1926, fig. 13). *Heterodontosaurus tucki* and *Fruitadens haagarorum* (Galton 2014, fig. 14E, F and 14M respectively) have their cnemial crest laterally bent. The cnemial crest appears thick and craniolaterally oriented in *Eocursor parvus* (Butler 2010, fig.16E).

314(*). Fibula, proximal head: moderately expanded at both sides (0), features a major anterior expansion of its anteroproximal corner (1) (new character).

Tenontosaurus tilletti (Forster 1990, fig. 20C), *Camptosaurus dispar* and *Camptosaurus aphanoecetes* (Carpenter and Wilson 2008, fig. 26Y, 26BB), *Iguanodon bernissartensis* (Norman 1980, fig. 69D) differ from dryosaurids and more basally stemming ornithopods in having a prominent anterior projection of their fibular head. This condition also occurs convergently in *Heterodontosaurus tucki* (Galton 2014, fig. 14B), but is absent in *Fruitadens haagarorum* (Carpenter and Galton 2018, fig. 5NN).

316(*). Fibula, distal end is strongly reduced and splint-like: absent (0), present (1) (Ösi et al. 2012 #225).

The distal fibula of *Yinlong downsi* is described by Han et al. (2017) as being persistently reduced toward the distal extremity, but not as much as what occurs for heterodontosaurids. We follow Han et al. (2017 #363, same character) and newly code (0) for *Yinlong downsi*. In *Tianyulong confuciusi* (Sereno 2012, p. 68) and *Stegoceras validum* (Gilmore 1924, pl. 22.2), the fibula tapers distally to a slender rod. *T. confuciusi* was corrected and coded (1).

317(*). Astragalus/calcaneum, indistinguishable and fused to one another: absent (0), present (1) (Ösi et al. 2012 #226).

Scheetz (1999, p. 68) states that the astragalus and calcaneum are indistinguishably fused in *Zephyrosaurus schaffi*, as also occurs for *Orodromeus makelai*. We followed Scheetz (1999) and newly coded (1) for *Z. schaffi*. *Kangnasaurus coetzeei* (Cooper 1985) has unfused proximal tarsals, so this taxon was corrected and coded (0).

318(*). Astragalus, anterior process: moderate to high, from tooth-like to wide anteriorly (0), low to absent (1) (modified from Brown et al. 2013 #118).

In *Jeholosaurus shangyuanensis* (Han et al. 2012, fig. 11O) the anterior ascending process of the astragalus is conspicuous and somewhat tooth-like. The anterior ascending process of astragalus was incorrectly thought to be high in the Vegagete ornithopod, because it was confounded with an anterodistal splint of bone (Dieudonné et al. 2016a, fig. 9D2). It is actually very low to absent in this taxon (pers. observation). *Zalmoxes robustus* (Weishampel et al. 2003, p. 94), *Muttaburrasaurus langdoni* (Bartholomai and Molnar, 1981, fig. 10D), *Tenontosaurus tilletti* (Forster 1990, fig. 20A), *Tenontosaurus dossi* (Winkler et al. 1997), *Talenkauen santacrucensis* (Cambiaso 2007, fig. 36A), *Anabisetia saldiviai* (Cambiaso 2007, fig. 119A), *Gasparinisaura cincosaltensis* (Cambiaso 2007, fig. 73B), and the dryomorphs *Dryosaurus altus* (Galton 1981, fig. 15A) and *Dysalotosaurus lettowvorbecki* (Janensch 1955, pl. 14-5A), *Camptosaurus dispar* (Gilmore 1909, p. 262), *Iguanodon bernissartensis*, Norman 1980, fig. 69A), all bear a low to absent anterior ascending process of astragalus. Such character is unknown and not formally described for *Zephyrosaurus schaffi* so far (Sues 1980, Scheetz 1999). *J. shangyuanensis* was corrected and coded (0). The Vegagete ornithopod, *M. langdoni*, *Z. robustus, T. tilletti*, *T. dossi*, *T. santacrucensis*, *A. saldiviai*, *G. cincosaltensis*, *D. altus*, *D. lettowvorbecki*, *C. dispar*, *I. bernissartensis* were corrected and coded (1). *Z. schaffi* was corrected and coded with a question mark.

319(*). Astragalus, posterior side size: low (0), high (1) (Brown et al., 2013 #117).

In *Nanosaurus agilis*, Galton and Jensen (1973) states that the calcaneum is almost identical to that of *D. Lettowvorbecki*, *D. altus*, and *H. foxii*. However, the first two were coded (1) and the latter was coded (0) in previous data-sets (Brown et al., 2013 #117). *Nanosaurus agilis* displays no astragalus posterior process when viewed from a medial view (Galton and Jensen 1973, fig. 5D), as *Hypsilophodon foxii* (Galton 1974*a*, fig. 57B) and contrary to *Dryosaurus*

altus (Galton 1981, fig. 18C, D). The astragalus posterior process appears either little developped or inexistent in *Hexinlusaurus multidens* (He and Cai 1984, fig. 18D), *Jeholosaurus shangyuanensis* (Han et al. 2012, fig. 11I, S), *Yinlong downsi* (Han et al. 2018, fig. 13B), *Fruitadens haagarorum* (Butler et al. 2012, fig. 14C, K), *Heterodontosaurus tucki* (Galton 2014, fig. 14H), *Homalocephale calathocercos* (Maryanska and Osmolska 1974, pl. 30-3A). The astragalus posterior process is well developped in *Orodromeus makelai* (Scheetz 1999, fig. 30B) as well as in the elasmarian *Talenkauen santacrucensis* (Cambiaso 2007, fig. 36). *N. agilis, H. Multidens, J. shangyuanensis, Y. downsi, F. haagarorum, H. tucki* were corrected and coded (0). *T. santacrucensis* and *O. makelai* were corrected and coded (1).

320(*). Astragalus, fibular facet on the lateral margin of the proximal surface: large (0), reduced to small articulation or absent (1) (rephrased from Ösi et al. 2012 #207).

The nature of such contact is not known in *Orodromeus makelai* (Scheetz 1999), *Psittacosaurus mongoliensis* (Osborn 1923, 1924) or *Psittacosaurus major* (Sereno et al. 2007; You et al. 2008). *O. makelai* and Psittacosauridae were newly corrected and coded with a question mark.

321(*). Calcaneum, tibial articular surface from a lateral view: facet for tibia absent (0), facet for tibia present and subequal in length to that for the fibula (1), facet for tibia longer than the facet for the fibula, and the posteroventral part of the calcaneum is elongated into a distinct caudal process (2) (modified from Ösi et al. 2012 #208, Rozadilla et al. 2016 #236).

Within Tyreophora, *Stegosaurus stenops* features a very wide fibular facet and would have had the very primitive trait of an absence of contact between the calcaneum and the lateral maleollus of tibia (Maidment et al. 2015). None of the previous publication concerning the proximal tarsals of *Scelidosaurus harrisonii* allow to code for this character state (Owen 1861; Newman 1968). In *Tenontosaurus tilletti*, the calcaneum lacks a posteroventral lip (Forster, pers. comm.). In *Archaeoceratops oshimai* (You and Dodson 2003, fig. 4E), a small

posterior lip is present but the facet for the contact with the tibial malleolus is subequal to shorter than that for the fibula. *Fruitadens haagarorum* (Butler et al. 2012, fig. 14L), as well as the dryomorphs *Dysalotosaurus lettowvorbecki* (Janensch 1955, pl. 14-7B) and *Dryosaurus altus* (Galton 1981, fig. 15C-D) display a posteroventrally expanded lip. The calcaneum of *Zalmoxes robustus* features a thick posteroventral expansion when seen from a lateral view (Weishampel et al. 2003, fig. 24). However, Weishampel et al. (2003) affirms the presence of a lateral thin edge lying between the concave lateral surface and the tibial facet, which should hinder the observation of a more pronounced posterior lip. The calcaneum of *Z. shqiperorum* would also be roughly similar to that of *Z. robustus* (Weishampel et al. 2003, cf. fig. 34E, F). Notwithstanding, the drawing doesn't allow to confirm the presence of such posteroventral expansion. A posteroventral expansion similar to that of *Z. robustus* is present in a yet undescribed calacaneum that belongs to the Vegagete rhabdodontid (pers. obs.). It will be fully described in a future publication. This feature is unfortunately not observable in *Heterodontosaurus tucki* (Galton 2014, fig. 14J), and the calcaneum is broken off posteroventrally in *Muttaburrasaurus langdoni* (Herne, pers. comm.). Stegosauria was corrected and coded (0). *A. oshimai*, *F. haagarorum*, *D. lettowvorbecki*, the Vegagete rhabdodontid were corrected and coded (2). *M. langdoni*, *S. harrisonii* as well as *Z. robustus* and *Z. shqiperorum* were corrected and coded with a question mark pending further verification.

322(*). Calcaneum, angle between the edge separating the tibial and fibular articular facets, and the lateral border of the calcaneum on the posterior side: greater than 110 degrees (0), less than 110 degrees (1) (modified from Brown et al. 2013 #119).

In *Hypsilophodon foxii* (Galton 1974*a*, fig. 57A) and *Thescelosaurus neglectus* (Galton 1974*b*, see fig. 3L) the angle between the fibular and tibial facets retains the plesiomorphic state and is higher than 110°. In *Talenkauen santacrucensis* (Cambiaso 2007, fig. 37C),

Tenontosaurus tilletti (Forster, pers. comm.), *Dysalotosaurus lettowvorbecki* (Janensch 1955, pl. 14-7A, B) the angle between the tibial and the fibular facet is less than 110°. No detailed description of this character is provided for *Nanosaurus agilis* (Galton and Jensen 1973), *Gasparinisaura cincosaltensis* (Coria and Salgado 1996; Salgado et al. 1997; Cambiaso 2007), *Tenontosaurus dossi* (Winkler et al. 1997), and *Parksosaurus warreni* (Parks 1926). *H. foxii* and *T. neglectus* were corrected and coded (0). *T. santacrucensis*, *T. tilletti* were corrected and coded (1). *N. agilis*, *G. cincosaltensis*, *T. dossi*, *P. warreni* were corrected and coded with a question mark. This character was also corrected and coded for the Vegagete rhabdodontid based on a new, yet unpublished specimen (pers. obs.).

323(*). Medial distal tarsal, shape: blocky in dorsal view (0), thin and rectangular (1), round (2) (Brown et al., 2013 #120).

Both the medial tarsal of *Heterodontosaurus tucki* (Galton 2014, fig. 15L) and *Goyocephale lattimorei* (Perle et al. 1982, pl. 44.5A) are blocky in dorsal view. In *Dysalotosaurus lettowvorbecki* the distal medial tarsal is roughly lozenge-shaped to sub-rectangular in outline (Janensch 1955, pl. 14-8). In *Muttaburrasaurus langdoni*, the metatarsals III and IV were formerly misinterpreted as metatarsals III and II (cf. Herne et al. 2018, fig. 32O; Herne, pers. comm.). The distal tarsal 2 was reported to be fully preserved above metatarsal III, and attached to a tiny, distal tarsal 1 (Bartholomai and Molnar, 1981). Owing to its position above the metatarsal, we consider that the distal tarsal 2 corresponds to the medial distal tarsal. The distal tarsal 2 is described as hexagonal, but is actually much rounded from the illustration (Bartholomai and Molnar, 1981, fig. 12A). One of the distal tarsals of *Parksosaurus warreni* (Parks 1926) is described as being roughly elliptical in outline. It would most probably represent the distal medial tarsal, but without any illustration it is very hazardous to code for this taxon. The medial distal tarsal of *Yinlong downsi* is told to have rounded borders. Though, this doesn't discriminate between either a possibly "blocky" or "rounded" distal

tarsal, so we left this taxon uncoded pending revision. *M. langdoni* was corrected and coded (2). *D. lettowvorbecki* was corrected and coded (1). *G. lattimorei* was corrected and coded (0). *P. warreni* was corrected and coded with a question mark.

324(*). Medial distal tarsal: articulates distally with metatarsal III only (0), articulates distally with metatarsals II and III (1) (Ösi et al. 2012 #209).

In *Homalocephale calathocercos*, Maryanska and Osmolska (1974, p. 92) state that the third lateral distal tarsal is preserved and articulated above the proximal articular surfaces of metatarsals II and III. Such position is unlikely for a third distal tarsal: it should in fact represent the medial distal tarsal, just as for *Goyocephale lattimorei* (Perle et al. 1982). No modification of character coding was required, which somewhat confirms that the medial distal tarsals of *H. calathocercos* and *G. lattimorei* contact both metatarsals II and III. Han et al. (2017, p. 19) state that the medial distal tarsal of *Yinlong downsi* articulates with metatarsal 3 only. *Heterodontosaurus tucki* was previously thought to bear 2 distal tarsals, one medial and one lateral (Sereno 2012). However, the medial tarsal in fact corresponds to two faintly separated tarsals (DT 1 and DT 2); *H. tucki* therefore bear 3 distal tarsals (Galton 2014) which articulate distally with metatarsals II, III, and a small part of metatarsal IV. Han et al. (2012) note that in *Jeholosaurus shangyuanensis* and *Orodromeus makelai* the medial tarsal probably represents distal tarsals 1 and 2. On the other hand, distal tarsal 3 remains in the same position – i.e. above metatarsal IV – in very distantly related ornithischians (e.g. *Dryosaurus altus* in Galton 1981, fig. 15E). We therefore consider here that the medial tarsal which is dealt about here corresponds to the contour of both DT 1 and DT 2 on juxtaposition. Owing to the earlier comment made on the medial distal tarsal of *M. langdoni* (cf. previous character), the medial distal tarsal of *M. langdoni* would articulates distally only with the third metatarsal. *M. langdoni* and *Y. downsi* were corrected and coded (0). *H. tucki* was corrected and coded (1).

325(*). Lateral distal tarsal, shape in dorsoventral view: square (0), kidney-shaped (1), sub-triangular (2) (modified from Brown et al. 2013 #122).

The lateral distal tarsal looks triangular in *Herrerasaurus ischigualastensis* (Novas 1994, fig. 9F-G), *Homalocephale calathocercos* (Perle et al. 1982, pl. 44.5) and *Heterodontosaurus tucki* (Galton 2014, fig. 15L). Note that it is also medially concave in the last two, and such concavity is more pronounced in *Heterodontosaurus tucki* (Galton 2014, fig. 15L). The lateral distal tarsal is kidney-shaped (i.e. with a straight to slightly concave medial contour and convex lateral contour) in *Dysalotosaurus lettowvorbecki* (Janensch 1955, pl. 14-10, 11). In *Yinlong downsi*, Han et al. (2017, p. 19) describes a lateral distal tarsal which is at the same time "sub-rectangular" and medially concave to accommodate the medial tarsal. Congruently with previous codification, this conformation strongly suggests a "kidney-shaped" rather than a merely "squarrish" distal lateral tarsal. The lateral distal tarsal is not preserved in *Muttaburrasaurus langdoni* (Bartholomai and Molnar, 1981). *G. lattimorei*, *H. tucki* and *H. ischigualastensis* were corrected and coded (2). *Y. downsi* and *D. lettowvorbecki* were corrected and coded (1). *M. langdoni* was corrected and coded with a question mark.

326(*). Metatarsal II/metatarsal III, morphology of the contact in proximal view: continuous, flat to smoothly concave anteroposteriorly (0), metatarsal II forms a lateral step over a proximal outgrowth on the ventro-medial side of the metatarsal III (1) (Dieudonné et al. 2016a #277).

In *Eocursor parvus*, the second metatarsal is dorsoventrally enlongated and devoid of any lateral step (Butler 2010, fig. 17B). In *Orodromeus makelai* (Scheetz 1999, p. 72), the proximolateral surface of MT II is flat and "snugly" articulates with MT III. In *Eousdryosaurus nanohallucis*, the second metatarsal is broadly and extensively concave laterally and overlaps the third metatarsal both ventrally and dorsally (Escaso et al. 2014, fig. 6), but without a marked lateral step. A lateral step is present in *Dryosaurus altus* although it seems fainter in *Dysalotosaurus lettowvorbecki* (Herne 2014, fig. 9.36). In *Morrosaurus*

antarcticus (Cambiaso 2007, fig. 52A; Rozadilla et al. 2016, fig. 5A) and *Kangnasaurus coetzeei* (Cooper 1985, fig. 19C) the posteromedial surface of the proximal third metatarsal remains smooth, as does the respective contact surface on the second metatarsal. Bartholomai and Molnar (1981, p. 338) stated that the proximal second metatarsal of *Muttaburrasaurus langdoni* "appeared more angular anterolaterally", a statement which made us score this taxon with character state (1) in Dieudonné et al. (2016a #277). Bell et al. (2019) stated that no evidence allowed for coding this taxon with character state (1), for which they corrected and coded this taxon with a question mark. However by that time, Herne et al. (2018, fig. 32O) had already figured a smooth proximal contact between metatarsals II and III for *Muttaburrasaurus langdoni.* The lack of step-like proximal contact is incongruent with the iguanodontian status of *M. langdoni* (Dieudonné et al. 2016a). Actually, only a few derived ornithopods such as the elasmarians *Kangnasaurus coetzeei* (Cooper 1985, fig. 19C) or *Morrosaurus antarcticus* (Cambiaso 2007, fig. 52A) feature a flat to smoothly concavo-convex and unimbricated proximal contact. In the Vegagete rhabdodontid, such step-like contact occurs only in the proximalmost extremity of the second metatarsal (pers. obs.). What recalls our attention is that Bell et al. (2019) should normally have coded *M. langdoni* with character state (0), but didn't. An important information is that the right metatarsals II and III figured by Herne et al. (2018, fig. 32O) are the same as those which Molnar (1996, fig. 10) mistakenly confounded with left MT-III and IV (Herne, pers. comm.). A proximal extremity of MT-III was described by Bartholomai and Molnar (1981, p. 337) as "waisted" in proximal appearance, although incompletely preserved proximally. Such description fits perfectly with the proximal extremity of MT-II that was figured by Herne et al. (2018, fig. 32O). Although this keeps being a supposition, the proximal extremity of MT-II might correspond to the proximal MT-III described by Bartholomai and Molnar (1981) and thus be incomplete in *M. langdoni*. On what regards *Talenkauen santacrucensis*, only diaphyseal fragments of

metatarsal II and III are present (Rozadilla et al. 2019). *E parvus*, *O. makelai*, *M. antarcticus*, *K. coetzeei* and *D. lettowvorbecki* were corrected and coded (0). *T. santacrucensis* was corrected and coded with a question mark. We followed Bell et al. (2019) and corrected and coded *M. langdoni* with a question mark.

327(*). Metatarsal II, width of proximal articular surface at mid dorsoplantar height (at the level of its lateral "step" whenever present): inferior to 75% the maximum width of MT III (0), exceeds 75%, but is still below 100% of MT III maximum width (1), equals or exceeds 100% the maximum width of MT III (2) (new character).

The width of MT II should be measured at mid-height, although whenever a lateral "step-like" process occurs (cf. character above), we here regard the width of MT II at the level of that lateral "step" (cf. previous character). This was specified as the second metatarsal of *Tenontosaurus tilletti* and *Iguanodon bernissartensis* is massive, but their lateral step occurs above 50% of the total dorsoplantar height of their MT II (Forster 1990, fig. 22A; Norman 1980, fig. 70). In *Thescelosaurus assiniboiensis*, the second metatarsal is relatively massive at mid-height but only two third the maximum width of MT III (Herne et al. 2018, fig. 32R). By contrast, the second metatarsal of *Parksosaurus warreni* (Herne et al. 2018, fig. 32Q) and *Convolodaurus marri* (Andrzejewski et al. 2019, fig. 26B), *Tenontosaurus tilletti* (Forster 1990, fig. 22A), *Muttaburrasaurus langdoni* (Herne et al. 2008, fig. 32O) and the Vegagete rhabdodontid (Dieudonné et al. 2016a, fig. 15C) appears very large with respect to MT III, so that it equals or exceeds its width. In *Talenkauen santacrucensis*, the proximalmost extremity of the third metatarsal is missing (Rozadilla et al. 2019) but it should not have enlarged much from the preserved portion. The second metatarsal clearly oversizes 75% of the maximum width of MT III (Herne et al. 2018, fig. 32P), unlike the condition found in most other elasmarians and dryosaurids.

328(*).Metatarsal III, dominance of proximal articular surface, width of MT III largely exceeds width of metatarsal IV (by omitting the eventual posteromedial process of MT IV and associated caudolateral notch on MT III): absent (0), present (1) (rephrased and modified from Rozadilla et al. 2016 #232).

The original definition stands for the presence/absence of a dominant third metatarsal between the second and fourth metatarsals. However we think of that definition as somewhat imprecise and vague, so we regard that a dominant and proximally massive metatarsal occurs when its width exceeds the width of metatarsal IV. The proximal third metatarsal of *Eocursor parvus* (Butler 2010, fig. 17G) is not dominant. *Talenkauen santacrucensis* (Cambiaso 2007, fig. 40A) has a markedly less imposing third metatarsal. Rozadilla *et al*. (2019) affirm that the third metatarsal of this taxon is smaller than the fourth proximally, although it is slightly incomplete proximally. Usually, the third metatarsal doesn't expand much proximally so it is reasonnable to think that it wouldn't have formed a central, dominant element. Brusatte et al. (2017, fig. 9) figure a proximal third metatarsal of *Zalmoxes shqiperorum* which looks quite similar to that of the Vegagete rhabdodontid because of its rectangular, dorosventrally tall proximal outline. In *Iguanodon bernissartensis* (Norman 1980, fig. 70C), the third metatarsal is not dominant either. The proximal extremity of the third metatarsal is large and dominant in *Anabisetia saldiviai* (Cambiaso 2007, fig. 120B) and *Valdosaurus canaliculatus* (Barrett et al. 2011, fig. 10D, F), *Gasparinisaura cincosaltensis* (Salgado et al. 1997, fig. 5.5), *Morrosaurus antarcticus* (Rozadilla et al. 2016, fig. 5A), *Kangnasaurus coetzeei* (Herne et al. 2018, fig. 32F), *Dryosaurus altus* and *Dysalotosaurus lettowvorbecki* (Herne et al. 2018, fig. 32H, I), *Camptosaurus dispar* (Carpenter and Galton 2018, fig. 26GG, JJ). The fourth metatarsal is for now not described in *Muttaburrasaurus langdoni* (Herne, pers. comm.).

E. parvus, *T. santacrucensis*, *Z. shqiperorum*, *D. lettowvorbecki* and *I. bernissartensis* were corrected and coded (0). *C. dispar*, *D. lettowvorbecki* and *Dryosaurus* were corrected and coded (1). *M. langdoni* was corrected and coded with a question mark.

329(*). Metatarsal III and IV proximal contact, dorsolateral notch on the proximolateral surface of MT III for eventual dorsomedial overlap of metatarsal IV: absent (0), present (1) (new character).

Eousdryosaurus nanohallucis (Escaso et al. 2014, fig. 6), *Thescelosaurus assiniboiensis* (Brown et al. 2011, fig. 22C), *Gasparinisaura cincosaltensis* (Salgado et al. 1997, fig. 5.5), *Kangnasaurus coetzeei* (Herne 2014, fig. 9.36), *Valdosaurus canaliculatus* (Barrett et al. 2011, fig. 9E) and *Anabisetia saldiviai* (Cambiaso 2007, fig. 120B), *Iguanodon bernissartensis* (Norman 1980, fig. 70C), *Camptosaurus dispar* (Carpenter and Galton 2018, fig. 26JJ) share the presence of a dorsolateral notch on the proximal extremity of their third metatarsal. *Dysalotosaurus lettowvorbecki* and *Dryosaurus altus* (Galton 1981, fig. 19E; Herne 2014, fig. 9.36) also appears to have had such a notch. *Camptosaurus aphanoecetes* (Carpenter and Galton 2018, fig. 26PP), *Tenontosaurus tilletti* (Forster 1990, fig. 22A), *Muttaburrasaurus langdoni* (Herne et al. 2018, fig. 32O) and the Vegagete rhabdodontid (Dieudonné et al. 2016a, fig. 15C) are all in marked difference from the above-mentionned taxa in that they lack an anterolateral notch on their proximal third metatarsal.

330(*). Metatarsal IV, proximal extremity: sends a prominent posteromedial process toward MT III, which is eventually hosted within a deep caudolateral notch on MT III: absent (0); present (1) (rephrased from McDonald 2012 #134; Dieudonné et al. 2016a #278).

There is no caudolateral notch on the proximal fourth metatarsal of *Hexinlusaurus multidens* (He and Cai 1984, fig. 20C), *Parksosaurus warreni* (Herne et al. 2018, fig. 32Q). The third metatarsal of *Muttaburrasaurus langdoni* features a proximally flat lateral surface for articulating with the fourth metatarsal, although a small posterolateral concavity – too small

so that it could be regarded as a proper notch – is present (Herne et al. 2018, fig. 32O). A proximal fourth metatarsal might be present in *M. langdoni* but was never described (Herne, pers. comm.). The posterolateral concavity on its third metatarsal likely didn't host any prominent posteromedial process from the fourth metatarsal, although this character cannot be inferred and such concavity could have served for a fifth metatarsal. Herne (2014, fig. 9.36) and Herne et al. (2018, fig. 32H) figure a deep caudolateral notch on the proximal third metatarsal of *Dysalotosaurus lettowvorbecki* for reception of a posteromedial process from the fourth metatarsal. Such a caudolateral notch is present in *Camptosaurus dispar*, but not in *Camptosaurus aphanoecetes* (Carpenter and Galton 2018, fig. 26JJ and 26PP respectively). There is a weak, but present posteromedial process in the proximal fourth metatarsal of *Talenkauen santacrucensis* (Rozadilla et al. 2019, fig. S10E), *Dryosaurus altus* (Galton 1981, fig. 15F), *Gasparinisaura cincosaltensis* (Salgado et al. 1997, fig. 5.6), *Camptosaurus dispar* (Carpenter and Galton 2018, fig. 26GG, JJ). *H. multidens* and *P. warreni* were corrected and coded (0). *C. dispar*, *G. cincosaltensis*, *T. santacrucensis*, *Dryosaurus* and *D. lettowvorbecki* were corrected and coded (1). *D. lettowvorbecki* was corrected and coded with a question mark.

331(*). Metatarsal III and IV, proximal contact: tightly adpressed, no notch is observed posteriorly between them (0), conspicuous concavity to either, or both, the posterolateral side of metatarsal III and the posteromedial side of metatarsal IV which can eventually host the fifth metatarsal (1) (Dieudonné et al. 2016a #279).

Cooper (1985, p. 310, fig. 18F) states that the posteromedial surface of the proximal fourth metatarsal is excavated to receive a vestigial fifth metatarsal in *Kangnasaurus coetzeei*. Such a vestigial fifth metatarsal hosted between the proximal posterior third and fourth metatarsals was observed in *Gasparinisaura cincosaltensis* (Salgado et al. 1997, fig. 5.6) and the Vegagete rhabdodontid (Dieudonné et al. 2016a, fig. 15C). A similar bone was figured in

Eousdryosaurus nanohallucis plantarly between the third and fourth metatarsal, although it was not formally recognized as from the fifth metatarsal (Escaso et al. 2014, fig. 6). We regard the posterolateral concavity on the proximal MT-III of *Muttaburrasaurus langdoni* (Herne et al. 2018, fig. 32O) as not deep enough for having received a prominent process from the fourth metatarsal. However, it is present and noteworthy in this taxon. A similar concavity excavate the plantar surface of the proximal third and fourth metatarsals in *Gideonmantellia amosanjuanae*, although the fifth metatarsal is not preserved in that space (cf. Ruiz-Omeñaca 1996, fig. 4.52). *M. langdoni* was corrected and coded (1).

334(*). Metatarsal I, proximal surface: developped into a distinct articular surface (0), proximally splint-like or devoid of any articular surface (1) (new character).

The proximal surface of the first metatarsal is splint-like in the Vegagete rhabdodontid (Dieudonné et al. 2016a, fig. 10), *Camptosaurus dispar* (Carpenter and Galton 2018, fig. 26GG), *Thescelosaurus neglectus* (Gilmore 1915, fig. 16). It is described as a "flattened rod" in *Iguanodon bernissartensis* so we regarded it as devoid of proximal articular surface (Norman 1980, fig. 70D). Janensch (1955, p. 169) describes the first metatarsal of *Dysalotosaurus lettowvorbecki* as a very small bone with respect to that of *Camptosaurus* and *Thescelosaurus*. The first metatarsal of *Nanosaurus agilis* (Galton and Jensen 1973, fig. 6C; Carpenter and Galton 2018, fig. 18E, H-L) has a much proximally reduced, practically absent articular surface. By contrast, there is a proximal articular surface in *Tenontosaurus tilletti* (Forster 1990, fig. 22A), *Talenkauen santacrucensis* (Rozadilla et al. 2019, fig. S7E), *Anabisetia saldiviai* (Coria and Calvo 2002, fig. 8), *Convolosaurus marri* (Andrzejewski et al. 2019, fig. 26B), *Eousdryosaurus nanohallucis* (Escaso, pers. comm.). Cambiaso (2007, p. 166) argues that the first metatarsal of *Gasparinisaura cincosaltensis* was proximally compressed, although it also makes more than 50% the height of the second metatarsal. This is unlike what was previously figured by Salgado et al. (1997, fig. 5.7, 5.8). In Cambiaso

(2007, fig. 76C) we note that although devoid of digits, the first metatarsal had a relatively developped proximal articular surface. From the available descriptions, it is impossible to define how reduced is the proximal articular surface of the first metatarsal in *Muttaburrasaurus langdoni* (Bartholomai and Molnar, 1981, fig. 12B) and *Fruitadens haagarorum* (Carpenter and Galton 2018, fig. 5QQ). We note that the relative sharpness of the proximal first metatarsal was only based on textual description in *Jeholosaurus shangyuanensis* (Han et al. 2012), *Changchunsaurus parvus* (Liyong et al. 2010) or *Haya griva* (Makovicky et al. 2011). However, interpretations of such trait might vary from an author to another. This character should be examined in an array of taxa in order to settle a quantitative boundary of proximal sharpness. Here, we regarded the lower limit for a developped proximal articular surface as that displayed by *Archaeoceratops oshimai* (You and Dodson 2003, fig. 5).

335(*). Pedal digit I, number of pedal phalanges on the first metatarsal: two phalanges (0), bears only one ungueal or does not bear digits at all (1) (modified from Ösi et al. 2012 #211; Brown et al. 2013 #123).

Dryosaurus altus (Carpenter and Galton 2018, fig. 31TT) and *Anabisetia saldiviai* (Coria and Calvo 2002, fig. 8) present two pedal phalanges on their first digit. *Eousdryosaurus nanohallucis* (Escaso et al. 2014, fig. 6) and *Gasparinisaura cincosaltensis* (Salgado et al. 1997) are remarkable for this feature as they bear one or no distal ungueal on their first metatarsal. On account of the well-developped distal articular surface of the first metatarsal, *Stegoceras validum* should have born four “functional” digits (Gilmore 1924, pl. 9.7). *Yinlong downsi* (Han et al. 2018, fig. 14B) and *Psittacosaurus mongoliensis* (Osborn 1924, fig. 4) bear four founctional digits. The distal articular surface of metatarsal I is well-developped and would have born two phalanges in the Vegagete ornithopod (Dieudonné et al. 2016a, fig. 10). The Vitrolles *Rhabdodon* bears at least four pedal digits as *Muttaburrasaurus langdoni* and

Tenontosaurus tilletti, but the exact number of phalanges on its first digit is unknown (Pincemaille-Quilleveré 2002). *Camptosaurus dispar* bears two phalanges on its first pedal digit (Galton 2009, fig. 21X). The Vegagete rhabdodontid, *C. dispar*, *Dryosaurus*, *A. saldiviai, Y. downsi* and *P. mongoliensis* were corrected and coded (0). *R.* sp1 was corrected and coded (0, 1) pending further examination of the material. *D. lettowvorbecki* was regarded as unknown for this character.

336(*). Pedal digit I, configuration: the first metatarsal is well-developed, distal end of last phalanx projects beyond the distal end of metatarsal II (0), metatarsal I reduced or absent, end of phalanx I-1 not extending beyond the end of metatarsal II (1) (modified from Ösi et al. 2012 #211).

The first digit is well-developped in *Yinlong downsi* (Han et al. 2018, p. 20, fig. 14B), but reduced in *Archaeoceratops oshimai* with the end of phalanx I-1 reaching only the very beginning of phalanx II-1 (You and Dodson 2003, Fig. 5). We removed character state (2) on this character as it relates to the number of pedal phalanges on digit 1, and not on the relative proximodistal extension of the first pedal digit. As seen above, *Dryosaurus altus* bears two pedal phalanges on its first metatarsal, but here this character gets worth it as the whole first digit is reduced (Carpenter and Galton 2018, fig. 31TT). This is unlike what occurs in *Camptosaurus dispar* (Carpenter and Galton 2018, fig. 26II) in which the phalanges from digit I extend beyond the end of the second metatarsal. In the Vegagete rhabdodontid, the end of the first metatarsal is rather robust and the two distal phalanges would have extended beyond the end of the second metatarsal (Dieudonné et al. 2016a, fig. 10). The relative extension of digit I is unknown in *Muttaburrasaurus langdoni* as it would only preserve a prowimal first metatarsal (Bartholomai and Molnar, 1981, p. 338). Every taxa previously coded (2) were now rescored with character state (1), except for *Dryosaurus* and *D. lettovorbecki*. *Y. downsi*, *C. dispar* and the Vegagete rhabdodontid were corrected and coded

(0). *A. oshimai* and *Dryosaurus* were corrected and coded (1). *D. lettowvorbecki* and *M. l angdoni* were corrected and coded with a question mark.

Supplemental material 3.2 – List of characters re-included and/or excluded from the raw data-matrix (Dieudonné et al. 2016a) with corresponding comments and explanations.

Characters reincluded after undue exclusion from the raw data-matrix

Characters #25 and #106 from Ösi et al. (2012) were unduely left apart in the data-matrix of Dieudonné et al. (2016a), so we reintegrated them here. Ösi et al. (2012 #106) deals with the lateral boss on the surangular and appears under an array of morphologies in a variety of taxa. Ösi et al. (2012 #25) relates to the anterior bulge in front of the anterior ascending process of the maxilla, and was accidentaly confounded with character #40 of Brown et al. (2013) which relates to the anterior premaxillary process itself.

Reported redundancies

Within the data matrix of Dieudonné et al. (2016a), characters #10 and #15, #20 and #24, #59 and #77, #72 and #73, #98 and #97, #122 and #125, #183 and #185, #218 and #222 were found mutually redundant. Characters #10 (from McDonald et al. 2010 #30) and #15 (from Ösi et al. 2012 #9) deal with the ventral inflection of the oral margin of premaxilla. Characters #20 (from Boyd 2015 #11) and #24 (from Ösi et al. 2012 #12) relate to the dorsal process of premaxilla and its contact with the nasals. Characters #59 (from Brown et al. 2013 #59) and #77 (from Ösi et al. 2012 #54) deal with the posteroventral expansion of the jugal wing with respect to the distal quadrate condyles. Characters #72 (Ösi et al. 2012 #47) and #73 (from Boyd 2015 #26) deal with the posterior expansion of the posterior jugal ramus. Characters #97 (Brown et al. 2013 #73) and #98 (McDonald et al. 2010 #76) deal with the presence of an anteroposteriorly extending median groove along the ventral surface of the basioccipital. Characters #122 (McDonald et al. 2010 #122) and #125 (Ösi et al. 2012 #103) deal with the position of the coronoid eminence with respect to the dentary dentition. Characters #183 (from Ösi et al. 2012 #216) and #185 (from Brown et al. 2013

#86 and Ösi et al. 2012 #217) deal with the presence of ossified epaxial tendons along the whole vertebral column for the former, and ossified hypaxial tendons along the tail for the latter. These two characters overlap as epaxial and hypaxial tendons are commonly found together along the tail. Character #218 and #222 from Dieudonné et al. (2016a, originally from Ösi et al. 2012 #168 and McDonald et al. 2010 #112 respectively) deals with the mediolateral expansion of the dorsal iliac margin. Character #155 from Dieudonné et al. (2016a, originally from Brown et al. 2013 #60) was merged with character #147 from Dieudonné et al. (2016a, originally from Brown et al. 2013 #41), and now deal with the shape of both maxillary and dentary teeth.

Within the datamatrix of Xu et al. (2006), characters #7, #8, #10, #16, #19, #27, #28, #31, #46, #59, #80, #85, #89, #97, #101 were omitted because of their mutual redundancies or because of other redundancies with characters from the raw datamatrix (Dieudonné et al. 2016). The snout height (#7) is closely related with the naris height (#8), and both of these characters are also redundant with character #22 from Dieudonné et al. (2016a). The presence of an epijugal ossification (#10) is typical of derived ceratopsids; this character is therefore beyond the scope of this data-matrix. The supraoccipital is not subrectangular (#16) in every ceratopsians (e.g. *Archaeoceratops oshimai*, You and Dodson 2003, fig. 1A), and this character is not observable in *Liaoceratops yanzigouensis* (Xu et al. 2002). The presence of a primary ridge on maxillary teeth (#19) is a very common character among neornithischians, and its relative prominence is much likely linked most of the time to the scarcer occurrence of secondary ridges rather than to any proper prominence *per se*. The presence of a flange on the dentary (#27) and a prominent medial expansion on the mandible (#28, and redundantly #89) could not be verified from the literature. The character (#31) deals with the anterior or posterior inclination parietal branch of the squamosal. It was found redundant with Xu et al. (2006, #60) which deals with the anterior or posterior position of the parietal relative to the squamosal. Character #46, which deals with the presence or absence of maxillae participation of internal nares, may conflict with character #9 from the same data-matrix (presence or absence of a

maxilla-vomer contact). Character #59 deals with the position and orientation of the quadratojugal foramen, and is redundant with Xu et al. (2006, #39). Character #80 deals with the transverse thickening of the jugal. It supposedly links heterodontosaurids with ceratopsians. However, in heterodontosaurids, the transverse thickening of jugal must be linked with the presence of the jugal boss (see illustrations from Norman et al. 2011, fig. 6B). For now, any homology between the jugal boss and the jugal transverse thickening has not been demonstrated. A reduced posterior exposure of the parietal was used to characterize neoceratopsians (Xu et al. 2006, #85). However, no much could be inferred for this character in *Archaeoceratops oshimai* (Dong and Azuma 1997; You and Dodson 2003) and *Liaoceratops yanzigouensis* (Xu et al. 2002), and this part of the skull is absent in *Chaoyangsaurus youngi* (Zhao et al. 1999). Character #97 dealt with the orientation of the basipterygoid processes articular facets. These basipterygoid articular facets appear laterally facing in *Yinlong* (Han et al. 2015, fig. 19D), but are in an intermediate anterolateral orientation in other ornithischians, including the pachycephalosaur *Goyocephale lattimorei* (Perle et al. 1982, pl. 42.2). Therefore, this character should not group *Yinlong* to other pachycephalosaurs, and was omitted in the present data-matrix. Character #101 from Xu et al. 2006 may refer to the dorsal squamosal ridge which served for the *adductor mandibulae externus superficialis* muscle attachment (e.g. Norman et al. 2011, fig. 34A for *Heterodontosaurus tucki*). The presence of such upper ridge on the temporal bar would have signified the presence of a powerful adductor musculature. However, such ridge is found in a wider variety of taxa than those coded in Xu et al. (2006 #101). This character could furthermore conflict with character #84 of Xu et al. (2006), which deals with a dorsolateral squamosal overhang.

Characters #234 and #235 from Dieudonné et al. (2016a, originally from characters #194 and #195 from Ösi et al. 2012), as well as #43 and #106 from Xu et al. (2006) all deal with the relative extension of the prepubic process and were all merged into a single character.

Characters definitively excluded

Character #96 from Dieudonné et al. (2016a, from Brown et al., 2013 #72) deals with the flat (0) or arched (1) nature of the basioccipital floor of braincase. It was removed from this data matrix, because the "flat" state of character could not be ascertained in any instances. The basioccipital of *Tenontosaurus tilletti* (Thomas 2015, fig. 1), *Dryosaurus altus* (Galton 1983, fig. 1B), *Iguanodon bernissartensis* (Norman 1980, p. 19) form a dorsally arched and concave floor of braincase. In *Camptosaurus dispar* (Gilmore 1909, fig. 4), the nature of such basioccipital floor appears relatively flat but it is hazardous to ascertain due to the perspective of the drawing. Original views of *Lesothosaurus diagnosticus* crania aren't available from a posterior view. However, a posterior reconstruction was produced by Sereno (1991) as a drawing. Neither Sereno's basioccipital description nor his drawing (1991, fig. 11C) allow to infer a flat basioccipital floor of braincase.

Character #124 from Dieudonné et al. (2016a, originally from Ösi et al. 2012 #102) deals with the participation of the dentary to the coronoid process. It was found incoherently coded and inconsistent with the observations drawn from the literature. *Herrerasaurus ischigualastensis* (Sereno and Novas 1993) and pachycephalosaurs such as *Wannanosaurus yansiensis* (Butler and Zhao 2009) and *Stegoceras validum* (Sues and Galton 1987) were coded as having their dentary swinging up onto the anterodorsal border of the coronoid eminence. We consider such coding as dubious in the former, and wrong in the latter. Actually, the presence or absence of a coronoid process cannot be determined in *Herrerasaurus ischigualastensis* (Sereno and Novas 1993, p. 459), and the dentary forms a non-significant part of the coronoid process in the pachycephalosaurs *W. yansiensis* (Butler and Zhao 2009, fig. 7A) and *Stegoceras validum* (Sues and Galton 1987, fig. 3A).

Character #172 from Dieudonné et al. (2016a, from Brown et al. 2013 #83) deals with the orientation of sacral neural spines. An anterior orientation was coded only for *Camptosaurus dispar* in the whole data-matrix.

Character #210 from Dieudonné et al. (2016a, from Ösi et al. 2012 #156) was originally coded to account for the relatively long manual phalanges of *Heterodontosaurus tucki* with respect to its humerus, a feature thought to be shared with *Herrerasaurus ischigualastensis* (Sereno 1993, fig. 13; Galton 2014, p. 113). However, in *Herrerasaurus ischigualastensis* the humerus is only known from its proximal and distal extremities (Sereno 1993, fig. 3-4), so this taxon could not be coded. Moreover and contrarily to what was previously coded, no manus is preserved in the taxon *Fruitadens haagarorum* (Butler et al. 2009). *H. tucki* ends-up being the only taxon that could be coded (1) within our data matrix so this character was omitted from the present data-matrix. We further discuss about the distribution of this character and arbitrarily choose to look at the first manual phalanx of digit III. In *H. tucki*, the length of manual phalanx III-1 is rhoughly about 18% the length of the humerus (Galton 2014, fig. 8B, E). *Tianyulong confuciusi* differs from *H. tucki* in that its manual digit III-1 forms less than 10% the length of the humerus (see Zheng et al. 2009, sup. info. and Sereno 2012, fig. 26). Long manual phalanges with respect to the humerus might therefore not even be homogeneously found in heterodontosaurids.

Character #262 from Dieudonné et al. (2016a, originally from Brown et al. 2013 #112) deals with the conformation of the proximal inner condyle of tibia with respect to the outer condyle. From what is currently described or figured, the inner and lateral proximal condyles of tibia are level with one another solely in the outgroup taxon (*Herrerrasaurus ischigualastensis*, Novas, 199, Fig. 8C). Within Ornithischia, the lateral condyle of tibia is always offset posteriorly on the proximal portion of the tibial shaft, so that the inner condyle looks slightly more anteriorly positioned (e.g. in *Eocursor parvus*, Butler 2010, fig. 16C; *Lesothosaurus diagnosticus*, Baron et al. 2016, fig. 15B; *Fruitadens haagarorum*, Galton 2014, fig. 14K; and derived ornithopods such as *Zalmoxes shqiperorum*, Godefroit et al. 2009, fig. 20A or *Tenontosaurus tilletti*, Forster 1990, fig. 20B). What's more, the hypothesis that the fibula's proximal head fitted against the inner proximal condyle of tibia (character state 2) was made in the case of the Vegagete ornithopod because the

subadult tibia had a very small inner condyle, but such hypothesis could not be really rulled out neither in the larger tibia of the same taxon (Dieudonné et al. 2016a, fig. 9A, B), nor in more taxa.

Character #257 from Dieudonné et al. (2016a, originally from Ösi et al. 2012 #203) and #258 from Dieudonné et al. (2016a, originally from McDonald et al. 2010 #127) deal respectively with the presence or absence of a distal extensor groove on the femur, and with its geometric nature. These characters were considered altogether into a newly formulated character.

Character #263 from Dieudonné et al. (2016a, originally from Brown et al. 2013 #114) deals with the triangular or rounded tibial cross-section. This character is problematic for three reasons: (1) the geometric nature of any tibial cross-section is difficult to ascertain externally, (2) the cross-section outline may vary wether we consider it more proximal or distal, and (3) this character was poorly described in the literature.

Character #268 from Dieudonné et al. (2016a, originally from Ösi et al. 2012 #226) deals with the presence or absence of fusion between the astragalus and fibula. Galton (2014, p. 121) claims that the fusion between the astragalus and calcaneum should be more phylogenetically informative. Butler et al. (2009, p. 6) affirm that *Fruitadens haagarorum* is a heterodontosaurid partly because of a fused astragalus and calcaneum, which also occurs for *Heterodontosaurus tucki* (Galton 2014). However, such fusion does not occur in the heterodontosaurid *Abrictosaurus consors* (Sereno 2012, fig. 37). A fusion between the astragalus and calcaneum occurs sporadically in ornithopods such as *Zephyrosaurus schaffi* and *Orodromeus makelai* (Scheetz 1999, p. 68). Pending further discussion, we decided to omit this character from the present data-matrix.

Characters temporarily excluded pending further re-examination

Character #27 from Dieudonné et al. (2016a, from Butler et al. 2008 #15) deals with the flat or 'arched' nature of the premaxilla-maxilla diastema. It results that its codings are much similar to those of the immediately anterior character, which deals with the presence or absence of a diastema

between the maxilla and premaxilla (Dieudonné et al. 2016 #26, from Butler et al. 2008 #14). It is very difficult to recognize an absence of diastema, from a 'diastema' which would correspond to a medially inset 'gap' of the anterior maxillary process.

Character #30 from Dieudonné et al. (2016a, originally from Brown et al. 2013 #40) deals with the nature of the maxillary anterior process and its contact with the premaxilla. The coding of this character suggests that only the anterior maxillary process of *Tenontosaurus* bears a dorsal sulcus for reception of the premaxilla (Thomas 2015, fig. 17). But this is far from being the case. For example it may also happen in *Talenkauen santacrucensis* (Cambiaso 2007, fig. 8C), and in *Hypsilophodon foxii* (Galton 1974*a*, p. 30-31), the 'lateal sheet' is reported to vary in width depending on the specimen, and to support the premaxilla dorsally. Most importantly, the exact shape of the anterior maxillary process could not be observed in many instances. This character deserves a close inspection in a wide array of taxa so that it could be reused further with confidence.

Character #33 from Dieudonné et al. (2016a, from Butler et al. 2008 #27) deals with the presence/absence of a maxillary notch for the lacrimal. Contra previous codifications, we could not find any description for a maxillary notch in *Dryosaurus altus* and *Dysalotosaurus lettowvorbecki* (e.g. Galton 1983). Such notch was only reported in *Agilisaurus louderbacki* (Peng 1997) and *Lesothosaurus diagnosticus* (Porro et al. 2015, p. 11). This character was never figured so it is momentaneously impossible to infer its presence in more taxa.

Character #37 from Dieudonné et al. (2016a, from Butler et al. 2008 #23; Boyd 2015 #92; Han et al. 2018 #35) deals with the presence/absence of an additional opening anteriorly within the antorbital fossa. It seems that such antorbital opening could be present in *Yinlong downsi* but no mention of this character is made (Han et al. 2015, fig. 2). Globally, many taxa were coded for the absence of an anterior antorbital opening but were never described or shown for bearing this character.

Character #50 from Dieudonné et al. (2016a, from Ösi et al. 2012 #49 and Brown et al. 2013 #20) deals with the postorbital orbital margin, being either smooth or bearing a distinct anterior boss or projection into the orbit. Norman et al. (2004, p. 400) report that the anterior margin of the postorbital is "often expanded and rugose" in basal ornithopods and could have served as an area of attachment for the postpalpebral. Maidment and Porro (2010) suppose that the slot between the palpebral and the anterior postorbital margin was spanned by connective tissue. The relative prominence of this boss largely varies between taxa, from a "discrete crest" (*Haya griva*, Makovicky et al. 2011) to a more rounded boss in *Thescelosaurus neglectus* (Boyd 2014). In *Heterodontosaurus tucki* (Norman et al. 2011, p. 203), the anterior surface of the postorbital is rugose but apparently does not show any anterior prominence. What's more, the presence of such boss could be under ontogenetic control: in *Jeholosaurus shangyuanensis*, the juvenile postorbital features a well visible boss anteriorly, but not the adult (Barrett and Han, 2009, fig. 3A, 7A, not described in the text description). We lack an accurate description of the texture/shape of the postorbital margin in other critical taxa. For all those reasons, and pending further examination of this character in more ornithischians, we did not use this character in this data matrix.

Character #70 from Dieudonné et al. (2016a, from Boyd 2015 #31) deals with the nature of the jugal-postorbital joint. In most of the cases, the jugal-postorbital joint faces both anteriorly and laterally, so it is very difficult to assess to which extent this junction was facing more to one side or to the other, without direct access to the specimen. Note that in *Heterodontosaurus tucki*, the postorbital-jugal joint is completely facing laterally (cf. Norman et al. 2011, see also fig. 4B), contrary to previous codification. This characteristic could not be observed in other taxa for the moment. Character state (2) was only attributed to the Kaiparowits orodromiines (Boyd 2015 #31), which are not yet part of this data-matrix. For all the above-mentionned reasons, this character was temporarily omitted, but could be reintroduced in the data-matrix if a more detailed examination is performed in the future.

Character #80 from Dieudonné et al. (2016a, from Boyd 2015, #53) deals with the point of dorsal expansion for the pterygoid wing of quadrate. We found hazardous and difficult to distinguish a pterygoid ramus starting from the dorsal head from another arising more ventrally on the quadrate shaft, because most of the time the pterygoid wing does not form a conspicuous break in slope with respect to the dorsal head of the quadrate, and this could lead to important misinterpretations. Moreover, the pterygoid wing of quadrate is not much visible in a large array of taxa.

Character #81 from Dieudonné et al. (2016a, from Boyd 2015, #54) – deals with the relative expansion of the pterygoid wing of quadrate. We omitted this character from the present data-matrix for the two following reasons. The first reason is because it is too unsuficiently known for a number of taxa. In *Parksosaurus warreni* (Galton 1973, fig. 1, 5) and *Orodromeus makelai* (Scheetz 1999, fig. 4, p. 24), the pterygoid wing of quadrate appears small from a lateral view but we have no way to check wether this is an optical illusion linked to the medial folding of the pterygoid wing, or if the pterygoid wing of quadrate was actually small. In *Jeholosaurus shangyuanensis* (Barrett and Han, 2009), *Haya griva* (Makovicky et al. 2011), *Changchunsaurus parvus* (Liyong et al. 2010), there is no illustration or description to allow saying wether the pterygoid wing was large or short anteroposteriorly. To what concerns the rhabdodontomorphs, the pterygoid wing of *Zalmoxes shqiperorum* (Godefroit et al. 2009, fig. 5) and *Zalmoxes robustus* (Weishampel et al. 2003, fig. 7) is broken, and that of *Muttaburrasaurus langdoni* is not visible (Bartholomai and Molnar, 1981, fig. 1). The second reason was that the vast majority of taxa for which the pterygoid wing of quadrate could be observed – by the only exception of *Gasparinisaura cincosaltensis* (Coria and Salgado 1996, fig. 2A) – display an unvariantly expanded pterygoid wing. This is the case for example of pachycephalosaurids (*Stegoceras validum*, Gilmore 1924 ; *Stegoceras validum*, *Prenocephale prenes*, *Homalocephale calathocercos*, Maryanska and Osmolska 1974, fig. 1A4, C4, D4), basal ceratopsians (*Yinlong downsi*, Han et al. 2015, fig. 17, p. 19), *Lesothosaurus diagnosticus* (Porro et al. 2015, fig. 6D-E), as well as in a variety of

ornithopods such as *Zephyrosaurus schaffi*, *Yandusaurus hongheensis*, *Thescelosaurus neglectus*, *Hypsilophodon foxii*, *Tenontosaurus tilletti* (Sues 1980, fig. 16 ; He and Cai 1984, fig. 24 ; Boyd 2014, fig. 8C, D, Galton 1974, fig. 4A ; Thomas 2015, fig. 15 and 17).

Character #212 of Dieudonné et al. 2016a (originally from #161 from Ösi et al. 2012) should be omitted pending further re-evaluation and pending an extension of the dataset to more taxa. The two folds relationship between the lengths of the first and second row of manual phalanges isn't true for *Camptosaurus dispar* (Carpenter and Galton 2018, fig. 24L) and *Tenontosaurus tilletti* (Forster 1990, fig. 14). Such character was unknown for *Muttaburrasaurus langdoni* (Bartholomai and Molnar, 1981) but Bell et al. (2019 #212) stated that the two folds relationships wasn't true either for this taxon. *Iguanodon bernissartensis* (cf. Norman 1980, fig. 60A, B) is the only taxon with *Hypsilophodon foxii* (Galton 1974*a*, fig. 41; Bell et al. 2019 #212) for which the manual phalanges of the second row are more than twice smaller than those from the first row.

Character #242 from Dieudonné et al. (2016a, from Ösi et al. 2012, #183), deals with the presence or absence of a dorsal groove on the dorsal surface of the ischial shaft. Butler (2010) states that "a distinct groove is present on the dorsolateral margin of the blade in *Lesothosaurus diagnosticus* (Sereno 1991), [its synonymous] *Stormbergia dangershoeki* (Butler, 2005), *Scutellosaurus lawleri* (UCMP 130580), *Agilisaurus louderbacki* (ZDM T6011), as well as in most basal dinosaurs". The heterodontosaurid *Tianyulong confuciusi* was also reported to bear such groove, but not *Heterodontosaurus tucki* (Galton 2014, p. 119). This character appears to be ontogenetically variable at least in some taxa (e.g. *Jeholosaurus shangyuanensis*, Han et al. 2012) and is also poorly described for many ornithischians. It was therefore omitted from this data-matrix.

Character #244 from Dieudonné et al. (2016a, from McDonald et al. 2010 #119) deals with the morphology and relative curvature of the ischial shaft. Character #246 from Dieudonné et al. (2016a, from Ösi et al. 2012 #182) deals with the presence/absence of a distal ischial boot. The relative curvature of the ischial shaft, and the presence/absence of a distal ischial boot are highly

homoplastic and varies even at the generic level. The footed shaft of *Dryosaurus altus* is smoothly curved toward the anterior side (Galton 1981, to fig. 10A, whereas the unfooted one is straight (Galton 1981, to fig. 10E). Conversely, the unfooted ischium of *Z. robustus* curves regularly along its whole length with a more distal break in slope (Weishampel et al. 2003, to fig. 22D, E). In *Z. shqiperorum*, the ischial shaft is straight, with a distal foot directed anteriorly (Weishampel et al. 2003, to fig. 31A, B). Both characteristics are also widely variable among iguanodontids (see also Gasca et al. 2014). The presence or absence of a distal boot (Nopcsa, 1929b), and the ischial shaft curvature could potentially represent either sexual dimorphism, or intraspecific variability. Pending further investigation on the subject, we omitted both characters from the present data-matrix.

Characters #13 and #99 from Xu et al. (2006) should be considered as a single character, as both deal with the possibility to observe the basal tubera of basisphenoid from a posterior view, and therefore, also deal with the relative coverage of the basal tubera by the basioccipital. Contra Xu et al. (2006 #99), the basal tubera of basispenoid in *Yinlong downsi* are completely covered anteriorly by a dorsoventral basioccipital extension (Han et al. 2015, fig. 19D). In almost all ornithischians, the anteroventral part of the basioccipital forms a dorsoventral extension which contacts the whole posterior surface of the basisphenoid basal tubera. Exceptions are *Lesothosaurus diagnosticus* (Porro et al. 2015; Sereno 1991), the pachycephalosaurs *Stegoceras validum*, *Prenocephale prenes*, *Homalocephale calathocercos* (Maryanska and Osmolska 1974, fig. 1A4, 1C4 and 2, 1D4 respectively), *Herrerasaurus ischigualastensis* (Sereno and Novas 1993) and *Heterodontosaurus tucki* (Norman et al. 2011). In *L. diagnosticus* and pachycephalosaurs, the basioccipital forms only part of the dorsolateral margins of the basal tubera. In the latter two, the basioccipital may not participate at all in the formation of the basal tubera, though this should be verified as it is not clearly specified in the descriptions. This character was temporarily omitted from this data-matrix, pending first-hand examination of the basicrania from *Herrerasaurus ischigualastensis* and *Heterodontosaurus tucki*.

Within Xu et al. (2006), character #26 was omitted but could potentially be interesting in future studies. Xu et al. (2006, #26) deals with the postpalatal part of the pterygoid and the relative prominence of its posterior process which fitted against the basisphenoid. It has been argued that this process was more pronounced in some psittacosaurs, *Liaoceratops yanzigouensis* and several other basal neoceratopsians (Xu et al. 2002). Contra Xu et al. (2006 #26), the pterygoid is not sufficiently known in *Archaeoceratops oshimai* (Dong and Azuma 1997; You and Dodson 2003) and *Psittacosaurus mongoliensis* (Osborn 1923, 1924), but *Psittacosaurus major* exhibits a prominent pterygoid posterior process (You et al. 2008, fig. 1C). The basal ceratopsian *Yinlong downsi* would present a reduced pterygoid posterior process (Han et al. 2015). This character is poorly known in other taxa, and it could be homplastic among different other ornithischian lineages. Actually, pachyephalosaurs display an expanded plate-like pterygoid posterior process (Maryanska and Osmolska 1974). *Tenontosaurus tilletti* also shows in its way a relatively prominent pterygoid posterior process (Thomas 2015, fig. 14). We should therefore await a better and fuller characterization of such character and its variety of shapes before considering once again its codification.

Charater #96 from Xu et al. (2006) deals with the oval or circular shape of the basipterygoid articular facets. A broad, circular articular facet was originally told to group ceratopsians and pachycephalosaurs together. Here, we observe that the articular facets of the basipterygoid processes are elongated and oval in both *Yinlong downsi* (Han et al. 2015, fig. 19) and *Psittacosaurus major* (You et al. 2008), which contrasts with previous codifications. *Liaoceratops yanzigouensis* (Xu et al. 2002) and *Archaeoceratops oschimai* neither (Dong and Azuma 1997 ; You and Dodson 2003) lack description and figuration of the basipterygoid processes. *Liaoceratops yanzigouensis* and *Archaeoceratops oshimai* would have basipterygoid processes lying very close to the basal tubera, as also occurs in more derived ceratopsians (Makovicky 2001 #48). This may explain why their exact morphology is obscured. Unfortunately, and as far as we are concerned, the

exact shape of the basipterygoid processes facets is not mentioned for pachycephalosaurs (Gilmore 1924; Maryanska and Osmolska 1974; Sues and Galton 1987). We accessorily note that in *Heterodontosaurus tucki* the basipterygoid processes may have born very small, circular articular facets (Norman et al. 2011, fig. 13). However, this character is too poorly known in a number of taxa so that it could be coded for the time.

Supplemental material 3.3 – Comments on changes made by other authors on their datasets (Pol et al. 2011; Rozadilla et al. 2016, 2019; Andrzejewski et al. 2019), and comments on changes brought by Bell et al. (2019) on the rax version of this datamatrix more particularly.

Remarks on changes from Pol et al. *(2011)*

Pol et al. (2011) based their phylogenetic analysis onto the same raw data-matrix as that used in this paper (Butler et al. 2009). Their modifications were not taken onto consideration in the subsequent analysis of Dieudonné et al. (2016a) so we briefly review them here. 8 characters were modified. One of those (#46) was omitted so its corresponding modifications were not considered. Character #46 dealt with the presence of a postorbital boss, but this cannot be well-substanciated and might be subject to some ontogenetic variation (cf. discussion herein concerning the removal of character #50 from Dieudonné et al. (2016a). Pol et al. (2011) further added three new characters (#228, #229, #230), which were all readily included in this dataset.

Remarks on changes from Rozadilla et al. *(2016)*

Rozadilla et al. (2016) appended characters (#231 to #237) to the dataset of Pol et al. (2011). Of these, characters (#231), (#232), (#234), (#236) and (#237) were already dealt with in our raw dataset, but characters (#233) and (#235) weren't. Character (#233) deals with the presence of longitudinal grooves ventral to the caudal centra. We did not use it and contest its reliability for the

three following reasons. First, Nopcsa (1929) remarked its intraspecific or intrageneric variability, and suggested that such character was sexually dimorphic. Second, very few caudal vertebrae are figured in ventral view or described for this character, so it is difficult to assess its taxonomic validity. Third, the disarticulated Vegagete ornithopod features a ventral groove only on the posterior caudal centra of one or many individuals out of five (Dieudonné et al. 2016a; personal observation), so such character might vary even within the tail of a single individual. Character (#235) deals with the presence of mineralized intercostal plates. We omitted this character for the following reasons. Intercostal plates are cartilaginous plates which are arranged between the distal dorsal ribs and might have played a role in ventilation (Butler and Galton 2008). They were disparately found amongst *a priori* unrelated ornithopods and could be found even in basal cerapods such as *Nanosaurus agilis* (Galton and Jensen 1973). The taxonomic validity of such intercostal plates is not in doubt. However, the fact that such plates were not recovered in an array of ornithopods might be the result of preservationnal bias, or incompletely achieved ossification or mineralization. We are unfortunately unable to rule out any of those two possibilities. We therefore temporarily omitted this character, expecting it could reach some better reliability in the future.

Remarks on changes from Andrzejewski et al. *(2019)*

Andrzejewski et al. (2019) used a data-matrix from Butler et al. (2008 *et seq.*), with the last contribution being that of Baron et al. (2016). Modifications brought by Baron et al. (2016) were also achieved in Dieudonné et al. (2016a) through the merging of characters coding of *Stormbergia dangershoeki* and *Lesothosaurus diagnosticus*. Andrzejewski et al. (2019) also considered 5 characters from Scheetz (1999), already dealt with in Dieudonné et al. (2016a) through the accounting of Boyd's (2015) data-matrix. Of note is that Character (#228) from Andrzejewski et al. (2019, from Scheetz 1999 #8, cf. Dieudonné et al. 2016a #80 and Boyd 2015, #53) was criticized above and omitted in this data-matrix. Actually, we believe that the emergence of the pterygoid

wing on the dorsal quadrate shaft is fairly difficult and hazardous to distinguish. Most of the time, the pterygoid wing does not form a conspicuous break in slope with respect to the dorsal head of the quadrate and its dorsal rise is often obscured when observed from a direct lateral view. Finally, the new character (#233) of Andrzejewski et al. (2019) is, as far as we are aware of, autapomorphic to *Convolosaurus marri*, so we did not use it in our data-matrix.

Remarks on changes from Rozadilla et al. *(2019)*

Rozadilla et al. (2019) used the data matrix of Boyd (2015). They modified characters #112, #166, #212, #216 and added four new characters (#256-259).

Their character #112 deals with the number of premaxillary teeth. Our taxonomic sampling is still incomplete and premaxillary teeth were lost independently a number of times within Ornithischia, which calls for cautiouness. We only dealt with the presence of three premaxillary teeth or less, or more than three premaxillary teeth (see character #159 from our revised datamatrix for further explanations). Coding this character with any further precision should lead to phylogenetic inconsistencies.

Their character #166 deals with the straight (0), modest (1) or pronounced (2) medial bowing of the humeral shaft from an anteroposterior view. In our dataset, we do not make a particular difference between the straight and modest medial bowing which we consider quite difficult to perceive, but we rather refer to the proximolateral margin of the humerus, which could be straight and aligned with the distolateral margin (0), or medially bowed (1) (modified from Ösi et al. 2012 #155).

The difference made by Rozadilla et al. (2019 #212) between the regularly convex (0) and flat (1) lateral surface of the greater trochanter was found too tenuous in some instances so that it could be reasonably differenciated in a number of taxa. For example, *Camptosaurus aphanoecetes* (Carpenter and Galton, 2008, fig. 30F), seems to display a flat lateral surface on its greater trochanter. In *Dryosaurus altus*, that surface is flat laterally but convex in its anterior and posterior

margins from a proximal view (Galton 1981, fig. 13E). Moreover, the sigmoid proximal outline is closely related to the length of the anterior protrusion of the greater trochanter, a character which we deal with in our dataset (Rozadilla et al. 2016 #231). We therefore kept the restricted definition originally given by Boyd (2015 #213), which deals with the mere presence or absence of a posterolaterally globular greater trochanter.

Character #216 from Rozadilla et al. (2019) deals with the relative closeness of the lesser trochanter with respect to the greater trochanter. As seen for the Vegagete ornithopod (Dieudonné et al. 2016a) this character is under strong ontogenetic control, so it shouldn't be used unless complete ontogenetic series are present in every taxon for which this character has to be coded.

Character #256 from (Rozadilla et al. 2019 #256) deals with a mediolaterally compressed proximal extremity of second metatarsal, but was temporarily omitted from this dataset. Such mediolateral compression was coded as present for *Anabisetia saldiviai, Gasparinisaura cincosaltensis, Morrosaurus antarcticus, Talenkauen santacrucensis, Kangnasaurus coetzeei*. However one the one hand, *Kangnasaurus coetzeei*, *Dryosaurus altus*, *Dysalotosaurus lettowvorbecki* and *Hypsilophodon foxii* don't seem to bear much difference in the relative proximal narrowness of their second metatarsal, at least from the figure given by Herne (2014, fig. 9.36). In *Gasparinisaura cincosaltensis*, the outline drawing of the second metatarsal is shown much narrower in Salgado et al. (1997, fig. 5.6) than in Herne (2014, fig. 9.36). On the other hand, several taxa shouldn't have been coded for this character. *T. santacrucensis* is solely reported to preserve a midshaft portion of its second metatarsal. However a personnal observation - at least valid on what regards the Vegagete rhabdodontid (Dieudonné et al. 2016a, fig. 10) - shows that the second metatarsal could be relatively wide proximally then drastically shrinks mediolaterally toward midshaft. Conservation of the proximal extremity of the second metatarsal is therefore necessary to code for a mediolateral compression of the proximal second metatarsal. As a last example, the second metatarsal of *Orodromeus makelai* was described as high and mediolaterally compressed (Scheetz 1999, p. 71),

but no proximal view is available and it was coded (0) in Rozadilla et al. (2019 #256). The proximal narrowness of the second metatarsal narrowness is undiscutable in at least some gondwanan elasmarians (e.g. *Morrosaurus antarcticus*, *Kangnasaurus coetzeei*, *Anabisetia saldiviai* in Rozadilla et al. 2016, fig. 5A; Cooper 1985, fig. 19C; Cambiaso 2007, fig. 120B). However we think that the overall distribution of this character is still too poorly known so that it be adequately coded. More photograph and/or measurements of the second metatarsal length/width ratio have to be performed to improve the overall picture of this character distribution.

Rozadilla et al. (2019 #257) deals with the presence or absence of mineralized intercostal plates. It corresponds to the previous character #235 of Rozadilla et al. (2016) and was omitted from the previous iteration of this analysis as we could not rule out wether the presence or absence of mineralized intercostal plates is a matter of preservational bias or not.

Rozadilla et al. (2019 #258) corresponds to the previous character #236 of Rozadilla et al. (2016), and was readily added to this data matrix.

Character #258 from Rozadilla et al. (2019) deals with the asymmetric distal expansion of the chevrons, but was already dealt with in character #144 from Ösi et al. (2012).

Remarks on changes from Bell et al. (2019)

N.B.: any character number referred to from within the datamatrix of Bell et al. (2019) corresponds to the same character number in the datamatrix of Dieudonné et al. (2016a).

Bell et al. (2019 #89) considered that *Muttaburrasaurus langdoni* had exoccipitals which restricted the contribution of the supraoccipital to the foramen magnum (1). However, Bartholomai and Molnar stated that the supraoccipital formed much of the dorsal margin of the foramen magnum in *Muttaburrasaurus langdoni*, a trait which appears confirmed from a quick observation at their figures (Bartholomai and Molnar, 1981, p. 321, fig. 1C). The supraoccipital contribution to the foramen magnum looks much more reduced in *Dryosaurus* sp. (Carpenter and Lamanna 2015, fig.

4E) and *Dryosaurus elderae* (Galton 1983, fig. 1B) than it does in *Camptosaurus dispar* (Carpenter and Lamanna 2015, fig. 7E).

Bell et al. (2019 #217, from the same character in Dieudonné et al. 2016a) deals with the relative lateral deflection of the preacetabular process of ilium (weak: <30° (0), or pronounced: >30° (1)). Bell et al. (2019 #217) regarded the preacetabular process of ilium of *Muttaburrasaurus langdoni* as weakly laterally deflected, an observation with which we actually concur (it makes roughly about 25° in *M. langdoni*, contra previous codification of Dieudonné et al. 2016a #217). Because of this and the general difficulty encountered for characterizing the relative deflection of the preacetabular process, we reactualized our datamatrix to deal with the dorsal outline of the ilium which is much more telling (straight, regularly concavo-convex, or sigmoid). Many ornithopods feature a dorsal iliac margin with a straight or regular and continuous curve from a dorsal view. However, only a few taxa are characterized by a sinuous dorsal iliac margin. This is notably the case of rhabdodontomorphs (Fig. 3C, #262(2)).

Bell et al. (2019 #218) deals with the dorsal thickening of the dorsal iliac margin above the acetabulum. Bell et al. (2019 #218) regards the dorsal iliac margin *of M. langdoni* as unexpanded dorsally, contra our previous codification. We disagree as, although missing its very dorsal margin, the preserved dorsal iliac margin looks distinctively thickened above the acetabulum in this taxon (Fig. 3C, #267(1)).

Disagreements on character #218 from Bell et al. (2019) also affect the changes made on their character #222 for *M. langdoni*. As stated above, the dorsal iliac margin of *M. langdoni* looks dorsally expanded from above the ischiac peduncle onward. Bell et al. (2019) also modified the scoring for *Camptosaurus dispar* from (0) to (1) on character #222. Gilmore (1909, p. 256) describes the dorsal margin of the iliac blade of *Camptosaurus dispar* as being characteristic of the genus and “rounded and thickened transversely”. However, a dorsal illustration of the ilium of *C. dispar* isn’t available. On the other hand, the dorsal margin of the iliac blade of *Camptosaurus*

aphanoecetes (Carpenter and Wilson 2008, fig. 13A) appears thin all along. For this reason we left *C. dispar* coded with a question mark.

Bell et al. (2019 #224) concerned the brevis shelf size, visibility and orientation from a lateral view. We interpret the brevis shelf as consisting in a very thin and smooth crest drawing a dorsally convex outline in *Muttaburrasaurus langdoni* and (see Fig. 3B). It is therefore almost absent and invisible from a lateral view. We could not accept their modification to character state (0) which deals with a ventrolaterally projecting brevis shelf. In *Hypsilophodon foxii*, the brevis shelf is slightly visible from a lateral view (Galton 1974*a*, fig. 49-51), which in the case of our interpretation of the character was considered as enough evidence to code it with character state (0). We further agree with their correction of *Koreanosaurus boseongensis* as being unknown for this character.

Character #252 from Bell et al. (2019) concerns the shape of the proximolateral edge of the greater trochanter. In *Muttaburrasaurus langdoni* (Bartholomai and Molnar, 1981, fig. 9F) or *Hypsilophodon foxii* (Galton 1974*a*, fig. 54E) the lateral surface of the greater torchanter doesn't appear globular and rounded (cf. Rozadilla *et al*. 2016). The rescoring of these two taxa to character state (0) is unsupported.

Bell et al. (2019) drew attention to the fact that character #93 from their and our previous data-matrix (Dieudonné et al. 2016a) was modified to deal with the relative contribution of the foramen magnum to the basioccipital condyle width. This character was told to be modified from Ösi et al. (2012 #79) and Brown et al. (2013 #71). However, as Bell et al. (2019) pointed out, this is not a modification from (Ösi et al. 2012 #79) but actually a modification from (Brown et al. 2013 #71) only. Ösi et al. (2012 #79) deals with the exclusion of the basioccipital from the ventral margin of the foramen magnum because of ventromedial contact between both exoccipitals, a feature not transcribed in the new character definition as it was coded as present solely for two neoceratopsians: *Archaeoceratops oshimai* and *Liaoceratops yanzigouensis*, two taxa formerly

absent in our dataset. Note however that the basioccipital is excluded from the foramen magnum in *A. oshimai* (You and Dodson 2003, p. 269), but it may still contact the foramen magnum in *L. yanzigouensis* (Xu et al. 2002, p. 315). We therefore made this character more inclusive to deal with either a narrow basioccipital contribution to the foramen magnum or to deal with its total exclusion by the exoccipitals.

Bell et al. (2019) judiciously suggested to rephrase their character #94 (from McDonald et al. 2010 #74), dealing with the "orientation" of the basioccipital condyle, or presence/absence of basioccipital condyle posteroventral expansion. We rephrased this character by referring to the presence of absence of a posteroventral neck and posterodistal expansion.

Character #131 dealt with the level of the quadratomandibular joint with respect to the the "level of the maxilla". They removed this character for the following belief: 'This is really a character of the quadratomandibular condyle on the quadrate, and thus should describe the maxillary occlusal margin' (Bell et al. 2019, supp. mat.). We do not understand why this plays in favor of rejecting the validity of this character. We also regarded this character as relating to the maxillary occlusal margin rather than to the 'maxilla', and readily rephrased it as such in the character definition.

They found characters #141 and #142 as redundant as both deal with apicobasally extending ridges on the labial and lingual surface of maxillary and dentary teeth respectively. We concur with this observation. In our dataset, we referred to this morphological trait in the newly implemented character #118 from Pol et al. (2011).

They interpreted the "lack of space" between maxillary teeth (#144) as correlative of imbricated teeth. We think this is not necessarily true. We added another character state, and differenciated a close tooth juxtaposition with their imbrication "*en echelon*" (cf. character #174 from the present dataset).

Bell et al. (2019) removed their character #188 dealing with the distal expansion of the scapular blade. They argued that there was no sufficient quantification to precisely know how to

differenciate the scoring for a distally expanded *versus* unexpanded scapular blade. However, although a quantitative appreciation of this character might be of help to diversify the number of states on this character, we argue that the difference called into question here is telling. As an example of reference, a distally unexpanded scapula should look like that of the Tyreophoran *Stegosaurus stenops* (Maidment et al. 2015, fig. 66).

Bell et al. (2019) removed character #191 because this character originally added within Dieudonné et al. (2016) was not clearly described. It was originally stated as: " Scapula, proximo-distal corner above glenoid cavity: elongated so that the distal edge turns to the horizontal posteriorly (0), forms a more obtuse angle, the distal edge is steep and does not expand posteriorly (1)". We agree that the "proximo-distal corner" is an incorrect and clumsy formulation that was intended to relate with the supraglenoid process. The "distal edge" relates to the distal edge above that process. As Jay Nair (pers. com.) notified to us, another problem relates to the orientation: in meaning "the horizontal" we were meaning a 90° curve with respect to an unnatural vertical orientation of the scapula. However, the scapula might be posterodorsally oriented over the rib-cage in a natural position, so we should not use the term "horizontal". This character was rephrased, and merged with a similar character that was already mentionned by Xu et al. (2006 #20). The proximo-posterior angle of the supraglenoid process was quantified with a 75° boundary between the "obtuse" and "actute" supraglenoid.

Bell et al. (2019) removed character #197, which deals with the presence or absence of an anterior bicipital sulcus on the proximal extremity of the humerus. The fact that one of the character states specifies the presence of a "varyingly developped" bicipital sulcus shouldn't be misleading, but rather understood as its presence to varying degrees. Any given bicipital sulcus might vary in depth from a very shallow to much more concave. By contrast, the absence of bicipital sulcus corresponds to a completely flat anterior surface on the proximal humeral shaft. We draw attention to the fact that we require our character be observed from a proximal view only, which means that we deals

with the proximo anterior surface of the humerus and not to the mid-shaft region. Bell et al. (2019) stated that there was not bicipital sulcus in the humerus of *Fostoria dhimbangunmal*. However it is not possible to know wether the anteroproximal surface of humerus of *F. dhimbangunmal* was actually flat or exhibited any degree of excavation for the flexor musculature, as it only preserves a mid-diaphysis fragment.

Bell et al. (2019) mentioned that character #203, dealing with a low (0), moderate (1) or prominent (2) olecranon process of ulna, did not allow to fully distinguish character state (1) from states (0) and (2). We somewhat agree with their observation but still, we think that a low olecranon process means its total absence, a moderate olecranon process means its presence in a moderate manner and a large process should be seen as a real and strong proximal eminence. Again, we think that visual inspection might still be enough to code this character unless other quantification method is found. We further agreed with changing the character scoring of *M. langdoni* from (1) to (0).

Bell et al. (2019) misinterpreted character #220 in their dataset, which deals with the presence or absence of a supra-acetabular flange. Such flange is present above the acetabulum itself, but not above the dorsal iliac, preacetabular or postacetabular margin.

Their character #222 deals with the absence of any dorsal bulging (0), presence of a dorsally bulging eminence (1), of a thikenned uneverted rim (2) or a dorsally thickened everted rim (3) along the dorsal iliac margin at the level above the ischial peduncle of ilium. Bell et al. (2019) found that character states 1, 2 and 3 were not necessarily always mutually exclusive and removed this character. They further argued that there was no special reason to order this character. We agree on the relatively little weight of character state (1), on the non-mutually exclusive relationship between character states (2) and (3). We also agree on the ordering of such character which is nothing more than an *a priori* assumption. This character was at any cases reworded within the present data-matrix to deal with the dorsal iliac thickening only at different levels along

the dorsal iliac margin, but not with any eversion of the dorsal margin which was regarded as a distinct character.

Character #224 deals with the orientation, size and morphology of the iliac brevis shelf. Character state (2) was added in Dieudonné et al. (2016a) to deal with the near absence of brevis shelf, which was observed in *Muttaburrasaurus langdoni* (Herne, pers. com., cf. also Fig. 3B) as well as all rhabdodontids preserving an ilium (i.e. *Zalmoxes robustus* and *Zalmoxes shqiperorum*, Weishampel et al. 2003; Godefroit et al. 2009). Bell et al. (2019) argued that the brevis shelf of *Muttaburrasaurus langdoni* corresponded to the surface upon which the sacral ribs were inserting. However, this isn't the way we interpret the position of the brevis shelf, as for example in *Hypsilophodon foxii* such shelf is present ventromedially to the fourth sacral rib insertion (Galton 1974*a*, fig. 50B, 51B). As told above, we interpret the brevis shelf in this taxon as well as in rhabdodontids as a very small, tiny ridge located ventromedial to the postacetabular process (Fig. 3B).

Character #250 deals with the relative height of the lesser trochanter. Bell et al. (2019) considered that this feature varied considerably within single OTUs and rejected its validity as a character. However, we are not aware of example that shows such variability. Yet, we agree that there might be some difficulties in characterizing the difference between a lesser trochanter below or slightly below the greater trochanter (character state 0), to a lesser trochanter that is exactly level with the greater trochanter (character state 1). Our new formulation of this character considers a lesser trochanter that is well below the greater trochanter (0) as usually occurs in basal ornithischians, below or slightly below (1) as occurs in most ornithopods, level or higher than the greater trochanter (2) as occurs in some elasmarians and dryosaurids.

Character #262 was added by Dieudonné et al. (2016a) and deal with the anteroposterior reduction of the outer proximal condyle of tibia. In the Vegagete ornithopod, the proximal head of fibula might have fitted directly onto the inner tibial condyle (Dieudonné et al. 2016a, fig. 9A-C), but

such bizarre feature remains questionable and wasn't reported in other rhabdodontids to date. We agree with Bell et al. (2019) on the necessity to remove this character until better first-hand observations are made on more taxa.

Character #279 deals with the presence of a notch excavated on either or both the ventromedial side of metatarsal IV and the ventrolateral side of metatarsal III. The fact that such notch hosted the fifth metatarsal or not was disregarded. Actually, there is no way to know wether a fifth metatarsal was hosted in that notch or not, and it might also have been there if it was not preserved or unossified. Bell et al. (2019) argues that this character is the same as character #278 which deals with the presence of a ventrolateral notch on the third metatarsal to host a ventromedial outgrowth of the fourth metatarsal. However, the ventromedial process of the proximal fourth metatarsal isn't always inserted on a notch, and is an outstanding feature that deserves a different character state. We transformed character #279 (character #331 in this dataset) to deal exclusively with the presence of a ventromedial outgrowth of the proximal fourth metatarsal.

Supplemental material 3.4 – Bibliography.

Andrzejewski KA, Winkler DA, and Jacobs LL. 2019. A new basal ornithopod (Dinosauria : Ornithischia) from the Early Cretaceous of Texas. PLoS ONE, 14, 1–44.

Averianov AO, Voronkevich AV, Leshchinskiy SV, and Fayngertz AV. 2006. A Ceratopsian dinosaur *Psittacosaurus sibiricus* from the Early Cretaceous of West Siberia, Russia and its phylogenetic relationships. Journal of Systematic Palaeontology, 4, 359–95.

Bakker RT, Galton PM, Siegwarth J, and Filla J. 1990. A new latest Jurassic vertebrate fauna, from the highest levels of the Morrison Formation at Como Bluff, Wyoming. Part IV. The dinosaurs: a new Othnielia-like hypsilophodontoid. Hunteria, 2, 8-19.

Bakker RT, Sullivan RM, Porter V, Larson P, and Saulsbury SJ. 2006. Dracorex hogwartsia, n. gen. n. sp., a spiked, flat-headed pachycephalosaurid dionsaur from the Upper Cretaceous Hell Creek Formation of South Dakota. New Mexico Museum of Natural History and Science Bulletin, 35, 331–45.

Baron MG, Norman DB, and Barrett PM. 2016. Postcranial anatomy of *Lesothosaurus diagnosticus* (Dinosauria : Ornithischia) from the Lower Jurassic of southern Africa : implications for basal ornithischian taxonomy and systematics. Zoological Journal of the Linnean Society, 179, 125-68.

Barrett PM. 2016. A new specimen of *Valdosaurus canaliculatus* (Ornithopoda : Dryosauridae) from the Lower Cretaceous of the Isle of Wight, England. Memoirs of Museum Victoria, 74, 29–48.

Barrett PM, Butler RJ, and Knoll F. 2005. Small-bodied ornithischians dinosaurs from the Middle Jurassic of Sichuan, China. Journal of Vertebrate Paleontology, 25, 823–34.

Barrett PM, Butler RJ, Mundil R, Scheyer TM, Irmis RB, and Sanchez-Villagra MR. 2014. A palaeoequatorial ornithischian and new constraints on early dinosaur diversification Proceedings of the Royal Society B: Biological Sciences, 281 : 20141147.

Barrett PM, Butler RJ, Novas FE, Moore-Fay SC, Moody JM, Clark JM, and Sanchez-Villagra MR. 2008. Dinosaur remains from the La Quinta Formation (Lower or Middle Jurassic) of the Venezuelan Andes. Palaeontologische Zeitschrift, 82, 163–77.

Barrett PM, Butler RJ, Twitchett RJ, and Hutt S. 2011. New material of *Valdosaurus canaliculatus* (Ornithischia, Ornithopoda) from the Lower Cretaceous of southern England. Special Papers in Palaeontology, 86, 131–63.

Barrett PM, Butler RJ, Yates AM, Baron MG, and Choiniere JN. 2016. New specimens of the basal ornithischian dinosaur *Lesothosaurus diagnosticus* Galton 1978 from the Early Jurassic of South Africa. Palaeontologia Africana, 50, 48–63.

Barrett PM, and Han F-L. 2009. Cranial anatomy of *Jeholosaurus shangyuanensis* (Dinosauria: Ornithischia) from the Early Cretaceous of China. Zootaxa, 2072, 31–55.

Bartholomai A, and Molnar RE. 1981. *Muttaburrasaurus*, a new iguanodontid (Ornithischia: Ornithopoda) dinosaur from the Lower Cretaceous of Queensland. Memoirs of the Queensland Museum, 20, 319–49.

Bell PR, Brougham T, Herne MC, Frauenfelder T and Smith ET. 2019. *Fostoria dhimbangunmal*, gen. et sp. nov., a new iguanodontian (Dinosauria, Ornithopoda) from the mid-Cretaceous of Lightning Ridge, New South Wales, Australia. Journal of Vertebrate Paleontology, 39 : e1564757.

Boyd CA. 2014. The cranial anatomy of the neornithischian dinosaur *Thescelosaurus neglectus*. PeerJ, 2 : e669.

Boyd CA. 2015. The systematic relationships and biogeographic history of ornithischian dinosaurs. PeerJ, 3, 1–62.

Brown CM and Druckenmiller P. 2011. Basal ornithopod (Dinosauria: Ornithischia) teeth from the Prince Creek Formation (early Maastrichtian) of Alaska. Canadian Journal of Earth Sciences, 48, 1342–54.

Brown CM, Evans DC, Ryan MJ and Russell AP. 2013. New data on the diversity and abundance of small-bodied ornithopods (Dinosauria, Ornithischia) from the Belly River Group (Campanian) of Alberta. Journal of Vertebrate Paleontology, 33, 495–520.

Brown B and Schlaikjer EM. 1943. A study of the troödont dinosaurs, with the description of a new genus and four new species. Bulletin of the American Museum of Natural History, 82, 115–50.

Brusatte SL, Dumbrava M, Vremir M, Csiki-Sava Z, Totoianu R and Norell MA. 2017. A catalog of *Zalmoxes* (Dinosauria : Ornithopoda) Specimens from the Upper Cretaceous of Nalat-Vad Locality, Hateg Basin, Romania. American Museum Novitates, 3884, 1–36.

Butler RJ. 2010. The anatomy of the basal ornithischian dinosaur *Eocursor parvus* from the lower Elliot Formation (Late Triassic) of South Africa. Zoological Journal of the Linnean Society, 160, 648–84.

Butler RJ and Galton PM. 2008. The 'dermal armour' of the ornithopod dinosaur *Hypsilophodon* from the Wealden (Early Cretaceous : Barremian) of the Isle of Wight : a reappraisal. Cretaceous Research, 29, 636–642.

Butler RJ, Galton PM, Porro LB, Chiappe LM, Henderson DM and Erickson GM. 2009. Lower limits of ornithischian dinosaur body size inferred from a new Upper Jurassic heterodontosaurid from North America. Proceedings of the Royal Society of London, Series B. 277, 375–81.

Butler RJ, Liyong J, Jun C, and Godefroit P. 2011. The postcranial osteology and phylogenetic position of the small ornithischian dinosaur *Changchunsaurus parvus* from the Quantou Formation (Cretaceous, Aptian-Cenomanian) of Jilin Province, north-eastern China. Palaeontology, 54, 667–83.

Butler RJ, Porro LB, Galton PM, and Chiappe LM. 2012. Anatomy and Cranial Functional Morphology of the Small-Bodied Dinosaur *Fruitadens haagarorum* from the Upper Jurassic of the USA. PLoS ONE, 7 : e31556.

Butler RJ, Smith RMH and Norman DB. 2007. A primitive ornithischian dinosaur from the Late Triassic of South Africa, and the early evolution and diversification of Ornithischia. Proceedings of the Royal Society of London, Series B., 274, 2041–2046.

Butler RJ and Sullivan RM. 2009. The phylogenetic position of the ornithischian dinosaur *Stenopelix valdensis* from the Lower Cretaceous of Germany and the early fossil record of Pachycephalosauria. Acta Palaeontologica Polonica, 54, 21–34.

Butler RJ, Upchurch P and Norman DB. 2008. The phylogeny of the ornithischian dinosaurs. Journal of Systematic Palaeontology, 6, 1–40.

Butler RJ and Zhao Q. 2009. The small-bodied ornithischian dinosaurs *Micropachycephalosaurus hongtuyanensis* and *Wannanosaurus yansiensis* from the late Cretaceous of China. Cretaceous Research, 30, 63–77.

Calvo J, Porfiri J and Novas F. 2007. Discovery of a new ornithopod dinosaur from the Portezuelo Formation (Upper Cretaceous), Neuquén, Patagonia, Argentina. Arquivos Do Museu Nacional, 65, 471–83.

Cambiaso AV. 2007. Los ornitópodos e iguanodontes basales (Dinosauria, Ornithischia) del Cretácico de Argentina y Antártida [The ornithopods and basal iguanodonts (Dinosauria, Ornithischia) from the Cretaceous of Argentina and the Antarctic] [dissertation]. Universidad de Buenos Aires, Facultad de Ciencias Exactas y Naturales, 410 pp. Spanish.

Carpenter K, Dicroce T, Kinneer B and Simon R. 2013. Pelvis of *Gargoyleosaurus* (Dinosauria : Ankylosauria) and the Origin and Evolution of the Ankylosaur Pelvis. PLoS ONE, 8 : e79887.

Carpenter K and Galton PM. 2018. A photo documentation of bipedal ornithischian dinosaurs from the Upper Jurassic Morrison Formation, USA. Geology of the Intermountain West, 5, 167–207.

Carpenter K and Lamanna MC. 2015. The braincase assigned to the ornithopod dinosaur *Uteodon* McDonald, 2011, reassigned to *Dryosaurus* Marsh, 1894 : implications for iguanodontian morphology and taxonomy. Annals of Carnegie Museum, 83, 149–65.

Carpenter K and Wilson Y. 2008. A new species of *Camptosaurus* (Ornithopoda: Dinosauria) from the Morrison formation (Upper Jurassic) of Dinosaur National Monument, Utah, and biomechanical analysis of its forelimb. Annals of Carnegie Museum, 76, 227–63.

Charig AJ. 1972. The evolution of the archosaur pelvis and hindlimb: an explanation in functional terms. 121–155. In Joysey KA and Kemp TS, editors. Studies in vertebrate evolution: essays presented to Dr. FR Parrington, FRS Oliver and Boyd, Edinburgh, 284pp.

Colbert EH. 1981. A primitive ornithischian dinosaur from the Kayenta Formation of Arizona. Museum of Northern Arizona Press, 53, 1–61.

Coombs WP. 1972. The Bony Eyelid of *Euoplocephalus* (Reptilia, Ornithischia). Journal of Vertebrate Paleontology, 46, 637-50.

Cooper MR. 1985. A Revision of the Ornithischian Dinosaur *Kangnasaurus coetzeei* Haughton, with a classification of the Ornithischia. Annals of the South African Museum, 95, 281–317.

Coria RA and Calvo JO. 2002. A new Iguanodontian Ornithopod from Neuquen Basin, Patagonia, Argentina. Journal of Vertebrate Paleontology, 22, 503–9.

Coria RA and Salgado L. 1996. A basal iguanodontian (Ornithischia, Ornithopoda) from the Late Cretaceous of South America. Journal of Vertebrate Paleontology, 16, 445–57.

Cruzado-Caballero P, Gasca JM, Filippi LS, Cerda I, Garrido AC. 2019. A new ornithopod dinosaur from the Santonian of Northern Patagonia (Rincón de los Sauces, Argentina), Cretaceous Research, 98, 211–29.

Dieudonne P-E, Tortosa T, Torcida Fernandez Baldor F, Canudo JI and Diaz-Martinez I. 2016a. An unexpected early rhabdodontid from Europe (Lower Cretaceous of Salas de los Infantes, Burgos Province, Spain) and a Re- Examination of basal iguanodontian relationships. PLoS ONE, 11 : e0156251.

Dieudonne P-E, Tortosa T, Ruiz-Omeñaca JI, Torcida-Fernandez-Baldor F, and Canudo JI. 2016b. The Gondwanan rhabdodontomorphans and the origins of the Rhabdodontidae. 65–68. VII Jornadas Internaciones sobre Paleontología de Dinosaurios y su Entorno. Salas de los Infantes, Burgos.

Dodson P, Madsen JH and Jr. (1981). On the Sternum of *Camptosaurus*. Journal of Paleontology, 55, 109-12.

Dong Z and Azuma Y. 1997. On A Primitive Neoceratopsian from the Early Cretaceous of China. Sino-Japanese Silk Road Dinosaur Expedition. China Ocean Press, Beijing, 1997, 68–89.

Escaso F, Ortega F, Dantas P, Malafaia E, Silva B, Gasulla JM, Mocho P, Narvaez I, Sanz JL. 2014. A new dryosaurid ornithopod (Dinosauria, Ornithischia) from the Late Jurassic of Portugal. Journal of Vertebrate Paleontology, 34, 1102–12.

Forster CA. 1990. The postcranial skeleton of the ornithopod dinosaur *Tenontosaurus tilletti*. Journal of Vertebrate Paleontology, 10, 273–94.

Galton PM. 1973. Redescription of the skull and mandible of Parksosaurus from the Late Cretaceous with comments on the family Hypsilophodontidae (Ornithischia). Life Science Contributions, Royal Ontario Museum, 89, 1–21.

Galton PM. 1974a. The ornithischian dinosaur *Hypsilophodon* from the Wealden of the Isle of Wight. Bulletin of the British Museum. Natural History. Geology Series, 25, 1–152.

Galton PM. 1974b. Notes on *Thescelosaurus*, a conservative ornithopod dinosaur from the Upper Cretaceous of North America, with comments on ornithopod classification. Journal of Paleontology, 1974b, 1048–67.

Galton PM. 1978. Fabrosauridae, the basal family of ornithischian dinosaurs (Reptilia: Ornithopoda). Paläontologische Zeitschrift, 52, 138.

Galton PM. 1981. Dryosaurus, a hypsilophodontid dinosaur from the Upper Jurassic of North America and Africa; postcranial skeleton. Palaeontologische Zeitschrift, 55, 271–312.

Galton PM. 1983. The cranial anatomy of *Dryosaurus*, a hypsilophodontid dinosaur from the Upper Jurassic of North America and East Africa, with a review of hypsilophodontids from the Upper Jurassic of North America. Geologica et Palaeontologica, 17, 207–43.

Galton PM. 2001. Endocranial casts of the plated dinosaur *Stegosaurus* (Upper Jurassic, Western USA): A Complete and undistorted cast and the original specimens of Othniel Charles Marsh. 105-29. In Carpenter K, editor. The armored dinosaurs, Indiana University Press, 526 pp.

Galton PM. 2009. Notes on Neocomian (Lower Cretaceous) ornithopod dinosaurs from England - *Hypsilophodon*, *Valdosaurus*, "*Camptosaurus*", "*Iguanodon*" - and referred specimens from Romania and elsewhere. Revue de Paléobiologie, 28, 211–73.

Galton PM. 2014. Notes on the postcranial anatomy of the heterodontosaurid dinosaur *Heterodontosaurus tucki*, a basal ornithischian from the Lower Jurassic of South Africa, Revue de Paléobiologie, 33, 97–141.

Galton PM and Jensen JA. 1973. Skeleton of a Hypsilophodontid Dinosaur (*Nanosaurus* (?) *rex*) from the Upper Jurassic of Utah. Brigham Young University Research Studies, Geology Series, 20, 137–57.

Gasca M, Canudo J-I, and Moreno Azanza M. 2014. On the diversity of Iberian iguanodont dinosaurs : New fossils from the lower Barremian, Teruel province, Spain. Cretaceous Research, 50, 264–72.

Gilmore CW. 1909. Osteology of the Jurassic reptile *Camptosaurus*, with a revision of the species of the genus, and description of two new species. Proceedings of the United States National Museum, 36, 197–332.

Gilmore CW. 1914. Osteology of the armored Dinosauria in the United States National Museum, with special reference to the genus *Stegosaurus*. Bulletin of the United State National Museum, 89, 1–143.

Gilmore CW. 1915. Osteology of *Thescelosaurus*, an orthopodous dinosaur from the Lance Formation, Wyoming. Proceedings of the United States National Museum, 49, 591–616.

Gilmore CW. 1924. On *Troodon validus*, an Orthopodous Dinosaur from the Belly River Cretaceous of Alberta, Canada. University of Alberta Press, 1, 1–58.

Godefroit P, Codrea V and Weishampel DB. 2009. Osteology of *Zalmoxes shqiperorum* (Dinosauria, Ornithopoda), based on new specimens from the Upper Cretaceous of Nalat-Vad (Romania). Geodiversitas, 31, 525–53.

Godefroit P, Sinitsa SM, Dhouailly D, Bolotsky YL, Sizov AV, Mcnamara ME, Benton MJ, Spagna P. 2014. A Jurassic ornithischian dinosaur from Siberia with both feathers and scales. Science, 345, 451–55.

Goloboff PA, Farris JS, Nixon K 2008. TNT, a free program for phylogenetic analysis. Cladistic, 24, 774–86.

Han F-L, Barrett PM, Butler RJ and Xu X. 2012. Postcranial anatomy of *Jeholosaurus shangyuanensis* (Dinosauria, Ornithischia) from the Lower Cretaceous Yixian Formation of China. Journal of Vertebrate Paleontology, 32, 1370–95.

Han F-L, Forster CA, Clark JM and Xu X. 2015. Cranial anatomy of *Yinlong downsi* (Ornithischia : Ceratopsia) from the Upper Jurassic Shishugou Formation of Xinjiang, China, 36 : e1029579.

Han F-L, Forster CA, Xu X and Clark JM. 2018. Postcranial anatomy of *Yinlong downsi* (Dinosauria : Ceratopsia) from the Upper Jurassic Shishugou Formation of China and the phylogeny of basal ornithischians. Journal of Systematic Palaeontology, 16, 1159–87.

Han F-L, Zheng W, Hu D, Xu X and Barrett PM. 2014. A New Basal Ankylosaurid (Dinosauria : Ornithischia) from the Lower Cretaceous Jiufotang Formation of Liaoning Province, China. PLoS ONE, 9 : e104551.

Haubold H. 1990. *Emausaurus ernsti*, ein neuer dinosaurier (Ornithischia, Thyreophora) aus dem Unteren Jura des nördlichen Mitteleuropa. Revue de Paléobiologie, 9, 149–77.

Haughton SH. 1915. On some dinosaur remains from Bushmanland. Transactions of the Royal Society of South Africa, 5, 259–64.

He X and Cai K. 1984. The Middle Jurassic Dinosaurian Fauna from Dashanpu, Zigong, Sichuan. Vol. I. The Ornithopod Dinosaurs. Sichuan Scientific and Technological Publishing House, 1–66.

Herne MC. 2014. Anatomy, systematics and phylogenetic relationships of the Early Cretaceous ornithopod dinosaurs of the Australian-Antarctic rift system [dissertation]. The University of Queensland, Brisbane, 335 pp.

Herne MC, Nair JP, Evans AR and Tait AM. 2019. New small-bodied ornithopods (Dinosauria, Neornithischia) from the Early Cretaceous Wonthaggi Formation (Strzelecki Group) of the Australian-Antarctic rift system, with revision of *Qantassaurus intrepidus*. Journal of Paleontology, 93, 543-584.

Herne MC, Tait AM, Weisbecker V, Hall M, Nair JP, Cleeland M and Salisbury SW. 2018. A new small-bodied ornithopod (Dinosauria, Ornithischia) from a deep, high-energy Early Cretaceous river of the Australian–Antarctic rift system. PeerJ, 5, e4113.

Horner JR and Goodwin MB. 2009. Extreme Cranial Ontogeny in the Upper Cretaceous Dinosaur *Pachycephalosaurus*. PLoS ONE, 4, 1-11.

Hou L. 1977. A primitive pachycephalosaurid from the Cretaceous of Anhui, China, *Wannanosaurus yansiensis* gen. et sp. nov. Vertebrata PalAsiatica, 15, 198–202.

Hübner TR and Rauhut OWM. 2010. A juvenile skull of *Dysalotosaurus lettowvorbecki* (Ornithischia : Iguanodontia), and implications for cranial ontogeny, phylogeny, and taxonomy in ornithopod dinosaurs. Zoological Journal of the Linnean Society, 160, 366-396.

Huh M, Lee D, Kim J, Lim J and Godefroit P. 2010. A new basal ornithopod dinosaur from the Upper Cretaceous of South Korea. Neues Jahrbuch Fuer Geologie Und Palaeontologie Abhandlungen, 259, 1–24.

Ibiricu LM, Martinez RD, Luna M and Casal GA. 2014. A reappraisal of *Notohypshilophodon comodorensis* (Ornithischia : Ornithopoda) from the Late Cretaceous of Patagonia, Argentina. Zootaxa, 3786, 401–22.

Janensch W. 1955. Der Ornithopod *Dysalotosaurus* der Tendaguruschichten [The ornithopod *Dysalotosaurus* from the Tendaguru]. Palaeontographica, Suppl. 7, 1955, 105–76. German.

Junchang L, Qiang J, Yubo G and Zhixin L. 2007. A New Species of the Ankylosaurid Dinosaur *Crichtonsaurus* (Ankylosauridae : Ankylosauria) from the Cretaceous of Liaoning Province, China. Acta Geologica Sinica, 81, 883–97.

Liyong J, Jun C, Shuqin Z, Butler RJ and Godefroit P. 2010. Cranial anatomy of the small ornithischian dinosaur *Changchunsaurus parvus* from the Quantou Formation (Cretaceous, Aptian-Cenomanian) of Jilin Province, northeastern China. Journal of Vertebrate Paleontology, 30, 196–214.

Maidment SCR, Brassey C and Barrett PM. 2015. The Postcranial Skeleton of an Exceptionally Complete Individual of the Plated Dinosaur *Stegosaurus stenops* (Dinosauria : Thyreophora) from the Upper Jurassic Morrison Formation of Wyoming, U.S.A. PLoS ONE, 10 : e0138352.

Maidment SCR and Porro LB. 2010. Homology of the palpebral and origin of supraorbital ossifications in ornithischian dinosaurs. Lethaia, 43, 95–111.

Makovicky PJ. 2001. A *Montanoceratops cerorhynchus* (Dinosauria: Ceratopsia) braincase from the Horseshoe Canyon Formation of Alberta. 243-62. In Tanke DH and Carpenter K, editors. Mesozoic Vertebrate Life, Indiana University Press, Bloomington and Indianapolis, 352 pp.

Makovicky PJ, Kilbourne BM, Sadleir RW and Norell MA. 2011. A new basal ornithopod (Dinosauria, Ornithischia) from the Late Cretaceous of Mongolia. Journal of Vertebrate Paleontology, 31, 626–640.

Mallon JC and Anderson JS. 2014. The Functional and Palaeoecological Implications of Tooth Morphology and Wear for the Megaherbivorous Dinosaurs from the Dinosaur Park Formation (Upper Campanian) of Alberta, Canada. PLoS ONE, 9 : e98605.

Marsh OC. 1887. Principal characters of American Jurassic dinosaurs; Part IX, The skull and dermal armor of *Stegosaurus*. American Journal of Science, 203, 413–17.

Maryanska T and Osmolska H. 1974. Pachycephalosauria, a New Suborder of Ornithischian Dinosaurs. Palaeontologia Polonica, 30, 45–102.

Mateus O and Antunes MT. 2001. *Draconyx loureiroi*, a new camptosauridae (Dinosauria, Ornithopoda) from the Late Jurassic of Lourinha, Portugal. Annales de Paléontologie, 87, 61–73.

Matheron P. 1869. Notice sur les reptiles fossiles des dépots fluvio-lacustres crétacés du bassin à lignite de Fuveau. Mémoire de l'Académie Impériale Des Sciences, Belles-Lettres et Arts de Marseille, 1–39.

Mcdonald AT. 2012. Phylogeny of basal iguanodonts (Dinosauria: Ornithischia): An update. PLoS ONE, 7 : e36745.

Mcdonald AT, Kirkland JI, Deblieux DD, Madsen SK, Cavin J, Milner ARC and Panzarin L. 2010. New basal iguanodonts from the cedar mountain formation of utah and the evolution of thumb-spiked dinosaurs. PLoS ONE, 5 : e14075.

Molnar RE. 1996. Observations on the australian ornithopod dinosaur *Muttaburrasaurus*. Memoirs of the Queensland Museum, 39, 639–52.

Newman BH. 1968. The Jurassic dinosaur Scelidosaurus harrisoni, Owen. Palaeontology, 11, 40–3.

Nopcsa FB. 1925. Dinosaurierreste aus siebenbürgen. IV. Die Wirbelsaule von Rhabdodon und Orthomerus. Palaeontologica Hungarica, 1, 273-316.

Nopcsa FB. 1929. Sexual differences in Ornithopodous dinosaurs. Palaeobiologica, 2, 187–201.

Norell MA and Barta DE. 2016. A new specimen of the ornithischian dinosaur Haya griva, cross-Gobi geologic correlation, and the age of the Zos Canyon beds. American Museum Novitates, 3851, 1-20.

Norman DB. 1980. On the ornithischian dinosaur *Iguanodon bernissartensis* from the Lower Cretaceous of Bernissart (Belgium). Mémoires de l'Institut Royal des Sciences Naturelles de Belgique, 178, 1-105.

Norman DB, Crompton AW, Butler RJ, Porro LB and Charig AJ. 2011. The Lower Jurassic ornithischian dinosaur *Heterodontosaurus tucki* Crompton and Charig, 1962 : cranial anatomy, functional morphology, taxonomy, and relationships. Zoological Journal of the Linnean Society, 163, 182–276.

Norman DB, Sues H-D, Witmer LM, Coria RA. 2004. Basal Ornithopoda. 393–412. In Weishampel DB, Sues H-D, Witmer LM and Coria RA, editors. The Dinosauria, 2nd edn. Berkeley: University of California Press, 861 pp.

Novas FE. 1994. New information on the systematics and postcranial skeleton of *Herrerasaurus ischigualastensis* (Theropoda : Herrerasauridae) from the Ischigualasto Formation (Upper Triassic) of Argentina. Journal of Vertebrate Paleontology, 13, 400–23.

Ösi A, Prondvai E, Butler R and Weishampel DB. 2012. Phylogeny, Histology and Inferred Body Size Evolution in a New Rhabdodontid Dinosaur from the Late Cretaceous of Hungary. PLoS ONE, 7 : e44318.

Osborn HF. 1923. Two Lower Cretaceous dinosaurs from Mongolia. American Museum Novitates, 95, 1–10.

Osborn HF. 1924. *Psittacosaurus* and *Protiguanodon*: two lower Cretaceous iguanodonts from Mongolia. American Museum Novitates, 127, 1–16.

Owen R. 1858. Monograph on the fossil Reptilia of the Wealden and Purbeck Formations. Part V. Lacertilia. Monographs of the Palaeontographical Society, 12, 31–39.

Owen R. 1861. Monographs on the British Fossil Reptilia from the Oolitic Formations. Part First, Containing *Scelidosaurus harrisonii* and *Pliosaurus grandis*. Monographs of the Palaeontographical Society, 13, 1-16.

Owen R. 1863. Monographs on the British Fossil Reptilia from the Oolitic Formations. Part Second, Containing *Scelidosaurus harrisonii* and *Pliosaurus grandis*. Monographs of the Palaeontographical Society, 14, 1-26.

Parks WA. 1926. *Thescelosaurus warreni*, a new species of orthopodous dinosaur from the Edmonton Formation of Alberta. University of Toronto Studies, Geological Series, 21, 1–42.

Paulina-Carabajal A, Lee Y-N and Jacobs LL. 2016. Endocranial Morphology of the Primitive Nodosaurid Dinosaur *Pawpawsaurus campbelli* from the Early Cretaceous of North America. PLoS ONE, 11 : e0150845.

Peng G. 1992. Jurassic ornithopod *Agilisaurus louderbacki* (Ornithopoda: Fabrosauridae) from Zigong, Sichuan, China. Vertebrata PalAsiatica, 30, 39–53.

Peng G. 1997. Fabrosauridae. 237-40. In CURRIE P and PADIAN K, editors. Encyclopedia of Dinosaurs, Academic Press, San Diego, 869 pp.

Perle A, Maryanska T and Osmolska H. 1982. *Goyocephale lattimorei* gen. et sp. n., a new flat-headed pachycephalosaur (Ornithischia, Dinosauria) from the Upper Cretaceous of Mongolia. Acta Palaeontologica Polonica, 27, 8–132.

Pincemaille-Quillevere M. 2002. Description d'un squelette partiel de *Rhabdodon priscus* (Euornithopoda) du Crétacé supérieur de Vitrolles (Bouches du Rhône, France) [Description of a partial skeleton of *Rhabdodon priscus* (Euornithopoda) from the Upper Cretaceous of Vitrolles (Bouches du Rhône, France)]. Oryctos, 4, 39–70. French.

Pol D, Rauhut OWM and Becerra M. 2011. A Middle Jurassic heterodontosaurid dinosaur from Patagonia and the evolution of heterodontosaurids. Naturwissenschaften, 98, 369–79.

Porro LB, Witmer LM and Barrett PM. 2015. Digital preparation and osteology of the skull of Lesothosaurus diagnosticus (Ornithischia : Dinosauria). PeerJ, 3 : e1494.

Rosenbaum JN and Padian K. 2000. New material of the basal Thyreophoran *Scutellosaurus lawleri* from the Kayenta Formation (Lower Jurassic) of Arizona. PaleoBios, 20, 13–23.

Rozadilla S, Agnolin FL, Novas FE, Aranciaga Rolando AM, Matias JM, Lirio JM and Isasi MP. 2016. A new ornithopod (Dinosauria, Ornithischia) from the Upper Cretaceous of Antarctica and its palaeobiogeographical implications. Cretaceous Research, 57, 311–324.

Rozadilla S, Agnolin FL, Novas FE. 2019. Osteology of the Patagonian ornithopod *Talenkauen santacrucensis* (Dinosauria, Ornithischia). Journal of Systematic Paleontology. 17, 1-47.

Rozadilla S, Cruzado-Caballero P, Calvo JO. 2020. Osteology of Ornithopod *Macrogryphosaurus gondwanicus* (Dinosauria, Ornithischia) from the Upper Cretaceous of Patagonia, Argentina, Cretaceous Research, https://doi.org/10.1016/j.cretres.2019.104311.

Ruiz-Omeñaca JI. 1996. Los dinosaurios hipsilofodontidos (Reptilia: Ornithischia) del Cretácico Inferior de Galve (Teruel) [The hypsilophodontid dinosaurs (Reptilia: Ornithischia) from the Lower Cretaceous of Galve (Teruel)]. Unpublished Bc Thesis, Universidad de Zaragoza, Zaragoza. Spanish.

Sachs S, Hornung JJ. 2005. Juvenile ornithopod (Dinosauria : Rhabdodontidae) remains from the Upper Cretaceous (Lower Campanian, Gosau Group) of Muthmannsdorf (Lower Austria). Geobios, 39, 415–25.

Salgado L, Canudo JI, Garrido AC, Moreno-Azanza M, Martinez LCA, Coria RA and Gasca JM. 2017. A new primitive neornithischian dinosaur from the Jurassic of Patagonia with gut contents. Nature Publishing Group, 7, 1–10.

Salgado L, Coria RA, Heredia SE. 1997. New materials of *Gasparinisaura cincosaltensis* (Ornithischia, Ornithopoda) from the Upper Cretaceous of Argentina. Journal of Paleontology, 71, 933–40.

Scheetz RD. 1999. Osteology of *Orodromeus malelai* and the phylogeny of basal ornithopod dinosaurs [dissertation]. Montana State University, Bozeman, 186 pp.

Senter P. 2007. Analysis of forelimb function in basal ceratopsians. Journal of Zoology, 273, 305–14.

Sereno PC. 1991. Lesothosaurus, “Fabrosaurids,” and the early evolution of Ornithischia. Journal of Vertebrate Paleontology, 11, 168–97.

Sereno PC. 1992. New data on parrot-beaked dinosaurs. 203-10. In Carpenter K and Currie PJ, editors. Dinosaur Systematics: Approaches and Perspectives, Cambridge University Press, 318 pp.

Sereno PC. 1993. The pectoral girdle and forelimb of the basal theropod *Herrerasaurus ischigualastensis*. Journal of Vertebrate Paleontology, 13, 425–50.

Sereno PC. 2000. The fossil record, systematics and evolution of pachycephalosaurs and ceratopsians from Asia. 480–516. In Benton MJ, Shishkin MA, Unwin DM and Kurochkin EN, editors. The Age of Dinosaurs in Russia and Mongolia, Cambridge University Press, 740 pp.

Sereno PC. 2010. Taxonomy, Cranial Morphology, and Relationships of Parrot-Beaked Dinosaurs (Ceratopsia: Psittacosaurus). In Ryan MJ, Chinnery-Allgeier BJ and Eberth DA, editors. New perspectives on horned dinosaurs: the Royal Tyrrell Museum Ceratopsian Symposium, Indiana University Press, 656 pp.

Sereno PC. 2012. Taxonomy, morphology, masticatory function and phylogeny of heterodontosaurid dinosaurs, 226, 1–225.

Sereno PC and Novas FE. 1993. The skull and neck of the basal theropod *Herrerasaurus ischigualastensis*. Journal of Vertebrate Paleontology, 13, 451–76.

Sereno PC, Shichin C, Zhengwu C and Chenggang R. 1988. *Psittacosaurus meileyingensis* (Ornithischia : Ceratopsia), a new psittacosaur from the Lower Cretaceous of northeastern China. Journal of Vertebrate Paleontology, 8, 366–77.

Sereno PC, Xijin Z, Brown L and Lin T. 2007. New psittacosaurid highlights skull enlargement in horned dinosaurs. Acta Palaeontologica Polonica, 52, 275–84.

Shepherd JD, Galton PM and Jensen JA. 1977. Additional Specimens of the Hypsilophodontid Dinosaur *Dryosaurus altus* from the Upper Jurassic of Western North America. Brigham Young University Research Studies, Geology Series, 24, 11–5.

Snively E and Theodor JM. 2011. Common Functional Correlates of Head-Strike Behavior in the Pachycephalosaur *Stegoceras validum* (Ornithischia, Dinosauria) and Combative Artiodactyls. PLoS ONE, 6 : e21422.

Sternberg CM. 1940. *Thescelosaurus edmontonensis*, n. sp. and classification of the Hypsilophodontidae. Journal of Paleontology, 14, 481–94.

Suberbiola XP and Sanz JL. 1999. The ornithopod dinosaur *Rhabdodon* from the Upper Cretaceous of Laño (Iberian Peninsula). Estudios Del Museo de Ciencias Naturales de Alava, 14 (Núm. Espec. 1), 257–72.

Sullivan RM. 2006. A taxonomic review of the Pachycephalosauridae (Dinosauria: Ornithischia). New Mexico Museum of Natural History and Science Bulletin, 35, 347-65.

Sues H-D. 1980. Anatomy and relationships of a new hypsilophodontid dinosaur from the Lower Cretaceous of North America. Palaeontographica Abteilung A, 169, 51–72.

Sues H-D and Galton PM. 1987. Anatomy and Classification of the North American Pachycephalosauria (Dinosauria: Ornithischia). Palaeontographica Abteilung A, 198, 1–40.

Tanoue K, You H-L and Dodson P. 2010. Mandibular Anatomy in Basal Ceratopsia. 234–250. In Ryan MJ, Chinnery-Allgeier BJ and Eberth DA, editors. New perspectives on horned dinosaurs: the Royal Tyrrell Museum Ceratopsian Symposium, Indiana University Press, 656 pp.

Tennant J. 2013. Osteology of a near-complete skeleton of *Tenontosaurus tilletti* (Dinosauria: Ornithopoda) from the Cloverly Formation, Montana, USA [master's thesis]. University of Manchester, Manchester, 195 pp.

Thomas DA. 2015. The cranial anatomy of *Tenontosaurus tilletti* Ostrom, 1970 (Dinosauria, Ornithopoda). Palaeontologia Electronica, 18, 1–99.

Thulborn RA. 1972. The post cranial skeleton of the Triassic ornithischian dinosaur *Fabrosaurus australis*. Palaeontology, 15, 29–60.

Thulborn RA. 1977. Relationships of the Lower Jurassic Dinosaur Scelidosaurus harrisonii. Journal of Paleontology, 51, 725–39.

Verdu F-J, Godefroit P, Royo-Torres R, Cobos A and Alcala L. 2017. Individual variation in the postcranial skeleton of the Early Cretaceous *Iguanodon bernissartensis* (Dinosauria : Ornithopoda). Cretaceous Research, 74, 65–86.

Weishampel DB and Heinrich RE. 1992. Systematics of hypsilophodontidae and basal Iguanodontia (dinosauria: Ornithopoda). Historical Biology: An International Journal of Paleobiology, 6, 159–84.

Weishampel DB, Jianu C-M, Csiki Z and Norman DB. 2003. Osteology and phylogeny of *Zalmoxes* (n. g.), an unusual Euornithopod dinosaur from the latest Cretaceous of Romania. Journal of Systematic Palaeontology, 1, 65.

Winkler DA, Murry PA and Jacobs LL. 1997. A new species of *Tenontosaurus* (Dinosauria; Ornithopoda) from the Early Cretaceous of Texas. Journal of Vertebrate Paleontology, 17, 330–48.

Xu X, Forster CA, Clark JM and Mo J. 2006. A basal ceratopsian with transitional features from the Late Jurassic of northwestern China. Proceedings of the Royal Society of London, Series B. 273, 2135–140.

Xu X, Makovicky PJ, Wang X, Norell MA and You H. 2002. A ceratopsian dinosaur from China and the early evolution of Ceratopsia. Nature, 416, 314–17.

You H-L and Dodson P. 2003. Redescription of neoceratopsian dinosaur *Archaeoceratops* and early evolution of Neoceratopsia. Acta Palaeontologica Polonica, 48, 261–72.

You H-L and Dodson P. 2004. Basal Ceratopsia. 478–93. In Weishampel DB, Sues H-D, Witmer LM and Coria RA, editors. The Dinosauria, 2nd edition, Berkeley: University of California Press, 861 pp.

You H-L, Tanoue K and Dodson P. 2007. A new specimen of *Liaoceratops yanzigouensis* (Dinosauria: Neoceratopsia) from the Early Cretaceous of Liaoning Province, China. Acta Geologica Sinica - English Edition, 81, 898–904.

You H-L, Tanoue K and Dodson P. 2008. New data on cranial anatomy of the ceratopsian dinosaur *Psittacosaurus major*. Acta Palaeontologica Polonica, 53, 183–96.

You H-L, Xu X and Wang X. 2003. A New Genus of Psittacosauridae (Dinosauria : Ornithopoda) and the Origin and Early Evolution of Marginocephalian Dinosaurs. Acta Geologica Sinica, 77, 15-20.

Zhao X, Cheng Z and Xu X. 1999. The earliest ceratopsian from the Tuchengzi Formation of Liaoning, China. Journal of Vertebrate Paleontology, 19, 681–91.

Zheng W, Jin X, Shibata M, Azuma Y and Yu F. 2012. A new ornithischian dinosaur from the Cretaceous Liangtoutang Formation of Tiantai, Zhejiang Province, China. Cretaceous Research, 34, 208–19.

Zheng X-T, You H-L, Xu X and Dong Z-M. 2009. An Early Cretaceous heterodontosaurid dinosaur with filamentous integumentary structures. Nature, 458, 333–36.

Supplemental material 6: Table of clades names, definitions and supporting characters.

Clade name and original author's defintion	Definition used	Phylogenetic definition	Diagnosis type	Common characters for each clade
Ornithischia, SEELEY 1887	Butler, Upchurch & Norman 2008	All dinosaurs more closely related to *Triceratops horridus* MARSH 1889 than to either *Passer domesticus* (Linnaeus 1758), or *Saltasaurus loricatus* BONAPARTE & POWELL 1980.	Stem	130(1) ; 145(1) ; 165(1) ; 168(1) ; 169(1) ; 172(1) ; 175(1) ; 177(1) ; 193(0) ; 204(1) ; 222(0) ; 223(0) ; 259(1) ; 278(1) ; 279(1) ; 284(1) ; 292(0) ; 301(2) ; 312(1) ; 313(1).
Genasauria SERENO 1986	Sereno 2005	*Ankylosaurus magniventris* BROWN 1908, *Stegosaurus stenops* MARSH 1877a, *Parasaurolophus walkeri* PARKS 1922, *Triceratops horridus* (Marsh 1889), *Pachycephalosaurus wyomingensis* (Gilmore 1931), their most recent common ancestor and all descendants.	Node	62(1) ; 251(0) ; 282(1) ; 311(0).
Tyreophora	Butler,	All genasaurians more closely related to	Stem	176(0) ;

NOPCSA, 1915	Upchurch & Norman 2008	*Ankylosaurus magniventris* BROWN 1908 than to *Parasaurolophus walkeri* PARKS 1922, *Triceratops horridus* MARSH 1889, or *Pachycephalosaurus wyomingensis* (Gilmore 1931).		218(1) ; 224(0) ; 227(0).
Neornithischia COOPER 1985	Butler, Upchurch & Norman 2008	All genasaurians more closely related to *Parasaurolophus walkeri* PARKS 1922 than to *Ankylosaurus magniventris* BROWN 1908 or *Stegosaurus stenops* MARSH 1877a.	Stem	33(1) ; 38(1) ; 63(0) ; 148(1) ; 185(1) ; 196(1) ; 207(1) ; 253(0) ; 273(2) ; 281(2) ; 283(1) ; 300(1) ; 321(1).
Cerapoda SERENO 1986	Butler, Upchurch & Norman 2008	*Parasaurolophus walkeri* PARKS 1922, *Triceratops horridus* MARSH 1889, their most recent common ancestor and all descendants.	Node	57(1) ; 132(2) ; 199(0) ; 204(2) ; 264(1) ; 296(1) ; 298(1) ; 299(1).
Marginocephalia SERENO 1986	Butler, Upchurch & Norman 2008	*Triceratops horridus* MARSH 1889, *Pachycephalosaurus wyomingensis* (Gilmore 1931), their most recent common ancestor and all descendants.	Node	29(1) ; 40(1) ; 69(1) ; 70(1) ; 104(2) ; 157(2) ; 159(1) ; 179(0) ; 195(1) ; 202(0) ; 222(1) ;

				270(1) ; 282(2) ; 288(2) ; 297(1) ; 329(1).
Pachycephalosauria MARYANSKA & OSMOLSKA 1974	Maryanska & Osmolska 1974	All marginocephalians closer to *Pachycephalosaurus* than to *Triceratops* MARSH 1889	Stem	4(0) ; 14(1) ; 28(1) ; 41(1) ; 72(1) ; 109(1) ; 113(1) ; 138(1) ; 141(0) ; 145(0) ; 162(0) ; 181(1) ; 183(1) ; 208(0) ; 209(1) ; 241(1) ; 244(2) ; 248(1) ; 251(1) ; 252(0) 254(1) ; 256(1) ; 290(1) ; 313(0) ; 316(1) ; 325(2).
Heterodontosaurinae KHUN 1966	Sereno 2012	The most inclusive clade containing *Heterodontosaurus tucki* CROMPTON & CHARIG 1962 but not *Tianyulong confuciusi* ZHENG *et al.* 2009, *Fruitadens haagarorum* BUTLER *et al.* 2010, *Echinodon becklesii* OWEN 1858.	Stem	161(0) ; 175(1) ; 177(0).
Pachycephalosauridae STERNBERG 1945	Sereno 1998	*Stegoceras*, *Pachycephalosaurus*, their most recent	Node	71(1) ; 158(1).

		common ancestor and all descendants		
Ceratopsia MARSH 1890	Sereno, 1998	All marginocephalian closer to *Triceratops* than to *Pachycephalosaurus*	Stem	1(1) ; 8(1) ; 20(0) ; 25(1) ; 34(1) ; 49(1) ; 66(1) ; 68(1) ; 72(2) ; 74(0) ; 83(1) ; 83(1) ; 114(1) ; 124(1) ; 128(1) ; 155(1) ; 160(1) ; 164(1) ; 170(1) ; 173(0) ; 174(1) ; 280(2) ; 281(1) ; 285(2).
Neoceratopsia SERENO 1986	Sereno, 1998	All ceratopsian closer to *Triceratops* than to *Psittacosaurus*	Stem	58(1) ; 89(2) ; 92(0) ; 136(1) ; 147(2) ; 152(1) ; 171(2) ; 172(0) ; 189(2).
Psittacosauridae OSBORN 1923	Sereno *et al.* 2005	The most inclusive clade containing *Psittacosaurus mongoliensis* OSBORN 1923 but not *Triceratops horridus* MARSH 1889	Stem	336(0).

Ornithopoda MARSH 1881	Marsh 1881	All genasaurians more closely related to *Parasaurolophus walkeri* PARKS 1922, than to *Triceratops horridus* MARSH 1889.	Stem	27(1) ; 37(1) ; 45(1) ; 100(1) ; 101(1) ; 115(1) ; 134(1) ; 142(1) ; 154(1) ; 158(1) ; 174(2) ; 211(1) ; 216(1) ; 280(1).
Clypeodonta NORMAN 2015	Norman 2015	*Hypsilophodon foxii* HUXLEY 1869, *Edmontosaurus regalis* LAMBE 1917, their most recent common ancestor, and all of its descendants.	Node	35(1) ; 38(2) ; 80(1) ; 92(0) ; 126(0) ; 139(1) ; 171(2) ; 172(0) ; 206(1) ; 336(0).
Hypsilophodontidae DOLLO 1882	Sereno 2005	All neornithischians more closely related to *Hypsilophodon foxii* Huxley 1869 than to *Parasaurolophus walkeri* Parks 1922.	Stem	ø
Parksosauridae BUCHHOLZ 2002	Boyd 2015	All neornithischians more closely related to *Parksosaurus warreni* PARKS 1926 than to *Hypsilophodon foxii* HUXLEY 1869, *Dryosaurus altus* (Marsh 1878), or *Parasaurolophus walkeri* PARKS 1922	Stem	194(0) ; 211(0) ; 216(0) ; 253(1) ; 270(1) ; 297(2).

Thescelosaurinae STERNBERG 1937	Boyd 2015	All neornithischians more closely related to *Thescelosaurus neglectus* Gilmore, 1913 than to *Orodromeus makelai* HORNER & WEISHAMPEL 1988 or *Parasaurolophus walkeri* PARKS 1922.	Stem	52(1) ; 107(1) ; 111(1) ; 212(1) ; 302(1).
Iguanodontia, DOLLO 1888	Sereno 2005	All ornithopods more closely related to *Parasaurolophus walkeri* PARKS 1922 than to *Hypsilophodon foxii* Huxley 1869 or *Thescelosaurus neglectus* GILMORE 1913.	Stem	19(0) ; 188(2) ; 190(1) ; 196(0) ; 244(1) ; 255(1) ; 307(1) ; 326(1).
Rhabdodontidae WEISHAMPEL, JIANU, CSIKI & NORMAN 2003	This study.	The most recent common ancestor of *Zalmoxes robustus*, *Rhabdodon priscus*, the Vegagete ornithopod and all the descendants of this common ancestor.	Node	178(1) ; 233(1) ; 234(1) ; 242(2) ; 306(0).
Rhabdodontomorpha DIEUDONNE, TORTOSA, TORCIDA FERNANDEZ-BALDOR, CANUDO, DIAZ-MARTINEZ 2016	Dieudonné, Tortosa, Torcida Fernández-Baldor, Canudo, Díaz-Martínez 2016	the most inclusive clade containing *Rhabdodon priscus* MATHERON 1869 and *Muttaburrasaurus langdoni* BARTHOLOMAI & MOLNAR 1981.	Node	86(1) ; 112(2) ; 113(0) ; 262(2) ; 267(1) ; 270(2) ; 275(1) ; 276(1) ; 331(1).
Dryomorpha SERENO 1986	Boyd 2015	*Dryosaurus altus* (Marsh 1878), *Parasaurolophus walkeri* PARKS 1922, their most recent	Node	171(1) ; 174(1) ; 188(1) ; 196(1) ; 244(0) ;

		common ancestor and all descendants.		282(0) ; 292(1) ; 305(2).
Dryosauridae MILNER & NORMAN 1984	Sereno 2005	All iguanodontians more closely related to *Dryosaurus altus* (Marsh 1878) than to *Parasaurolophus walkeri* PARKS 1922.	Stem	40(1) ; 43(0) ; 46(0) ; 62(0) ; 63(1) ; 82(1) ; 115(1) ; 130(0) ; 208(2) ; 224(0) ; 298(2) ; 309(0) ; 330(1).
Elasmaria CALVO, PORFIRI & NOVAS 2007	Calvo, Porfiri & Novas 2007 *sensu* Rozadilla, Agnolin, Novas, Aranciaga Rolando, Motta, Lirio, Isasi 2016	*Talenkauen santacrucensis* NOVAS, CAMBIASO & AMBROSIA 2004 and *Macrogryphosaurus gondwanicus* CALVO, PORFIRI & NOVAS 2007, their most recent common ancestor and all descendants.	Node	198(2) ; 203(0) ; 212(1) ; 231(3) ; 236(2) ; 270(1) ; 300(0) ; 330(1).
Ankylopollexia SERENO 1986	Sereno 2005	*Camptosaurus dispar* (Marsh 1879), *Parasaurolophus walkeri* PARKS 1922, their most recent common ancestor and all descendants.	Node	142(2) ; 145(2) ; 226(0) ; 246(1) ; 250(1) ; 270(1) ; 276(1) ; 314(1).

Characters supporting each clade were obtained through the « Map Common Synapomorphies » and « Character mapping » options of TNT (Goloboff *et al.* 2008) onto the semi-strict consensus tree with removal of the wildcard taxon *Yandusaurus hongheensis* (see

Supplemental material 1 for accessing corresponding character description). We remarked that the « Common Synapomorphies » referred to in TNT do not consider those synapomorphic characters when one or several closely related sister taxa are unknown for the state of that character. We revised each character one by one by activating the « Character mapping option » and completed our list of common characters manually to include those characters which distribution actually support the clade, despite of being unknown in one or several closely related sister taxa (written in blue font). We should also point out that taxonomic sampling is non-exhaustive. For this reason, those listed characters do not constitute an official synapomorphy list, but rather provide a broad picture of character support for each clade.

BIBLIOGRAPHY

Bonaparte JF and Powell JE. 1980. A continental assemblage of tetrapods from the Upper Cretaceous bed of El Brete, northwestern Argentina (Sauropoda-Coelurosauria-Carnosauria-Aves). Mémoires de la Société Geologique, France 139, 19–28.

Boyd CA. 2015. The systematic relationships and biogeographic history of ornithischian dinosaurs. PeerJ, 3, 1–62.

Brown B. 1908. The Ankylosauridae, a new family of armored dinosaurs from the Upper Cretaceous. Bulletin of the American Museum of Natural History, 24, 187–201.

Buchholz PW 2002. Phylogeny and biogeography of basal Ornithischia. In Brown DE, editor. The Mesozoic in Wyoming. Casper, Wyoming: Tate Geological Museum, 18–34.

Butler RJ, Upchurch P and Norman DB 2008. The phylogeny of the ornithischian dinosaurs. Journal of Systematic Paleontology, 6, 1–40.

Calvo JO, Porfiri JD and Novas FE. 2007. Discovery of a new ornithopod dinosaur from the Portezuelo Formation (Upper Cretaceous), Neuquen, Patagonia, Argentina. Arquivos do Museu Nacional, 65, 471–483.

Cooper MR. 1985. A revision of the ornithischian dinosaur *Kangnasaurus coetzeei* Haughton with a classification of the Ornithischia. Annals of the South African Museum, 95, 281–317.

Dollo L. 1882. Première note sur les dinosauriens de Bernissart. Bulletin de Museum Royal de Histoire Naturelles de Belgique, 1, 161–180.

Dollo L. 1888. Iguanodontidae et Camptonotidae [Iguanodontidae and Camptonotidae]. Comptes Rendus de Académie des Sciences, 106, 775–777. French.

Gilmore CW. 1913. A new dinosaur from the Lance Formation of Wyoming. Smithsonian Miscellaneous Collections, 61, 1–5.

Gilmore CW. 1931. A new species of troodont dinosaur from the Lance Formation of Wyoming. Proceedings of the United States National Museum, 79, 1–6.

Goloboff P, Farris JS, Nixon K. 2008. TNT, a free program for phylogenetic analysis. Cladistic, 24, 774–86.

Horner J and Weishampel DB. 1988. A comparative embryological study of two ornithischian dinosaurs. Nature, 332, 256–257.

Huxley TJ. 1869. On *Hypsilophodon*, a new genus of Dinosauria. Abstracts of the Proceedings of the Geological Society of London, 204, 3–4.

Kuhn O. 1966. Die Reptilien. System und Stammesgeschichte [The reptiles. System and tribal history], Verlag Oeben, Krailling bei München, 154 pp. German.

Lambe LM. 1917. A new genus and species of crestless hadrosaur from the Edmonton Formation of Alberta. The Ottawa Naturalist, 31, 65–73.

Linnaeus C. 1758. Systema Naturae per regna tria naturae. Volume 1 Regnum Animale. 10th Edition. London: Trustees, British Museum (Natural History), 823 pp.

Marsh OC. 1877. New order of extinct Reptilia (Stegosauria) from the Jurassic of the Rocky Mountains. American Journal of Science, Series 3, 14, 513–514.

Marsh OC. 1878. Principal characters of American Jurassic dinosaurs. American Journal of Science, Series 3, 16, 411–416.

Marsh OC. 1879. Notice of new Jurassic reptiles. American Journal of Science, Series 3, 18, 501–505.

Marsh OC. 1881. Principal characters of American Jurassic dinosaurs. Part V. American Journal of Science, Series 3, 21, 417–423.

Marsh OC. 1889. Notice of gigantic horned Dinosauria from the Cretaceous. American Journal of Science, Series 3, 38, 173–175.

Marsh OC. 1890. Additional characters of the Ceratopsidae, with notice of new Cretaceous dinosaurs. American Journal of Science, 39 (233), 418–429.

Nopcsa F. 1915. Die Dinosaurier der siebenbürgischen Landesteile. Mitteilungen aus dem Jahrbuche der Koniglich-Ungarischen Geologischen Reichsanstalt, 23, 1–26.

Norman DG. 2015. On the history, osteology, and systematic position of the Wealden (Hastings group) dinosaur *Hypselospinus fittoni* (Iguanodontia: Styracosterna). Zoological Journal of the Linnean Society, 173, 92–189.

Novas FE, Cambiaso AV and Ambrosio A. 2004. A new basal iguanodontian (Dinosauria, Ornithischia) from the Upper Cretaceous of Patagonia. Ameghiniana, 41, 75–82.

Owen R. 1858. Monograph on the fossil Reptilia of the Wealden and Purbeck Formations. Part V. Lacertilia. Monographs of the Palaeontographical Society, 12, 31–9.

Parks WA. 1922. *Parasaurolophus walkeri*, a new genus and species of crested trachodont dinosaur. University of Toronto Studies, Geological Series, 13, 1–32.

Seeley HG. 1887. On the classification of the fossil animals commonly named Dinosauria. Proceedings of the Royal Society of London, 43, 165–171.

Sereno PC. 1986. Phylogeny of the bird-hipped dinosaurs. National Geographic Research, 2, 234–256.

Sereno PC. 1998. A rationale for phylogenetic definitions with application to the higher-level taxonomy of Dinosauria. Neues Jahrbuch für Geologie and Paläeontologie Abhandlungen, 210, 41–83.

Sereno PC. 2005. The logical basis of phylogenetic taxonomy. Systematic Biology, 54, 595–619

Sereno PC, McAllister S, and Brusatte SL. 2005. TaxonSearch: A relational database for suprageneric taxa and phylogenetic definitions. PhyloInformatics, 8, 1–20.

Sternberg CM. 1937. A classification of *Thescelosaurus*, with a description of a new species. Proceedings of the Geological Society of America (for 1936), 375.

Sternberg CM. 1945. Pachycephalosauridae proposed for dome-headed dinosaurs, *Stegoceras lambei* n. sp., described. Journal of Paleontology, 19, 534–538.

Weishampel DB, Jianu C-M, Csiki Z and Norman DB. 2003 Osteology and phylogeny of *Zalmoxes* (n. g.), an unusual euornithopod dinosaur from the latest Cretaceous of Romania. Journal of Systematic Palaeontology, 1 (2), 65–123.

Supplemental material 5 – Templeton tests for three phylogenetic hypotheses against the reference tree.

Templeton tests were run using the TNT script developed by Alexander N. Schmidt-Lebuhn (2016). The test of Templeton (1983) is a one-tailed Wilcoxon signed-rank test which challenges the null hypothesis that the second hypothetical tree to be tested fits the data as well as the first one which was obtained from maximum parsimony. The reference tree and alternative trees topologies were successively recreated in TNT as the first and second tree in memory by unlocking those trees and modifying their topologies.

Hypothesis 1. Heterodontosauridae (((*Fruitadens haagarorum*; (*Lycorhinus angustidens*; (*Heterodontosaurus tucki*; *Abrictosaurus consors*))); (*Echinodon becklesii*; *Tianyulong confuciusi*))) are set as a basal monophyletic sister group of Genasauria.

Rank	Difference	Rankscore
1	-1.000000	-36.500000
2	1	36.500000
3	-1.000000	-36.500000
4	1	36.500000
5	1	36.500000
6	1	36.500000
7	1	36.500000
8	-1.000000	-36.500000
9	-1.000000	-36.500000
10	1	36.500000
11	-1.000000	-36.500000
12	1	36.500000
13	-1.000000	-36.500000
14	1	36.500000
15	1	36.500000
16	1	36.500000
17	-1.000000	-36.500000
18	-1.000000	-36.500000
19	-1.000000	-36.500000
20	1	36.500000
21	1	36.500000
22	-1.000000	-36.500000
23	1	36.500000
24	1	36.500000
25	1	36.500000
26	1	36.500000
27	1	36.500000

28	1	36.500000
29	1	36.500000
30	1	36.500000
31	1	36.500000
32	1	36.500000
33	-1.000000	-36.500000
34	1	36.500000
35	1	36.500000
36	1	36.500000
37	1	36.500000
38	1	36.500000
39	-1.000000	-36.500000
40	1	36.500000
41	1	-36.500000
42	1	36.500000
43	1	36.500000
44	1	36.500000
45	-1.000000	36.500000
46	1	36.500000
47	-1.000000	-36.500000
48	1	36.500000
49	-1.000000	-36.500000
50	-1.000000	-36.500000
51	-1.000000	-36.500000
52	1	36.500000
53	-1.000000	-36.500000
54	1	36.500000
55	1	36.500000
56	1	36.500000
57	1	36.500000
58	-1.000000	-36.500000
59	1	36.500000
60	1	36.500000
61	1	36.500000
62	1	36.500000
63	1	36.500000
64	1	36.500000
65	-1.000000	-36.500000
66	1	36.500000
67	1	36.500000
68	1	36.500000
69	1	36.500000
70	-1.000000	-36.500000
71	1	36.500000
72	1	36.500000
73	-2.000000	-73.000000

Sum of negative ranks 839.500000

Number of non-zero scores 73

Critical value is 1177 for 5 percent, 1051 for 5 percent, 994 for 2.5 percent, and 927 for 1 percent. The risk of erroneously rejecting the null-hypothesis that both tree topologies fit the

data as well is significant at the 1 percent level ($p < 0.01$).

Hypothesis 2. Rhabdodontomorpha (as resolved in the 50% MRC) as the closest sister group of Ankylopollexia (comprising *Camptosaurus aphanoecetes*, *Camptosaurus dispar* and *Iguanodon bernissartensis*).

Rank	Difference	Rankscore
1	1	14.500000
2	1	14.500000
3	-1.000000	-14.500000
4	1	14.500000
5	1	14.500000
6	1	14.500000
7	1	14.500000
8	1	14.500000
9	1	14.500000
10	1	14.500000
11	1	14.500000
12	1	14.500000
13	-1.000000	-14.500000
14	-1.000000	-14.500000
15	1	14.500000
16	-1.000000	-14.500000
17	1	14.500000
18	1	14.500000
19	-1.000000	-14.500000
20	1	14.500000
21	-1.000000	-14.500000
22	1	14.500000
23	-1.000000	-14.500000
24	-1.000000	-14.500000
25	1	14.500000
26	1	14.500000
27	-1.000000	-14.500000
28	1	14.500000

Sum of negative ranks 130.500000
Number of non-zero scores 28
Critical value is 130 for 5 percent, 116 for 2.5 percent, and 101 for 1 percent. The risk of erroneously rejecting the null-hypothesis that both tree topologies fit the data as well is not significant.

Hypothesis 3. Breakage of Rhabdodontomorpha with *Muttaburrasaurus langdoni* and *Fostoria dhimbangunmal* set as the closest monophyletic sister group of Ankylopollexia (comprising *Camptosaurus aphanoecetes*, *Camptosaurus dispar* and *Iguanodon bernissartensis*), and Rhabdodontidae left in the same position as in the reference tree.

Rank	Difference	Rankscore
1	-1.000000	-17.500000
2	1	17.500000
3	1	17.500000
4	1	17.500000
5	1	17.500000
6	1	17.500000
7	1	17.500000
8	1	17.500000
9	1	17.500000
10	-1.000000	17.500000
11	-1.000000	-17.500000
12	-1.000000	-17.500000
13	-1.000000	-17.500000
14	1	17.500000
15	-1.000000	-17.500000
16	-1.000000	-17.500000
17	1	17.500000
18	1	17.500000
19	1	17.500000
20	1	17.500000
21	1	17.500000
22	1	17.500000
23	1	17.500000
24	1	17.500000
25	-1.000000	-17.500000
26	1	17.500000
27	1	17.500000
28	1	17.500000
29	-1.000000	-17.500000
30	-1.000000	-17.500000
31	-1.000000	-17.500000
32	1	17.500000
33	1	17.500000
34	1	17.500000

Sum of negative ranks 192.500000
Number of non-zero scores 34
Critical value is 200 for 5 percent, 182 for 2.5 percent, and 162 for 1 percent. The risk of erroneously rejecting the null-hypothesis that both tree topologies fit the data as well is significant at the 5 percent level ($p < 0.05$).

Cretaceous
Jurassic
Triassic
Maastrichtian
Campanian
Santonian
Coniacian
Turonian
Cenomanian
Albian
Aptian
Barremian
Hauterivian
Valanginian
Berriasian
Tithonian
Kimmeridgian
Oxfordian
Callovian
Bathonian
Bajocian
Aalenian
Toarcian
Pliensbachian
Sinemurian
Hettangian
Rhaetian
Norian
Carnian
66.
72.1 ± 0.2
83.6 ± 0.2
86.3 ± 0.5
89.8 ± 0.5
93.9
100.5
~113.0
~125.0
~129.4
~132.9
~139.8
~145.0
152.1 ± 0.9
157.3 ± 1.0
163.5 ± 1.0
166.1 ± 1.2
168.3 ± 1.3
170.3 ± 1.4
174.1 ± 1.0
182.7 ± 0.7
190.8 ± 1.0
199.3 ± 0.3
201.3 ± 0.2
~208.5
~227
Herrerasaurus ischigualastensis
Eocursor parvus
Laquintasaura venezuelae
Lesothosaurus diagnosticus
Scutellosaurus lawleri
Emausaurus ernsti
Scelidosaurus harrisonii
Ankylosauria
Stegosauria
Isaberrysaura mollensis
Agilisaurus louderbacki
Hexinlusaurus multidens
Liaoceratops yanzigouensis
Archaeoceratops oshimai
Stenopelix valdensis
Yinlong downsi
Chaoyangsaurus youngi
Psittacosaurus major
Psittacosaurus mongoliensis
Fruitadens haagarorum
Lycorhinus angustidens
Heterodontosaurus tucki
Abrictosaurus consors
Tianyulong confuciusi
Echinodon becklesii
Wannanosaurus yansiensis
Goyocephale lattimorei
Homalocephale calathocercos
Prenocephale prenes
Stegoceras validum
Pachycephalosaurus wyomingensis
ORNITHOPODA
100
79
58
95
79

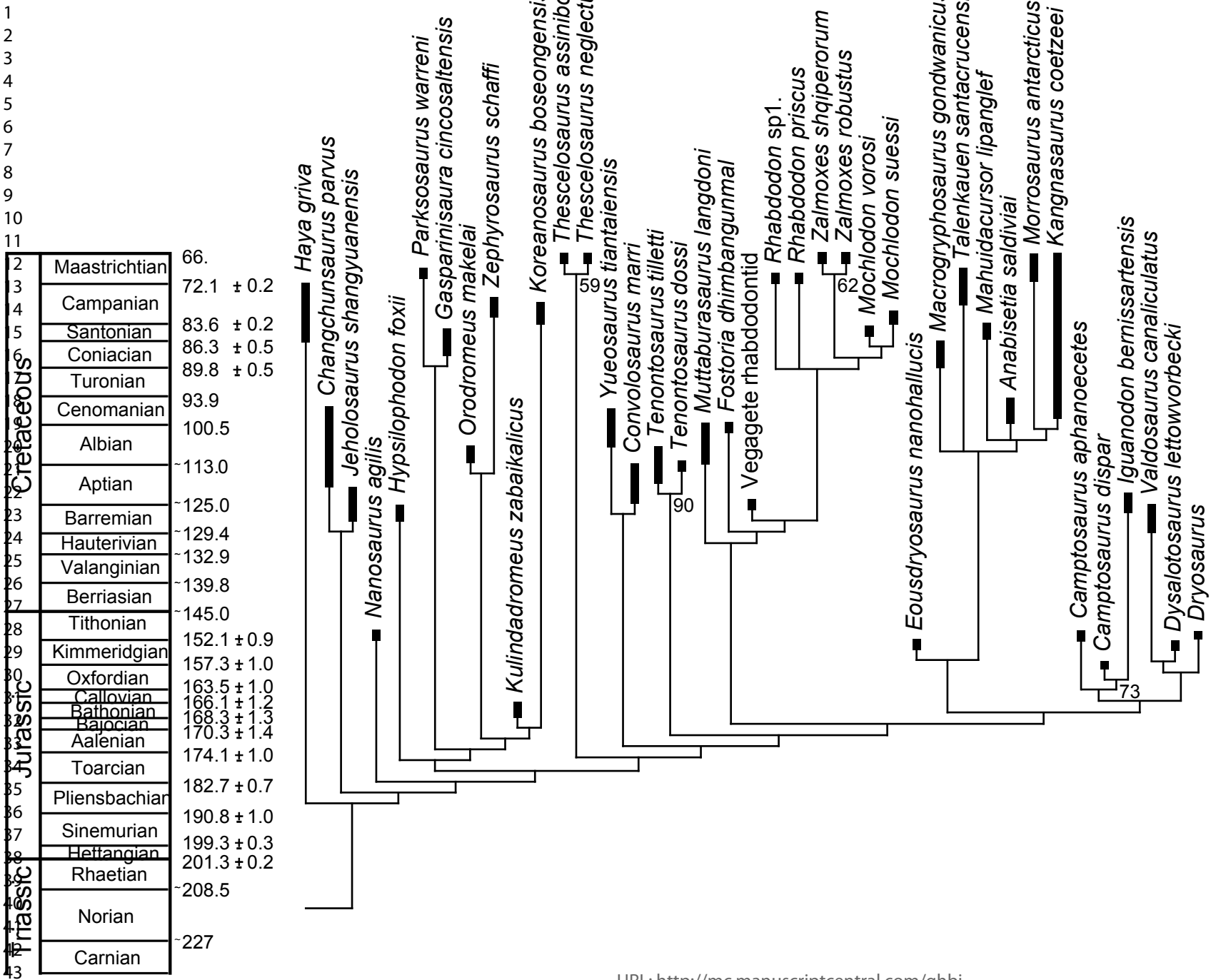
Haya griva
Changchunsaurus parvus
Jeholosaurus shangyuanensis
Nanosaurus agilis
Hypsilophodon foxii
Parksosaurus warreni
Gasparinisaura cincosaltensis
Orodromeus makelai
Zephyrosaurus schaffi
Kulindadromeus zabaikalicus
Koreanosaurus boseongensis
Thescelosaurus assiniboiensis
Thescelosaurus neglectus
59
Yueosaurus tiantaiensis
Convolosaurus marri
Tenontosaurus tilletti
Tenontosaurus dossi
90
Muttaburrasaurus langdoni
Fostoria dhimbangunmal
Vegagete rhabdodontid
Rhabdodon sp1.
Rhabdodon priscus
Zalmoxes shqiperorum
Zalmoxes robustus
62
Mochlodon vorosi
Mochlodon suessi
Eousdryosaurus nanohallucis
Macrogryphosaurus gondwanicus
Talenkauen santacrucensis
Mahuidacursor lipanglef
Anabisetia saldiviai
Morrosaurus antarcticus
Kangnasaurus coetzeei
Camptosaurus aphanoecetes
Camptosaurus dispar
Iguanodon bernissartensis
73
Valdosaurus canaliculatus
Dysalotosaurus lettowvorbecki
Dryosaurus
Cretaceous
Jurassic
Triassic
Maastrichtian
Campanian
Santonian
Coniacian
Turonian
Cenomanian
Albian
Aptian
Barremian
Hauterivian
Valanginian
Berriasian
Tithonian
Kimmeridgian
Oxfordian
Callovian
Bathonian
Bajocian
Aalenian
Toarcian
Pliensbachian
Sinemurian
Hettangian
Rhaetian
Norian
Carnian
66.
72.1 ± 0.2
83.6 ± 0.2
86.3 ± 0.5
89.8 ± 0.5
93.9
100.5
~113.0
~125.0
~129.4
~132.9
~139.8
~145.0
152.1 ± 0.9
157.3 ± 1.0
163.5 ± 1.0
166.1 ± 1.2
168.3 ± 1.3
170.3 ± 1.4
174.1 ± 1.0
182.7 ± 0.7
190.8 ± 1.0
199.3 ± 0.3
201.3 ± 0.2
~208.5
~227

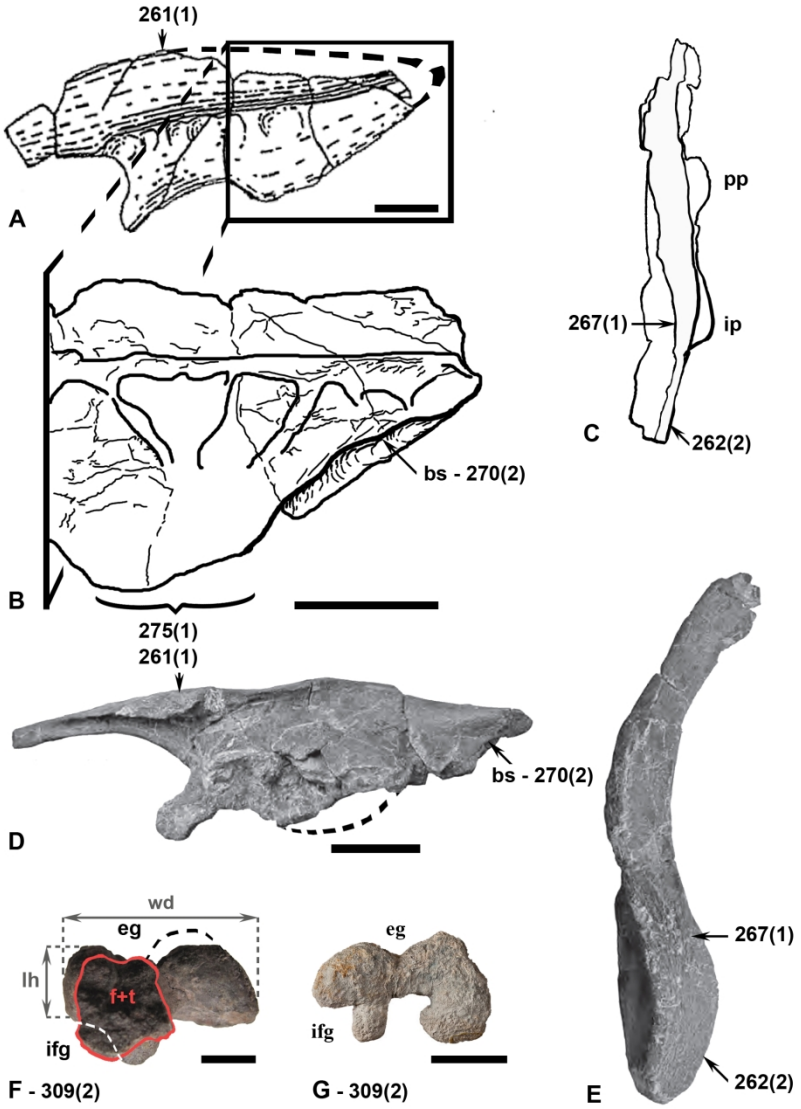

Figure 3 : Rhabdodontomorphans features. A-C : right ilium QM F6140 of Muttaburrasaurus langdoni in A, lateral; B, medial (with close-up of postacetabular process); C, dorsal views. D-E: left (UBB NVZ1-17) and right (UBB NVZ1-16) ilium of Zalmoxes shqiperorum in D, medial (reversed to right) ; E, dorsal views. F, right femur MDS-VG, 135 of the Vegagete rhabdodontid in distal view. G, right femur LRF 3050.V of Fostoria dhimbangunmal in distal view. A proceeds from Bartholomai & Molnar (1981, fig. 8C). B and C are line-drawing outlines made-up from photos of Muttaburrasaurus' ilium kindly provided by Matthew Herne. D and E proceed from Godefroit et al. (2009, fig. 18B, C). F is a distal view of the largest distal femur of the Vegagete ornithopod (cf. same bone in posterior view in Dieudonné et al. 2016a, fig. 8C). G proceeds from Bell et al. (2019, fig. 8E). Abbreviations : bs, brevis shelf ; eg, extensor groove ; ifg, iliofibularis groove ; ip, ischiac peduncle ; pp, pubic peduncle. Characters numbers are referred with their state in parentheses. We precise that state 2 of character #309 occurs in F and G as lh (lateral width) divided by wd (distal width) is inferior to 40%. Scales bars are 15 cm (A-C), 5 cm (D, E and G), and 5 mm (F).

166x246mm (300 x 300 DPI)